

Role of Lectin Receptors in recognition of Pseudomonas aeruginosa biofilms

Thesis submitted to the University of Nottingham

for the degree of Doctor of Philosophy

Yasir Saleh I Almuhanna

September 2020

Abstract

Colonisation and chronic lung infection by the opportunistic pathogen *Pseudomonas aeruginosa* (PA) is the leading cause of morbidity and mortality in cystic fibrosis patients. A critical key determinant of PA pathogenicity is the switch from planktonic to the biofilm mode of growth, which facilitates chronic infections and makes PA eradication extremely difficult. Biofilms are aggregates of microorganisms in which the cells are enclosed in an extracellular polymeric substance (EPS) that contains proteins, extracellular DNA (eDNA) and exopolysaccharides. Psl and Pel are two important exopolysaccharides utilised by PA to construct biofilms. While Psl is composed of D-mannose, D-glucose, and L-rhamnose, Pel contains N-acetylgalactosamine (GalNAc) and N-acetylglucosamine (GlcNAc).

C-type lectins receptors (CLRs) are pattern recognition receptors (PRRs) that recognise carbohydrate motifs and are expressed by innate immune cells, including dendritic cells (DCs), macrophages and neutrophils. The overarching aim of this thesis is to investigate the interplay between PA and innate immune cells and how it is affected by biofilm formation. We hypothesise that engagement of CLRs through recognition of carbohydrate structures within PA biofilms could modulate the immune response and interfere with innate immune cells function, hence facilitating the persistence of infection.

Previously, our lab demonstrated that PA biofilms and biofilm-associated carbohydrates purified from the Pel-deficient mutant Δ*wspF* Δ*pel*, engage two CLRs, Dendritic Cell-Specific Intercellular adhesion molecule-3-Grabbing Non-integrin (DC-SIGN, CD209) and Mannose receptor (MR, CD206). In this study, we show that Dectin-2 (CLEC6A) is another CLRs that binds PA biofilms and purified biofilm carbohydrates; Dectin-2 binds to biofilms formed by PA strains with different EPS composition as well as biofilms formed by PA wound isolates. Similarly to MR and DC-SIGN, Dectin-2 also recognised purified biofilm-associated carbohydrates. High and low molecular fractions of purified biofilm carbohydrates were tested in this study and Dectin-2, together with DC-SIGN and MR preferentially bound to the HMW preparations. Biofilm-associated HMW carbohydrates did not induce Dectin-2 signalling on huDectin-2 reporter cells or HEK-Blue™ mDectin-2 cells but showed antagonistic activity blocking the response of muDectin-2 reporter cells to the Dectin-2 ligand zymosan.

To microscopically examine the distribution of CLRs ligands within the biofilms and to study the interaction of immune cells with biofilm, we optimised biofilm generation in substrates suitable for microscopic examination. Confocal analysis shows DC-SIGN, Dectin-2 and, weakly, MR ligands within PAO1 biofilms concentrated into discrete clusters with additional DC-SIGN ligands dispersed among bacteria aggregates. Monocyte-derived DCs (moDCs)

(DC-SIGN+ and MR+) cultured with biofilms formed by strains that overexpress Psl (Δ*wspF* and Δ*wspF* Δ*pel*) tend to display round morphology and similar findings were noted when moDCs were incubated with purified biofilm carbohydrates. In a different set of experiments cytokine production by human moDCs in response to biofilms was tested and no differences were seen among biofilms with different carbohydrate compositions or after addition of purified biofilm carbohydrates. Taken together, these data indicate that DC-SIGN, MR and Dectin-2 are receptors for PA biofilms and biofilm-associated carbohydrates. The results of this research support the idea that CLRs engagements upon biofilm recognition by innate immune cells might modulate immune cells function.

As the first responder cells of the innate immune system, neutrophils possess a unique set of migration features. Several studies found that neutrophils were not able to eradicate infection caused by biofilm-forming PA, which might indicate that biofilm formation was hindering neutrophil's activity. Here, we describe an *in vitro* assay that allows us to examine neutrophil behaviour, using live and confocal microscopy, following their interaction with PA, as a planktonic or biofilm cultures. Using live microscopy analysis, we observed that (1) biofilms reduced neutrophil velocity, net distance covered and the mean square displacement. Using confocal microscopy analysis, we observed that (2) neutrophils appeared unable to release granules when incubated with biofilms. Finally, (3) preliminary observations indicated that cells exhibit higher circularity when incubated with biofilm formed by strains expressing Psl or Psl-deficient biofilms in the presence of purified biofilm carbohydrates.

The findings from this study have gone some way towards enhancing our understanding of the potential impact of biofilm formation on innate immune cells which might open new avenues for therapeutic approaches.

Acknowledgements

First and foremost, I would like to thank almighty Allah for giving me the strength, ability, and opportunity to conduct and complete this project.

To my sponsors, the Government of Saudi Arabia, the Saudi Arabian Cultural Bureau in the United Kingdom, and Shaqra University, I say a very big thank you for the financial support and offering me a scholarship to fulfil my dream.

I would like to express my deep and sincere gratitude to my principal supervisor, Dr. Luisa Martinez-Pomares for her expert advice, supervision, support, mentoring and inspiration throughout this research. It was a great privilege and honor to work and study under her guidance. I am also extremely thankful to Professor Miguel Cámara, my second supervisor, for all his contributions and support.

I would like to say thanks to all amazing previous and current members of the lectin biology group (Darryl Jackson, Sonali Singh, Sirina Muntaka, Mohammad Alshahrani, Diego De Medeiros Costa, Kelly Lee, Oliver Chan, Philemon Gyasi-Antwi and Farah Hussein) for the help, support and the demonstration of some technical procedures. A special thanks goes to Sonali Singh for all her assistance and cooperation throughout this project. I am also grateful for the assistance given by Dr Chris Gell with confocal and live microscopy examinations.

I would especially like to thank my family. I cannot begin to express my thanks to my Mum (Norah Almoshwah), for the love, prayers, caring, and the encouragements to follow my dreams. I would like to also present my sincere thankfulness to my deceased father (Saleh Almuhanna), for his great role in my life and his numerous sacrifices. My success in all aspects of my life would not have been possible without the support and nurturing of my parents. I would also like to extend my deepest gratitude to my wife (Wejdan Aljurays) for giving me all the support, motivation, prayers, understanding and being there for me always. You will always

be my guiding light. I also wish to thank all my brothers and sisters (Yazeed, Wejdan, Reem, Abdullah and Abdulaziz) for all your encouragements and prayers.

I am also truly grateful to each of my friends for all the support that I have received from them. I am extremely grateful and thankful to all of you.

Declaration

1. Co-Authorship

I hereby declare that this thesis incorporates material that is result of joint research, as follows:

A. Some sections of Chapter 5 (5.4.1.2, 5.4.2 and 5.4.3) were co-authored with Dr. Sonali Singh under the supervision of Dr. Luisa Martinez-Pomares. The contribution of co-authors (Yasir Almuhanna and Sonli Singh) is detailed in the table below:

<table>
<tr><th rowspan="2">Sections co-authoerd jointly</th><th colspan="2">Contripution</th></tr>
<tr><th>Yasir Almuhanna</th><th>Sonali Singh</th></tr>
<tr><td>5.4.1.1 RNAseq analysis of DC-SIGN, MR, Dectin-1 and Dectin-2 expression on human macrophages</td><td>Performed analysis of a novel RNAseq data set produced in the lab by Dr. Sirina Muntaka, unpublished</td><td>Did not contribute</td></tr>
<tr><td>5.4.1.2 Flow cytometry analysis of DC-SIGN, MR, Dectin-1 and Dectin-2 expresion on huDCs.</td><td>Performed all the assays</td><td>Contributed to the statistical analysis and generation of graphs</td></tr>
<tr><td>5.4.2 Effect of the biofilms with different carbohydrate composition on cytokine responses by moDCs</td><td colspan="2" rowspan="2">Both co-authors contributed equaly</td></tr>
<tr><td>5.4.3 Cell survival assay (LDH)</td></tr>
<tr><td>5.4.4 Biofilm carbohydrate interferes with the function of cell-associated DC-SIGN and MR</td><td>Did not contribute</td><td>Performed and analysed all the assays</td></tr>
</table>

5.4.5 The effect of biofilm carbohydrate on morphological characteristics of human dendritic cells	Performed and analysed all the assays	Did not contribute

B. Chris Gell contributed only in the microscopy settings of data presented in:

- Chapter 4 (4.4.3 Distribution of C-type lectin receptor ligands on PAO1 biofilms).

- Chapter 6 (6.4.4 Optimisation experiments to study neutrophil-PA interaction and 6.4.5 Live microscopy analysis of neutrophil responses to PA biofilms).

I am aware of the University of Nottingham Policy on Authorship and I certify that I have properly acknowledged the contribution of other researchers to my thesis.

I certify that, other than the above mentioned, this thesis, and the research to which it refers, is the product of my own work.

II.Previous Publication

This thesis includes [1] original preprint previously uploaded to bioRxiv that was referred to in the introduction of Chapter 4 (4.1.7. Data leading to this study).

Full citation of the priprent: SINGH, S., ALMUHANNA, Y., ALSHAHRANI, M. Y., LOWMAN, D., RICE, P. J., GELL, C., MA, Z., GRAVES, B., JACKSON, D., LEE, K., KELKAR, R., KORANTENG, J., MITCHELL, D., SILVA, A. D., HUSSAIN, F., YILMAZ, G., MASTROTTO, F., IRIE, Y., WILLIAMS, P., WILLIAMS, D., CAMARA, M. & MARTINEZ-POMARES, L. 2020. *Pseudomonas aeruginosa* biofilms display carbohydrate ligands for CD206 and CD209 that interfere with their receptor function. bioRxiv, 2020.04.20.051292.

List of publication

Published / In review

- S. Singh, **Y. Almuhanna**, M. Y. Alshahrani, D. Lowman, P. J. Rice, C. Gell, Z. Ma, B. Graves, D. Jackson, K. Lee, R. Kelkar, J. Koranteng, S. Muntaka, D. Mitchell, A. C. da Silva, F. Hussain, G. Yilmaz, F. Mastrotto, Y. Irie, P. Williams, D. Williams, M. Camara, and Luisa Martinez-Pomares (2020). Pseudomonas aeruginosa biofilms display carbohydrate ligands for CD206 and CD209 that interfere with their receptor function. bioRxiv, 2020.04.20.051292 (Published)
- S. Muntaka, **Y. Almuhanna**, A. Asante, M. Camara and L. Martinez-Pomares (2019). Gamma Interferon and Interleukin-17A Differentially Influence the Response of Human Macrophages and Neutrophils to Pseudomonas aeruginosa Infection. Infection and Immunity (Published)

Selected posters and presentations at conferences

- M. Y. Alshahrani, T. Rahman, **Y. Almuhanna**,Y. Irie, M. Camara, L. Martinez Pomares (2016), The interaction between Pseudomonas aeruginosa and C-Type Lectins. 5th UK Cystic Fibrosis Microbiology Consortium Meeting. November 29th, 2016. Jury's Inn, Liverpool, UK (Poster)
- S. Muntaka, **Y. Almuhanna**, M. Cámara and L. Martinez-Pomares (2017). L-17A And IFN-γ establish the balance between inflammatory potential and bacteria killing by human phagocytes during bacterial Infection. Microbes Research Group Forum. March 15th, 2017. University of Nottingham, Nottingham, UK. (Poster presentations)
- S. Muntaka, **Y. Almuhanna**, M. Cámara and L. Martinez-Pomares (2017). Regulation of IL-1β secretion by IFN-γ in Human Macrophage Neutrophil co-cultures During

Pseudomonas aeruginosa Infection. 5th Mol Micro & 4th M4 Meeting. September 13th-14th, 2017. University of Birmingham, Birmingham, UK. (Poster presentations)

- **Y. Almuhanna**, S. Singh, C. Gell, Y. Irie, M. Cámara and L. Martínez-Pomares (2018). The interaction between Pseudomonas aeruginosa biofilms and neutrophils. The Young Microbiologist Symposium, August 27th-28th, 2018. Queen's University Belfast, Belfast (Poster presentation)
- **Y. Almuhanna**, S. Singh, M. Alshahrani, R. Kelkar, C. Gell, Y. Irie, A. Silva, P. Williams, M. Cámara and L. Martínez-Pomares (2019). Modulation of immune cell activation by Pseudomonas aeruginosa biofilms; potential role of C-type lectin receptors. 6th Eurobiofilms ESGB meeting, September 3rd-6th, 2019. The Technology and Innovation Centre, Glasgow, UK. (Oral and Poster presentations)
- **Y. Almuhanna**, S. Singh, M. Alshahrani, R. Kelkar, C. Gell, Y. Irie, A. Silva, P. Williams, M. Cámara and L. Martínez-Pomares (2019). Recognition of Pseudomonas aeruginosa biofilms by DC-SIGN, Mannose receptor and Dectin-2 modulate the immune response. British Society for Immunology Congress, December 2–5th, 2019. The Arena and Convention Centre (ACC), Liverpool, UK. (Poster presentation)
- S. Singh, **Y. Almuhanna**, M. Y. Alshahrani, D. Lowman, P. J. Rice, C. Gell, Z. Ma, B. Graves, D. Jackson, K. Lee, R. Kelkar, J. Koranteng, S. Muntaka, D. Mitchell, A. C. da Silva, F. Hussain, G. Yilmaz, F. Mastrotto, Y. Irie, P. Williams, D. Williams, M. Camara, and Luisa Martinez-Pomares (2020). Pseudomonas aeruginosa biofilms display carbohydrate ligands for CD206 and CD209 that interfere with their receptor function. The Young Microbiologist Symposium, Virtual, August 26th-27th, 2020. (Poster presentation)

Table of Contents

Abstract 1
Chapter 1. Introduction 21
1.1. General introduction to *P. aeruginosa* 21
1.2. Clinical Importance of *P. aeruginosa* 25
1.2.1. Skin-associated infections 25
1.2.2. Ventilator-associated pneumonia (VAP) 26
1.2.3. Cystic fibrosis (CF) 26
1.3. Virulence determinants of *P. aeruginosa* 28
1.3.1. Flagella and pili 29
1.3.2. Type III secretion system (T3SS) 31
1.3.3. Lectins 33
1.3.4. Lipopolysaccharide 34
1.3.5. Quorum sensing (QS) 36
1.4. Biofilm formation in *P. aeruginosa* 39
1.4.1. Role of proteins in biofilm formation: 41
1.4.2. Role of eDNA function in biofilm formation: 43
1.4.3. EPS function in the biofilm formation: 44
1.5. The role of the innate immune system during PA infection: 51
1.5.1. Immune recognition of PA via pattern recognition receptor (PRRs): 51
1.5.2. Toll-Like receptors: 51
1.5.3. Nod-Like receptors: 54
1.5.4. C-type lectins (CLRs): 55
1.6. The role of innate immune cells during PA Infection: 63
1.6.1. Dendritic Cells (DCs): 63
1.6.2. Macrophages: 66
1.6.3. Neutrophils: 67
1.7. Hypothesis and aims 69
Chapter 2. Materials and Methods 71
2.1. Bacterial strains and generation of mid-log phase cultures: 71
2.2. Genotyping of Wspf, Psl, and Pel mutation using polymerase chain reaction (PCR) 74
2.3. Biofilm formation and quantification assay (Crystal violet assay). 74
2.4. Analysis of the adhesion of planktonic PA to plastic 75
2.5. Lectin binding assays (Enzyme-Linked immunosorbent assay, ELISA). 75
2.6. Generation of Biofilms for microscopic analysis 76
2.6.1. Generation of PA biofilms on CELLview™ cell culture slides. 76
2.6.2. Generation of PA biofilms on µ-Slide VI 0.4 slides. 77
2.6.3. Generation of PA biofilms under flow condition using a peristaltic pump system. 77
2.6.4. Generation of PA biofilms under standardized flow conditions using the syringe pump system. 78

2.7. Study of lectin binding to PA biofilms by confocal microscopy 79
2.8. Isolation of human monocytes (CD14+ cells) 80
2.9. Preparation of human monocyte-derived dendritic cells (moDCs) 81
2.10. Purification of human neutrophils 82
2.11. Analysis of cell surface markers using flow cytometry 83
2.12. Analysis of Dectin-2 expression by western blot 84
2.13. Analysis of changes in moDCs morphology after incubation with HMW-Psl or PA biofilms 84
2.14. Analysis of changes in neutrophil morphology after incubation with HMW-Psl or PA biofilms 85
2.15. Analysis of the effect of biofilms or purified HMW-Psl on cytokine production by moDCs86
2.16. Cytokine quantification 87
2.17. Cell survival (LDH assay) 88
2.18. CLRs blocking on moDCs 88
2.19. Dectin-2 reporter cells assay 88
2.20. Biofilm-human neutrophils live microscopy assay 89
2.21. Analysis of biofilm-human neutrophils live microscopy assay using TrackMate 90
2.22. Quantification of neutrophils motility parameters 90
2.23. Statistical analysis 91
Chapter 3. Generation and Characterisation of *Pseudomonas aeruginosa* biofilms 92
3.1. Introduction 92
3.2. Hypothesis 96
3.3. Aims 96
3.4. Results 97
3.4.1. Validation of the PAO1 strains, Δ*wspF*, Δ*wspF*Δ*psl*, Δ*wspF*Δ*pel* and Δ*wspF*Δ*pel*Δ*psl*97
3.4.2. Analysis of biofilm formation on 96 wells plates by PAO1, Δ*wspF* mutants and clinical isolates using the CV assay 99
3.4.3. Visualisation of biofilm formation using confocal microscopy 102
3.5. Summary 110
3.6. Discussion: 112
3.6.1. The use of X-Vivo-15: 113
3.6.2. Biofilm formation using the syringe pump system 114
Chapter 4. Recognition of *Pseudomonas aeruginosa* biofilms and purified biofilm-associated carbohydrate by Dectin-2 118
4.1. Introduction 118
4.1.1. Structure of Dectin-2 119
4.1.2. Ligands of Dectin-2 120
4.1.3. Dectin-2 involvement in fungi recognition 121
4.1.4. Role of Dectin-2 in recognition of mycobacteria 122
4.1.5. Dectin-2 Signalling 124
4.1.6. Role of Dectin-2 in Disease 126
4.1.7. Data leading to this study 126

4.2. Hypothesis 130
4.3. Aims 130
4.4. Results 130
4.4.1. Biofilms formed by PAO1 and Δ*wspF* mutants are recognised by the CRD domain of Dectin-2 130
4.4.2. Biofilms formed by PA wound clinical isolates are recognised by Dectin-2-Fc, DC-SIGN-Fc and MR (CTLD-4-7-Fc) 133
4.4.3. Distribution of C-type lectin receptor ligands on PAO1 biofilms 135
4.4.4. Dectin-2 Fc binds Psl purified from PA biofilms 137
4.4.5. Binding of Dectin-2 to Psl is calcium-dependent 138
4.4.6. Manα-1-2Man inhibits binding of Dectin-2 to purified HMW-Psl 140
4.4.7. Confirmation of Dectin-2 binding to Psl using biolayer interferometry 142
4.4.8. Dectin-2 Fc does not bind PA planktonic cells 144
4.4.9. Psl does not induce Dectin-2 signalling 147
4.4.10. Psl acts as an antagonist for Dectin-2 150
4.5. Summary 151
4.6. Discussion 151
4.6.1. Binding of Dectin-2 to *P. aeruginosa* biofilms 152
4.6.2. Binding of Dectin-2 to biofilms purified carbohydrates 155
4.6.3. Antagonistic activity of HMW-Psl against Dectin-2 157
Chapter 5. Interaction of human Dendritic cells with PA Biofilms 160
5.1. Introduction 160
5.2. Hypothesis 162
5.3. Aims 164
5.4. Results 165
5.4.1. Analysis of DC-SIGN, MR, Dectin-1 and Dectin-2 expression on human myeloid cells 165
5.4.2. The effect of biofilm carbohydrate on the cytokine response of human dendritic cells 170
5.4.3. Cell survival (LDH assay) 180
5.4.4. Biofilm carbohydrate interferes with the function of cell-associated DC-SIGN and MR 182
..... 183
5.4.5. The effect of biofilm carbohydrate on morphological characteristics of human dendritic cells 185
5.5. Summary 195
5.6. Discussion 196
5.6.1. moDCs express high level of DC-SIGN and MR but not Dectin-2. 197
5.6.2. Biofilm-moDC co-cultures in the presence and absence of Psl show high variability in cytokine production. 199
5.6.3. The possible adverse impact of bacterial fixation and donor variability on the cytokines results. 206
5.6.4. Recommend adjustments on the current models and an alternative mouse model could be used to follow up this research 209

5.6.5. Concluding remarks 211
Chapter 6. Analysis of biofilm-human neutrophils interactions 213
6.1. Introduction 213
6.2. Hypothesis 215
6.3. Aims 215
6.3.1. Set up an assay to study neutrophil-PA biofilm interactions. 215
6.3.2. Utilise this assay to determine neutrophil morphological and behavioural changes following their interaction with PA biofilms. 215
6.4. Results 216
6.4.1. Optimisation of neutrophil PA co-culture for microscopic analysis 216
6.4.2. Neutrophils isolation using negative selection 216
6.4.3. Analysis of Dectin-2 expression by neutrophils. 217
6.4.4. Optimisation experiments to study neutrophil-PA interaction 220
6.4.5. Live microscopy analysis of neutrophil responses to PA biofilms 225
6.4.6. Confocal microscopy analysis of changes in neutrophil phenotype in response to PA biofilms 235
6.4.7. Investigation of neutrophils circularity following incubation with PA 239
6.5. Summary 242
6.6. Discussion 242
6.6.1. Motility and biofilms 242
6.6.2. Lack of attachment 247
6.6.3. HHA labelling and granules content 249
6.6.4. Circularity 250
6.6.5. Final conclusions 252
Chapter 7. General discussion and future perspective 255
7.1. Generation and Characterisation of PA biofilms (Chapter 3) 256
7.2. Recognition of *Pseudomonas aeruginosa* biofilms and purified biofilm-associated carbohydrate by Dectin-2 (Chapter 4). 257
7.3. Interaction of human Dendritic cells with PA Biofilms (Chapter 5) 260
7.4. Analysis of biofilm-human neutrophils interactions (Chapter 6) 262
7.5. Future prospects 264
7.5.1. Examination of the innate immune response to polymicrobial biofilms: 264
7.5.2. Examination of the possibility of other lectins to also contribute to PA recognition: 266
7.5.3. Examination of the synergistic response of CLRs with other PPRs such as TLR-9: 268
References 270

List of Figures

Figure 1.1 Major infections caused by PA. 22

Figure 1.2 Summary of main Gac/Rsm cascade components. 24

Figure 1.3 Selected virulence factors in PA. 28

Figure 1.4 The process of biofilm formation in PA 41

Figure 1.5 Main polysaccharides in PA biofilms 45

Figure 1.6 TLRs signalling pathways. 54

Figure 1.7 Schematic representation of the structure and signalling of MR, DC-SIGN, Dectin-1, Dectin-2 and Mincle 57

Figure 3.1 Confirmation of mutations in wspF and psl and/or pel operons using PCR. 98

Figure 3.2 Measurement of biofilm formation of PAO1 and Δ*wspF* strains in X-vivo-15 media using the crystal violet method. 100

Figure 3.3 Biofilm formation of PA clinical isolates in X-vivo-15 media using the crystal violet method. 101

Figure 3.4 Visualisation of biofilm formation of Δ*wspF* strains using confocal microscopy. 104

Figure 3.5 Comparison between three coating plates. 106

Figure 3.6 Biofilm formation by Δ*wspF* in ibidi µ-Slide VI 0.4 slides under flow conditions generated with a peristaltic pump. 107

Figure 3.7 Process for pre-gassing of X-Vivo-15 media. 109

Figure 3.8 Standardised conditions applied to generate biofilms using a syringe pump system. 110

Figure 3.9 Generation of PAO1 biofilms under standardised flow conditions. 112

Figure 3.10 Biofilms characteristics after 18 and 24 hr culture. 108

Figure 3.11 Analysis of biofilm components in mushroom-shaped structures within PAO1 biofilms. 109

Figure 3.12 Summary of the work done in this chapter to optimise biofilm formation using the syringe pump system. 115
Figure 4.1 Structure of Dectin-2 119
Figure 4.2 Man-LAM structure 123
Figure 4.3 Dectin-2 signalling pathway 125
Figure 4.4 Recognition of DC-SIGN and MR-CTLD-4-7 to PAO1 biofilm 127
Figure 4.5 Size analysis and binding to DC-SIGN and MR-CTLD4-7 of *P. aeruginosa* biofilm-associated carbohydrate 128
Figure 4.6 Characterisation of high molecular weight biofilm carbohydrates 129
Figure 4.7 Binding of Dectin-2-Fc to PA biofilms. 132
Figure 4.8 Assessment of binding of DC-SIGN-Fc, Dectin-2-Fc and MR (CTLD4-7-Fc) to biofilms formed by PA clinical isolates. 134
Figure 4.9 Distribution of DC-SIGN, MR, and Dectin-2 ligands in PAO1 biofilms. 136
Figure 4.10 Binding of Dectin-2-Fc and MR (CTLD4-7-Fc) to purified Psl. 138
Figure 4.11 Binding of Dectin-2-Fc and MR (CTLD4-7-Fc) to purified HMW-Psl$^{(LPS\text{-}free)}$ is calcium-dependent. 139
Figure 4.12 Inhibition of Dectin-2-Fc binding to purified HMW-Psl-2$^{(LPS\text{-}free)}$ by Manα-1-2Man. 141
Figure 4.13 Dectin-2 binding using BLI 143
Figure 4.14 Dectin-2-Fc does not bind to planktonic PA and purified LPS in ELISA. 145
Figure 4.15 Dectin-2 does not bind planktonic PA in an immunofluorescence assay. 146
Figure 4.16 huDectin-2 2B4-NFAT-GFP reporter cells do not respond to purified Psl 148
Figure 4.17 mDectin-2 reporter cells and hDectin-1 reporter cells incubation with HMW-Psl-2 149
Figure 4.18 HMW-Psl-2$^{(LPS\text{-}free)}$ inhibits Dectin-2-mediated cellular activation. 150
Figure 5.1 Role of lectin receptors during PA infection. 163
Figure 5.2 mRNA levels of DC-SIGN, MR, Dectin-1 and Dectin-2 on M-CSF-Macrophages 166

Figure 5.3 Flow cytometry analysis of DC-SIGN, MR, Dectin-2 and Dectin-1 expression on moDCs 168
Figure 5.4 Characterisation of HMW carbohydrate preparations. 172
Figure 5.5 Effect of HMW-Psl-2$^{(LPS\text{-}free)}$ on moDCs responses to PA Psl-deficient biofilm and planktonic cultures 173
Figure 5.6 Analysis of cytokine production by moDCs in response to Psl+/Pel+, Psl+/Pel-, Psl-/Pel+ biofilms 175
Figure 5.7 Confirmation of CLRs blocking using flow cytometry donor 2 177
Figure 5.8 Confirmation of CLRs blocking using flow cytometry donor 3 178
Figure 5.9 Effect of blocking CLRs on moDCs responses to PA biofilms 179
Figure 5.10 Lactate Dehydrogenase (LDH) assay indicated neither fixed PA biofilms or HMW-Psl-2$^{(LPS\text{-}free)}$ cues moDCs cell death. 181
Figure 5.11 Inhibition of sugar uptake by MR and DC-SIGN expressing cells by HMW-Psl-1 and HMW-Psl-2. 183
Figure 5.12 Polymyxin B does not affect HMW-Psl-1 and HMW-Psl-2 mediated inhibition of Lewis^{x} uptake by moDCs. 184
Figure 5.13 Visualisation of DC-SIGN on moDCs 187
Figure 5.14 Comparison of moDCs DC-SIGN expression using two different anti-DC-SIGN antibodies 188
Figure 5.15 Optimisation of DC-SIGN staining using PEM buffer 189
Figure 5.16 Visualisation of moDC morphology after incubation with PA biofilms 191
Figure 5.17 Changes in unpermeabilised moDCs morphology in the presence of biofilm-associated carbohydrate, Psl. 193
Figure 5.18 Specific detection of DC-SIGN in permeabilised moDCs in the presence and absence of Psl. 194
Figure 6.1 Neutrophil purification and analysis of Dectin-2 expression 218
Figure 6.2 First live microscopy monitoring of neutrophil-biofilm interaction indicated neutrophil were active throughout 2 hr incubation. 222

Figure 6.3 Analysis of neutrophil labelling intensity during live imaging 223
Figure 6.4 Summarised workflow of the microscopy-based assay to study neutrophil and PA interaction. 224
Figure 6.5 fixed stage coordinate used in this assay 227
Figure 6.6 Neutrophil tracking using TrackMate 228
Figure 6.7 Analysis of mean velocity and net distances in neutrophils cultured under different conditions 229
Figure 6.8 Mean square displacement (MDS) and average speed in neutrophils cultured under different conditions 232
Figure 6.9 Neutrophils were phagocytic against both, biofilms and planktonic cells. 233
Figure 6.10 Total neutrophils per location 234
Figure 6.11 Confocal microscopy analysis of neutrophil PA interaction 238
Figure 6.12 Neutrophils incubated with biofilms or Psl tend to retain circular morphology compared to those incubated with planktonic cultures 242
Figure 6.13 Suggested model for future assays 246

List of Tables

Table 1 Strains used in the study 72

Table 2 *P. aeruginosa* wound clinical isolates used in the study.....73

Table 3 Primers used to confirm specific mutations in the *wspF* mutants 74

List of Abbreviations

AHL	N-acylhomoserine lactones
AprA	Alkaline protease
BSA	Bovine serum albumin
c-di-GMP	Cyclic dimeric guanosine monophosphate
CF	Cystic fibrosis
CFTR	Cystic Fibrosis Transmembrane Conductance Regulator gene
CLRs	C-type lectin receptors
CTLDs	C-type lectin-like domains
CPA	Common polysaccharide antigen
DCs	Dendritic cells
DC-SIGN	Dendritic Cell-Specific Intercellular adhesion molecule-3-Grabbing Non-integrin
Dectin-1	Dendritic cell-associated C-type lectin-1
Dectin-2	Dendritic cell-associated C-type lectin-2
DGCs	Diguanylate cyclases
eDNA	Extracellular DNA
EPS	Extracellular polymeric substance
ETA	Exotoxin A
ET	Endotracheal Tube
F1gE	Flagellar hook protein
GAC	Global activator of antibiotic and cyanide
GAP	GTPase activating protein
HHA	Hippeastrum hybrid Amaryllis
HHQ	2-Heptyl-4-quinolone
HIV	Human immunodeficiency virus
HptB	Histidine phosphotransfer protein B
ITAM	Immunoreceptor tyrosine-based activation motif
IRF	Interferon regulatory transcription factor
ITAM	Immunoreceptor tyrosine-based activation motif
LB	Luria-Bertani
LPS	Lipopolysaccharide
LRRs	Leucine-rich repeats

LTB4	Leukotriene B4
LARG	Leukemia-Associated RhoGEF
LSP1	leukocyte-specific protein 1
MAPK	Mitogen-activated protein kinases
MPO	Myeloperoxidase
MR	Mannose receptor
MyD88	Myeloid differentiation 88
NETs	Neutrophil extracellular traps
NF-κB	Nuclear Factor kappa-light-chain-enhancer of activated B cells
NLRP	Nucleotide-binding oligomerization domain, Leucine-rich Repeat and Pyrin domain
NLRs	Nucleotide-binding oligomerization domain (NOD)-like receptors
NOD	Nucleotide-binding oligomerization domain
GalNAc	N-acetylgalactosamine
GlcNAc	N-acetylglucosamine
3O-C12-HSL	N-3-oxo-dodecanoyl-L-homoserine
OSA	O-specific antigen
PA	Pseudomonas aeruginosa
PAMPs	Pathogen associated molecular patterns
PLC	Phospholipase C
PMNs	Polymorphonuclear leukocytes
PQS	2-Heptyl-3-hydroxy-4-quinolone
PRR	Pattern recognition receptors
Psl	Polysaccharide synthesis locus
PYD	Pyrin domain
Pld	Phospholipase D
PPAR-γ	Proliferator-activated receptor-gamma
QS	Quorum sensing
GM-CSF	Granulocyte macrophage colony–stimulating factor
RhoA	Ras homolog gene A
RLRs	Retinoic acid-inducible gene (RIG)-I-like receptors
ROS	Reactive oxygen species
RsmA	RNA-binding regulatory protein
RsmY	Small regulatory RNA Y
RsmZ	small regulatory RNA Z

SyK	Spleen tyrosine kinase
SagS	surface attachment and growth sensor hybrid
T3SS	Type III secretion system
T6SS	Type VI secretion system
TIR	Toll/IL-1 receptor
TIRAP	TIR-associated protein
TLRs	Toll-like receptors
TNF-α	Tumour necrosis factor- α
TRAM	TRIF-related adaptor molecule
TRIF	TIR domain-containing adaptor protein-inducing IFN-β
STAT	Transcription of signal transducer and activator of transcription
WFL	*Wisteria floribunda* lectin

Chapter 1. Introduction

1.1. General introduction to *P. aeruginosa*

Pseudomonas aeruginosa (PA) is a gram-negative rod-shaped bacterium and a common cause of nosocomial infections (Mulcahy et al., 2014). PA highly adaptable to different environments and mainly found in habitats with intense human contact (Crone et al., 2020). This bacterium is part of the human natural microflora and rarely causes infection in healthy individuals (Cogen et al., 2008). However, PA is considered a significant threat and can cause devastating infections in patients suffering underlying disease (e.g. cancer and cystic fibrosis (CF)) or individuals with disrupted non-specific host defences (e.g. burns, catheters, ventilators and surgery) (Driscoll et al., 2007, Lyczak et al., 2000). Several factors account for the ability of PA to cause these infections. Besides its ability to adapt to different environments, the bacterium is intrinsically resistant to a broad spectrum of antimicrobial agents (Lister et al., 2009). The World Health Organization (WHO) ranked antibiotic-resistant PA as number one on a list of antibiotic-resistant "priority pathogens" that pose the greatest threat to human health (Tacconelli et al., 2017). Furthermore, PA can form biofilms and utilize a vast arsenal of virulence determinants to interfere with the immune system (Gellatly and Hancock, 2013).

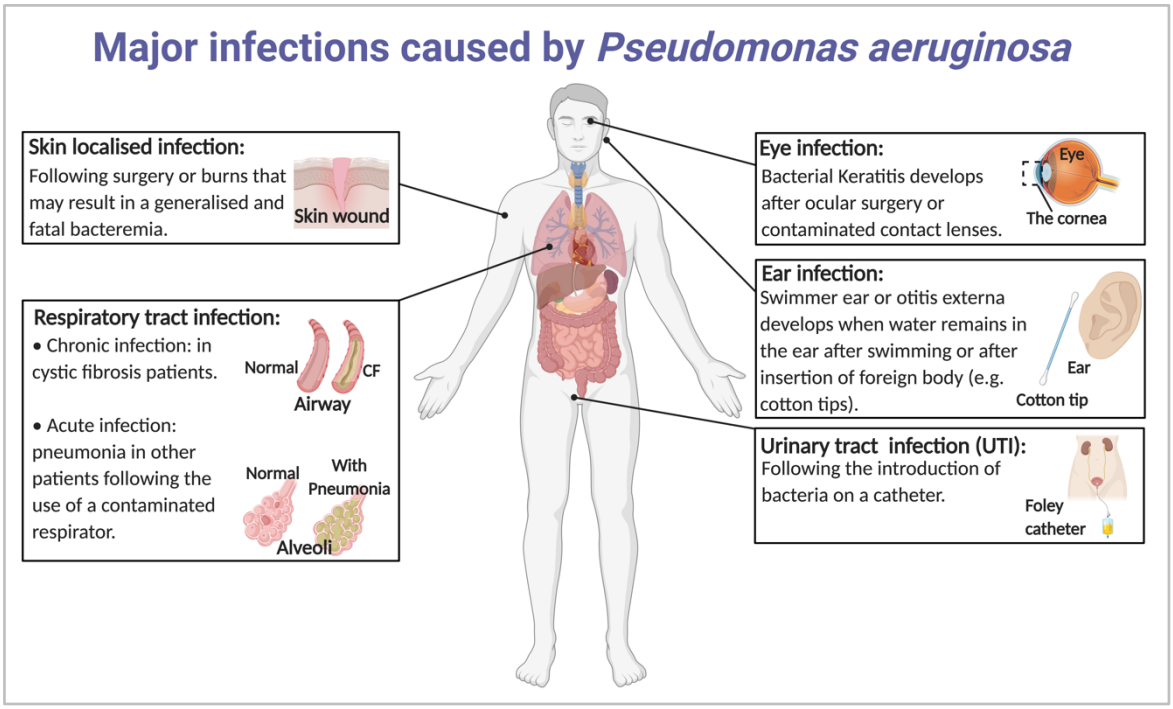


Figure 1.1 Major infections caused by PA.

Illustration of the major clinical diseases caused by the opportunistic pathogen PA. For the most part, infections are facilitated by the presence of underlying disease, e.g. cancer and CF or breakdown in non-specific host defences, e.g. burns, catheters, ventilators and surgery (Driscoll et al., 2007, Lyczak et al., 2000). Created with BioRender.com.

PA can cause acute or chronic infection (Klockgether and Tümmler, 2017). Acute infections are associated with the single-cell free-living mode of growth called planktonic (Furukawa et al., 2006). Planktonic cells are usually armed with various aggressive host-invasion strategies needed to establish infection and initial bacterial survival in the host (Valentini et al., 2018). In this living style, PA establishes the infection after bacteria bind to host epithelial cells utilising its adhesive molecules flagella and type IV pili. This binding of the flagella and type IV pili to the host epithelial cells elicit an inflammatory response (Gellatly and Hancock, 2013). This contact with mucosal surfaces causes devastating tissue damage in immunocompromised individuals triggered by the translocation of bacterial cytotoxic effectors exoenzymes released by the Type III Secretion System (T3SS) into the host cells along with the production of other extracellular virulence factors (Berube et al., 2016). Eventually, the release of these virulence

factors disturbs the integrity of the endothelial barrier, which allows PA to grow and disseminate rapidly within the host (Berube et al., 2016). To clear the infection, activation of macrophages and recruitment of neutrophils and monocytes to the site of infection takes place (Lund-Palau et al., 2016). As a strategy to evade host defence and facilitate its persistence, PA adapts to the host environment and undergoes modifications that facilitate bacterial tolerance and host defence evasion (Bragonzi et al., 2009). This adaptation process commonly involves the loss of major PA characteristics associated with planktonic cells, like motility or T3SS, and/or the conversion to a biofilm mode of growth which is associated with chronic infection (Bragonzi et al., 2009). The biofilm mode of growth plays a significant role in PA persistence and chronic disease (Furukawa et al., 2006).

In contrast to the planktonic/acute phase of infection, in the biofilm/chronic mode of growth, bacteria exhibit lower cytotoxic and immunogenic ability and persist for an extended period (Valentini et al., 2018). Additionally, the biofilm mode of growth is associated with resistance to antibiotics (Høiby, 2011). A binary regulatory switch was proposed to control the shift between both PA living styles and infection types (Furukawa et al., 2006). Mainly, the GAC/RSM global regulatory network of PA gene expression summarised in (Figure 1.2) plays a key role in the bacterial shift from acute to chronic infection (Goodman et al., 2004).

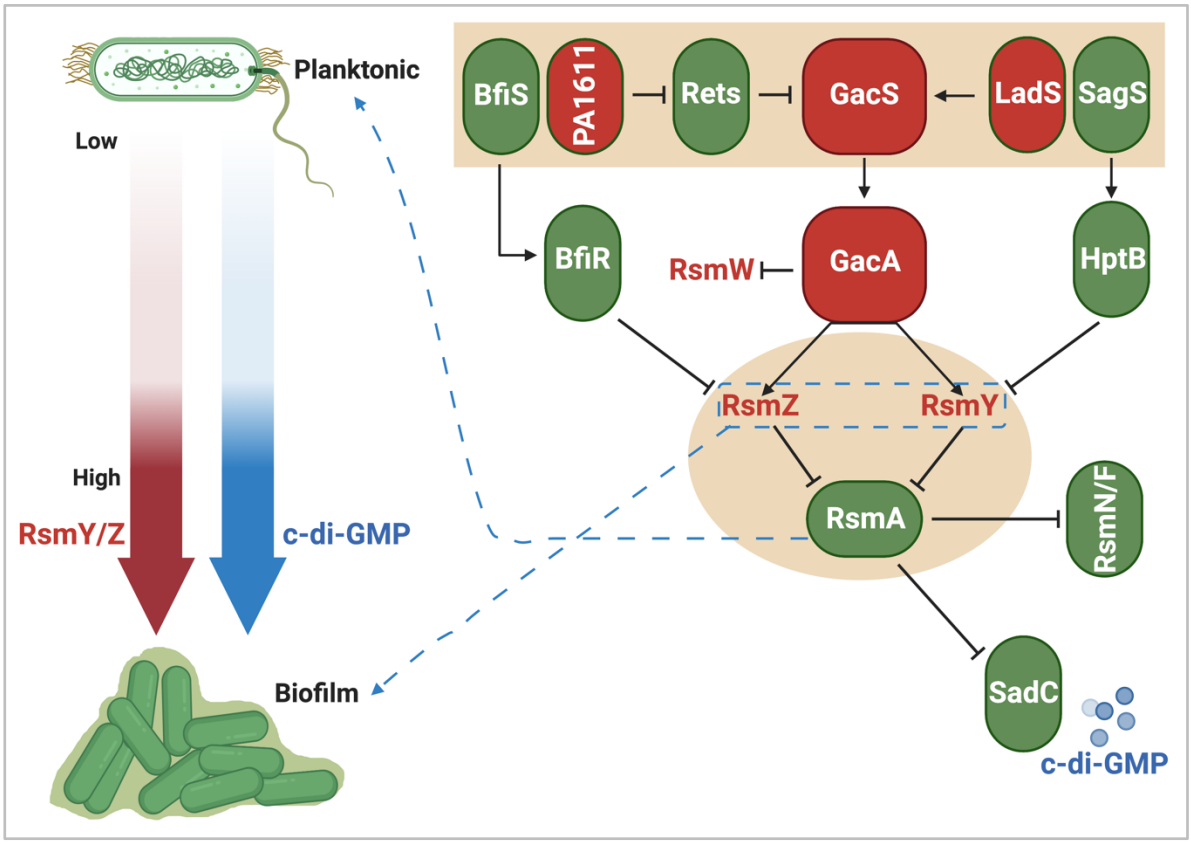


Figure 1.2 Summary of main Gac/Rsm cascade components.

The Gac/Rsm gene regulatory network consist of multiple regulatory components with different regulatory action (→ activation, —┤ repression). The pathways converge on the RNA-binding regulatory protein (RsmA) which binds to 5′untranslated region of mRNA and represses the translation of several genes in PA including psl (Irie et al., 2010). Along with RsmA, the backbone of the Gac/Rsm network comprises the two-component system GacS/GacA that upon activation upregulates the expression of the small regulatory RNAs (RsmZ and RsmY). These two-small regulatory RNAs (RsmY/Z) possess multiple RsmA-binding motifs that act to sequester RsmA from target mRNAs and relieving the mRNAs. Sequestration of RsmA by RsmY/Z eventually reduce RsmA availability and induce preferential expression of virulence factors associated with biofilm/chronic infection. Other proteins with different regulator actions also feeds into the Gac/Rsm cascade. The hybrid sensor histidine kinase RetS is reported to suppress biofilm formation while the histidine kinase LadS antagonizes the effect of RetS and promote phosphorylation of GacS (Rasamiravaka et al., 2015). The hybrid sensor kinase PA1611 interact with RetS, which inhibits it from suppressing GacS (Francis et al., 2017). The surface attachment and growth sensor hybrid (SagS), is involved in the motile-sessile switch and antibiotic resistance. SagS regulates RsmY through phosphorylation of the Histidine phosphotransfer protein B (HptB). The two-component system BfiS is essential for the switch to cells irreversible attachment during the process of biofilm formation and reported to regulate levels of RsmZ (Francis et al., 2017). The second messenger cyclic di-GMP (c-di-GMP) is an important regulator in the switch between planktonic and biofilms. RsmA repress SadC which is one

of the five diguanylate cyclases (DGCs) that are required for c-di-GMP synthesis. Diagram adapted from (Valentini et al., 2018) and created with BioRender.com.

1.2. Clinical Importance of *P. aeruginosa*

The International Consortium for the Control of Nosocomial Infections reported that nosocomial PA infections had become a global health problem (Rosenthal et al., 2016). PA is particularly important as it is the leading cause of morbidity and mortality in CF patients (Moradali et al., 2017). Additionally, PA is also usually linked to hospital-acquired infections such as ventilator-associated pneumonia, wound-burn infection and catheter-surgical related infections (Edwardson and Cairns, 2019).

1.2.1. Skin-associated infections

PA skin infections generally occur following an incident that causes a defect in the skin epithelial barrier such as burns, wounds, or the implementation of medical devices such as catheters (Turner et al., 2014). Naturally existing in the human skin microflora, PA rarely causes infection in the skin of healthy individuals; however, in chronic wounds, this pathogen is one of the most often isolated bacteria (Ruffin and Brochiero, 2019). The risk of PA skin infection is larger in immunocompromised patients, or individuals with an underlying condition, such as diabetes (Serra et al., 2015). PA infections can lead to a failure to heal skin injuries and therefore promote development of chronic wounds. It has been shown that PA usually forms biofilms on the surface of epithelial layers (Brandenburg et al., 2015). Once established, PA biofilm-associated chronic wound infections are hard to eradicate (Ruffin and Brochiero, 2019). Utilizing a 3D model of reconstituted human epidermis that imitate the human's multi-layered epithelial structure of the skin, Garcia et al. (2018) demonstrated that wild type (WT) PA could be detected in almost all layers of the epidermis including the deeper layers. In contrast, strains lacking flagellin failed to invade the epidermis tissue suggesting a fundamental role for flagella in the initial establishment of skin infection (Garcia et al., 2018).

1.2.2. Ventilator-associated pneumonia (VAP)

VAP can occur if patients in the intensive care unit are placed under mechanic ventilation via an endotracheal tube (ET) for longer than 48 hr (Pneumatikos et al., 2009). PA is one of the most frequently isolated bacterial pathogens in all VAP cases (Cisneros et al., 2019) and associates with a high mortality rate that can reach up to 69% (Bouglé et al., 2017). Additionally, VAP caused by PA is also associated with a high recurrence rate that can reach 30% of cases after treatment with appropriate antibiotics (Planquette et al., 2013). The establishment of PA-VAP occurs after the bacteria access and then adheres to the lower respiratory tract, causing persistent infection (Safdar et al., 2005). It has been indicated that ET serves as a facilitator for VAP pathogens to establish biofilms (Diaconu et al., 2018). Within hours following insertion, ET is rapidly colonized by PA that forms a biofilm on its surface, leading to poor prognosis (Diaconu et al., 2018). In a study conducted on a group of VAP patients showed that patients with PA expressing T3SS showed the worse clinical outcomes (Hauser, 2009).

1.2.3. Cystic fibrosis (CF)

CF is a life-threatening recessive genetic disorder caused by a mutation in the gene encoding the CF transmembrane conductance regulator (CFTR) protein (O'Sullivan and Freedman, 2009). The incidence of CF is approximately 1 of every 2,500 Caucasians live births (Welsh et al., 1995). CFTR protein found on the apical membrane of the cells lining the airways and functions primarily by regulating the chloride ions which are moved by the CFTR ion channel from the inner cell to the outside of the cell (Saint-Criq and Gray, 2017). After they are outside the cell, chloride ions attract a layer of water which is important as it allows cilia on the surface of the lung cells to move back and forth. This movement sweeps mucus up and out of the airways, which helps to clear the airway from inhaled particles and microorganisms (Saint-Criq and Gray, 2017). Mutations in CFTR result in disturbance of this chloride channel (Koch and Hoiby, 1993, Schwiebert et al., 1999, Sheppard and Welsh, 1999). In the lung this

disturbance in the salt/water balance of cellular secretions eventually results in the production of thick mucus which will hinder the “mucociliary elevator” of the bronchial lining (Rowe et al., 2005). Gradually, different infectious bacteria, including *Staphylococcus aureus*, *Haemophilus influenza*, *Burkholderia cepacia* and PA, become permanent residents and colonize the lower airway (Cullen and McClean, 2015). Chronic PA infection is considered an important determinant of mortality and morbidity in CF patients (Lavoie et al., 2011). Evidence of PA colonization have been found at earlier stages in CF patients; PA has been isolated from sputum samples taken from teens and children aged 3 (Burns et al., 2001). As described above PA is a very adaptable organism; it has been demonstrated that during the course of infection PA adapts to different conditions within the CF lung such as oxygen deficiency, antibiotic pressure and bacterial competition (Sousa and Pereira, 2014). One of the most important adaptive mechanisms and a critical key determinant of PA pathogenicity is the switch from planktonic to the biofilm mode of growth which, as mentioned above, facilitates chronic infection and makes PA eradication extremely difficult or even impossible (Hogardt and Heesemann, 2010, Schelstraete et al., 2013).

1.3. Virulence determinants of *P. aeruginosa*

PA possess an arsenal of virulence factors, enabling the organism to manipulate the immune system and destroy the host cells to establish an infection (Figure 1.3) (Gellatly and Hancock, 2013). PA can adapt to the airway environment by accumulating mutations that allow the bacteria to persist (Moradali et al., 2017). Isolates from acute infections express a high number of virulence determinants, whereas isolates from chronic CF lung infections show a deficiency in some of those virulence determinants (Valentini et al., 2018).

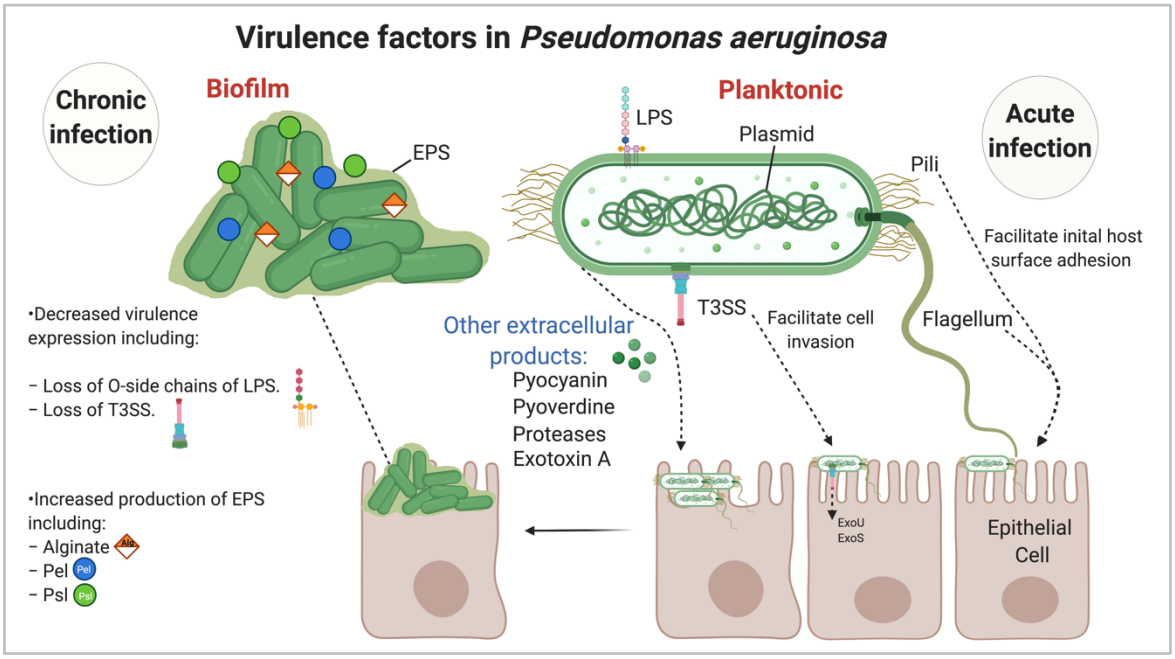


Figure 1.3 Selected virulence factors in PA.
Infection by PA is mediated by different virulence factors used to interfere with the host defences. Flagella and type IV pili facilitate host surface adhesion by binding to an epithelial ganglioside, asialoGM1. Besides lipopolysaccharide, these surface accessories are also highly inflammatory. After contact with host epithelial cells, the T3SS can be activated, and injects cytotoxins directly into the host cell such as ExoS and ExoU, which lead to disruption of actin cytoskeleton. Other virulence determents are secreted by PA and have different effects on the host. Pyocyanin, the blue-green pigment, can interfere with host cell electron transport pathways causing oxidative damage, whereas pyoverdine is critical for iron chelation. Also, several proteases are produced that can destroy host complement factors and disrupt tight junctions between epithelial, thus facilitating dissemination of the bacteria. Figure adapted from (Vilaplana and Marco, 2020) and created with BioRender.com.

1.3.1. Flagella and pili

PA possess two types of appendages, flagella and type IV pili which are required for motility, and play a key role in mediating cellular attachment and biofilm establishment (Bucior et al., 2012). PA movement has been classified into three different methods, swimming, swarming and twitching motility (Rashid and Kornberg, 2000). Swimming motility is PA movement in aqueous environments and in low agar (0.4%) facilitated by its flagella. When the fluid becomes thicker (semisolid), such as viscous media containing (0.4 to 0.7%) agar, the swimming bacteria becomes elongated and may possess two polar flagella to facilitate the movement on the semisolid surface, this movement called swarming motility (Köhler et al., 2000, Overhage et al., 2008). To reduce tension and aid swarm motility on the surface PA reported to produce and secrete the biosurfactant molecule rhamnolipids (Morris et al., 2011). Twitching motility is the bacterial movement on the solid surface mediated by the retraction and elongation of its pili (Burrows, 2012).

The major component of the single polar flagellum (flagellin), is recognized by the pattern recognition receptor Toll-like receptor (TLR)-5 (Feuillet et al., 2006) and promotes inflammation during PA acute infection (Balloy et al., 2007). Additionally, flagellin was found to activate TLR-dependent inflammatory responses in alveolar macrophages and airway epithelial cells (Raoust et al., 2009) Furthermore, the flagellin-mutant PA strains failed to activate nuclear factor kappa-light-chain-enhancer of activated B cells (NF-κB) in human airway epithelial cells (Zhang et al., 2005). The flagellar cap protein FliD was suggested to be the part of flagella involved in the initial attachment of PA to the human respiratory mucin (Arora et al., 1998).

Despite the important role of flagella in facilitating the initial bacterial colonization of the CF airways, flagellin expression is significantly downregulated during chronic infection (Mahenthiralingam et al., 1996, Wolfgang et al., 2004). Some PA strains isolated from CF lack flagella (Deligianni et al., 2010). PA suppression or downregulation of flagellin synthesis

promotes immune evasion and reduces phagocytosis (Jyot et al., 2007, Wolfgang et al., 2004). The process occurs as a result of the release of neutrophil elastase which degrades the PA flagellar hook protein F1gE. Low levels of F1gE triggers the aggregation of the anti-sigma factor F1gM within the bacterium suppressing the flagellin encoding gene fliC (Jyot et al., 2007). Several studies have shown that cyclic di-GMP is a crucial player in facilitating the transition of the bacterium from motile to sessile lifestyle (Hengge, 2009). Flagellin expression is influenced by c-di-GMP; while low levels of c-di-GMP promote bacterial motility by enhancing flagella formation and bacterial dispersion (Merighi et al., 2007), higher levels of c-di-GMP down-regulate flagellin expression (Baraquet and Harwood, 2013).

The Type IV pili (TFP) are polarly localised and composed of *pilin* subunits assembled to form hair-like filamentous structures (Leighton et al., 2015). Functionally, TFP are essential for initial surface sensing and adhesion and tissue colonisation (Doig et al., 1988). Additionally, TFP facilitates twitching motility (Mattick, 2002) and biofilm formation (Van Schaik et al., 2005, O'Toole and Kolter, 1998a). Through twitching motility pili assist surface exploration and it has been reported that pili interact with Psl deposited on the surface to guide bacterial gathering for biofilm formation (Zhao et al., 2013). TFP also plays a crucial role in cell-cell interactions and cell-surface interactions that are necessary for bacterial pathogenesis (Brill-Karniely et al., 2017). The initial PA colonization of epithelial cells is promoted by pili binding to asialoGM1 at the epithelial cell membrane (Alarcon et al., 2009). This interaction triggers the activation of NF-κB and mucin production (Li et al., 2003). Non-piliated strains showed decreased virulence as they failed to colonise host cells and initiated less severe infection (Tang et al., 1995). Similar to the flagellum, some PA-CF Isolates were found to lack pili (Deligianni et al., 2010). As pili and flagella were shown to bind asialoGM1 at the membrane of the epithelial cells (DiMango et al., 1995), it was speculated that it forms a complex with TLR-2 which might amplify the signalling capability of TLR-2 (Soong et al., 2004).

1.3.2. Type III secretion system (T3SS)

T3SS is a needle-like structure found on the surface of different gram-negative bacteria that allows bacterial effector proteins to be translocated directly into the host cell cytoplasm, bypassing the extracellular environment (Coburn et al., 2007). The PA T3SS is controlled by 43 genes grouped into five clustered operons that are involved in the biogenesis and regulation of the type III secretory apparatus (Veesenmeyer et al., 2009). Four effector proteins of the PA T3SS have been reported: exoS, exoT, exoU and exoY (Hauser, 2009). While the genes for T3SS are present in all PA strains, the expression of the effector proteins varies among PA strains with only few strains expressing all four effector proteins (Kroken et al., 2018). Examination of over 100 PA clinical isolates from different infections indicated the presence of the exoS gene in 58–72% of isolates, exoU gene in 28–42%, exoY gene in 89% and exoT gene in 92–100%. For an unexplained reason, an inverse relationship between exoS or exoU was noted with all strains containing either exoS or exoU but not both (Feltman et al., 2001).

Following their injection inside the host cells, T3SS exoenzymes function as follows: ExoS is a bi-functional protein which has GTPase activating protein (GAP) and ADP-ribosyltransferase (ADPRT) activities (Rangel et al., 2015). These two activities are reported to alter the actin cytoskeleton (leading to round morphology) and interfere with host cell functions, including phagocytosis, endocytosis, and DNA synthesis (Hauser, 2009). Recently Garai et al. (2019) reported an interesting observation, using confocal microscopy they found that intracellular PAO1 were able to lyse human macrophages in a T3SS dependent manner that relies mainly on ExoS (Garai et al., 2019). Similar to ExoS, ExoT also has GAP activity that disrupts actin cytoskeleton and leads to cell rounding (Garrity-Ryan et al., 2000, Kazmierczak and Engel, 2002). Additionally, ExoT GAP activity was found to inhibit cell migration, phagocytosis and epithelial cell wound repair (Garrity-Ryan et al., 2000, Cowell et al., 2000, Wood et al., 2015). ExoY has adenylate cyclase activity reported to cause an increase of the concentration of intracellular Cyclic adenosine 3',5'-monophosphate (cAMP) GAC, which is known to regulate

a high number of host cells genes (Hauser, 2009). Although ExoY is expressed in 89% of PA clinical isolates, its contribution in PA pathogenicity is largely controversial and remains unclear (Kloth et al., 2018, Munder et al., 2018). Several *in vivo* and *in vitro* experiments showed that injection of ExoU into mammalian host cells leads to rapid cellular necroptosis, attributed to ExoU phospholipase activity against the plasma membrane (Foulkes et al., 2019). During infection, epithelial cells release the neutrophil chemo-attractant hepoxilin A3 that triggers neutrophils migration. Following initial migration recruited neutrophils produce leukotriene B4 (LTB4) to increase the recruitment process. Production of the eicosanoid LTB4 depends on phospholipase activity which is enhanced in the presence of ExoU. Therefore presence of ExoU promotes LTB4 synthesis and neutrophil recruitment (Pazos et al., 2017).

The T3SS is not constitutively expressed by PA and is activated either under low calcium conditions or after contact with host cells (McMackin et al., 2019). Expression of T3SS is often associated with acute infection and positively correlates with a high mortality rate (Hauser, 2009). Additionally, expression of the T3SS was reported to be hindered by high levels of c-di-GMP (Bailin, 2017) and another study found that c-di-GMP signalling requires rsmYZ to facilitate the switch between T3SS and Type VI secretion system (T6SS) gene expression based on western blot analysis (Moscoso et al., 2011).

Three T6SS have been described in PA, H1-, H2-, and H3-T6SSs (Sana et al., 2016). Functionally, H1-T6SS was found to act only on prokaryotic cells, releasing effector toxins such as Tse1 and Tse3 that provide fitness advantage for PA in competition with other bacteria (Cianfanelli et al., 2016, Russell et al., 2011). H2-T6SS and H3-T6SS on the other hand was indicated to target both prokaryotic and eukaryotic cells (Sana et al., 2016). For example, the phospholipase D (Pld)A and PldB effectors released by H2-T6SS and H3-T6SS respectively were shown to facilitate both, PA killing of competitor bacteria and the internalisation and invasion of epithelial cells (Bleves et al., 2014, Jiang et al., 2014, Sana et al., 2012). Chen et al. (2020) reported a significantly higher expression of all three T6SS genes (hcp1, hcp2, and hcp3) in PAO1 biofilm compared to planktonic cells, suggesting an association between T6SS

and biofilm formation (Chen et al., 2020). Based on regulatory molecules such as RetS and LadS and the stage of infection, PA can switch between chronic/biofilm and acute/ planktonic mode of growth (Goodman et al., 2004). Both, RetS and LadS are influenced by the c-di-GMP pathway to inversely regulate motility and T3SS, which are associated with acute infection, and biofilm formation and T6SS, which are related to chronic disease (Moscoso et al., 2011).

1.3.3. Lectins

PA produces two types of carbohydrate-binding lectins, the galactose-binding lectin LecA and the fucose and mannose-binding lectin LecB. Both lectins bind ligands in a calcium-dependent manner (Mitchell et al., 2005, Sabin et al., 2006) LecA and LecB were initially found and characterized in the PA cytoplasm (Chemani et al., 2009, Glick and Garber, 1983). However, significant quantities of both lectins were also present on the outer membrane of the bacteria, suggesting that they may play an important role in bacterial adhesion (Tielker et al., 2005). PA strains which produce elevated levels of these lectins exhibited a higher virulence (Funken et al., 2012). LecA has been reported to induce a dose-dependent cytotoxic effect on respiratory epithelial cells *in vitro*, which might lead to lung injury during PA infection (Bajolet-Laudinat et al., 1994).

It has been shown that LecA interferes with intestinal epithelial permeability, leading to increased absorption of the cytotoxic virulence factor exotoxin A (ETA) by those cells (Laughlin et al., 2000). LecB was reported to induce NF-kB-mediated inflammation and reduces the migration and proliferation of respiratory epithelial cells (Cott et al., 2016). Additionally, LecB was reported to prevent ciliary beating in human airways (Adam et al., 1997) and inhibits tissue repair processes in lung epithelial cells (Cott et al., 2016). Both lectins have been suggested to contribute to bacterial aggregation during the process of biofilm formation, and LecA and LecB mutants form thin biofilms compared to the WT strain (Diggle et al., 2006, Rasamiravaka et al., 2015). It was reported that the application of solutions containing LecA- and LecB-

specific sugars significantly decreased PA CFU in the sputum of CF patients (Hauber et al., 2008) and successfully eliminated the organism in patients with PA airway infection (Von Bismarck et al., 2001). It was suggested that these sugar solutions probably act as inhibitors of lectin-mediated bacterial adhesion to host cells (Funken et al., 2012). The expression of these two lectins was reported to be controlled by the rhl Quorum Sensing (QS) system (Winzer et al., 2000).

1.3.4. Lipopolysaccharide

Lipopolysaccharide (LPS), is the major outer membrane component of Gram-negative bacteria (Silhavy et al., 2010). Structurally, LPS is composed of three different domains: (1) lipid A, (2) core oligosaccharide and (3) O-antigen (Caroff and Novikov, 2019). Because of its localisation and structure, LPS is a key virulence factor that plays a significant role in PA infection (Huszczynski et al., 2020). As mentioned above, the World Health Organization named multi-drug resistant PA a number 1 priority critical pathogen for new antibiotics (Tacconelli et al., 2017) and many researchers attribute PA antibiotic resistance to be mediated by LPS (Huszczynski et al., 2020). What follows is a summary of the main functions of each LPS components in PA pathogenesis.

Lipid A is the outer membrane-anchored part of the LPS. It is composed of an acylated O- and N- di-glucosamine with distinct fatty acids attached to the di-glucosamine backbone (King et al., 2009). It is the main immune stimulatory part of LPS, contributing to the life-threatening septic shock syndrome resulting from over-activation of the innate immune system (Weiss and Barker, 2018). LPS elicits immune signalling through the MD-2/TLR-4 receptor complex (Park et al., 2009). This activity leads to the activation of the transcription factors IRF3 and NF-κB, which result in a cascade of inflammatory cytokines, including TNF-α, IL-1β, IL-6 and type 1 IFNs (Weiss and Barker, 2018). LPS-MD2/TLR4 interaction is mainly through Lipid-A acyl chains (Park et al., 2009). Although the general structure and synthesis of lipid A are generally conserved, the number of acyl chains can vary and may have significant implications for the

bacterium-host interaction (Korneev et al., 2015). The acylation level of lipid-A was found to significantly influence PA pathogenicity (Korneev et al., 2015, Hajjar et al., 2002). Isolates from CF patients with hexa- and hepta-acylated lipid A were found to be very potent in triggering an inflammatory response compared to the penta-acylated lipid A usually found in laboratory strains or those obtained from non-CF-related diseases (Huszczynski et al., 2020, Ernst et al., 1999, Ernst et al., 2006). Additionally, PA isolates taken from later stage CF patients were hepta-acylated, suggesting acylation might be an important indication of the infection severity (Ernst et al., 2003, SenGupta et al., 2016).

The core oligosaccharide of PA consists of heptose, 3-deoxy-D-manno-oct-2-ulosonic acid, D-galactosamine, D-glucose, and L-rhamnose (Kocincova and Lam, 2011). In a mouse model, (Schroeder et al., 2002) reported that CFTR expressed by lung epithelial cells bound to the core oligosaccharide of LPS. This interaction leads to the translocation of NF-κB, which facilitated the eradication of bacteria (Schroeder et al., 2002). Experiments using epithelial cell lines carrying either the WT or mutated CFTR indicated a reduction in bacterial internalization in the mutated cell line, suggesting that CFTR mutations may promote PA infection (Fraser-Pitt and O'Neil, 2015).

O-antigen is the outermost part of LPS and is composed of a repetitive carbohydrate polymer attached to the core oligosaccharide (Huszczynski et al., 2020). O-antigen polymers consist of repeating sugar units that vary among PA strains; such distinctive structure is the reason for the O-serogroups classification, which categorise each strain based on the O-antigen structure (Lam et al., 2011). PA is able to produce two types of O-antigen: a homopolymer of D-rhamnose trisaccharide repeats called the common polysaccharide antigen (CPA) which is conserved and a heteropolymer composed of repeating units of 3-5 different sugars named O-specific antigen (OSA) which is variable (Bystrova et al., 2006, Yokota et al., 1987). The O-antigen is not present in all PA strains; strains with LPS containing O-antigen are called smooth or capped while strains with LPS lacking O-antigen are called rough or uncapped (Silhavy et al., 2010). Isolates from CF patients often contain rough LPS (Schurek et al., 2012).

It has been shown that certain O-antigen serotypes induce NETs formation by human neutrophils (Pieterse et al., 2016) which is linked to host tissue damage and worsen the disease condition (Yousefi and Simon, 2016).

LPS alteration is suggested to be a key factor in the adaptation and immune evasion of PA during the course of infection (Cigana et al., 2009). Analysis of sequential variants of PA showed changes in O-antigen (Lee et al., 2005) and lipid A alterations which lead to diminished MD-2/TLR-4 signalling (Cigana et al., 2009). In a mouse model, Lorè et al. (2012) show that early PA variants were lethal to mice, whereas late strains displayed reduced virulence (Lorè et al., 2012). Furthermore, LPS structure is highly dynamic during the process of biofilm formation (Huszczynski et al., 2020). In the lung of CF patients, OSA expression is usually lost due to genetic mutation, whereas expression of CPA is more stable (Lam et al., 1989). It was indicated that mutation of the CPA synthesis but not OSA disrupts biofilm maturation (Beveridge et al., 1997). Changes in LPS O-antigen are regulated by the c-di-GMP, a molecule that regulates a wide variety of chronic infection phenotypes, including biofilm formation as mentioned earlier (McCarthy et al., 2017).

1.3.5. Quorum sensing (QS)

QS is a gene regulatory system that regulates PA functions including production of virulence factors and biofilm formation, depending on the density of the bacterial population and environmental cues. QS is mediated by self-generated extracellular signalling molecules (Williams and Cámara, 2009, Lee and Zhang, 2015). This bacterial cell-cell communication mechanism is essential for PA adaptation to different environments (Passador et al., 1993, Davies et al., 1998). Four distinct QS systems have been identified in PA: Las, Rhl, PQS and Iqs (Lee and Zhang, 2015). Both Las and Rhl are activated by increased cell density within a bacterial population, and both utilise N-acylhomoserine lactone (AHL) molecules as signals for communication (Lee and Zhang, 2015). Two different AHL are produced by PA: while LasI mediates production of N-3-oxo-dodecanoyl-L-homoserine (3O-C12-HSL) which is detected

by LasR, RhlI produces N-butyryl-L-homoserine lactone (C4-HSL) which is detected by RhlR (Papenfort and Bassler, 2016, Schuster and Greenberg, 2006). The PQS is triggered by iron limitation within the cell population (McKnight et al., 2000). In the PQS system, the *PqsABCDE* operon produces the precursor 2-heptyl-4-quinolone (HHQ), and PqsH catalyses the conversion of HHQ to 2-heptyl-3-hydroxy-4-quinolone (PQS), which is detected by PqsR (Heeb et al., 2011). The last discovered system is Iqs, which is activated through phosphate starvation and signals through 2-(2-hydroxyphenyl)-thiasole-4-carbaldehyde which seems to be produced by *AmbBCDE* with no known sensor molecule (Lee et al., 2013a). The QS system regulates a large number of PA virulence factors (Turkina and Vikström, 2019). The different QS system work in a hierarchical manner (Lee and Zhang, 2015). Briefly, at the top of the QS hierarchy the Las system regulating the expression of PQS, Rhl and Iqs systems. In addition to Las, the Rhl system is also under the control PQS (Lee and Zhang, 2015). Examples of virulence factors controlled by QS are described in the following section.

PA produces several extracellular proteases, including LasB, which degrades host tissues components including elastin, collagen, laminin and fibronectin leading to tissue injury and haemorrhage during acute infection (Yang et al., 2015). Moreover, during chronic infection, LasB was found to interfere with the host immune response, degrading components such as TNF-α, IL-2 and IFN-γ (Suarez-Cuartin et al., 2017). The production of LasB and the other PA produced protease LasA is under the control of the Las and Rhl QS systems (Li and Lee, 2019). Additionally, PA secretes ETA into the extracellular milieu, which after secretion, enters host cells through binding to CD91 and inactivates cellular protein biosynthesis (Kounnas et al., 1992). Similar to the proteases, ETA regulation is also influenced by the Las and Rhl QS systems (Michalska and Wolf, 2015). Pyocyanine is a toxic product released by PA reported to increase intracellular levels of reactive oxygen species (ROS), which leads to oxidative stress, enzyme inhibition, damage to DNA, and cellular death (Hall et al., 2016). Pyocyanine production is regulated by Las, Rhl and PQS (Wagner et al., 2003). PA also produces rhamnolipids reported to induce neutrophils necrosis (Jensen et al., 2007) and dissolve dynein

(Hastie et al., 1986) essential for cilia movement to clean the lung airway of inhaled particles (Tilley et al., 2015). Rhamnolipids production is Las and RhL controlled (Shrout et al., 2006).

Additionally, PA produces three extracellular phospholipases C (PLC), PLC-H, PLC-N, and PLC-B, which hydrolyse lipids in host pulmonary membranes and cause lung dysfunction (Wargo et al., 2011). Only the production of PLC-B is regulated by AHL dependent QS (Wagner et al., 2003, Schuster et al., 2003). QS also controls the release of LPS and T3SS, a very potent PA virulence factor, as explained previously (Nakamura et al., 2008).

QS signalling molecules not only regulate the virulence of PA but are also reported to modulate the functions of several mammalian host cells. A recent study reveals that 3O-C12-HSL produced by LasI induced mitochondrial dysfunction and apoptosis of human neutrophils (Singh et al., 2019). 3O-C12-HSL is also reported to induce downregulation of the pro-inflammatory cytokine TNF-α, and up-regulation of the anti-inflammatory cytokine IL-10 in LPS-stimulated murine macrophages (Glucksam-Galnoy et al., 2013). Similarly, addition of exogenous PQS reduced TNF-α and IL-6 production in WT and Δ*pqsA*-infected Calu-3-ALI cells (Liu et al., 2018). Furthermore, PQS diminished the ability of bone marrow-derived DCs to activate antigen-induced T-cell proliferation *in vitro* (Skindersoe et al., 2009).

The QS system controls various aspects of PA biofilm formation process. For example, extracellular DNA (eDNA) has been suggested to play a crucial role in the early stages of biofilm development, working as a cell-to-cell interconnecting compound (Allesen-Holm et al., 2006, Flemming and Wingender, 2010, Whitchurch et al., 2002). Allesen-Holm et al. (2006) reported that the release of eDNA in PA cultures and biofilms is controlled by the PQS QS system (Allesen-Holm et al., 2006). Another important biofilm component is the carbohydrate Pel which plays an essential role in biofilm stability and integrity. Pel was shown to be significantly diminished in lasI and rhlI mutants (Sakuragi and Kolter, 2007). Biofilm formation is a multistage process including initial attachment and transition from planktonic to sessile lifestyle. Motility assists bacterial surface exploration and facilitates the interaction with

surfaces and host cells (Zhao et al., 2013). QS is reported to control PA swarming motility as cells with mutations in the las system showed reduced swarming behaviour, and rhl mutants completely lost the ability to swarm (Haiko and Westerlund-Wikström, 2013). While the interaction between c-di-GMP and QS in PA is not yet fully understood, a recent study indicated that the rhl and pqs QS operons in cells with low c-di-GMP levels were upregulated (Lin Chua et al., 2017, Srivastava and Waters, 2012). This upregulation enhanced the expression of Rhl and PQS controlled virulence such as rhamnolipids and pyocyanin, which enhanced bacterial intracellular survival rates and cytotoxicity in murine macrophages (Lin Chua et al., 2017).

1.4. Biofilm formation in *P. aeruginosa*

Biofilms are multicellular communities of microorganisms in which the cells adhere to each other and/or to a surface or interface. Cells in biofilms are enclosed in a self-produced extracellular polymeric substance (EPS) (Borlee et al., 2010, Costerton et al., 1999). Biofilms are widely distributed, a recent analysis estimated that 40–80% of microorganisms on earth reside in biofilms (Flemming and Wuertz, 2019) and biofilms have been found in very high (50^{o}C) (Jones et al., 2010) and low temperatures (glacier samples) (Yang et al., 2009). In some agricultural and other industrial settings, biofilm formation has a beneficial impact (Rosche et al., 2009). For example, biofilms are used to enhance crop production (Timmusk et al., 2017), degrade hazardous material (Irankhah et al., 2019) and treat wastewater (Ali et al., 2018). Despite the positive effect of biofilms, the formation of biofilm in other situations is harmful (Muhammad et al., 2020). For instance, biofilms formed by pathogens associated with foodborne infection such as *Bacillus cereus*, *Enterohemorrhagic Escherichia coli*, *Listeria monocytogenes*, *Salmonella enterica*, and *Staphylococcus aureus*, has been found in food processing factories, threatening consumers health (Galie et al., 2018). Also, biofilm presence has been associated with chronic infection in human, animals and plants (Costerton et al., 1987). Moreover, over 60% of all hospital-related infections are caused by biofilms established on medical devices (Shirtliff et al., 2009) such as contact lenses, mechanical heart valves and

urinary catheters (Wu et al., 2015) as well as CF mucus plugs (Donlan, 2002, Ma et al., 2009, Stoodley et al., 2002). In addition to the strains associated with foodborne infection mentioned earlier, other human pathogens display biofilm formation capacity including *Candida albicans*, *Vibrio cholera*, *Klebsiella pneumonia*, *Enterobacter*, *Campylobacter spp*., and *PA* (Donlan, 2002, Stoodley et al., 2002, Flemming et al., 2016). Bacterial communities inside these biofilms develop several properties which might not be found in the planktonic (free-living) bacteria, such as antibiotic tolerance, immune evasion and cell to cell communication (Flemming et al., 2016).

Biofilm formation is a multi-stage process initiated (1) by reversible cell attachment to the surface, (2) irreversible attachment followed by EPS creation, (3) generation of mature biofilm and (4) dispersal and release of planktonic bacteria from the mature biofilm to colonise a new location or remain in the planktonic mode of growth (Figure 1.4) (Stoodley et al., 2002). PA biofilm architecture fundamentally depends on the production of EPS, and it is thought that the EPS holds these communities together working as glue, and contributes to the persistence of bacterial infections by protecting against host immune response and antimicrobial agents (Stoodley et al., 2002). In PA, the EPS mainly consists of exopolysaccharides, eDNA and proteins (Rybtke et al., 2015b).

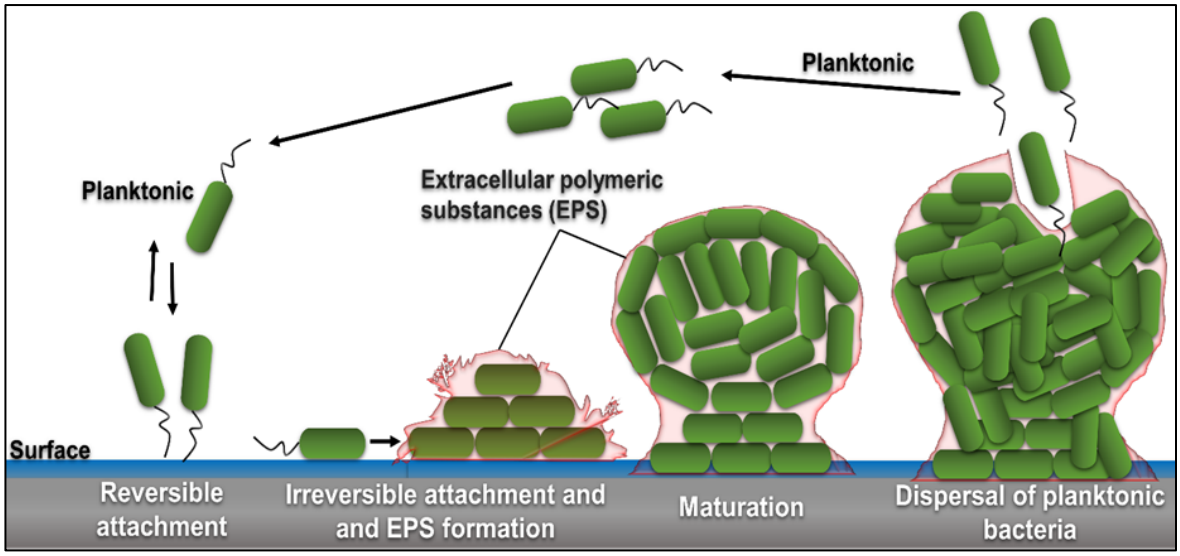


Figure 1.4 The process of biofilm formation in PA

Biofilm formation is a multi-stage process initiated (1) by reversible cell attachment to surface, (2) irreversible attachment followed by EPS production, (3) generation of mature biofilm and (4) dispersal and release of planktonic bacteria from the mature biofilm. Figure adapted from (Ma et al., 2009).

1.4.1. Role of proteins in biofilm formation:

Proteins play different functions during the process of biofilm formation, including assistance to cellular attachment to surfaces and the maintenance of biofilm integrity and stability through interactions with EPS components (Fong and Yildiz, 2015). The most studied protein linked to biofilm formation is the extracellular adhesin CdrA which is exclusively found in the PA EPS matrix and is absent in planktonic cell fractions (Toyofuku et al., 2012). Western blot analysis revealed the presence of two forms of CdrA, a cellular fraction form (220 kDa) and a supernatant fraction form (150 kDa) (Borlee et al., 2010). The cleavage by the periplasmic protease LapG of cell surface CdrA was reported to mediate the release of the CdrA into the supernatant (Rybtke et al., 2015a). The expression of CdrA is c-di-GMP dependent which also controls other genes essential for biofilm formation such as those involved in Psl and Pel synthesis (Borlee et al., 2010, Filloux, 2011, Hickman and Harwood, 2008). Structurally, CdrA is suggested to have a carbohydrate-binding domain (Borlee et al., 2010). It was reported that

through its carbohydrate-binding domains CdrA binds Psl, and this interaction promotes biofilm stability and bacterial aggregation (Borlee et al., 2010). This interaction was also found to enhance aggregate integrity offering protection against self-produced and exogenous proteases (Borlee et al., 2010).

Additionally, the localization of Psl at the biofilm periphery was reported to be controlled by CdrA (Borlee et al., 2010). It was reported that CdrA could facilitate bacterial aggregation and biofilm formation even in the absence of Psl due to CdrA-CdrA interactions which were shown to offer protection against mechanical stress (Reichhardt et al., 2018). Recently, it was reported that CdrA interacts with another important biofilm carbohydrate, Pel, and this interaction protects against proteases, as described for the CdrA-Psl interaction mentioned above (Reichhardt et al., 2020). Due to the low amount of information on the CdrA and Pel structure, it is uncertain whether CdrA binds to Psl and Pel through the same or different binding site (Reichhardt et al., 2020).

Along with CdrA additional proteins were reported to have a role in the biofilm formation, including the Type IV pili, which binds to eDNA and facilitates the establishment of biofilms (Van Schaik et al., 2005). Other proteins reported to mediate bacterial attachment to surfaces during initial biofilm formation are the CupA, CupB, CupC, CupD fimbriae (Vallet et al., 2001, Kulasekara et al., 2005). Additionally, overexpression the Fap amyloid was shown to increase biofilm biomass (Dueholm et al., 2013). The lectin LecB assist the biofilm structure by facilitating the attachment of cells to each other and to the host surface (Vallet et al., 2004, Tielker et al., 2005). Recently LecB was shown to bind to Psl resulting in enhanced retention of cells and EPS in the biofilm (da Silva et al., 2019). Similar to the CdrA, the DNA-binding protein HU protein was also only found in the biofilm matrix and is absent in planktonic cells (Toyofuku et al., 2012); however the exact function of this protein has not yet been established. It was suggested that HU might stabilise DNA in extreme environments to prevent denaturation (Stover et al., 2000).

1.4.2. Role of eDNA function in biofilm formation:

eDNA is a fundamental component of biofilms; treatment with DNase completely prevented biofilms formation by PAO1 (Swartjes et al., 2013). eDNA has been suggested to play a key role in the early stage of biofilm development, working as a cell-to-cell interconnecting compound (Allesen-Holm et al., 2006, Flemming and Wingender, 2010, Whitchurch et al., 2002). eDNA was shown to facilitate the mass transit of cells toward the edge of actively expanding biofilms, preventing traffic jams through maintaining the coherent of cells alignments (Gloag et al., 2013). Additionally, it was reported that bacteria utilise eDNA as a nutrient source during starvation (Mulcahy et al., 2010, Finkel and Kolter, 2001). As mentioned above Pel cross-links eDNA via an ionic binding mechanism, and this interaction was suggested to partially affect the localization of Pel to the biofilm stalk, which enhances biofilms structure (Allesen-Holm et al., 2006). eDNA also enhances biofilms stability, protecting it from mechanical stress, antibiotics, and detergents (Flemming and Wingender, 2010, Mulcahy et al., 2008).

The source of eDNA in biofilms was initially reported to be autolysis of bacteria subpopulations within the biofilm community (Turnbull et al., 2016, Montanaro et al., 2011) which was supported by the detection of full bacterial genomic DNA in the EPS of a PAO1 biofilms (Deng et al., 2020). This controlled cell death of bacterial cells was suggested to mainly take place in the central part of the microcolonies, releasing large amounts of eDNA that concentrate primarily in the stalk (Allesen-Holm et al., 2006). However, a recent study has found that PAO1 Δ*wspF* displayed a distinct mechanism of eDNA release independent of the suicidal path as previously reported in PAO1 (Deng et al., 2020). In this case the eDNA in biofilms formed by PAO1 ∆*wspF* contains only parts of the whole bacterial genome, opposite of what been reported with WT PAO1. This fragmented eDNA was shown to enhance biofilms resistance to DNase treatment (Deng et al., 2020).

1.4.3. EPS function in the biofilm formation:

In addition to proteins and eDNA, PA utilises three polysaccharides to construct biofilms: alginate, Psl, and Pel (Figure 1.5) (Ma et al., 2009). Expression of these polysaccharides within the EPS matrix and their importance for biofilms structural stability varies depending upon the strain and the infection stage (Colvin et al., 2012). For instance, alginate, Psl, and Pel are thought to be expressed during various stages of PA CF lung infections (Reichhardt and Parsek, 2019, Martin et al., 1993). Generally, these EPS polysaccharides function as a structural platform facilitating cell-cell and cell-surface interactions maintaining biofilms integrity and shielding it from antibiotic treatment (Wei and Ma, 2013). A more detailed account of alginate, Psl, and Pel is given in the following section.

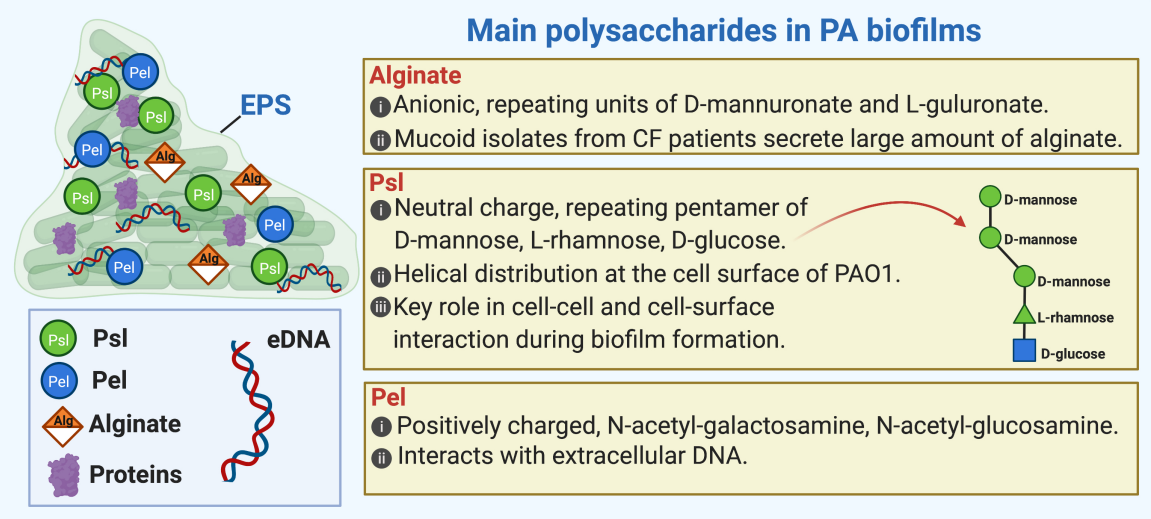


Figure 1.5 Main polysaccharides in PA biofilms

PA biofilms are embedded in EPS matrix that contains eDNA, proteins and polysaccharides. Three main polysaccharides are reported in PA biofilms alginate, Pel and Psl. Each of these polysaccharides have distinct structure and function. Generally, these EPS polysaccharides function as a structural platform facilitating cell-cell and cell-surface interactions (Wei and Ma, 2013). Created with BioRender.com.

1.4.3.1. Alginate:

Alginate is an anionic linear polymer composed of β-D-mannuronic acid and α-L-guluronic acid (Zhao et al., 2016). It is the predominant polysaccharide in biofilms formed by mucoid PA strains while non-mucoid PA strains mainly relay on Psl and Pel (Franklin et al., 2011). Mucoid strains overproduce alginate and these strains are associated with chronic infection of the CF lung. Non-mucoid strains are isolates taken from initial infection or a reverted mucoid variant that converted to a nonmucoid phenotype (Rao et al., 2011). Nonmucoid revertants were recovered from CF lungs. PA have been reported to have a selective benefit of the coexistence in both mucoid and nonmucoid in the CF lung as both variants interact with each other to evade the immune response and for the persistence of the infection (Malhotra et al., 2018). Although alginate is not essential for biofilm formation (Nivens et al., 2001, Wozniak et al., 2003), it was shown to protect against host defence and antimicrobial agents (Alkawash et al., 2006, Boyd and Chakrabarty, 1994). Aggregates formed by the alginate overproducing mutant

strain *mucA* showed higher antibiotic tolerance compared to aggregates formed by WT bacteria (Goltermann and Tolker-Nielsen, 2017). Alkawash et al. (2006) showed that using alginate lyase to treat PA biofilms boosted the bacterial killing capacity of gentamicin (Alkawash et al., 2006). At the early stages of infection, nonmucoid strains colonise CF lungs, but as the infection persists, mucoid forms begin to appear and become the dominant strains (Hay et al., 2009, Lee et al., 2005). The transformation from a non-mucoid to mucoid phenotype is attributed to alginate production and frequently due to mutations in the mucA gene (Hay et al., 2009, Lee et al., 2005). The presence of the mucoid form in the CF lung highly correlates with the deterioration of the patients' condition (Li et al., 2005). CF lung infection causes the recruitment of inflammatory cells into the infection site, where reactive oxygen species are released. Alginate scavenges these free radicals released by active macrophages and neutrophils offering protection from phagocytic clearance (Pier, 1998, Govan and Deretic, 1996).

Furthermore, alginate was reported to protect biofilms from IFN-γ mediated killing by macrophages (Leid et al., 2005). While high titers of alginate antibodies are present in the sera of chronically infected CF patients (Pier et al., 1987), these antibodies were found not to facilitate phagocyte-dependent bacterial killing or increase protection against infection (Pier et al., 2004). Additionally, in a model of CF respiratory infection, alginate overproduction assists in the coexistence of PA with *S. aureus* as it was shown to reduce the synthesis of tools utilised by PA to kill *S. aureus* such as siderophores and rhamnolipids (Limoli et al., 2017).

1.4.3.2. Psl:

Psl is a neutral pentasaccharide composed of repeating units of D-mannose, D-glucose and L-rhamnose in an approximate ratio of 3:1:1. (Byrd et al., 2009). The *psl* locus is composed of fifteen genes, eleven of which (*pslACDEFGHIJKL*) are essential for Psl polysaccharide biosynthesis (Byrd et al., 2009). While the structures and functions of the majority of these proteins remain largely unknown, a recent study on PslG which is localised on the inner membrane and periplasm, reported its critical role in the biosynthesis of Psl with the

periplasm/inner membrane ratio of PslG determining the amount of secreted Psl (Wu et al., 2019).

Psl is found in two forms (1) cell-associated form with high molecular weight and (2) a low molecular weight soluble form (Byrd et al., 2009, Mann and Wozniak, 2012). It was indicated that the cell-associated form is helically distributed around the cell surface (Ma et al., 2009).

Although the mechanism that regulates the helical pattern of Psl is not yet understood, this distribution of Psl was found to facilitate the interactions with Psl on adjacent bacteria (Ma et al., 2009). Several studies indicated the importance of Psl during the initial attachment of bacterial cells to biotic and abiotic substrates (Friedman and Kolter, 2004b, Jackson et al., 2004, Ma et al., 2006, Ryder et al., 2007). Overproduction of Psl further increases bacterial surface attachment and production of biofilm (Colvin et al., 2012, Ma et al., 2006). Also, Psl increases the crosslinking and elasticity of the EPS matrix, strengthens the scaffolding and enhances the formation of microcolonies (Byrd et al., 2009, Mann and Wozniak, 2012, Reichhardt and Parsek, 2019). It has been suggested that mutation in Psl synthesis increased the viscosity of the biofilms, which in turn resulted in more diffused biofilm structure (Chew et al., 2014).

Researchers widely utilised a lectin called *Hippeastrum hybrid* lectin (HHA) to detect Psl, which suggested to bind specifically to Psl (Ma et al., 2007). Interestingly, it has been shown that PA deposits a trail of Psl as it moves on surfaces that guides the subsequent movement of the upcoming cells. Furthermore, cells with highest Psl expression serve as the founders of microcolonies (Zhao et al., 2013). In mature biofilms Psl was localised in the centre (Huq et al., 2005) and the periphery (Ryder et al., 2007). The peripheral localisation has been attributed to the interaction of Psl with CdrA as mentioned in an earlier section (Reichhardt et al., 2018).

Using continuous flow and static biofilm experiments Billings et al. (2013) have shown that Psl represents the first line of biofilm defence against antibiotic treatment (Billings et al., 2013).

Overexpression of Psl was found to promote resistance of Polysorbate 80, which is a detergent that inhibits biofilm formation by PA and is well tolerated in human tissues (Zegans et al., 2012). Additionally, Billings et al. (2013) showed that Psl-mediated protection against antibiotics extends to other bacterial species such as *E. coli* and *S. aureus* in co-culture biofilms (Billings et al., 2013).

Psl inhibits effective complement opsonisation, which resulted in a reduction in neutrophil ROS production, and reduced bacterial killing activity by neutrophils and macrophages (Mishra et al., 2012). Recently, it was reported that the serine protease inhibitor ecotin, produced by PA, binds to Psl within the biofilms, and this binding protects biofilms from neutrophil elastase-mediated killing (Tseng et al., 2018). In addition, neutrophils failed to penetrate biofilms containing Psl at ocular surfaces (Kugadas et al., 2019). Since 99% percent of PA clinical isolates were shown to produce Psl (Zegans et al., 2016, Tabor et al., 2018), the therapeutic and prophylactic effects of anti-Psl antibodies have been widely explored (DiGiandomenico et al., 2012). Recently three different anti-Psl antibodies named I, II and III that target different Psl epitopes were identified (Ray et al., 2017). Using confocal microscopy Ray et al. (2017) showed that each of these anti-Psl antibodies targets specific locations within the biofilms and exhibit differential abilities to inhibit early biofilm formation and reduce the biomass of mature biofilms (Ray et al., 2017).

1.4.3.3. Pel:

Pel is a cationic positively charged polysaccharide, composed of acetylated 1→4 glycosidic linkages of N-acetylgalactosamine (GalNAc) and N-acetylglucosamine (GlcNAc) (Jennings et al., 2015). The pel locus is composed of seven genes (*pelABCDEFG*) necessary for Pel polysaccharide biosynthesis (Friedman and Kolter, 2004a, Vasseur et al., 2005). Similar to Psl, transcription of the *pel* operon is also controlled by c-di-GMP (Hickman and Harwood, 2008, Baraquet et al., 2012). A recent study showed that after 30 min of surface attachment, *pelA* transcript levels increased 10-fold compared to planktonic cells as a result of the rise in c-di-GMP levels (Armbruster et al., 2019). It has been proposed that the Pel biosynthesis

machine uses enzymes involved in the synthesis pathways of other carbohydrates to provide necessary sugar precursors to Pel (Franklin et al., 2011).

The function of Pel in biofilm development was first recognised in an screen for mutants deficient in pellicle formation, which is the floating layer formed on top of standing cultures (Friedman and Kolter, 2004a). A more explicit description of the role of Pel in biofilm development indicated that the contribution of this carbohydrate depends on the strain (Jennings et al., 2015). Deletion of Pel in strains where Psl is the dominant carbohydrate such as PAO1 did not affect biofilm development (Colvin et al., 2012), on the other hand strains incapable of producing Psl such as the highly virulent laboratory strain PA14 fundamentally relies on Pel as the primary biofilm matrix polysaccharide (Colvin et al., 2012). Although Psl is the dominant EPS in PAO1 as mentioned earlier, in its absence, Pel is upregulated to compensate for the lack of Psl (Jennings et al., 2015). Furthermore, Pel localization within the biofilms was found to be strain-dependent as well (Jennings et al., 2015). Using the Pel-specific lectin *Wisteria floribunda* lectin (WFL), which has specificity to GalNAc moieties, Jennings et al. (2015) found that in Pel-dominant strains including PA14 and PAO1Δ*wspF* Δ*psl,* Pel was observed in both the biofilm periphery and stalks, whereas it was found only in the biofilm stalk of the Psl-dominant strains such as PAO1 and Δ*wspF* (Jennings et al., 2015). As mentioned earlier Psl was reportedly located inside and in the periphery of PAO1 biofilms, Interestingly, in its absence, Pel was found in the periphery suggesting a necessity of either Pel or Psl in the periphery of PAO1 biofilms (Reichhardt and Parsek, 2019). The stalk region is rich in eDNA, and it was suggested that Pel binds eDNA in the stalk region of the biofilm through ionic interactions aiding to biofilms structure (Jennings et al., 2015). Pel is reported to be essential for maintaining cell-to-cell interactions in a PA14 biofilm and provides resistance to aminoglycoside antibiotics (Colvin et al., 2011). Additionally, increased production of Pel in PAO1 and PA14 enhanced tolerance to gentamicin and tobramycin compared to WT strains, indicating that Pel could improve resistance to antibiotics (Khan et al., 2010).

1.4.4. Role of wspF gene in biofilm formation:

PA with mutations in the Wsp operon, mainly wspF, are frequently detected in isolates from CF sputum (Starkey et al., 2009, Smith et al., 2006). This chemosensory system, Wsp, controls c-di-GMP levels in response to surface sensing (O'Connor et al., 2012). The wspF gene is a member of the wsp operon, which consists of eight genes, wspA-R (Hickman et al., 2005). The methyl-accepting chemotaxis protein (MCP), WspA, is methylated by the methyltransferase, WspC, after PA makes contact with a surface. WspA then interacts with the histidine kinase, WspE, which phosphorylates WspR, a diguanyl cyclase (DGC), leading to the synthesis of c-di-GMP.WspF is a methylesterase that removes methyl groups from WspA, thereby decreasing its signalling activity to WspR. Hence a mutation in WspF will lead to WspA becoming constitutively activated. This results in boosted WspR phosphorylation, causing elevation of c-di-GMP levels. C-di-GMP has been recognized as a key regulator of PA biofilm formation (Maunders and Welch, 2017). Overproduction of c-di-GMP is associated with increased production of the biofilm matrix components psl and pel (Ha and O'Toole, 2015). Addtionaly, increased c-di-GMP levels promote eDNA level and bacterial adhesins (Chua et al., 2015).

1.5. The role of the innate immune system during PA infection:

1.5.1. Immune recognition of PA via pattern recognition receptor (PRRs):

The innate immune system senses pathogens by a variety of non-clonally expressed receptors termed, Pattern Recognition Receptors (PRRs), which have the ability to bind highly conserved molecular complexes called Microbe-Associated Molecular Patterns (MAMPS) also referred to in the literature as Pathogen-Associated Molecular Patterns (PAMPs) (Benko et al., 2008, Medzhitov, 2007). These MAMPS are not only found on pathogens and could be components of the bacterial cell wall (LPS and peptidoglycan), flagella and DNA or RNA (Medzhitov, 2007, Mogensen, 2009). Additionally, PRRs recognize endogenous molecules released after damage to the host cells known as Damaged Associated Molecular Patterns (DAMPs) (Takeuchi and Akira, 2010). PRRs are expressed by a wide range of immune and structural cells, which include macrophages, neutrophils, DCs, monocytes, lymphocytes, endothelial cells, epithelial cells and others (Hartl et al., 2012). Four major classes of PRRs have been discovered: Toll-Like receptors (TLRs), NOD (Nucleotide-binding Oligomerization Domain receptors)-like receptors (NLRs), C-type lectins receptors (CLRs) and the retinoic acid-inducible gene (RIG)-I-like receptors (Takeuchi and Akira, 2010).

1.5.2. Toll-Like receptors:

Members of the TLR family consist of two domains, an extracellular domain containing leucine-rich repeats (LRR) which take part in ligand binding (Opitz et al., 2010) and a cytoplasmic Toll/IL-1 receptor homology (TIR) domain that mediates downstream signalling (Janssens and Beyaert, 2003). Four TLRs have been identified to have roles in PA recognition: TLRs 2, 4, 5 and 9 (Williams et al., 2010). TLR-2 is possibly involved in the detection the extracellular slime-glycolipoprotein (slime-GLP) (Lagoumintzis et al., 2008), alginate (Flo et al., 2002), and ExoS

(Epelman et al., 2000). TLR-2 is known to facilitate the interaction between PA flagella and asialoGM1 (Adamo et al., 2004). TLR-4 and 5 are responsible for the recognition of LPS and flagella, respectively (Hayashi et al., 2001, Janeway and Medzhitov, 2002). In contrast to TLR-2, 4 and 5 which are expressed at the plasma membrane, TLR 9 is endosomal and able to sense unmethylated CpG DNA (Vollmer, 2006). TLRs are highly expressed by different host inflammatory cells including, macrophages, DCs, lung epithelial cells and endothelial cells (Williams et al., 2010, Opitz et al., 2010). Following the identification of bacterial ligands, TLRs initiate signalling though the MyD88 adaptor protein causing the activation of NF-kB and production of pro-inflammatory cytokines (Parker and Prince, 2011). The significance in host defence of MyD88 signalling was observed experimentally using MyD88(-/-) mice infected with a low dose of PA as these mice become very susceptible, with 100% of mice dying within 48 h (Ramphal et al., 2005).

As mentioned in (1.3.4) the main immune stimulatory part of LPS, Lipid A elicits immune signalling through interaction with the MD-2/TLR-4 receptor complex, leading to the initiation of TIRAP-MyD88-pathway and the activation of the transcription factor NF-κB, which result in a cascade of inflammatory cytokines (Weiss and Barker, 2018). This interaction is mainly through Lipid-A acyl chains, and optimal inflammatory activity of LPS was shown to require six lipid chains (Park and Lee, 2013). Isolates from CF patients with hexa- and hepta-acylated lipid A were found to be very potent in triggering an inflammatory response compared to the penta-acylated lipid A usually found in laboratory strains or those obtained from non-CF-related diseases (Huszczynski et al., 2020, Ernst et al., 1999, Ernst et al., 2006). TLR-4 also signals through TRIF-TRAM pathway, following TLR-4 endocytosis TRAF3 is activated which trigger IRF3 activation leading to IFNs (Figure 1.6). In addition to TRAF3 role in promoting TRIF-dependent pathway, activation of TRAF3 inhibit the MyD88-dependent pathway (Kawasaki and Kawai, 2014), suggested to be initiated to avoid septic shock and multiple organ failure (Kuzmich et al., 2017). It was reported that CFTR mutation in murine macrophages leads to the blocking of the endosomal-lysosomal TLR-4 trafficking in

macrophages causes a reduced TLR-4 degradation and an enhanced plasma membrane TLR-4 expression, which results in higher inflammatory response to LPS (Bruscia et al., 2011)

TLR-5 recognition of flagellin activate the mitogen activated protein kinase (MAPK) and NF-κB (Tallant et al., 2004). This activation seems to protect against PA infection through initiation of IL-8 production (Zhang et al., 2007). Flagellin-mutant PA strains failed to activate nuclear factor NF-κB in human airway epithelial cells (Zhang et al., 2005). As mentioned earlier (1.3.1), PA undergoes downregulation of flagellin during chronic infection (Mahenthiralingam et al., 1996, Wolfgang et al., 2004). This suppression or downregulation of flagellin synthesis by PA promotes immune evasion and diminishes phagocytosis (Jyot et al., 2007, Wolfgang et al., 2004). Some PA strains isolated from CF lack flagella (Deligianni et al., 2010). It was reported that PA produce alkaline protease (AprA) which work as a TLR-5 signalling inhibitor that obstructed NF-κB activation (Kuzmich et al., 2017). Additionally, AprA reported to degrade free flagellin monomers and thus assisting PA to avoid immune recognition (Bardoel et al., 2011).

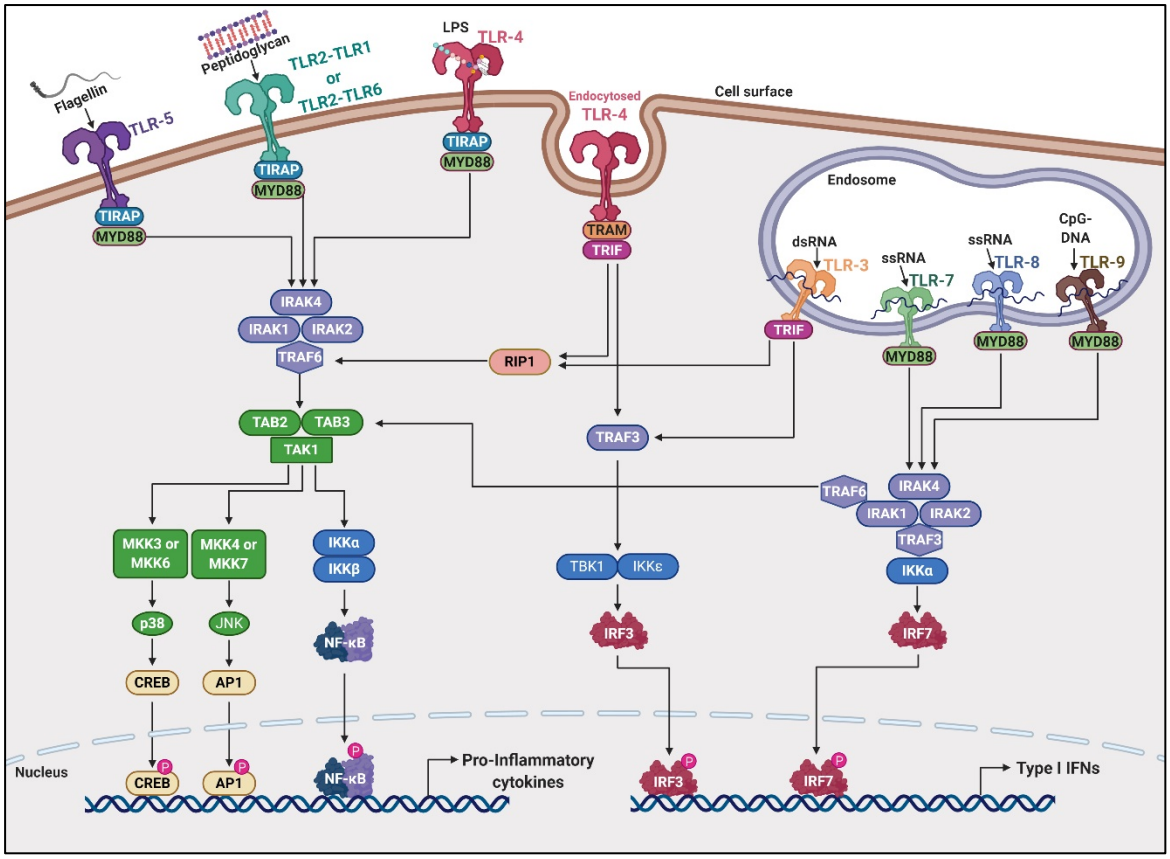


Figure 1.6 TLRs signalling pathways.

Membrane TLRs (TLR-2, TLR-4, and TLR-5) detect ligands such as gram-positive peptidoglycan, gram-negative LPS and flagellin respectively. On the other hand TLRs localised in the endosomal compartment (TLR-3, TLR-7, TLR8 and TLR-9) recognise ligands such as double strand RNA (dsRNA) for TLR-3, and single strand RNA (ssRNA) for TLR-7 and TLR-8, and CpG for TLR-9. TLR-4 could be endocytosed in a process mediated by CD14. All TLRs utilise MyD88-dependent pathway, except TLR3 which employs the TRIF -dependent pathway. Recognition of ligands by TLRs initiates signalling through the two main downstream adaptor proteins TRIF and MyD88, leading to the production of inflammatory cytokines. TIRAP directs the signal from TLR-2, -4 to MyD88 while TRAM facilitate signalling from TLR-4 to TRIF within endosomes. Activation of MyD88-dependent pathway leads to the activation of IKK complex-NF-κB and MAP Kinases while initiation of the TRIF- signalling activates NF-κB, MAPKs, IRF3, and IRF7. Following activation, NF-κB subunits and IRF3,7 are relocated to nucleus to initiate inflammatory cytokines (NF-κB, CREB and AP1) and type I interferons transcription (IRF3 and IRF7) (Fitzgerald and Kagan, 2020, Kawasaki and Kawai, 2014). Created with BioRender.com.

1.5.3. Nod-Like receptors:

All 22 members of the NLR family consist of a central nucleotide-binding oligomerization (NOD) domain and C-terminal LRRs which are possibly involved in ligand binding. NLRs

contain different N-terminal effector binding domain including caspase recruitment domains (CARD), pyrin domains (PYD), or baculovirus inhibitor repeats (BIR) (Fritz et al., 2006, Chen et al., 2009). The CARD-containing molecules NOD1 and NOD2 bind gamma-glutamyl diaminopimelic acid and muramyl dipeptide, respectively, which are present in peptidoglycan in gram-positive and gram-negative bacteria including PA (Travassos et al., 2005, Lipinski et al., 2009). Similar to TLR, when NOD 1 and 2 are engaged, they activate NF-kB (Williams et al., 2010). NLRP 1–4 forms a subgroup of NLRs receptors characterized by displaying the PYD some of which have the capacity to form inflammasomes (Kofoed and Vance, 2011). Inflammasomes regulate Caspase-1 activity which in turn mediates the processing and secretion of IL-1β and IL-18. The production of IL-1β is controlled by another signal, which came from TLRs, through activation of an NF-κB–dependent synthesis of inactive pro–IL-1β (Opitz et al., 2010). NLRP-1 in murine macrophages is activated in response to PA pilin, the main protein constituent of bacterial type IV pili. (Arlehamn and Evans, 2011). It has been indicated that PA triggers, through T3SS, the activation of another member of the NLR family called NLRC4 which contains a CARD domain instead of the PYD domain, leading to IL-1β and IL-18 secretion (Faure et al., 2014). NLRC4 activation induced by PA expressing T3SS decreases the clearance of this extracellular pathogen. The proposed underlining mechanism was that when NLRC4 is activated by T3SS it will trigger IL-18 secretion, which will induce high neutrophil recruitment and, in turn, host damage. Furthermore, IL-18 will downregulate IL-17 secretion in the lung, decrease the expression of antimicrobial peptides by lung epithelial thereby hindering bacterial clearance (Faure et al., 2014).

1.5.4. C-type lectins (CLRs):

CLRs are a family of PRRs that includes soluble and transmembrane proteins capable of binding carbohydrate ligands, and with one or more C-type lectin-like domains (CLTDs) (Zelensky and Gready, 2005, Weis et al., 1998). CLRs play a critical role in the control and regulation of infection (Geijtenbeek and Gringhuis, 2009) triggering multiple cellular and immunological responses, which include cell adhesion, pathogen recognition, complement

activation and phagocytosis (Kerrigan and Brown, 2009). CLRs are categorised into 17 groups based on phylogeny and structural features (Zelensky and Gready, 2005). This thesis will focus on four CLRs members, which are relevant for the present study, one from the Group VI, mannose receptor (MR, CD206), two from Group II, dendritic cell-specific ICAM-3-grabbing non-integrin (DC-SIGN, CD209) and dendritic cell-associated C-type lectin-2 (Dectin-2), and one from Group V dendritic cell-associated C-type lectin-1 (Dectin-1) (Figure 1.7).

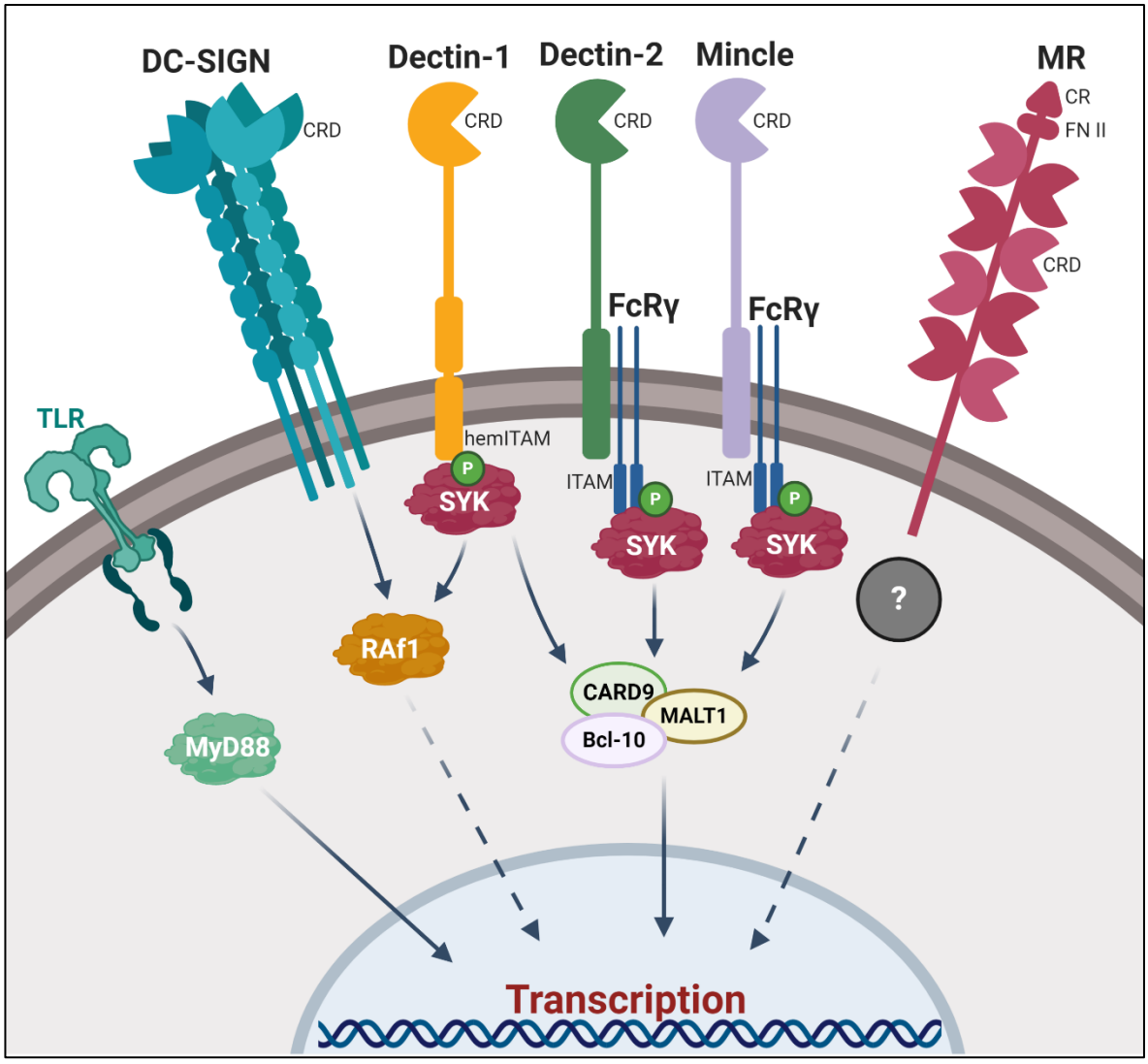


Figure 1.7 Schematic representation of the structure and signalling of MR, DC-SIGN, Dectin-1, Dectin-2 and Mincle

Mannose receptor is composed of three main extracellular regions: cysteine-rich domain (CR), fibronectin type II domain (FNII), and 8 CTLDs. The cytosolic region contains an internalisation motif. DC-SIGN is a tetrameric transmembrane protein composed of a single CTLD followed by a stalk region, a transmembrane region, and a terminal cytoplasmic domain. Dectin-1 has a single CTLD attached to a stalk region and ends with a cytoplasmic tail, that consists of a motif similar to the immunoreceptor tyrosine-based activation motif (ITAM) called hemITAM. Dectin-2 and Mincle are composed of one CTLD domain and both associate with the ITAM containing FcRγ chain to transduce intracellular signalling for the phosphorylation and activation of the spleen tyrosine kinase (SYK). Dectin-1 directly activates SYK via hemITAM. SYK activation begins the protein kinase C delta (PKCδ) pathway, which initiates the caspase-associated recruitment domain (Card9)- B-cell lymphoma (Bcl10)- mucosa-associated lymphoid tissue lymphoma translocation (Malt1) complex. Dectin-1 employ the serine and threonine kinase Raf-1 for signalling to activate NF-κB. DC-SIGN also was reported to trigger the activation of Raf-1, which consequently leads to activation of the NF-

κB subunit p65, but only after TLR-induced activation of NF-κB (Gringhuis et al., 2007). Although MR is reported to activate intracellular signalling, MR signalling mechanism remain unclear. CLRs engagement not necessarily induce signalling by themselves but rather modulate signalling by other PRRs such as TLRs (Shibata et al., 2012).

1.5.4.1. Mannose receptor (MR, CD206):

MR is a 175 kDa transmembrane protein belonging to the mannose receptor family, which is a subgroup of CLRs (Martinez-Pomares, 2012). MR has three extracellular regions: a cysteine-rich domain (CR), a fibronectin type-II domain (FNII), and eight CTLDs. The CR domain recognises sulphated sugars, the FNII domain collagen, and the CTLDs are responsible for binding to carbohydrates terminated in mannose, fucose, or N-acetyl glucosamine; binding of these sugars occurs only in the presence of calcium (Martinez-Pomares, 2012). The MR cytoplasmic tail does not contain an ITAM or ITIM motif but does have a tyrosine residue which is essential for facilitating endocytosis (Schweizer et al., 2000). It has been shown that the binding affinity of CTLDs (4–8) is the same as for the complete MR receptor (Gazi and Martinez-Pomares, 2009, Taylor et al., 2005a). MR is found in macrophages, DCs, endothelial cells of the liver, splenic sinusoids, microvascular endothelial cells of the dermis, cells of Kaposi's sarcoma, human keratinocytes, and retinal pigment epithelium (Jahagirdar et al., 2019). Additionally, macrophage and DCs differentiation pattern influence the expression of MR. Differentiated macrophages and DCs have abundant expression of the receptor, whereas CD14+ monocytes lack MR (Martinez-Pomares, 2012). Only less than 20% of MR is present at the cell surface, whereas the remaining is located intracellularly within early endosomes (Jahagirdar et al., 2019). The expression of MR is upregulated by IL-4, IL-10, and IL-13, and down-regulated by IFN-γ and LPS (Kerrigan and Brown, 2009). MR performs several functions, which include enhancing antigen presentation, clearance and cellular activation (Martinez-Pomares, 2012). It is well established that the ITAM – containing adaptor molecule FcRγ-chain is required for the cell surface expression and signalling of several CLRs such as MCL, Mincle and Dectin-2 (Miyake et al., 2013, Yamasaki

et al., 2008). Recently, (Rajaram et al., 2017) reported that MR binds FcRγ-chain, and this binding is essential for the cell surface localisation of MR on human monocyte-derived macrophages (Rajaram et al., 2017). Additionally, the same authors reported that the activation of MR expressed on monocyte-derived macrophages by *Mycobacterium tuberculosis* (MTB) results in phosphorylation of the tyrosine residue in the MR. (Rajaram et al., 2017) also showed that Syk, is phosphorylated upon MR activation, suggesting that Syk is possibly activated through MR binding to the FcRγ-chain, which contains an ITAM motif (Rajaram et al., 2017). It is important to note that Syk activation in this case might possibly mediated by Dectin-1, which also reported to recognise MTB (Wagener et al., 2018).

Different studies have described the role of MR as a homeostasis regulator by binding and removing endogenous unwanted molecules from circulation including lysosomal enzymes, neutrophil-myeloperoxidase, the anterior pituitary hormone lutropin as well as thyroid-stimulating hormone (Allavena et al., 2004, Taylor et al., 2005a). Similarly, MR has an endocytic activity to internalise a wide range of allergens including house dust mite (Martinez-Pomares, 2012, Gazi and Martinez-Pomares, 2009). Additionally, MR can recognise different microorganisms through the CTLDs including MTB, *Candida albicans*, *Leishmania*, HIV, dengue virus, *Klebsiella pneumonia*, and *Streptococcus pneumonia* (Gazi and Martinez-Pomares, 2009). These pathogens might bind MR to trigger an anti-inflammatory/immune-suppressive response and cause a persistent infection (Jahagirdar et al., 2019). For example, in the case of MTB, a component of the cell wall called Mannose-capped lipoarabinomannan (ManLAM), possess a terminal mannose structure that can bind MR (Schlesinger et al., 1994). MR binding of ManLAM is reported to induce upregulation of the transcription regulatory factor peroxisome proliferator-activated receptor-gamma (PPAR-γ) causing increase in the transcription of signal transducer and activator of transcription (STAT)-5α (Turner and Torrelles, 2018). High level of PPAR-γ was reported to be associated with ManLAM-dependent suppression of macrophage apoptosis, decrease of nitric oxide (NO) and oxygen radicals and restricting proinflammatory cytokine production (Turner and Torrelles, 2018).

Furthermore, MR binding by MTB obstructs phagosome-lysosome fusion in the macrophage, which facilitate the dissemination of MTB infection (Le Cabec et al., 2005).

While MR was implicated in the recognition and phagocytosis of different pathogens such as *P. carinii*, *Saccharomyces cerevisiae*, *Leishmania*, MTB, and *C. albicans* (Gorvel, 2004), no differences were observed in the response of MR-deficient mice to *C. albicans* (Lee et al., 2003) or *Leishmania* (Akilov et al., 2007). A possible explanation is that although the signalling mechanisms of MR is still unclear, it is possible that MR biological response depends on the co-activation of other receptors (Gazi and Martinez-Pomares, 2009). Bernardo et al. (1998) showed that the capacity of macrophages to generate a calcium response following exposure to ManLAM requires engagement of both CD14 and MR (Bernardo et al., 1998). In agreement with this, MR reportedly cooperates with TLR-4 for the proliferation and differentiation of CD4+ and CD8+ T lymphocytes into Th17/Tc17 cells in response to *P. brasiliensis*-challenged DCs (Loures et al., 2015).

1.5.4.2. Dendritic Cell-Specific Intercellular adhesion molecule-3-Grabbing Non-integrin (DC-SIGN, CD209):

DC-SIGN is a type II transmembrane protein that belongs to group II C-type lectin receptors and is expressed by DCs and some macrophage subpopulations (Kerrigan and Brown, 2009). Structurally, DC-SIGN is composed of a CTLD domain followed by a stalk region, a transmembrane region, and a cytoplasmic domain (Kerrigan and Brown, 2009). The cytoplasmic tail of DC-SIGN contains a di-leucine motif reported to mediate antigen uptake and internalization (Engering et al., 2002, Azad et al., 2008). In addition, this cytoplasmic area contains tyrosine residue that functions as a dock for several proteins that are essential for cellular responses and intracellular trafficking such as Leukemia-Associated RhoGEF (LARG), Ras homolog gene A (RhoA), and leukocyte-specific protein 1 (LSP1) (Gringhuis et al., 2009, Gringhuis et al., 2014, Hodges et al., 2007). DC-SIGN activation after binding to mannose structures induces a complex chain of events that eventually cause the phosphorylation and activation of Raf-1 leading to the modulation of NF-κB signalling in response to other PRRs.

This modulation enhances the transcription of the immunosuppressive cytokine IL-10 (Yamasaki, 2016).

The stalk region forms α-helices that mediate the spontaneous formation of tetramers reported to enhance binding avidity (Frison et al., 2003). The CTLDs facilitate binding to mannose and fucose structures in a calcium-dependant manner (Garcia-Vallejo and van Kooyk, 2013). Expression of DC-SIGN is induced by IL-4 and is down-regulated by IFN-γ, TGFβ, and dexamethasone (Relloso et al., 2002).

Functionally, DC-SIGN binds high fucose and mannose, as well as blood group Lewis antigens in a calcium-dependent manner (Ehlers, 2010, Geijtenbeek et al., 2000b). DC-SIGN has been indicated to recognise pathogens containing mannose structures such as HIV-1, HCV, Ebola, and MTB (Gringhuis et al., 2009, Pöhlmann et al., 2003, Lin et al., 2003), as well as those containing fucose structure, such as *Schistosoma mansoni* and *H. pylori* (Gringhuis et al., 2014). Similar to MR, DC-SIGN is involved in recognition of ManLam and induction of an immunosuppressive response characterised by enhanced IL-10 release and neutralization of the TLR-4-dependent pro-inflammatory response (van Kooyk and Geijtenbeek, 2003). DC-SIGN is also important in facilitating DCs antigen presentation and T-cell differentiation (Švajger et al., 2010). DCs internalise antigen and facilitate presentation by MHC to CD4+ and CD8+ T cells. DC-SIGN on DCs bind with ICAM-3 on T-Cell, which contains high mannose oligosaccharides and this binding facilitates the scanning of MHC by TCRs, leading to T cell activation and differentiation (Švajger et al., 2010). It has been shown that the presence of biofilms in chronic rhinosinusitis correlates positively with the accumulation of DCs expressing CD209 (Karosi et al., 2013).

1.5.4.3. Dendritic-Cell-Associated C-type lectin-1 (Dectin-1, CLEC7A):

Dectin-1 is primarily expressed by DCs, macrophages, and neutrophils (Taylor et al., 2002). The structure of Dectin-1 contains a single CTLD attached to a stalk region and end with a cytoplasmic tail, that consists of a motif similar to the immunoreceptor tyrosine-based

activation motif (ITAM) termed by some authors hemITAM (Brown, 2006). Dectin-1 found in two isoforms A and B. A-isoform is the full-length Dectin-1 protein, with 247 amino acid, single transmembrane and spanning protein. On the other hand, B-isoform lacks 46 amino acid with long stalk region between the CRD and the transmembrane domains (Fischer et al., 2017). The most-reported Dectin-1 ligand is the β-1, 3-linked glucan found in of MTB, *C. albicans*, *Aspergillus fumigatus*, and zymosan, *Saccharomyces cerevisiae* cell wall component (Tone et al., 2019). Engagement of Dectin-1 by its ligand binding trigger the activation of Syk-CARD9 signalling pathways which provokes expression of chemokines and cytokines, including TNF-α, CXCL2, IL-2, IL-10 and IL-12 (Dostert and Tschopp, 2007). Along with cytokine secretion, Dectin-1 binding reported to facilitate phagocytosis and ROS production (Goodridge et al., 2011). Mutation of Dectin-1 increased mouse susceptibility to *C. albicans* infection due to impaired immune response, including phagocytosis (Taylor et al., 2007). In adaptive immunity, Dectin-1 reported to mediate recruitment of MHC II molecules to phagosomes, promoting fungal-derived antigen presentation to CD4 T cells (Ma et al., 2012). Additionally, Dectin-1 plays an important role in promoting Th17, Th1 and Th2 differentiation (Tone et al., 2019). Dectin-1 deficiency associated with impaired *C. albicans* clearance, dysregulated cytokine production and reduced Th17 response (Carvalho et al., 2012). Ferwerda et al. (2009) have indicated that humans with Dectin-1 deficiency are more susceptible to *C. albicans* mucosal infection (Ferwerda et al., 2009).

1.5.4.4. Dendritic-Cell-Associated C-type lectin-2 (Dectin-2, CLEC6A):

Dectin-2 has been shown to be crucial for protective host immunity against *C. albicans* (Robinson, Osorio et al. 2009, Saijo, Ikeda et al. 2010). Similar to MR and DC-SIGN, Dectin-2 is capable of detecting ligands bearing high mannose structures, but with 10-fold lower affinity (McGreal et al., 2006). Dectin-2 is reviewed in detail in chapter 4.

1.6. The role of innate immune cells during PA Infection:

1.6.1. Dendritic Cells (DCs):

DCs are specialised antigen presenting cells essential in orchestrating adaptive immunity against different pathogens such as bacteria, viruses and fungi (Geginat et al., 2015). DCs are found throughout the body located mainly in barrier sites including lung, spleen, gut and skin as well as circulating in the blood (Durand and Segura, 2015, Guilliams et al., 2016). Two main DCs subtypes have been identified in human and mouse, plasmacytoid dendritic cells (pDCs) and conventional dendritic cells (cDC). Both DC populations originate from proliferating progenitor cells in the bone marrow (Auray et al., 2016, Guilliams et al., 2016, Heidkamp et al., 2016) and can be distinguished from each other by their surface markers and functionality (Swiecki and Colonna, 2015) . While pDCs are particularly important in the initiation of IFN-induced antiviral responses during viral infections (Swiecki and Colonna, 2015), cDC are professional antigen-presenting cells, utilising MHC molecules to present antigen to naïve T cell and facilitate Th1, Th2, Th17 and Treg polarisation (Merad et al., 2013). Under some conditions cDCs are associated with the production of high IL-12p70, promoting cytotoxic T cells polarisation (Merad et al., 2013). DC research has benefited from the use of DCs generated *in vitro* by culturing monocytes in GM-CSF and IL-4, known as monocyte-derived (mo)DCs (moDCs) (Sichien et al., 2017). These cells are thought to represent DCs subpopulations that differentiate from blood monocytes in response to inflammation or infection (Segura et al., 2013, Reynolds and Haniffa). The relevance of moDCs is a controversial area, however, due to the low number of pDCs and cDCs, their isolation is challenging and time-consuming (Sichien et al., 2017). Thus, in human studies, moDCs have been used extensively as a tool to study DCs function *in vitro* (Lutz et al., 2017). The culture of CD14+ monocytes with GM-CSF and IL-4 generate a large number of cells that exhibit immature DCs characteristics (Lutz et al., 2017, Dauer et al., 2003). DCs exist mainly in two functional states: immature and mature. Immature DCs are typically located in peripheral

tissues and characterised by high endocytic activity and low surface expression of MHC II and costimulatory molecules. Immature DCs are regarded as weak inducers of T cells proliferation and activation (Harding and Song, 1994); however, these cells display high ability for antigen recognition and capture due to their high expression of PRRs including DC-SIGN and MR (Geijtenbeek et al., 2000b, Sallusto et al., 1995). Following the recognition of exogenous and endogenous signals by PRRs such as TLRs, DCs undergo maturation (Dalod et al., 2014). DCs maturation alters cellular metabolic, and genetic transcription systems enabling mature DCs migration from peripheral tissues to secondary lymphoid organs and upregulation of MHCII and costimulatory molecules to present antigen to naive CD4+ T cell and induce T cell activation and proliferation (Dalod et al., 2014).

Efficient pathogen-specific immunity involves T cell differentiation induced by complex cytokine profiles, established following recognition of pathogens and cell damage by antigen-presenting cells such as DCs and macrophages (Mogensen, 2009). Moss et al. (2000) demonstrated that T cells from patients with CF produce lower levels of IFN-γ, a Th1 cytokine, and higher levels of IL-10, a Th2 cytokine (Moss et al., 2000). Additionally, Moser et al. (2000) reported that a Th2 type immune response is most common in CF patients with chronic PA lung infection, characterised by high level of IL-4 and decreased lung function. In the other hand, a Th1-dominated immune response associated with higher IFN-γ production and better lung function was observed in CF patients with no chronic PA infection (Moser et al., 2000).

Several studies suggested that the engagement of DCs during PA infection might facilitate the bacterial long-lasting repression of inflammatory responses and could impact T cell response and polarization. It was reported that production of pulmonary DCs to IL-10 cytokine is important for the inhibition of Th1 responses (Akbari et al., 2001). Whiteson et al. (2017) exposed human moDCs to culture supernatant from five PA strains including mucoid and non-mucoid PA, *Streptococcus pneumonia*, *S. salivarius* and *Rothia mucilaginosa*. These organisms are found commonly in the oral and respiratory tract of CF patients and associate with CF pathology (Whiteson et al., 2017). The data in Whiteson et al. (2017) indicated that

PA supernatants from both mucoid and nonmucoid strains induced the highest release of the anti-inflammatory cytokine IL-10 compared to all other bacteria tested (Whiteson et al., 2017). Additionally, it was reported that two PA QS molecules 3-oxo-C12-HSL and PQS reduced IL-12 production in LPS-stimulated murine DCs. These murine DCs showed reduced capability of inducing T cell proliferation and activation (Skindersoe et al., 2009). It was indicated that Th2 response is due to pulmonary DC-mediated inhibition of Th1 responses via IL-6 production which negatively regulate the expression of IL-12 (Dodge et al., 2003).

In a mouse model of chronic PA pulmonary infection characterized by bacteria growing as biofilm, Damlund et al. (2016) reported that activated DCs were detected in the lung after day one of infection, and in the regional lymph nodes by day three of infection. Damlund et al. (2016) suggested this is could be attributed to migration of DCs to the regional lymph nodes after they encounter and process PA in the lungs. The author isolated DCs from both, the lung and regional lymph nodes and assessed cytokines expression in response to PA-LPS. Data indicated constant increase of IL-10 production from day one through days two and three to day seven in both DCs isolated. Similar gradual increase from day one up to day seven were detected in IL-6. On the other hand, the author reported that IL-12 concentration in the lungs decreased at day three which correlate with the increase in IL-6 and IL-10, both IL-12 inhibitors (Damlund et al., 2016).

Airway epithelial cells are particularly important in the initiation of IFN-α and IFN-β signalling cascade that are crucial in the activation of innate immune cells including DCs and the elimination of different pulmonary bacterial pathogens, including *Streptococcus pneumoniae*, *S. aureus* and PA (Cohen and Prince, 2012). It has been reported that due to CFTR dysfunction, CF airway epithelial cells displayed diminished activation capability of pulmonary DCs in response to PA infection (Parker et al., 2012a).

1.6.2. Macrophages:

Macrophages are critical players in host defence by initiating and regulating innate immune responses. Generally, macrophages act as scavengers of foreign particles and are able to sense intruders as well as tissue dysfunction (Williams et al., 2010). Macrophages are found in all human tissues, with different types of macrophages in each tissue displaying a high degree of heterogeneity in morphology, phenotype and life span (Ovchinnikov, 2008). This heterogeneity is due to the stimulation from nearby cells and components of the extracellular matrix (Gordon and Martinez-Pomares, 2017). There are different subsets of tissue-resident macrophages (TRMs) depending on the organ they are located in. For example, alveolar macrophages are located in the lung alveoli, microglia in the brain, Kupffer cells in the liver, renal macrophages in the kidneys, while osteoclasts are the macrophages in bone, and dermal macrophages reside in the skin (Xu and Shinohara, 2017). Upon injury/infection, circulating monocytes can migrate to the site of inflammation where they can differentiate into macrophages or DCs depending on the local cytokine environment (Smith et al., 2018b). The contribution of monocytes in circulation to the pool of resident tissue macrophages is tissue-dependent. In the case of AMs, they originate from fetal embryonic monocytes, and their differentiation requires GM-CSF (Gordon and Martinez-Pomares, 2017, McGovern et al., 2015). Following recruitment, the number of AM is maintained by cell division (Aberdein et al., 2013), in contrast, due to their short half-life the dermal resident macrophage are continuously replaced upon monocyte recruitment (McGovern et al., 2014). Macrophages can be activated through two main pathways, the classical activation or M1 activation where macrophage are activated with IFN-γ, a major Th1 cytokine, and/or PAMPs. The other macrophage activation route is the alternative pathway or M2 macrophages, where macrophages are activated with IL-4, IL-10, or IL-13 (Gordon and Martinez, 2010). These populations are thought to represent different stages of macrophage activation during inflammation, with M1 viewed as pro-inflammatory and M2 as anti-inflammatory and pro-resolution.

The potential role of macrophages in controlling PA infection have been addressed in several studies (Speert et al., 1988, Speert and Gordon, 1992, Heale et al., 2001, Kannan et al., 2008). Previous results by our group have showed treatment of macrophages with IL-17 enhanced macrophages killing of PA compared to macrophages treated with IFN-γ (Muntaka et al., 2019). However, it was indicated that peripheral blood mononuclear cells (PBMCs) from CF patients with PA chronic infection production of IFN-γ positively correlated with lung function, in contrast IL-17A levels tended to correlate negatively with lung function. Treatment of human macrophages with IFN-γ lead to up-regulation of IL-6, MCP-1 and TNF-α, and down-regulation of IL-10 expression by infected macrophages (Singh et al., 2015).

A possible role for alveolar macrophages in recruiting neutrophils during PA infection has been supported by different studies (Hashimoto et al., 1996, Kooguchi et al., 1998). Kooguchi et al. (1998) stated that when lung macrophages were depleted it negatively correlated with neutrophil recruitment to the site of infection (Kooguchi et al., 1998), same effects were seen in a study by Hashimoto and his colleagues (Hashimoto et al., 1996). An *in vitro* study showed that alveolar macrophages display phagocytic competency against PA; however, it failed to phagocyte un-opsonized PA (Cheung et al., 2000).

There is a growing body of literature showing that CF macrophages have reduced capability to clear pathogens (Ratner and Mueller, 2012). Some studies have indicated that CF macrophages hindered killing ability might be attributed to the disturbance in phagosome acidification caused by the CFTR mutation (Deriy et al., 2009, Di et al., 2006). It was reported that macrophages treated with CFTR-specific inhibitors have increased intracellular calcium (Ca_{2+}) levels, which might hampered macrophage activity (Shenoy et al., 2011).

1.6.3. Neutrophils:

Neutrophils constitute about 50–70% of all circulating white blood cells in humans. Neutrophils originated from myeloid precursor cells in the bone marrow (Doeing et al., 2003, Mestas and Hughes, 2004). These cells play an essential role in the complete resolution of lung infection

as they function as effective phagocytic cells against extracellular bacteria and fungi (Segal, 2005). Granulocyte colony-stimulating factor (G-CSF) controls neutrophil proliferation, differentiation and their release from the bone marrow (Shochat et al., 2007). G-CSF is produced in response to IL-17A (Ley et al., 2006), which regulates the severity of inflammatory diseases and contributes to host immunity against bacterial and fungal infection by indirectly promoting neutrophil recruitment (Korn et al., 2007, Iwakura et al., 2011). The main source of IL-17A is Th17 cells; however, neutrophil could also produce IL-17A after stimulated by MAMPs such as LPS (Ferretti et al., 2003, Lin et al., 2011). It has been indicated that treatment of neutrophils with both IL-6 and IL-23 were required for IL-17 production in neutrophils as IL-17 expression was inhibited in the presence of anti-IL-6 or anti-IL-23 (Taylor et al., 2014).

Tissue resident macrophages and DCs act as sentinel cells through the action of PRRs, such as those mentioned above, and could initiate neutrophil recruitment through several process such as the production of IL-23 and increasing blood vessels permeability (Kolaczkowska and Kubes, 2013). It had been indicated that deletion of macrophage or dendritic cells significantly reduced neutrophil infiltration into infected tissues (Ajuebor et al., 1999, Vieira et al., 2009).

Neutrophils can eliminate pathogens by different means, both intracellularly and extracellularly (Kolaczkowska and Kubes, 2013). When neutrophils encounter a pathogen, the pathogen is phagocytosed and becomes encapsulated inside a phagosome (Kolaczkowska and Kubes, 2013). In order to kill these pathogens neutrophil employ NADPH oxygen-dependent mechanism or antibacterial proteins such as cathepsins, defensins, lactoferrin and lysozyme (Borregaard, 2010, Häger et al., 2010). To aid the elimination of pathogens neutrophils generate neutrophil extracellular traps (NETs) (Kolaczkowska and Kubes, 2013). NET is a meshwork of DNA structures consisting of chromatin-associated with different antimicrobial peptides with potent bactericidal activity including myeloperoxidase, elastase, lactoferrin, histones, cathepsin, gelatinase, and proteinase 3 (Papayannopoulos, 2018). NETs continued presence can, however, result in tissue damage (Castanheira and Kubes, 2019).

The important role of neutrophil against PA infection have been stated by several studies, were neutrophil-depleted mice showed high vulnerability and mortality rates (Koh et al., 2009, Tsai et al., 2000, Fujimoto et al., 2002). It was reported recently that 3O-C12-HSL induces neutrophils apoptosis (Singh et al., 2019). Induction of NETs was reported during PA infection; however, several studies indicate that PA was able to resist neutrophils NETs antimicrobial activity (Geddes-McAlister et al., 2019). In a mouse model of PA infection in the cornea, even though PA biofilms were reported to resist neutrophils killing and antibiotic treatment, NETs formed a barrier restricting bacteria to the external corneal environment, and preventing bacterial dissemination into the brain (Thanabalasuriar et al., 2019). In a mouse PA infection model, Hirche et al. (2008) showed that neutrophil elastase is necessary for the elimination of PA (Hirche et al., 2008). CF patients experience persistent bacterial infection associated with massive neutrophil infiltration because of the excessive IL-17A release, resulting in pulmonary injury. Singh et al. (2015) found that the production of IL-17A by circulating immune cells correlates negatively with pulmonary function (Singh et al., 2015). Additionally, CFTR mutation was proposed to diminish neutrophils phagocytic and killing capacity (Ratner and Mueller, 2012, Painter et al., 2010, Painter et al., 2008).

1.7. Hypothesis and aims

The overarching aim of this project is to investigate the interplay between PA and innate immune cells and how it is affected by biofilm formation. This thesis investigates the innate immune cells-biofilms from three directions:

a) Previous work in the lab (Tamanna Rahman and Mohammad Alshahrani, PhD theses) indicated that PA biofilms bind MR and DC-SIGN and that DC-SIGN bound to PA biofilms significantly better than MR. In addition, MR and DC-SIGN recognise purified biofilm carbohydrate. Therefore, we hypothesized that

Dectin-2 is another CLR that could bind PA biofilms and purified biofilm carbohydrate

b) Because of its high carbohydrate content EPS could modulate immune activation through the engagement of C-type lectin receptors.

The specific aims for directions A and B are:

- Set up a system to generate PA biofilms under flow conditions to investigate the distribution of C-type lectin ligands within PA biofilms.
- Determine the capability of Dectin-2, to interact with PA biofilms and purified EPS components.
- Identify how recognition of EPS by C-type lectins influence the immune response to PA.

c) As the first responder cells of the innate immune system, neutrophils possess a unique set of migration features. Several studies found that neutrophils were not able to eradicate infection caused by biofilm-forming PA, which might indicate that biofilm formation was hindering neutrophils activity. The establishment of an *in vitro* model suitable for imaging will enable us to examine neutrophil morphological and behavioural changes following their contact with PA biofilms.

The aims of direction C are:

- Set up an assay to study neutrophil-PA biofilm interactions.
- Utilise this assay to determine neutrophil morphological and behavioural changes following their interaction with PA biofilms.

Chapter 2. Materials and Methods

2.1. Bacterial strains and generation of mid-log phase cultures:

All the strains (Table 1 and Table 2), unless otherwise stated, were grown on Lysogenic Broth (LB) agar plates from glycerol stocks stored at -80°C and incubated overnight at 37°C. The following day, a single colony was selected and inoculated into 5 ml of X-Vivo-15 media (LZBE02-061Q, Lonza) and incubated overnight at 37°C, at 200/220 rpm. The OD_{600nm} of cultures was adjusted to 0.01 in 20 ml of media in a 250 ml flask and incubated for 3 hr at 37°C, shaking at 200/220 rpm in order to reach mid log phase. Strains in (Table 1) were kindly provided by Dr. Yasuhiko Irie, University of Tartu, Estonia. Strains in (Table 2) were kindly provided by Dr. Ana da Silva, University of Nottingham, UK.

Table 1 Strains used in the study

Strain	Features	Source
PAO1	• (WT) Laboratory strain from Parsek's laboratory • Normal cellular level of c-di GMP • Expresses Psl and Pel	(Holloway et al., 1979)
ΔwspF	• PAO1 Δ*wspF.* • High cellular levels of c-di GMP • Expresses Psl and Pel	(Hickman et al., 2005)
Δ*wspF*Δ*pel*	• PAO1 Δ*wspF*Δ*pel* • High cellular levels of c-di GMP • Overexpresses Psl • Lacks Pel	(Irie et al., 2010)
Δ*wspF*Δ*psl*	• PAO1 Δ*wspF*Δ*psl* • High cellular levels of c-di GMP • Overexpresses Pel • Lacks Psl	
Δ*wspF*Δ*pel*Δ*psl*	• PAO1Δ*wspF*Δ*pel*Δ*psl* • High cellular levels of c-di GMP • Lacks Psl and Pel • Biofilm deficient	(Borlee et al., 2010)
Δ*wspF GFP*	• PAO1 Δ*wspF*. • High cellular levels of c-di GMP • Expresses Psl and Pel • Expressing chromosomally labelled constitutive GFP	(Irie et al., 2017)
Δ*wspF*Δ*pel*Δ*psl GFP*	• PAO1Δ*wspF*Δ*pel*Δ*psl* • High cellular levels of c-di GMP • Lacks Psl and Pel • Biofilm deficient • Δ*wspF* Δ*pel* Δ*psl* expressing chromosomally labelled constitutive GFP	

Table 2 *P. aeruginosa* wound clinical isolates used in the study

Strain	Description	Source
CW2 B40	Isolated from bone	(Singh et al., 2020)
CW5 B1		
CW3 T40	Isolated from wound tissue	
CW6 T4		
CW7 T1		
CW5 S1	Isolated from blood	

2.2. Genotyping of Wspf, Psl, and Pel mutation using polymerase chain reaction (PCR)

Table 3 Primers used to confirm specific mutations in the *wspF* mutants

***WspF* gene**	**Primer sequence (5'-3')**
Forward primer	AAGATTCAGAACGTCGGCTG
Reverse primer	GATGTGATTGTTGGTCCCCG
PslC* and *PslD	**Primer sequence (5'-3')**
Forward primer	GGTCTACCATTCCCACGATTAC
Reverse primer	TCAGCTCGTTGGCGATTT
PelA	**Primer sequence (5'-3')**
Forward primer	CCCTATCCGTTCCTCACCTC
Reverse primer	TACTGGGCCTCGAAGTTCTC

PCR was used to confirm the mutations in (Table 1) strains. Primers were designed to target the mutated gene(s) (Table 3). PCR reactions were carried out in 25 µl reaction containing 1 µl of overnight bacterial culture in X-Vivo-15 media, 0.1 µM each of reverse and forward primers, and 1x of GoTaq G2 green master mix (M7822, Promega). The amplification process was as follows: a denaturation cycle at 96 °C for 5 min, followed by 30 cycles of denaturation at 95 °C for 30 s, annealing at 55 °C for 30 s and extension at 72 °C for 30 s. This process was completed by an extra extension cycle at 72 °C for 5 min. PCR products (15 µl) were loaded into 0.1% agarose gel containing 0.01% of Syber safe DNA gel stain (S33102, Invitrogen) in Tris-acetate-EDTA (TAE) buffer and electrophoresed for 1 hr at 100 volts.

2.3. Biofilm formation and quantification assay (Crystal violet assay).

After mid log phase (3 hr) cultures were generated as described above, absorbance was measured at OD_{600nm} in 1 ml samples using an spectrophotometer (Thermo Scientific Biomate 3) before adjusted to OD_{600nm} 0.04 in X-vivo-15 media (Lonza) and kept on ice. Then 100 µl of adjusted OD_{600nm} cultures were added to each well of a UV-sterilised 96-well plate (MaxiSorp™, 439454, Nunc immune-plate), Cell culture 96-well plate (0030730135,

eppendorf) or CELLview™ slide (543979, Greiner Bio-One). To quantify the biomass, cultures incubated for 24 hr at 37°C, 5%CO_2 were washed three times with 200 µl of HPLC water and stained with 125 µl of 1% (w/v) crystal violet (1 hr, room temperature (RT)). After washing three times in water, the stain was solubilised by adding 200 µl of 70% ethanol for 15 min; 125 µl was transferred into a clean 96-well MaxiSorp plate to measure the absorbance at 595 nm using a Multiskan FC (Thermo Scientific).

2.4. Analysis of the adhesion of planktonic PA to plastic

Overnight PA cultures in X-Vivo-15 were centrifuged at 16,000 × g for 5 min at 4°C, washed twice with phosphate buffered saline (PBS), and re-suspended in 4% paraformaldehyde (PFA, 15710-S, Electronic Microscopy Sciences, USA) in PBS for 30 min at 4°C. After fixation, cultures were washed once with PBS, adjusted to 0.5 OD_{600nm} in PBS, and pipetted onto 96-well Maxisorp plates (50 µl/well) and incubated overnight at 4°C. After washing three times with PBS blocking was carried out by adding 50 µl of 3% (w/v) bovine serum albumin (BSA) (80400-100, Alpha diagnostics) prepared in PBS. Rabbit anti-PA polyclonal antibody (50 µl/well, ab68538, Abcam) 10µg/ml in PBS was added and incubated for 90 min at RT. After three washes in PBS, the plate was incubated with 50 µl of goat anti-rabbit IgG conjugated to alkaline phosphatase diluted 1:2000 (A3687, Sigma) in PBS for 1 hr at RT. After three washes with AP buffer (100 mM Tris-HCl, 100 mM NaCl, 1 mM MgCl2, pH 9.5), 50 µl of p-nitrophenyl phosphate substrate solution (N2770, Sigma) were added to each well and incubated for 30-40 min at room temperature in the dark. Absorbance was measured at 405 nm using a Multiskan FC (Thermo Scientific).

2.5. Lectin binding assays (Enzyme-Linked immunosorbent assay, ELISA).

Assays for the binding of chimeric proteins to fixed PA biofilms, fixed planktonic PA cells and purified carbohydrate were performed as follows. Biofilms were grown on a (MaxiSorp™,

439454, Nunc immune-plate) over 24 hr and fixed with 100 µl of 4% PFA in PBS for 10 min at 4°C. For fixed PA cells, wells of Maxisorp plates were coated with fixed bacteria (100 µl/per well) and incubated at 4°C overnight. Purified biofilm carbohydrate was added to Maxisorp plates overnight (50 µl/well in 154 mM NaCl, 37°C). In all instances, plates were washed three times with TBS (10 mM Tris-HCl, pH 7.5, 10 mM CaCl2, 154 mM NaCl and 0.05% (v/v) Tween 20). Chimeric proteins MR-CTLD4-7 (CTLD-4-7-Fc, prepared in house, (Linehan et al., 2001)), Dectin-2-Fc (ALX-522-126-C050, Enzo) and DC-SIGN-Fc(161-DC, R&D) (50 µl/well in TBS) were added and incubated for 2 hr at RT. After three washes with TBS, anti-human Fc-conjugated to alkaline phosphatase (A9544, Sigma) was added (50 µl/well) and incubated for 1 hr, RT (1:1000 dilution). After washing three times with TBS, alkaline phosphatase activity was measured as above. Inhibition assays were carried out as above but using TSB buffer containing 1M NaCl (TSB-high salt). MR-CTLD4-7 and Dectin-2 were pre-incubated with different concentrations of the Manα1-2Man (M202, Dextra) in TSB-high salt for 30 min at RT. After pre-incubation, proteins were added to appropriate wells containing biofilms. Polymers containing D-mannose, L-fucose, D-galactose (2-5 µg/ml, 50 µl per well, Lectinity) or Heat killed *Candida albicans* ($4x10^6$ PA/well, 50 µl per well, kindly provided by Mohammad Alshahrani) were used as controls.

2.6. Generation of Biofilms for microscopic analysis

2.6.1. Generation of PA biofilms on CELLview™ cell culture slides.

Mid log phase (3 hr) cultures generated as described above, were diluted to OD_{600nm} 0.04 in X-Vivo-15 medium (Lonza) and used to inoculate CELLview™ slide (100 µl per well, 543979, Greiner Bio-One). Slides were incubated at 37°C, 5% CO_2 for 24 hr. To visualize PA biofilms, following 24 hr incubation supernatants were removed, and cultures fixed with 4% PFA in PBS at 4°C for 10 min before washing three times with PBS. The wells then were blocked with 5% normal goat serum (Sigma-Aldrich) in PBS for 30 min. Next the blocking buffer was removed and rabbit polyclonal anti- *Pseudomonas aeruginosa* prepared in blocking buffer (4.5µg/ml,

Abcam) was added and incubated for 1hr before doing three washes with PBS. Biofilms were then labelled with a mixture of the following: (green) Goat anti-rabbit antibody conjugated to Alexa Fluor 488 (10 µg/ml, A-11008, Molecular Probes) to stain the bacteria and (Blue) DAPI (1 µg/ml, D9542, Sigma-Aldrich) to stain DNA. The staining mixture was prepared in 5% goat serum (100µl per well) and incubated for 30 min. Excess dye was removed by washing three times with PBS. Each well of the CELLview™ cell culture slides were then filled with 0.1% NaN_3 prepared in PBS before confocal microscopy examination. Confocal images were acquired using Zeiss LSM 710 using a 40x /1.2 water objective. Fluorescence emission was collected between 405- 457 nm (DAPI) and 488-525 nm (Alexa Fluor 488). Presented Z-Stack (212.55 µm, y: 212.55 µm, z: 0.44 µm). Images were processed using Fiji (Schindelin et al., 2012).

2.6.2. Generation of PA biofilms on µ-Slide VI 0.4 slides.

Mid log phase (3 hr) cultures generated as described above were diluted to OD_{600nm} 0.04 in X-vivo-15 medium (Lonza) and used to inoculate µ-Slide VI 0.4 channels (30 µl per channel, Ibidi, tissue culture treated) and incubated at 37°C, 5% CO_2 for 24 hr. To visualize PA biofilms, following 24 h incubation supernatants were removed, and cultures fixed with 4% PFA in PBS at 4°C for 10 min before being washed three times with PBS. Next, biofilms were labelled with (Blue) DAPI at 1 µg/ml to stain DNA. Confocal images were acquired using Zeiss LSM 710 using a 40x /1.2 water objective. Fluorescence emission was collected between 415- 496 nm (DAPI). Presented Z-Stack (212.55 µm, y: 212.55 µm, z: 5.5.35 - 12.311 µm). Images were processed using Fiji (Schindelin et al., 2012) and biofilm parameters were quantified using Comstat (Heydorn et al., 2000b).

2.6.3. Generation of PA biofilms under flow condition using a peristaltic pump system.

Mid log phase (3 hr) cultures generated as described above, were diluted to OD_{600nm} 0.04 in X-Vivo-15 medium (Lonza) and used to inoculate µ-Slide VI 0.4 channels (30 µl per channel,

Ibidi, tissue culture treated) and incubated at 37°C for 1 hr to allow bacterial attachments to the surface. Slides were fitted into the peristaltic pump system, and exposed to flow (4.5 ml/hr, bacterial culture 0.04 OD_{600nm} in X-vivo-15 medium, 15 hr) at 37°C, 5% CO_2. After culture, supernatants were collected, biofilms fixed with 100 µl of 4% PFA in PBS for 10 min at 4°C. After fixation, biofilms were washed gently 3 times with 120 µl of PBS. Membranes were labelled with FM™ 1-43 FX (100 µl per channel, F35355, Thermo Fisher, 5 µg/ml, 15 min, on Ice) and DNA with DAPI (100 µl per channel, Thermo Fisher, 2 µg/ml, 15 min, RT). After incubations slides were washed gently 3 times with 120 µl of PBS. Finally, slides were filled with ibidi mounting medium (50001, ibidi). Confocal images were acquired using Zeiss LSM 710 using a 40x /1.2 water objective. Fluorescence emission was collected between 415- 496 nm (DAPI), 506-554 nm (FM 1-43FX), 603-690 nm (HHA). Presented Z-Stack (212.55 µm, y: 212.55 µm, z: 15.257 µm). Images were processed using Fiji and biofilm parameters were quantified using Comstat (Heydorn et al., 2000b).

2.6.4. Generation of PA biofilms under standardized flow conditions using the syringe pump system.

Mid log phase (3 hr) cultures generated as described above, were diluted to OD_{600nm} 0.04 in X-Vivo 15 medium (Lonza, pre-gassed for 48 h at 37°C / 5% CO_2) and used to inoculate µ-Slide VI 0.4 channels (30 µl per channel, Ibidi, tissue culture treated) and incubated at 37°C for 1 hr to allow bacterial attachment to the surface. Slides were fitted into the syringe pump system, and exposed to flow (1.6 µl/hr, pre-gassed X-Vivo-15, 18 or 24 hr) at 37°C, 5% CO_2. After culture, supernatants were collected, biofilms fixed with 100 µl of 4% PFA in PBS for 10 min at 4°C. After fixation, biofilms were washed gently 3 times with 120 µl of PBS. Mannose-rich carbohydrate was labelled with HHA-conjugated to Texas red (100 µl per channel, T-8008-1, EYlabs, 100 µg/ml, 2 hr, RT). Membranes were labelled with FM™ 1-43 FX (100 µl per channel, F35355, Thermo Fisher, 5 µg/ml, 15 min, on Ice) and DNA with DAPI (100 µl per channel, Thermo Fisher, 2 µg/ml, 15 min, RT). After incubations slides were washed gently 3 times with 120 µl of PBS. Finally, slides were filled with ibidi mounting medium (50001, ibidi).

Confocal images were acquired using Zeiss LSM 710 using a 40x /1.3 oil objective. Fluorescence emission was collected between 415- 496 nm (DAPI), 506-554 nm (FM 1-43FX), 603-690 nm (HHA). Presented Z-Stack (212.55 µm, y: 212.55 µm, z: 7.5-19.181 µm). Images were processed using Volocity (PerkinElmer Inc.) and biofilm parameters were quantified using Comstat (Heydorn et al., 2000b).

2.7. Study of lectin binding to PA biofilms by confocal microscopy

Biofilms generated under flow on µ-Slide VI 0.4 (80606, Ibidi) as described above (section 6.4), were fixed with 4% PFA in PBS (100 µl per channel, 10 min, 4°C), and washed three times with TSB buffer. In some instances, wells were stained with FM 1-43 FX membrane dye (100 µl per channel, 5 µg/ml, F35355, Thermofisher) in PBS for 15 min on ice. Following three washes with TSB buffer MR-CTLD4-7 (CTLD-4-7-Fc, prepared in house, (Linehan et al., 2001), MR-CR-FNII-CTLD1-3, prepared in house (Martinez-Pomares et al., 2006), Dectin-2-Fc (ALX-522-126-C050, Enzo) or DC-SIGN-Fc (161-DC, R&D) (30 µl per channel, 10 µg/ml in TSB buffer) were added and incubated for 2 hr at RT. After washing three times with TSB buffer, 100 µl of TSB containing 10 µg/ml goat anti-Human IgG conjugated to Alexa fluor 647 (A21445, Invitrogen) and 3%(v/v) Goat serum (G9023, Sigma) in TBS were added and incubated for 1 hr at RT. Following three washes with TSB, DNA was labelled with DAPI (100 µl per channel, 2 µg/ml, D9542, Sigma-Aldrich) in PBS for 15 min, RT. The plates were washed with TSB and mounted in Ibidi mounting media (50001, Ibidi) before storing at 4°C in the dark. Confocal images were acquired using Zeiss LSM 880 using a 40x /1.20 water objective, the collection was not done with filters. Fluorescence emission was collected between 434 and 515 nm (DAPI), 469-538 nm (FM 1-43FX), 641-688 nm (AF 647). Stack size (49.43 µm, y: 49.43 µm, z: 7.5-12.9 µm). Presented single slice size (49.43 µm, y: 49.43 µm, z: 0.288-0.293 µm). Images were processed using Fiji (Schindelin et al., 2012).

2.8. Isolation of human monocytes (CD14+ cells).

Buffy coats from the Blood Transfusion Service, Sheffield, UK were used to isolate monocytes (CD14+ cells) by positive selection. Use of buffy coats was approved by the Faculty of Medicine and Health Sciences Research Ethics Committee. After decontaminating the blood bags with 70% alcohol, the buffy coats were transferred into a T75 flask and diluted up to 140 ml with Dulbecco's Phosphate Buffered saline (DPBS) without Ca^{2+} and Mg^{2+} (Invitrogen). The diluted buffy coat was layered into four Falcon tubes (BD Biosciences or CellStar), each containing 15 ml Histopaque-1077 (10771, Sigma). The tubes were centrifuged at 800 x g for 30 min, acceleration 3, deceleration 3 using an Allegra X- 15R centrifuge (Beckman Coulter). Following centrifugation, the peripheral blood mononuclear cells (PBMC) layer was gently collected and transferred into new falcon tubes using a sterile pipet and washed once in PBS (centrifuged – 350 x g for 10 min). Following centrifugation, if pellet looked contaminated with red blood cells (RBC), RBC lysis buffer (11814389001, Roche) was used as follows. RBC lysis buffer was added at 1:3 dilution (for example if the pellet is in 5 ml, 10 ml of lysis buffer was added) and incubated at RT 10 min on tube roller. The tubes were then centrifuged 350 x g for 5 min accel 1 decel 1 or minimum. In all instance tubes were washed twice with in PBS each centrifugation – 350 x g for 10 min. Cells were counted, before being re-suspended in pre-cold MACs buffer (80 µl per 10^7 cells) and incubated with CD14-magnetic beads (10 µl per 10^7 cells, Miltenyi Biotec) on ice, in the dark for 15 min to obtain the monocyte (CD14+ cells) fraction by positive selection. CD14+ cells were washed with MACS buffer at 350 x g for 5 min and applied through a LS MACS column following the manufacturer's protocol.

2.9. Preparation of human monocyte-derived dendritic cells (moDCs)

After numbers of monocytes and cell viability were determined using automated cell counter (TC20, BIO-RAD), Purified monocytes were resuspended in RPMI complete medium [RPMI-1640 (R0883, Sigma), 15% (v/v) human AB serum (PAA Laboratories, UK), 2 mM L-glutamine (G7513, Sigma), 10 mM HEPES (15630056, Gibco), 50 ng/ml recombinant human granulocyte macrophage colony–stimulating factor (rhGM-CSF) (130-093-865, Miltenyi Biotec), and 50 ng/ml rh interleukin (IL)-4 (130-093-921, Miltenyi Biotec)] at density of 1.5 x 10^6 monocytes/ml. Monocytes were seeded in each well of 24 well flat bottom tissue culture plates (EP0030722116-60EA, Eppendorf; at 750,000 cells per well) and cultured at 37°C, 5%CO2 for 6 days. On Day 3, fresh RPMI complete media containing growth factors was added to each well. To collect moDCs at Day 7, the 24 well plates were placed on ice for 20 min, then using 1 ml pipette, the cells were gently flushed and transferred into 15 ml falcon tubes and placed on ice. Wells were observed microscopically to ensure complete harvest of the moDCs. If there were any cells still attached to the wells, then 500 µl of the media to be used was added to the wells and the plate was incubated for 5 min on ice. Then cells were flushed off gently with 1 ml pipette and transferred to the 15 ml falcon tube. In all cases, cell suspensions in the 15 ml falcon tubes were centrifuged at 350 x g, 4°C, acceleration 3, deceleration 3, for 5 min to pellet moDCs. These were then washed 2 times with fresh X-Vivo-15 before re-suspended in appropriate media per assay. Cells were counted and adjusted to densities as appropriate per assay.

2.10. Purification of human neutrophils

Human blood samples were obtained by venipuncture from healthy donors under an ethics protocol approved by the University of Nottingham. Informed written consent form was obtained from all participants. Neutrophils were purified from whole blood using negative selection following manufacturer's instruction (STEMCELL, 19666). Whole blood collected in EDTA tube (2 ml) was transferred to an isolation round button tube and incubated for 5 min at RT with 50 µl/ml of both, (1) antibody isolation cocktail and (2) magnetic RapidSpheres. The tube was then toped up to 10 mL with Hank's buffer without Ca^{2+} and Mg^{2+} before being mixed gently 3 times with a 10 ml pipette. Next the tube was placed (without lid) into the magnet ("The Big Easy", Catalog #18001, STEMCELL) and incubated for 5 min at RT. After incubation, the magnet and tube were picked and in one continuous motion were inverted to pour the cell suspension into a new tube . Then, same volume of magnetic RapidSpheres used earlier were mixed and incubated with the cell suspension (5 min at RT). The tube was then placed in the magnet and incubated for further (5 min at RT) before being poured into new tube. The new tube was placed in the magnet and incubated for (5 min at RT). Finally, the magnet and tube were picked and in one continuous motion were inverted to pour the purified neutrophils into new tube .

Neutrophils purity were determined by cytospin preparations. Cell suspensions were placed onto a glass slide already inserted into cytofunnels (EZ Single Cytofunnel, Ref: A78710020, Fisher Scientific) and centrifuged at 200 rpm, 20 min, low acceleration using a cytospin (Cytospin 2, Shandon). Slides were air dried, labelled with Hemacolor (MERCK) following the manufacturer's procedure (solution 1: applied for 30 seconds, solution 2 for 3 seconds and solution 3 for 6 seconds), air dried, mounted with DPX (Sigma-Aldrich). The stained slides were examined under a bright field inverted microscope fitted with a camera.

In only one experiment (Figure 6.3), labelling for PKH67 was performed following manufacture instructions. First, purified neutrophils were washed twice in fresh X-Vivo-15 and (centrifuged

– 350 x g for 5 min) at RT. 500 µl of diluents C was added to the cell pellet, and gentle pipetting was performed to ensure complete dispersion. A dye solution was prepared by mixing 4 µm of PKH67 dye solution (Sigma-Aldrich, PKH67GL-1KT) into 500 µl of diluent C in a 15 ml falcon tube. 500 µl of the cell suspension in Diluent C was added to 500 µl of dye solution and mixed immediately by pipetting and incubated for 5 minutes at RT. Staining was stopped by adding an equal volume of BSA (1ml) and incubating for 1 min at RT C to allow binding of excess dye. Cells were washed three times with X-Vivo-15 media and (centrifuged – 350 x g for 5 min) at RT and re-suspended in X-Vivo-15 medium for further experimentation.

2.11. Analysis of cell surface markers using flow cytometry

Cells were re-suspended in X-vivo-15 media in a 15 ml falcon tube at a density of 1×10^6 cells /ml, centrifuged at 350 x g, for 5 min, acceleration and deceleration 3, at 4°C and re-suspended in 1 ml of 5% (v/v) human serum (PAA Laboratories Ltd) in PBA solution [0.5% (w/v) BSA and 0.1% (w/v) sodium azide (S2002, Sigma) prepared in PBS], and incubated for 1 hr at 4°C. After washing the cells with cold PBA three times, the cell density was adjusted to 100,000 cells/100µl of PBA. Then the cells were incubated with anti-human monoclonal antibodies or their matched isotype controls: CD206 (MMR)-Allophycocyanin (APC) (321109, Biolegend), DC209 (DC-SIGN)-APC (330107, Biolegend), CLEC6A (Dectin-2)-APC (FAB3114A, R&D), CLEC7A (Dectin-1)-APC (144306, Biolegend), CD66b-FITC (REA306, Miltenyi Biotec), APC Mouse IgG1 (MR) Isotype Ctrl (400120, Biolegend), APC Mouse IgG2a (DC-SIGN) Isotype Ctrl (400222, Biolegend), APC Mouse IgG1 (Dectin-2) Isotype Ctrl (IC002A, R&D), APC Rat IgG1 (Dectin-1) Isotype Ctrl (400411, Biolegend) or human IgG1 FITC-REA (CD66b) control Ab (130-113-437, Miltenyi Biotec) for 1 hr at 4°C. The cells were washed twice with cold PBA and re-suspended in fresh cold PBA and fixed with 0.5% PFA (15710-S, Electronic Microscopy Sciences, USA) in PBS at 4°C. Cells were analysed using a FC500 Beckman Coulter flow cytometer; 10,000 events were collected. Data were analysed using Kaluza Software 1.5a.

2.12. Analysis of Dectin-2 expression by western blot

For western blot analysis, cells were lysed in lysis buffer [10 mM Tris-HCl, pH8.2, 150 mM NaCl, 5 mM EDTA, 2% Triton X-100 and two tablets of protease inhibitor (11836170001, Roche)] for 30 min on ice. Lysates are then clarified by centrifugation at 13,000g for 30 min before the supernatants were collected. Protein concentration was determined by the BCA assay (Bio-Rad Laboratories). Samples were boiled at 100°C for 5 mins before different amounts of protein were electrophoresed on SDS–polyacrylamide gel. A 10-230 kDa Protein Ladder were used to determine molecular weight. The gels were then electro-blotted onto nitrocellulose membranes. After blocking with 5% milk in PBS with 0.1% tween 20, membranes were incubated with primary antibody against human Dectin-2 (Anti-Dectin-2 antibody (ab107572, abcam)) at 5 µg/ml. Finally, the relevant protein was visualized by incubating with IRDye 800CW anti mouse Licor at 1:5000 for 1 hr at room temperature. The bands were detected by using an Odyssey Imager (LI-Cor biosciences).

2.13. Analysis of changes in moDCs morphology after incubation with HMW-Psl or PA biofilms

Assays for the analysis of changes in moDCs morphology after incubation with HMW-Psl or PA biofilms were performed as follows. Biofilms were grown on µ-Slide VI 0.4 slides over 24 hr using the syringe pump system described above and fixed with 100 µl of 4% PFA in PBS for 10 min at 4°C. Purified biofilm carbohydrate was added to µ-Slide VI 0.4 slides (10 µg/ml, in X-vivo-15) overnight at 4°C. After washing, and addition of moDCs (5×10^4 cells per channel in X-vivo 15 containing GM-CSF and IL-4) cultures were incubated for 24 hr at 37°C, 5% CO_2. Samples were fixed in 4% PFA (15710-s, EM Grade) in PEM (Cytoskeleton-preserving buffer PIPES-EGTA-Magnesium, 80 mM PIPES pH 6.8, 5 mM EGTA, 2 mM $MgCl_2$) for 15 min, RT. Slides were washed in PEM, and blocked with 5% donkey serum (D9663, Sigma) in PEM in the presence or absence of 0.25% Triton X-100. After 3 washes in PEM, cells were incubated

with rabbit polyclonal to DC-SIGN (10 µg/ml overnight at 4°C) (ab5715, Abcam) in blocking buffer and then with Alexa Fluor® 647 AffiniPure Donkey Anti-Rabbit IgG (H+L)) (jacksonimmuno, 711-605-152) 1:500 in blocking buffer. After 3 washes in PEM cells were labelled with DAPI (1.5 µg/ml in PBS, Sigma-Aldrich, D9542), washed in PBS and mounted in Ibidi mounting media (Ibidi, 50001). Confocal images were acquired using Zeiss LSM 710 under 40x /1.3 oil objective, without filters. Fluorescence emission was collected between 410 and 585 nm (DAPI) and 638-755 nm (AF 647). Image size (212.55 µm, y: 212.55 µm, z: 0.406 µm). Images were analysed using Fiji (Schindelin et al., 2012). Raw Integrated density and cell perimeter were measured by manually following the contour of the cell using the segmented line tool (width=12 nm). Circularity (the ratio between longer and shortest axes for each cell) was determined by manually following the contour of the cell using the free hand line tool. The selected areas were then saved in the ROI manager for analysis. Single per unit area was calculated by (Raw Integrated density / area selected using the segmented line tool (width=12 nm) = single per unit area).

2.14. Analysis of changes in neutrophil morphology after incubation with HMW-Psl or PA biofilms

Assays for the analysis of changes in neutrophils morphology after incubation with biofilm cultures of PAO1, Δ*wspF*, Δ*wspF*Δ*pel*Δ*psl* or Δ*wspF*Δ*pel*Δ*psl* + (High molecular weight (HMW))-Psl were performed as follows. Bacterial cultures were placed on µ-Slide VI 0.4 slides under shear stress for 18 hr using the syringe pump system described above and fixed with 100 µl of 4% PFAe in PBS for 10 min at 4°C, washed twice using PBS with Ca^{2+} and Mg^{2+}, purified biofilm carbohydrate was added to fixed Δ*wspF*Δ*pel*Δ*psl* (10 µg/ml in X-vivo-15 for 1 hr) and removed prior addition of neutrophils. After addition of neutrophils (5 x 10^4 cells per channel in X-vivo 15) cultures were incubated for 2 hr at 37°C, 5% CO_2. Neutrophils-PA co-cultures were fixed (4% PFA in PBS 10 min at 4°C), washed twice with PBS and permeabilised with 0.15% Triton X-100 in PBS for 10 min, washed twice with PBS and blocked with 1% BSA

in PBS for 30 min. Cells were stained with 1:500 rhodamine phalloidin at RT for 30 min followed by HHA-conjugated to Texas red (100 µl per channel, T-8008-1, EYlabs, 100 µg/ml, 2hr, RT), before stained with DAPI (100 µl per channel, 2 µg/ml, D9542, Sigma-Aldrich) 5 min at RT. After each staining step slides were washed twice with PBS. Slides were then mounted with Ibidi mounting media (50001, Ibidi) before storing at 4°C in the dark. Confocal images were acquired using Zeiss LSM 710 using a 40x /1.3 oil objective. Fluorescence emission was collected between 405- 459 nm (DAPI), 488-549 nm F-actin (phalloidin (P)-AF488), 594-645 nm (HHA). Acquired Z-Stack (212.55 µm, y: 212.55 µm, z: 15.257-18 µm). Presented Z-Stack (32.38 µm, y: 31.97 µm, z: 15.257-18 µm). Images were processed using Fiji (Schindelin et al., 2012). F-actin intensity and circularity (the ratio between longer and shortest axes for each cell) were determined by manually following the contour of the cell using the free hand line tool. The selected areas were then saved in the ROI manager for analysis.

2.15. Analysis of the effect of biofilms or purified HMW-Psl on cytokine production by moDCs

Assays for the analysis of cytokines production by moDCs incubated with fixed PA biofilms and purified carbohydrate were performed as follows. Biofilms were grown on a cell culture 96-well plate (0030730135, eppendorf) over 24 hr and fixed with 100 µl of 4% PFA in PBS for 10 min at 4°C. Then wells were washed three times with 200 µl of PBS before 50 µl of X-vivo 15 was added to each well. For assays to test the effect of HMW-Psl (LPS-free) on moDCs responses to PA Psl-deficient biofilm and planktonic cultures, HMW-Psl was added at different concentration in 50 µl X-vivo-15 and incubated 1 hr (37 °C/ 5% CO_2). Next moDCs (10 x10^4 in 50 µl X-vivo-15 + 50 ng/ml IL-4 and 50 ng/ml GM-CSF) were added to each well and incubated 4 hr at 37 °C, 5% CO_2). Next, plates were centrifuged 350 x g for 5 min accel 3 decel 3 and supernatants were collected in 1.5 ml centrifuge tubes and stored at -80 °C prior cytokines quantification.

2.16. Cytokine quantification

Magnetic luminex assay kit (LXSAHM-7, R&D) was used to measure IL-1β, IL-6, TNF-α,IL-10, MCP-1 and IL-23 cytokines in supernatant collected from the assays described above. Color-coded magnetic micro-particles coated with specific cytokines antibodies were added to wells (50 µl), same volume of supernatant and standards (50 µl) were added to appropriate wells and incubated for 2 hr at RT on a shaker at 800 rpm. Wells were washed three times with the provided washing buffer following the manufacturer protocol. Next, 50 µl biotinylated antibody cocktail was added to each well and incubated for 1 hr at RT on a shaker at 800 rpm. After washing three times, 50 µl of streptavidin conjugated to phycoerythrin (PE) were added and incubated for 30 min at room temperature on a shaker at 800 rpm. The wells were washed three times and the micro-particles were re-suspended in 100 µl of the washing buffer per well and incubated for 2 min RTon a shaker at 800 rpm. Samples and standard were read using Bio-Rad Bio-Plex 200 system. Data was analysed with Microsoft Excel and GraphPad Prism.

ELISA was used for the analysis of TNF-α, MCP-1 and Gro- α (Duoset, R&D). Assays were conducted following manufacturer's protocol. Briefly, 96 well plate (MaxiSorp™, 439454, Nunc immune) was coated with 100 µl of capture antibody before sealed and incubated overnight at RT. Next the, plate was washed three times with the washing buffer provided. Wells were blocked with 300 µl of reagent diluent, incubated for 1 hr, and then washed three times with the washing buffer. Supernatants or standard (100 µl), both diluted with reagent diluent, were added and incubated for 2 hr at RT. The plate was then washed three times with the washing buffer before 100 µl of detection antibody was added and incubated for 2 hr at RT. After, the plate was washed three times with the washing buffer and Streptavidin-HRP was added and incubated for 20 min at RT. The plate was then washed three times with the washing buffer before 100 µL of Substrate Solution was added and incubated for 20 min at RT. Reaction was stopped by adding , 50 µl/well of the Stop Solution. Optical density was immediately measured using a using a Multiskan FC (Thermo Scientific) set to 450 nm. Readings at 595 nm was

taken and subtracted from 450 nm for wavelength correction as recommended. Data was analysed with Microsoft Excel and GraphPad Prism.

2.17. Cell survival (LDH assay)

Cell supernatants were tested for the release of lactate dehydrogenase (LDH) using an LDH cytotoxicity detection kit (11644793001, Roche) following the manufacturers' protocol. An LDH positive control (cells incubated with 2% Triton X-100) was also used alongside the test samples. In brief, equal volumes of test samples and reaction mixture were mixed and incubated for 30 min in the dark before reading. The plate was read using a microplate reader (Multiskan FC, Thermo Scientific) at 492nm and wavelength correction at 620nm. Data was analysed with Microsoft Excel and GraphPad Prism.

2.18. CLRs blocking on moDCs

Blocking of CLRs on moDCs was performed as follows, moDCs generated from CD14+ monocytes as described above were incubated with X-vivo-15 only or anti-hMR (40 µg/ml, 15-2, 321102, Biolegend), anti-hDC-SIGN (40 µg/ml, AZN-D1, kindly provided by Prof van Kooyk, VUMC), anti-hDectin-2 (20 µg/ml, mabg-hdect2, InvivoGen) or isotype-matched control antibody for 1 hr, 37 ˚C, 5% CO_2. To confirm the blocking capability of each anti-CLR used, moDCs (incubated with one, two or all anti-CLRs) were tested for MR, DC-SIGN, and Dectin-2 expression by flow cytometry as described above.

2.19. Dectin-2 reporter cells assay

2B4-NFAT-GFP reporter cells expressing human Dectin-2 and FcR-γ, or FcR-γ only were kindly provided by Dr. Sho Yamasaki (Osaka University, Japan) and grown in Ultra-Low attachment cell culture flasks (CLS3815, Sigma) in 10 ml of RPMI-1640 medium (R0883, Sigma) containing 10% (v/v) foetal bovine serum (FBS, F9665, Sigma), 50,000 U Penicillin,

50 mg streptomycin (11074440001, Roche) and (55 µM) 2-mercaptoethanol (M6250, Sigma) at 37°C, 5% CO_2. The media were changed when the cells are about 80% confluent. Cells were harvested by pipetting then centrifugated at 250 x g for 5 min before washed once in RPMI-1640 medium, re-suspended in RPMI-1640 medium containing supplements and adjusted to 4 $x10^5$/ml. To determine whether Dectin-2 recognition of biofilm-associated carbohydrates would induce Dectin-2-mediated signalling, cell culture 96-well plate (0030730135, eppendorf) were pre coated with purified HMW-Psl (500 µg/ml) or HKCA ($4x10^6$ particles/well) prepared in PBS with Ca^{2+} and Mg^{2+} for 24h at 4° C. Reporter cells expressing human Dectin-2 + FcR-γ, or FcR-γ only were added at 4 $X10^4$ /100µl into the wells and incubated at 37°C, 5% CO_2 for 20 hr. Cells were collected and GFP expression were assessed using a FC500 Beckman Coulter flow cytometer; 10,000 events were collected. Data were analysed using Kaluza Software 1.5a.

2.20. Biofilm-human neutrophils live microscopy assay

Assays for the live microscopy analysis of neutrophils behaviour after incubation with PA biofilms were performed as follows. Bacteria were cultured in µ-Slide VI 0.4 and placed under shear stress for 18 hr using the syringe pump system explained earlier, fixed with 4% PFA in PBS (100 µl, 10 min at 4°C), washed twice using 100 µl of PBS with Ca^{2+} and Mg^{2+}. The slide was kept with 100 µl of PBS with Ca^{2+} and Mg^{2+} in 4°C while neutrophil isolation was performed. Next, purified neutrophils were washed twice with HBSS with Ca^{2+} and Mg^{2+}, diluted in fresh X-Vivo-15 and added to the slide (the opposite side of the original shear stress, 50,000 cells in 30µl). Immediately 60 µl of fresh X-Vivo-15 were added simultaneously in each reservoir to reduce the tendency of neutrophils to move by capillarity as a result of surface tension. Cellular behaviour was monitored live using a DeltaVision microscope under Olympus U-Plan S-Apo 40X/0.95 objective. Time lapse images (15) were taken every 8 min from each condition. To increase accuracy of the data generated using this system and to aid in the experimental design, neutrophils movements were monitored in exactly 5 fixed locations.

These locations were stored with known stage coordinates and were applied in all experiments conducted as shown in (Ch.6, Figure 6.5).

2.21. Analysis of biofilm-human neutrophils live microscopy assay using TrackMate

Analysis of the time laps images collected as explained earlier was conducted as follow. To increase the detection capability of TrackMate the background of each video was subtracted before being uploaded to Fiji software. To start TrackMate, Plugins was pressed from the top list of options, then Tracking, then TrackMate. To recognize the cells, LoG Detector was selected with an estimated blob diameter of 10 µm, Threshold: 00, Use median filter: No, Do sub-pixel localization: Yes, then next. For Initial thresholding Auto Quality were chosen then next. (5) For the view: Hyperstack Display were selected then Next. (5) Quality filters were applied to filter unwanted spots. (6) to track the cells Simple LAP tracker was chosen with linking max distance: 50 µm and 15 gap-closing max frames. (7) Software were run to process the cell tracking. (8) no filter was set on tracks. (9) Data generated were saved in EXCEL format.

2.22. Quantification of neutrophils motility parameters

Velocity and net distance were automatically generated by Trackmate. For calculation of the other neutrophils motility parameter, Mean squared displacement (MSD) and cell speed we utilised DiPer, which is an Excel based program developed by (Gorelik and Gautreau, 2014). Briefly, MSD and cell speed were calculated as follow, the migration trajectory (Frame number, Position_X and Position_Y) previously generated using TrackMate were copied and pasted in DiPer excel file. To run the macros in order to compute cell migration parameters, Developer tab was clicked then Macros. From the list that will appear, MSD or Speed were selected.

Then Run were pressed and the displayed results were saved in excel with MSD or Speed graph automatically generated.

2.23. Statistical analysis

Statistical analysis was performed in GraphPad Prism as follows:

In Chapter 4 significance was calculated using Two-way ANOVA followed by Tukey's multiple comparisons test or Dunnett's multiple comparisons test. Parametric statistical tests were used because the number of repeats for the Fc chimericproteins binding to PA biofilms were too low (N=2-3) to assess normality, henece we assumed they followed a normal distribution. In addition the standard deviation was the same for each group. In all instances significance was calculated by comparing every mean with every other mean (Tukey's test). In only one condition as a result of high binding of DC-SIGN to clinical isolates the data was presented in a different graph and the binding mean of each Fc chimeric protein was compared to the mean of the control, thus the Dunnett test was applied.

In Chapter. 5 significance was calculated using One-way ANOVA followed by Tukey's multiple comparison test. Parametric statistical tests were used because the number of repeats for the Fc chimericproteins binding to PA biofilms were too low (N=7) to assess normality, henece we assumed they followed a normal distribution.

In Chapter. 6 significance was calculated using the Kruskal Willis test. A non-parametric statistical tests was used because the sample sizes were different and data were not normally distributed.

Chapter 3. Generation and Characterisation of *Pseudomonas aeruginosa* biofilms

3.1. Introduction

Biofilms are responsible for 80% of chronic microbial infection in humans (Römling and Balsalobre, 2012). In addition to the challenge of diagnosing biofilm infections, they are antibiotic resistances and capable of immune evasion, leading to high morbidity and mortality rates (Lynch and Robertson, 2008, Wolcott et al., 2010). These significant threats of biofilms have encouraged researchers to develop methods to study biofilms characteristic and host interaction. Several methods have been used to study biofilms, for the purpose of this thesis mainly two methods well be discussed below, (1) the microtiter plates (2) the continuous flow. In addition, other biofilm formation methods well discussed briefly. Moreover, highlight well be given on confocal microscopy as a biofilm studying tool.

(1) Commonly called the 96-well plate assay, the microtiter plates were originally used to assess *staphylococcus* adherences to plastic tissue culture plates (Christensen et al., 1985). The protocol published by Christensen et al. (1985) was then used to culture biofilm of many bacterial and fungal organisms with modification of growth times, media used, and ODs based on microorganism analysed (Genevaux et al., 1996, O'Toole, 2011, O'Toole and Kolter, 1998b). In brief, cells are cultivated for a certain period, and then the wells are washed to remove planktonic cells. Following, the remaining cells attached to the wells are stained with crystal violet (CV) that enables the attachment pattern to be visualised. The CV is then solubilised by ethanol and quantified by spectrophotometry to evaluate the formed biofilm. Studies have shown that motile bacteria, such as PA, *Escherichia coli* and *Vibrio cholera*, tend to aggregate at the top layer (the air-liquid interface) (Gomes et al., 2014). In contrast, non-motile cocci, such as enterococci (except for motile species *Enterococcus casseliflavus* and

Enterococcus gallinarum) and *staphylococci*, develop aggregates at the bottom layer of the microtiter plate (Frank et al., 2013, Liesse Iyamba et al., 2011).

Researchers mainly use the microtiter plate method because of its rapid, uncomplicated and reproducible results. However, there are several disadvantages to consider, such as the inability to generate highly mature biofilms due to nutrient reduction over incubation besides some clinical isolates reported to be poorly attached to the abiotic surface, thus unable to form biofilm (Magana et al., 2018, Azeredo et al., 2017). One of the most used techniques to assess biofilm formation on microtiter plates is the crystal violet (CV) assay, which facilitates visualisation of biofilm thickness and quantification of biofilm biomass. However, the technique is not appropriate for measuring the viability (Costerton et al., 1999, Stepanović et al., 2000). Besides, CV is not sensitive and highly variable; this might be due to the colour binds to negatively charged molecules unspecifically or is inaccurately extracted by ethanol (Magana et al., 2018, Azeredo et al., 2017).

Besides microtiter plates, there are other methods to form static biofilms, including, the Calgary biofilm device (CBD), which is a technique that enables the formation of biofilms on pegs attached to 96 wells plate lid (Ceri et al., 1999). The pegs lid is mounted in 96 wells plate with a standardised optical density of bacterial inoculum. The plate then placed at a rocking station to generate shear forces for a particular time and temperature. In this framework, biomass quantitation usually involves the retrieval of bacterial cells from pegs by sonification, which have some limitations. Only a fraction of the sessile population can be suspended through sonification, usually between 5% and 90% of the biofilms (Edmonds et al., 2009, Muller et al., 2011). Second, disruption caused by this process could modify the biofilms' properties exhibited on the pegs (Grand et al., 2011).

Another method widely used is the biofilm ring test, which is a tool to detect the formation of biofilms on modified 96-well plates using magnetic microbeads and a plate reader. When beads are dispersed after application of the magnet field, biofilm-associated adherence is

determined, and in contrast, beads are immobilised in the middle of the well in the presence of planktonic cells (Chavant et al., 2007).

(2) Continuous flow cultures allow mature biofilms to be formed in chambers connected to plastic tubes fitted with peristaltic or syringe pumps. The flow generated by the pump helps fresh growth medium to circulate while eliminating planktonic cells and waste (Magana et al., 2018). The biofilm formed can be monitored microscopically after injection of fluorescent proteins or reporter genes such as Green Fluorescent Protein (GFP) (Starek et al., 2011). The opportunity to analyse the effects that different media, oxygen concentrations, temperature changes, and substances exert on a biofilm at all developmental phases is one of the benefits of continuous-flow models (Azeredo et al., 2017, Magana et al., 2018). Such models also provide an evaluation of the effects of transient molecules, such as antibiotics or adhesion inhibitors, on biofilms (Azeredo et al., 2017, Magana et al., 2018). Biofilms are reported to exist in aqueous environments subjected to a shear force (Thomen et al., 2017, Hall-Stoodley et al., 2004). This might also be applicable in some clinical settings, for example in bacterial endocarditis it was speculated that the turbulent flow might promote biofilms formation as biofilm aggregates respond to the turbulent flow of the cardiac environment by producing more EPS (Donlan and Costerton, 2002). The technological drawbacks of continuous-flow biofilms, however, include increased experimental complexity, cost as well as potential air bubble trapping in the setup tubing (Crusz et al., 2012, Wolfaardt et al., 1994).

Several microscopic models have been utilised to study biofilm characteristic and have contributed to enrich our understating of microbial biofilms such as light, fluorescent, scanning and confocal microscopy. Here, for the purpose of this thesis, we give special attention to confocal laser scanning microscopy (CLSM). CLSM is a useful tool for the analysis of biofilms, and several laboratories have widely applied CLSM to the study of biofilms cultivated in flow chambers (Borlee et al., 2010, Tseng et al., 2013, Jennings et al., 2015, Colvin et al., 2012). This approach has several benefits, including that it is a reproducible format for biofilm culture, live biofilms can be imaged non-destructively at different times and three-dimensional details

about cell and matrix distribution can be obtained (Heydorn et al., 2000a). Antibodies and/or lectin-conjugated dyes can also be used for the characterisation and identification of the biofilm components. Furthermore, by using COMSAT, the image analysis software (Heydorn et al., 2000b) image acquired can be used to analyse the biofilm matrix and adherent biomass quantitatively, while location and specific amounts of matrix components can also be calculated (Neu et al., 2001, Berk et al., 2012). Furthermore, the gradual effects of various nutrient conditions or antimicrobial therapies can also be monitored (Tseng et al., 2013, Sønderholm et al., 2017).

As mentioned above, there are different tools to study biofilms that vary between each other. Thus, researchers need to assess which approach is better for each study based on the research questions and other different factors, including budget. As this study aimed to study PA biofilms and C-type lectin interaction, in this chapter and for the purpose of this study and to utilise in the following chapters we (1) confirmed and quantified biofilm formation by PA Δ*wspF* strains and clinical isolates on microtiter plates and (2) optimised PA biofilm formation on microscopy slides to better understand changes in biofilm structure.

3.2. Hypothesis

Generation of biofilms in substrates suitable for microscopic examination will provide a platform for accurate analysis of:

1. Biofilm structure (this chapter).
2. Distribution of ligands for immune lectin receptors (Chapter 4).
3. Immune cells-biofilm interactions (Chapters 5 and 6).

3.3. Aims

The specific aims for this chapter are:

1. Confirm and quantify biofilm formation by PA Δ*wspF* strains and clinical isolates on two types of microtiter plates using a defined eukaryotic media; these biofilms will be utilised to test binding of C-type lectins and incubation with innate immune cells (Chapters 4 and 5, respectively).

2. Optimise PA biofilm formation on microscopy slides to better understand changes in biofilm structure with time. These useful tools will be exploited to study biofilm-myeloid cells interactions (Chapters 4, 5 and 6).

3.4. Results

3.4.1. Validation of the PAO1 strains, Δ*wspF*, Δ*wspF*Δ*psl*, Δ*wspF*Δ*pel* and Δ*wspF*Δ*pel*Δ*psl*

Extracellular polymeric substances (EPS) are a key component of the biofilm matrix (Stoodley et al., 2002). The contribution of the carbohydrates components, Pel and Psl to mature biofilm structure vary among PA strains, and either one or both can serve as the primary biofilm matrix polysaccharide (Colvin et al., 2012). wspF controls c-di-GMP levels, and Δ*wspF* mutants have increased amounts of intracellular c-di-GMP, leading to enhanced biofilm formation (Hickman et al., 2005). Intracellular c-di-GMP controls expression of genes involved in the production of exopolysaccharides in PA; c-di-GMP upregulates the *pel* and *psl* operons (Hickman et al., 2005). The overarching aim of this study is to study the interaction of myeloid cells with PA biofilms and how it is affected by carbohydrate composition. Therefore, it was essential to employ different PA strains that vary in the expression of the biofilm-associated genes involved in the synthesis of Pel and Psl; Δ*wspF*, Δ*wspF*Δ*pel*, Δ*wspF*Δ*psl* and Δ*wspF*Δ*pel*Δ*psl* (Table 1). The generation of the *wspF* gene deletion in the PAO1 (WT) was described by (Hickman et al., 2005). The mutations of the biofilm-associated operons *pel* and *psl* in the Δ*wspF* background were characterised by (Starkey et al., 2009, Kirisits et al., 2005), respectively.

Mutations in *wspF* and the *pel* and *psl* biosynthesis pathways were analysed by PCR (Figure 3.1). Using primers that target *wspF* (Table 3), we confirmed the mutation in *wspF* in all the strains except PAO1 (WT). To validate the mutation in the *psl* operon, primers that target *pslC* and *pslD* were used. Results indicated the presence of the mutation in only two strains Δ*wspF*Δ*psl* and Δ*wspF*Δ*pel*Δ*psl*. Finally, the *pel* operon mutation was tested using primers that target *pelA*. The *pel* mutation was detected only in two strains Δ*wspF*Δ*pel* and Δ*wspF*Δ*pel*Δ*psl* (Figure 3.1).

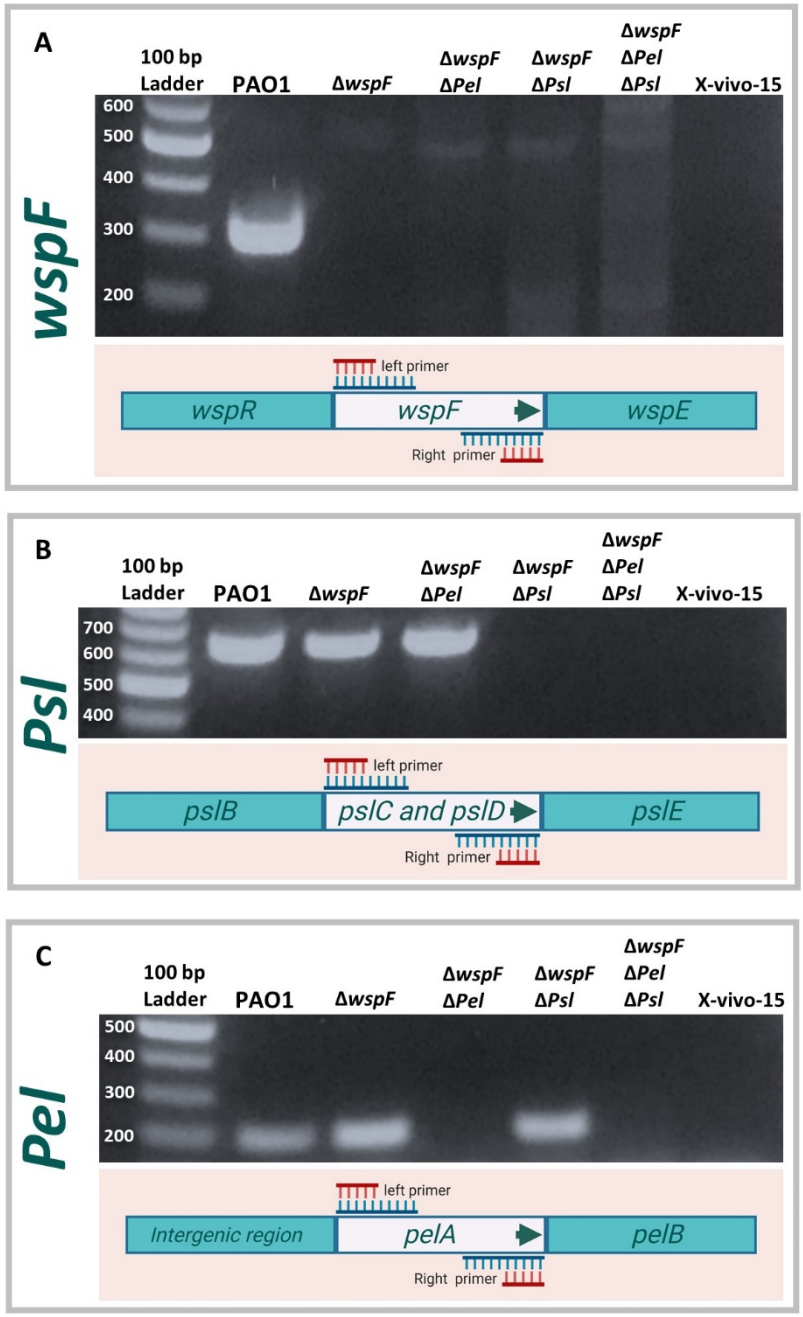


Figure 3.1 Confirmation of mutations in wspF and psl and/or pel operons using PCR.

PCR reactions were carried out in 25 µl reactions containing 1 µl of overnight culture, 0.1 µM of each of the reverse and forward primers, and 1X of GoTaq G2 green master mix in nuclease-free water. The amplification started with a denaturation cycle at 96 °C for 5 min, followed by 30 cycles of denaturation at 95 °C for 30 s, annealing at 55 °C for 30 s, and extension at 72 °C for 30 s. Then a new extension cycle at 72 °C for 5 min was performed. PCR products (10 µl) were loaded into 1% agarose gel containing 0.01% of Sybergreen safe stain in Tris-acetate-EDTA (TAE) buffer and electrophoresed for 60 min at 100 volts. A 100 bp marker was used. The figure shows representative images from 3 independent experiments.

3.4.2. Analysis of biofilm formation on 96 wells plates by PAO1, Δ*wspF* mutants and clinical isolates using the CV assay

Following PCR confirmation of their genetic mutation, the different Δ*wspF* strains were tested for their ability to form biofilms on 96 wells plates (MaxiSorp™) when incubated in X-Vivo-15, a serum-free cell culture media used in the laboratory for the proliferation of human myeloid cells. One of the main aims of this thesis is to explore the potential of C-type lectins to recognise PA biofilms. In order to assess the binding of C-type lectins to the biofilms using ELISA, it was necessary first to assess the ability of PA to form biofilm on 96 wells plates compatible with the ELISA (Martinez-Pomares et al., 2006). Biofilm formation was assessed by measuring biomass using the crystal violet assay. The diagram in (Figure 3.2A) summarises the basic steps of the assay performed as described in (2.3). Data shows that all the strains that express pel or/and psl displayed variable ability to form a biofilm. All Δ*wspF* strains produce more biofilms than PAO1 except the biofilm-deficient strain, Δ*wspF*Δ*pel*Δ*psl* (Figure 3.2B), confirming that the Δ*wspF* mutation led to higher biomass. The strains that overexpress Psl, Δ*wspF* and Δ*wspF*Δ*pel*, produced higher biofilm biomass than Δ*wspF*Δ*psl*, supporting the role of Psl as an essential component of the PA matrix (Figure 3.2B). This result confirmed the ability of all the strains to form biofilms on (MaxiSorp™) plates. The potential of C-type lectins to recognise PA biofilms will be tested in chapter 4 and 5.

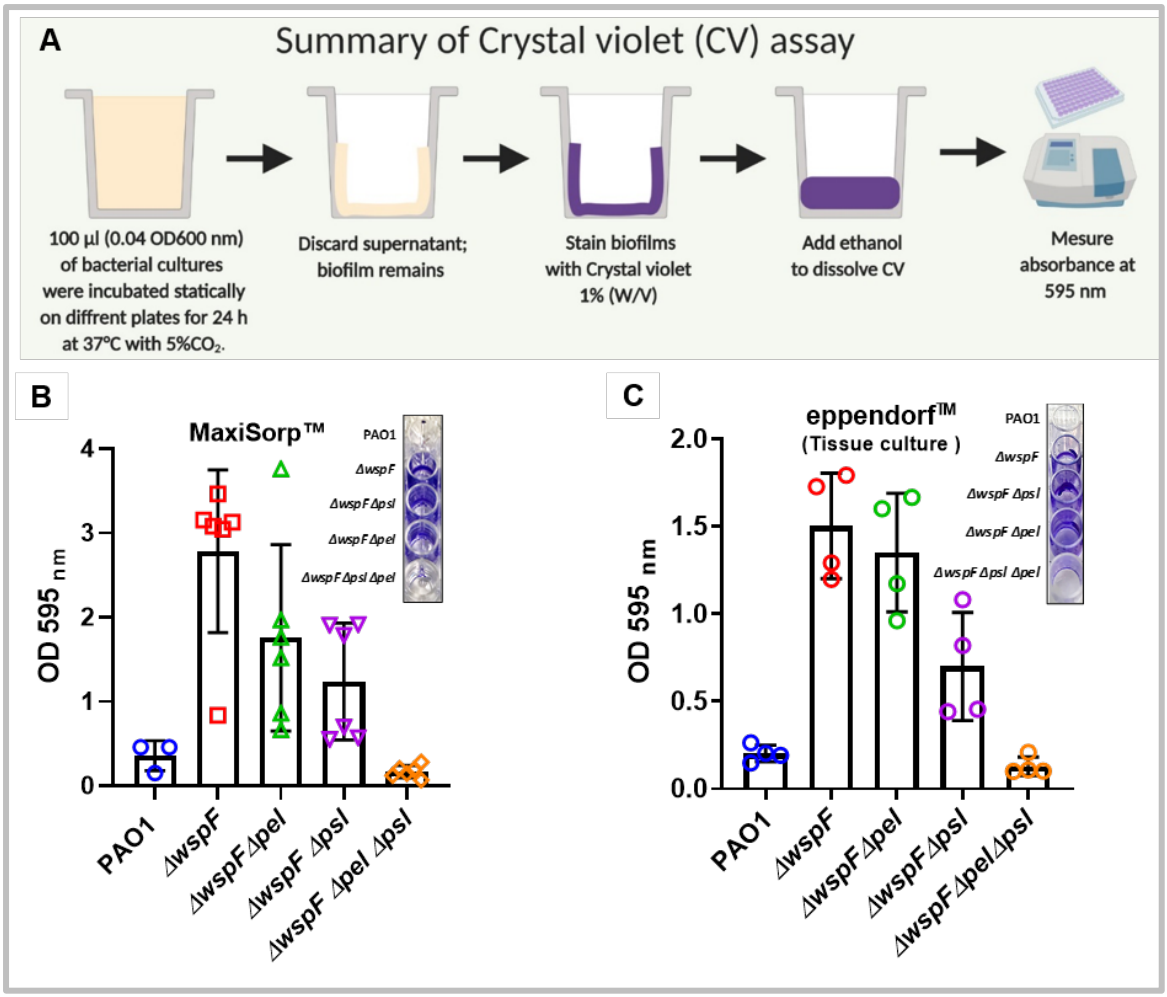


Figure 3.2 Measurement of biofilm formation of PAO1 and Δ*wspF* strains in X-vivo-15 media using the crystal violet method.

(A) Schematic representation of the crystal violet assay. Bacterial cultures in X-Vivo-15 with 0.04 OD_{600nm} were incubated statically on (B) MaxiSorp or (C) tissue culture-treated plates for 24 hr at 37°C with 5%CO_2. Non-adherent material was washed with HPLC water, and the amount of biofilm was quantified by staining with 1% crystal violet and measuring the absorbance at OD_{595nm} (A). Error bars indicate the standard deviation (SD) of at least three independent repeats with five technical replicates.

After testing the biofilm formation of Δ*wspF* mutant strains on MaxiSorp™, they were next tested for their capacity to form biofilm on tissue culture-treated plates. One of the main objectives of this project is to investigate the interaction of human monocyte-derived dendritic cells with PA biofilms to perform cytokine analysis. Thus, it was essential to form biofilms on plates where we can add human cells. Using the crystal violet assay, a similar pattern as that found in MaxiSorp™ was observed in tissue culture-treated plastic, although biofilm biomass was lower (Figure 3.2 C). Clinical isolates from a patient suffering from a chronic wound (Table 2) were also tested in this assay and showed differential ability for biofilm formation with bone isolates (B) displaying increased biomass compared to tissue (T) and blood isolates (S) (Figure 3.3).

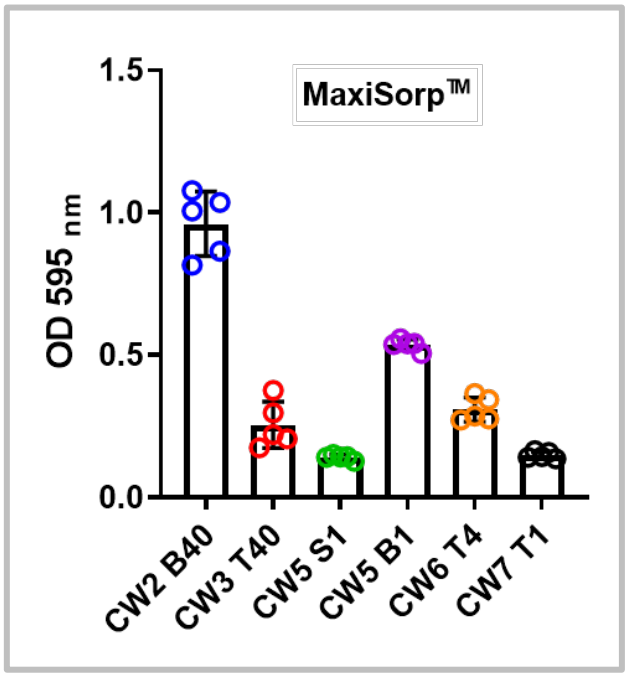


Figure 3.3 Biofilm formation of PA clinical isolates in X-vivo-15 media using the crystal violet method.

Bacterial cultures in X-vivo-15 with 0.04 OD_{600nm} were incubated statically on MaxiSorp for 24 h at 37°C, 5%CO_2. Non-adherent material was washed with HPLC water, and the amount of biofilm was quantified by staining with 1% crystal violet and measuring the absorbance at OD_{595nm}. Error bars indicate the standard deviation (SD) of five independent repeats with five technical replicates.

3.4.3. Visualisation of biofilm formation using confocal microscopy

Biofilms are multidimensional communities in which bacteria is covered by a self-derived extracellular matrix (Borlee et al., 2010, Costerton et al., 1999). With the aim of utilising microscopy to study the interaction of myeloid cells and PA biofilms in our lab, we tested different techniques to develop biofilms in a reproducible manner on microscopic slides. The goal was for these biofilms to mimic as much as possible the shape and the size of biofilms found chronic infection.

3.4.3.1. Biofilm formation in cell view slide

In the previous section 3.4.2), it was demonstrated that PA from different mutant strains were able to form biofilms on 96 wells plates using X-Vivo-15. In order to visualise the biofilms under confocal microscopy, it was essential to first test biofilm formation on an appropriate slide compatible with confocal microscopy. For this, PA biofilms were generated in CELLview™ cell culture slides using the same protocol as 96 wells plate summarised in (Figure 3.4 A) and crystal violet staining was performed to measure biofilm biomass as described (2.3). Results from biofilms generated in this system for 24 hr showed that, as above, all Δ*wspF* strains produce more biofilm biomass than PAO1 except the biofilm-deficient strain, Δ*wspF* Δ*pel* Δ*psl* (Figure 3.4 B). These results indicate that PA, particularly strains lacking *wspF* that express Pel and/or Psl form biofilms on CELLview™ slides (Figure 3.4 B).

To visualise PA biofilms generated on CELLview™ cell culture slides, biofilms were stained with three labels; rabbit anti-PA and goat anti-rabbit antibody conjugated to Alexa Fluor488 to label bacterial cells (green) and DAPI to label extracellular DNA (blue) (Figure 3.4 C). Biofilms formation (green) extracellular DNA (Blue) were observed on all tested strains (Figure 3.4 C) except for the biofilm deficient strains Δ*wspf*Δ*pel*Δ*psl* (data not shown). Confocal images showed formation of biofilms by Δ*wspf* with formation of microcolonies all around the field (Figure 3.4 C, upper row). Images of Δ*wspf*Δ*psl* and Δ*wspf*Δ*pel* showed biofilm formation (Figure 3.4 C, middle and last row, respectively) although larger bacterial aggregates were

observed in Δ*wspf*Δ*pel* as bacterial cells seemed to gather and concentrate in two specific locations. Furthermore, the rest of the bacterial cells seemed to be directed towards these two locations to join in the underdevelopment biofilms (Figure 3.4 C, last row). Interestingly, this behaviour was not detected in Δ*wspf*Δ*psl* as this strain displayed formation of small and scattered microcolonies (Figure 3.4 C, middle row). Large quantities of eDNA were observed in biofilms formed by Δ*wspf* and Δ*wspf*Δ*pel* with most eDNA accumulated within biofilms. In contrast, in Δ*wspf*Δ*psl* cultures, scattered eDNA was distributed all around the field (Figure 3.4.C). This result represents the first time we observed how Δ*wspf* mutants organise themselves during biofilm formation.

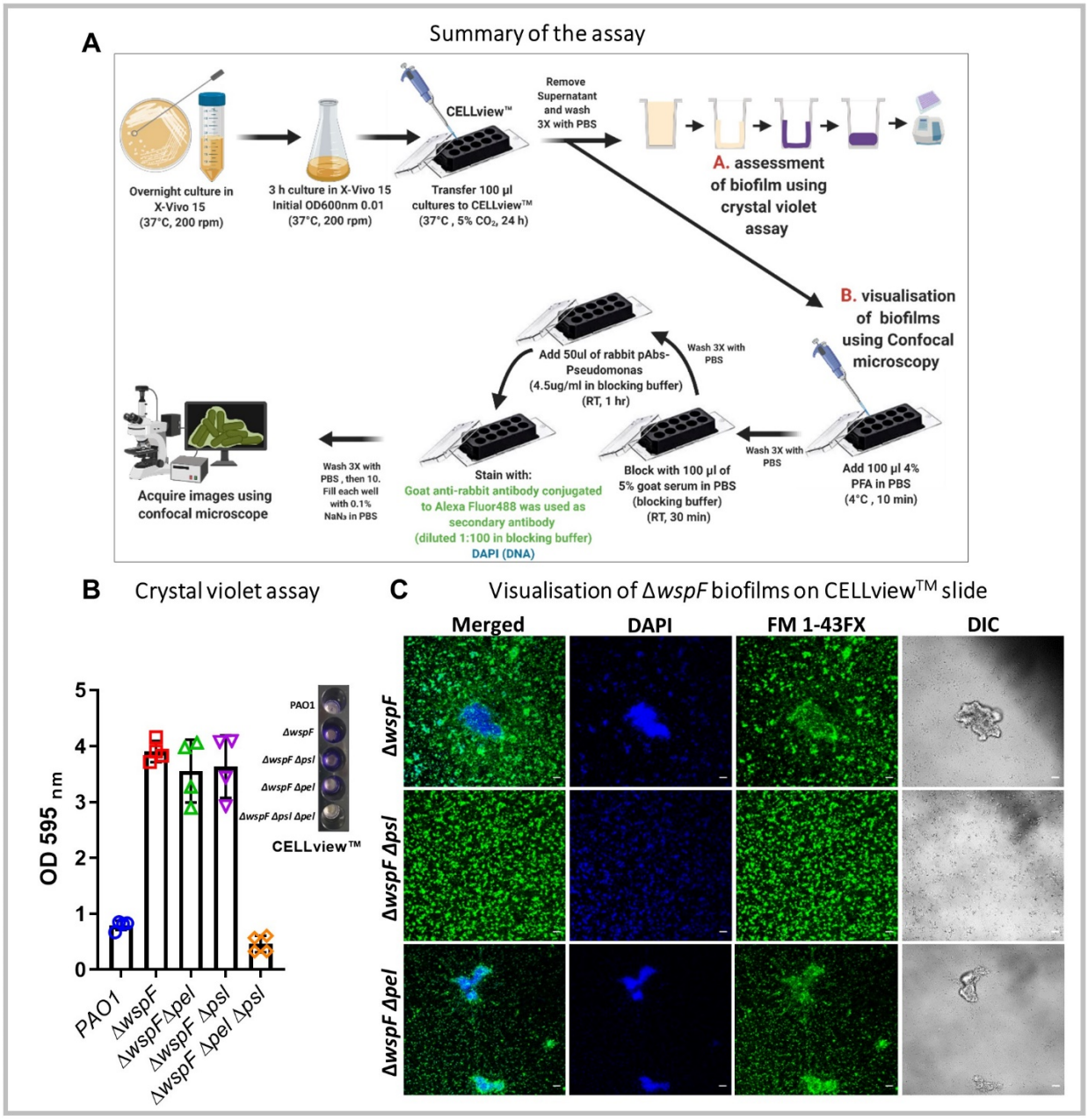


Figure 3.4 Visualisation of biofilm formation of Δ*wspF* strains using confocal microscopy.
Bacteria were grown on CELLview™ Slides for 24 hr at 37°C, 5% CO_2, as shown above (A). Following incubation, biofilms were either stained with crystal violet to assess biomass (B) or fixed with 4% PFA in PBS for visualisation using confocal microscopy (C). Biofilm was dual labelled with (green) rabbit anti-PA and goat anti-rabbit conjugated to Alexa Fluor 488 and (blue) DNA stain, DAPI. Z-stack combined images were taken using a Zeiss 710 confocal microscope, water x40 objective. Alexa Fluor 488 (green) was detected using excitation at 488 nm. Nucleic acid staining was revealed using excitation at 561 nm. Images were processed using Fiji (Schindelin et al., 2012). Images are representative of a single experiment.

3.4.3.2. Biofilm formation in ibidi µ-Slide VI 0.4

After testing biofilm formation on Cell view slides, a major disadvantage was observed. Specifically leaking from wells was noticed, and this would affect the future assays such as labelling for ligands for different lectins and cultures with immune cells in the same slide. Besides the Cell view slides did not provide us with the possibility of developing biofilms under flow conditions. Thus, it was decided to search for a system that supported biofilm formation without the risk of leaking and where the wells could be subjected to flow. Based on these requirements, ibidi µ-Slide VI 0.4. was selected. In the first instance, slides with different coatings were tested in the absence of flow for PA biofilm formation. Three options were tested: uncoated, tissue culture (TC)-treated and collagen-coated. Briefly, mid-log phase cultures in X-Vivo-15 medium (Lonza) were diluted to OD_{600nm} 0.04 and used to inoculate (30 µl per channel) and incubated statically at 37°C / 5% CO_2 for 24 hr. After culture, supernatants were collected, biofilms fixed with 100 µl of 4% paraformaldehyde in PBS for 10 min at 4°C. After fixation, biofilms were washed gently 3 times with 120 µl of PBS. DNA was labelled with DAPI (2 µg/ml, 15 min, RT). After incubations slides were washed gently 3X with 120 µl of PBS, mounted using ibidi mounting medium and examined binding under confocal microscopy LSM710, 40X oil. Images were processed using Fiji (Schindelin et al., 2012), and biofilm parameters were quantified using Comstat (Heydorn et al., 2000b). Preliminary results indicated that Δ*wspF* could form biofilms on µ-Slide VI 0.4 slides with higher biofilm formation observed on TC-treated slides compared to the uncoated and collagen-coated surfaces (Figure 3.5).

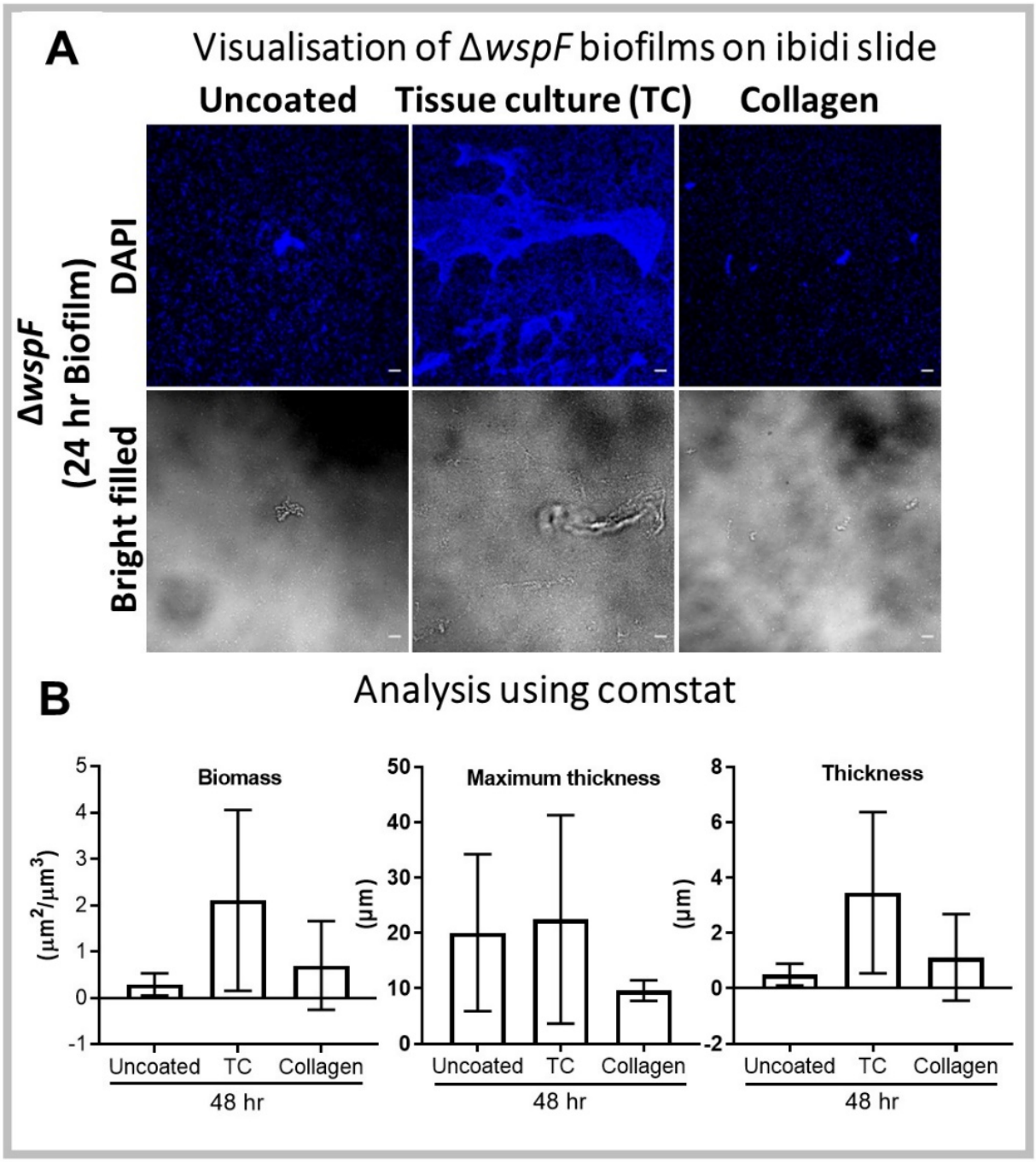


Figure 3.5 Comparison between three coating plates.

(A) Representative images of Δ*wspF* biofilms cultured statically for 24 hr on three different μ-Slide VI 0.4 plates (uncoated, tissue culture treated and collagen). (B) Preliminary results indicated higher biofilm observed on TC-treated slides compared to the uncoated and collagen-coated surfaces. Results represent images from one repeat; three images of each condition from one single expermint were analysed using comstat (Heydorn et al., 2000b).

3.4.3.3. Generation of Δ*wspF* biofilms in ibidi µ-Slide VI 0.4 under flow conditions, generated using a peristaltic pump

Continuous-flow cultures enable the formation of mature biofilms in chambers covered with coverslips or latex tubes fitted to a device that controls the flow rate such as a peristaltic or syringe pump. The pump facilitates the flow of fresh growth medium, whereas planktonic cells and waste are removed. In an attempt to improve biofilm formation in ibidi µ-Slide VI 0.4 slides bacteria were exposed to shear stress using a peristaltic pump. Results indicated higher biofilm formation even with shorter incubation time (Figure 3.6).

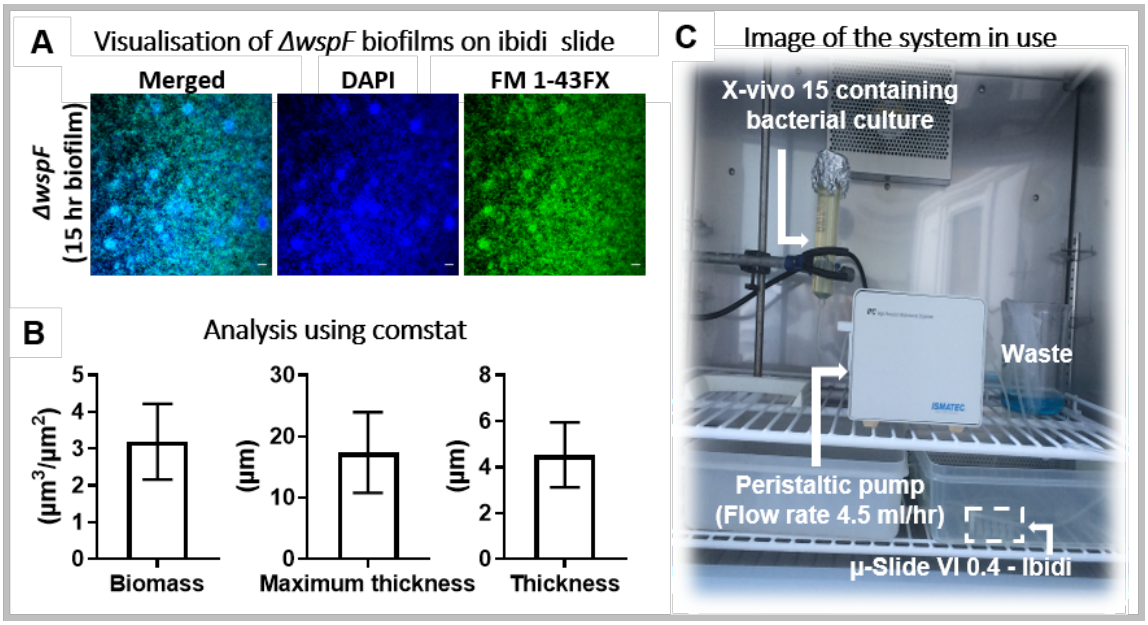


Figure 3.6 Biofilm formation by Δ*wspF* in ibidi µ-Slide VI 0.4 slides under flow conditions generated with a peristaltic pump.

Mid-log phase cultures in X-Vivo-15 medium were diluted to OD_{600nm} 0.04 and used to inoculate µ-Slide VI 0.4 channels (30 µl per channel, Ibidi, tissue culture treated) and incubated at 37 °C for 1 hr. Slides were fitted into the syringe pump system, and exposed to flow (4.5 ml/hr, bacteria culture in X-Vivo-15, 15 hr) at 37 °C. After culture, supernatants were collected, biofilms fixed with 100 µl of 4% paraformaldehyde in PBS for 10 min at 4 °C. After fixation, biofilms were washed gently 3 times with 120 µl of PBS. Membranes were labelled with FM™ 1-43 (5 µg/ml, 15 min, on Ice) and DNA with DAPI (2 µg/ml, 15 min, RT). After incubations slides were washed gently 3X with 120 µl of PBS, mounted using ibidi mounting medium and examined binding under confocal microscopy LSM880C, 40X oil. Images were processed using Volocity, and biofilm parameters were quantified using Comstat five images from one single expermint were analysed (Heydorn et al., 2000b).

3.4.3.4. Optimisation of biofilms formation in ibidi µ-Slide VI 0.4 under flow conditions, generated using a syringe pump

Although the peristaltic pump was suitable to generate flow that supported biofilm formation, the system was not considered optimal because it was difficult to control the flow rate and sterility. Therefore, we choose to apply a syringe pump flow system, which allowed for full control of flow rate and maintenance of sterile conditions. Among the advantages of the syringe pump system is the ability to compare the effects of different media, CO_2 concentrations, incubation time and flow rate on a biofilm at all developmental phases. Different experiments were conducted using the syringe pump system to select the best flow rate and incubation time for the bacteria to form biofilm evenly on the surface of µ-Slide VI 0.4 slides. First, three flow rates were compared [0.8, 1.6 and 3.2 ml/hr]. Results indicated that the best flow rate that maintains sufficient shear stress on the bacteria without affecting the structure of the biofilm is 1.6 ml/hr (data not shown). Second, we compared the effect of flowing media, which contain bacterial culture versus flowing fresh media. Results showed that flowing of fresh X-Vivo-15 media after initial bacterial attachment instead of bacteria cultures enhanced the biofilm biomass (data not shown). Third, because the syringe system is closed, we tested the effect of pre-gassing X-Vivo 15 prior use for 48 hr at 37 °C/5% CO_2 as described in (Figure 3.7). Results indicated that biofilm formed by PAO1 was increased after the use of the pre-gassing media (data not shown). Finally, to minimise biofilm biomass variability among repeats confocal microscopy images were taken from the area of homogeneous shear stress (Figure 3.8 C).

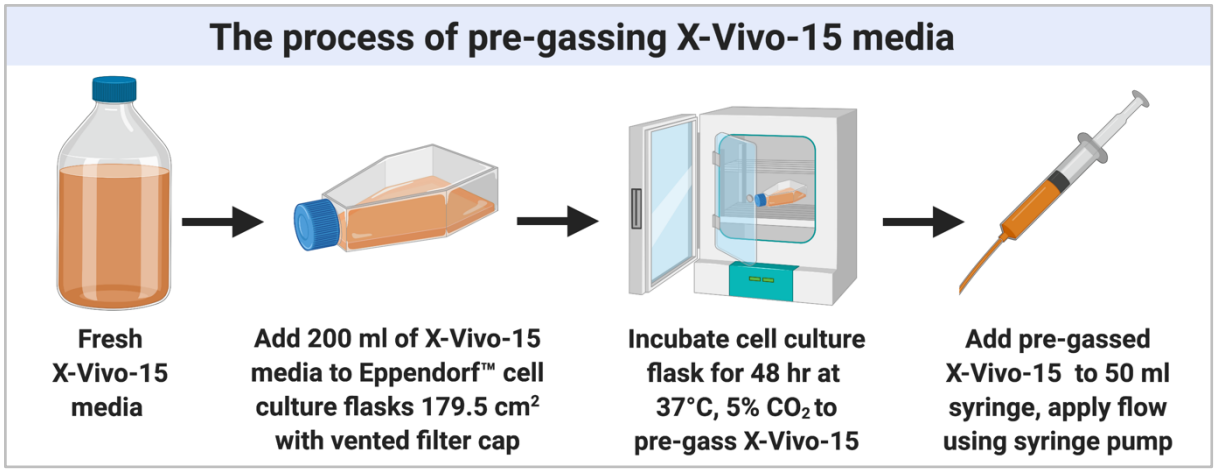


Figure 3.7 Process for pre-gassing of X-Vivo-15 media.

200 ml of X-Vivo-15 media was transferred to 1 L tissue culture vented flask (T175) with 179.5 cm^2 growth area and incubated at 37 °C/5% CO_2 for 48 hr. Media was then transferred to a 50 ml syringe pump before use. Created with BioRender.com.

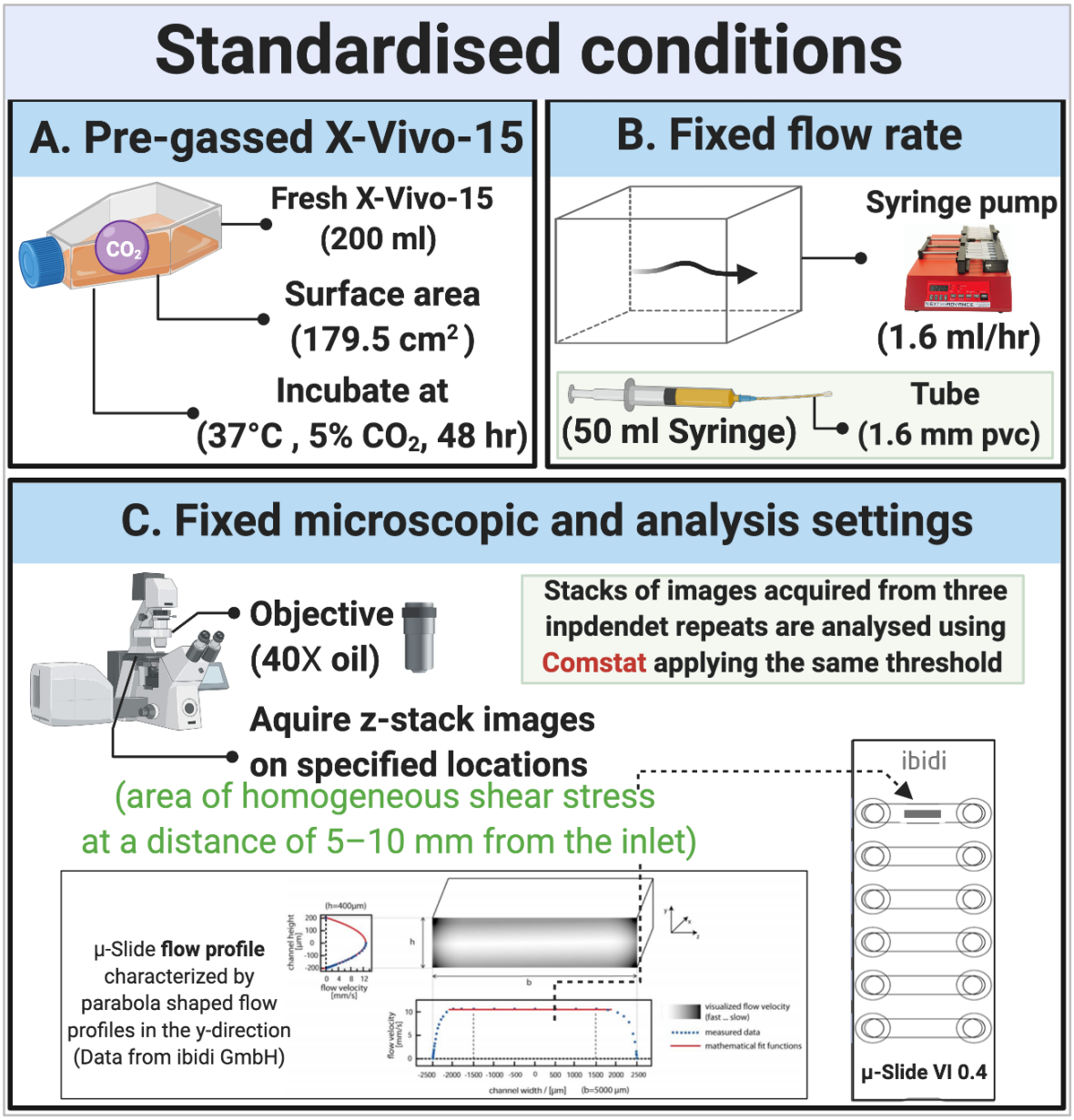


Figure 3.8 Standardised conditions applied to generate biofilms using a syringe pump system. 1) media was pre-gassed for 48 hr. 2) Pre-gassed media was transferred to 50 ml syringe connected with 1.6 mm PVC tube and placed on the syringe pump with a fixed flow rate at 1.6 ml per hr. 3) images were taken using 40x oil objective at the area of homogeneous shear stress to minimise variability among repeats (arrow pointed). Created with BioRender.com.

3.4.3.5. Generation and analysis of PAO1 biofilms in ibidi µ-Slide VI 0.4 under standardised flow conditions using a syringe pump

Confocal laser scanning microscopy has been used extensively in the field to study biofilms cultured under continuous flow (Borlee et al., 2010, Tseng et al., 2013, Jennings et al., 2015, Colvin et al., 2012). In our lab, the aim was to utilise this method to better understand the interaction of biofilms with myeloid cells. According to work presented in previous sections to optimise and grow biofilms under flow, the best conditions to grow PAO1 biofilms utilising the syringe pump system were (1) 1.6 ml/hr flow rate, (2) pre-gassed X-Vivo-15 (Figure 3.8). These conditions were applied in all assay afterwards as summarised in the (Figure 3.9).

It is important to clarify that we were not able to calculate the shear stress reported as (dynes/cm2). This is because we were not able to identify the viscosity of X-Vivo-15 either by direct communication with the manufacturer or by having access to a viscometer. Therefor, all data presented in this thesis shows the flow rate (volume/time) that the cultures were exposed to. To calculate the shear stress in µ-Slide VI 0.4 we can use the following formula:

Shear stress (dyn/cm2) = Dynamical viscosity (dyn s/cm2) X 176.1 (Factor dependent on the slide used and provided by ibidi) x Flow rate (0.0266 ml/min).

For example, if we assume that the Dynamical viscosity $^{(dyn\ s/cm2)}$ of X-vivo-15 is the same as water in 37°C the shear stress is = 0.0068 x 176.1 x 0.0266 = 0.0319 (dyn/cm^2).

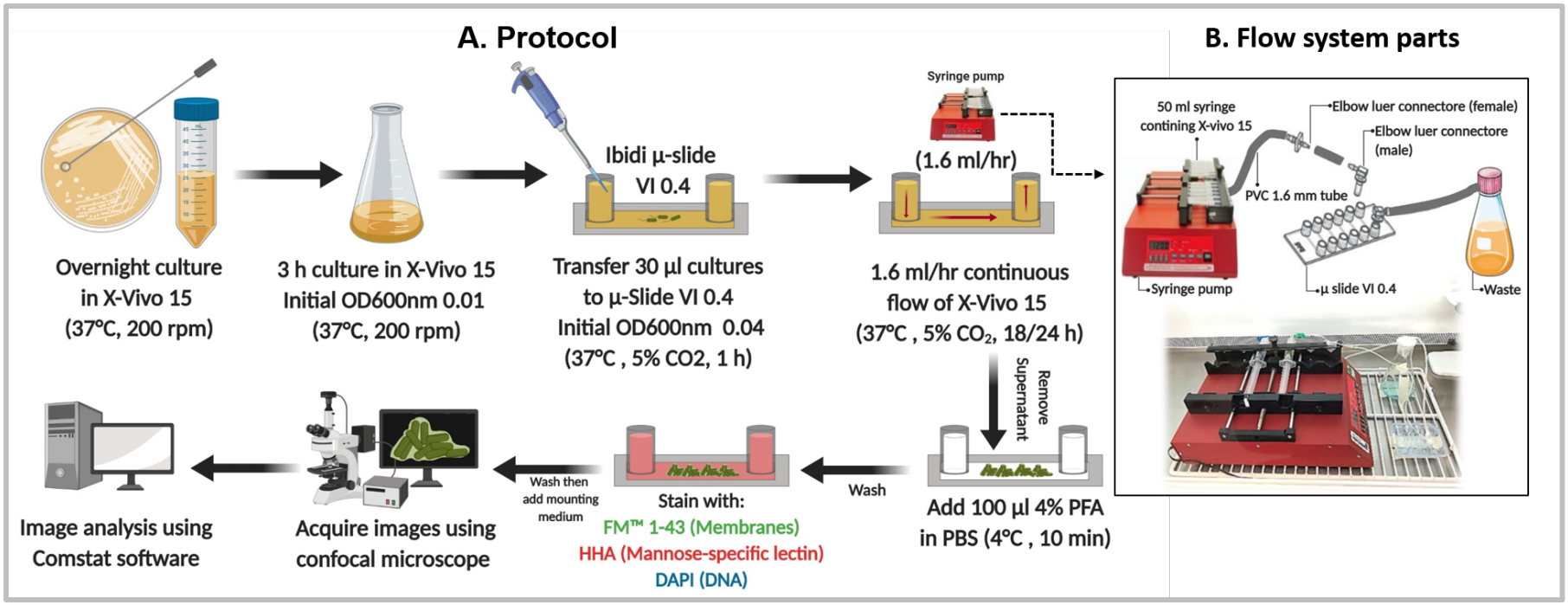


Figure 3.9 Generation of PAO1 biofilms under standardised flow conditions.

(A) Mid-log phase cultures in X-Vivo 15 medium (Lonza, pre-gassed for 48 hr at 37°C / 5% CO_2) were diluted to OD_{600nm} 0.04 and used to inoculate µ-Slide VI 0.4 channels (30 µl per channel, Ibidi, tissue culture treated) and incubated at 37 °C for 1 hr. Slides were fitted into the syringe pump system (B), and exposed to flow (1.6 ml/h, pre-gassed X-Vivo-15, 18 or 24 hr) at 37 °C, 5% CO_2. After culture, supernatants were collected, biofilms fixed with 100 µl of 4% paraformaldehyde in PBS for 10 min at 4 °C. After fixation, biofilms were washed gently 3 times with 120 µl of PBS. Mannose-rich carbohydrate were labelled with HHA-conjugated to Texas red (100 µg/ml). Membranes were labelled with FM™ 1-43 Fx (5 µg/ml, 15 min, on Ice) and DNA with DAPI (2 µg/ml, 15 min, RT). After incubations, slides were washed gently 3X with 120 µl of PBS, filled using ibidi mounting medium and examined using confocal microscopy, 40X oil. Images were processed using Volocity or Fiji, and biofilm parameters were quantified using Comstat. Diagram designed using Biorender.

3.4.3.6. Analysis of PAO1 biofilm formation in ibidi µ-Slide VI 0.4 using the standardised conditions confirms the reproducibility of the culture system

To study how PAO1 biofilms affect immune cells, it was considered essential to test the reproducibility of the optimised culture system. Therefore, biofilms generated as described above were fixed and stained for three components, HHA-Texas Red was used to label mannose-rich carbohydrate (likely Psl). This lectin was shown to be specific for Psl in a previous study (Ma et al., 2007). The bacterial cells were counterstained with the membrane stain FM 1-43 Fx, while eDNA was stained with DAPI. Five representative images from three independent experiments were taken from area of homogeneous shear stress as described in (Figure 3.8) and analysed using Comstat. PAO1 biofilms grown in µ-Slides VI 0.4 displayed increased biomass, carbohydrate and DNA at 24 hr compared to 18 hr (Figure 3.10). Biofilms cultured for 24 hr showed almost complete coverage of the slides with high cellular density (Figure 3.10 A). At 18 hr, PAO1 formed numerous cellular aggregates with numerous bacteria-free spaces (Figure 3.10 A) which would be consistent with increased roughness (Figure 3.10 B). All three labels co-localised on areas of high cellular density and increased to a similar degree at 24 hr compared to 18 hr (Figure 3.10).

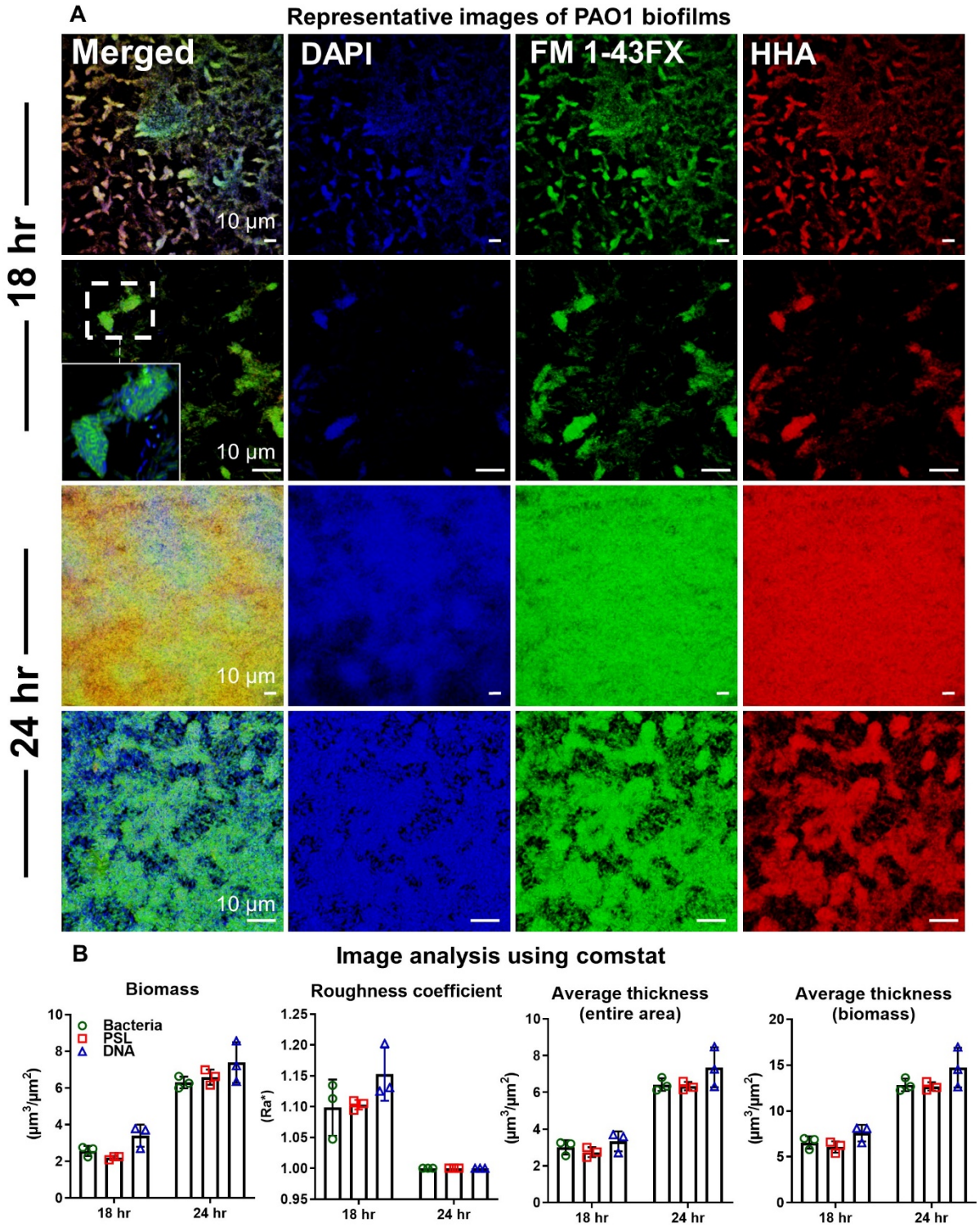


Figure 3.10 Biofilms characteristics after 18 and 24 hr culture.

(A) Representative images of PA biofilms cultured for 18 or 24 hr under flow. (B) Thickness and biomass increased at 24 hr culture compared to 18 hr when assessing membrane, carbohydrate (HHA/Psl) or DNA labelling. With additional incubation roughness coefficient diminished slightly. Results represent images from three independent repeats, five images of each repeat were analysed using comstat (Heydorn et al., 2000b).(Ra= Roughness average of the surface).

One of the main advantages of confocal microscopy is that it can be used to localise the matrix components of the biofilms 3D structure (Swerhone et al., 2001; Berk et al., 2012). Although it is acknowledged that mushroom-shaped biofilms are an unlikely feature of biofilms *in vivo*, the few mushroom-like structures seen on PAO1 biofilms provided us with the opportunity to test the specificity of the different labels. Hence in slides stained for bacteria with FM 1-43 Fx, for carbohydrate with HHA and DNA with DAPI, we could observe eDNA forming the base of the structure (arrow B), while Psl was found on the periphery of the mushroom-shaped biofilms and seemed to support the structure (arrow A) (Figure 3.11).

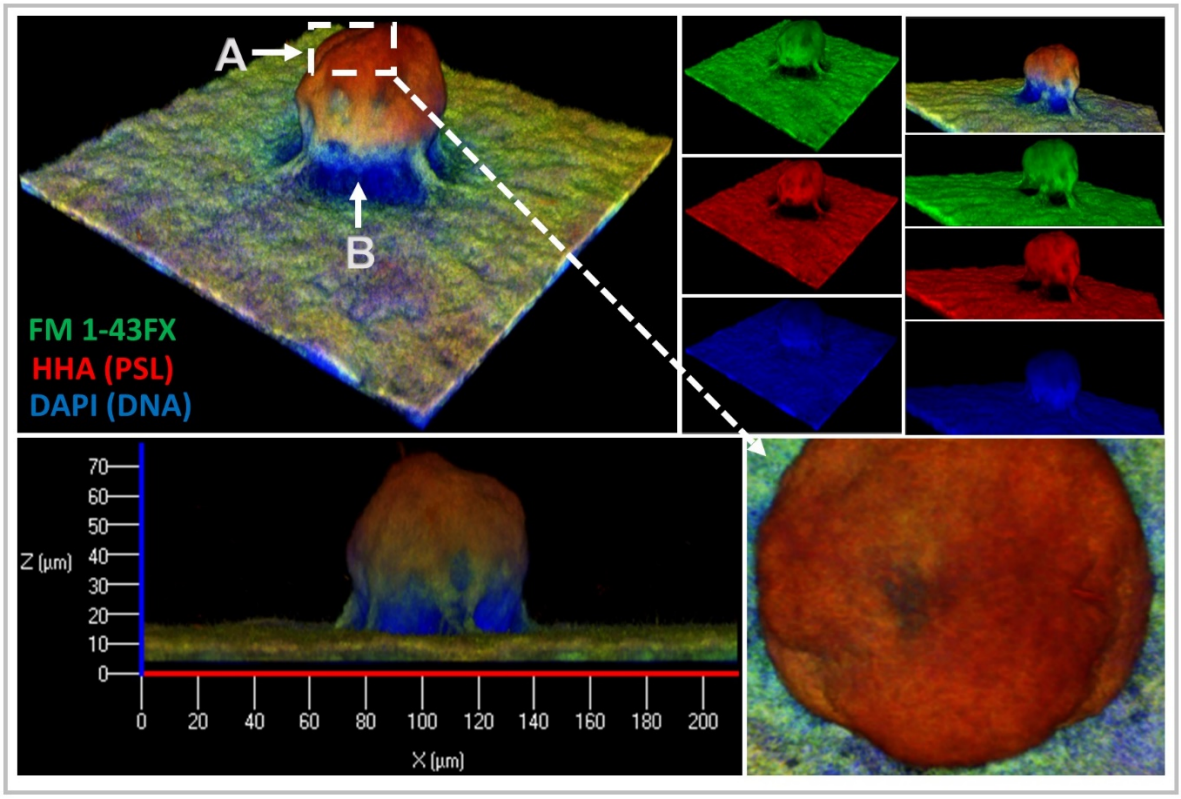


Figure 3.11 Analysis of biofilm components in mushroom-shaped structures within PAO1 biofilms.

PAO1 biofilms were generated as described above, and Psl was stained using HHA (red). The bacterial cells were counterstained with the membrane stain FM 1-43 Fx (green), while DNA was stained with DAPI. Figure shows one representative image of three independent analysis of these structures.

3.5. Summary

To summarise data presented in this chapter:

- PCR analysis confirmed mutation of Δ*wspF*, Δ*wspF*Δ*psl*, Δ*wspF*Δ*pel* and Δ*wspF*Δ*pel*Δ*psl.*
- PAO1, Δ*wspF* mutants and clinical isolates were tested for biofilm formation on (MaxiSorp™) plates:
    - PAO1, Δ*wspF*, Δ*wspF*Δ*pel*, Δ*wspF*Δ*psl* but not Δ*wspF*Δ*pel*Δ*pel* were able to form biofilms on (MaxiSorp™) plates, supporting that, without at least (Pel and/or Psl) PA cannot form biofilms (Figure 3.2 B).
    - All clinical isolates tested exhibited the ability to form biofilms on (MaxiSorp™) with different biomass (Figure 3.3).
- PAO1, Δ*wspF* mutants were tested for biofilm formation on tissue culture-treated plates:
    - Data showed a similar pattern as observed with (MaxiSorp™), though with lower biofilms biomass (Figure 3.2 C).
- PAO1 biofilm was optimised to generate biofilms under flow condition in ibidi µ-Slide VI 0.4. After several optimisation experiments summarised in the schematic (Figure 3.12) data (Figure 3.10) revealed that the best biofilm generation conditions are as follows:
    - (1) ibidi µ-Slide VI 0.4 tissue culture coated (Figure 3.5)
    - (2) Flow rate 1.6 ml/hr using a syringe pump
    - (3) Media: X-Vivo 15 pre-gassed 48 hr as described (Figure 3.7).
- These fixed measures mentioned above were applied to form PAO1 biofilm, data indicated increased biofilms structure by incubation time and reproducible results (Figure 3.10).

- This useful tool could be used to study biofilms components such as Psl and eDNA (Figure 3.11) and will be exploited to study biofilm-myeloid cells interactions (Chapters 4, 5 and 6).

3.6. Discussion:

Biofilms are multicellular communities of microorganisms in which the cells are adherent to each other and/or to a surface or interface; these cells are enclosed in a self-produced EPS (Borlee et al., 2010). Biofilm formation is a multi-stage process initiated by planktonic cells reversible and irreversible attachment to the surface followed by EPS creation and generation of mature biofilm, that ends with the dispersal and release of planktonic bacteria from the mature biofilm to colonies a new location or retain the planktonic mode of growth (Klapper et al., 2002). The main aim of this project is to investigate the interaction between PA and innate immune cells and how it is affected by biofilm formation. As this study investigates innate immune cells and biofilm interaction mainly through CLRs-EPS recognition, we employed different PAO1 strains that express either Psl and/or Pel to test whether CLRs bind PA biofilms and display selective bindings to EPS components. As mentioned earlier, strains employed in this study express the same high levels of c-di-GMP, resulted from the mutation of *wspF (Borlee et al., 2010)*. The high levels of c-di-GMP stimulate the expression of EPS and correlate with the tendency of bacteria to form biofilms (Hengge, 2009).

Confirmation of the genetic mutations in the strains utilised in this research prior the establishment of the study was considered a good starting point to ensure that the PAO1 strains used correctly possess the *wspF* and/or *psl* and *pel* mutations. Thus, we confirmed the genetic mutation in all strains employed (Figure 3.1). We also confirmed and quantified biofilm formation by PA Δ*wspF* strains (Figure 3.2) and clinical isolates (Figure 3.3) on microtiter plates to be used for testing binding of CLRs (Chapter 4) and incubation with innate immune cells in (Chapter 5). We also optimised a procedure to generate and analyse PA biofilms on microscopy slides (Figure 3.9, Figure 3.10) to better understand biofilm structure and study biofilm-myeloid cells interactions (see Chapters 4, 5 and 6). This chapter discussion will focus mainly on (1) the use of the defined serum-free medium X-Vivo-15 and (2) biofilm formation using the syringe pump system which are unique aspects of the biofilms developed in our lab.

3.6.1. The use of X-Vivo-15:

Researchers have been using multiple types of bacteriological or synthetic media supplemented with different nutrients or growth factors to study PA biofilms *in vitro* (Reichhardt and Parsek, 2019). To establish PA biofilms in a media suitable for the assessment of immune cell responses, we generated PA biofilms in X-Vivo-15. This media is generally used for the generation and proliferation of eukaryotic cells but not for prokaryotic cells (Bethke et al., 2002, Dasgupta et al., 2007, Earle et al., 2005). X-Vivo-15 was extensively used by previous members of our laboratory group to study innate immune cells interaction with PA. It was indicated that this medium supports the growth of PA and the bacterium capability to express quorum sensing molecules and virulence factors (Singh et al., 2015). Tamanna Rhamman, and Mohammad Y. Alshahrani (PhD thesis) established the optimisation of PA biofilm formation in X-Vivo-15 and found that this medium supports the formation of PA biofilms (Alshahrani, 2018, Rahman, 2016). Likewise, measurements of the biofilm biomass of PAO1, *wspF* mutant strains and clinical isolates after staining with CV dye and quantifying the absorbance of bound dye re-confirmed the capability of PA to form biofilms in X-Vivo-15 (Figure 3.2 Figure 3.3). Furthermore, confocal microscopy analyses, performed following 18 and 24 hr of incubation of PA in such medium, clearly demonstrated the presence of biofilm structure (Figure 3.10).

Although the composition of X-Vivo-15 is not available, email communication with the manufacturing company (Lonza) confirmed lack of mannose structures in X-Vivo-15. This was essential to make sure that no components in the media can elicit an immune response or alter the CLRs-biofilm binding assays conducted in Chapters 4, 5 and 6. Our lab has previously compared the growth of PAO1 in X-Vivo-15 medium to LB broth. Data revealed similar values of log phase and stationary phase optical density in both media (Singh et al., 2015). However, the LB broth contains yeast extract that could activate the immune cells and affect the assays; this was the main reason to favour X-Vivo-15 over the LB broth. The growth media TSB is widely used to generate PA biofilms (Colvin et al., 2012, Powell et al., 2018). Nevertheless, it

was found that TSB did not support macrophage growth and induced cell death (Hanke and Kielian, 2012). On the other hand, media that support innate immune cells generation and differentiation, such as RPMI 1640 medium were found not to support PA adhesion and planktonic growth (Wijesinghe et al., 2019). Therefore, the use of X-Vivo-15 was considered appropriate for this study.

3.6.2. Biofilm formation using the syringe pump system

As mentioned in the introduction, the significant threats represented by biofilms have encouraged researchers to develop several methods to study biofilms characteristics and interactions with the host. In this study, in addition to the confirmation of biofilm formation statically on 96 well plates, we optimised a system to generate biofilms under flow conditions in microscopy slides, ibidi µ-Slide VI 0.4. The main aim for developing this model was to better understand changes in biofilm structure in X-Vivo-15 with time, and utilise this useful tool to study biofilm-myeloid cells interactions (Chapters 4, 5 and 6). Additionally, it had been suggested previously that culturing PA CF isolates under shear stress induced the expression of phenotypic and molecular genetic traits in PA similar to those observed *in vivo* (Dingemans et al., 2016). Several optimisation experiments were conducted (summarised in the schematic (Figure 3.12)) which concluded that the best biofilm generation conditions among all tested were: (1) PA culture inoculated in tissue culture coated slide and subjected to (2) continuous flow (1.6 ml/hr) of (3) pre-gassed X-Vivo-15 [48 hr prior usage as described in (Figure 3.7)]. The flow of pre-gassed X-Vivo-15 was controlled using a syringe pump which has been preferred over the use of a peristaltic pump because it allows better flow control in a sterile environment. We compared three flow rates, 0.8, 1.6 and 3.2 ml/hr with the aim to select the flow rate that maintains sufficient shear stress on the bacteria without affecting the structure of the biofilm and 1.6 ml/hr was selected.

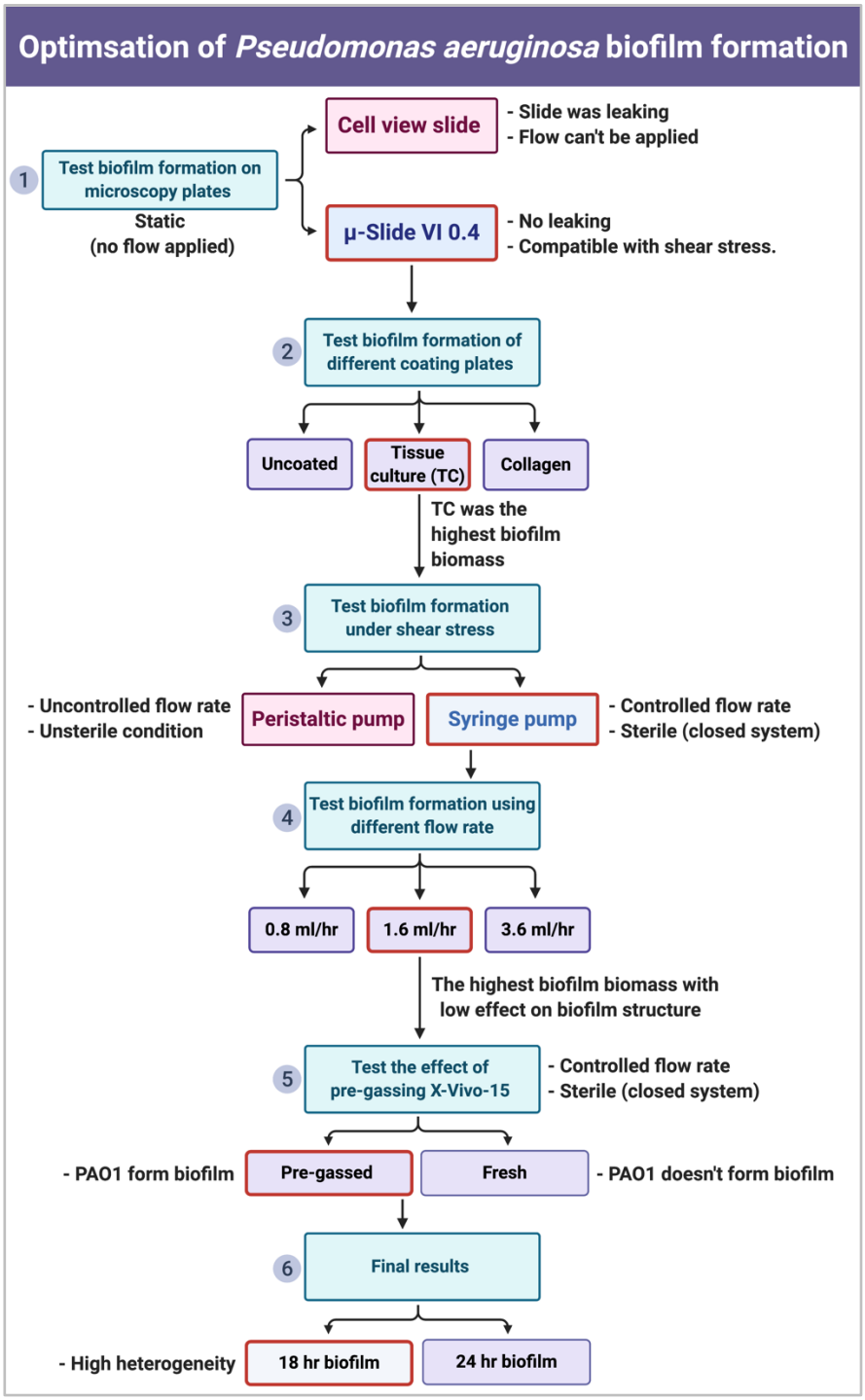


Figure 3.12 Summary of the work done in this chapter to optimise biofilm formation using the syringe pump system.

(1) The initial biofilm visualisation was done using cell view slides. Due to leaking problems, it was then substituted with ibidi u-slides. (2) After forming biofilms on three different coating options, TC coating was chosen because of high biomass formation. (3) Following that, flow was applied, and the syringe pump was chosen as it provides sterility and full control of the flow rate. (4) After applying the fixed flow rate and using (5) a pre-gassed media, we choose to use the (6) 18 hr biofilms as it provides higher heterogeneity. Diagram designed using Biorender.

In CF lungs and chronic wounds, PA grows in dense suspended separated aggregates with no mushroom-shaped structures or high biomass (Bjarnsholt et al., 2013) as observed at 24 hr (Figure 3.11). In our study, we observed enhanced biofilm formation that correlated with the introduction of the shear force and incubation time. Biofilms grown for 18 hr showed increased roughness (Figure 3.10) thus higher heterogeneity. Therefore, to better mimic the *in vivo* conditions of PA in chronic infections, we employed the 18 hr biofilms to study host-biofilms interaction in Chapters 4 and 5. The microcolonies observed in the 18 hr biofilms showed similar structure to PA aggregates observed in lungs from CF patients (Kragh et al., 2014) and chronic wounds (Bjarnsholt et al., 2013).

While it is well established that culturing biofilms under controlled shear stress produce higher biofilm biomass compared to static condition (Azeredo et al., 2017), as far as we know no study had evaluated the effect of CO_2 on the growth of PA as biofilm. A negative linear correlation was reported between the concentration of CO_2 and the growth rate of PA; the author attributed this low growth to lower enzymatic activity (King Jr and Nagel, 1975). Similarly, it was reported that CO_2 reduced the growth rate of a strain within the *Pseudomonas* genus *P. fluorescens* (Gill and Tan, 1979). It was indicated that the slow growth rate is a shared common characteristic of bacteria growing in biofilms triggered as a defensive mechanism in response to stimulation or nutrient limitation (Jefferson, 2004). Mohammad Y. Alshahrani (PhD thesis) evaluated the growth rate of PAO1 *wspF* mutant strains in X-Vivo-15 and based on the growth curves, wspF mutant strains that overexpress Psl and/or Pel, including Δ*wspF*, Δ*wspF*Δ*Pel*, and Δ*wspF*Δ*Psl* showed lower growth rate compared to PAO1 and Δ*wspF*Δ*Pel*Δ*Psl* (Alshahrani, 2018) which could relate to their increase ability to form biofilms. It has been indicated that CO_2 in high concentration might work as an antimicrobial against PA biofilms at concentrations greater than 5% (King Jr and Nagel, 1975). Therefore, it is possible that the introduction of CO_2 in the media worked as a stress mechanism that might trigger the enhanced biofilm generation of PAO1 strain. However, further research

should be undertaken to investigate the growth rate of PAO1 in both fresh and pre-gassed X-Vivo-15 and whether the pre-gassing of the media affects the PA metabolic activity.

As mentioned earlier, the architecture of the PA biofilms fundamentally relies on the production of EPS consisting mainly of polysaccharides, proteins, eDNA (1.4). The extracellular polysaccharides are probably the most studied macromolecules within the EPS (Vu et al., 2009). Fluorescent-conjugated lectins are commonly utilised as a tool to stain the extracellular microbial polysaccharides (Neu et al., 2001, Zhang et al., 2015). These lectins are proteins derived from a wide range of natural sources including seeds, plants, animals, fungal and bacterial cells (Strathmann et al., 2002). Several lectins have been employed to visualise different PA EPS components including the *Wisteria floribunda* lectin (WFL) isolated from Japanese Wisteria seeds and HHA obtained from the Amaryllis plant (Jennings et al., 2015). While WFL demonstrated specificity for GalNAc moieties which were indicated to be part of the Pel structure, HHA reportedly recognises 1,3- or 1,6-linked mannosyl units in Psl (Jennings et al., 2015).

As this study explored the interaction of CLRs, known to bind high mannose structures, and PA biofilms we utilised HHA to visualise the distribution of Psl within the biofilms along with the use of DAPI for DNA and FM 1-43 Fx for bacterial cells. In the case of mushroom-shaped biofilms, we observed eDNA forming the base of the structure (Figure 3.11), which correlates with the results reported in (Allesen-Holm et al., 2006). We also observed localisation of Psl on the periphery of the mushroom-shaped biofilms (Figure 3.11). These results correlate with Ma et al. (2009), who also utilising HHA, reported the peripheral localisation of Psl (Ma et al., 2009). These results confirmed the specificity of the staining utilised to assess the reproducibility of the system utilising the biofilms analysis software COMSTAT.

Overall, the optimised biofilm production system presented in this chapter will be utilised as a tool to study PA biofilms-CLRs interaction in the following chapters.

Chapter 4. Recognition of *Pseudomonas aeruginosa* biofilms and purified biofilm-associated carbohydrate by Dectin-2

4.1. Introduction

The dendritic cell-associated C-type lectin-2 (Dectin-2) (Clec4n, CLEC6A) was originally identified as a Langerhans cell-specific C-type lectin (Ariizumi et al., 2000), but following studies found Dectin-2 expression in other myeloid cells, including monocytes, macrophages, neutrophils and other populations of dendritic cells (McDonald et al., 2012, Robinson et al., 2009, Seeds et al., 2009, Taylor et al., 2005b). Expression of Dectin-2 in these cells is relatively low and is augmented by inflammatory stimuli (Miura et al., 2019, Kerscher et al., 2013, Saijo and Iwakura, 2011). However, specific molecular mechanisms regulating Dectin-2 expression have not been identified. The gene encoding Dectin-2 is located on chromosome 6F in mouse and chromosome 12q13 in humans, alongside other C-type lectins that comprise the Dectin-2 cluster (Balch et al., 2002, Fujikado et al., 2006). In the mouse, the Dectin-2 cluster contains nine C-type lectins that share a similar structure; these include, Dectin-2 (Clec4n), Macrophage C-type lectin (MCL, Clec4d), and Mincle. In humans fewer genes are found within the Dectin-2 cluster, these include Dectin-2 (CLEC6A), BDCA-2 (CLEC4C), DCIR (CLEC4A), MCL (CLECSF8), and Mincle (CLEC4E) (Yamasaki, 2016). Considering the shared similarity in gene structure by the receptors and the variability among cluster members between different species, it was hypothesised that this gene cluster might have resulted from gene duplication (Yamasaki, 2016). Interestingly, the chromosome area where the Dectin-2 cluster is located has been associated by linkage studies to several autoimmune diseases such as type I autoimmune diabetes, pernicious anaemia, systemic lupus erythematosus, multiple sclerosis and rheumatoid arthritis (Fujikado et al., 2006, Wandstrat and Wakeland, 2001). Therefore, C-type lectins may contribute to such diseases (Caliz et al., 2013). In this

section, we summarise the observations made on Dectin-2 with regards to structure, ligand recognition and contribution to disease. Then we finish with data leading to this study.

4.1.1. Structure of Dectin-2

Dectin-2 is a transmembrane type II glycosylated protein; the C-terminal end encodes the extracellular region and the N-terminal the cytoplasmic region (Ariizumi et al., 2000). This protein is composed of four parts: (1) a single extracellular Carbohydrate Recognition Domain (CRD) domain, (2) a stalk region, (3) a transmembrane region and (4) a short cytoplasmic domain without a known signalling motif (Figure 4.1). Such structures are found in other C-type lectins of the Dectin-2 cluster except for DCIR and DCIR2, which have an immunoreceptor tyrosine-based inhibitory motif (ITIM) in their cytoplasmic region. To transduce signalling, Dectin-2 engaged the adapter molecule Fc receptor common γ chain (FcRγ, Fcer1g) that contains an immunoreceptor tyrosine-based activation motif (ITAM) (Figure 4.1) (Yamasaki, 2016).

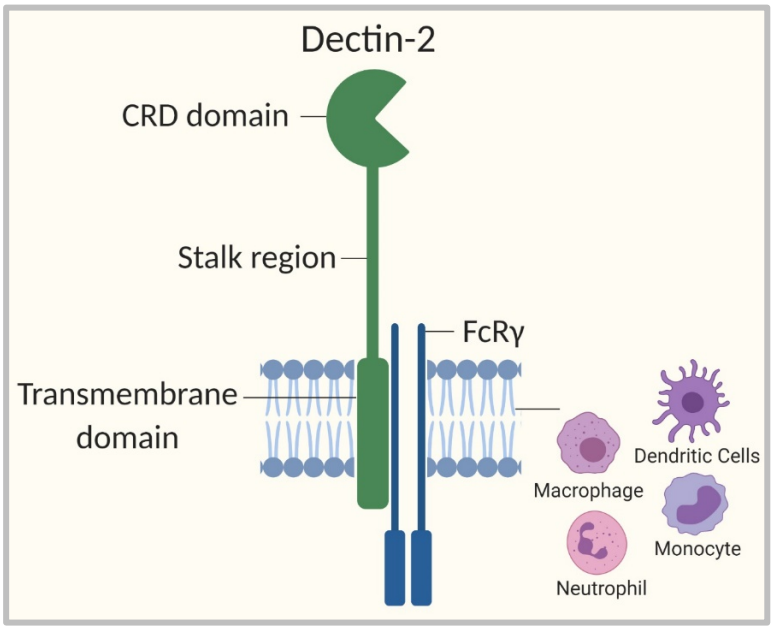


Figure 4.1 Structure of Dectin-2

Dectin-2 is composed of four parts: (1) a single CRD domain in the extracellular area, (2) a stalk region, (3) a transmembrane region and (4) a short cytoplasmic domain without a known signalling

motif. To transduce signalling upon ligand ligation, Dectin-2 links with the adapter molecule Fc receptor common γ chain. Created with BioRender.com.

While Dectin-2 contains an arginine residue, which often mediates interactions with immunoreceptor tyrosine-based activation motif (ITAM)-containing adaptor molecules in the transmembrane region, the interaction between Dectin-2 and FcRγ these two molecules does not depend on the arginine residue, unlike other FcRγ-coupled receptors, but instead involves the membrane-proximal region of the cytoplasmic tail of Dectin-2 (Sato et al., 2006). It has been reported that Dectin-2 might form disulfide-linked homodimers and heterodimers with the C-type lectin Dectin-3 via the preserved cysteine residue in its stalk region, with heterodimers displayed a greater affinity to the *C. albicans* hyphae than the homodimers (Zhu et al., 2013). The requirement of the cysteine residue of Dectin-2 for heterodimerisation and the molecular mechanism for dimer formation is still unknown.

4.1.2. Ligands of Dectin-2

Dectin-2 raised considerable interest as a pattern recognition receptor (PRR) as it possesses a glutamic acid – proline – asparagine (EPN) motif in its CRD domain, known to facilitate mannose, glucose, N-acetylglucosamine and fucose binding in a calcium-dependent manner (Fernandes et al., 1999). Competition binding studies indicated that the Dectin-2 CRD binds to monosaccharides with modest affinity and that affinity was greatly enhanced for mannose-linked (1–2) or (1– 4) to a second mannose residue. Glycan array analysis confirmed selective binding of the CRD to glycans that contain α-(1–2)-linked mannose epitopes (Feinberg et al., 2017). A study using a glycan array showed that Dectin-2 binds to high-mannose complexes present across a wide range of organisms, including fungi, bacteria and mammals (McGreal et al., 2006). In line with these findings Dectin-2 binds to a number of pathogenic microorganisms, including Candida spp., *Saccharomyces cerevisiae*, *Cryptococcus neoformans*, *Trichophyton rubrum*, *Paracoccidioides brasiliensis*, Malassezia spp., *Aspergillus fumigatus*, Mycobacterium spp., *Streptococccus neoformans*, *Streptococcus*

pneumoniae, and Ebola virus. In all instances, their surface cell wall polysaccharides contain a high mannose structure (McGreal et al., 2006, Sato et al., 2006, Barrett et al., 2009, Brudner et al., 2013, Miyasaka et al., 2013, Ritter et al., 2010).

4.1.3. Dectin-2 involvement in fungi recognition

C. ablicans cell wall is composed of cell wall proteins decorated with N- and O-linked glycansosylations known as mannans (Calderone and Clancy, 2011). Mannans account for 40% of the total cell wall polysaccharides. Mannans are composed of an N-glycan core, an α-(1,6)-mannoside backbone, and side chains that contain α-(1,2) or (1,3) linked oligomannosides (Graus et al., 2018). It was reported that culturing *C. albicans* under carbon-limiting, low pH and low-temperature conditions prevents the release of β-1,2-linked mannose residues, but not α-1,2-mannose residues that are secreted as water-soluble fractions into the medium (Shinohara et al., 2006). The α-1,2-mannose was found to be the primary ligand of Dectin-2 (Feinberg et al., 2017). *C. albicans*-derived α-mannans were used to stimulate wild type, and Dectin-2-deficient mouse bone marrow-derived DCs (BMDCs) and Dectin-2 deficient cells were unable to produce IL-6 and TNF-α indicating that Dectin-2 is a *C. albicans* α-mannans receptor. Depending on growth conditions, *C. albicans* can exist in yeast or hyphal form (Saijo et al., 2010) and Dectin-2 binds better to the hyphal form (Sato et al., 2006). Stimulation of Dectin-2- deficient BMDCs with *C. albicans* hyphae decreased significantly but not completely, cytokine production compared to wild type cells (Sato et al., 2006). On the other hand, absence of Dectin-2 abolished cytokine secretion in response to the yeast form of *C. albicans* (Sato et al., 2006).

The skin opportunistic pathogen *Malassezia furfur* is another fungus recognised by Dectin-2 (Ishikawa et al., 2013). Fractionation methods found that the hydrophilic cell wall components of Malassezia, the O-linked mannobiose-rich protein which contains α-1,2-mannosyl residues, is a distinct binding ligand for Dectin-2. Accordingly, the Malassezia α-1,2-mannosyl residues

activated Dectin-2-expressing reporter cells (Ishikawa et al., 2013). Dectin-2 deficiency reduced TNFα release by BMDCs after stimulation with *M. furfur* (Ishikawa et al., 2013).

It has been reported that Dectin-2 recognises the terminal mannose of N-linked glycan (McGreal et al., 2006). Based on the analysis of different Malassezia sp. (Ishikawa et al., 2013) define Dectin-2 ligands as a multivalent terminal α-1,2-mannose attached to glycans, proteins, and presumably any kind of scaffold. In line with this hypothesis, *C. guilliermondii* and *S. cerevisiae* were not recognised by Dectin-2, most likely because the cell wall of these fungi contains α-1,2-mannose masked with β-1,2-mannose and α-1,3-mannose, respectively (Romero et al., 1999, Shibata et al., 1996).

4.1.4. Role of Dectin-2 in recognition of mycobacteria

Mycobacteria (M.) display cell wall components that influence the host immune responses such as lipoarabinomannan (LAM). LAM is structured in four parts: (1) the anchor, a mannosyl-phosphatidyl-myoinositol (MPI), (2) the mannose backbone, (3) the arabinan domain and (4) the capping moieties located at the terminal extremity of the arabinan domain (Zhou et al., 2019).

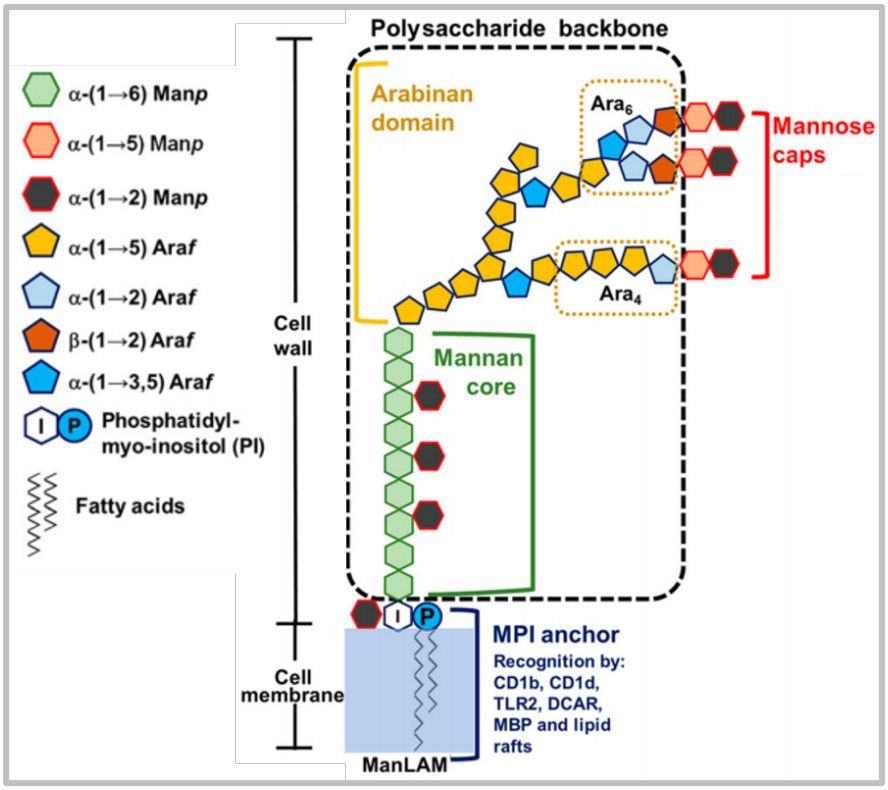


Figure 4.2 Man-LAM structure

LAM is structured in four parts: (1) the anchor a mannosyl-phosphatidyl-myo-inositol (MPI), (2) the mannose backbone, (3) the arabinan domain and (4) the capping moieties located at the terminal extremity of the arabinan domain. Figure and information adapted from (Zhou et al., 2019).

These capping moieties differ among mycobacterial species, and can include mannose as found in mannose-capped lipoarabinomannan (Man-LAM) (Figure 4.2) produced by *M. tuberculosis*, *M. leprae*, and *M. bovis* (Turner and Torrelles, 2018). Man-LAM from the pathogen *M. tuberculosis* causes wide effects on host immunity (Mishra et al., 2011) including suppression (Briken et al., 2004). Dectin-2 recognises mycobacterial Man-LAM, and this recognition induces both anti- and pro-inflammatory responses including IL-10 production during mycobacterial infection, which was abrogated in Dectin-2 deficient DCs (Yonekawa et al., 2014). It is important to note that another Mincle and MCL who share the same gene cluster with Dectin-2 recognise another mycobacterial cell wall component, trehalose-6,60-dimycolate (TDM) (Miyake et al., 2013, Ishikawa et al., 2009).

4.1.5. Dectin-2 Signalling

Dectin-2 recognition of carbohydrates structures triggers a sequence of cellular responses through the association of the ITAM-containing adaptor molecule FcR-γ. The process starts with phosphorylation of Spleen tyrosine kinase (Syk), which activates the Caspase recruitment domain family member 9 (CARD9)– B-Cell lymphoma 10 (BCL10)– Mucosa-associated lymphoid tissue lymphoma translocation protein 1 (MALT1) (CBM) cluster, leading to nuclear factor (NF)-κB activation (Hara et al., 2007, Saijo et al., 2010) NF-κB activation leads to the translation of cytokines such as IL-23 and pro-IL-1β. Simultaneously, the activation of Syk induces the production of reactive oxygen species (ROS). ROS are essential for pathogen eradication and activation of the NLRP3 inflammasome. The NLRP3 inflammasome that facilitates the processing of pro-IL-1β into mature IL-1β (Ritter et al., 2010). At the same time, the mitogen-activated protein kinases (MAPK) pathway is activated (Ritter et al., 2010), although the biological significance of MAPKs signalling in Dectin-2-mediated host defence is unknown (Figure 4.3).

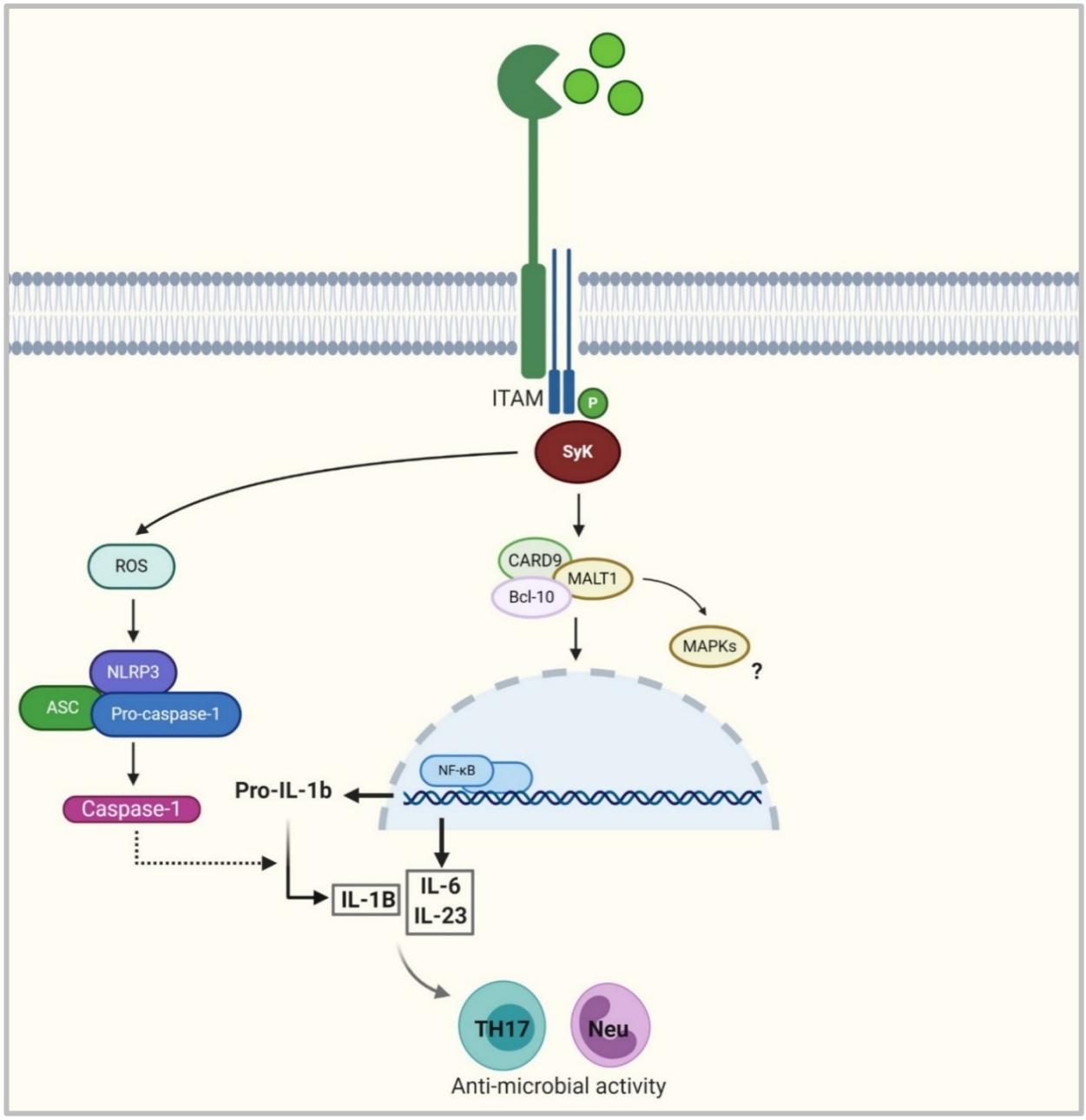


Figure 4.3 Dectin-2 signalling pathway

The interaction of the Dectin-2 with carbohydrates triggers cytoplasmic signalling and a number of cellular responses through association with FcR-γ chain. The process initiates after phosphorylation of Syk, which associates with the CARD9–BCL10–MALT1 complex, resulting in the production of pro-inflammatory cytokines and induction of T-cell immunity.

4.1.6. Role of Dectin-2 in Disease

The importance of Dectin-2 in antifungal immunity has been shown in mouse models (Robinson et al., 2009). Dectin-2-deficient mice showed decreased survival after *C. albicans* infection and displayed increased fungal growth in the kidney (Saijo et al., 2010). These results suggest an important role for Dectin-2 in pathogen eradication, but the mechanism remains unclear. One explanation is that the pro-inflammatory cytokines secreted by myeloid cells expressing Dectin-2 improve lymphocytic IL-17 production. Mice that are deficient in IL-17A and deficient in IL-23-p19 are more vulnerable to *C. albicans* infection indicating that IL-17A is essential to host defence against this fungus (Saijo et al., 2010, Kagami et al., 2010). Furthermore, mutations influencing human IL-17F and IL-17-receptor A (IL-17RA) function lead to the development of chronic fungal infection because of a compromised IL-17-mediated immunity (Puel et al., 2011).

Dectin-2 recognises MAN-LAM from *M. tuberculosis;* MAN-LAM has modulatory effects on host immunity as mentioned above (Briken et al., 2004, Gringhuis et al., 2009, Mazurek et al., 2012). Yonekawa et al. (2014) reported that bone marrow-derived dendritic cells (BMDCs) stimulated with Man-LAM produce both pro- (TNF-α, IL-6) and anti- (IL-10) inflammatory cytokines, which was completely abrogated in Clec4n–/– BMDCs. The author suggested that this production of pro- and anti-inflammatory cytokines are beneficial for host organisms to maintain balanced immune responses (Yonekawa et al., 2014). Dectin-2 deficient mice displayed augmented lung pathology in response to mycobacterial infection compared to WT mice suggesting Dectin-2 involvement in host defence against mycobacteria (Yonekawa et al., 2014).

4.1.7. Data leading to this study

As mentioned in the main introduction, colonisation and persistent infection by *Pseudomonas aeruginosa* (PA) are important causes of mortality and morbidity in individuals with underlining conditions such as cystic fibrosis (Moradali et al., 2017). The adaptability of PA enabling the

bacteria to switch from planktonic growth to biofilms contributes to chronic infection (Valentini et al., 2018). Biofilms are enclosed in an extracellular polymeric substance (EPS) (Costerton et al., 1999, Borlee et al., 2010) and the polysaccharides Psl and Pel are important EPS components that promote biofilm formation (Ma et al., 2009). Our lab reported binding of two CLRs to PA biofilms, DC-SIGN and the CTLD-4-7 fragment of MR (Figure 4.4). These results suggest the existence of a ligand recognised by CLRs within the biofilms, binding was (A) inhibited by specific sugars and (B) calcium-dependent (Figure 4.4) (Singh et al., 2020), preprint.

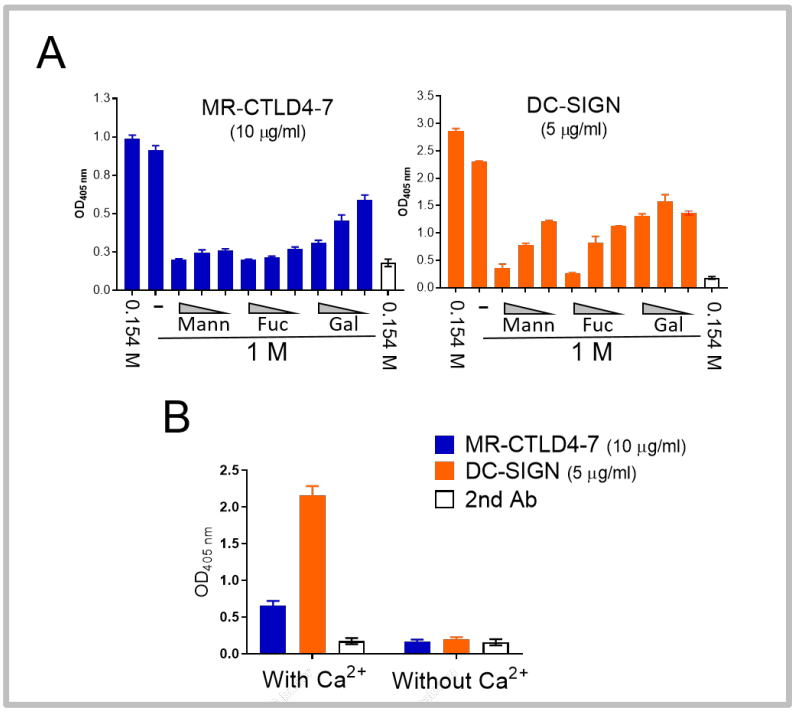


Figure 4.4 Recognition of DC-SIGN and MR-CTLD-4-7 to PAO1 biofilm

PA biofilms generated in 96 well plates for 24 hr were fixed and incubated with MR-CTLD4-7-Fc or DC-SIGN-Fc followed by anti-human Fc antibody conjugated to alkaline phosphatase. A. DC-SIGN and MR-CTLD4-7 bind to PAO1 biofilms and binding is selectively inhibited by Mannose and Fucose. Binding assays were performed in two NaCl concentrations (0.154 M and 1M), and for the 1M condition, incubation with Fc chimeric proteins was performed in the presence of different concentration of monosaccharides (1, 0.2 and 0.04 M). Binding at 1M NaCl was comparable to that observed at 0.154 M. Mann: Mannose, Fuc: Fucose; Gal: Galactose. N=3 in triplicate. Graphs show mean +/- SEM. B. DC-SIGN and MR-CTLD4-7 binding to PAO1 biofilms is Ca^{2+} dependent. N=2 in triplicate.

Furthermore, our lab purified Psl from the Pel deficient mutant Δ*wspF*Δ*pel* (two independent preparations) to determine whether the PA biofilm-associated carbohydrate was recognised by CLRs (Singh et al., 2020). The Δ*wspF* background causes high cyclic di-GMP levels that promote biofilm formation and a phenotype similar to small colony variants reported during chronic infections (Pestrak et al., 2018). Psl was fractionated into high (> 45 kDa, HMW-Psl) and low molecular weight (< 45 kDa, LMW-Psl) preparations using gel filtration chromatography (Bales et al., 2013). Gel permeation chromatography (GPC) confirmed differences in size (15,370 Da for LMW-Psl-1 and 182,300 Da and 132,670 Da, for HMW-Psl-1 and HMW-Psl-2, respectively) (Figure 4.5 A). No major protein or DNA contamination was detected based on Coomassie and Silver staining and spectrophotometry, respectively (data not shown).

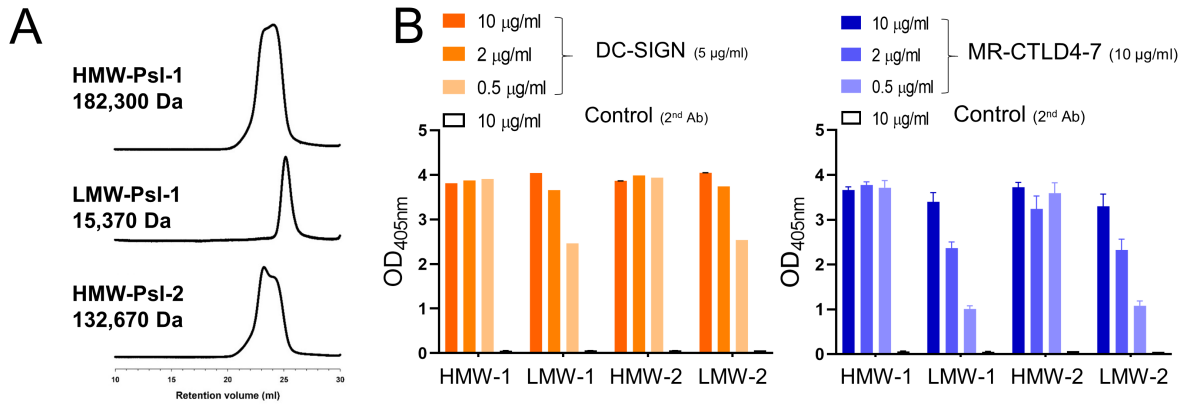


Figure 4.5 Size analysis and binding to DC-SIGN and MR-CTLD4-7 of *P. aeruginosa* biofilm-associated carbohydrate.

A. GPC analysis of HMW-Psl-1, LMW-Psl-1 and HMW-Psl-2 confirms successful fractionation into high and low MW forms. HMW-Psl-2 contained two peaks poorly resolved. This indicates that this sample is comprised of two components that are similar in MW and perhaps conformation. The MW for HMW-Psl-2 reflects the average MW for the entire sample. B. Lectin binding assays demonstrate binding of MR-CTLD4-7 and DC-SIGN to HMW-Psl-1, LMW-Psl-1, HMW-Psl-2 and LMW-Psl-2. Robust binding of HMW-Psl-1 and 2 was observed at 0.5 µg/ml while binding of LMW-Psl-1 and 2 at this concentration was substantially reduced. Dose-dependent binding of HMW-Psl-1 and HMW-Psl-2 to MR-CTLD4-7 and DC-SIGN occurs at lower doses. Fc-chimeric proteins and anti-human Fc-secondary antibody conjugated to alkaline phosphatase were used. Graphs show Mean ± SEM of 2 independent repeats done in duplicate.

Ligand binding assays demonstrated binding of HMW-Psl and LMW-Psl preparations to MR and DC-SIGN. Binding of HMW-Psl was stronger (Figure 4.5 B). The hydrolysed carbohydrates monomer compositions in moles % for HMW-Psl-1 was 74.9% mannose, 14.7% glucose, 7.4% galactose, and 3.0% rhamnose and for HMW-Psl-2 was 87.2% mannose, 15.3% glucose, 3.3% galactose, and 3.2% rhamnose. The ^{1}H-NMR spectra of HMW-Psl-1 and HMW-Psl-2 are very similar (Figure 4.6 A) and show that mannose, the major monomer present, arose from mannan segments in the polymer (Lowman et al., 2011). Both HMW exopolysaccharide preparations contain a small proportion of galactose, and there is a high proportion of 1-6-linked-α-mannose with some 1-2 linkages. Mannose-rich composition of HMW-Psl preparations is in agreement with previous findings (Byrd et al., 2009) and supported by its recognition by Hippeastrum Hybrid Amaryllis (HHA) lectin (Figure 4.6 B) commonly used to detect the mannose-rich carbohydrate Psl within *PA* (Reichhardt and Parsek, 2019).

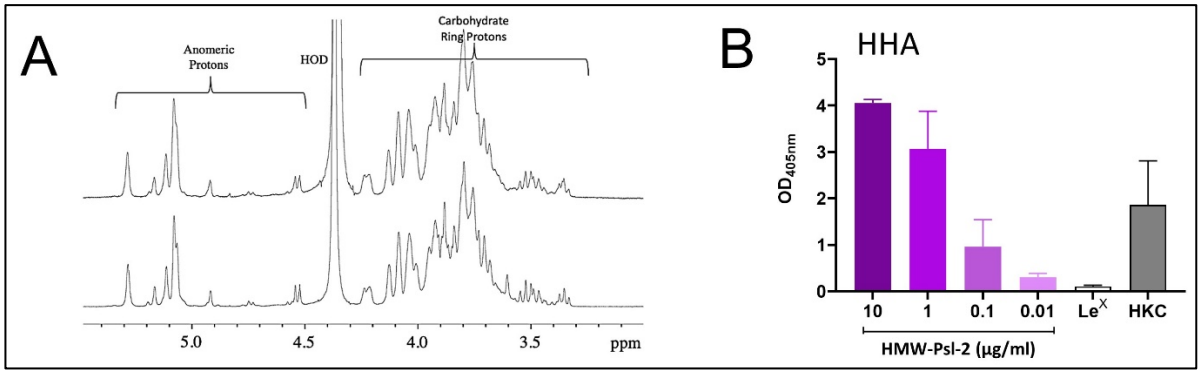


Figure 4.6 Characterisation of high molecular weight biofilm carbohydrates

A. 1H-NMR spectra from HMW-Psl-1 and HMW-Psl-2 demonstrate that they are very similar and contain primarily carbohydrates composed of α(1-6) linked mannose segments. Small amount of lipid and a trace of protein were also detected. B. HMW-Psl-2 bound the mannose-specific lectin HHA. HHA recognises both (1-3) and (1-6) α-linked mannose structures. HMW-Psl-2LPS-free (more details on Chapter 5) and HHA conjugated to alkaline phosphatase were used in these assays. Lewisx-PAA and Heat-Killed Candida albicans (HKC) were negative and positive controls, respectively. Graph shows Mean ± SEM of two independent repeats done in duplicate.

4.2. Hypothesis

The previous results demonstrate that PA biofilms directly engages CRLs expressed by human immune cells Mannose Receptor (CD206, MR) and DC-SIGN (CD209), this attracted our attention to the potential of other CLRs to bind PA biofilms. Taking into consideration that a common feature among C-type lectin receptors that bind mannose is the presence of the EPN amino acid triplet in their CRD in a Ca^{2+}-dependent manner; we hypothesised that other EPN-containing C-type lectins, such as Dectin-2 expressed by myeloid cells, might also contribute to the recognition of PA biofilms by immune cells.

4.3. Aims

This part of the project aims to:

1. Determine the capability of Dectin-2 to interact with PA biofilms and purified EPS components.
2. Identify how recognition of EPS by this C-type lectin influences the immune response to PA.

4.4. Results

4.4.1. Biofilms formed by PAO1 and Δ*wspF* mutants are recognised by the CRD domain of Dectin-2

Previously, our lab demonstrated binding of two CLRs to PA biofilms, DC-SIGN and the CTLD-4-7 fragment of MR. These results suggest the existence of a ligand recognised by CLRs within the biofilms (Singh et al., 2020). As a result, we explored the potential of the CLR Dectin-2 to recognise PA biofilms. Towards this aim, we performed a lectin ELISA assay as described in (2.5). In this study, we used two chimeric proteins containing either the extracellular domain of Dectin-2 (aa 44-209) or the CTLD4-7-region of mouse MR fused to the Fc portion of human

IgG1 (Linehan et al., 2001). The binding capability of Dectin-2-Fc was tested against a combination of PA strains with different EPS composition and different biofilms biomass, as shown in (Figure 4.7 inlet).

Dectin-2-Fc exhibited binding capacity to all tested strains except to the biofilm deficient strain Δ*wspF*Δ*pel*Δ*psl* (Figure 4.7 A). Dectin-2-Fc showed a binding pattern similar to MR (CTLD-4-7-Fc); however, MR binding was slightly higher. Dectin-2-Fc bound better to wells containing biofilms formed by Psl overexpressing strains Δ*wspF* and Δ*wspF*Δ*pel* compared to Δ*wspF*Δ*psl* and PAO1. These findings indicated that the presence of Psl promotes Dectin-2-Fc binding. Binding of Dectin-2-Fc and MR to biofilms formed by the strain lacking Psl (Δ*wspF*Δ*psl*) indicates that both receptors might bind to another ligand within biofilms that are independent of Psl. To assess whether the binding observed is through the CRD domain of Dectin-2, we simultaneously tested the effect of removing calcium from the assay buffer (10 mM vs 0 mM $CaCl_2$). As shown in (Figure 4.7 A), Dectin-2 and MR binding was significantly reduced by calcium removal. These results indicate the existence of a ligand recognised by Dectin-2 within PA biofilms recognised in a calcium-dependent manner. In all experiments, binding of Dectin-2-Fc to heat-killed candida (HKC) and different commercial carbohydrates were tested as controls. Results indicated high binding of Dectin-2 to HKC at $4x10^6$ particles /well (Figure 4.7 B) and moderate or no binding to mannose-containing polymers at 2 µg/ml (Figure 4.7 C).

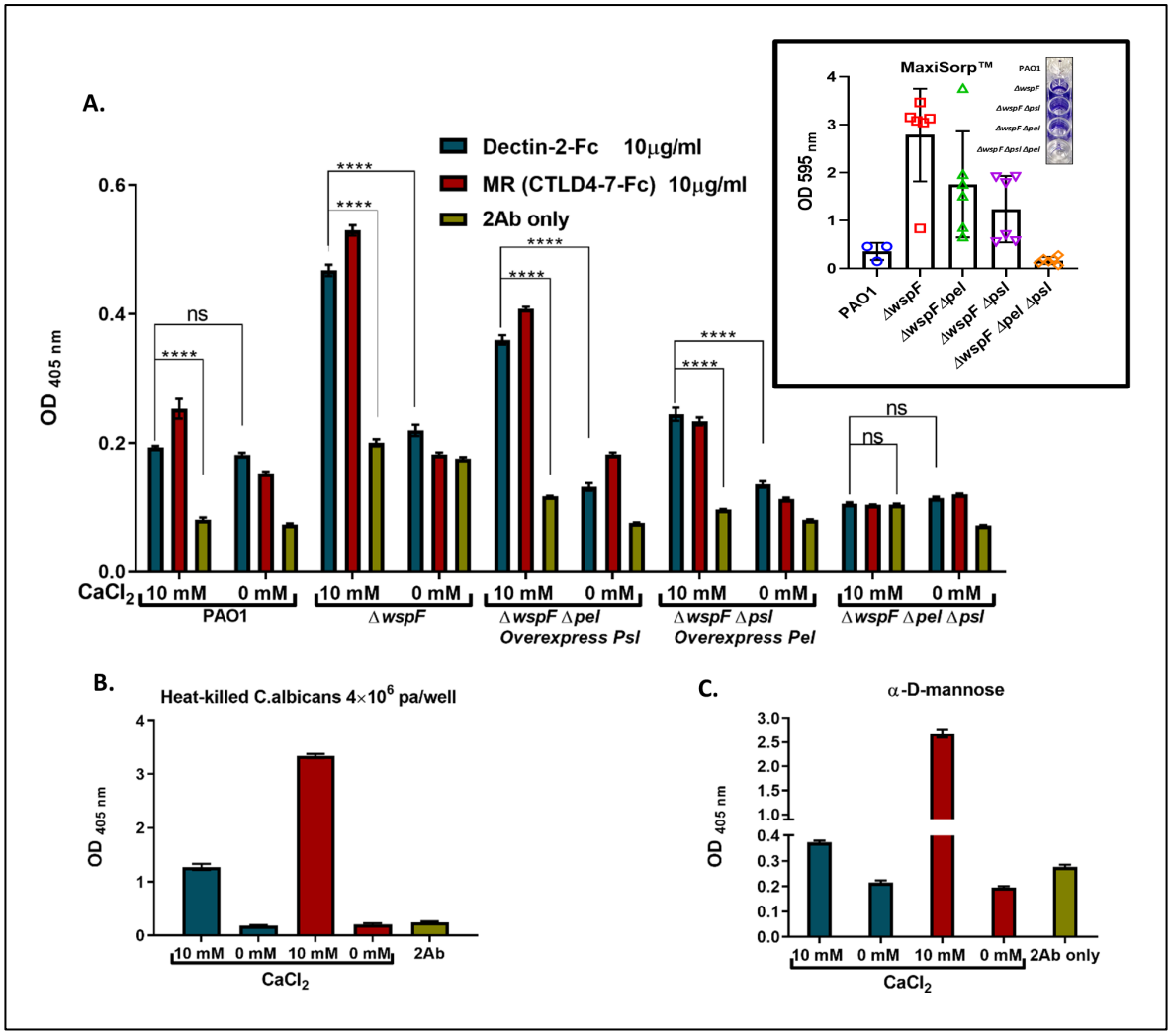


Figure 4.7 Binding of Dectin-2-Fc to PA biofilms.

(A) Biofilms from different strains (inlet), developed over 24 hr using Maxisprop plates as described (2.3), (B) Mannose-containing polymers at 2 µg/ml or (C) HKC at $4x10^6$ particles /well, were incubated with 10 µg/ml of Dectin-2-Fc or MR (CTLD-4-7-Fc) chimeric proteins prepared in TSB buffer with or without calcium ($CaCl_2$) for 2 hr at RT. The binding was determined using anti-human IgG Fc-specific antibody conjugated to AP (1:1000 dilution). Absorbance was read at $OD_{405\ nm}$. N=3 in triplicate. The analysis was done using two way ANOVA applying Tukey's multiple comparisons test. Graphs show mean +/- SEM. Inlet (black box) show the biofilm formation of PA lab strains which was presented earlier in (Chapter.3, Figure 3.2).

4.4.2. Biofilms formed by PA wound clinical isolates are recognised by Dectin-2-Fc, DC-SIGN-Fc and MR (CTLD-4-7-Fc)

To confirm that the binding of Dectin-2-Fc and MR (CTLD4-7-Fc) to biofilms occurred when using strains other than lab strains, biofilms generated by clinical PA isolates were also tested for DC-SIGN-Fc, Dectin-2-Fc and MR (CTLD4-7-Fc) binding. Biofilm formation by these PA clinical isolates (Table 2) was confirmed using crystal violet assay, as shown in (Figure 4.8 inlet). We used a collection of PA wound clinical collected from bone (CW2 B40 and CW5 B1), wound tissue (CW3 T40, CW6 T4 and CW7 T1) and blood (CW5 S1). Results showed that Dectin-2-Fc, MR (CTLD4-7-Fc) (Figure 4.8 A), DC-SIGN-Fc (Figure 4.8 B), bind to biofilms formed by clinical isolates and that, as seen previously [(Alshahrani, 2018), PhD thesis; (Singh et al., 2020), preprint], DC-SIGN-Fc binds significantly better than Dectin-2-Fc and MR (CTLD4-7-Fc) to all samples (Figure 4.8).

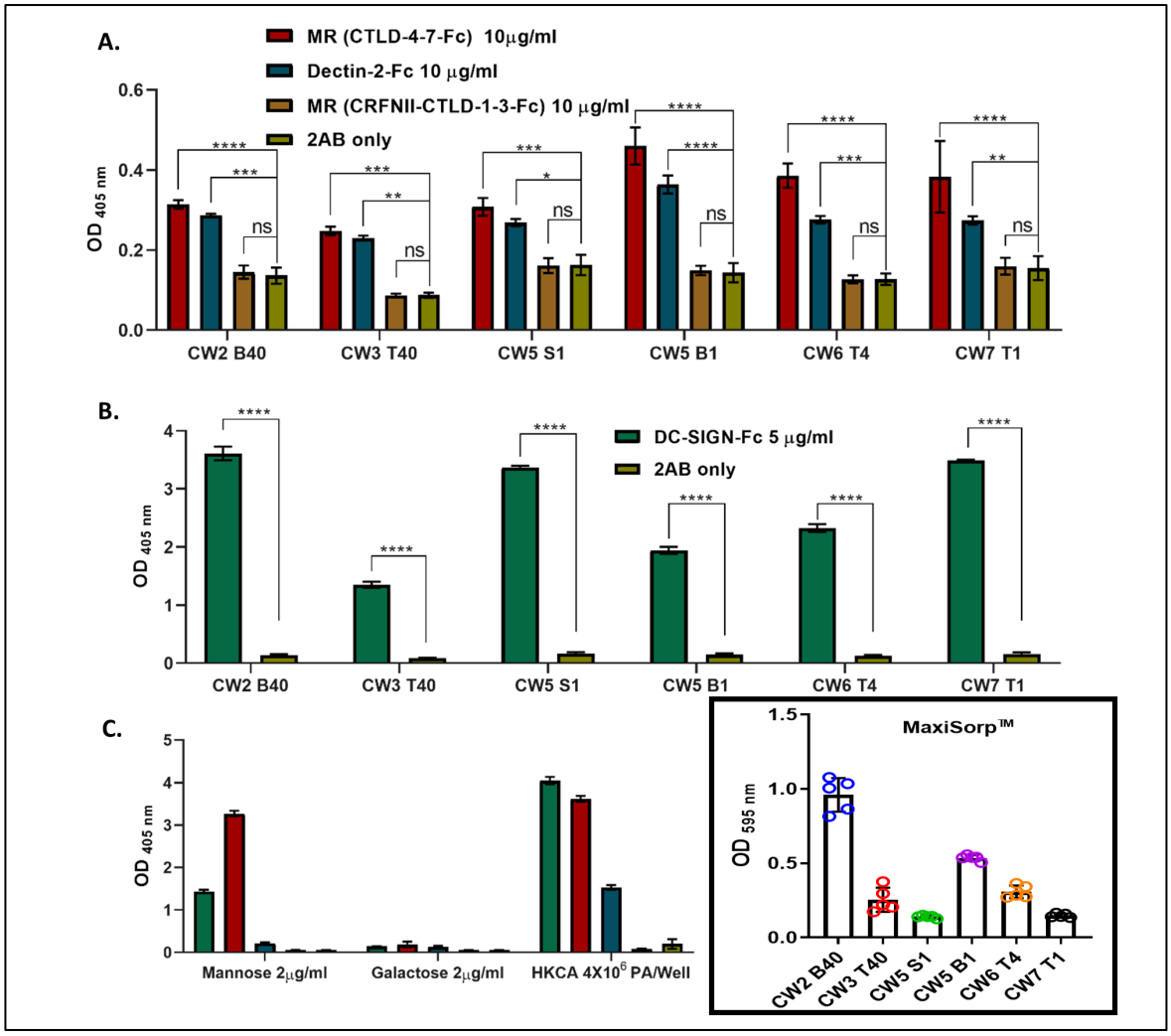


Figure 4.8 Assessment of binding of DC-SIGN-Fc, Dectin-2-Fc and MR (CTLD4-7-Fc) to biofilms formed by PA clinical isolates.

Formation of biofilms by PA clinical isolates was assessed using the crystal violet method (inlet). Biofilms were developed over 24 hr in Maxisorp plates as described in (2.3). Biofilm (A and B) or Maxisorp plates pre-coated with Mannose-containing polymers at 2 μg/ml or HKC at $4x10^6$ PA/well (C), were incubated with 10μg/ml MR (CTLD4-7-Fc) and 10μg/ml Dectin-2-Fc and 5μg/ml DC-SIGN-Fc for 2 hr at RT. The binding was determined using anti-human IgG Fc-specific antibody conjugated to AP (1:1000 dilution). Absorbance was read at $OD_{405\ nm}$. N=3 in triplicate. The analysis was done using two way ANOVA applying Dunnett's multiple comparisons test. Graphs show mean +/- SEM. Inlet (black box) show the biofilm formation of PA clinical isolates which was presented earlier in (Chapter.3, Figure 3.3).

4.4.3. Distribution of C-type lectin receptor ligands on PAO1 biofilms

After we confirmed the ability of Dectin-2-Fc to bind PA biofilms by ELISA using different lab and clinical strains, we then examined the distribution of ligands for Dectin-2 alongside that of DC-SIGN and MR on PAO1 biofilms developed on microscopic chamber slides as described in Chapter 3 (Figure 3.9). In brief, PAO1 biofilms formed under flow using the syringe pump system were fixed and incubated with Fc chimeric proteins used in ELISA assays. Binding was detected with a secondary antibody coupled to a fluorescent dye. Each lectin receptor displayed differing binding profiles to PAO1 biofilms. DC-SIGN-Fc showed abundant and dispersed binding, reaching substantial density in some areas located in the upper regions of the biofilm (Figure 4.9, top panel). MR (CTLD4-7-Fc) and Dectin-Fc ligands were less abundant (laser intensity was increased for their detection) (Figure 4.9, second and last panels respectively). Dectin-2-Fc showed more restricted binding, which concentrated in areas between bacterial aggregates. In the other hand, MR (CTLD4-7-Fc) showed a more diffused and lower binding compared to Dectin-2-Fc in terms of intensity. No binding was observed with the control protein CR-FNII-CTLD1-3-Fc or 2Ab (Figure 4.9, third panel). These results supported the display of DC-SIGN, MR and Dectin-2 ligands by PA biofilms and indicated that each C-type lectin bound to different areas within PA biofilms.

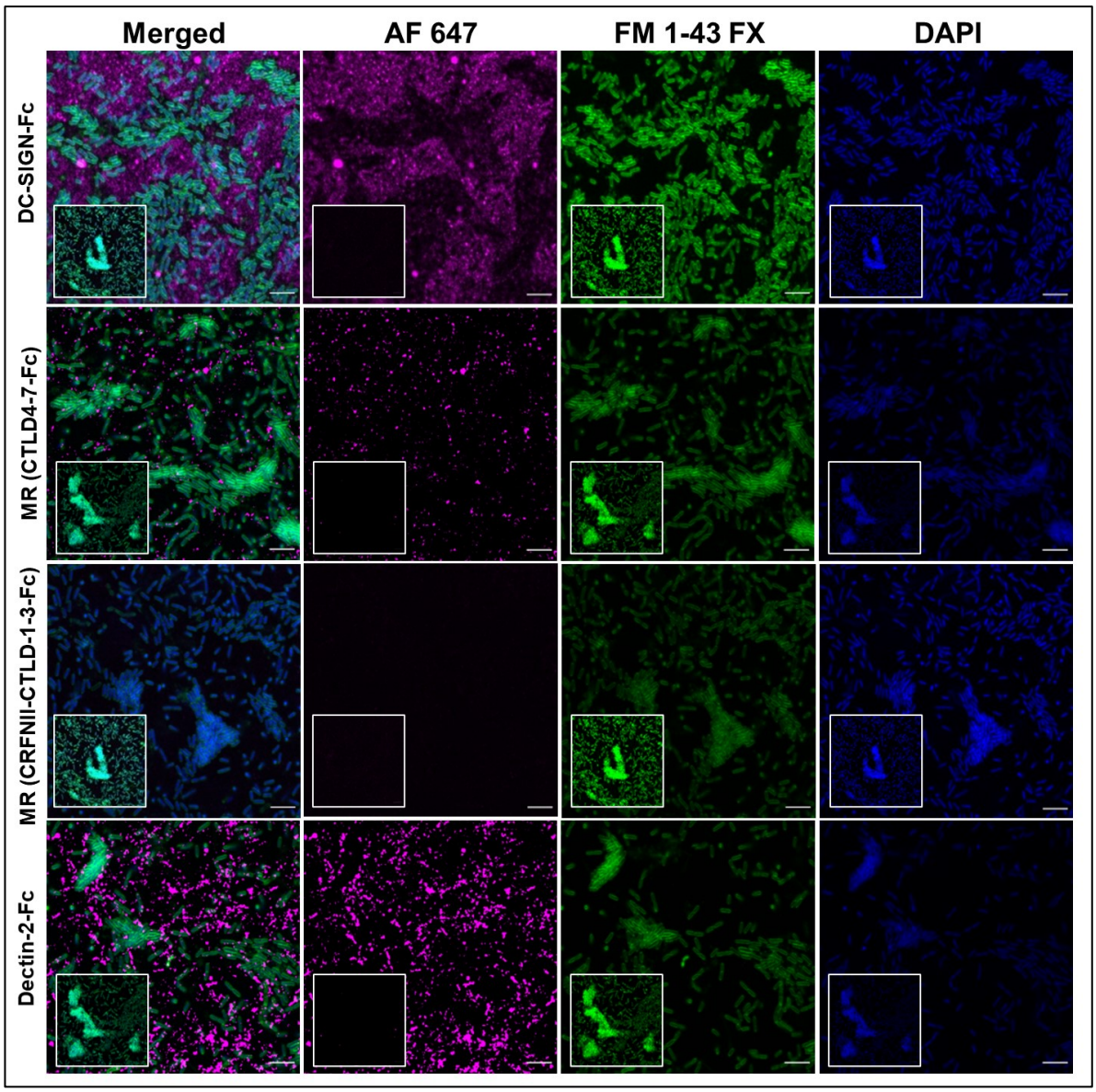


Figure 4.9 Distribution of DC-SIGN, MR, and Dectin-2 ligands in PAO1 biofilms.

PAO1 biofilms generated under flow conditions for 18 hr as described in (Figure 3.9) were incubated with 10 µg/ml DC-SIGN and 10 µg/ml MR-CTLD4-7-Fc and Dectin-2 Fc-chimeric proteins followed by anti-human Fc-secondary antibody conjugated to Alexa 647 (magenta) and counterstained with DAPI (DNA, blue) and FM1-43 Fx (bacteria, green). Z-stacks were acquired for all samples using confocal microscopy. Figure shows slice 9 for DC-SIGN-Fc, 16 for MR (CR-FNII-CTLD1-3-Fc) and 12 for corresponding secondary Ab control, and slice 12 for MR (CTLD4-7-Fc), 9 for Dectin-2-Fc and 12 for its control. Settings for image acquisition and processing were maintained constant for test and control samples. Inset shows biofilms incubated with corresponding secondary antibody only. No specific labelling was seen with MR (CR-FNII-CTLD1-3-Fc) chimeric protein. Size bar is 4 µm.

4.4.4. Dectin-2 Fc binds Psl purified from PA biofilms

The mannose-rich carbohydrate Psl is a major component of EPS in PA biofilms. Several studies have shown that Psl plays a major role in the development of biofilms through the promotion of cell aggregation and surface attachment. In our lab, a previous study indicated that carbohydrate purified from Δ*wspF*Δ*pel* biofilms bind MR (CTLD4-7 region) and DC-SIGN in a calcium-dependent manner. Thus, after we confirmed that Dectin-2-Fc bound to PA biofilms and Psl promoted binding, we assessed whether Dectin-2-Fc chimeric protein bound to new preparations of carbohydrate purified from Δ*wspF*Δ*pel* following the protocol by Bales et al. (2013). We examined three independent preparations, Psl-1, Psl-2 and Psl-3, which contained similar carbohydrate ratios (Singh et al., 2020). Each preparation was divided based on molecular weight after gel filtration into (A) high and (B) low molecular weight (Figure 4.5 and Figure 4.6). Results showed robust binding of Dectin-2-Fc and MR (CTLD4-7-Fc) to purified carbohydrate in a dose-dependent manner and that, as seen for total biofilms, CTLD4-7-Fc recognised this purified carbohydrate better than Dectin-2-Fc in all instances. In addition, both CLRs bound better to the higher molecular weight carbohydrates (A) (Figure 4.10). Initial 1H-NMR analysis indicated increased level of impurities in LMW-Psl-1 compared to HMW-Psl-1 and HMW-Psl-2 (data not shown), hence further work focused on HMW-Psl preparations.

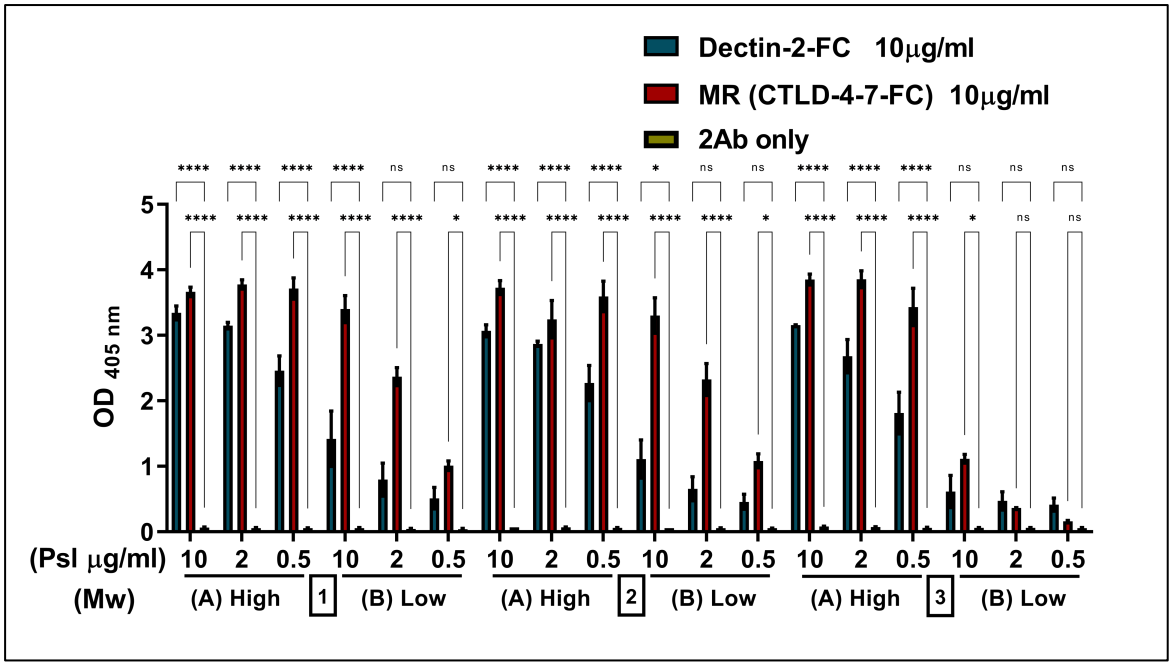


Figure 4.10 Binding of Dectin-2-Fc and MR (CTLD4-7-Fc) to purified Psl.

Maxisorp plates were coated with different preparations of carbohydrate purified from the Pel-deficient mutant Δ*wspF*Δ*Pel* diluted in 154mM NaCl overnight at 37°C. MR (CTLD4-7-Fc) and Dectin-2-Fc chimeric proteins were incubated for 2 hr at RT in TSB buffer. The binding was determined using anti-human IgG Fc-specific antibody conjugated to AP (1:1000) dilution. Absorbance was read at $OD_{405\,nm}$. Graphs show mean +/- SEM of two independent repeats.

4.4.5. Binding of Dectin-2 to Psl is calcium-dependent

In order to confirm that the binding of these lectins to purified carbohydrates or positive controls such as mannose and HKCA is calcium-dependent as observed earlier (Figure 4.7), the binding assay was carried out in TSB buffer, with and without calcium. It is important to note that in this assay and all subsequent assays in this chapter, LPS free preparations of HMW-Psl were used unless otherwise stated and will be referred to as HMW-Psl$^{(LPS\text{-}free)}$. This issue is discussed in details in Chapter 5 (5.4.2.1).

Results indicated that Dectin-2-Fc and MR (CTLD4-7-Fc) strongly bound to HMW-Psl-1$^{(LPS\text{-}free)}$, HMW-Psl-2$^{(LPS\text{-}free)}$ and HKCA in TSB buffer with calcium, and a significant reduction of lectin binding occurred in the absence of calcium (Figure 4.11). Data suggest that calcium is

necessary for the binding of Dectin-2 and MR to purified carbohydrate. LPS removal did not affect the binding of Dectin-2-Fc to HMW-PsI$^{(LPS\text{-}free)}$ (Figure 4.11).

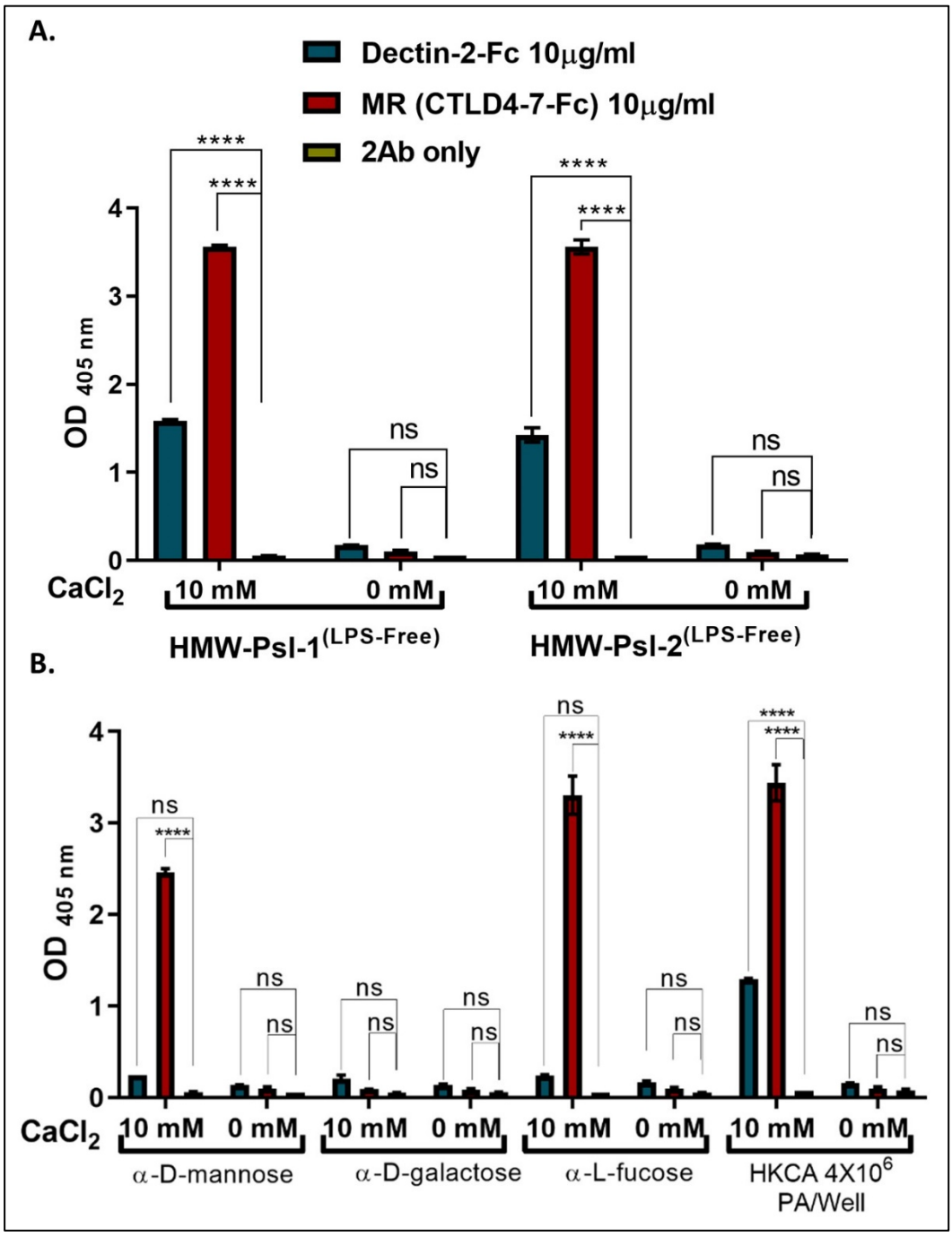


Figure 4.11 Binding of Dectin-2-Fc and MR (CTLD4-7-Fc) to purified HMW-PsI$^{(LPS\text{-}free)}$ is calcium-dependent.

Maxisorp plates were coated with different preparations of carbohydrate purified from the Pel-deficient mutant Δ*wspF*Δ*Pel* diluted in 154 mM NaCl overnight at 37 °C. Dectin-2-Fc and MR (CTLD4-7-Fc) chimeric proteins were added for 2 hr at RT in TSB buffer with or without calcium. The

binding was determined using anti-human IgG Fc-specific antibody conjugated to AP (1:1000) dilution. Absorbance was read at $OD_{405\ nm}$. The analysis was done using two way ANOVA applying Tukey's multiple comparisons test. Graphs show mean +/- SEM of two independent repeats.

4.4.6. Manα-1-2Man inhibits binding of Dectin-2 to purified HMW-Psl

As was mentioned in the chapter introduction, Dectin-2 binds specifically to high mannose structures (Ligands of Dectin-2). Therefore, to confirm that the binding of Dectin-2-Fc to Psl is specific to mannose, we performed inhibition assays in a high salt buffer; the high salt concentration improves the robustness of the inhibition assay (McGreal et al., 2006). We tested the binding of Dectin-2-Fc and MR (CTLD4-7-Fc) to purified HMW-Psl-$2^{(LPS\text{-}free)}$ in either TSB with normal salt (0.154 M) or in TSB with high salt concentration (1M) as described in (2.5). We found that the high salt buffer increases the binding of Dectin-2-Fc while MR (CTLD4-7-Fc) binding was not affected (Figure 4.12 A). Initially, the monosaccharides mannose was tested for its ability to inhibit the binding of Dectin-2-Fc and CTLD4-7-Fc to HMW-Psl-$2^{(LPS\text{-}free)}$ or controls, HKCA $4x10^6$ and α-D-galactose. Pre-incubation of Dectin-2-Fc with a very high concentration of monosaccharides (90mM) in TSB buffer with normal salt (0.154 M) for 30 min at RT did not inhibit the binding of Dectin-2-Fc (data not shown). Recent data indicated selective binding of Dectin-2-Fc to glycans that contain Manα-1-2Man epitopes (Feinberg et al., 2017). As mentioned in the introduction, our lab analysis of our purified HMW-Psl preparation indicated the presence of Manα-1-2Man. To investigate whether Dectin-2-Fc binding to HMW-Psl-$2^{(LPS\text{-}free)}$ observed earlier is through binding to Manα-1-2Man, we tested the binding of Dectin-2-Fc pre-incubated with different concentration of Manα-1-2Man for 30 min at RT prior addition to 96 Maxisorp plates containing purified HMW-Psl-$2^{(LPS\text{-}free)}$ as described in (2.5). Data indicated that Manα-1-2Man was able to inhibit the binding of Dectin-2-Fc and MR (CTLD4-7-Fc) to the purified HMW-Psl-$2^{(LPS\text{-}free)}$ (Figure 4.12 A). The inhibition was dose-dependent, and complete inhibition was reached at the concentration of 36.5 mM. Also, Manα-1-2Man was able to inhibit the binding of Dectin-2 and CTLD4-7-Fc to HKCA (Figure 4.12 B). MR and dectin-2 did not bind galactose-PAA (Figure 4.12 C). These data

indicate that Dectin-2-Fc bind to Manα-1-2Man within our purified HMW-Psl-2$^{(LPS\text{-}free)}$ preparation.

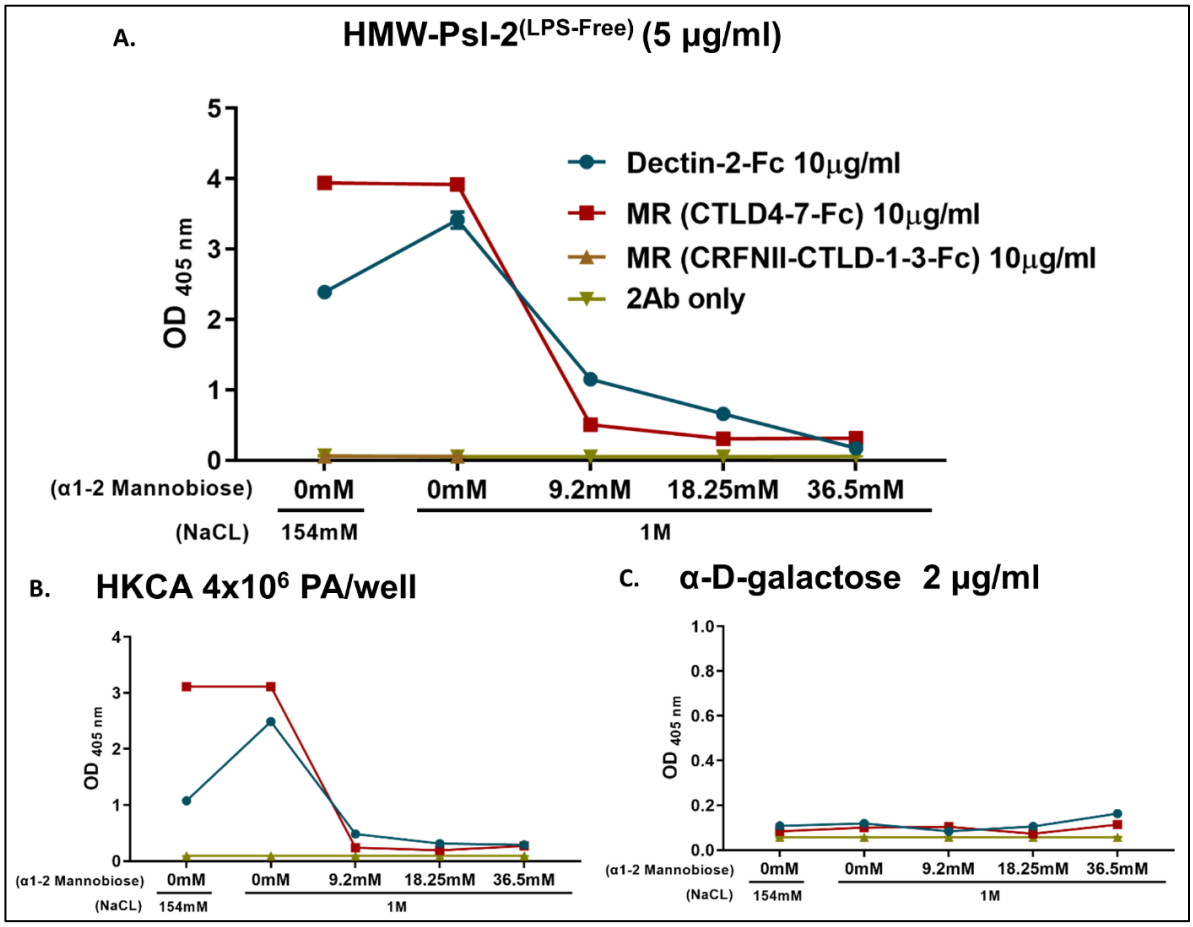


Figure 4.12 Inhibition of Dectin-2-Fc binding to purified HMW-Psl-2$^{(LPS\text{-}free)}$ by Manα-1-2Man.

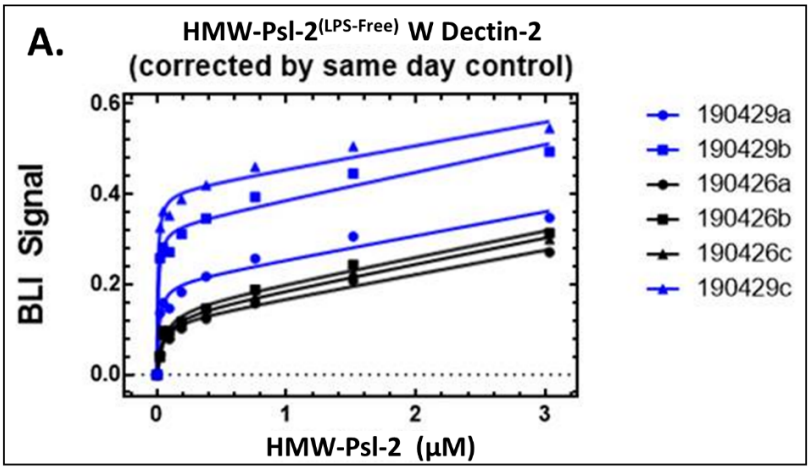
Maxisorp plates were coated with (5 µg/ml) carbohydrate purified from the Pel-deficient mutant Δ*wspF*Δ*pel* diluted in 154mM NaCl overnight at 37°C. Dectin-2-Fc and CTLD4-7-Fc chimeric proteins were pre-incubated with different concentration of Manα-1-2Man in TSB with high salt (1 M NaCl) for 30 min at RT before incubated for 1.5 hours at RT in TSB buffer with high salt. The binding was determined using anti-human IgG Fc-specific antibody conjugated to AP (1:1000) dilution. Controls in 154 mM NaCl were included. Absorbance was read at $OD_{405\ nm}$. Graphs show mean +/- SEM of two independent repeats.

4.4.7. Confirmation of Dectin-2 binding to Psl using biolayer interferometry

After we showed that both Dectin-2-Fc and MR (CTLD4-7-Fc) bind to purified Psl using ELISA, we wanted to confirm the binding using another approach. Our collaborator at East Tennessee State University, Prof David L. Williams, tested the binding of full-length human Dectin-2 (rhDectin-2) against HMW-Psl-2$^{(LPS\text{-}Free)}$ using biolayer interferometry. Results indicated very strong binding of rhDectin-2 to this preparation in a dose-dependent manner (Figure 4.13 A).

After testing the binding of Dectin-2 using biolayer interferometry our collaborator, David L. Williams, kindly compared the binding kinetics of rhDectin-2 against HMW-Psl-2 to other CLRs, biotinylated tetrameric DC-SIGN and full-length human MR (rhMR) and Dectin-1 (rhDectin-1). Analysis of the binding kinetics revealed two interesting observations. First, rhDectin-1 unexpectedly showed binding to HMW-Psl-2$^{(LPS\text{-}Free)}$ considering the fact that Dectin-1 was not reported to bind high mannose (Figure 4.13 B, the third one in the table). Second, Kd for Dectin-2 binding was lower (0.020 mM)) compared to DC-SIGN, MR and Dectin-1 (0.103 mM, 0.114 mM, and 0.091 mM respectively), indicating that in this experimental setting Dectin-2 binding showed the highest binding affinity (Figure 4.13 B).

A.



B.

Receptor	K_D [1] (microMolar)	B_{MAX} [3] (BLI)	$K_{NON-SPECIFIC}$ [4] (BLI/microMolar)
rhDC-SIGN	0.103 (0.062 – 0.143)[2]	0.100 (0.052 – 0.148)	0.0007828 (0.005647 – 0.01001)
rhMR	0.114 (0.088 – 0.147)	0.517 (0.271 – 0.764)	0.009623 (-0.00087 – 0.020116)
rhDectin-1	0.091 (0.066 – 0.126)	0.567 (0.385 – 0.749)	0.02118 (0.01362 – 0.02874)
rhDectin-2	0.020 (0.010 – 0.041)	0.223 (0.129 – 0.317)	0.05556 (0.04893 – 0.06219)

[1]K_D–Equilibrium dissociation constant for the receptor ligand interaction in µM.
[2]95% Confidence intervals in µM.
[3]Bmax – receptor density on the biosensor surface. This value also is indicative of the relative number of receptors bound.
[4]$K_{non-specific}$ – Non-specific binding.

Figure 4.13 Dectin-2 binding using BLI

Tetrameric hDC-SIGN, biotinylated and immobilised on a streptavidin sensor and rhMR, rhDectin-1 and rhDectin-2 immobilised on a Ni-sensor were incubated with different HMW-Psl-2$^{(LPS-free)}$ concentrations. (A) Saturation binding curves for rhDectin-2 are shown. (B) Comparison of the recognition and binding of HMW-Psl-2$^{(LPS-free)}$ by four human full-length pattern recognition receptors. The table shows equilibrium dissociation constants for the receptor-ligand interaction in mM (KD); receptor density on the biosensor surface (BMAX) and non-specific binding (KNON-SPECIFIC). 95% Confidence intervals in mM are shown within brackets. N=6 replicates.

4.4.8. Dectin-2 Fc does not bind PA planktonic cells

To explore the potential of Dectin-2 to bind planktonic PA, we tested binding of Dectin-2-Fc to planktonic bacteria using an ELISA assay as described in (2.5). Results showed no binding of Dectin-2 to planktonic PA (Figure 4.14 A) and confirmed negative MR binding previously described in Alshahrani (2018). Adherence of planktonic cells to the wells was confirmed by ELISA using an antibody against PA (anti-PA) as described in (2.4), results showed the ability of PA to attach to maxisorp plate (Figure 4.14 B).

As mentioned in the introduction, LPS is the major outer membrane component of Gram-negative bacteria (Silhavy et al., 2010) and composed of three different domains: lipid A, core oligosaccharide and O-antigen (Caroff and Novikov, 2019). Dectin-2 was reported to recognise mannosylated O-antigens from several Gram-negative bacteria such as *Hafnia alvei* and *E. coli* (Wittmann et al., 2016). For this, in addition to testing Dectin-2-Fc binding to planktonic cells, we tested Dectin-2-Fc binding to commercially available LPS of PA serotype 10.22 as described in (2.5). Data indicated no binding of Dectin-2 to purified LPS (Figure 4.14 A).

Confocal microscopy was utilised to further validate no binding of Dectin-2-Fc observed with ELISA (Figure 4.14 A). In this assay, DC-SIGN-Fc was used as a positive control, as Alshahrani (2018) indicated that DC-SIGN binds to PA planktonic cells, and binding was independent of Psl. Results confirmed no binding of Dectin-2-Fc observed with ELISA (Figure 4.15)

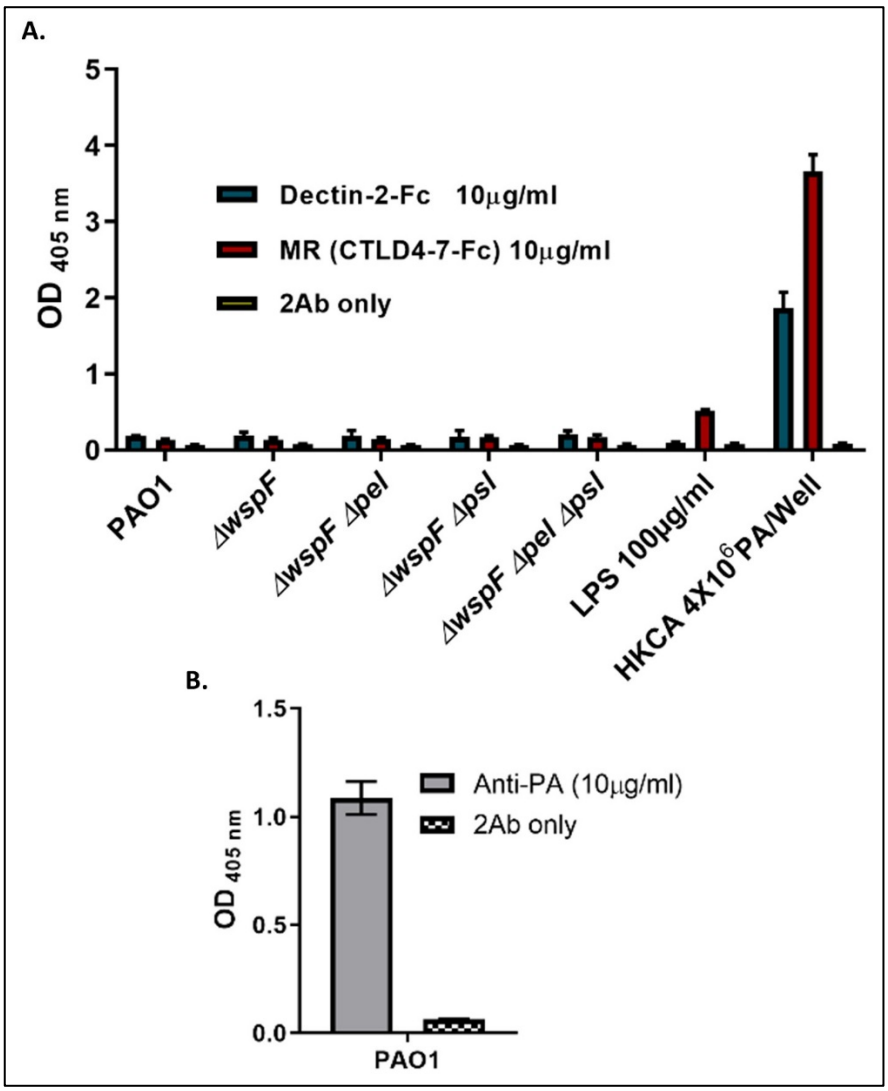


Figure 4.14 Dectin-2-Fc does not bind to planktonic PA and purified LPS in ELISA.

(A) Wells of maxisorp plates were coated over night with 100 µl of (fixed PA suspension adjusted to 0.5 OD_{600nm} in PBS), (LPS at 100µg/ml) and (HCKA 4X10^6 PA/Well) at 4 °C. Dectin-2-Fc or MR (CTLD4-7-Fc) both at (50 µl per well, 10 µg/ml in TSB buffer) were incubated for 2 hr at RT to assess the binding to whole bacteria, LPS or HCKA. The binding was determined using anti-human IgG Fc-specific antibody conjugated to AP (1:1000 dilution). Absorbance was read at $OD_{405\ nm}$. Graphs show mean +/- SEM of three independent repeats. (B) Adherence of planktonic cells to the wells was confirmed by ELISA. Wells of maxisorp plates coated over night with 100 µl of fixed PA suspension adjusted to 0.5 OD_{600nm} in PBS were incubated with rabbit anti-PA polyclonal antibody (10µg/ml in PBS) for 90 min at RT. The binding was detected using anti-rabbit IgG Fc-specific antibody conjugated to AP (1:2000 dilution) for 1 hr at RT. Absorbance was read at $OD_{405\ nm}$. N=2. Graphs show mean +/- SEM of two independent repeats.

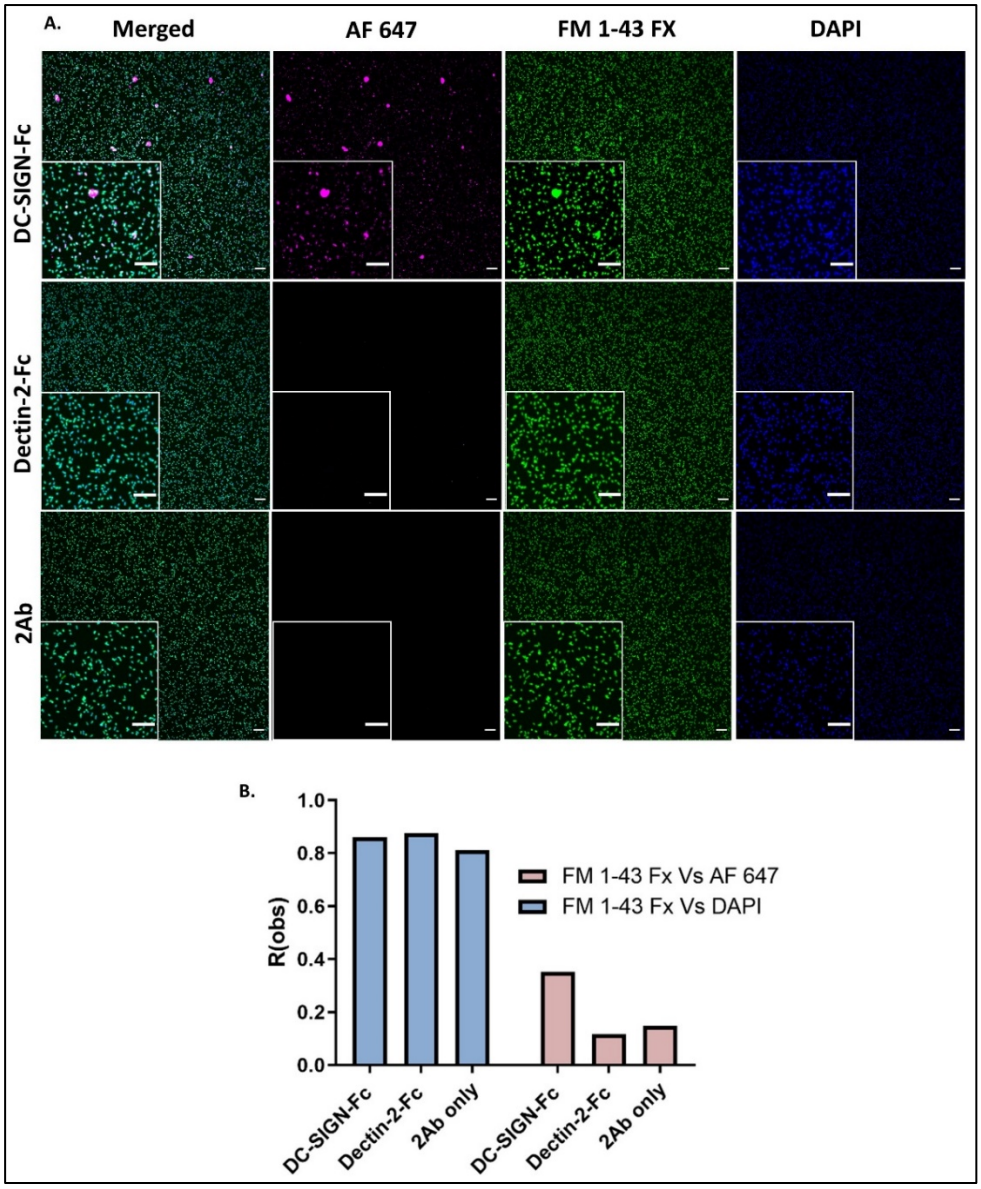


Figure 4.15 Dectin-2 does not bind planktonic PA in an immunofluorescence assay.

A. Channels of Ibidi µ-Slide VI 0.4 slides were coated overnight with 100 µl of fixed PA suspension adjusted to 0.5 OD_{600nm} in PBS) at 4°C. Bacteria cells were stained with FM 1-43 FX before incubated with Dectin-2-Fc or DC-SIGN-Fc (30 µl per channel, 10 µg/ml in TSB buffer) for 2 hr at RT. The binding was determined using goat anti-Human IgG conjugated to Alexa fluor 647 (100 µl per channel, 10 µg/ml in TSB containing 3%(v/v) Goat serum, incubated for 1 hr at RT). DNA was then labelled with DAPI before cultures were mounted in ibidi mounting media and stored at 4°C in the dark. Figure shows one image of each condition acquired using confocal microscopy. No specific labelling was seen with Dectin-2-Fc chimeric protein. Size bar is 4 µm. B. Assessment of the colocalisation of FM 1-43 FX channel with either DAPI (DNA) or Magenta (Fc proteins) was carried using a Fiji plugin that calculates Pearson's correlation coefficient for the two selected channels in each condition (Robs). N=1.

4.4.9. Psl does not induce Dectin-2 signalling

As was pointed out in the introduction to this chapter (Figure 4.3), Dectin-2 binding to high mannose structures trigger signalling through association with FcR-γ. We examined whether Dectin-2 strong binding of HMW-Psl observed in (Figure 4.10, Figure 4.11 and Figure 4.13) would induce Dectin-2-mediated signalling. For this, we utilised 2B4-nuclear factor of activated T-cell (NFAT)-GFP reporter cells expressing both, human Dectin-2 (hDectin-2) and FcR-γ. Activation of these cells induces nuclear translocation and transcriptional activity of NFAT, which can be detected through GFP activity (Ishikawa et al., 2013). FcR-γ-expressing reporter cells were used as a negative control. 2B4-NFAT-GFP reporter cells were cultured with HMW-Psl-1 (LPS contaminated) 500 µg/ml or HKCA 4x10^6 particles/well for 20 hr at 37°C, 5% CO_2. NAFT-GFP activity was assessed using flow cytometry as described (2.19). As shown in (Figure 4.16), GFP expression on hDectin-2-reporter cells was only induced after co-culture with HKCA, which is opposite of what was expected.

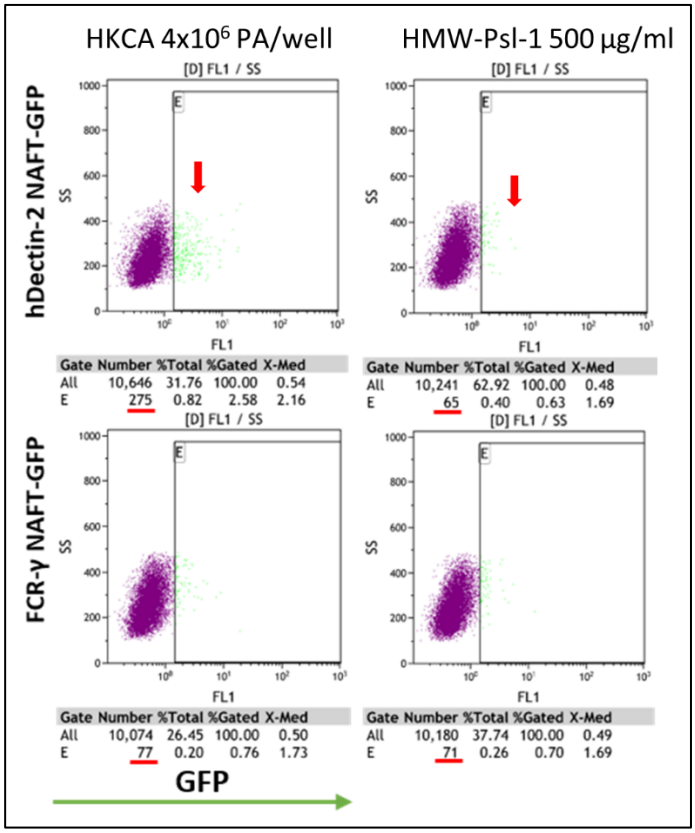


Figure 4.16 huDectin-2 2B4-NFAT-GFP reporter cells do not respond to purified Psl

Wells of maxisorp plates were coated overnight with 100 µl of HMW-Psl-1 (LPS contaminated) 500 µg/ml or HCKA $4x10^6$ PA/Well. Following day 50.000 cells of 2B4-NFAT-GFP reporter cells that either express both hDectin-2 + FcR-γ, or FcR-γ only were incubated for 20 hr. GFP expression was assessed using flow cytometry as described in (2.19). Representative images of three independent repeats.

To confirm our observation seen in figure (Figure 4.16), our collaborator at East Tennessee State University, Prof David L. Williams, tested whether the effect of biofilm-associated carbohydrate on another form of Dectin-2 reporter cells. They employed HEK-Blue™ mDectin-2 cells, an engineered human embryonic kidney HEK293 cells that stably express high levels of murine Dectin-2 as well as the genes of the Dectin-2 signalling pathway. These cells stably express an NF-κB-inducible secreted alkaline phosphatase (SEAP) reporter gene. Upon stimulation of Dectin-2 ligands, the cells express a SEAP, which are measurable by a simple colourimetric assay as described by the manufacturer. As a negative control, they used HEK-Blue™ Null1-v cells, which lacks Dectin-2. Results surprisingly correlated with previous observation presented in (Figure 4.16) and indicated no effect of the HMW-Psl-$2^{(LPS\text{-}free)}$ on Dectin-2 reporter cells which showed a visible response to zymosan particles (Figure 4.17 A).

Along with incubation with Dectin-2 reporter cells, Prof Williams' lab tested whether Dectin-1 reporter cells would show activation in response to biofilm carbohydrates following previous observation of Dectin-1 binding to HMW-Psl-$2^{(LPS\text{-}free)}$ (Figure 4.13). Using cells expressing the two major Dectin-1 isoforms a full-length A isoform and a 'stalkless' B isoform (Heinsbroek et al., 2006), HEK-Blue™ hDectin-1b and HEK-Blue™ hDectin-1a cells, results indicated activation of HEK-Blue™ hDectin-1a but not HEK-Blue™ hDectin-1b reporter cells after incubation with high concentration of HMW-Psl-$2^{(LPS\text{-}free)}$ (100µg/ml) (Figure 4.17 B). This results confirms the earlier observation of hDectin-1 binding to HMW-Psl-$2^{(LPS\text{-}free)}$ (Figure 4.13) and indicate the capability of high concentration of HMW-Psl-$2^{(LPS\text{-}free)}$ to induce Dectin-1 activation (Figure 4.17 B).

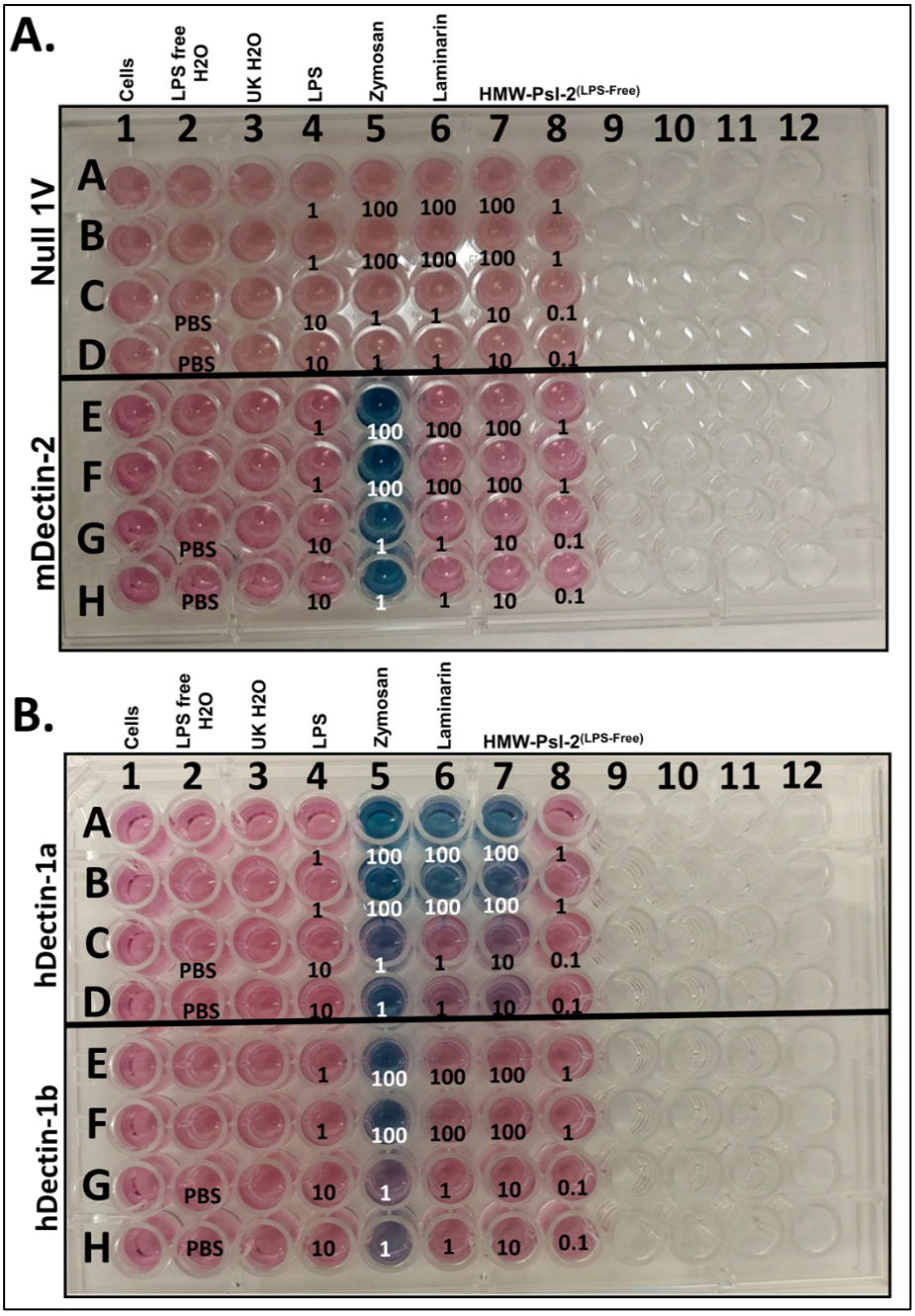


Figure 4.17 mDectin-2 reporter cells and hDectin-1 reporter cells incubation with HMW-Psl-2

(A) Murine Dectin-2 reporter cells (HEK-blue mDectin-2) and control cells (Null 1V), (B) human Dectin-1 reporter cells (HEK-Blue™ hDectin-1a) and control cells (HEK-Blue™ hDectin-1b). All reporter cells were exposed (5 x10^4 cells per well) to different stimuli [LPS (1 and 10 µg/ml), Zymosan (1 and 100 µg/ml), laminarin (100 and 1 µg/ml) and HMW-Psl-2$^{(LPS\text{-}free)}$ (100, 10, 1 and 0,1 µg/ml)] for 18 hr. Plates were read at $OD_{645\,nm}$. Image shows a representative image from 2 independent repeats.

4.4.10. Psl acts as an antagonist for Dectin-2

Even though Dectin-2 displayed high affinity towards HMW-Psl-2$^{(LPS\text{-}Free)}$ (Figure 4.13), the observation in (Figure 4.16 and Figure 4.17) shows that HMW-Psl-2$^{(LPS\text{-}Free)}$ failed to induce Dectin-2 signalling. Therefore, an alternative outcome for the interaction between Dectin-2 and HMW-Psl-2$^{(LPS\text{-}Free)}$ is for these carbohydrates to act as receptor antagonists.

Prof Williams' lab tested this hypothesis; HEK-Blue™ mDectin-2 cells were exposed to different concentrations of HMW-Psl-2$^{(LPS\text{-}Free)}$ before being stimulated with zymosan. Interestingly, results indicated that HMW-Psl-2$^{(LPS\text{-}Free)}$ inhibited the response of Dectin-2 reporter cells to high zymosan doses correlating with the possibility of HMW-Psl-2$^{(LPS\text{-}Free)}$ to act as an antagonist. This inhibition was obtained at lower dose of HMW-Psl-2$^{(LPS\text{-}Free)}$ (0.1, 1 and 10 µg/ml) in agreement with the high affinity detected between Dectin-2 and HMW-Psl-2$^{(LPS\text{-}Free)}$ (Figure 4.13).

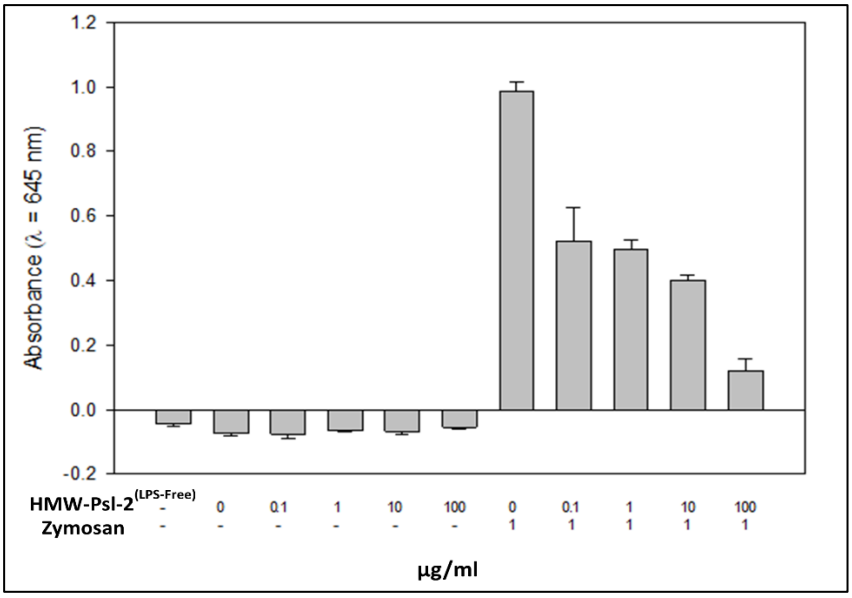


Figure 4.18 HMW-Psl-2$^{(LPS\text{-}free)}$ inhibits Dectin-2-mediated cellular activation.
(A) Dectin-2 reporter cells (5 x10^4 cells per well) were pre-incubated with different concentrations of HMW-Psl-2$^{(LPS\text{-}Free)}$ for 1 hr and then exposed to zymosan (1 µg/ml), for 18 hr. Plates were read at $OD_{645\ nm}$. N=3.

4.5. Summary

- Using a combination of strains with similar high level of cyclic di-GMP and different carbohydrate EPS components, we demonstrated that the recombinant protein Dectin-2-Fc comprising the mannose-binding region of Dectin-2 fused to the Fc portion of human IgG1 binds to biofilms formed by PAO1 and wound isolates.
- Binding of Dectin-2-Fc is highest towards biofilms formed by strains that overexpress Psl, Δ*wspF* and Δ*wspF*Δ*pel*. Nevertheess, data indicated that Dectin-2 bound to strains that lack Psl, indicating that Dectin-2-Fc could bind ligands present in biofilms that are independent of Psl.
- Data indicate no binding of Dectin-2-Fc to PA planktonic cells or to PA10 LPS which suggest that PA expresses ligands for Dectin-2 only when growing as a biofilm.
- In agreement with these findings, two different forms of recombinant Dectin-2 bound to the biofilm purified carbohydrate, Psl.
- Finally, Psl acts as a Dectin-2 antagonist.

4.6. Discussion

In this chapter, we have demonstrated that the C-type lectin receptor Dectin-2 is (1) a direct receptor for PA biofilms and purified Psl, and (2) purified Psl acts as an antagonist for Dectin-2. To our knowledge, this is the first study that reports direct recognition of PA biofilms by Dectin-2. As mentioned in the introduction, Dectin-2 is a transmembrane type II glycosylated protein; the C-terminal end encodes the extracellular region and the N-terminal the cytoplasmic region (Ariizumi et al., 2000). This protein is composed of four parts: (1) a single extracellular CRD domain, (2) a stalk region, (3) a transmembrane region and (4) a short cytoplasmic domain. To transduce signalling upon ligand ligation, Dectin-2 links with the adapter molecule Fc receptor common γ chain (Hara et al., 2007, Saijo et al., 2010).

Dectin-2 reportedly binds several pathogenic microorganisms, and in all instances, the cell wall polysaccharides of these organisms contain high mannose structures (McGreal et al., 2006, Sato et al., 2006, Barrett et al., 2009, Brudner et al., 2013, Miyasaka et al., 2013, Ritter et al., 2010). Competition binding studies indicated that the Dectin-2 CRD binds to monosaccharides with modest affinity and that affinity was significantly higher for mannose-linked (1–2) or (1– 4) to a second mannose residue (Feinberg et al., 2017).

4.6.1. Binding of Dectin-2 to *P. aeruginosa* biofilms

In this chapter, we used two chimeric proteins containing either the extracellular domain of Dectin-2 (aa 44-209) or the CTLD4-7 region of mouse MR fused to the Fc portion of human IgG1. ELISA binding-assays showed binding of Dectin-2-Fc to biofilms of all tested lab strains except to the biofilm deficient strain Δ*wspF*Δ*pel*Δ*psl* (Figure 4.7). When 96 well plates were coated with planktonic cultures of these strains, no binding was detected. This observation was confirmed with confocal microscopy (Figure 4.14). No binding of Dectin-2 to LPS was also observed (Figure 4.14). This finding is in agreement with previous findings showing no binding of Dectin-2 to PA LPS (Wittmann et al., 2016). The same study reported that Dectin-2 recognise mannosylated O-antigen found in two gram-negative bacteria, *Hafnia alvei* and *E. coli* (Wittmann et al., 2016). Altogether, these data suggest that PA display ligand(s) for Dectin-2 only as a biofilm.

The binding pattern of both proteins towards PA biofilms formed by lab strains was similar, with MR (CTLD-4-7)-Fc binding being slightly higher (Figure 4.7). Our data indicated that Dectin-2 preferentially binds Psl overexpressing strains Δ*wspF* and Δ*wspF*Δ*pel* rather than the Pel overexpressing strain Δ*wspF*Δ*psl* (Figure 4.7). This enhanced binding could relate that the biofilms formed by Psl overexpressing strains Δ*wspF* and Δ*wspF*Δ*pel* displayed more ligands for Dectin-2.

As mentioned in the introduction, Dectin-2 possesses an EPN motif in its CRD domain which was reported to facilitate binding to high mannose structures in a calcium-dependent manner

(McGreal et al., 2006, Gavino et al., 2005). Removal of calcium from the assay buffer significantly reduced Dectin-2-Fc binding to PA biofilms, confirming the existence of a mannose structure within PA biofilms recognised by the CRD domain of Dectin-2 (Figure 4.7). Our data also showed minor binding of Dectin-2-Fc and MR to biofilms formed by the strain lacking Psl (Δ*wspF* Δ*psl*) which might indicate that both receptors bind to another ligand within the biofilms that are independent of Psl (Figure 4.7).

Pel is a polymer of N-acetylglucosamine (GlcNAc) and N-acetylgalactosamine (GalNAc) (Jennings et al., 2015). Since Dectin-2 was not reported to bind GlcNAc or GalNAc it is unlikely that the binding was through Pel. This data could be further confirmed in the future using Pel dependent strains such as PA14 and PA14 with Δ*wspF* mutation. The mutation Δ*wspF was* shown to increase the biofilm formation (Hickman et al., 2005). Thus, it would be of interest to investigate if biofilms formed by PA14 Δ*wspF* would exhibit more ligands for Dectin-2. This might further confirm the presence of ligands of Dectin-2 in PA biofilms independent of Psl.

Studies have found that >90% of clinical isolates are capable of expressing Psl under *in vitro* conditions; thus it was essential to test binding of CLRs against biofilms formed by wound clinical isolates (DiGiandomenico et al., 2012, DiGiandomenico et al., 2014, Thaden et al., 2015). Our data show that the binding of DC-SIGN-Fc, Dectin-2-Fc and MR (CTLD4-7-Fc) to biofilms is not restricted to lab strains, but also biofilms generated by a collection of PA wound clinical isolates isolated from different sites (Figure 4.8). As seen previously [(Alshahrani, 2018), PhD thesis], DC-SIGN-Fc binds significantly better than Dectin-2-Fc and MR (CTLD4-7-Fc) to all samples (Figure 4.8). This is possibly attributed to DC-SIGN binding to planktonic cells in addition to biofilms which was reported in (Alshahrani, 2018), PhD thesis.

Examination of the distribution of ligands for DC-SIGN, Dectin-2 and MR on PAO1 biofilms developed on microscopic slides confirmed the enhanced binding of DC-SIGN compared to Dectin-2 and MR and showed that each receptor exhibited different binding profiles (Figure 4.9). Opposite of what seen in the ELISA, we observed enhanced Dectin-2 binding compared

to MR (Figure 4.9). Since biofilm cultured on μ-Slide VI 0.4 slides were subjected to a continuous flow of media opposite of the static condition on 96 well plate, it seems possible that the different binding profiles are due to the two different biofilm generation method which might alter biofilm structure (Azeredo et al., 2017).

The different binding profiles exhibited by DC-SIGN, Dectin-2 and MR might also be due to the different binding affinity towards different high mannose structure within the biofilms. Li et al. (2013) reported the presence of three distinct epitopes in Psl (class I, II, and III), each targeted with different monoclonal antibodies (mAbs) (Li et al., 2013). In a later study, these three antibodies identified the different location of these Psl epitopes within mature PAO1 biofilms as each antibody used showed different staining profile (Ray et al., 2017). Therefore, it is possible that each CLRs may bind a different Psl epitope.

As mentioned in the introduction, Psl is found in two forms (1) cell-associated form with high molecular weight and (2) a low molecular weight soluble form (Byrd et al., 2009, Mann and Wozniak, 2012). Our results in (Chapter 3, Figure 3.10) using the mannose-specific lectin HHA indicated production of Psl in PAO1, which was also confirmed by others using the same lectin (Jennings et al., 2015). HHA binding to PAO1 biofilms was described as a “coating shell” (Ma et al., 2009). In agreement with this, a polyclonal antibody against Psl was reported to bind to the surface of the biofilms (Jones and Wozniak, 2017).

Several studies have shown that for Dectin-2 to bind, ligands need to be terminally exposed based on the analysis of different *Malassezia* species (Ishikawa et al., 2013). Dectin-2 ligands consist of a multivalent terminal α-1,2-mannose attached to glycans, proteins and, presumably, any kind of scaffold. In line with this, even though the cell wall of *C. guilliermondii* and *S. cerevisiae* contains α-1,2-mannose, it is not recognised by Dectin-2, most likely because the α-1,2-mannose is masked with β-1,2-mannose and α-1,3-mannose, respectively (Romero et al., 1999, Shibata et al., 1996). Therefore, it is possible that the observed Dectin-2-Fc binding to PA biofilms is to Psl exposed on the outer biofilm structure.

4.6.2. Binding of Dectin-2 to purified carbohydrates from biofilms

As stated earlier, in this chapter, three independent preparations of the mannose rich carbohydrate Psl were employed (Psl-1, Psl-2 and Psl-3). Preparations 1 and 3 contained similar carbohydrate ratios and all were divided based on molecular weight after gel filtration into high (HMW) and low (LMW) molecular weight (Figure 4.5 and Figure 4.6).

Dectin-2-Fc and MR (CTLD4-7-Fc) exhibited robust binding to all preparations, and both CLRs bound better to the higher molecular weight carbohydrates (Figure 4.10). These results might correlate with the biofilm binding observed by confocal microscopy (Figure 4.9) since both CLRs exhibited binding to aggregates which are possibly the location of the biofilm-associated/high molecular weight Psl (Byrd et al., 2009, Mann and Wozniak, 2012). The fact that removal of the calcium caused a significant reduction of Dectin-2-Fc and MR (CTLD4-7-Fc) binding to high molecular weight Psl confirm that the binding occurs through the CRD domain of each lectin (Figure 4.11).

EPS-associated proteins such as LecB and CrdA have been reported to bind Psl and contribute to the biofilm formation (Borlee et al., 2010, da Silva et al., 2019). As was pointed out in the Data leading to this study, no major protein contamination was detected in all Psl preparation used in this study. Therefore, it is possible that the moderate lectin binding to biofilms compared to the robust binding to purified Psl might be due to the competition of Psl binding from other EPS-associated Psl binding proteins such as LecB and CrdA.

As mentioned earlier, Feinberg et al. (2017) reported selective binding of Dectin-2-Fc to glycans that contain Manα-1-2Man epitopes. Analysis of our purified Psl preparation indicated the presence of Manα-1-2Man (Singh et al., 2020). In the current study, pre-incubation of Dectin-2-Fc and MR (CTLD4-7-Fc) with Manα-1-2Man prior to performing the Psl-binding assay inhibit the binding of Dectin-2-Fc and CTLD4-7-Fc to purified Psl (Figure 4.12). This result correlates with Dectin-2 specificity to Manα-1-2Man mentioned in (Feinberg et al., 2017) and might indicate that both receptors were binding to the Manα-1-2Man structure within the

Psl preparation although the sugar specificity for MR-CTLD4-7 is broader (Martinez-Pomares, 2012).

Binding of Dectin-2 to HMW-Psl was further confirmed by Prof David L. Williams, at East Tennessee State University, utilising the full-length rhDectin-2 (Figure 4.13 A). Binding of rhDectin-2 to HMW-Psl was compared to other CLRs, biotinylated tetrameric DC-SIGN and full-length rhMR and rhDectin-1(Figure 4.13 B). Analysis of the binding kinetics revealed two interesting observations. First, rhDectin-1 unexpectedly showed binding to Psl despite the fact that Dectin-1 was not reported to bind high mannose structures. Second, the affinity for Dectin-2 binding was (0.020 mM) compared to DC-SIGN, MR and Dectin-1 (0.103 mM, 0.114 mM and 0.091 mM, respectively), indicating that in this experimental setting Dectin-2 binding showed the highest binding affinity.

As mentioned in the main introduction, the most-reported Dectin-1 ligand is the β-1, 3-linked glucan found in MTB, *C. albicans*, *Aspergillus fumigatus*, and zymosan a *Saccharomyces cerevisiae* cell wall component (Tone et al., 2019). It is somewhat surprising that Dectin-1 binding to HMW-Psl-2 was noted in this assay (Figure 4.13). This finding was further confirmed using hDectin-1a reporter cells that were activated using high Psl doses (Figure 4.17). The underlying cause of this binding is unclear; however, a possible explanation for these results may be the presences of β-glucan in our purified Psl. Because the activation of Dectin-1 reported cells was only observed with a high concentration of Psl, it might indicate that the β-glucan concentration in our Psl preparation could be so low that is below the level of detection. The presence of β-glucan in PA was previously reported (Lequette et al., 2007). A later study confirmed the presence of 1,3-β-D-glucan in seven PA isolates from the blood of immunocompromised patients, which might alter the diagnosis of invasive fungal infection and lead to false-positive results (Mennink-Kersten et al., 2008). In future investigations, it might be possible to utilise the 1,3-β-D-glucan reactivity assay to assess the presence of β-glucan in Psl preparations.

4.6.3. Antagonistic activity of HMW-Psl against Dectin-2

In this study, Dectin-2 exhibited very high affinity towards HMW-Psl$^{(LPS\text{-}Free)}$ characterised by the low 0.020 mM KD value (Figure 4.13). Contrary to expectations, incubation of HMW-Psl$^{(LPS\text{-}Free)}$ with hDectin-2-NAFT-GFP reporter cells and HEK-Blue™ mDectin-2 cells failed to induce Dectin-2-mediated signalling when compared to other Dectin-2 ligands HKCA and Zymosan used in (Figure 4.16 and Figure 4.17) respectively. These findings led us to test the possibility of HMW-Psl to work as an antagonist. A competition assay incubating the HEK-Blue™ mDectin-2 with different concentration of the known Dectin-2 agonist, Zymosan (McGreal et al., 2006) after incubating with different concentration of HMW-Psl$^{(LPS\text{-}Free)}$ showed inhibition of zymosan-medited activation of HEK-Blue™ mDectin-2 cells in agreement with the high affinity detected between Dectin-2 and HMW-Psl-2$^{(LPS\text{-}Free)}$ (Figure 4.7). This might suggest for the first time an antagonistic effect for Psl against Dectin-2 and suggests that no signalling resulted from Dectin-2 and Psl ligation.

One possible explanation of this antagonistic activity is that in addition to high mannose structures in the purified carbohydrate (HMW-Psl-2$^{(LPS\text{-}Free)}$) the preparation might contain a minimal amount of a particular molecule that interferes with Dectin-2 signalling. A similar observation was noted with Laminarin ((1→3)-β-D-glucans), which was initially described as an antagonist of Dectin-1 (Brown and Gordon, 2001); however, subsequent studies indicated that it also works as Dectin-1 agonist (Goodridge et al., 2007). A recent study compared different preparations of laminarin and indicated that differences in agonist and antagonist activity depend on the physicochemical properties, purity and structure of the laminarin preparation (Smith et al., 2018a).

It has been suggested that different gram-negative bacteria are capable of releasing molecules that interfere with the activity of Syk. For example, *Salmonella* secretes protein tyrosine phosphatases SptP which prevent the phosphorylation of Syk in mast cells and

suppresses degranulation (Choi et al., 2013). In PA, it was shown that the Las QS system indirectly controls c-di-GMP levels through the tyrosine phosphatase TpbA (Ueda and Wood, 2009). TpbA was found to also contribute to biofilm formation by positively regulating the eDNA release and bacterial cell lysis (Ueda and Wood, 2010). It is possible that the preparation might contain a very low amount of TpbA, which might interfere with Dectin-2 signalling, but was below detection. To test this hypothesis, future studies could incubate the HMW-Psl with cell lines that express a certain receptor that signals through Syk, but does not bind to HMW-Psl. The idea would be to activate the receptor with the receptor-ligand in the presence of HMW-Psl to confirm that no molecule in the HMW-Psl preparation that interferes with Syk phosphorylation.

Both Dectin-1 and Dectin-2 trigger signalling through Syk (Saijo and Iwakura, 2011). However, Dectin-1 activates Syk directly through an hemITAM at its cytosolic domain, while Dectin-2 activates Syk through association with the ITAM-containing FcR-γ (Robinson et al., 2009). Ligation of Dectin-1 or Dectin-2 by β-glucan or *C. albicans* respectively, leads to the phosphorylation of ITIM-bearing receptors, which recruit the Src homology 2 (SH2). Phosphorylated SHP-2 then works as a scaffold protein recruiting Syk to Dectin-1 or Dectin-2-FcR-γ, leading to the activation of Syk and Syk-dependent signalling cascade (Deng et al., 2015). SHP-2 possesses two SH2 domains at the N-terminus, N-SH2 and C-SH2 domain (Deng et al., 2015). It was indicated that SHP-2 is recruited to Dectin-1 hemITAM via its N-SH2 domain as deletion of the N-SH2 domain only, stopped the association of SHP-2 and Dectin-1. On the other hand, both SH2 domains N-SH2 and C-SH2 were found to be essential in recruiting Syk to FcR-γ (Deng et al., 2015). Thus it could be speculated that the carbohydrate preparation might contain molecules that interfere with C-SH2 only but not N-SH2 as Dectin-1 induced signalling upon stimulation with HMW-Psl.

Additionaly, further research should be undertaken to investigate the fate of Psl upon binding to Dectin-2. For example, Dectin-2 expressing cell line or human monocytes (highly expressing Dectin-2) could be employed and stained with LysoTracker to track the fate of Psl

upon ligation as shown in (Sato et al., 2006). Further work needs to be done to determine to wither Dectin-2 binding to HMW-PSI induces Syk, SHP-2 and ITAM phosphorylation.

Overall, the results of this chapter indicate that PA biofilms display ligand for Dectin-2 and that binding of these ligands inhibit receptor activity. The potential consequences of Dectin-2, DC-SIGN, and MR binding to biofilms and Psl will be discussed on the following chapter with suggestions for future work and describe how the findings might translate to in vivo situations. (Chapter 5).

Chapter 5. Interaction of human Dendritic cells with PA Biofilms

5.1. Introduction

Dendritic cells (DCs) are essential in orchestrating adaptive immunity against different pathogens such as bacteria, viruses and fungi (Geijtenbeek and Gringhuis, 2009). DCs and macrophages express pattern recognition receptors (PRRs) to detect pathogens and trigger innate signalling pathways leading to cells activation and cytokine release that impact on the ensuing T cell activation and differentiation. Such PRRs include Toll-like receptors (TLRs) and C-type lectins receptors (CLRs). Following pathogen binding, TLRs trigger signalling pathways through MyD88 or TRIF adapter proteins, leading to activation of transcription factors such as NF-κB (Kawasaki and Kawai, 2014). This research focus on a subset of PRRs (CLRs), which play an important role in pathogen recognition and induction of adaptive immunity (Geijtenbeek and Gringhuis, 2009). CLRs are able to independently induce immunity or modulate responses that are triggered by other PRRs (Zelensky and Gready, 2005).

Efficient pathogen-specific immunity involves T-cell differentiation induced by complex cytokine profiles, established following PRRs recognition of pathogen-associated molecular patterns (PAMPs) (Mogensen, 2009). Growing evidence supports the idea that signalling cascades generated by myeloid cells through CLRs engagement might have adverse effects on the outcome of infections. It has been shown that several CLRs recognise different viruses and promote viral spread and transmission (Geijtenbeek et al., 2000a, Lambert et al., 2008, Simmons et al., 2003). HIV, CMV, HCV and Ebola enter DCs through binding to DC-SIGN, where they are protected from lysosomal degradation, facilitating the transmission of these viruses to T-Cells (Geijtenbeek et al., 2000a, Halary et al., 2002, Ludwig et al., 2004, Alvarez et al., 2002). This feature is not exclusive to DC-SIGN, MR binding to HIV in macrophages also protects the virus and favour transmission of the virus to T-cells (Nguyen and Hildreth,

2003). LPS induces DC maturation through TLR-4 signalling (Ardavín et al., 2001). It was reported that ManLAM binding to DC-SIGN prevents mycobacteria- or LPS-induced DC maturation, suggesting that DC-SIGN, upon binding of ManLAM, interferes with TLR-mediated signals and suppress DC function (Geijtenbeek et al., 2002).

As mentioned in the main introduction, the opportunistic pathogen PA is considered a threat as can cause devastating infections in patients suffering underlying disease (e.g. cancer and cystic fibrosis (CF)) or individuals with disrupted non-specific host defences (e.g. burns, catheters, ventilators and surgery). Several factors account for the ability of PA to cause these infections. Besides its ability to adapt to different environments, the bacterium is intrinsically resistant to a broad spectrum of antimicrobial agents (Lister et al., 2009). In addition, PA is able to generate biofilms and use a wide array of virulence determinants to interact with the immune system (Gellatly and Hancock, 2013). Biofilms promote PA survival by increasing resistance to antimicrobial agents and immune assault (Mulcahy et al., 2014). Within biofilms, bacterial cells are enclosed in extracellular polymeric substances (EPS) consisting of carbohydrates, nucleic acids and proteins (Colvin et al., 2012, Irie et al., 2012). Three major carbohydrates are produced by PA: Psl, Pel and alginate, with Psl and Pel playing a key role in biofilm structure in a strain-dependent manner (Colvin et al., 2012, Irie et al., 2012, Franklin et al., 2011). Psl is neutral and mannose-rich (Byrd et al., 2009). Pel is cationic and largely composed of N-acetyl-galactosamine and N-acetyl-glucosamine (Jennings et al., 2015).

Bacteria-induced cellular activation and subsequent release of cytokines have been generally regarded as a protective mechanism by the immune system (Steichen et al., 2013, Dorhoi et al., 2010). In the case of PA biofilm infections, though, these reactions are very deleterious, leading to enhanced tissue damage and decreased bacterial clearance (Palomo et al., 2014, Rowe et al., 2005). Here we tested the hypothesis that the carbohydrate composition of PA biofilms affects the activation of human myeloid cells. Our data presented in Chapter 4, indicated strong binding of PA biofilms and purified Psl to three CLRs MR, DC-SIGN and Dectin-2. We hypothesized that engagement of CLRs expressed by human myeloid cells

through EPS recognition constitute a host factor granting an advantage to PA and facilitate the establishment of chronic infection. In this chapter, we first investigated the expression of DC-SIGN, MR, Dectin-1 and Dectin-2 on two populations of human myeloid cells moDCs and M-CSF macrophages. Second, we assessed the capability of PA biofilms and/or purified Psl to influence the activation of moDCs. A combination of flow cytometry, cytokine and confocal analysis were employed to investigate these questions. Most of the work in this chapter was generated together with Dr. Sonali Singh, unless otherwise stated.

5.2. Hypothesis

Our data in (Chapter 4, section 4.1.7 and 4.5) showed that the CTLD4-7 region of MR, the extracellular domain of DC-SIGN and the CRD of Dectin-2 recognise PA biofilms and purified EPS carbohydrate. In this chapter we aim to investigate whether the carbohydrate composition of PA biofilms affect the activation of human myeloid cells through CLR engagement. We hypothesized that engagement of CLRs through EPS recognition provides an advantage to the bacteria by modulating the immune cells towards a regulatory phenotype, hence facilitating the establishment of chronic infection (Figure 5.1).

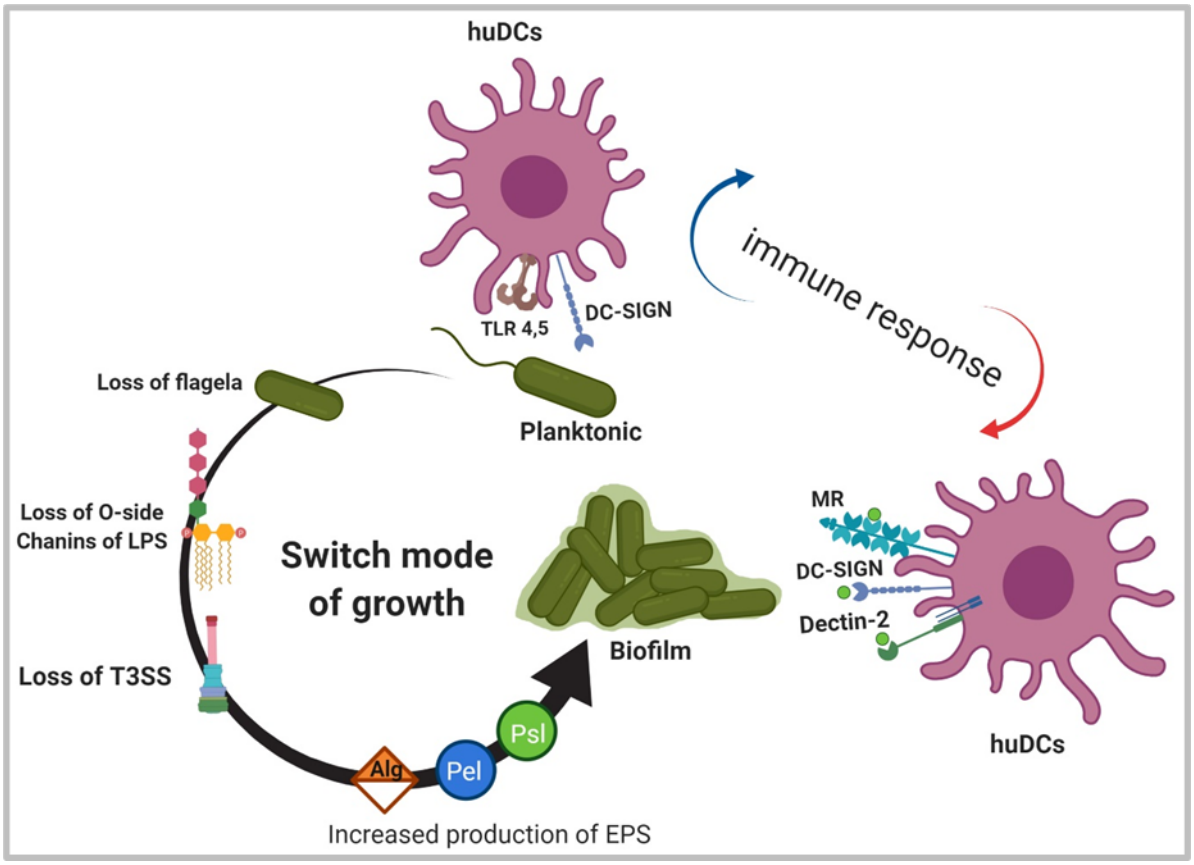


Figure 5.1 Role of lectin receptors during PA infection.

Bacteria are present in two separate ways: planktonic (free floating) and biofilms (cells aggregated embedded in a matrix). Planktonic bacteria display traits associated with enhanced cytotoxicity (T3SS+) and capacity to activate immune cells (Flagellin+) and may trigger several signalling pathways by interaction with PRRs (TLRs are shown as an example). In this case, DC-SIGN, possibly through the recruitment of Raf-1, will modulate cell activation and lead to an increase in the development of IL-10 (as seen in other pathogens). Biofilms co-stimulates DC-SIGN (through biofilm-associated carbohydrate and ligands in planktonic cells), MR and Dectin-2 (through biofilm carbohydrates). In addition, biofilm-associated bacterial cells display decreased capacity to induce cytotoxicity and activate pattern recognition receptors. In this case, MR, DC-SIGN and Dectin-2 may modulate the already altered cell activation, which will possibly contribute to more immune modulation away from the pro-inflammatory Th1-dominated reactions.

5.3. Aims

1. Investigate the expression of DC-SIGN, MR, Dectin-1 and Dectin-2 on M-CSF macrophages and moDCs.
2. Assess the capability of PA biofilms to influence the activation of moDCs by:
    a. Testing the effect of biofilms with different EPS components on moDCs.
    b. Test how highly purified HMW-Psl preparations modulate the activation of moDCs incubated with PA biofilms formed by strains lack Psl.
    c. Testing the contribution of DC-SIGN, MR and Dectin-2 on moDCs-biofilm interaction.

5.4. Results

5.4.1. Analysis of DC-SIGN, MR, Dectin-1 and Dectin-2 expression on human myeloid cells

5.4.1.1. RNAseq analysis of DC-SIGN, MR, Dectin-1 and Dectin-2 expression on human macrophages.

After we confirmed that the CTLD4-7 region of MR, the extracellular domain of DC-SIGN and the CRD of Dectin-2 recognise PA biofilms and purified EPS carbohydrate (Chapter 4, section 4.1.7 and 4.5), it was essential to search for human myeloid cells expressing the CLRs employed in this study. These cells can then be utilised to assess the contribution of CLRs on the immune recognition of PA biofilms. The first set of experiments aimed to analyse the expression of CLRs investigated in this study on human myeloid cells. We exploited a novel RNAseq data set produced in the lab to explore the expression of DC-SIGN, MR, Dectin-1 and Dectin-2 at the transcriptional level in human monocyte-derived macrophages (Sirina Muntaka, unpublished).

Results include macrophages generated in the presence of M-CSF and left untreated (M-CSF-Macrophages) or treated with LPS, IFN-γ, IL-4 or IFN-γ+LPS. Samples were collected at 4 h post-treatment. Data indicated that in M-CSF-macrophages highest expression was observed for MR followed by DC-SIGN and Dectin-1 respectively (Figure 5.2). DC-SIGN gene expression was relatively low compared with MR and enhanced with the addition of IL-4. Data also showed positive effect of IL-4 on the expression of MR and Dectin-1. Levels of Dectin-2 transcripts were very low compared to MR, and LPS had a small positive effect on Dectin-2 levels. In the other hand, data showed negative effect of LPS (with or without IFN-γ) on the expression of DC-SIGN, MR and Dectin-1. Treatment with IFN-γ showed no effect on any of CLRs expect for MR, which increased (Figure 5.2). These data suggest that human macrophages would possibly be applicable to establish MR contribution to biofilm recognition, but not the contribution of DC-SIGN and Dectin-2.

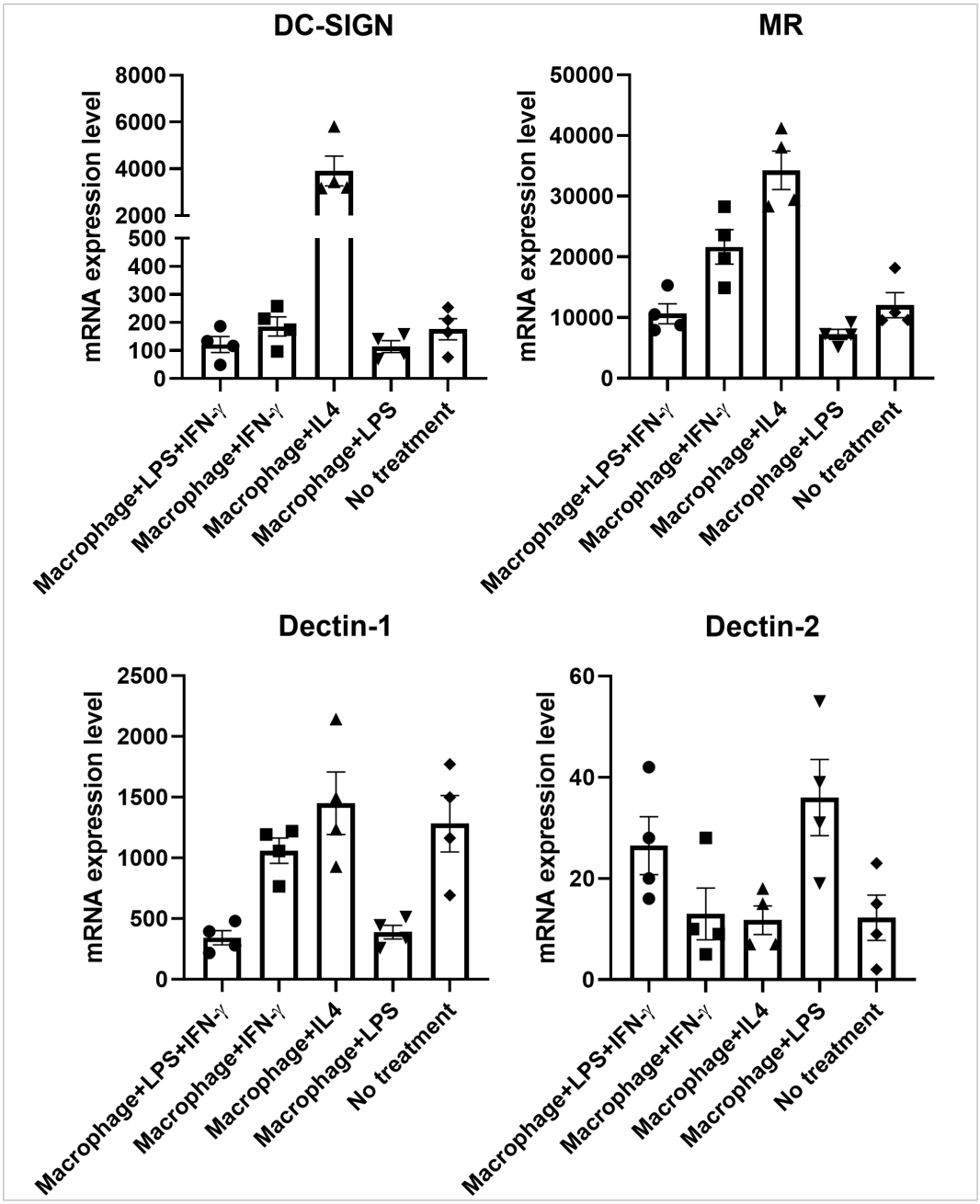


Figure 5.2 mRNA levels of DC-SIGN, MR, Dectin-1 and Dectin-2 on M-CSF-Macrophages

Cells generated from CD14+ monocytes in the presence of M-CSF (50 ng/ml) for 6 days were harvested and seeded (1.2 x 10^6 cells/well) on 6 well TC plate for overnight incubation at 37 °C. On day 7 cell were treated with (20 ng/ml) of LPS, IFN-γ and/or IL-4 for 4 hr at 37 °C. Following incubation total cellular RNA were extract using (ReliaPrep™ miRNA Cell and Tissue Miniprep System) following manufacture's protocol. Gene expression profiles were determined by RNAseq. Graphs show mean +/- SEM of four independent repeats. (Sirina Muntaka, unpublished).

5.4.1.2. Flow cytometry analysis of DC-SIGN, MR, Dectin-1 and Dectin-2 expression on huDCs

After we found that human macrophages are not suitable to establish the contribution of DC-SIGN and Dectin-2 to biofilm recognition (Figure 5.2); we explored the expression of these receptors along with the expression of MR in moDCs using flow cytometry. CD14+ monocytes purified as described in (2.8) were differentiated into moDCs in the presence of GM-CSF and IL-4 (Sallusto and Lanzavecchia, 1994, Chapuis et al., 1997), harvested on day 6, and analysed by flow cytometry (2.11) using commercial antibodies specific for MR, DC-SIGN, Dectin-2 and Dectin-1. Unstained and relevant antibody isotypes were used as controls.

Results demonstrated that DC-SIGN, MR, Dectin-1 and Dectin-2 were present in all moDCs tested (Figure 5.3 A). Expression of MR and DC-SIGN is higher than that of Dectin-1 and Dectin-2, with MR showing the highest MFI (Figure 5.3 B). The MFI values of MR range from (47.2262) to (387.6422) with most values being between (200) and (300). The MFI values of DC-SIGN range from (12.96591) to (60.21333) with most values being between (20) and (30). Expression of Dectin-1 was lower than MR and DC-SIGN with MFI ranging from (4.929825) to (9.829932) with most values being between (5) and (8) (Figure 5.3 B). Findings confirmed previous observation of relatively low expression of Dectin-2 on moDCs (Carter et al., 2006) with MFI of Dectin-2 being the lowest and ranging from (2.189873) to (3.935484) with most values being between (2.5) and (3.5). As both Dectin-1 and Dectin-2 expression were relatively low, it is important to note that the data presented need to be validated using positive control cells and/or RNA analysis. In terms of the number of cells positive for each CLR, almost 100% of the cells express MR, 80-90% express DC-SIGN, while Dectin-2 is expressed by 40-60% of the cells and Dectin-1 was the lowest with a negligible number of the cells express it (Figure 5.3 B). These data indicate that moDCs are best suited to investigate the contribution of MR and DC-SIGN to biofilm recognition but would not for investigating Dectin-2 contribution.

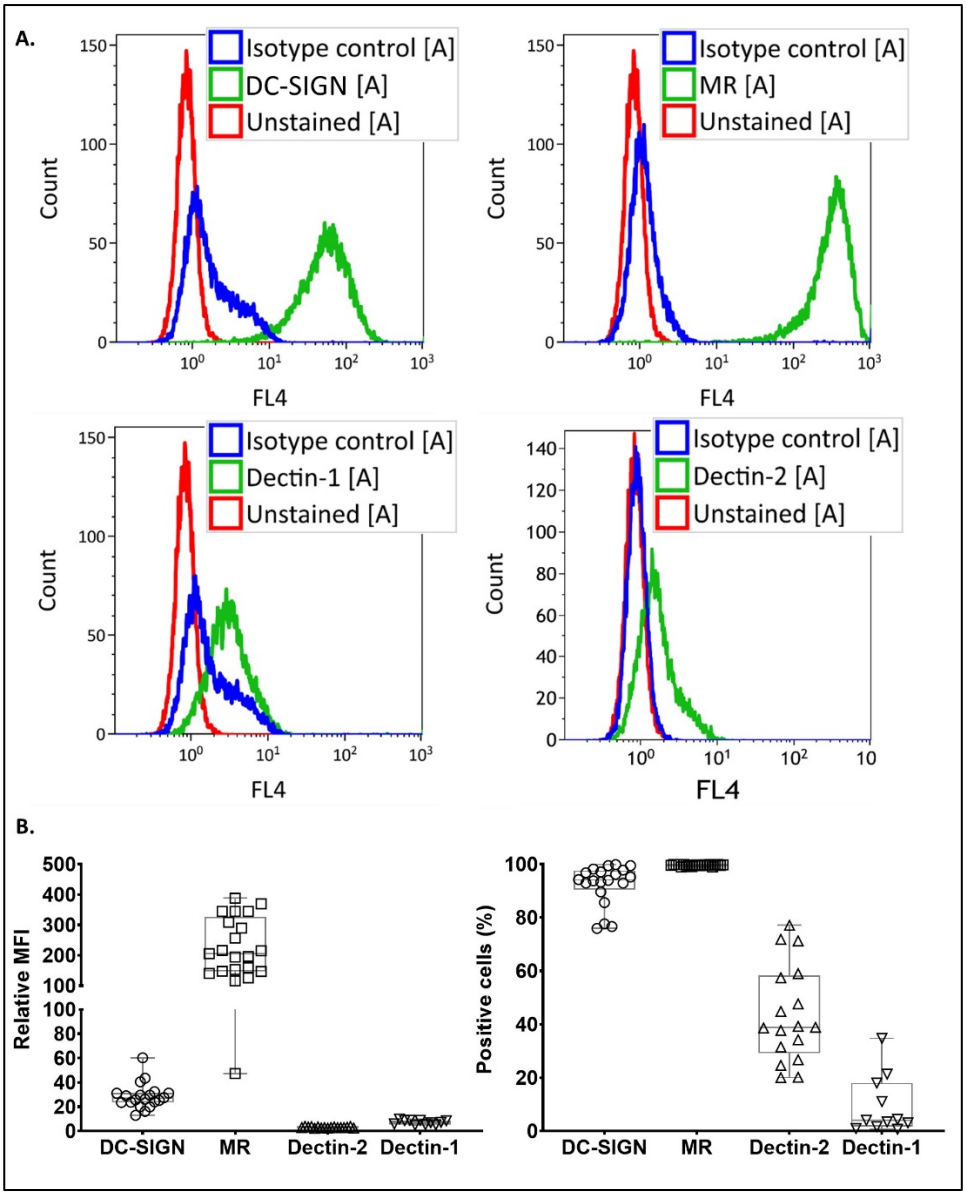


Figure 5.3 Flow cytometry analysis of DC-SIGN, MR, Dectin-2 and Dectin-1 expression on moDCs

moDCs generated from CD14+ monocytes in the presence of GM-CSF and IL-4 (50 ng/ml) for 6 days were tested for MR, DC-SIGN, Dectin-1 and Dectin-2 expression by flow cytometry. moDCs were re-suspended in X-Vivo-15 media in a 15 ml falcon tube at a density of 1×10^6 cells/ml, centrifuged and re-suspended in 1 ml of 5% (v/v) human serum in PBA solution, and incubated for 1 hr at 4°C. After washing, the cell density was adjusted to 100,000 cells/100µl of PBA and cells were incubated with mouse anti-human monoclonal antibodies or their matched isotype controls: CD206 (MMR)-Allophycocyanin (647), CD209 (DC-SIGN)-647, CLEC6A (Dectin-2)-APC, or CLEC7A (Dectin-1)-APC for 1 hr at 4°C. Cells were then washed and fixed with 0.5% (v/v) PFA and analysed using a FC500 Beckman Coulter flow cytometer; 10,000 events were collected. Data were analysed using Kaluza Software 1.5a. Data are from 25 independent preparations and show consistent expression of both MR and DC-SIGN in all instances and low expression of Dectin-2 and Dectin-1. A. Representative histograms for each labelling. B. Representation of relative MFI and the percentage of positive cells for all markers. Relative MFI was calculated as the MFI obtained by the specific antibody divided by the MFI obtained for the isotype control. Percentage of positive cells

was claucated by the following. First, A dot plots of the markers vs. side scatter for the isotype control, unstained, and stained conditions was made. Then the quadrants were set such that in the isotype control the positive cells were <= 1% (% Gated cells in the plots). These same quadrants were copied to the stained condition. The value obtained for % gated cells in the positive quadrant is what was reported as "% positive cells" for the marker.

5.4.2. The effect of biofilm carbohydrate on the cytokine response of human dendritic cells

5.4.2.1. Effect of purified Psl on cytokine production by moDCs

Before proceeding to examine the effect of purified Psl on cytokine production by moDCs it is important to return (briefly) to the work done by Sonali Singh to characterize and purify Psl form PA biofilms (4.1.7). As previously stated, Psl preparation generated were divided into high (>45 kDa, HMW-Psl) and low molecular weight (<45 kDa, LMW-Psl) based on protein standards by gel filtration chromatography (4.1.7). DC-SIGN and MR-CTLD4-7 was shown to bind to HMW-Psl and LMW-Psl from different preparations but binding to HMW-Psl was stronger (Figure 4.5). Initial NMR analysis indicated an increased level of impurities in LMW-Psl compared to HMW-Psl (data not shown), hence further work largely focused on HMW-Psl preparations. Silver staining of two preparation of HMW-Psl highlighted large LPS contamination (Figure 5.4 A). Thanks to substantial efforts placed by our lab members (Sonali, Singh and Darrel Jackson), LPS removal from HMW-Psl was finally achieved using an endotoxin removal column and confirmed using SDS-PAGE (Figure 5.4 B) and TLR4-transduced cells (Data not shown). ELISA binding assay indicated that HMW-Psl$^{(LPS\text{-}free)}$ retained the ability to bind DC-SIGN and MR-CTLD4-7 (Figure 5.4 C).

After we confirmed the expression of DC-SIGN and MR on moDCs (Figure 5.3) and based on the data presented in (Figure 4.5), which indicated strong binding of PA biofilms and purified Psl to MR and DC-SIGN, we explored the possibility of the mannose-rich HMW-Psl-2$^{(LPS\text{-}free)}$ to induce cytokines production by moDCs (DC-SIGN+, MR+, Dectin-1^{low}, Dectin-2$^{low/-}$, Figure 5.3). Data indicated that HMW-Psl-2$^{(LPS\text{-}free)}$ (10, 1, 0.1 µg/ml) in isolation did not induce cytokine production by moDCs nor modified the response of moDCs to purified *E. coli* LPS (data not shown).

Following this observation, we explored the possibility of HMW-Psl-2$^{(LPS\text{-}free)}$ altering the cytokine production of human moDCs in response to biofilms that lack Psl (Δ*wspF*Δ*pel*) and

planktonic cultures (Δ*wspF*Δ*pel*Δ*psl*). For this, cultures of Δ*wspF*Δ*Psl* and Δ*wspF*Δ*Pel*Δ*Psl* were prepared in 96 wells TC plates as described in (2.3) and shown in (Figure 3.2 A). Following 24 hr incubation, cultures were fixed with 4% PFA in PBS for 10 min at 4°C and washed. Then HMW-Psl-2$^{(LPS\text{-}free)}$ was added at different concentration (0, 0.01, 0.1, 1, 10 µg/ml) and incubated for 1 hr before moDCs (5 x 10^4 per well) were added and incubated for 4 hr at 5% CO_2/37°C. Following incubation, supernatants were collected and stored at -80°C until analysis for cytokine release. Multiplex assay was used as described in (2.16) to analyse IL-1β, IL-23, IL-6 and IL-10, and ELISA was used as described (2.16) to analyse TNF-α, MCP-1 and Gro-α.

Results presented in (Figure 5.5 B) confirmed previous observation that moDCs stimulated with different concentration of HMW-Psl-2$^{(LPS\text{-}free)}$ (0.01, 0.1, 1 or 10 µg/ml) did not induce any of the tested cytokines. Additionally, information in (Figure 5.5 B) demonstrated that there is a considerable variation among different donors in terms of cytokines release upon stimulation with bacterial cultures in the presence and absence of different concentrations of HMW-Psl-2$^{(LPS\text{-}free)}$. Although, certain cytokines exhibited a downward or an upward trend after treatment with different concentration of HMW-Psl-2$^{(LPS\text{-}free)}$, no statistical significance could be detected in any conditions. From the data in (Figure 5.5 B) it can be seen that IL-1β production increased when moDCs were incubated with Δ*wspF*Δ*psl* cultures compared to *ΔwspFΔpelΔpsl* cultures, addition of HMW-Psl-2$^{(LPS\text{-}free)}$ didn't altered this response significantly. Overall, these findings suggest that HMW-Psl-2$^{(LPS\text{-}free)}$ in isolation did not induce cytokine production by moDCs nor modified the response of moDCs to PA biofilms or planktonic cells.

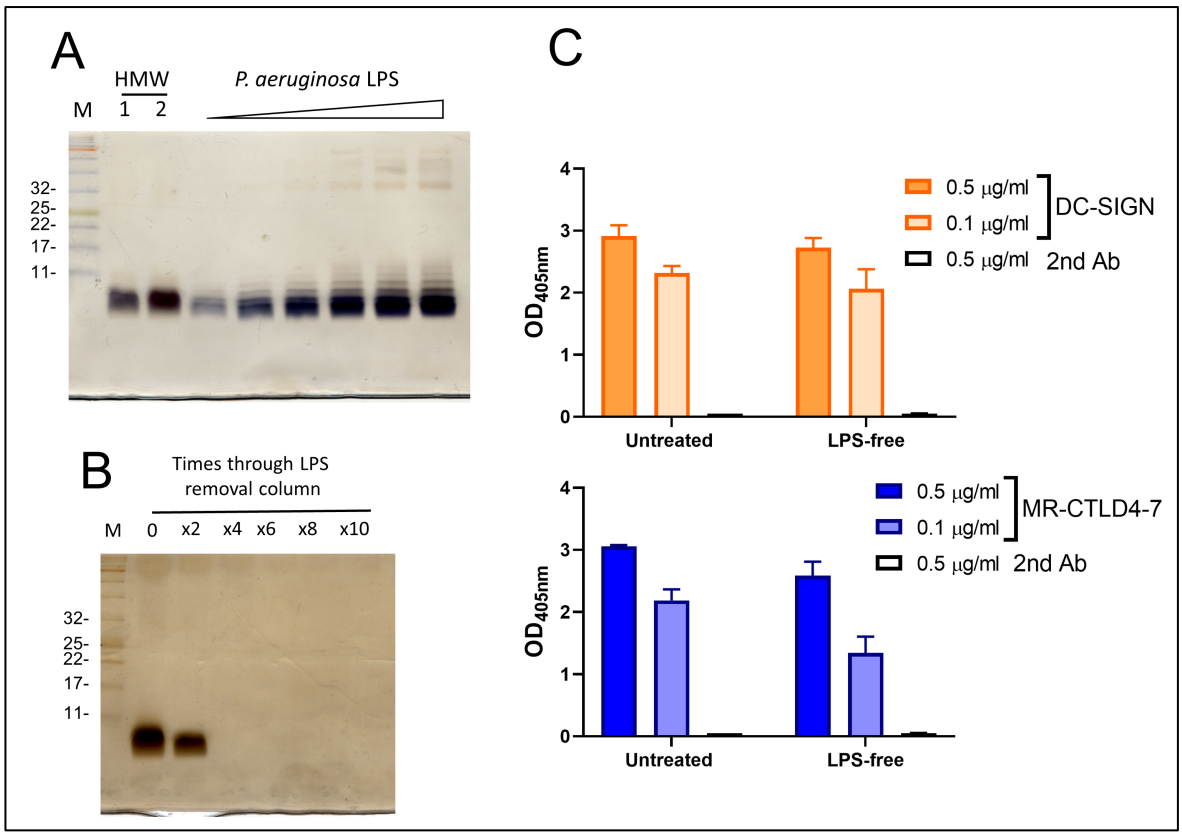


Figure 5.4 Characterisation of HMW carbohydrate preparations.

A. Estimation of LPS contamination in two HMW-Psl preparations by SDS-PAGE and silver staining. Both preparations (37.5 µg) were electrophoresed under reducing conditions alongside different amounts of purified PA LPS (1, 2, 4, 6, 8 and 10 µg, Sigma L8643) in a 15% SDS-PAGE and silver stained using PlusOne Silver Staining kit, (71-71777-00, GE Healthcare). HMW-Psl-1 contained approx. 2 µg/37.5 µg. HMW-Psl-2 contained approx. 4 µg/37.5 µg. B. Successful removal of LPS contamination in HMW-Psl-2 through repeated passages by a LPS-removal column (Pierce ™ High Capacity Endotoxin Removal Spin Columns (0.5ml) Cat No 88274). To ensure lack of contamination 10 passages were performed. The x10 passage preparation (HMW-Psl-2$^{(LPS\text{-}free)}$) did not induce cytokine production by human monocyte-derived dendritic cells (data not shown). C. Binding of DC-SIGN and MR-CTLD4-7 is maintained after LPS removal. Maxisorp plates were coated with Untreated- and LPS-free HMW-Psl-2 and incubated with DC-SIGN-Fc or MR-CTLD4-7-Fc. Binding was detected with anti-human Fc antibody conjugated to alkaline phosphatase. N=1. (Singh et al., 2020).

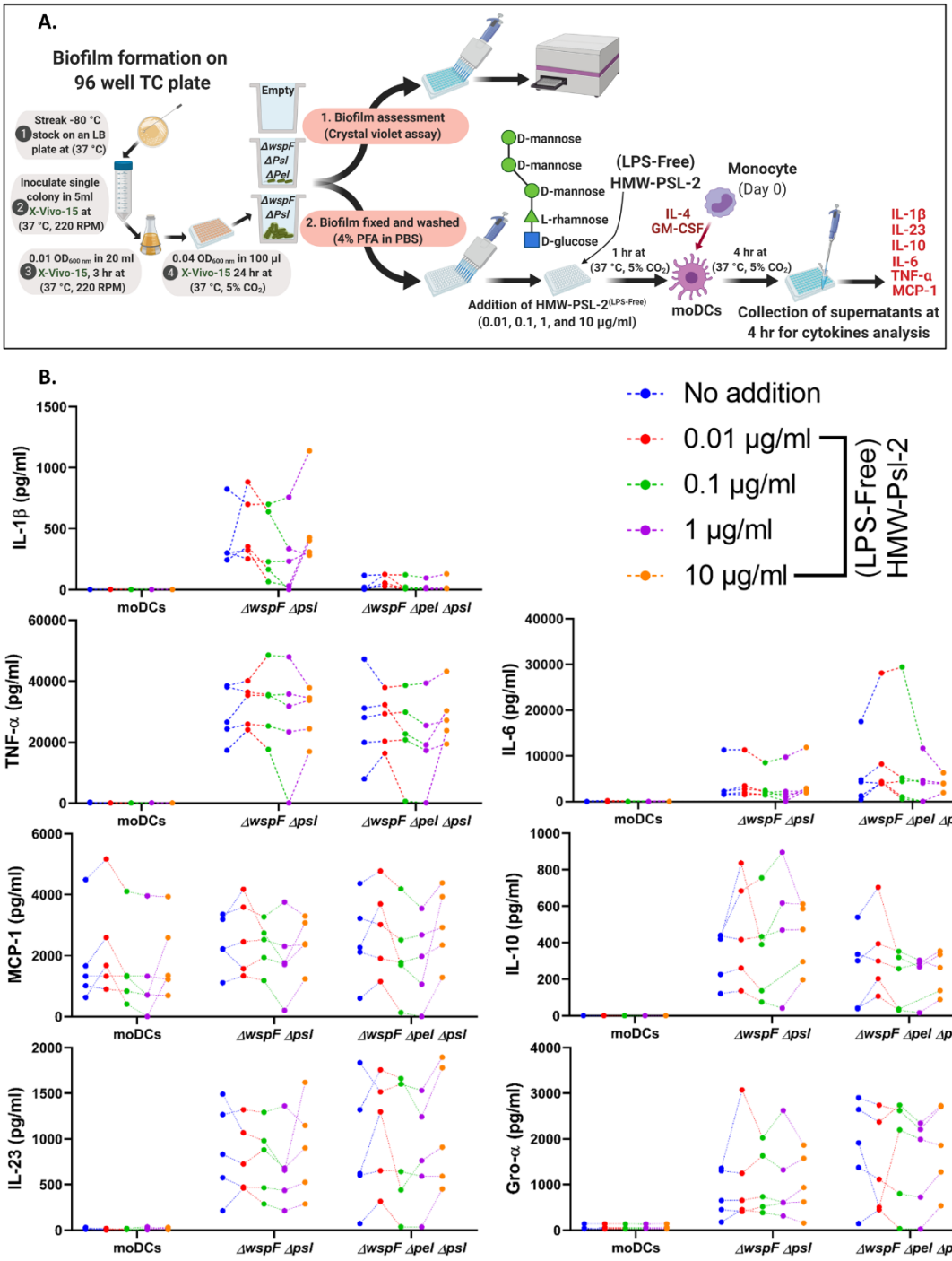


Figure 5.5 Effect of HMW-Psl-2$^{(LPS\text{-}free)}$ on moDCs responses to PA Psl-deficient biofilm and planktonic cultures

(A) Flow chart summarises the assay conditions. Different concentration of HMW-Psl-2$^{(LPS\text{-}free)}$ were added to wells that either were (1) empty, (2) contained biofilms or (3) contained cultures of PA unable to form biofilms. moDCs were added at 5 x 10^4 cells per well for 4 hr, 5% CO_2/37°C before supernatants were collected for analysis. (B) Multiplex assay was used to analyse IL-1β, IL-6, TNF-α,IL-10, MCP-1 and IL-23. ELISA was used to analyse TNF-α, MCP-1 and Gro- α. Data represented using GraphPad Prism, N=5. Flow chart created using Biorender.

5.4.2.2. Effect of biofilms with different carbohydrate composition on cytokine responses by moDCs

After we earlier found that HMW-Psl-2$^{(LPS\text{-}free)}$ did not induce cytokine production by moDCs nor altered their response to PA biofilms, planktonic cells or LPS, we next questioned whether exposing moDCs to biofilms with different carbohydrate components would induce different cytokine responses. For this, biofilms of PAO1 and different Δ*wspF* mutant strains with different EPS components were formed on TC 96 wells plates as described in (2.3) and shown in (Figure 5.6 A) and incubated with moDCs. As summarised in the flow diagram (Figure 5.6 A), 1 x 10^5 moDCs per well were incubated 4 hr with fixed 24 hr PA biofilms; following incubation, supernatants were collected and stored in -80 °C before analysis for cytokines release as described in 2.15). Multiplex assays were used to analyse IL-1β, IL-23, IL-6, IL-10, and ELISA was used to analyse TNF-α and MCP-1 as described in (2.16).

Results show that levels of all cytokines tested expect MCP-1, were higher in infected cells than uninfected cultures (Figure 5.6 B). Similar to previous observations, IL-1β levels were significantly higher when moDCs were exposed to biofilms forming strains compared to low/no biofilm strains (Figure 5.6 B). No significant difference was observed in IL-1β production induced by Psl and/or Pel producing biofilms. IL-23, IL-6, IL-10, TNF-α, and IL-10 levels in stimulated moDCs cultures did not differ significantly when biofilms were formed by Δ*wspF,* Δ*wspF*Δ*pel* or Δ*wspF*Δ*psl*, and low/no forming biofilms strains PAO1 and Δ*wspF*Δ*pel*Δ*psl*. A trend towards reduced IL-1β production was observed when Psl was missing in biofilms while the opposite was true for IL-23 (Figure 5.6). To conclude, although certain cytokines exhibited a downwards or an upwards trend as in IL-1β and IL-23 as described above, apart from IL-1β which was biofilms specific, no significant effect of different EPS components on cytokine production by moDCs was observed (Figure 5.6). Indicating that carbohydrate composition does not influence cytokine production by moDCs under these experimental conditions.

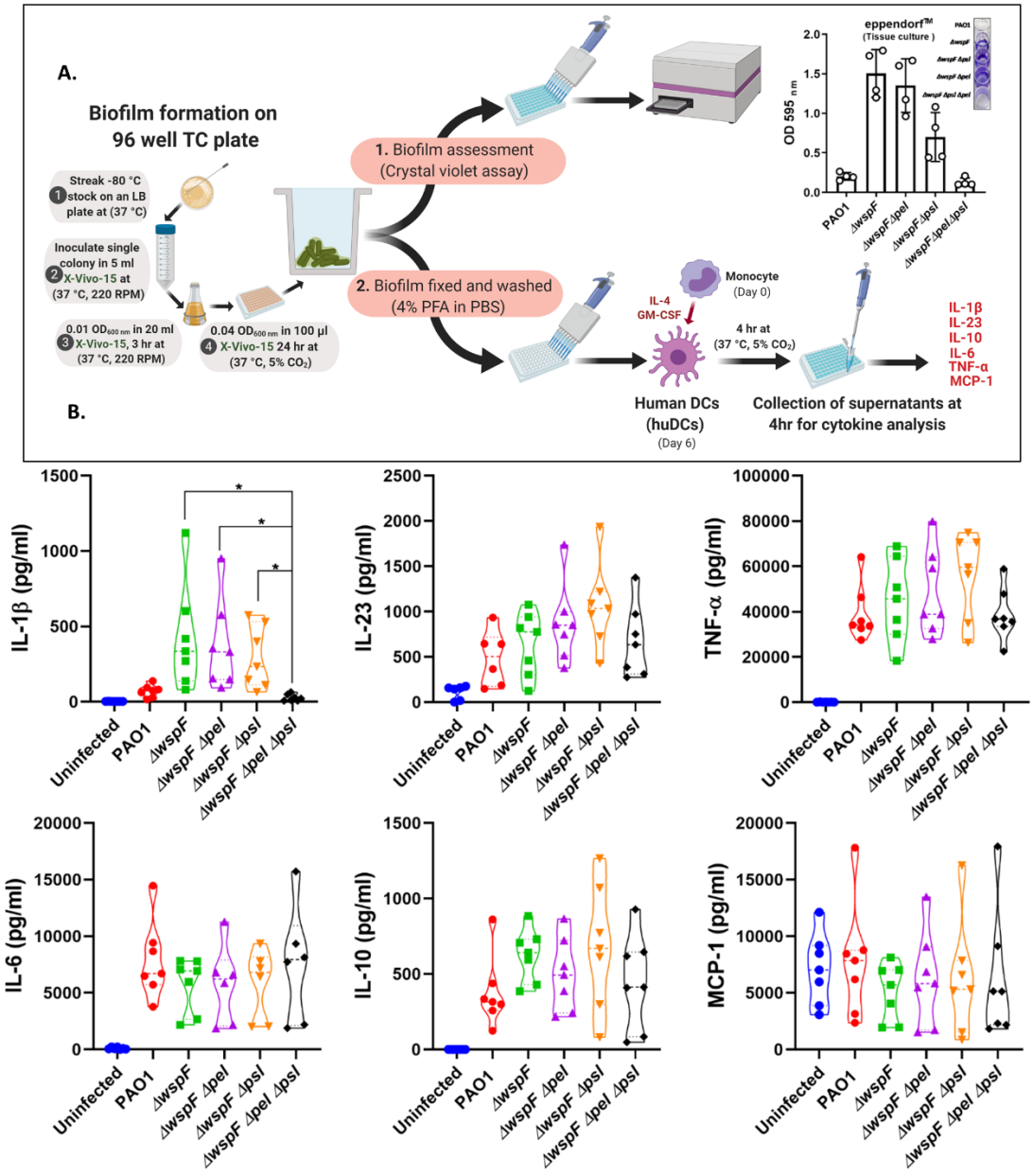


Figure 5.6 Analysis of cytokine production by moDCs in response to Psl+/Pel+, Psl+/Pel-, Psl-/Pel+ biofilms .

(A) Flow chart of experimental methods including biofilm growth for 24 hr and (1.) assessment of biofilm formation using CV assay as described in (2.3), and (2.) stimulation of moDCs with fixed PA biofilms for 4 hr as described in (2.15). Supernatants were collected for cytokines analysis using multiplex assay (IL-1β, IL-6, IL-23, IL-10) and ELISA (TNF-α and MCP-1). (B) Violin plots showings the level of cytokines released by moDCs stimulated with fixed PA biofilms with different EPS components. Dashed lines (----) denote median, dotted lines (…..) denote the two quartile lines of the highest and smallest value and width denote frequency. N=7. Significance analysis was done using GraphPad Prism 8.3.0 and one-way ANOVA with Tukey's multiple comparison test. Flow chart created using Biorender.

5.4.2.3. Contribution of DC-SIGN, MR and Dectin-2 to the cytokine response of moDC to PA biofilms

Although previous findings indicate that carbohydrates do not dominate the early cytokine response of moDCs to PA biofilms, we completed this investigation by assessing the effect of blocking DC-SIGN, MR and/or Dectin-2 on the cytokine response of moDCs to PA biofilms. For this, Δ*wspF* biofilms were generated on TC 96 well plates for 24 hr, fixed, washed and kept at 4°C prior addition of moDCs (2.15). The moDCs added were pre-incubated either with X-Vivo-15 only or at least with one or more of the anti-CLRs blocking antibodies or the respective isotype control as described in (2.18) for 1 hr at 5% CO_2/37 °C. To validate blocking of CLRs on moDCs, we utilised flow cytometry, two donors out of four were tested. Results confirmed blocking of MR and DC-SIGN in both donors tested (Figure 5.7) & (Figure 5.8) respectively. Dectin-2 data is from one donor and indicated no effect of the blocking reagent as the isotype control showed a similar effect (Figure 5.7). This result confirmed previous observations (Figure 5.3) regarding the lack of Dectin-2 expression by moDCs. moDCs (DC-SIGN+, MR+, Dectin-1^{low} and Dectin-2$^{low/-}$) cells were then incubated with biofilms for 4 hr when supernatants were collected for cytokine analysis.

Similar to results observed in (Figure 5.5 and Figure 5.6) data demonstrated high level of variation between different donors. Cytokine values (Figure 5.9) were normalised to show the fold change. No statistically significant changes could be detected; however, certain cytokines exhibited a downward or an upward trend when CLRs were blocked but there was a great deal of inconsistency. Taken together, all results presented earlier (Figure 5.5, Figure 5.6 and Figure 5.9) suggest that these experimental conditions might not be suitable for testing our hypothesis.

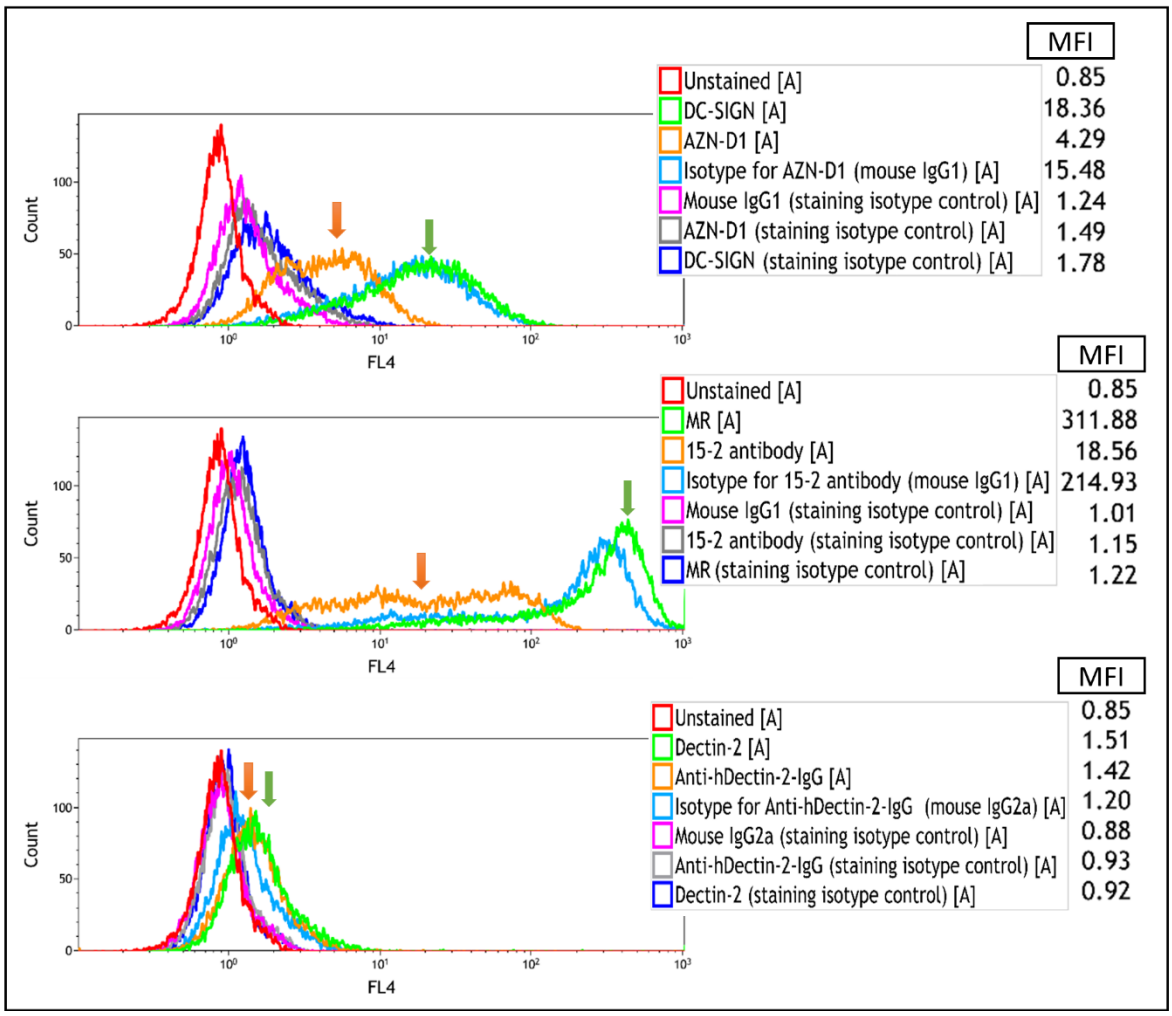


Figure 5.7 Confirmation of CLRs blocking using flow cytometry donor 2

moDCs generated from CD14+ monocytes in the presence of (50ng/ml) GM-CSF and IL-4 for 6 days were pre-incubated either with X-Vivo-15 only or at least with one or more of the anti-CLRs blocking antibodies (mouse anti-human DC-SIGN Ab (AZN-D1) for DC-SIGN, mouse anti-human MR Ab (15.2) for MR and mouse anti-hDectin-2-IgG for Dectin-2) or their respective isotype controls as described in (2.18) for 1 hr, 5% CO_2/37 °C. After incubation, moDCs were tested for MR, DC-SIGN, and Dectin-2 expression by flow cytometry as follows. moDCs were re-suspended in X-Vivo-15 media in a 15 ml Falcon tube at a density of 1 ×10^6 cells/ml, centrifuged and re-suspended in 1 ml of 5% (v/v) human serum in PBA solution, and incubated for 1 hr at 4°C. After washing, the cell density was adjusted to 100,000 cells/100µl of PBA and cells were incubated with mouse anti-human monoclonal antibodies or their matched isotype controls: CD206 (MMR)-Allophycocyanin (647), CD209 (DC-SIGN)-647 or CLEC6A (Dectin-2)-APC for 1 hr at 4°C. Cells were washed and fixed with 0.5% (v/v) PFA and analysed using a FC500 Beckman Coulter flow cytometer; 10,000 events were collected. Data were analysed using Kaluza Software 1.5a. Data are from 1 independent experiment and show blocking of the expression of both MR and DC-SIGN.

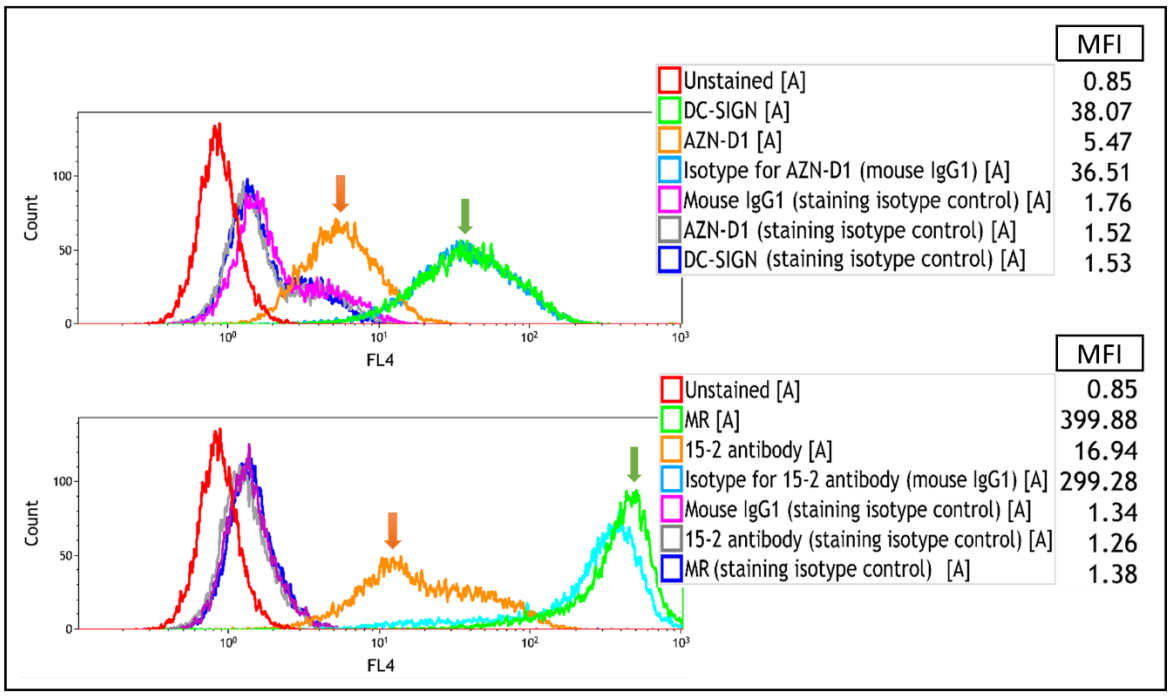


Figure 5.8 Confirmation of CLRs blocking using flow cytometry donor 3

Similar to donor 2 presented in (Figure 5.7), following incubation with blocking antibodies. moDCs were tested for MR and DC-SIGN expression by flow cytometry. Data indicated effective blocking of both MR and DC-SIGN. Data were analysed using Kaluza Software 1.5a. Data are from 1 independent experiment.

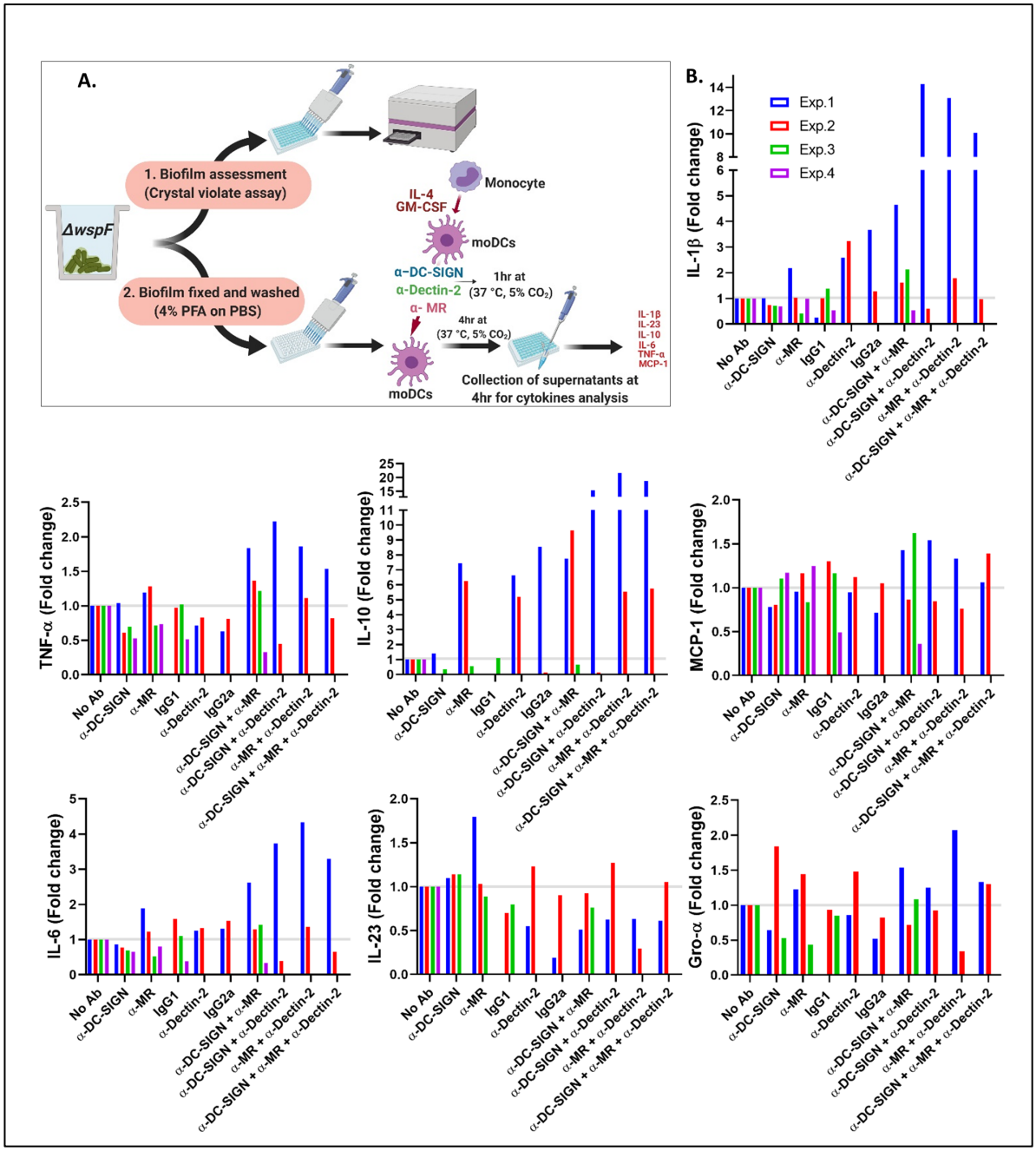


Figure 5.9 Effect of blocking CLRs on moDCs responses to PA biofilms

(a) Flow chart summarising the assay conditions. moDCs were pre-incubated either with X-Vivo-15 only or at least with one or more of the anti-CLRs blocking antibodies or their respective isotype controls as described in (2.18) for 1 hr, 5% CO_2/37 °C before being added to fixed Δ*wspF* biofilms. Following 4 hr of incubation at 5% CO2/37 °C supernatants were collected for analysis. (B) cytokines were analysed using multiplex assay (IL-1β, IL-6, IL-23, IL-10) and ELISA (TNF-α, MCP-1 and Gro-α). Cytokine values were normalised to show the fold change. Data represented using GraphPad Prism, N=4. Flow chart created using Biorender.

5.4.3. Cell survival (LDH assay)

To confirm all cytokines assays conducted above were not affected by differential cell death resulting from necrosis or pyroptosis, the Lactate Dehydrogenase (LDH) assay was performed as described in (2.17). LDH is a soluble cytoplasmic enzyme found in nearly all cells that is released into the extracellular space after membrane damage (Burd and Usategui-Gomez, 1973). The assay measures the amount of LDH released in supernatants as a result of cytotoxicity. Results showed minimal cytotoxicity of all assay performed, some data are not included as it was done using an expired LDH assay kit, which showed the same LDH levels under all assays conditions even with positive and negative control. Analysis using a new LDH kit (11644793001, Roche) in (Figure 5.10), showed neither fixed biofilms or HMW-Psl-$2^{(LPS\text{-}free)}$ have a cytotoxic effect on moDCs after 4 hr incubation. These results confirmed also that the assay condition of using 5 $x10^5$ cells in one well were not inducing cell death.

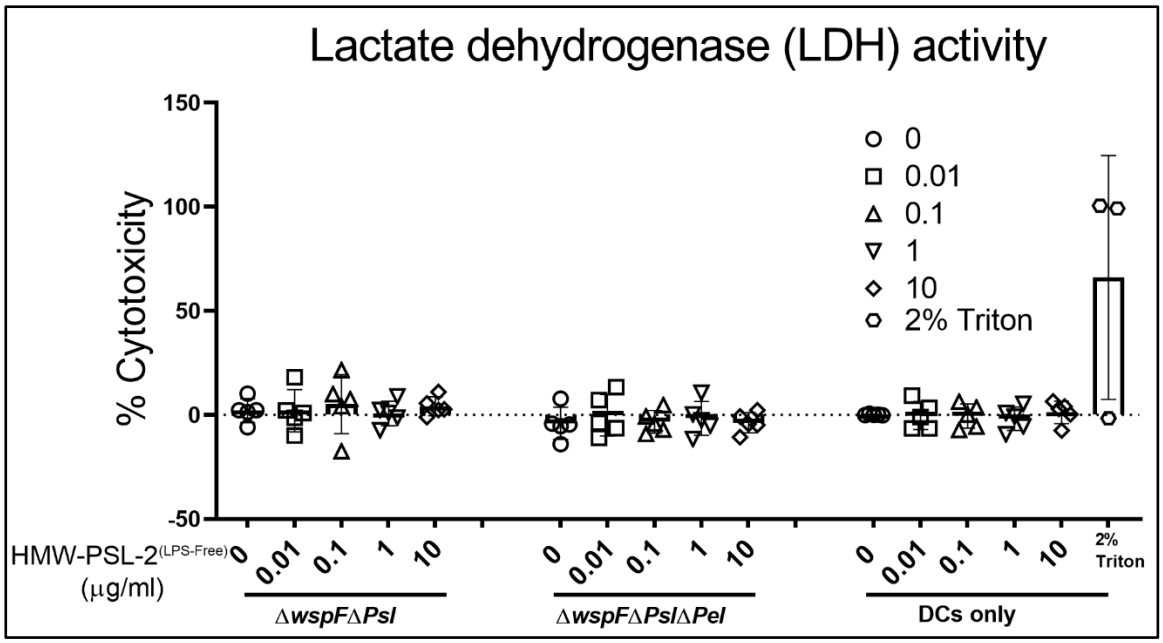


Figure 5.10 Lactate Dehydrogenase (LDH) assay indicated neither fixed PA biofilms or HMW-Psl-2$^{(LPS\text{-}free)}$ cues moDCs cell death.

moDCs were either (1) unstimulated (DCs only) or stimulated with (2) fixed PA biofilms (Δ*wspF* Δ*psl*), or (3) fixed PA planktonic cells (Δ*wspF*Δ*pel*Δ*psl)* in the presence and absence of different concentrations of HMW-Psl-2$^{(LPS\text{-}free)}$. After incubation for 4 hr, 5% CO_2/37 °C supernatants were collected. LDH assay was performed following the manufacturer's instructions as described in (2.17). Results showed that neither fixed planktonic cells, biofilms or HMW-Psl-2$^{(LPS\text{-}free)}$ have a cytotoxic effect on moDCs after 4 hr incubation. N=at least 3.

5.4.4. Biofilm carbohydrate interferes with the function of cell-associated DC-SIGN and MR

The previous work showed that our model to study moDCs-PA biofilm interactions did not provide any information suggesting an important role for carbohydrates on the interaction of biofilms with immune cells. In order to determine whether HMW-Psl could modulate different characteristics of moDCs, a series of endocytosis experiments were performed by Dr. Sonali Singh. MR and DC-SIGN are important endocytic receptors expressed by the antigen presenting cells, moDCs (Garcia-Vallejo and van Kooyk, 2013, Martinez-Pomares, 2012). The ability of two different HMW-Psl preparations HMW-Psl-1 and HMW-Psl-2 to interfere with moDCs endocytic activities were evaluated. moDCs internalise fucose-PAA-FITC (model ligand for MR and DC-SIGN), Lewis^{x}-PAA-FITC (model ligand for DC-SIGN) and, poorly, galactose-PAA-FITC (not recognised by MR or DC-SIGN).

Presence of HMW-Psl-1 and HMW-Psl-2 (contaminated with LPS) partially inhibits uptake of Lewis^{x}-PAA-FITC but not that of fucose-PAA-FITC or galactose-PAA-FITC by moDCs (Figure 5.11). These findings were not affected by Polymyxin B (100 µg/ml) (Figure 5.12) suggesting that these observations are LPS-independent. These results indicate specific ability of HMW-Psl-1 and HMW-Psl-2 to modulate DC-SIGN-mediated endocytosis in moDCs.

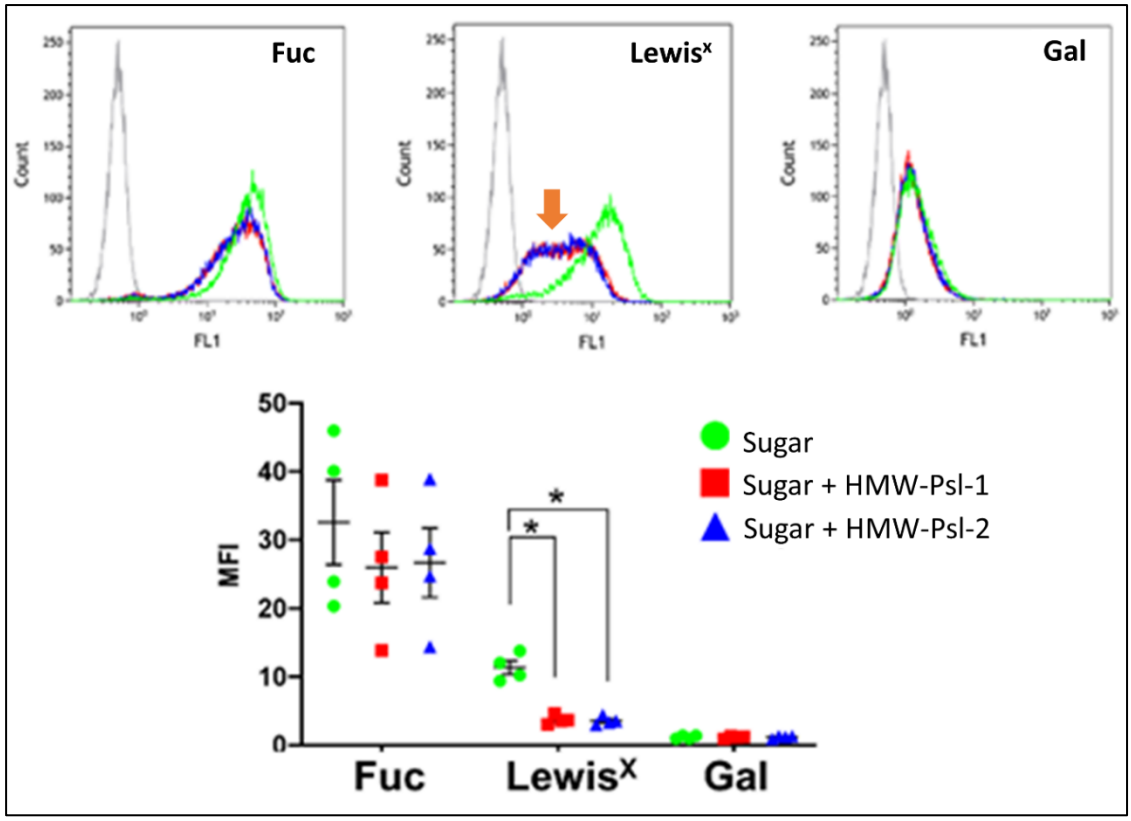


Figure 5.11 Inhibition of sugar uptake by MR and DC-SIGN expressing cells by HMW-Psl-1 and HMW-Psl-2.

moDCs (DC-SIGN+, MR+, Dectin-1^{low} and Dectin-2$^{low/-}$, Figure 5.3) were treated with HMW-Psl-1 and HMW-Psl-2 (10 µg/ml) for 1 hr, then fluorescently labelled sugars were added for a further 1 hr. Association of fluorescent sugars to cells was measured by flow cytometry. Representative histograms and scatter plots depicting mean ± SEM of MFI are shown. moDCs internalise fucose (Fuc), Lewis^x and galactose (Gal) PAA-FITC polymers but only Lewis^x uptake was reduced by HMW-Psl-1 and HMW-Psl-2, N=4. Repeated-measures ANOVA was performed to determine statistical significance; *, ≤0.05. Fuc: fucose; Gal: galactose.

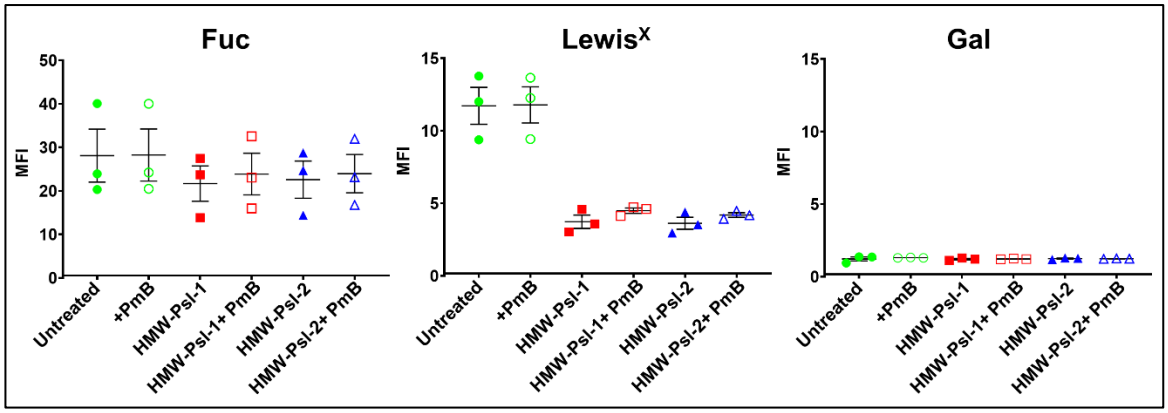


Figure 5.12 Polymyxin B does not affect HMW-Psl-1 and HMW-Psl-2 mediated inhibition of Lewis^x uptake by moDCs.

moDCs were treated with HMW-Psl-1 or HMW-Psl-2 (10 µg/ml) for 1 hr in the presence or absence of Polymyxin B (100 µg/ml, PmB), then fluorescently labelled sugar polymers (5 µg/ml) were added for a further 1 hr. Association of fluorescent sugars to cells was measured by flow cytometry. Representative scatter plots depict mean ± SEM of median fluorescence intensity (MFI) are shown. N=3. Fuc, Lewis^x and Gal refer to polymers bearing fucose, Lewis^x or galactose, respectively.

5.4.5. The effect of biofilm carbohydrate on morphological characteristics of human dendritic cells

5.4.5.1. Visualisation of DC-SIGN expression on huDCs; a comparison of two different anti-DC-SIGN antibodies.

The fact that HMW-Psl modulate DC-SIGN-mediated endocytosis in moDCs encouraged us to establish a microscopy-based model to determine whether HMW-Psl, could affect other aspects of moDCs biology. Thus, we investigated whether incubation with biofilms and/or biofilm-associated carbohydrates could alter DC-SIGN distribution on moDCs. The first step in this process was to optimise DC-SIGN staining for confocal analysis. To reveal the localisation of DC-SIGN on moDCs, we employed two different anti-DC-SIGN antibodies (Figure 5.13 A), (1) mouse anti-human DC-SIGN Ab (AZN-D1), kindly provided by Prof van Kooyk, VUMC (Bashirova et al., 2001), and (2) rabbit polyclonal anti-DC-SIGN antibody (Rb pAb) (ab5715, Abcam). After CD14+ cells were differentiated to moDCs for 6 days as described in (2.9) they were harvested and seeded into µ-Slide VI 0.4 TC treated channels (5 x 10^5 per channel) and incubated for 24 hr at 37 °C, 5% CO_2 prior fixation with 4% PFA prepared in PBS for 10 min at 4°C. After fixation, cells were either permeabilised and blocked with 0.25% Triton X-100 in blocking buffer [5% normal donkey serum (NDS) in PBS], or blocked with blocking buffer in the absence of 0.25% Triton X-100 for 15 min at 4°C. After that, cells were washed and incubated with AZN-D1 or Rb pAb (10 µg/ml in blocking buffer) overnight at 4°C. After incubation, secondary antibodies were added prepared in blocking buffer. To label the nucleus, samples were incubated with DAPI, before being washed and mounted in Ibidi mounting media (Figure 5.13 B).

Examination of samples using confocal microscopy revealed that DC-SIGN labelling with both antibodies used was identical (Figure 5.14). Permeabilised cells showed slightly lower cell surface expression compared with none permeabilised. Furthermore, the DC-SIGN was mostly detected at the cell surface, which is in agreement with previous findings (Horrevorts

et al., 2018). However, data showed unexpected DC-SIGN staining in the nucleus, which was more obvious in permeabilised cells (Figure 5.14).

Since DC-SIGN was never reported in the literature to be expressed in the nucleus, we questioned the use of PBS buffer in our assay. Thus, to overcome this problem, we tested the use of a different fixative: PIPES-EGTA-Magnesium (PEM). Fixation with freshly prepared 4% PFA in PEM [80 mM PIPES pH 6.8, 5 mM EGTA, 2 mM $MgCl_2$] has been recently reported to be better than PBS in preserving cells characteristics with minimum effect on the cytoskeleton (Leyton-Puig et al., 2016, Pereira et al., 2019).

Results (Figure 5.15) using the PEM fixation confirmed the previous observation of DC-SIGN expression associated with the cell membrane. More importantly, there was no sign of DC-SIGN staining in the nucleus, which indicated that the previous observation might be related to the use of PBS buffer (Figure 5.15). Overall, these results indicate that DC-SIGN localised mostly at the cell membrane and highlighted the importance of using of PEM for fixing, staining and blocking the moDCs to rule out any labelling artefacts.

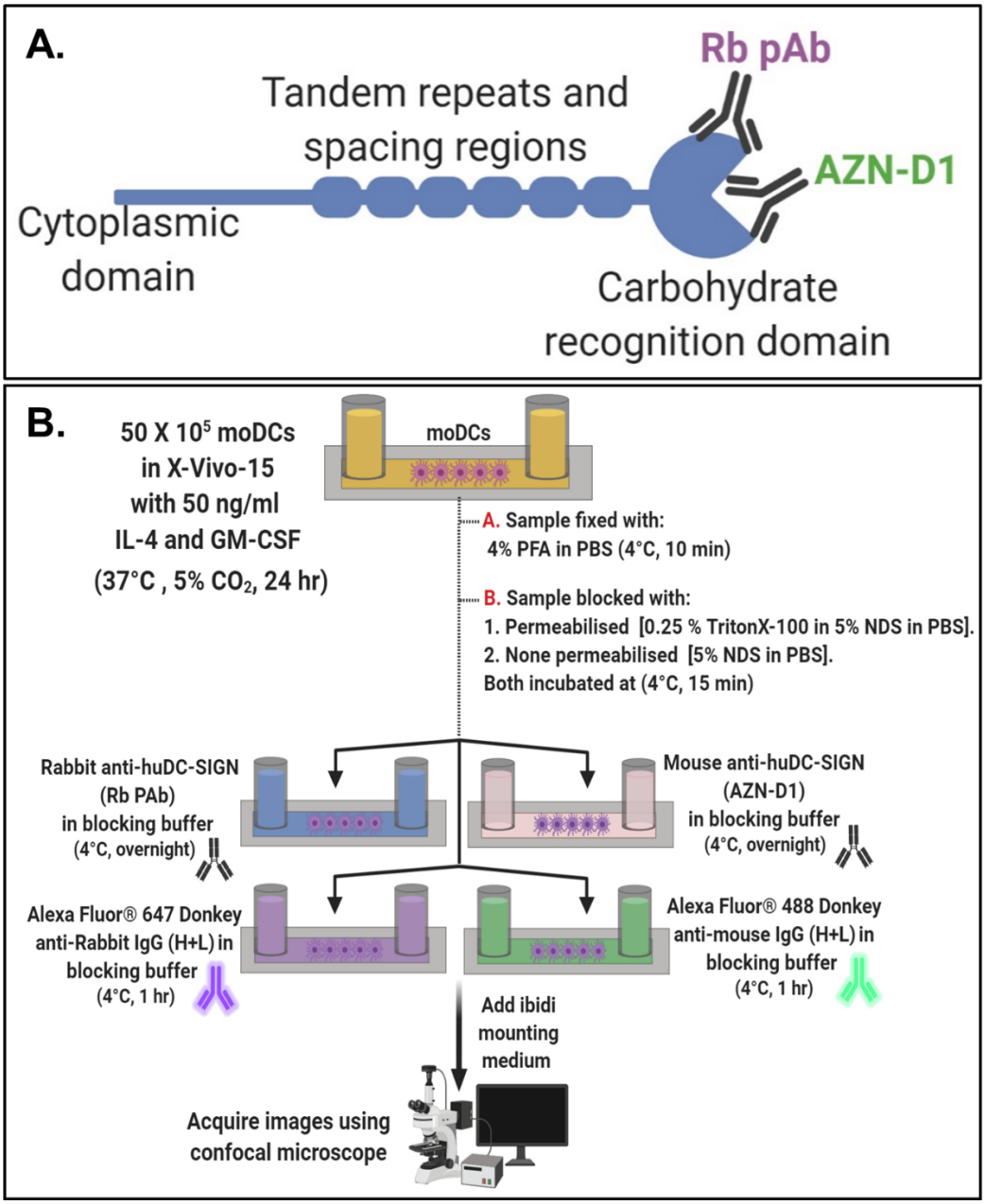


Figure 5.13 Visualisation of DC-SIGN on moDCs

(A) Summary of the two anti-DC-SIGN antibodies employed in this study, (1) anti-DC-SIGN mouse Ab (AZN-D1), kindly provided by Prof van Kooyk, VUMC, and rabbit anti-DC-SIGN antibody (Rb pAb) (ab5715, Abcam). Both antibodies target the CRD domain of human DC-SIGN. (B) Flow chart summarizes the process to localise DC-SIGN in moDCs using confocal microscopy. More details of the process are available in (2.13).

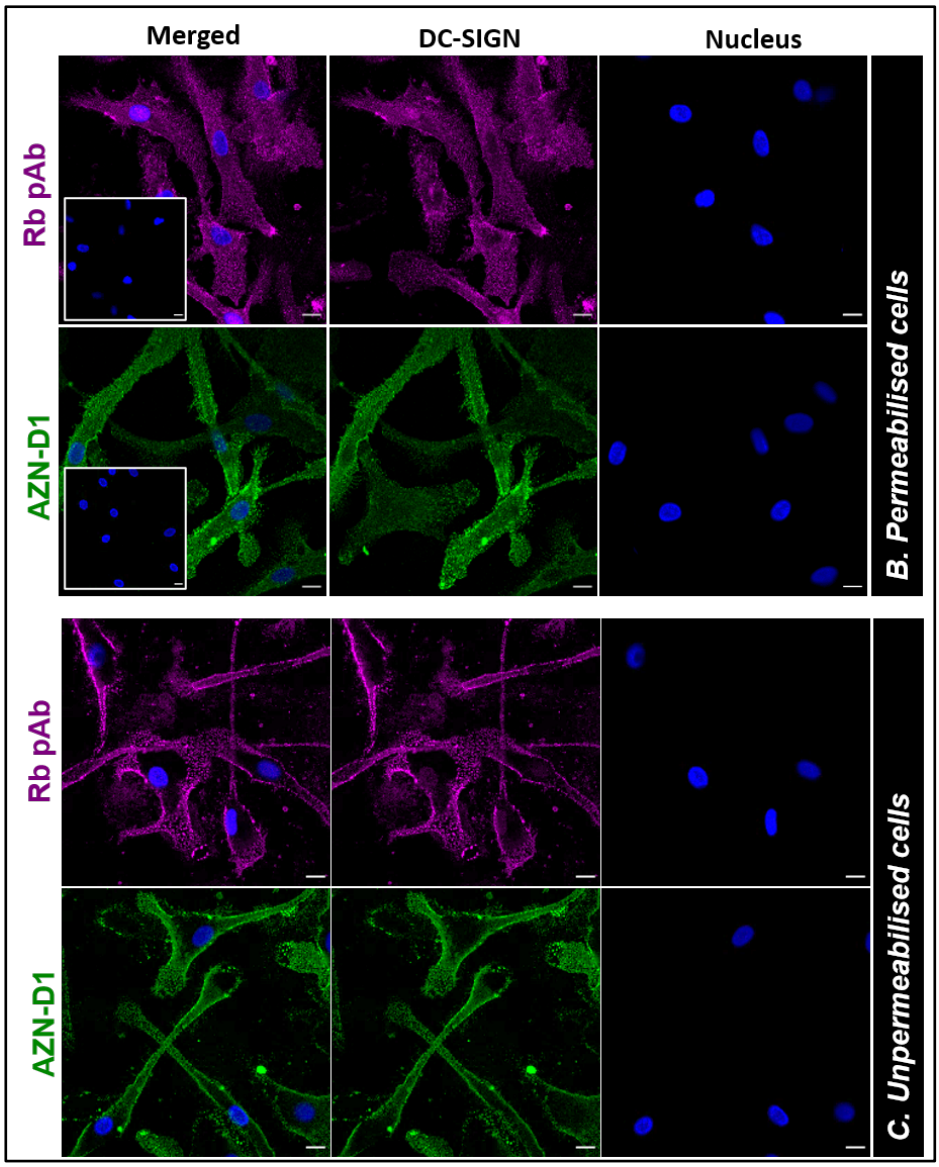


Figure 5.14 Comparison of moDCs DC-SIGN expression using two different anti-DC-SIGN antibodies

moDCs (5 x 10^5 cells per channel) in X-Vivo-15 with IL-4 and GM-CSF (50 ng/ml) were added to chambers of µ-slide VI 0.4 and incubated overnight at 37°C, 5% CO_2. Samples were then fixed with 4% PFA prepared in PBS for 10 min at 4°C. Afterward, permeabilised cells (A) were, blocked and permeabilised with [0.25% triton in 5% NDS] for 15 min at 4°C. For non-permbilised cells (B), cells were just blocked with the same buffer lacking 0.25% Triton X-100. Next samples were stained for DC-SIGN with 10 µg/ml of AZN-D1 (green) or Rb pAb (magenta), and nuclei were labelled with 1.5 µg/ml DAPI (blue). Experiment were repeated independently twice; the images shown are representative of one experiment and showing one slice of z-stack images. Scale bar 10 µm.

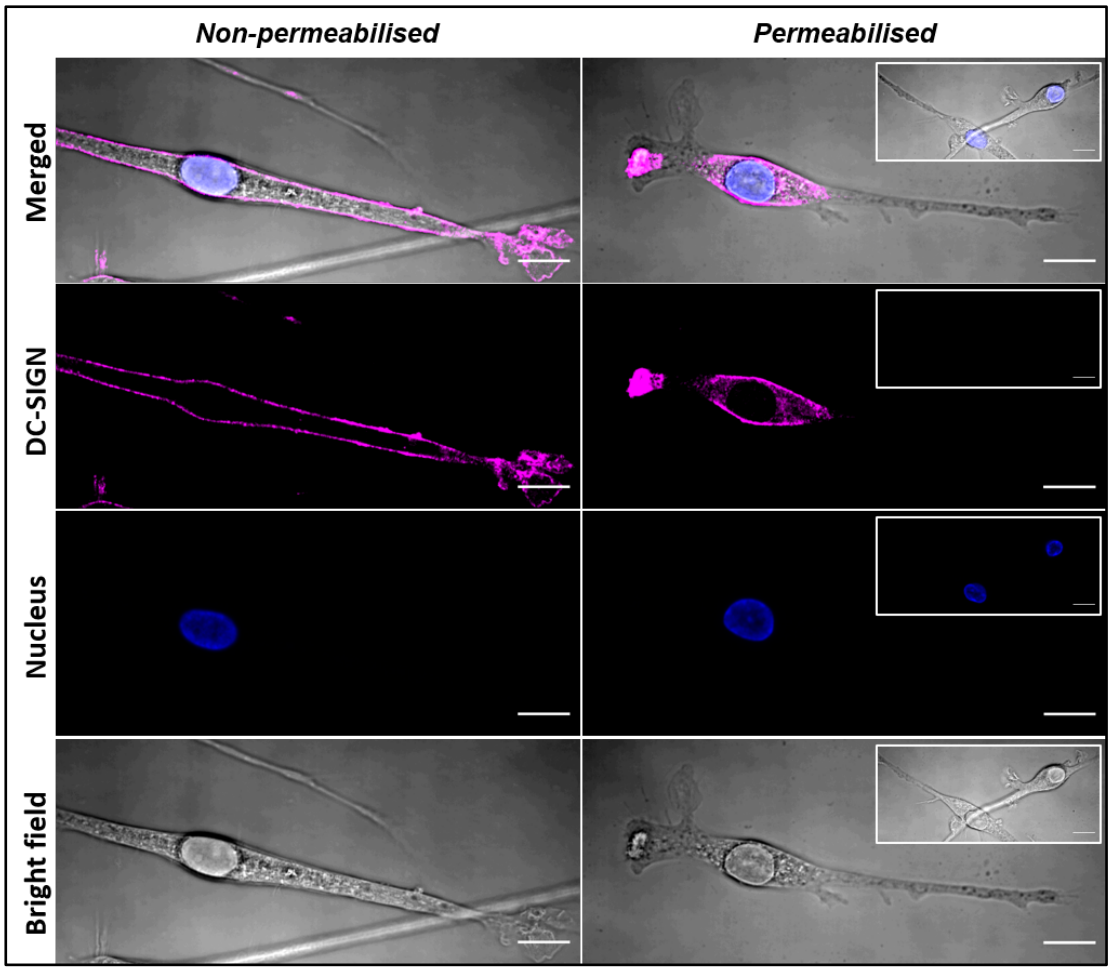


Figure 5.15 Optimisation of DC-SIGN staining using PEM buffer

Analysis of DC-SIGN in moDCs using Rb pAb anti-DC-SIGN. (Right panels) Permeabilised cells blocked with 0.25% Triton X-100 in blocking buffer [5% normal donkey serum (NDS) in PEM] for 20 min at RT. (Left panels) Non-permeabilised cells were incubated with blocking buffer without 0.25% Triton X-100 for 20 min at RT. Samples were stained for DC-SIGN with 10 µg/ml of Rb pAb and anti-rabbit secondary antibody (magenta). Nuclei were labelled with 1.5 µg/ml DAPI (blue). Experiment was repeated independently twice; the images shown are one single slice form one independent experiment. Insets show secondary antibody only controls. Scale bar 10 µm.

5.4.5.2. Phenotypic changes in moDCs incubated with Psl+/Pel+, Psl+/Pel-, Psl-/Pel+ biofilms

After we confirmed the localisation of DC-SIGN distribution on moDCs we performed an initial screening experiment to gain a preliminary data on what would happen to moDCs incubated with to biofilms with different EPS components. For this, biofilms of Δ*wspF* mutant strains with different EPS components were formed on to µ-Slide VI 0.4 TC treated as described in (2.6.4) for 15 hr. The 15 hr time point was chosen because the Δ*wspF* mutant strains if exposed to 1.6 ml/hr shear stress longer than 15 hr form high biomass biofilms that block the µ-Slide channels causing leakage (data not shown). Thus, biofilms generated for 15 hr were fixed, washed, and incubated with moDCs (5×10^4 cells per channel) for 24 hr. Following incubation, samples were fixed, permeabilised, and stained for DC-SIGN (PBS fixation) as described in (2.13). It is important to clarify that at the time this experiment was conducted PEM fixation had not been evaluated.

Preliminary results (n=1) (Figure 5.16) indicated that moDCs adopt different morphologies when incubated with different Δ*wspF* strains. moDCs cultured with strains that overexpress Psl (Δ*wspF* and Δ*wspF*Δ*pel*) tend to display rounder shapes. On the other hand, the strain that lacked Psl (Δ*wspF*Δ*psl*) induced a stretched phenotype in moDCs with numerous membrane ruffles. Cells incubated with planktonic cells (Δ*wspF*Δ*pel*Δ*psl*) were also stretched and seemed to express less DC-SIGN. Low numbers of moDCs were detected in wells with strains that overexpress Psl (Δ*wspF* and Δ*wspF*Δ*pel*) compared to the strains that lack Psl (Δ*wspF* Δ*psl* and Δ*wspF*Δ*pel*Δ*psl*) (Figure 5.16, based on nucleus (DAPI) stain). Overall, these preliminary observations indicated that presence of Psl in biofilms may induce phenotypical changes on moDCs that could possibly influence their shape and affect their attachments.

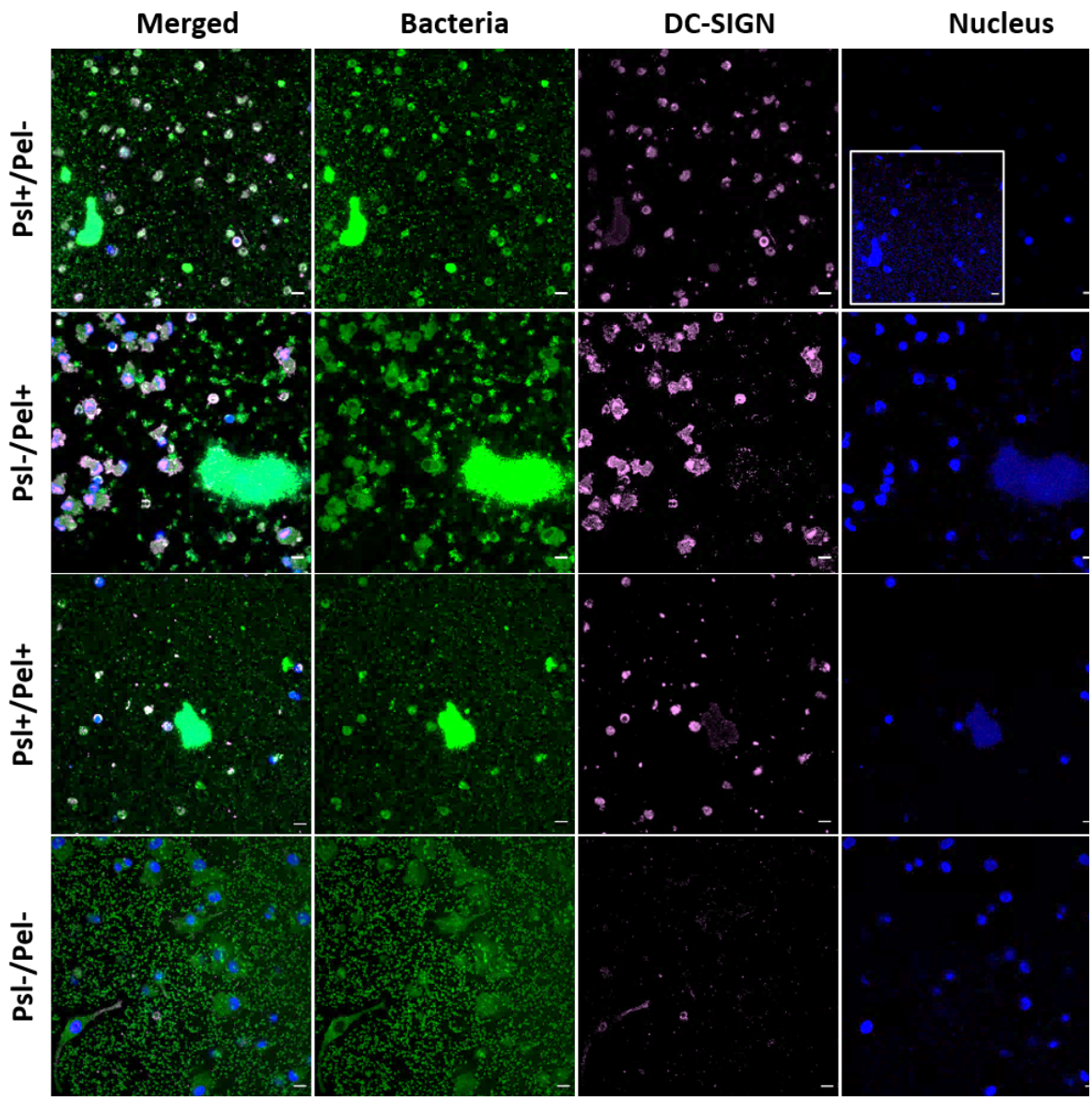


Figure 5.16 Visualisation of moDC morphology after incubation with PA biofilms

Biofilms formed by different Δ*wspF* mutants in chambers of µ-slide VI 0.4 as described in (2.6.4) for 15 hr were fixed with 4% PFA in PBS for 10 min at 4°C. moDCs (5 x 10^4 cells per channel) were added and incubated for 24 hr. After incubation, moDCs-biofilm co-cultures were fixed with 4% PFA in PBS. Samples were blocked and permeabilised with [0.25% Triton X-100 in 5% NDS] in PBS before stained for DC-SIGN with 10 µg/ml of Rb pAb and anti-rabbit secondary antibody 1:500 (DC-SIGN, magenta), FM1-43 Fx (membranes day label both bacteria and moDCs, green) and DAPI (nucleus, blue). Data are representative images from one experiment. Image processed using Fiji. Scale bar 10 µg/ml. Inlet increased brightness of DAPI channel to show bacteria.

5.4.5.3. Effect of purified Psl on moDC phenotype

Following on previous findings, we explored the possibility of HMW-Psl$^{(LPS\text{-}free)}$ altering the phenotype of human moDCs (DC-SIGN+, MR+, Dectin-1^{low} and Dectin-2$^{low/-}$, Figure 5.3). Thus we examined if moDCs incubated with HMW-Psl$^{(LPS\text{-}free)}$ would also adopt the round morphology observed earlier with Psl-containing biofilms. Towards this aim we investigated morphological changes in moDCs and DC-SIGN surface distribution (Figure 5.15) after incubation on HMW-Psl-coated surfaces as described in (2.13). Both HMW-Psl and HMW-Psl$^{(LPS\text{-}free)}$ were tested. moDCs cultured on HMW-Psl$^{(LPS\text{-}free)}$ for 24 hr display a rounder morphology, characterised by increased circularity index and reduced perimeter (Figure 5.17), suggesting changes in the cytoskeleton related to maturation state. These morphological changes were less apparent when using crude Psl indicating that LPS can partially reverse this effect. Analysis of DC-SIGN surface expression showed reduced DC-SIGN labelling (Raw Integrated Density) in cells cultured in the presence of Psl (both HMW-Psl and HMW-Psl$^{(LPS\text{-}free)}$). When adjusting for cell size (Signal per Unit Area), only the LPS-containing samples showed reduced surface DC-SIGN labelling (Figure 5.17), which is compatible with a more classical moDC activation (Relloso et al., 2002). These findings support the ability of biofilm-associated carbohydrates to influence moDCs function in the absence of LPS.

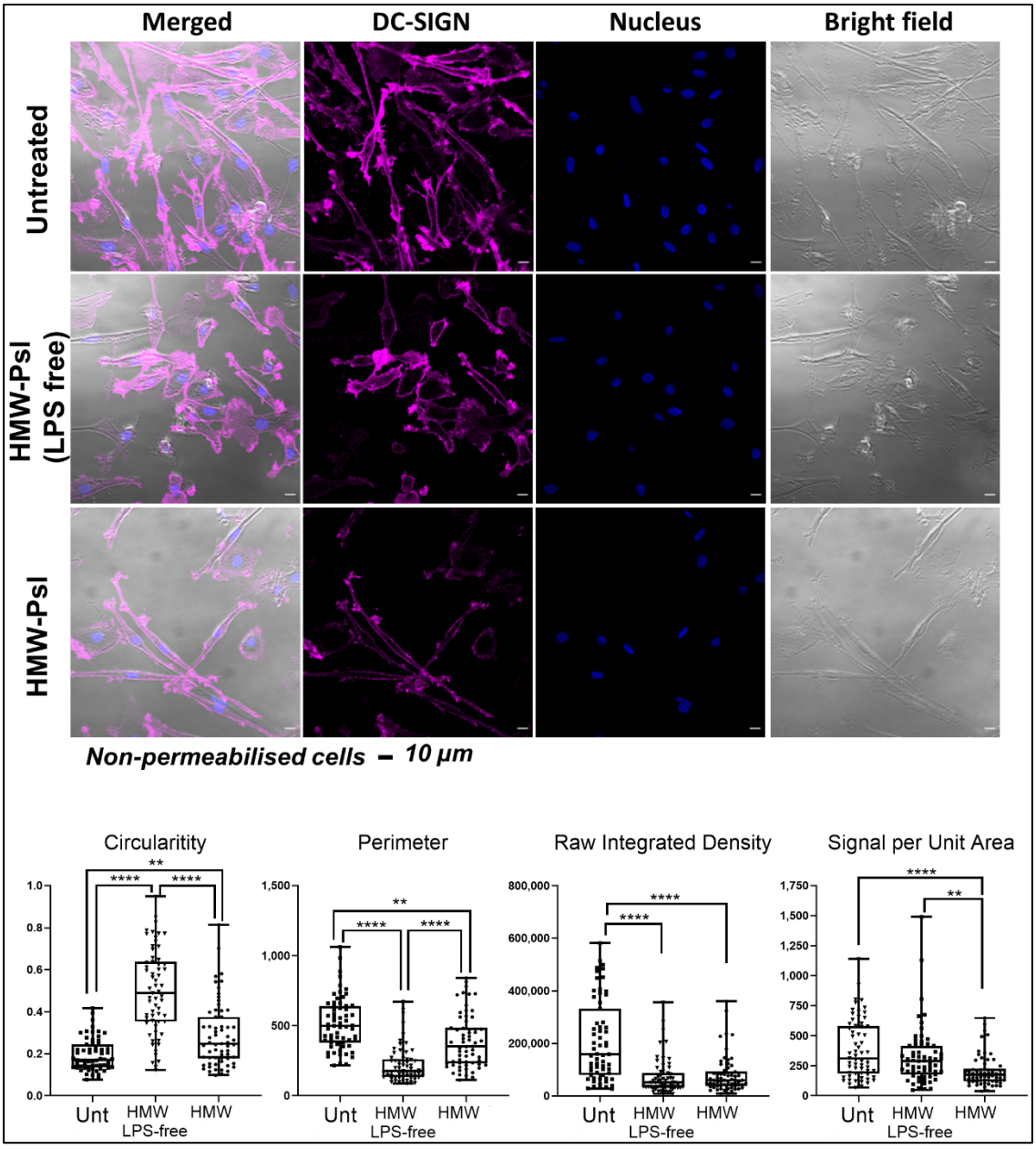


Figure 5.17 Changes in unpermeabilised moDCs morphology in the presence of biofilm-associated carbohydrate, Psl.

HMW-Psl (with and without LPS contamination) diluted in X-Vivo-15 (10 µg/ml) were used to coat chambers of µ-slide VI 0.4 overnight at 4°C. moDCs (5 x 10^4 cells per channel) were added and incubated for 24 hr. Samples were then fixed and stained for DC-SIGN with 10 µg/ml of Rb pAb and anti-rabbit secondary antibody 1:500 (DC-SIGN, magenta), and 1.5 µg/ml DAPI (nucleus, blue). Top panels show representative images from unpermeabilised samples of one repeat. Permeabilised samples from the same repeat are shown in (Figure 5.18). Bottom panels show analysis for changes in shape (Circularity Index), size (Perimeter) and DC-SIGN labelling intensity (Raw Integrated Density and Signal per Unit Area). Data derive from 3 independent experiments, 20 cells per experiment were analysed. Statistical significance assessed using Kruskal-Wallis test corrected for multiple comparison using a Dunn's multiple comparison test.

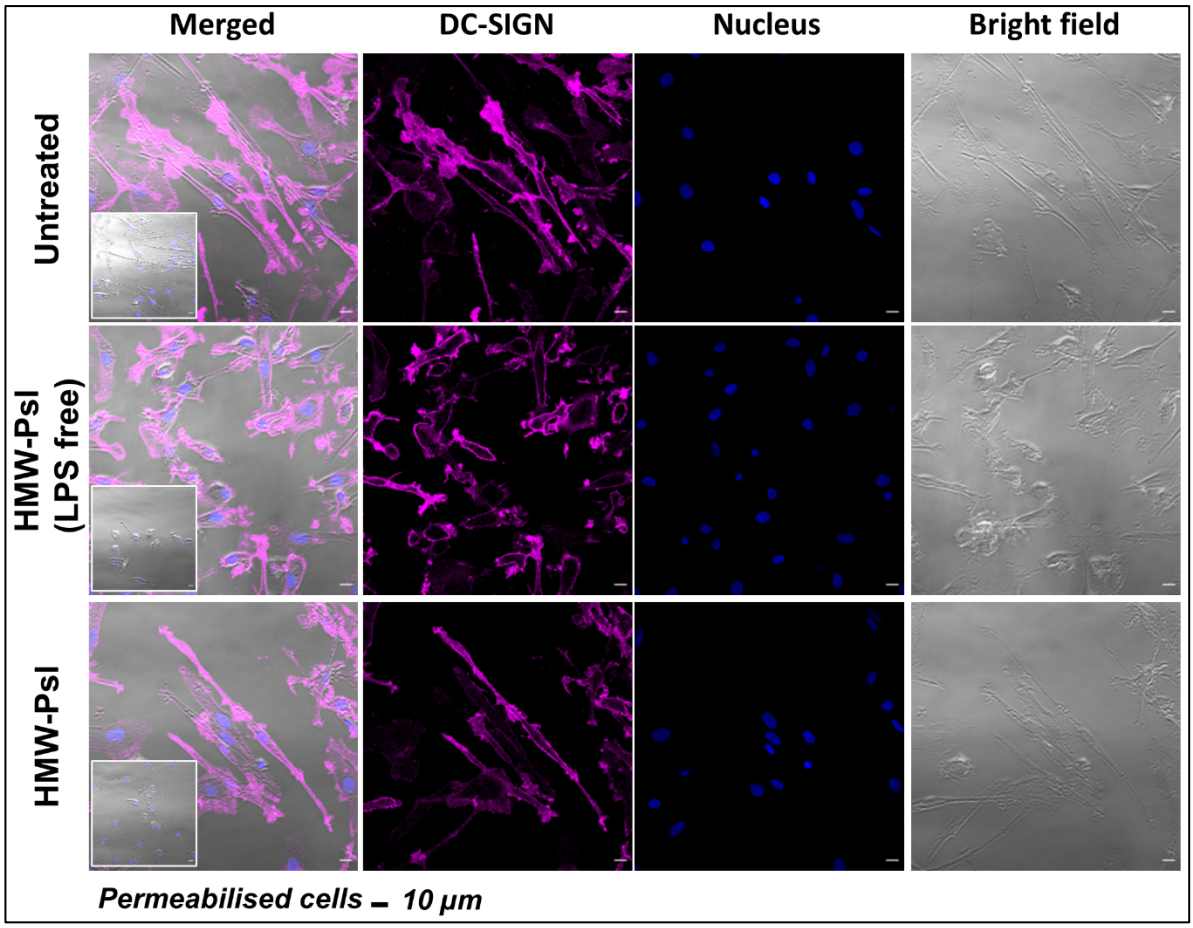


Figure 5.18 Specific detection of DC-SIGN in permeabilised moDCs in the presence and absence of PsI.

PsI (with and without LPS contamination) diluted in X-Vivo-15 (10 µg/ml) was used to coat chambers of µ-slide VI 0.4 flow slides for 24 h. moDCs (5 x 10^4 cells per channel) were added and incubated for 24 hr. Samples were then fixed before blocked and permeabilised with 0.25% Triton X-100 in blocking buffer [5% normal donkey serum (NDS) in PEM] for 20 min at RT. Permeabilised samples were then stained for DC-SIGN with 10 µg/ml of Rb pAb and anti-rabbit secondary antibody 1:500 (DC-SIGN, magenta), and 1.5 µg/ml DAPI (nucleus, blue). Insets in show labelling with secondary antibody only of permeabilised samples. Image processed using Fiji. Size bars: 10 µm.

5.5. Summary

To summarize data presented in this chapter:

- Flow cytometry analysis indicated high expression of DC-SIGN and MR by moDCs (Figure 5.3).
- Biofilm-moDC co-culture studies in the presence and absence of Psl show high variability in cytokine production, and suggest either a minor role for carbohydrates in dictating the early responses of moDCs to biofilms, or the model used is not the right approach to study this interaction (Figure 5.5, Figure 5.6 and Figure 5.9).
- Confocal analysis of DC-SIGN on cells incubated with Psl-containing biofilms or HMW-Psl-2$^{(LPS\text{-}free)}$ revealed rounded cells morphology (Figure 5.16, Figure 5.17 and Figure 5.18). These results agree with specific ability of two HMW-Psl preparations to modulate DC-SIGN-mediated endocytosis in moDCs (Figure 5.11 and Figure 5.12).

5.6. Discussion

Our data in (Chapter 4, section 4.1.7 and 4.5) showed that the CTLD4-7 region of MR, the extracellular domain of DC-SIGN and CRD domain of Dectin-2 recognise PA biofilms and purified EPS carbohydrate. In this chapter, we have utilised moDCs (DC-SIGN+, MR+, Dectin-1^{low} and Dectin-$2^{low/-}$, Figure 5.3) to study the effect of CLRs engagement in the immune recognition of PA biofilms and Psl. This is, to our knowledge, the first attempt to utilise human DCs expressing DC-SIGN and MR to investigate the engagement of CLRs through EPS recognition. We hypothesised such engagements would provide an advantage to the bacteria by modulating the immune cells towards a regulatory phenotype, hence facilitating the establishment of chronic infection.

Biofilms are critical players in bacterial pathogenesis. Several reports indicated an immune-modulatory effect of PA biofilms (Jones and Wozniak, 2017, Mulcahy et al., 2014, Rasamiravaka et al., 2015). MR and DC-SIGN are known as promotors of immune regulatory responses intended to mitigate inflammatory harm and MR and/or DC-SIGN binding is regarded as mechanisms of immune evasion during infection (Garcia-Vallejo and van Kooyk, 2013, Martinez-Pomares, 2012). Based on the fact that biofilms are generally linked to chronic disease, it is possible to speculate that a biofilm mode of growth will offset immune attacks after early infections started by planktonic cells while tuning immunity to non-resolving, ineffective immunity as shown earlier in (Figure 5.1).

Our strategy in this chapter was to use human myeloid cells that express all CLRs being investigated to determine their response to PA biofilms or purified Psl. Using human moDCs (DC-SIGN+, MR+, Dectin-1^{low}, Dectin-$2^{low/-}$, Figure 5.3), we have shown that (i) Biofilm-moDC co-culture studies in the presence and absence of HMW-Psl-$2^{(LPS\text{-}free)}$ show high variability in cytokine production and suggest either a minor role for carbohydrates in dictating the early responses of moDCs to biofilms or the model used is not the right approach to study this interaction (Figure 5.5, Figure 5.6 and Figure 5.9). More importantly, we have shown (ii)

specific ability of HMW-Psl-1 and HMW-Psl-2 to modulate DC-SIGN-mediated endocytosis in moDCs (Figure 5.11Figure 5.12), and (iii) confocal analysis of DC-SIGN on cells incubated with Psl-containing biofilms or HMW-Psl-2$^{(LPS\text{-}free)}$ revealed that cells adopt a rounded morphology (Figure 5.16, Figure 5.17 andFigure 5.18).

5.6.1. moDCs express high level of DC-SIGN and MR but not Dectin-2.

Taking advantage of novel RNAseq data set produced in the lab by Dr Sirina Muntaka (unpublished), we explored the expression of several CLRs at the transcriptional level in human monocyte-derived macrophages (5.4.1.1). M-CSF is a key inducer of macrophage differentiation (Hamilton, 2008); it is constitutively expressed under steady-state conditions leading to resident M2-like macrophages, while GM-CSF is enhanced during inflammation and promotes pro-inflammatory M1-like macrophages (Hamilton, 2008).

For the RNAseq study, CD14+ monocytes were differentiated into macrophages using M-CSF (Martinez and Gordon, 2014). Data indicate that in M-CSF-Macrophages highest expression was observed for MR followed by DC-SIGN and Dectin-1, respectively (Figure 5.2). This result agrees with studies showing that DC-SIGN expression is not restricted to human dendritic cells (Soilleux et al., 2002, Domínguez-Soto et al., 2011, Garcia-Vallejo and van Kooyk, 2013). However, levels of Dectin-2 transcripts were very low, consistent with previous observations (Miura et al., 2019, Taylor et al., 2005b). Although macrophages treated with LPS exhibited higher Dectin-2 compared to untreated consistent with previous research (Miura et al., 2019, Taylor et al., 2005b), levels of Dectin-2 were still very low indicating a major limitation that prevented the use of macrophages in this study (Figure 5.2).

As DC-SIGN expression has been described in DCs (Garcia-Vallejo and van Kooyk, 2013), we explored the expression of these CLRs on moDCs a well-known antigen-presenting cells (Rossi and Young, 2005). Culturing of mouse bone marrow cells with the cytokine GM-CSF is widely used to generate mouse bone marrow DCs in large numbers (Inaba et al., 1992,

Steinman and Inaba, 1999, van de Laar et al., 2012, Zhan et al., 2012a, Zhan et al., 2012b). In humans, the differentiation of moDCs was found to be dependent on IL-4 (Romani et al., 1996, Sallusto and Lanzavecchia, 1994, Bender et al., 1996). A strong relationship between IL-4 and both DC-SIGN and MR expression has been reported in the literature. It was indicated that IL-4 primarily induces DC-SIGN expression during the monocyte-DC differentiation pathway and GM-CSF cooperates with IL-4 to up-regulate DC-SIGN expression during moDCs differentiation (Relloso et al., 2002). Additionally, it was reported that interleukin IL-4 up-regulated MR surface expression (Stein et al., 1992). The RNAseq results are in agreement with these observations as both MR and DC-SIGN transcripts are upregulated by IL-4 (Figure 5.2).

In our study, we generated moDCs after culturing human CD14+ monocyte for 6 days in RPMI media containing IL-4 and GM-CSF as described in (2.9). While the addition of GM-CSF with IL-4 has shown to induce the expression of DC-SIGN and MR, the addition of these two cytokines did not promote Dectin-2 expression. Flow cytometry analysis (Figure 5.3 A) indicated that moDCs are best suited to investigate the contribution of MR and DC-SIGN to biofilm recognition, but would not be efficient for investigating Dectin-2 contribution. Our data (Figure 5.3 A) showed relatively low expression of Dectin-2 on moDCs, which is consistent with a previous observation (Carter et al., 2006). It seems possible that these results are due to the downregulation effect of IL-4 on Dectin-2 expression on moDCs (Gavino et al., 2005).

Although it was reported that IL-4 and GM-CSF would stimulate the expression of Dectin-1 (Willment et al., 2003), similar to Dectin-2 our data showed low expression of Dectin-1 in moDCs (Figure 5.3 A). These data must be interpreted with caution as the expression of both Dectin-1 and Dectin-2 were relatively low; therefore, there is a need for data validation with known positive controls of both lectins.

Since our data suggest that neither human monocyte-derived macrophages or DCs would not be suitable to establish Dectin-2 contribution to biofilm recognition, to develop a full picture of

Dectin-2 function in recognition of PA biofilms, future research should include the use of different primary cells with high expression of this receptor. For example, possible human cell types include monocytes and neutrophils as it was indicated to express Dectin-2 (McDonald et al., 2012). Additionally, as mentioned in the main introduction and chapter 4 introduction, mouse models might offer a good tool to explore the contrition of Dectin-2 in PA biofilms recognition. Further general recommendations for future research using mouse models is covered in (5.6.4.2).

5.6.2. Biofilm-moDC co-cultures in the presence and absence of Psl show high variability in cytokine production.

As stated in the introduction, biofilms are defined as bacterial cells enclosed in extracellular polymeric substances (EPS) which consist of proteins, nucleic acids and carbohydrates (Colvin et al., 2012, Irie et al., 2012). The three main carbohydrates produced by PA are Psl, Pel and alginate, with Psl and Pel playing a key role in biofilm structure in a strain-dependent manner (Colvin et al., 2012, Irie et al., 2012, Franklin et al., 2011). While the structure of Pel known to be largely composed of N-acetyl-galactosamine and N-acetyl-glucosamine (Jennings et al., 2015) Psl is described as mannose-rich exopolysaccharide (Byrd et al., 2009).

One of the keys aims of our lab MRC-funded project to study CLRs-PA biofilm interaction was to extract and purify the mannose-rich Psl from PA biofilms. Dr. Sonali Singh efforts in our lab resulted in the production of several Psl preparations from Δ*wspF*Δ*pel* biofilms which lack Pel and overexpress Psl (4.1.7). Based on protein standards, Psl preparations were divided into high (>45 kDa, HMW-Psl) and low molecular weight (<45 kDa, LMW-Psl) (Figure 4.5). This is consistent with a previous study indicating the presence of both LMW-Psl and HMW-Psl (Byrd et al., 2009). As stated earlier, due to the high level of unknown impurities in LMW-Psl compared to HMW-Psl detected by ^{1}H-NMR analysis (data not shown), we only utilised HMW-Psl preparations in this study. ^{1}H-NMR spectra of two HMW-Psl preparation indicates high

level of similarity and shows that mannose, is the major monomer present and accounts for 74.9%-87.2% of the hydrolysed carbohydrates monomer compositions in moles (Figure 4.6).

Silver staining of both HMW-Psl preparations highlighted large LPS contamination (Figure 5.4 A) (Singh et al., 2020). Since LPS is known as a potent cellular activator as mentioned in (1.3.4), there was a critical need to remove LPS from HMW-Psl preparation prior assessment of cellular responses. LPS removal from HMW-Psl was achieved and confirmed using SDS-PAGE (Figure 5.4 B) as a result of significant efforts placed by our lab members (Dr. Sonali, Singh and Darryl Jackson), ELISA binding assays indicated that HMW-Psl$^{(LPS\text{-}free)}$ retained the ability to bind DC-SIGN and MR-CTLD4-7 (Figure 5.4 C). With this information in hand, we moved to assess the interaction between DC-SIGN and MR and HMW-Psl$^{(LPS\text{-}free)}$ on the cellular level.

5.6.2.1. Different experiments performed to assess cytokine release.

The analysis presented in (Figure 5.3) confirms that DC-SIGN and MR are highly expressed in all moDCs tested, although there was a donor to donor variability. As stated above, a series of different experiments were performed to assess cytokine profiles (5.4.2). We quantified IL-1β, IL-23, IL-6, IL-10, MCP-1, Gro-α and TNF-α) in supernatants collected following 4 hr incubation.

Both DC-SIGN and MR binding were reported in the literature not directly to lead to the induction of immune responses; instead, the engagement of these receptors was reported to modulate signalling induced by other PRRs such as TLRs significantly. Contrary to expectations based on the strong binding of MR and DC-SIGN to HMW-Psl$^{(LPS\text{-}free)}$ which was confirmed by several methods (ELISA, Figure 5.4 C and BLI, Figure 4.13 B), results indicated that HMW-Psl$^{(LPS\text{-}free)}$ in isolation did not induce cytokine production by moDCs nor modified the response of moDCs to purified *E. coli* LPS (data not shown). These findings raise intriguing questions about the nature of DC-SIGN and MR interaction with HMW-Psl$^{(LPS\text{-}free)}$ and the possibility of such interaction requiring the presence of other ligands within the PA

biofilms or on planktonic cells to trigger a modulatory effect. However, the addition of different concentration of HMW-Psl$^{(LPS\text{-}free)}$ to PA biofilms formed by Psl-deficient strain or Psl-, Pel-deficient planktonic cells did not alter moDCs response (Figure 5.5).

ManLAM is a known ligand for both MR and DC-SIGN (Geijtenbeek et al., 2002, Kang et al., 2005). Rivière et al. (2004) have reported that the modulatory effect resulted from the engagement of both MR or DC-SIGN is only achieved by ManLAM clusters and not by monomers ManLAM (Rivière et al., 2004). Therefore, to rule out the possibility that the structure of our purified HMW-Psl$^{(LPS\text{-}free)}$ does not resemble that of Psl within PA biofilms, we exposed moDCs to PA biofilms formed by wspF mutant strains with different EPS components. Data showed no evidence that the presence of Psl influenced moDCs cytokine response to biofilms (Figure 5.6). Taken together, these results suggest that there is either no role for Psl on the modulation of moDCs responses or the models implemented in this study are too limited.

DC-SIGN induces signalling events that modulate TLR responses (Horrevorts et al., 2018). In the last attempt to use this model, we evaluated the effect of blocking DC-SIGN and/or MR well alter moDCs response to PA biofilms. Flowcytometry analysis validated the blocking capability of both anti-DC-SIGN (AZD-1), and anti-MR (15-2) used (Figure 5.7Figure 5.8). Similar to data observed with the earlier two assays, there was no clear effect of blocking either DC-SIGN, MR or/and Dectin-2 on the response of moDCs to PA biofilms (Figure 5.9). Thus far, the most obvious findings to emerge from using this model is that HMW-Psl$^{(LPS\text{-}free)}$ does not stimulate cytokines production of moDCs (Figure 5.5).

While we were conducting the experiments discussed above, Dr. Sonali Singh was carrying another set of tests aimed to determine whether HMW-Psl could affect different characteristics of moDCs. As stated in the literature, both MR and DC-SIGN are considered important endocytic receptors expressed by the antigen-presenting cells (Garcia-Vallejo and van Kooyk, 2013, Martinez-Pomares, 2012). Thus, the ability of two different HMW-Psl preparations

HMW-Psl-1 and HMW-Psl-2 to interfere with moDCs endocytic activities were evaluated. Presence of HMW-Psl-1 and HMW-Psl-2 (contaminated with LPS) partially inhibits the uptake of Lewisx-PAA-FITC (Figure 5.11) with no effect resulted from Polymyxin B (Figure 5.12) indicating specific ability of HMW-Psl to modulate DC-SIGN-mediated endocytosis in moDCs independent of LPS. These results triggered the establishment of the microscopy model to study moDCs- HMW-Psl interaction.

5.6.2.2. Rounded cells morphology when moDCs incubated with Psl-containing biofilms or purified HMW-Psl.

CLRs expressed by DCs facilitate pathogen internalisation and subcellular trafficking to endosomal compartment (Yamasaki, 2016). In particular, it has been well established in the literature that the interaction of DC-SIGN with mannose-rich ligands triggers internalisation (Engering et al., 2002). For example, it was reported that DC-SIGN binding to HIV-1 gp120 leads to internalisation and cytoskeleton remodelling that mediate subsequent transmission of HIV-1 to T cells (Smith et al., 2007, Moris et al., 2006). As our purified HMW-Psl showed capability to modulate DC-SIGN-mediated endocytosis in moDCs independent of LPS, we examined if HMW-Psl$^{(LPS\text{-}free)}$ could modulate other aspects of moDCs biology. Towards this aim, we first localised and optimised DC-SIGN staining.

Previous studies evaluated DC-SIGN expression on moDCs observed exclusive receptor expression at the extracellular membrane (Horrevorts et al., 2018, Cambi et al., 2004). In this research, we utilised anti-DC-SIGN mouse Ab (AZN-D1), kindly provided by Prof van Kooyk, VUMC, and rabbit polyclonal anti-DC-SIGN antibody (Rb pAb), both antibodies target the CRD domain of DC-SIGN. AZN-D1 is widely used in the literature to target and block DC-SIGN (Tacken et al., 2011, Geijtenbeek et al., 2000a) while only one previous study used the commercially available rabbit polyclonal anti-DC-SIGN antibody (Rb pAb) (Moutsopoulos et al., 2014).

Examination of samples using confocal microscopy revealed that DC-SIGN labelling with both antibodies used was identical (Figure 5.14), confirming that both target the same receptor. In agreement with earlier findings, our data revealed that the DC-SIGN was mostly detected at the cell surface (Horrevorts et al., 2018, Cambi et al., 2004). However, initial experiments demonstrated unexpected DC-SIGN staining in the nucleus (Figure 5.14), which was more obvious in permeabilised cells. Since DC-SIGN was never reported in the literature to be expressed in the nucleus, this finding raises an intriguing question regarding the use of PBS buffer in our assay to fix the cells prior staining for DC-SIGN.

PFA crosslinks the amino groups without modifying the tertiary protein structure, thus keeping epitopes in place for the detection by antibodies (Fujiwara, 1980, Robinson and Snyder, 2004). Proper PFA sample fixation was reported to be critical in microscopic analysis and play a crucial role in the introduction of artefacts (Pereira et al., 2019). Ideal fixation was shown to be important not only in preserving the structural properties of the cells but also minimising photobleaching that might result from using different fluorochromes for labelling (Endesfelder and Heilemann, 2014, Ha and Tinnefeld, 2012, van de Linde et al., 2010). Recent studies suggested that PFA fixation demonstrates better ability to preserve the architecture of the actin cytoskeleton and to facilitate the localization of various membrane-associated protein when it is dissolved in PEM compared to PBS (Leyton-Puig et al., 2016, Pereira et al., 2019).

In this study, we tested the effect of fixation with freshly prepared 4% PFA in PEM; results confirmed the previous observation of DC-SIGN expression associated with the cell membrane (Figure 5.15). More importantly, this time, there was no sign of DC-SIGN staining in the nucleus, which indicated that the previous observation highly likely related to the use of PBS buffer. To conclude, results of this investigation show that (1) DC-SIGN expression associated on the membrane of moDCs (Figure 5.14 and Figure 5.15), (2) both anti-DC-SIGN antibodies used showed identical staining for DC-SIGN, confirming that both target the same location, thus they can be used in further analysis (Figure 5.14), (3) artefact of nuclear staining of DC-SIGN was resolved by the using of PEM (Figure 5.15).

Previous studies evaluating the morphological characteristics of moDCs reported a significant increase in size, irregular shape and multiple dendritic projections, including podosomes, invadopodia and circular dorsal ruffles, following six days of culture in the presence of GM-SCF and IL-4 (Tang et al., 2005, Nguyen et al., 2015, McRae et al., 2000). Importantly, the irregular shape membrane structures, podosomes, are involved in many cellular activities. In addition to their role in attachment, podosomes allow DCs to migrate through the extracellular matrix and control the cells actin arrangement through complex mechanisms (Linder and Aepfelbacher, 2003, Buccione et al., 2004).

Preliminary results indicated that moDCs (DC-SIGN+, MR+, Dectin-1^{low}, Dectin-2$^{low/-}$, Figure 5.3) adopt rounded morphologies when incubated with biofilms formed by strains that overexpress Psl (Δ*wspF*, Δ*wspF*Δ*pel*) (Figure 5.16). Swetman Andersen et al. (2006) reported that DCs with rounded morphology have reduced adherence ability. In this preliminary assay (5.4.5.2), even though the same number of cells were added in all conditions, lower number of moDCs was noticed in wells containing Psl overexpressing strains (Δ*wspF*, Δ*wspF*Δ*pel*) (Figure 5.16). These results would seem to suggest that the rounded morphology observed in moDCs incubated with Psl^{+} biofilms could interfere with moDCs adhesion ability. Similar to the rounded cells observed with Psl^{+} biofilms, moDCs cultured with HMW-Psl$^{(LPS\text{-}free)}$ for 24 hr displayed a rounder morphology (Figure 5.17 and Figure 5.18), characterised by increased circularity index and reduced perimeter (Figure 5.17), suggesting changes in the cytoskeleton related to maturation state.

These morphological changes were less apparent when using HMW-Psl contaminated with LPS indicating that LPS can moderately reverse this effect (Figure 5.17 and Figure 5.18). Analysis of DC-SIGN surface expression showed reduced DC-SIGN labelling (Raw Integrated Density, Figure 5.17) in cells cultured in the presence of HMW-Psl (both with LPS or LPS-free preparations). When adjusting for cell size (Signal per Unit Area, Figure 5.17), only the LPS-containing samples showed reduced surface DC-SIGN labelling which is compatible with a more classical moDCs activation (Relloso et al., 2002) and recent published data which

showed reduction of DC-SIGN on moDCs following stimulation with LPS (Horrevorts et al., 2018). These findings support the possible ability of HMW-Psl to influence moDCs function in the absence or the presence of LPS, though the later need to be validated with LPS only control.

Podosomes contain proteins involved in adhesion and actin-regulating, including integrins, kinases, and GTPases (Murphy and Courtneidge, 2011, Foxall et al., 2016, Di Martino et al., 2016). DC-SIGN stimulation with antibody or HIV, a known DC-SIGN ligand, led to increased GTPase activity (Hodges et al., 2007). Once activated, GTPases are known to bind a variety of effectors and some actin-binding proteins that directly or indirectly affect the local assembly or disassembly of filamentous (F)-actin (Sit and Manser, 2011). Earlier studies report that PA activates GTPase in lung endothelial, epithelial and macrophages cells (Kazmierczak and Engel, 2002, Ganter et al., 2009). Interestingly although this activation is through the type three secretion protein ExoT, it induces morphological changes in macrophages similar to those observed in this study (cell rounding and detachment, Figure 5.16 and Figure 5.17) (Kazmierczak and Engel, 2002). Additionally, a previous study reported a rounded morphology in neutrophils incubated with PA biofilms which resulted in reduced neutrophil phagocytic ability (Jesaitis et al., 2003).

Immuno-gold labelling for various PRRs on moDCs confirmed localisation of PRRS such as DC-SIGN, MR, Dectin-1 and DCIR on moDCs podosomes with 3-fold (DC-SIGN) and 9-fold (MR) enrichment on podosome compared to other part of cell membrane (Baranov et al., 2014). It was reported that absence of podosomes, reduced 10 fold the DCs uptake ability (Gawden-Bone et al., 2010). Additionally, there are similarities between the moDCs' morphology caused by Psl in this study and those described by (Swetman Andersen et al., 2006). The study showed that DCs blocked with antibodies against CD209 adopted rounded morphology. Furthermore, cells treated with cytoskeleton inhibitor cytochalasin B and colchicine adopted a rounded shape as well (Swetman Andersen et al., 2006). Taken together, these studies support the notion that rounded cellular morphology might result from Psl binding

to DC-SIGN. The rounded cell morphology also was found to reduce the endocytic uptake by DCs through DC-SIGN significantly (Swetman Andersen et al., 2006); thus, it might be an evading mechanism of bacteria.

In summary, moDCs incubated with HMW-Psl$^{(LPS\text{-}Free)}$ adopted rounded morphology (Figure 5.17), suggesting that Psl capability to interfere with moDCs activity, possibly through modulation of cytoskeleton.

5.6.3. The possible adverse impact of bacterial fixation and donor variability on the cytokines results.

The clearest findings to emerge from this chapter is that HMW-Psl$^{(LPS\text{-}Free)}$ does not stimulate cytokines production of moDCs. However, the presence of HMW-Psl$^{(LPS\text{-}Free)}$ alters moDCs in two ways (1) stops Lewis^{x} uptake (Figure 5.11) and (2) induces a round morphology (Figure 5.17). Analysis of moDCs cytokines responses during different stimulation with PA biofilms and/or HMW-Psl$^{(LPS\text{-}Free)}$ did not show any modulatory effect (5.4.2). Hence, the question was, how can we observe an effect of HMW-Psl on Lewis^{X} uptake and the changes in morphology that does not translate into changes in cytokines release?. These results might indicate that the strategy followed in this chapter to study moDCs activation is not effective when studying the dynamics of moDCs interactions with PA biofilms and/or EPS components. This could be due to (1) biofilms were not fixed properly and/or (2) donors' variability.

Fixation techniques could be categorized into two types: additive and denaturing fixatives (St-Laurent et al., 2006). Additive fixatives (also known as cross-linking solutions) which include formaldehyde and paraformaldehyde, work by forming covalent bonds between proteins (Dapson, 2007). This approach largely maintains and preserve the proteins structures (Meade et al., 2010). On the other hand, denaturing fixatives such as methanol and ethanol, act by reducing protein solubility and/or interfering with hydrophobic association, thereby altering and denaturing protein structures and inactivating enzymes (St-Laurent et al., 2006). An issue that

was not addressed in this study was whether the fixation implemented in this study using 4% PFA for 10 min is enough for the full fixation of bacterial cells within biofilms.

Previous research comparing the effect of different fixation methods on the EPS found that fixation with 4% PFA highly preserves the bacterial EPS whereas glutaraldehyde or ethanol significantly removed the EPS (Chao and Zhang, 2011). One study explored the impact of fixating PA biofilms with 4% PFA found that Psl epitopes on PA biofilms are conserved indicating no effect of fixation on Psl within biofilms (Ray et al., 2017). All this information support the use of our fixation approach.

However, our fixation technique might not be effective in stopping the bacterial growth, and that may be mirrored in the high cytokines variability. The reason could be due to the fact that biofilm matrix is composed of 97% water (Zhang et al., 1998). The amount of water retained within PA biofilms is not fully studied but expected to be very high (Mann and Wozniak, 2012). It was speculated that this large amount of water might possibly disturb fixation process, leading to large variability between experiments when compared to other biofilms forming organisms such as *S. aureus* and *C.albicans* (Peeters et al., 2008).

Throughout this research, we endeavoured to apply identical procedures of growing, handling and fixing all the biofilms developed in 96-wells plates before the addition of moDCs in all assays. Consequently, different biofilms biomass which might contain different quantity of water might respond differently to the fixative added. Thus, the concentration of the added fixation might not be as anticipated as it might be diluted by the amount of water already present within the biofilms (Mann and Wozniak, 2012). Additionally, researchers reported that biofilms formed by PA showed a high degree of variability not only between each experiment but also between neighboured wells (Kragh et al., 2019).

In literature, biofilms are referred to as a defensive structure protecting the bacteria from antibiotics; in this state, bacteria within biofilms might be resistant to the fixation when compared to their planktonic counterparts. Our data showed IL-1β levels were significantly

higher when moDCs were exposed to biofilms forming strains compared to low/no biofilm strains with no influence of different EPS components on IL-1β release (Figure 5.6). LDH analysis of the supernatants collected showed that moDCs incubated with PA biofilms induced similar LDH levels to untreated samples, indicating IL-1β release is not due to cell death (Figure 5.10). It might appear like IL-1β release is biofilms specific, but it is highly anticipated that what we are observing is not biofilm-related but rather, related to the presence of live bacteria. PhD student Kelly Lee successfully recovered live bacteria from PA biofilms fixed with 4% PFA for 30 min, which suggested that our fixation approach was not efficient.

Unfixed bacteria might continue quorum sensing (QS) signalling. Several researchers have demonstrated that QS signals, when administered *in vitro*, can modulate the production of proinflammatory cytokines by macrophages (Glucksam-Galnoy et al., 2013). Moreover, as bacteria continue to grow, it will eventually increase the number of ligands associated with IL-1β release in PA infection such as T3SS or flagellin (Miao et al., 2008, Sutterwala et al., 2007, Miao et al., 2010, Faure et al., 2014). Therefore, we believe that the presence of live bacteria might be played a role in the high variability noticed in our cytokines data as fixation of bacteria cells for 10 min with 4% PFA was not effective in stopping the bacterial growth.

Another uncontrolled factor that might have influenced the results in our model is the work with primary human cells, which could introduce a high degree of biological variance (Li et al., 2016). This issue is a significant challenge for researchers. In our case, DCs are found in very low number in the blood. Thus, it is challenging to work with directly isolated DCs from blood (Plantinga et al., 2015). Alternatively, scientists have been culturing monocytes with GM-CSF and IL-4 to generate moDCs in large numbers as a tool to study DCs functions *in vitro* (Romani et al., 1996, Sallusto and Lanzavecchia, 1994, Bender et al., 1996, Inaba et al., 1992, Steinman and Inaba, 1999, van de Laar et al., 2012, Zhan et al., 2012a, Zhan et al., 2012b).

Primary human cells derived from different donors can behave differently in culture conditions depending on various factors, including genetics and age of individuals from whom that buffy

coat or tissue was derived (Li et al., 2016). In the case of infection, studies have shown that different donors might respond differently to bacteria and fungi due to genetic variations. For example, measurement of seven different cytokines after stimulation of PBMCs from 71 healthy donors with 10 different bacterial and fungal stimuli revealed inter-individual variability ($P < 0.01$) in cytokine secretion following stimulation (Li et al., 2016). Additionally, (Mummidi et al., 2001) reported significant donor variability of DC-SIGN expression in DCs, which might affect the interpretation of data when studying DC-SIGN-pathogen interactions and their influence on cytokines levels. In this chapter, we recognised a little to medium degree of variability in the expression of DC-SIGN and MR among donors tested, which in addition to the issue of bacterial fixation, add to the variability observed in cytokines.

In summary, it has been shown from this section that insufficient biofilms fixation and donor variability might have affected the cytokines data generated. Therefore, what is now needed is a full controlled model to study CLRs and PA biofilms interaction. The next section will introduce recommend adjustments on the current models and alternative models that could be used to follow up this study.

5.6.4. Recommended adjustments on the current models and an alternative mouse model that could be used to follow up this research

5.6.4.1. Revised model

Recognition of pathogen structures by TLRs induces signalling from either MyD88 or TRIF adaptor proteins leading to the activation of NF-kB and other transcript factors which influence the immune response (Fitzgerald and Kagan, 2020). Signals emerging from CLRs, including DC-SIGN, modulate TLR response (Geijtenbeek et al., 2002). A strong association was reported between DC-SIGN-mediated Raf-1 activation in response to several mannose-expressing pathogens, including *M. tuberculosis* and HIV-1, and the modulation of TLR immune responses (Gringhuis et al., 2007). DC-SIGN activation of RaF-1 in response to mannose structures was shown to modulate TLR-4 signalling by augmenting the expression

of IL-10, IL-12 and IL-6 (Gringhuis et al., 2007). In our model, in the context of cytokines analysis, we did not observe any modulatory effect of Psl on moDCs (DC-SIGN+, MR+, Dectin-1^{low}, Dectin-$2^{low/-}$, Figure 5.3) in any of the assays conducted (Figure 5.5, Figure 5.6 or Figure 5.9) Implementation of further controlled measures on bacterial fixation and donors variability could minimize the variability and improve the quality of the data generated using the current system. This could include both (1) the use of effective fixation technique and stratification of the donors based on DC-SIGN and MR expression profiles.

In regard to fixation, as stated above, current work in our lab is undergoing to evaluate different fixation approaches. The use of 4% PFA was reported to highly preserve the bacterial EPS compared with other fixatives (Chao and Zhang, 2011). More importantly, it conserved Psl epitopes on PA biofilms (Ray et al., 2017). All this information indicating our fixation approach was not altering the EPS composition as we aimed. However, with the fact that PA biofilms contain large amount of water (Mann and Wozniak, 2012) that could interfere with fixation process (Peeters et al., 2008); it could be recommended to use different PFA concentrations and time of incubation to reach the optimum condition that stops the bacterial growth and negligibly affect the EPS components. Inclusion of UV inactivation is currently being explored.

To reduce donor variability, moDCs generated from different donors could be divided into different groups. For example, after stimulation of moDCs with Psl, PA-biofilms and/or LPS, based on the cytokines profiles, individuals could be grouped to either a high or low responders. In support of this suggestion, measurement of seven different cytokines after stimulation of PBMCs from 71 healthy donors with 10 different bacterial and fungal stimuli reviled inter-individual variability ($P < 0.01$) in cytokine secretion following stimulation (Li et al., 2016). The same study also found that one particular individual could be a high responder in terms of one set of cytokines, but a low responder for other cytokines (Li et al., 2016). In general, based on these natural variations, it seems not possible to claim that the response of an individual to certain stimuli is similar to all other donors. Hence, grouping of donors based on high and low responders is highly recommended.

5.6.4.2. The use of mouse models

The physiological role of several CLRs has been well studied utilizing the targeted deletion of their homologs in mice (Yamasaki, 2016). However, with the absence of DC-SIGN homologs in mice and to address the functional role of human DC-SIGN in response to PA biofilms or Psl under *in vivo* condition, researchers applied the use of DC-SIGN transgenic mice as solution (Garcia-Vallejo and van Kooyk, 2013). However, mouse cells express other lectins such as DCIR which also binds high mannose structures (Yamasaki, 2016). Co-stimulation of CLRs was found to affect the internalisation of high mannose ligands. Particularly, DC-SIGN internalisation and antigen presentation to T-Cells was reduced when DCIR was triggered simultaneously (García-Vallejo et al., 2015). In our study, we found a ligand within the PA biofilms that bind three CLRs, MR, DC-SIGN and Dectin-2, it is possible that DCIR could also be involved in biofilm recognition. Current available models using only one CLRs knockout might provide a preliminary indication of the role of that CLR in PA EPS recognition, however, such model might miss the effect of the costimulation of other CLR which might have an impact on the data generated with that model. To fully understand the role of CLRs in PA infection, the need for a comprehensive mouse model that allows the study of multiple CLRs is essential.

5.6.5. Concluding remarks

Several questions remain to be answered, one of which is whether incubation of DCs stimulated with Psl with or with LPS would influence the differentiation of naive T-cell. Future work could focus on this area. Also, recognition of pathogen structures by TLR induce signalling from either MyD88 or TRIF adaptor proteins leading to the activation of NF-kB and other transcript factors which influence the immune responses (Fitzgerald and Kagan, 2020). Signals emerging from CLRs, including DC-SIGN, modulate TLR responses. A strong relationship was reported between DC-SIGN Raf-1 activation and the modulation of TLR signalling. DC-SIGN activation of Raf-1 in response to mannose structure was shown to modulate TLR-4 signalling by augmenting the expression of IL-10, IL-12 and IL-6 (Gringhuis

et al., 2007). Work will need to be done to determine whether Psl with or without LPS, induce Raf-1 activation.

Despite its limitations, this study certainly adds to our understanding of the interaction between biofilm-associated carbohydrates and CLRs and opens the possibility for these receptors to contribute to the establishment of chronic infections.

Chapter 6. Analysis of biofilm-human neutrophils interactions

6.1. Introduction

Different types of cells participate in the immune response to PA, including epithelial cells, neutrophils, macrophages, lymphocytes and DCs (Gellatly and Hancock, 2013). Neutrophils, however, are regarded as the most important cells in the defence against PA infection (Williams et al., 2010) and their contribution to PA clearance is considered more important than that of other cells, particularly during acute infection (Ojielo et al., 2003). For example, neutrophil-depleted mice were much more susceptible to PA infection even when very small bacterial numbers were used (Koh et al., 2009). Depletion of neutrophils in mice results in higher mortality during PA-induced pneumonia (Tsai et al., 2000). However, there is evidence of PA overcoming neutrophil-mediated killing *in vitro* and reports of PA utilising neutrophil-released DNA for biofilms formation (Walker et al., 2005, Laharrague et al., 1984).

Neutrophils follow a variety of signals to reach sites of infection (de Oliveira et al., 2016). Neutrophils recognition of PA biofilms is facilitated by several pathogen recognition receptors that detect several ligands such as LPS, peptidoglycan, bacterial DNA and other PAMPs (Madianos et al., 2005, Bass et al., 2008, Newton and Dixit, 2012). Additionally, there are reports of neutrophils being attracted to biofilms by different potent chemo-attractant such as the quorum sensing molecules N-acyl homoserine lactones (AHL) and formyl-Met-Leu-Phe (Karlsson et al., 2012, Holm and Vikström, 2014).

As the first responder cells of the innate immune system, neutrophils possess a unique set of migration features. These include high velocity, and both ability for transmigration, shared by other leukocytes across endothelia, and reverse migration (Vestweber, 2015, Wang et al., 2017). Neutrophil nuclei are considered key determinants of neutrophil migration as it transmits traction force through cells as they migrate (Manley et al., 2018). Neutrophils can

migrate within a short space of time through different extravascular environments through polarisation and repeated cycles of adhesion, extension, contraction and adhesion (Sheetz et al., 1998). There were indications based on in vitro experiments that the local physical environment also modifies neutrophils migration properties (Bershadsky et al., 2003, Toyjanova et al., 2015). Throughout migration process, neutrophils integrate multiple extracellular signals from several source to direct their migration (Van Haastert and Devreotes, 2004).

Several studies on the interaction of neutrophils with biofilms report migration of neutrophils towards biofilms and neutrophils localised within, around or on biofilms. Neutrophils are reported to remain phagocytic and able to release granule contents and form nets (Jesaitis et al., 2003). The same study reported that although neutrophils were phagocytic when settled on PA biofilms, they become immobilised and acquired a rounded morphology (Jesaitis et al., 2003). Using time-lapse microscopy to monitor the dynamic interactions between PA and neutrophils in a mouse model of bacterial keratitis, Thanabalasuriar et al. (2019) found that neutrophils were not able to eradicate infection caused by biofilm-forming PA. In contrast neutrophils were efficient at clearing biofilm-deficient bacteria. The authors also demonstrated that anti-biofilm antibodies that target Psl blocked biofilm formation and reduced ocular infection and pathology while preventing bacterial dissemination (Thanabalasuriar et al., 2019). Indicating that biofilm formation was hindering neutrophils activity. In line with this it has been indicated that extensive amounts of eDNA and biofilm EPS found in mucus obtained from CF patients restricted neutrophils movements (Stewart, 2014). Similarly, it has been suggested that biofilm mechanics may assist resistance to phagocytic clearance by neutrophils (Kovach et al., 2017). Considering the clinical relevance of this opportunistic pathogen, it is essential to better understand neutrophil-biofilm interplay.

Here, we describe an *in vitro* assay that allows us to examine neutrophils' behaviour, as determined by live and confocal microscope following their interaction with PA, as a planktonic or biofilms. Using live microscopy analysis, we observed that (1) biofilms reduced neutrophil

velocity, net distance covered and the mean square displacement (MSD). Using confocal microscopy analysis, we observed that (2) neutrophils appeared unable to release granules when incubated with biofilms. Finally (3) preliminary observations indicated that cells exhibit higher circularity when incubated with biofilm formed by strains expressing Psl or Psl-deficient biofilms in the presence of HMW-PSL.

6.2. Hypothesis

The establishment of an *in vitro* model suitable for imaging will enable us to examine neutrophil morphological and behavioural changes following their contact with PA biofilms.

6.3. Aims

6.3.1. Establish an assay to study neutrophil-PA biofilm interactions.

6.3.2. Utilise this assay to determine neutrophil morphological and behavioural changes following their interaction with PA biofilms.

6.4. Results

6.4.1. Optimisation of neutrophil PA co-culture for microscopic analysis

After having produced consistent biofilms using the syringe pump system described in (2.6.4) and applying this system to determine the distribution of CLRs ligands within biofilms (4.4.3) and investigate DCs-biofilm interactions (5.4.5) we employed this system to establish a model to study biofilms and neutrophil interaction. A first step towards this aim was the optimisation of the procedure and several testing experiments were carried out aimed to standardise the assay to generate reproducible data.

6.4.2. Neutrophil isolation using negative selection

First, although when this study established, there was a neutrophil isolation technique already used in the lab (Muntaka et al., 2019), a reliably quicker neutrophil isolation technique was required to reduce duration of the isolation process and the time neutrophil left on the bench due to short neutrophil half-life (Summers et al., 2010). The purification procedure should also provide high purity neutrophils with minimum or no activation (Oh et al., 2008). Therefore, we employed a neutrophil isolation technique commercially available that enable the isolation of non-activated neutrophils directly from whole blood using negative selection (STEMCELL, 19666). Briefly as described in (2.10), whole blood collected in EDTA was transferred to an isolation round button tube and mixed with antibody Isolation cocktail and magnetic RapidSpheres, which target all cells in the blood except neutrophils. The tube is then placed in a magnet, which pulls unwanted cells to the side of the tube, and the purified neutrophils can be poured from the tube (Figure 6.1 A.). Cytospin analysis using a bright field inverted microscope indicated successful neutrophil isolation (Figure 6.1 A.). It was reported that purified neutrophils require Ca^{2+} and Mg^{2+} for activation (Estensen et al., 1976). As mentioned in (2.10) during the isolation process, we used Hank's buffer without Ca^{2+} and Mg^{2+} as a dilution solution aiming not to activate the neutrophils. However, prior addition to biofilms cells were washed twice with Hank's buffer with Ca^{2+} and Mg^{2+} before being suspended in X-Vivo-

15 and added to biofilms. Our data indicated that this method generates highly purified neutrophils in a short time, thus we employed this procedure in all assays conducted in our study.

6.4.3. Analysis of Dectin-2 expression by neutrophils.

Following neutrophil isolation, along with our efforts in assessing Dectin-2 expression in human macrophages and DCs presented in (Figure 5.2 and Figure 5.3, respectively), we also explored whether human neutrophils offer a suitable model to study the biological consequences of the Dectin-2-biofilm interaction reported in (4.5). For this, the expression of Dectin-2, along with the expression of the known neutrophil marker CD66b (Eades-Perner et al., 1998), was assessed by flow cytometry using commercial antibodies (FAB3114A, R&D) and (130-104-395, Miltenyi Biotec), respectively. Unstained and relevant antibody isotypes were used as controls. Results demonstrate low/negative expression of Dectin-2 and high expression of CD66b (Figure 6.1 B.). This result is in agreement previous observation of relatively low expression of Dectin-2 on human neutrophils (McDonald et al., 2012) and high expression of CD66b (Eades-Perner et al., 1998). Data of Dectin-2 expression must be interpreted with caution because when the same Dectin-2 antibody stock was used to stain monocytes and/or Dectin-2 expressing cell lines (Ishikawa et al., 2013), similar results were observed, which is opposite of what was expected (data not shown) (Taylor et al., 2005b). Thus, further work is required to validate these findings.

In addition, we studied the expression of Dectin-2 on human neutrophils by western blotting. For this, cells were lysed as described (2.12), and total protein concentration was determined by the BCA assay. Four serial dilutions of the lysate were electrophoresed, and Dectin-2-Fc was used as a positive control. Anti-Dectin-2 antibody mouse monoclonal antibody (IMG3D1) was used as a primary Ab at 2 µg/ml. IRDye 800CW anti-mouse was used as secondary Ab at 1:5000. Dectin-2 was detected as a 40 kDa band in a dose-dependent manner (Figure 6.1 C.), this is higher than the full-length Dectin-2 expected size which is 27 kDa (Ariizumi et al.,

2000). Furthermore, results showed a high molecular weight band (Figure 6.1 C.) which might indicate either cross-reactivity of the anti-Dectin-2 antibody or presence of Dectin-2 heterodimers with other lectin(s), such as Dectin-3 which has been reported in the literature (Zhu et al., 2013).

Overall, these preliminary observations suggest that Dectin-2 appears to be expressed by human neutrophils, although further work is required to validate these data as there were concerns regarding the quality of the antibodies. Additionally, further studies on western blotting analysis need to be undertaken in future, including the use of a secondary antibody only control.

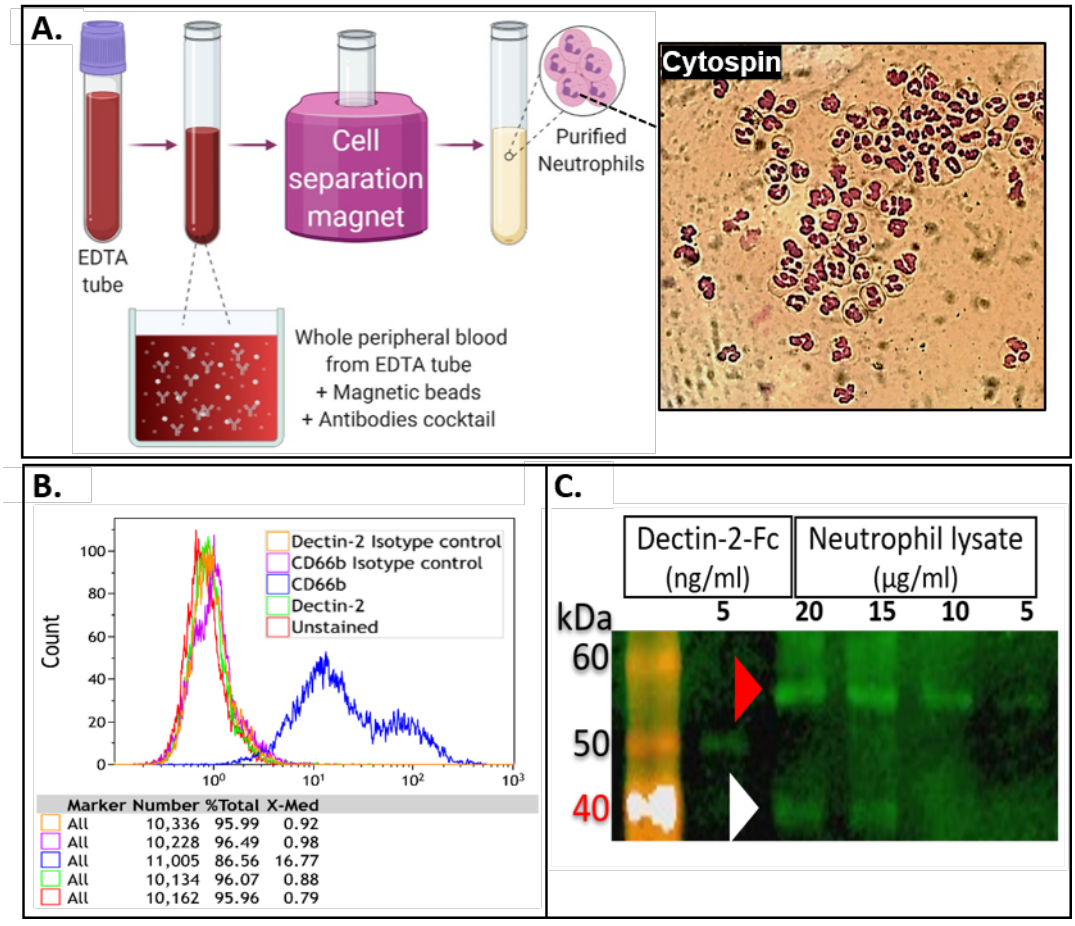


Figure 6.1 Neutrophil purification and analysis of Dectin-2 expression

(A.) Schematic flow chart of the process of immunomagnetic negative isolation of neutrophil directly from peripheral blood collected in a tube containing EDTA. Briefly, peripheral blood was mixed in a round-bottom tube with both antibody Isolation cocktail (50 µl/ml), and the magnetic RapidSpheres (50 µl/ml) following manufacturers' instructions. The tube then was placed in a magnet, and purified

neutrophils were poured into a fresh tube. The purity of the isolated neutrophil was verified by cytospin, as shown in the representative image taken using a bright-field inverted microscope. Cell suspensions were placed onto a glass slide already inserted into cytofunnels (EZ Single Cytofunnel, Ref: A78710020, Fisher Scientific). This was then spun at 200 rpm, 20 min, at low acceleration using a cytospin (Cytospin 2, Shandon). Slides were air-dried, labelled with Hemacolor (MERCK) following the manufacturer's procedure (solution 1: applied for 30 seconds, solution 2 for 3 seconds and solution 3 for 6 seconds), air-dried, mounted with DPX (Sigma-Aldrich). The stained slides were examined under a bright field inverted microscope fitted with a camera. **(B.)** Neutrophils isolated by negative selection were tested for Dectin-2 and CD66b expression by flow cytometry. Cells were re-suspended in X-Vivo-15 media in a 15 ml Falcon tube at a density of 1×10^6 cells/ml, centrifuged and re-suspended in 1 ml of 5% (v/v) human serum in PBA solution, and incubated for 1 hr at 4°C. After washing, the cell density was adjusted to 100,000 cells/100µl of PBA and cells were incubated with mouse anti-human monoclonal antibodies or the matched isotype control of CLEC6A (Dectin-2)-APC, or CD66b-FITC (REA306, Miltenyi Biotec, Germany) or the matched recombinant antibody (REA) control for 1 hr at 4°C. Cells were washed and fixed with 0.5% (v/v) PFA and analysed using a FC500 Beckman Coulter flow cytometer; 10,000 events were collected. Data were analysed using Kaluza Software 1.5a. Data are from 1 preparation and show histograms for each labelling which show expression of CD66b but low/no expression of Dectin-2. **(C.)** Analysis of Dectin-2 expression in human neutrophil by western blot. Cells were lysed in lysis buffer (10 mM Tris-Hcl, pH 8.2, 150 mM NaCl, 5 mM EDTA, 2% Triton X-100 and protease inhibitors). Different amounts of protein were electrophoresed on SDS–PAGE. A 10-230 KbP Protein ladder was used to determine molecular weight. The gels were then electroblotted onto nitrocellulose membranes. After blocking, membranes were incubated with specific primary anti-human antibodies against Dectin-2. The relevant protein was visualised by staining with IRDye 800CW anti-mouse Licor for 1 hr at room temperature. Bands were visualised using Odyssey Imager (LI-Cor biosciences). Data are from 1 preparation and show expression of Dectin-2 at 40 kDa in a dose-dependent manner (white arrow). However, there was unexplained high band at 57 kDa detected which might indicate cross-reactivity of the anti-Dectin-2 antibody used (red arrow) or the presence of Dectin-2 heterodimers with other lectin(s), such as Dectin-3 which has been reported in the literature (Zhu et al., 2013).

6.4.4. Optimisation experiments to study neutrophil-PA interaction

Several optimisation experiments were carried out to explore the possibility of using live microscopy to investigate the interaction of neutrophils with PA biofilms. In the first optimisation experiments, PAO1 biofilms generated under flow conditions in ibidi µ-Slide VI 0.4 for 15 hr as described in (2.6.4), fixed with 4% PFA in PBS for 10 min at 4°C and washed with PBS with Ca2+ and Mg2+ before the addition of human neutrophils at (5 x 10^5 cells /channel) suspended in X-Vivo-15. Neutrophils behaviour was monitored by live microscopy using DeltaVision microscope under Olympus U-Plan S-Apo 40X/0.95 objective.

Live microscopy exanimation and settings in the first optimisation assay and all assays presented in this chapter were performed by Dr. Chris Gell from the School of Life Sciences Imaging Facility. In the first optimisation experiments (Figure 6.2), the microscope was set up to take time-lapse images every 1 min for 2 hr from 10 different locations in the middle of the channel (area of homogenise shear stress as shown in Figure 3.8). Locations were 2 mm apart from each of other. Preliminary observations presented in (Figure 6.2 A) of individual frames from a continuous time-lapse movie show disappearance of PAO1 biofilms during incubation. Zoomed area of one single cell showed neutrophil engulfing biofilm material (Figure 6.2 B.). This preliminary observation indicated neutrophils cultured with fixed PAO1 biofilms in X-Vivo-15 were active during the time of incubation (2 hr) with no observed cells death. Our data also showed that cells were clearly detected with the Olympus U-Plan S-Apo 40X/0.95 objective, confirming our microscopic settings.

In an attempt to explore the possibility of labelling neutrophils using live cells staining prior incubation with PA biofilms, 5 x 10^4 PKH67-labelled neutrophils were added to fixed 15 hr PAO1 biofilms, and the interaction monitored live as explained earlier. Wells containing Δ*wspF* Δ*psl*Δ*pel* cultures were used as controls. Preliminary observation indicated neutrophils lost the staining during incubation (Figure 6.3 A.). To confirm this observation, we analysed PKH intensity over time. Briefly, using a rectangular selection tool in Fiji, the whole imaging area

were selected, and the mean intensity of all pixels within the selected area was calculated. Data indicated a reduction of the green intensity over time of incubation (Figure 6.3 B). Data also indicated that the standard deviation of the area selected (StdDeV) was very high at the first imaging point this is because of the large differences in intensity between neutrophils and other areas in the field (areas without neutrophils). However, the StdDev reduced during incubation, which means the difference in intensity is reduced over time of incubation (Figure 6.3 C.). This reduction in intensity could be caused by quenching of the signal caused by the laser. There were also concerns about the possibility of neutrophils being stressed by laser exposure. Therefore, all subsequent experiments were performed with unlabelled neutrophils, aiming to not exposed the cells to any form of stress that might influence the assay outcomes.

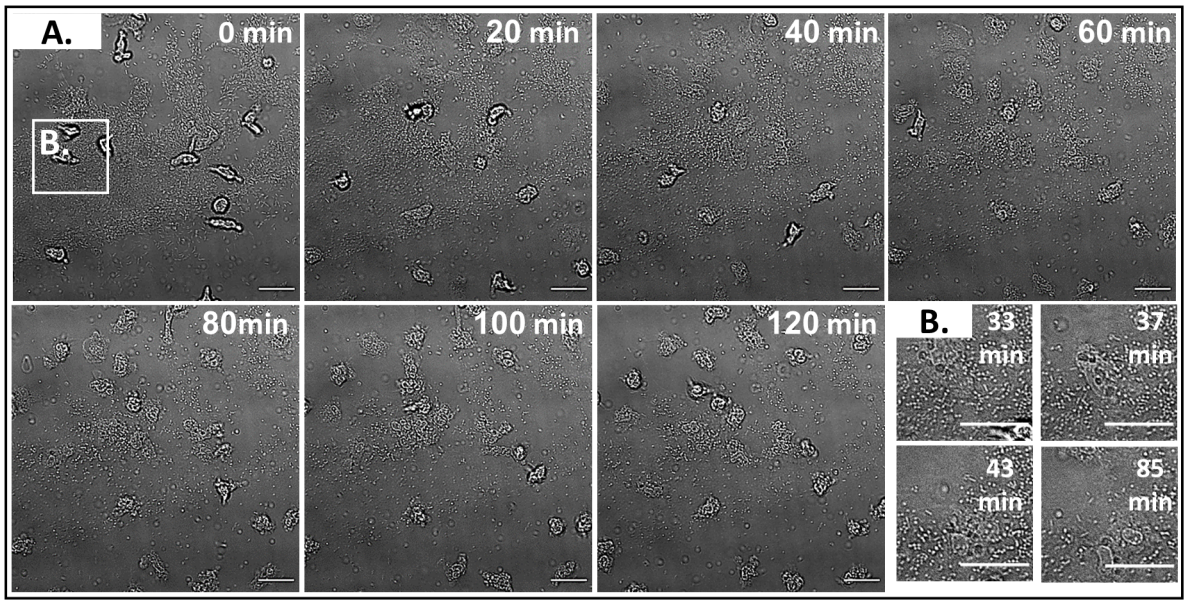


Figure 6.2 First live microscopy monitoring of neutrophil-biofilm interaction indicated neutrophil were active throughout 2 hr incubation.

PAO1 biofilms generated under flow conditions for 15 hr as described in (2.6.4) were fixed with 4% PFA in PBS for 10 min at RT and washed with PBS with Ca2+ and Mg2+ before addition of human neutrophils ($50x10^4$ cells per channel). Time-lapse images were taken every 1 min for 2 hr from 8 different location using a DeltaVision microscope under Olympus U-Plan S-Apo 40X/0.95 objective (please see videos of 8 location). **(A)** individual frames from a continuous time-lapse movie shown disappearance of PA biofilms overtime of incubation. **(B)** zoomed area of a single neutrophil engulfing PAO1 biofilm material. n = 1. (Scale bars: 20 μm.) Relative time is displayed in min.

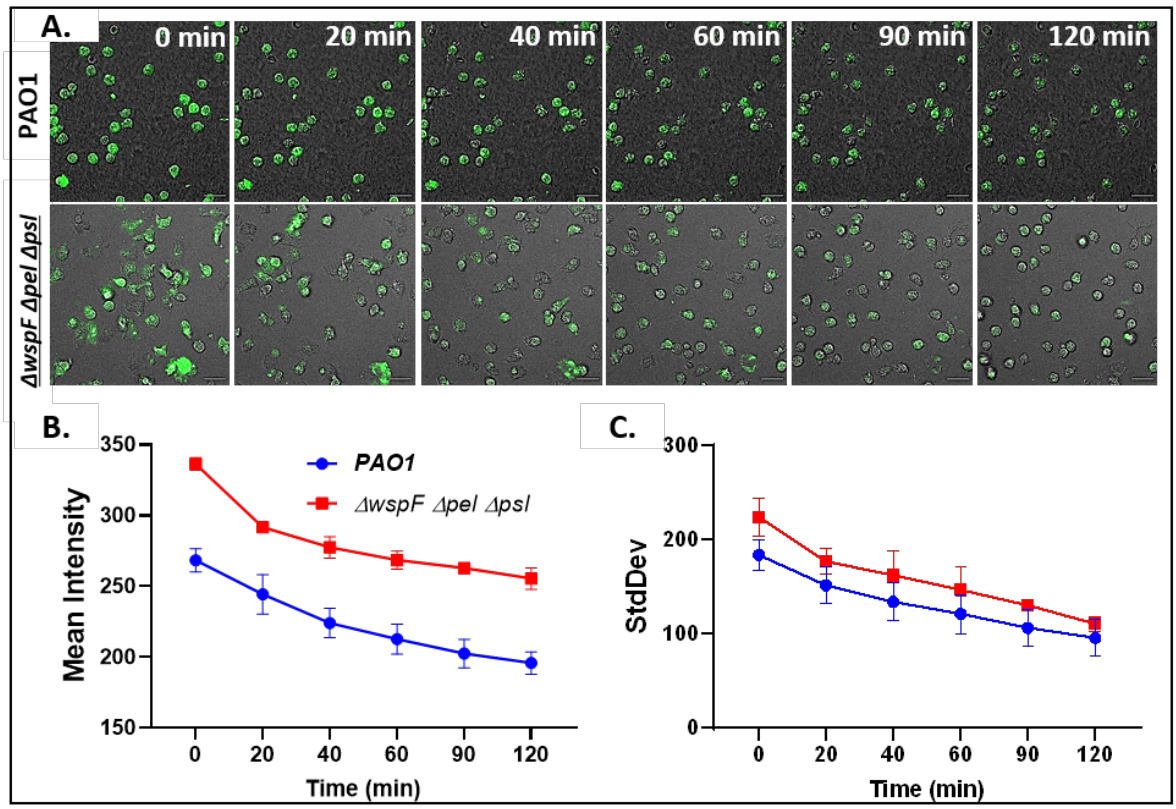


Figure 6.3 Analysis of neutrophil labelling intensity during live imaging

Human neutrophils pre-labelled with PKH (green) (2.10) (50.000 in 30 µl X-Vivo-15) were added to fixed PAO1 biofilms or Δ*wspF*Δ*pel*Δ*psl* bacteria cultured under flow condition in ibidi µ-Slide VI 0.4 for 15 hr as described in (2.6.4). Interaction was monitored live using DeltaVision microscope under Olympus U-Plan S-Apo 40X/0.95 objective. In this experiment images were acquired every 130 sec on the DeltaVision Elite. Scale bar, 20 µm. **(A)** Results indicated neutrophil lost staining and were not moving (please see the video) as compared to previous experiments. **(B)** Mean intensity of PKH stain indicates that neutrophils labelling became less bright over time. **(C)** Standard deviation of the area selected (StdDeV) was very high at the first time point this is because of the large variation in intensity observed in neutrophils compared of other filed area. However, the StdDev reduced over the time point of incubation, which means the difference in intensity is reduced over time of incubation. n = 1. (Scale bars: 20 µm.) Relative time is displayed in min.

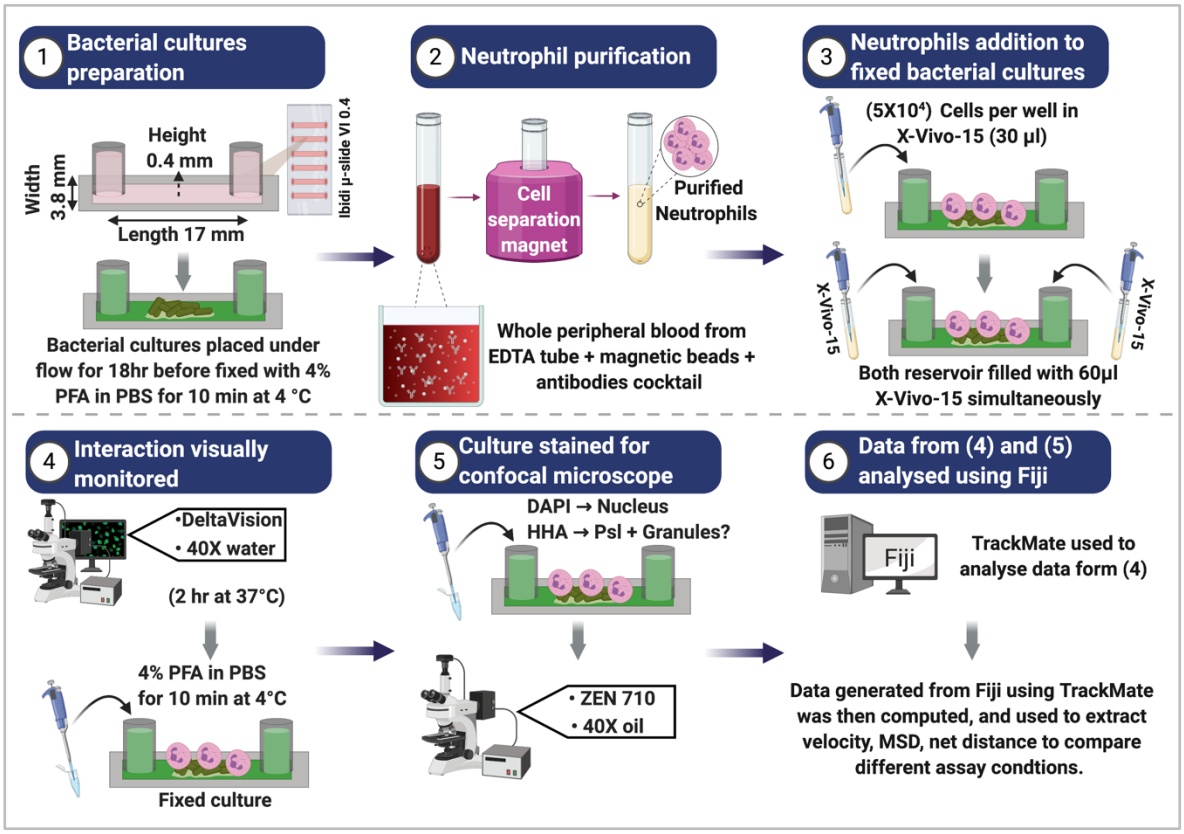


Figure 6.4 Summarised workflow of the microscopy-based assay to study neutrophil and PA interaction.

(1) Bacteria were cultured in µ-Slide VI 0.4 under flow for 18 hr to enable biofilm formation, fixed with 4% PFA in PBS (10 min at 4°C), washed twice with PBS with Ca^{2+} and Mg^{2+}. The slide was kept in 4°C while neutrophil isolation was performed. **(2)** Neutrophils were isolated by negative selection following manufacturers' protocol, as summarised earlier. In this process, we used Hank's buffer (HBSS) without Ca^{2+} and Mg^{2+} as a dilution solution aiming not to activate the neutrophils. However, prior addition to bacterial cultures cells were washed twice with HBSS with Ca^{2+} and Mg^{2+} before suspended in X-vivo-15 and added to biofilms. **(3)** Purified neutrophils were transferred to µ-Slide VI 0.4 (with or without fixed bacterial cultures, $5x10^4$ cells per channel). Following neutrophils inoculation 60 µl of fresh X-vivo-15 were added from both sides of the channel simultaneously (total volume 120 µl). **(4)** Neutrophil-PA co-cultures were incubated for 2 hr at 37°C. Interaction was monitored live by taking time-lapse images every 8 min using a DeltaVision microscope under Olympus U-Plan S-Apo 40X/0.95 objective. **(5)** Following 2 hr incubation co-cultures were fixed with 4% PFA prepared in PBS (10 min at 4°C) before being washed and stained for confocal analysis. **(6)** Microscopy images are processed for subsequent data analysis and interpretation using Fiji. Time laps analysis was performed by applying computational image-processing algorithms following tracking using the Fiji free plugin TrackMate.

6.4.5. Live microscopy analysis of neutrophil responses to PA biofilms

Following examination of different assay parameters as presented above, we standardised the assay conditions with the aim to generate reproducible data as shown in (Figure 6.4). In brief, bacterial cultures were placed under shear stress for 18 hr using the syringe pump system presented in (Figure 3.9). Three strains were used in this assay, PAO1, Δ*wspF* GFP and Δ*wspF*Δ*pel*Δ*psl GFP*. The GFP expressing Δ*wspF* GFP and Δ*wspF*Δ*pel*Δ*psl GFP* mutants were validated in the lab by Kelly Lee using PCR (data not shown).

After incubation bacterial cultures were fixed with 10 % PFA prepared in PBS for 10 min at 4°C and washed twice using PBS containing Ca^{2+} and Mg^{2+}. At this point bacterial cultures were left in PBS with Ca^{2+} and Mg^{2+} at 4°C while neutrophil isolation was conducted. After isolated neutrophils were washed twice with HBSS with Ca^{2+} and Mg^{2+}, diluted in fresh X-Vivo-15 and added to the slide (the opposite side of the original shear stress, 50,000 cells in 30 µl). Immediately 60 µl of fresh X-Vivo-15 were added simultaneously in each reservoir to reduce the tendency of neutrophils to move by capillarity as a result of surface tension. Cellular behaviour was monitored live using a DeltaVision microscope under Olympus U-Plan S-Apo 40X/0.95 objective. Time-lapse images (15) were taken every 8 min from each condition. To increase accuracy of the data generated using this system and to aid in the experimental design, we monitored the neutrophils movements in exactly 5 fixed locations for both repeats. These locations were stored with known stage coordinates and were applied in both experiments conducted as shown in (Figure 6.5).

After time lapse images were collected, data were uploaded to Fiji to conduct tracking analysis to perform statistical analysis of the microscopy data. For this we used TrackMate, an open source Fiji plugin for the automated tracking of single-particles (Tinevez et al., 2017). TrackMate uses algorithms that identify moving neutrophils and creates linkages between the same neutrophil from different time laps images and then provides neutrophils tracks that represents cells movements throughout the µ-Slide VI 0.4 over the 2 hr incubation. TrackMate

directly generates useful data for each individual cell such as mean velocity and net distances, data of each individual cell also can be exported for further analysis.

The tracking process by TrackMate involves several stages and we followed a protocol widely used for tracking cellular migration (Gorelik and Gautreau, 2014, Visweshwaran and Maritzen, 2019). First to differentiate the neutrophils on the time-lapsed images a detection process was established. The LOG detector was selected based on TrackMate developers' recommendation. This step will detect and draw a 10 μm estimated blob diameter around each cell in the track but will also select unwanted spots. To filter these unwanted spots to focus on the neutrophils, quality filters were applied. Second, to track the cells, simple lap tracker was applied with 50 micron linking max distances and gap closing distances and 16 gap closing frame. Next, data was generated after images were computed using algorithms written in detail at the original paper describing TrackMate.

In our study we compared different neutrophils motility parameters to investigate whether biofilms influence cellular motility. Velocity and net distance data were directly obtained from information generated from tracking analysis. Our data showed that neutrophils' velocity was lower when cells were incubated with biofilms-forming strains (PAO1, Δ*wspF*) compared to cells incubated with the planktonic strain (Δ*wspF* Δ*pel* Δ*psl)* or left untreated (Figure 6.7 A). A similar trend was also observed with another motility parameter, the net distance covered (Figure 6.7 B). These data indicate that biofilms limit neutrophils movement.

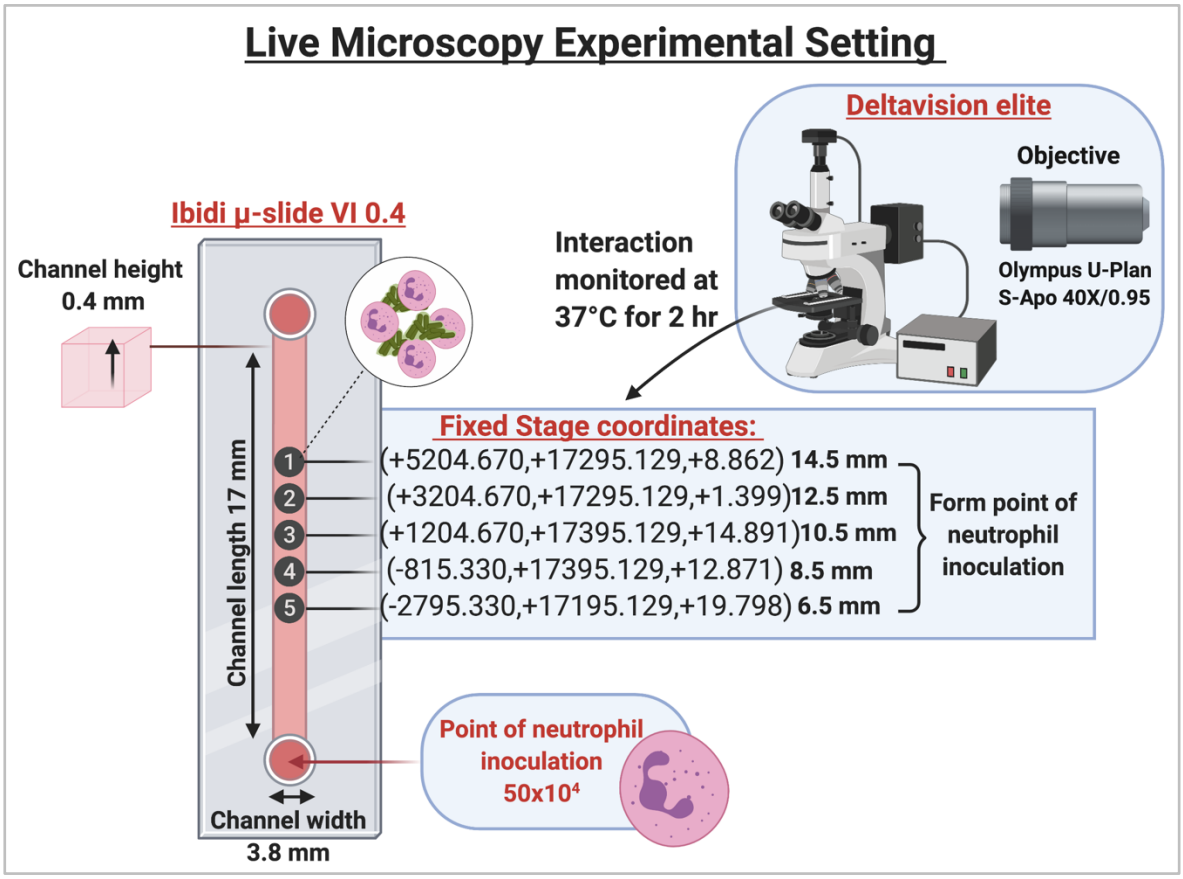


Figure 6.5 fixed stage coordinate used in this assay

Schematic chart designed using Biorender showing the fixed stage coordinates used in this assay.

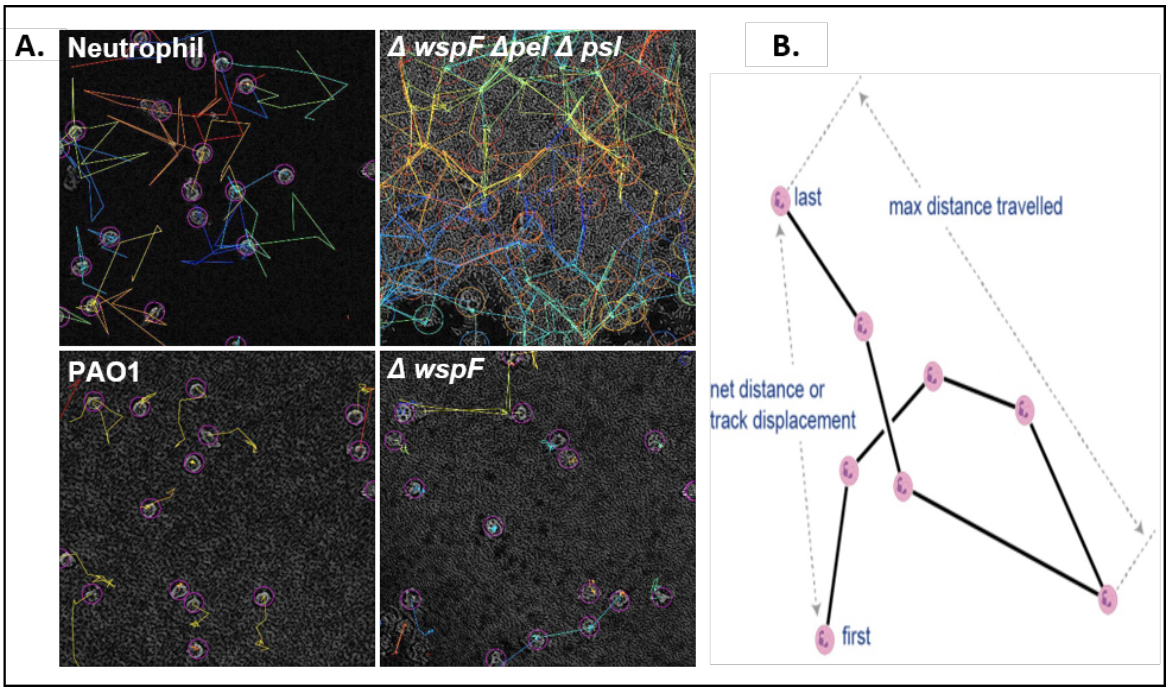


Figure 6.6 Neutrophil tracking using TrackMate

Following the acquisition of time-lapse images, data were uploaded to Fiji to conduct tracking analysis aiming to translate the microscopy data into numbers. Using TrackMate, an open-source Fiji plugin for the automated tracking of single-particles which uses algorithms that identify moving neutrophils and creates linkages between the same neutrophil from different time-lapse images and then gathers neutrophils tracks that represent cells movements throughout the µ-Slide VI 0.4 over the 2 hr incubation **(A.)** Examples taken from one location of the tracking results obtained by TrackMate Fiji plugin. Results show neutrophils exposed to fixed PAO1, Δ*wspF* and Δ*wspF*Δ*pel*Δ*psl* cultures or untreated (Neutrophils). Videos of the tracked image stacks available upon click on this link. The colour of the tracks represents the track index detected. Neutrophils are represented as spheres with an initially constant radius (10µm). **(B.)** TrackMate directly generates useful data for each cell such as mean velocity and net distances; data of each cell also can be exported for further analysis.

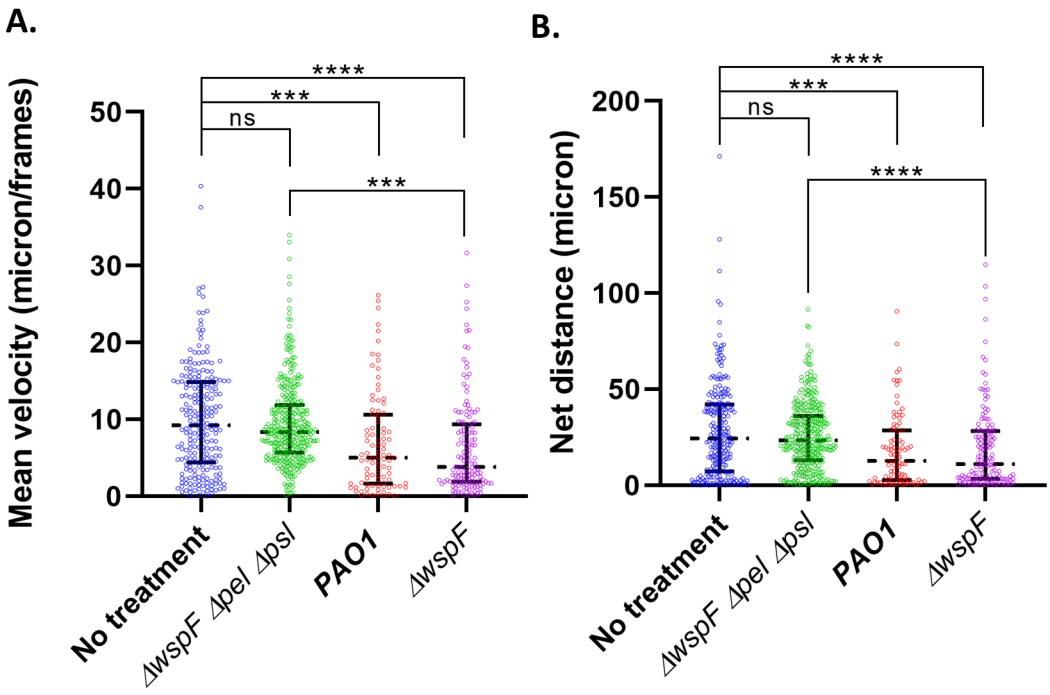


Figure 6.7 Analysis of mean velocity and net distances in neutrophils cultured under different conditions

Cultures of PAO1, Δ*wspF* and Δ*wspF*Δ*pel*Δ*psl* exposed to shear stress on µ-Slide VI 0.4 for 18 hr were fixed before neutrophils were added and incubated for 2 hr. Neutrophil movement was monitored live using a DeltaVision microscope, and 15-time laps images were taken every 8 min from each condition. To increase the accuracy of our data, we monitored the neutrophils movements in five fixed locations for both experiments conducted. After time-lapse images were acquired, data were uploaded to Fiji to conduct tracking analysis using TrackMate to calculate mean velocity and net distances. **(A.)** Mean velocity values calculated using the link velocity. The link velocity (or velocity) is defined for a single link between two spots (distance between the two spots divided by the time difference). Our data indicated that neutrophils incubated with biofilm-forming strains PAO1 and Δ*wspF* displayed lower velocity compared to neutrophils incubated with the biofilm-deficient strain, Δ*wspF*Δ*pel*Δ*psl*, or uninfected cells **(B.)** Similarly, the distance travelled by neutrophils is reduced in the presence of biofilms compared to untreated neutrophils or neutrophils exposed to planktonic cultures. (Neutrophils, 215 cells; Δ*wspF* Δ*pel* Δ*psl*, 339 cells; PAO1, 82 cells; Δ*wspF*, 134 cells; data pooled from 2 independent experiments). Graphs and analysis were generated in GraphPad Prism, and bars show median values with interquartile range. Significant calculated using Kruskal Willis test.

To further analyse the characteristics of the cellular motion we calculated the mean square displacement (MSD). The MSD is used in physics to relate displacement of objects; particularly MSD describes average square displacements over increasing time intervals between positions within a migration route (Gal et al., 2013). In the context of cell migration, MSD is a good measure of the surface area explored by cells over time, which relates to the overall efficiency of migration. For this we utilised DiPer, the custom-made open-source suite of a computer program created by Gorelik & Gautreau (Gorelik and Gautreau, 2014). Our data indicate that the slope of movement for control neutrophils continuously increased until 72 min time of incubation when the slope started to decrease indicated reduction in cellular movement. This was less apparent for all other conditions (Figure 6.8 A.). Data also revealed that neutrophils incubated with biofilm-forming strains showed lower MSD compared to uninfected cells or neutrophils incubated with planktonic cultures which suggests that biofilms disturb cellular migration (Figure 6.8 A.). We also utilised DiPer to computer the average speed for each cell as average of its instantaneous speeds. Results indicated that the average speed of neutrophils incubated with biofilms were lower compared to cells uninfected or incubated with planktonic cultures.

As described earlier, we acquired data from precisely five fixed stage coordinates in both experiments, and these locations are 2mm apart from each other (Figure 6.5). As neutrophils were inoculated from the slide's inlet close to location 5, they probably reached location 5 first before moving to 4,3,2 and 1 respectively (Figure 6.10 A). To assess whether neutrophils were attracted to a specific location, we compared the total number and percentages of cells appeared within the time of incubation, in these five locations. Results showed that the numbers of control neutrophils in the locations (5,4 and 3) that first reached 'theoretically' were more than the remote sites (location 2 and 1) (Figure 6.10 B). The opposite was seen with neutrophils incubated with PAO1 with interestingly no cells detected in location 5 while the majority of cells attracted to location 1, the furthest location monitored. A similar observation can be seen in cells incubated with (Δ*wspF* and Δ*wspF*Δ*pel*Δ*psl*) (Figure 6.10 B). This might

indicate that the presence of bacterial cells encouraged cells to travel to distant locations. The data also revealed that total numbers of cells from all five locations of neutrophils incubated with biofilms forming strains (PAO1 and Δ*wspF*) were lower than controls and cells incubated with the planktonic strain (Δ*wspF*Δ*pel*Δ*psl*). This might indicate that biofilms might influence neutrophils attachments.

Overall data generated from live microscopy and tracking analysis indicated that although neutrophils appear phagocytic when incubated with biofilms (Figure 6.9 A. and Figure 6.9 C.), incubation of neutrophils with biofilms might limit cellular movement and alter cells attachments.

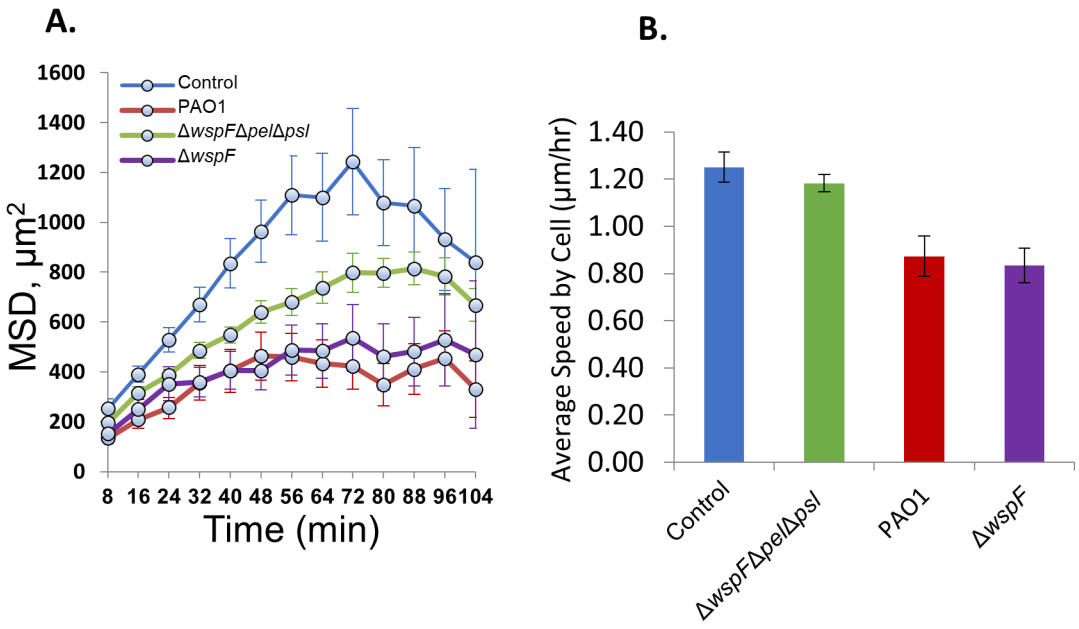


Figure 6.8 Mean square displacement (MDS) and average speed in neutrophils cultured under different conditions

(A.) MSD, i.e the amount of space neutrophils have explored in the channel is plotted on a linear scale from neutrophils incubated with PAO1, Δ*wspF* and Δ*wspF* Δ*pel* Δ*psl* cultures or empty channels (Control). Data revealed that neutrophils incubated with biofilms (PAO1, Δ*wspF* cultures) displayed lower MSD compared to neutrophils uninfected (controls) or incubated with planktonic cultures(Δ*wspF* Δ*pel* Δ*psl*). **(B.)** Average neutrophil speed was calculated using Diper applying the Fürth's formula. Data indicate that cells incubated with biofilms (PAO1, Δ*wspF* cultures) exhibited lower average speed compared to those incubated with planktonic counterparts (Δ*wspF* Δ*pel* Δ*psl*) or controls indicating that biofilm structures might reduce neutrophils motility. Data computed using DiPer. Graphs were performed in Excel. (Neutrophils, 215 cells; ΔwspF Δpel Δpsl, 339 cells; PAO1, 82 cells; ΔwspF, 134 cells; data pooled from 2 independent experiments). Data is represented as mean +/- SEM.

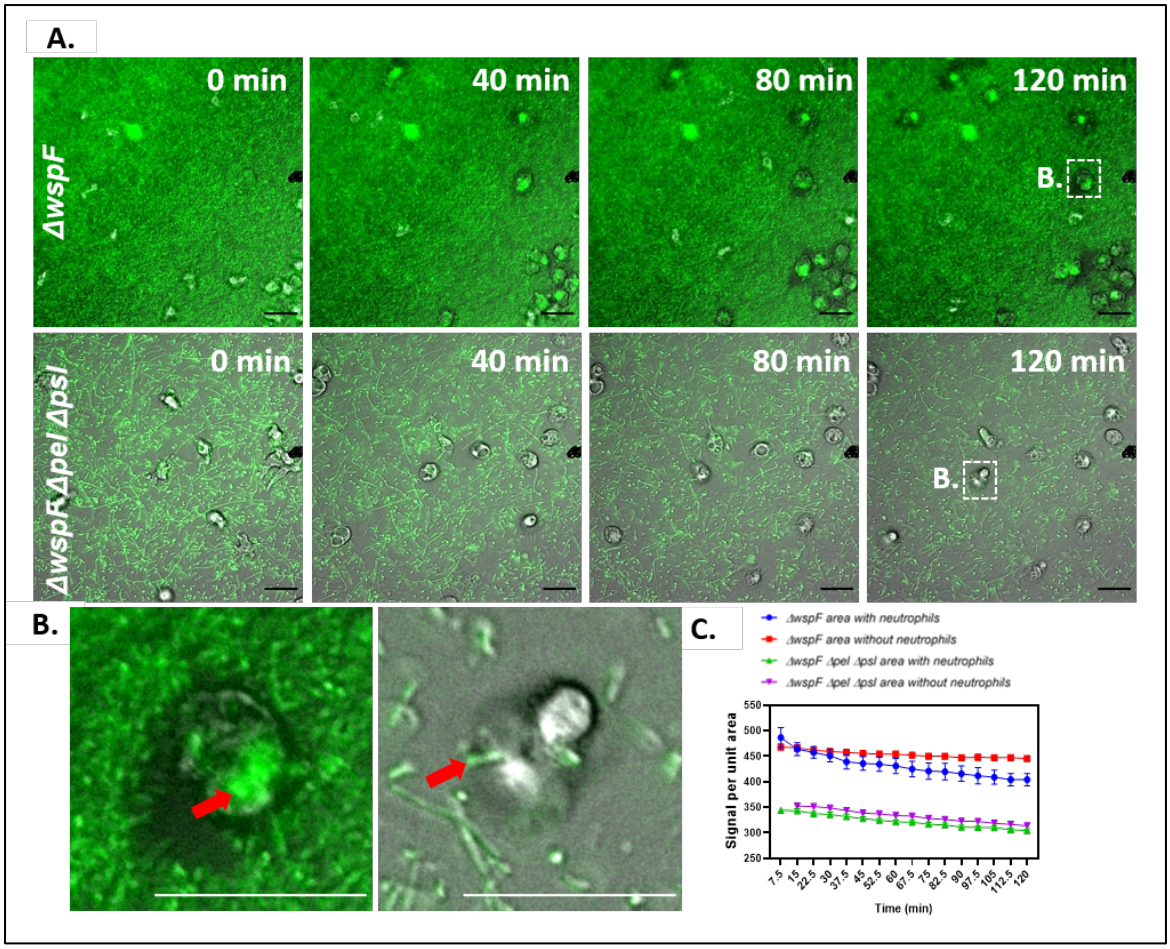
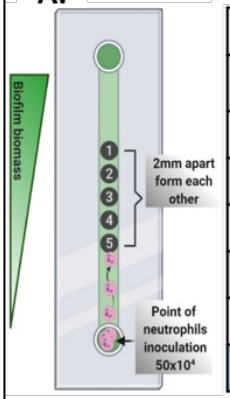


Figure 6.9 Neutrophils were phagocytic against both, biofilms and planktonic cells.

(A) Representative images of one location showing human neutrophils introduced to fixed bacterial cultures of Δ*wspF* GFP (biofilm-forming strain) and Δ*wspF*Δ*pel*Δ*psl* GFP (biofilm-deficient strain). (B) Magnified images showing the presences of GFP-labelled bacteria within the neutrophils (Red arrow). (C) The intensity of GFP in the area with (Δ*wspF* GFP, Blue and Δ*wspF*Δ*pel*Δ*psl* GFP, Green) or without (Δ*wspF* GFP, Red and Δ*wspF*Δ*pel*Δ*psl* GFP, Purple) neutrophils was calculated using Fiji. Results show signal per unit area plotted over time of incubation. Data displayed small reduction in GFP expression over time in both areas with or without neutrophils, suggesting neutrophils activity in clearing bacteria in the presence or absence of biofilms. The reduction in GFP signal in the presence and absence of neutrophils, might indicate that neutrophils alongside engulfing the bacteria the may perhaps produce free radicals and released bactericidal molecules in the extracellular milieu to eliminate bacteria. (Scale bars: 20 μm.) Relative time is displayed in min.

A.



B.

	Control		*ΔwspF Δpel Δpsl*		PAO1		*ΔwspF*	
locations	No.	%	No.	%	No.	%	No.	%
1	28	13.02	114	33.62	37	45.12	34	25.37
2	30	13.95	46	13.56	21	25.6	6	4.47
3	44	20.4	45	13.27	14	17	30	22.38
4	62	28.8	94	27.72	10	12.19	35	26.11
5	51	23.72	40	23.72	0	0	29	21.6
Total	215	100%	339	157.67%	82	38.14%	134	62.32%

Percentage of total number of cells as compered to control (215 = 100%)

Figure 6.10 Total neutrophils per location

Time-lapse images were taken from precisely five fixed stage coordinates for each condition numbered as location 1,2,3,4 and 5. Neutrophils probably reached location 5 first before moving to locations 4, 3, 2 and 1 sequentially **(A.)**. After time-lapse images were acquired, data were uploaded to Fiji to conduct tracking analysis using TrackMate aiming to calculate the total number of neutrophils appeared in each location. **(B)** Total number of neutrophils appearing in each position (No.) and the percentage of cells (%) over the 2 hr incubation. N=2

6.4.6. Confocal microscopy analysis of changes in neutrophil phenotype in response to PA biofilms

Following our earlier observation of neutrophils reduced migration capabilities based on reduced velocity, net distance, MSD and speed when incubated with biofilm cultures (PAO1, Δ*wspF*) compared to cells incubated with planktonic cultures (Δ*wspF*Δ*pel*Δ*psl)* or empty channels (Figure 6.7 and Figure 6.8), we utilised confocal microscopy to further assess neutrophils biofilm interaction. For this, after the interaction of neutrophils and PA (PAO1, Δ*wspF* or Δ*wspF*Δ*pel*Δ*psl*) was recorded using live microscopy, cultures were fixed with 4% PFA prepared in PBS for 10 min at 4°C, washed and stained with DAPI and HHA prior analysis by confocal microscopy. It is important to note that at the time these experiments were conducted, fixation using PEM had not been introduced.

As Psl contains high mannose structures, our initial aim was to stain with HHA to explore the possibility of neutrophils being attracted to areas with higher Psl deposition. Surprisingly, data showed that neutrophils were labelled with HHA and that labelling intensity was significantly low in neutrophils incubated with planktonic strains compared to neutrophils incubated with biofilms forming strains. Non-infected neutrophils displayed an intermediate phenotype. Recent study reported the presence of high mannose structures (paucimannosidic proteins) within neutrophils azurophilic granules that can be released upon activation (Thaysen-Andersen et al., 2015). This could explain the changes in HHA staining observed. Our data suggest that HHA stains high mannose proteins within neutrophils' azurophilic granules with possible translocation of these components to the plasma membrane in the presence of PA biofilms. It is important to note the need for future validation of this observation using a known staining of neutrophils granules and permeabilised and non-permeabilised conditions.

Images presented in (Figure 6.11 A) indicated that neutrophils incubated with Δ*wspF* mutant strains exhibited clustering behaviour. Therefore, in order to confirm this observation, we utilised a concept in biology named the nearest neighbour distance (NND) (Mao, 2016). It is a

tool that measures the distance between each cell and its nearest neighbours to observe whether this could be different in cells incubated with biofilms compared to planktonic cells. We utilised a Fiji plugin to calculate the NND (Mao, 2016). Our data indicate that NND of cells incubated with the Δ*wspF* mutant was significantly lower compared to Δ*wspF* Δ*pel* Δ*psl* or untreated neutrophils. While the PAO1 data was not statically different when compared to control cells, analysis indicated that the NND of PAO1 was statically different when compared to planktonic strains Δ*wspF*Δ*pe*Δ*psl.* However, the difference is lower than the difference noticed between Δ*wspF* and Δ*wspF*Δ*pel*Δ*psl*, this could be due to that PAO1 biofilms being more heterogeneous compared to Δ*wspF* biofilms, which were more homogenous due to the higher biomass. These observations need further validation.

All together this section indicated that neutrophils, although phagocytic when encountered biofilms, might display increased capability of granular release and clustering behaviour.

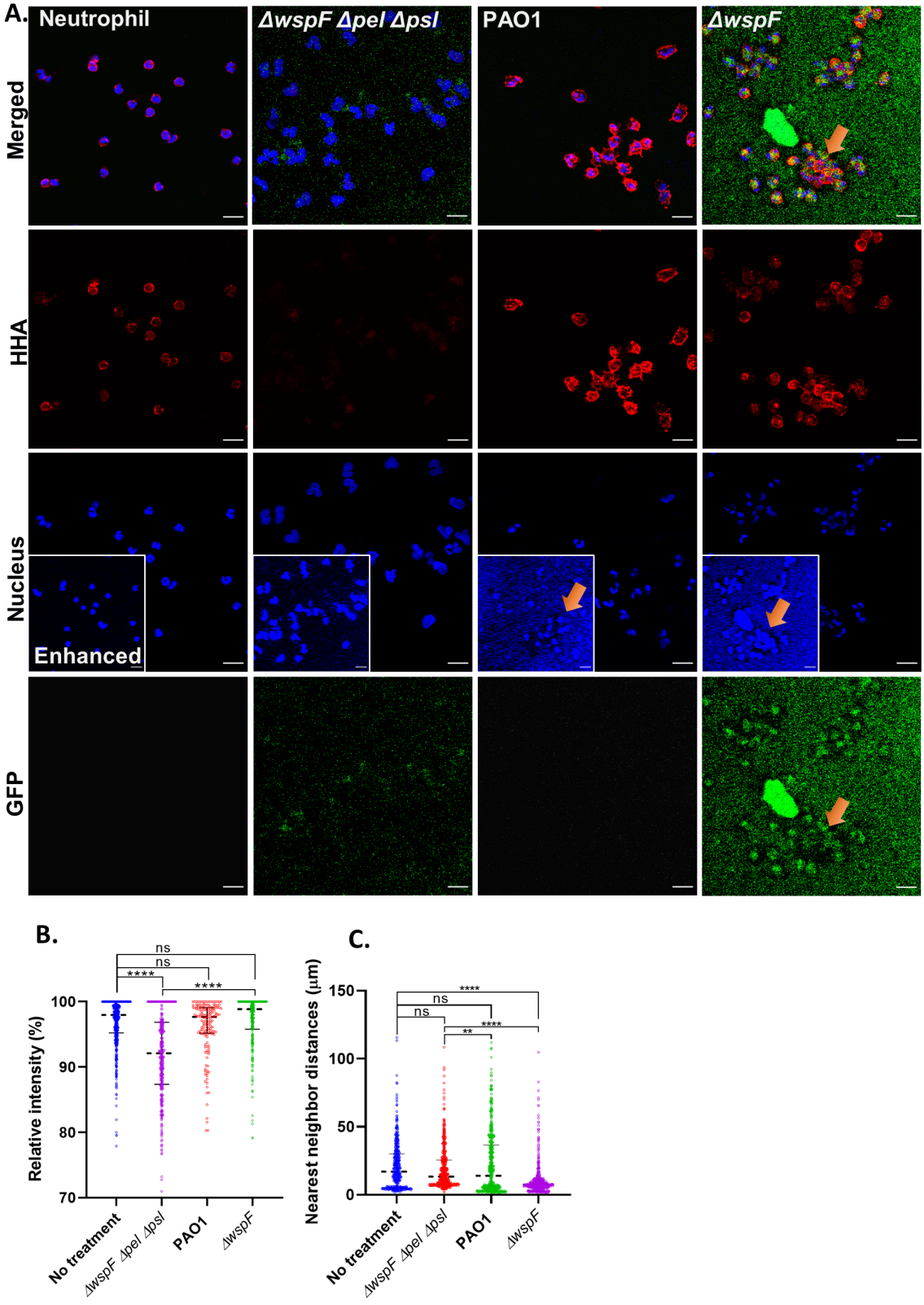

A.
Neutrophil
ΔwspF Δpel Δpsl
PAO1
ΔwspF
Merged
HHA
Nucleus
Enhanced
GFP
B.
Relative intensity (%)
100
90
80
70
ns
ns
****
****
No treatment
ΔwspF Δpel Δpsl
PAO1
ΔwspF
C.
Nearest neighbor distances (μm)
150
100
50
0
****
ns
ns
****
**
No treatment
ΔwspF Δpel Δpsl
PAO1
ΔwspF

Figure 6.11 Confocal microscopy analysis of neutrophil PA interaction

Biofilms of PAO1 and *ΔwspF* GFP in chambers of µ-slide VI 0.4 as described in (M&M) for 18 hr were fixed with 4% PFA in PBS for 10 min at 4°C. Following biofilms fixation, neutrophils (50.000 cells per channel) in 30 µl X-Vivo-15 were added and incubated for 2 hr. After incubation, neutrophils-biofilm co-cultures were fixed with 4% PFA in PBS. Following, samples were stained with DAPI (nucleus or bacterial DNA, blue) and HHA (Psl and granules, red). **(A.)** representative images from one donor. Image processed using Fiji. Scale bar 20 um. **(B.)** Relative intensity of HHA staining of each neutrophils measured as described in M&M. Data were normalised to cells with the highest HHA intensity (250). **(C.)** Nearest neighbour distances (µm) were measured using Fiji applying a plugin (Mao, 2016) that compute the distance between centroids for each cell. Graphs and analysis were generated in GraphPad Prism, and bars show median values with interquartile range. Significant calculated using Kruskal Willis test.

6.4.7. Investigation of neutrophils circularity following incubation with PA

In an earlier chapter, we observed that moDCs adopted a rounded morphology when exposed to PA biofilms or HMW-Psl (Figure 5.16Figure 5.17). Similarly, it has been reported that neutrophils display rounded morphology only when exposed to PA biofilms (Jesaitis et al., 2003). Here, we examined whether neutrophils would also adopt a circular morphology when exposed to PA biofilms, and whether addition of the biofilm purified component, HMW-Psl to planktonic cells would influence neutrophils shape. To investigate these possibilities neutrophils were incubated (2 hr, 37 ^{o}C/ 5% CO_2) with fixed bacterial cultures of PAO1, Δ*wspF*, Δ*wspF*Δ*pel*Δ*psl* and Δ*wspF*Δ*pel*Δ*psl* + HMW-Psl (10 µg/ml added in X-Vivo-15 for 1 hr and removed prior addition of neutrophils). Neutrophils-PA co-cultures were fixed with 4% PFA in PBS, washed and permeabilised. Samples were labelled with Alexa Fluor 488-phalloidin for F-actin (green) and DAPI for DNA (blue), and HHA for Psl (and possibly neutrophils' granules (Red)). Sample were examined under confocal microscopy. Images acquired were then uploaded to Fiji for the calculation of circulatory following the same protocol used with moDCs explained earlier (Figure 5.17) and (2.14). These initial observations indicate that neutrophils exhibited reduced circular morphology when incubated with biofilms or planktonic cultures with HMW-Psl, with this effect being more apparent in the case of planktonic cultures with HMW-Psl. In this case, HMW-Psl addition shows a possible trend to increases circularity. These data also confirmed our earlier observation of increased HHA labelling in neutrophils incubated with biofilms. In this instance, as cells were permeabilised, it is possible that the total amount of HHA+ material within the neutrophils increases in the presence of biofilms. We also assessed the intensity of Alexa Fluor 488-phalloidin for F-actin (green) using Fiji as explained in (2.13), data indicated that biofilms tend to increase the intensity of phalloidin while planktonic reduced it with the addition of HMW-Psl reverse the decrease of intensity. It is possible that this observation is due to high motility observed with planktonic strains observed earlier with live

microscopy analysis (Figure 6.7 and 4.8) while the opposite with planktonic strains and addition of HMW-Psl might have an influence on neutrophils' movements.

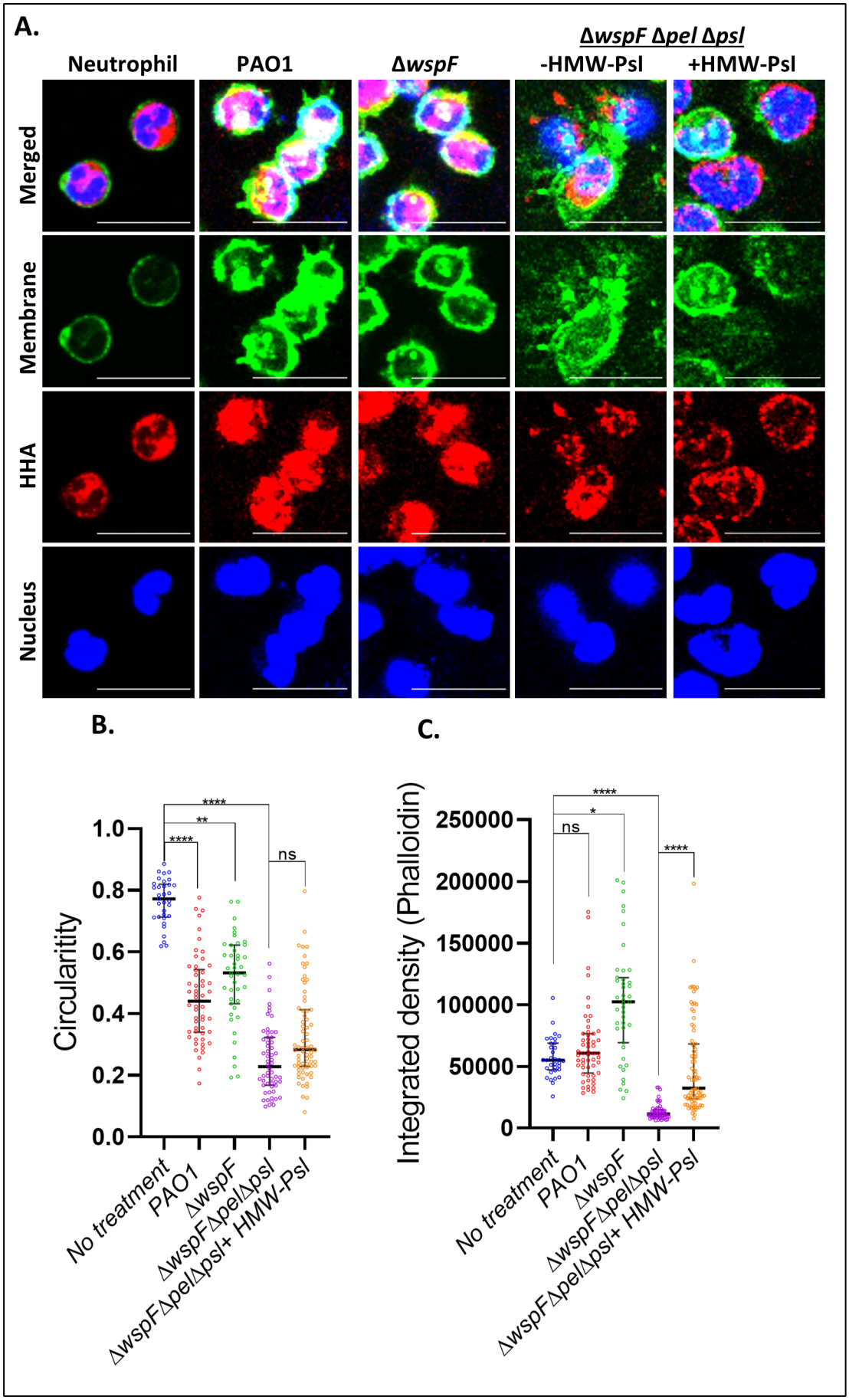

A.
ΔwspF Δpel Δpsl
Neutrophil
PAO1
ΔwspF
-HMW-Psl
+HMW-Psl
Merged
Membrane
HHA
Nucleus
B.
Circularitity
1.0
0.8
0.6
0.4
0.2
0.0
****
**
****
ns
No treatment
PAO1
ΔwspF
ΔwspFΔpelΔpsl
ΔwspFΔpelΔpsl+ HMW-Psl
C.
Integrated density (Phalloidin)
250000
200000
150000
100000
50000
0
****
*
ns
****
No treatment
PAO1
ΔwspF
ΔwspFΔpelΔpsl
ΔwspFΔpelΔpsl+ HMW-Psl

Figure 6.12 Neutrophils incubated with biofilms or Psl tend to retain circular morphology compared to those incubated with planktonic cultures

After growing PA biofilms for 18 h under shear stress, cultures were fixed with 4% PFA. Neutrophils were then isolated from human healthy donors using negative selection were added at 50,000 cell/channel and incubated with biofilm forming strains (PAO1, Δ*wspF)* or biofilm deficient strain (Δ*wspF*Δ*pel*Δ*psl)* with or without purified HMW-PSL for 2hr. After incubation samples were fixed and nucleus stained with DAPI, F-actin stained with phalloidin (P)-AF488 and mannose structures stained with HHA-TR. **(A.)** Single slice of images processed with Fiji from each condition. **(B.)** analysis of cellular circularity calculated based on the F-actin (membrane). **(C.)** analysis of integrated density of phalloidin calculated with Fiji. Scale bar 20 μm. (Neutrophils, 33 cells; Δ*wspF*Δ*pel*Δ*psl*, 58 cells; Δ*wspF*Δ*pel*Δ*psl*+HMW-Psl, 71 cells; PAO1, 54 cells; Δ*wspF*, 43 cells; data from 1 experiments).

6.5. Summary

1. Live microscopy analysis indicated that biofilms significantly reduced neutrophils motility determined as reduced velocity, net distance, MSD and speed. Biofilms also induce neutrophil clustering.

2. Preliminary observations indicate that (i) neutrophils were not retained on biofilms (lower total numbers in 5 fields), (ii) neutrophils display structures labelled with the HHA lectin, (iii) HHA labelling in neutrophils was affected by the presence of biofilms and planktonic cells and (iv) retained circular-shaped after exposed to biofilms or HMW-Psl + (V) displayed higher intensity of phalloidin, suggesting modulation of the cytoskeleton.

6.6. Discussion

6.6.1. Motility and biofilms

Neutrophils migrate towards attractive molecules released by microorganisms (de Oliveira et al., 2016, Wagner and Roth, 2000). Such migration requires an allowable matrix (Wagner and Roth, 2000). Several studies on the interaction of neutrophils with biofilms report migration of neutrophils towards biofilms and neutrophils localised within, around or on biofilms (Jesaitis et al., 2003). Using time-lapse microscopy to monitor the dynamic interactions between PA and

neutrophils in a mouse model of bacterial keratitis, Thanabalasuriar et al. (2019) found that neutrophils were not able to eradicate infection caused by biofilm-forming PA. In contrast, neutrophils were efficient at clearing biofilm-deficient bacteria (Thanabalasuriar et al., 2019). Biofilms are encapsulated in EPS matrix, which is composed mainly of protein, eDNA and polysaccharides (Limoli et al., 2015). The EPS generally described as highly viscoelastic material (Böl et al., 2013, Gloag et al., 2018, Klapper et al., 2002, Stewart, 2014, Wilking et al., 2011).

In this study, we examined neutrophils behaviour using live microscopy, following their interaction with PA, as a planktonic and biofilms (encapsulated by EPS). Results of this study (Figure 6.7 and 6.8) showed that biofilms significantly reduced neutrophils motility observed as reduced velocity, net distance, MSD and speed. Our results reflect those of Jesaitis et al. (2003) who investigated human neutrophils response to biofilms and reported that neutrophils were partially active when encountered biofilms and displayed limited degranulation ability and reduced motility (Jesaitis et al., 2003). A possible explanation for this might be that the reduced motility is due to the biofilm biomass working as a trap for neutrophils. It was reported that the size of biofilms biomass works adversely on human neutrophils migration. Hänsch et al. (2008) reported that neutrophils migrated only in the case of low biomass biofilms, while neutrophils migration was significantly inhibited when incubated with higher biomass biofilms. In the same study, Hänsch et al. (2008) also tested neutrophils migration on purified EPS and stated that neutrophils were "stuck" when incubated with a high concentration of EPS (Hänsch et al., 2008).

In a mouse model, Rich (2016) used a strain that was engineered with the thermo-sensing diguanylate cyclase (tdcA) gene to facilitate biofilm production when inoculated into the mouse. This diguanylate cyclase acts on the development of c-di-GMP as the temperature increases to 37 °C, which then facilitates EPS overproduction. The diguanylate cyclase is inactive at 28 °C, which allows the PA strains to be grown at lower temperatures and suspended planktonically to a standardised inoculum to ensures that aggregates are not being

introduced into the lung and strains with a functional copy of tdcA will then be induced to produce EPS at the murine body temperature, 37 °C. Following mouse infection with different PAO1 strains that either overproduce biofilms or lack Psl or Pel, Rich (2016) have tracked neutrophils movements in the mouse lung using live microscopy. Rich (2016) reported that only the strains that produce Psl show significant reduction in neutrophils motility. The average speed of neutrophils incubated with strains overproduce Psl were slower compared to the control (uninfected). Neutrophils incubated with strain that overproduce both Pel and Psl showed lower track length, displacement and velocity compared to all other strains. Overall, the author suggests that EPS expression reduced neutrophil activity (Rich, 2016).

Similar to biofilms, many host biological materials are viscoelastic as well (Levental et al., 2007, Stewart, 2014) For example, It was reported that neutrophils, were able to migrate in normal airway mucus (1.5–2.5% dry weight) but showed reduced migration capacity in thick mucus (6.5%) (Matsui et al., 2005), which is similar to the mucus found in CF lung (Hill et al., 2018). Additionally, Parkhurst and Saltzman (1994) reported that neutrophils migrated effectively in cervical mucus. The same scientists also measured human neutrophil motility in collagen gels and found that motility reduced dramatically after the concentrations of collagen were increased and were immobilised in very high concentration (Parkhurst and Saltzman, 1992). It was speculated that the viscoelasticity of in vivo biofilms is higher than the biofilms formed in vitro (Stewart, 2014). It is now understood that a number of host materials could be incorporated by the bacteria into the biofilm structure such as secreted mucus, necrotic tissue, DNA released from dead neutrophils (Parks et al., 2009, Siddiqui and Bernstein, 2010, Wolcott et al., 2008). Therefore, these structures might increase biofilm rigidity, and such increases could possibly further reduce phagocyte mobility (Stewart, 2014).

Substantial progress has been made in understanding the mechanisms that control neutrophil migration in different diseases utilising live microscopy (de Oliveira et al., 2016). The majority of the work has involved the use of mouse neutrophils and these models mainly focus on mouse tissues that can be imaged under microscope, such as cornea, lung and ear

(Mantopoulos et al., 2010, Looney et al., 2011, Ng et al., 2011). Despite the useful data generated from these models, they do not fully reflect the situation in humans. For example, using a mouse model, it was indicated that Ly6G is a key regulator of neutrophil migration (Wang et al., 2012). However, human neutrophils lack Ly6G (Lee et al., 2013b); thus, the need for human cell-based assay is essential to understand neutrophils biofilms interaction.

Neutrophils normally circulate in the bloodstream (Balamayooran et al., 2010). At the time of infection, they migrate rapidly to the infection sites (Balamayooran et al., 2010). Migration from the blood to the site of infection can occur through migration of neutrophils either directly through or between endothelial cells (de Oliveira et al., 2016). One limitation of our system is that we introduced neutrophils to biofilms directly and did not take in consideration the endothelial barrier. To fully understand neutrophils biofilm interaction, it would be recommended to establish a model which contain a membrane that reflects endothelial cells and separate neutrophils from the biofilms. At the same time, it would be very time saver to utilise the syringe pump system already established and optimised in Chapter.3.

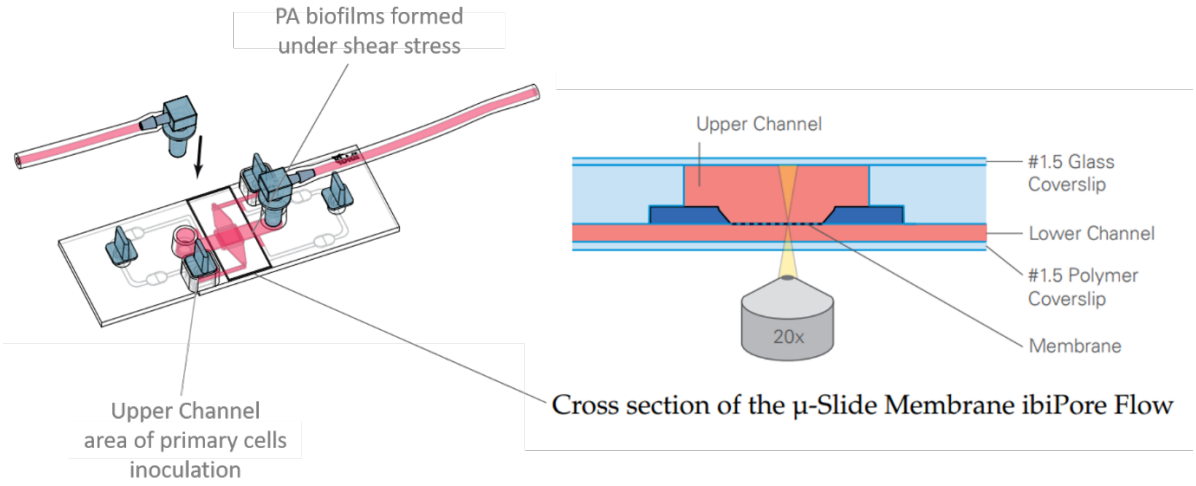


Figure 6.13 Suggested model for future assays

Schematic of a suggested model to study neutrophils biofilms interaction for future analysis. Biofilms could be formed on µ-Slide Membrane ibiPore slide from ibidi. This slide offer two channel, lower channel where we could culture the biofilms under shear stress and an upper channel where we could inoculate the neutrophils after biofilms formation and fixation. For neutrophils to move from the upper channel to the lower channel they need to pass through a membrane which resemble the epithelial cells (3-5 um pore size). Image curtesy of ibidi.

For example, biofilms could be formed on µ-Slide Membrane ibiPore slide from ibidi. This slide contains two independent channels that allow us to generate PA biofilms in the lower area and inoculate the cells in the upper channel. For the cells to move to the lower channel, they need to cross a membrane, resembling neutrophils migration from the blood to the site of infection through endothelial cells.

Neutrophils don't work alone, their initial recruitment, activation and survival is facilitated by airway epithelial cells and macrophages through the release of different cytokines and chemokines (Linden et al., 2005, Mantovani et al., 2011). In addition to neutrophils recruitment, macrophages could also induce a "switch-off" response to clear neutrophils and restore the organ function (Soehnlein and Lindbom, 2010, Grainger et al., 2013, Muntaka et al., 2019). Macrophages can also react to and incorporate neutrophil products, particularly myeloperoxidase, which activates macrophages further (Silva, 2011). Models allowing interactions between macrophages and neutrophils, therefore provide a physiologically

relevant experimental framework to investigate an effective immune response to PA biofilms (Muntaka et al., 2019). We previously studied neutrophils and morphogens interaction in response to PA as a planktonic. However, that model is limited to planktonic cells as it might affect the structure of the biofilm (Muntaka et al., 2019). The above-suggested model enables us to pre incubate macrophages with fixed biofilms at the lower channel, following incubation we could introduce neutrophils at the top channel to assess neutrophils ability in migration and their behaviour in the presence or absence of macrophages.

Despite the need to incorporate and develop complex models that take inconsideration the effect of the epithelial cells and macrophages on neutrophils migration. Data presented in this chapter showed that biofilms significantly reduced neutrophils motility determined as reduced velocity, net distance, MSD and speed.

6.6.2. Lack of attachment

In our study, as explained earlier, we measured the total number of neutrophils appeared in 5 different location in the 4 conditions tested. We observed that the total number of neutrophils incubated with biofilms forming strains (PAO1 and Δ*wspF*) were lower than the total number of neutrophils incubated with planktonic strains (Δ*wspF*Δ*pel*Δ*psl*) or controls cells. We pointed in an earlier chapter that we observed lower number in moDCs incubated with biofilms compered to planktonic (Figure 5.16). It is possible that biofilms affect the ability of neutrophils to adhere on the surface. It was reported that biofilms reduce the ability of neutrophils to adhere, Guenther et al. (2009) showed that neutrophils adhered less on *S. epidermidis* biofilms compered to *S. aureus* biofilms and *S. epidermidis* had little susceptibility to phagocytic destruction by neutrophils. The author suggested that this could be due to *S. epidermidis* biofilms rigidity is higher than *S. aureus* biofilms (Guenther et al., 2009). Another study showed that neutrophils surround biofilm and become activated, but were not able to migrate into the biofilm, probably because of a lack of a chemotactic signal as well as by hindrance of migration into the “slimy” material (Arciola et al., 2012). Thus, the inability of

neutrophils to penetrate biofilm results in progression of implant-related infections (Arciola et al., 2012). In case of PA, although there is no clear explanation of why would this happen, based on the data in the literature, there are, however, possible explanations.

First biofilms could possibly produce materials that kill the cells. For instance, rhamnolipids, which play a role into PA biofilm formation, are reported to be toxic to neutrophils and the host tissues at the site of biofilm infections (Mulcahy et al., 2014). Alhede et al. (2014), showed that both in vitro and in vivo PA biofilms produce a shield of rhamnolipids, that protect bacteria from neutrophils (Alhede et al., 2014). Second, as mentioned earlier, that neutrophils are attracted towards the site of infection through chemotactically active molecules (Balamayooran et al., 2010). These molecules may either found on the bacteria as explained in the introduction or released by several immune cells at the site of infection, such as epithelial cells macrophages (Linden et al., 2005, Mantovani et al., 2011). Biofilms could possibly reduce the diffusion of these chemoattractant molecules; thus, neutrophils were not encouraged to move forward and reach the examined site.

To understand this in future, we could utilise the system suggested earlier which equipped with 300-nm-thick membrane with 3-μm pores as explained previously. After development of biofilms on those slides similar to explained in chapter 3 we could possibly monitor neutrophils transmigration from the upper channel (empty) to the lower channel (biofilms or planktonic cells) through the pores to understand whether neutrophils well be attracted to biofilms compared to wells containing planktonic cells or empty wells. Similar works on neutrophils transmigration were already performed on these slides to study neutrophils transmigration to neutrophils chemoattractant molecules N-formylmethionyl- leucyl-phenylalanine (fMLP) (Rohwedder et al., 2019).

Overall these data might indicate that biofilm might affect neutrophil attachment.

6.6.3. HHA labelling and granules content

As covered earlier in the introduction of this chapter and in main introduction, neutrophils are a key effector cells in the innate immune system, working as the first line of defence against invading microorganisms. Neutrophils utilise several defensive mechanisms to tackle these foreign pathogens. In addition to its ability to produce inflammatory cytokines and chemokines they contain compounds that can kill pathogens, called granules. Granule content can also be released into the extracellular environment when the granule membrane fuses with the plasma membrane through a process known as degranulation (Cowland and Borregaard, 2016). As mentioned in the main introduction, Four types of neutrophil granules have been categorised and referred to as primary (or azurophil), secondary (or specific), tertiary (or gelatinase) granules and secretory vesicles (Cowland and Borregaard, 2016). Once released outside of the cells, those granule contents play a role in the elimination of extracellular pathogens (Pham, 2006). Content of these granules were discussed in details in the main introduction (1.6.3). It is known that LPS causes neutrophil degranulation (DeLeo et al., 1998, Ward et al., 2000, Ruchaud-Sparagano et al., 2014).

In our study, we observed that neutrophils were stained with the HHA which was reported that it is specific for high mannose structure (Balzarini et al., 2004) and where shown to stain paucimannose from *Trypanosoma brucei* (Castillo-Acosta et al., 2013). It was reported that azurophilic granule proteins contain paucimannosidic N-linked carbohydrate structures (Thaysen-Andersen et al., 2015). Furthermore, Shepherd and Hoidal (1990) reported uptake of MPO by MR (Shepherd and Hoidal, 1990). Additionally, Reiding et al. (2019) recently characterised the structure of MPO in neutrophils from healthy human donors; the author confirmed the presence of high mannose structure in MPO (Reiding et al., 2019). Therefore, it can thus be suggested that possibly HHA stain the azurophilic granules which contain mannose structures, though this needs to be verified in future studies using stain specific for neutrophils azurophilic granule protein MPO (Allen, 2014). Analysis of the HHA stain intensity showed that neutrophils incubated with biofilms forming strains (PAO1 and Δ*wspF*) have

similar intensity values to control (uninfected neutrophil). On the other hand neutrophils incubated with planktonic strain (Δ*wspF*Δ*pel*Δ*psl*) showed lower intensity when compared to controls and biofilms forming strains. These results might suggest that neutrophils when encountered with planktonic strains, were able to release the granules content, but was not the case when countered the biofilms, thus it might be possible that biofilms restrict neutrophils granules release.

LPS is a major component of the outer membranes of all Gram-negative bacteria (Aguiniga et al., 2016). As mentioned earlier, it is known that LPS causes neutrophil degranulation (DeLeo et al., 1998, Ward et al., 2000, Ruchaud-Sparagano et al., 2014). However, it was indicated that PA undergoes LPS alteration when forming biofilms, most importantly, lipid A (Ciornei et al., 2010). Relatively, It was reported that PA lipid A mutant isolated from CF patients showed lower ability in triggering neutrophil degranulation (SenGupta et al., 2016). Additionally, it was indicated that extracellular DNA, a major proinflammatory part of PA biofilm reduces the release of neutrophils azurophilic granules component, MPO and treating the biofilms with DNase increase the MPO activity (Bass et al., 2010). Together, this may perhaps explain the results shown earlier were neutrophils incubated with biofilms strains showed higher intensity of HHA staining compared with planktonic strains.

Overall, these data showed that HHA might possibly stain neutrophils azurophil granules and HHA labelling in neutrophils was affected by the presence of biofilms and planktonic cells, biofilms might restrict the release of the granules content.

6.6.4. Circularity

In the previous chapter, we reported round cells morphology of moDCs incubated with biofilms and purified HMW-Psl (Figure 5.16 and Figure 5.17). Similarly, preliminary observation in this chapter indicated neutrophils incubated with biofilms forming strains (PAO1 and Δ*wspF*) showed higher circularity compared to neutrophils incubated with planktonic strains and addition of purified HMW-Psl tend to increase circulatory of neutrophils incubated with

planktonic strains (Figure 6.12). Relatively, Neutrophils were reported to retained round morphology when incubated with PA biofilms which resulted in reduced neutrophil phagocytic ability (Jesaitis et al., 2003). Additionally, *Pseudomonas* contain proteins involved in adhesion and actin-regulating, including integrins, kinases, and GTPases (Murphy and Courtneidge, 2011, Foxall et al., 2016, Di Martino et al., 2016). We also analysed the intensity of phalloidin, data indicated that biofilms tend to increase the intensity of phalloidin while planktonic reduced it with the addition of HMW-Psl reverse the decrease of intensity observed with planktonic strains. It is possible that both circulatory and high intensity of phalloidin observed with neutrophils incubated with biofilms or with neutrophils incubated with planktonic cells +HMW-Psl affects its motility through changes in cytoskeleton.

Cytoskeleton alterations by bacterial pathogens been reported as a tool to impair neutrophils phagocytosis following neutrophil recognition (Bros et al., 2019). Different gram-negative bacteria utilise the T3SS to inject GTPase activating proteins (GAPs) into the host cell to facilitate the establishment of infection. Throughout all situations, host actin dynamics are modified by bacteria manipulating RHO GTPases, such as ROS, RAC1 and cycle 42 cell division. RHO GTPases act as molecular switches by regulating the actuin-related protein 2/3 complex 26 in the control of actin dynamics. For instance, it was reported that PA utilise ExoS to cause cells rounding in epithelial cells (Frithz-Lindsten et al., 1998). Similarly, Yersinia uses YopE to target small RhoA family G proteins affecting the actin cytoskeleton, thus actively inhibiting phagocytosis (Rolán et al., 2013). Yersinia also expresses another type III effector protein tyrosine phosphatase (PTPase), YopH, which, together with YopE, has recently been shown to interfere with neutrophil degranulation (Taheri et al., 2016). In addition, Salmonella enterica SptP target the actin cytoskeleton through GTPase activation (Galán and Zhou, 2000).

It is possible that the alteration of the cytoskeleton characterised by high circularity and high intensity of phalloidin after neutrophils incubation with PA biofilms or planktonic strains + HMW-Psl is through changes in GTPase, which is similar to the morphological changes

observed with moDCs in earlier chapter. Innate immune cells such as neutrophils, macrophages and DCs share an overlapping range of functions (Bros et al., 2019). Thus, it was speculated, RhoA-specific functions that have been elucidated in one myeloid cell type may generally be applicable to other cells as well (Bros et al., 2019). As we observed similar changes in both cells, neutrophils and moDCs incubated with biofilms or EPS, future analysis might focus on analysis of GTPase in both cells to unveil the mechanism behind the round morphology. In addition, neutrophil function involves numerous processes that are also regulated by Rho GTPases such as phagocytosis, degranulation including MPO release and NETs formation (McCormick et al., 2019). This also added to the important of investigating GTPases in future analysis.

6.6.5. Final conclusions

To develop a full picture of neutrophils biofilms interaction, additional studies will be needed on two important neutrophils defence strategies, MPO and NETs.

MPO is the most abundant enzyme within the neutrophils and important in the host defence (Van der Veen et al., 2009). Mainly, MPO is released into the phagosome to support in the degradation of opsonised pathogens, and 30% could be released into the extracellular space following degranulation (Parker et al., 2012b). In this study after incubation of neutrophils with fixed bacteria, supernatants were collected, we aim to analyse MPO activity utilising a commercial assay kit (abcam, ab111749). However, we didn't detect any MPO released in the supernatants neither in neutrophils incubated with planktonic cells or with biofilms (data not shown). This finding was unexpected and suggested that there was a problem with the supernatants collected, as the assay positive control was working (data not shown). Despite the results reported by Bass et al. (2010) of reduced MPO activity with biofilms, our data are not concordant with previous data as neutrophils MPO activity was reported with planktonic PA as well (Mathy-Hartert et al., 1996). It is possible that our negative results were due to the long-time supernatants were stored in -80 °C prior to analysis, as a result, MPO enzymes

might have lost their activity. For future analysis, it might be recommended to assess MPO as soon as supernatant collected.

NETs are large, extracellular, web-like structures composed of DNA and granule proteins, such as neutrophil elastase, MPO, and cathepsin G. (Papayannopoulos, 2018). Most of DNA in NETs is derived from the nucleus, and NETs also enriched in mitochondrial DNA (Papayannopoulos, 2018, Lood et al., 2016). Neutrophils release NETs to catch, trap and kill different pathogens including bacteria (Brinkmann et al., 2004), fungi (Urban et al., 2006) and viruses (Saitoh et al., 2012). Nevertheless, if dysregulated, NETs can contribute to the progression of disease (Papayannopoulos, 2018). It was indicated that different PA strains induce NETs that contain different structures suggesting that the composition of NETs varies depending on the stimulus (Dwyer et al., 2014). Additionally, It was reported that mucoid strains of PA, seem to be moderately resistant to neutrophil NETs–mediated killing (Young et al., 2011). Furthermore, some bacterial biofilms were able to either inhibit NETs (Ma et al., 2017) or to be protected inside biofilms and resisted NETs (Hong et al., 2009, Wartha et al., 2007). Therefore, it was essential to investigate NETs release in our study.

Therefore, along with our efforts to assess MPO we examined neutrophils' release of NETs utilising microscopy and using the DNA staining DAPI. Although NETs release assessment utilising DNA stain DAPI is widely used method (Rebernick et al., 2018, Gomez-Lopez et al., 2017), we encountered a problem which is DPAI stain both bacteria and neutrophils and it was difficult to adjust the microscopic setting to clarify NETs. Therefore, we were unable to observe any NETs formation. Future studies should utilise specific staining for NETs only that target several granule components, for example, myeloperoxidase or elastase, which have also been shown to be present at high amounts within NETs to be able to assess NETs release accurately, with the addition of NETs positive controls (de Buhr and von Köckritz-Blickwede, 2016).

To end, analysis performed in this study were based on free available program that need the interventions of human factor, which might reduce the reproducibility and take a very long time for analysis. To increase the data accuracy, and reduce the analysis time, for future analysis it would be highly recommended to utilise the current available artificial intelligence programs based on machine learning. These programs currently are opening new horizons in biomedical research and promises to revolutionise the microscopy field (von Chamier et al., 2019).

Overall, despite its limitation presented earlier, this study adds up to our understanding on human neutrophils and PA biofilms interaction and identified possible factors that might affected neutrophils ability in eliminating biofilms.

Chapter 7. General discussion and future perspective

The opportunistic pathogen *Pseudomonas aeruginosa* (PA*)* is believed to play a key role in the long-lasting infections of immunocompromised individuals, including patients with cystic fibrosis (Moradali et al., 2017). One of the most important adaptive factors that facilitate chronic infection is the switch from planktonic to the biofilm mode of growth which makes PA eradication extremely difficult or even impossible (Hogardt and Heesemann, 2010, Schelstraete et al., 2013). Biofilms consist of bacterial communities interconnected and coated by a self-produced extracellular polymeric substance (EPS) (Costerton et al., 1999, Borlee et al., 2010). PA produces two major carbohydrates within the EPS, Psl and Pel; the presence of at least one is essential for biofilms formation (Franklin et al., 2011). Structurally, Psl contains D-mannose, D-glucose, and L-rhamnose (Byrd et al., 2009) and Pel is composed of N-acetylgalactosamine (GalNAc) and N-acetylglucosamine (GlcNAc) (Jennings et al., 2015).

It is understood that the immune response to planktonic PA is triggered through the engagement of multiple PRRs able to detect specific PA antigens, including TLR-4 and TLR-5 which bind LPS and flagellin, respectively (Hayashi et al., 2001, Janeway and Medzhitov, 2002). During the process of biofilm formation, PA undergoes phenotypic changes, including the loss of LPS O-antigen, downregulation of flagellin, and loss of T3SS (Bragonzi et al., 2009) that might alter PRR engagement and, in turn, immune responses. So far, very little attention has been paid to the immune response to biofilms and the role of PRRs, including C-type lectin receptors (CLRs), in this process. Therefore, the overarching aim of this thesis was to investigate the interplay between PA and innate immune cells and how it is affected by biofilm formation from three different angles presented in Chapters 4, 5 and 6, respectively.

First, data from previous work in the lab (Tamanna Rahman and Mohammad Alshahrani, PhD theses) revealed that two CLRs, MR and DC-SIGN recognise PA biofilms and purified biofilm

carbohydrates. The main aim of Chapter 4 was to determine the capability of another CLR, Dectin-2, to interact with PA biofilms and purified EPS components. Second, as mentioned in Chapter 5, the hydrolysed carbohydrates monomer compositions in moles % for HMW-Psl-1 was 74.9% mannose. Hence this chapter mainly aimed to determine how recognition by C-type lectins (DC-SIGN and MR) of this high mannose compound influences immune responses. Third, in Chapter 6 we set up an assay to study neutrophil-PA biofilm interactions, particularly neutrophil morphological and behavioural changes following contact with PA biofilms. Neutrophils are first responder cells of the innate immune system that play a major role in the control of bacterial infections.

To study the interaction of myeloid cells with PA biofilms and how it is affected by carbohydrate composition, we employed different PA strains that vary in the expression of genes involved in the synthesis of Pel and/or Psl; Δ*wspF*, Δ*wspF*Δ*pel*, Δ*wspF*Δ*psl* and Δ*wspF*Δ*pel*Δ*psl.* These strains express the same high levels of c-di-GMP, resulted from the mutation in *wspF* (Borlee et al., 2010). The high levels of c-di-GMP stimulate the expression of EPS and correlate with the tendency of bacteria to form biofilms (Hengge, 2009). Confirmation of the genetic mutations in the strains utilised in this research prior initiating the study was considered a good starting point to ensure that these PAO1 strains possessed the correct *wspF* and/or *psl* and *pel* mutation (Figure 3.1). What follows is a brief summary of the aims and main findings of this thesis.

7.1. Generation and Characterisation of PA biofilms (Chapter 3)

Chapter 3 described the biofilm generation methods used in this investigation to study the interaction of innate immune cells with biofilms. The main aim was to optimise biofilm generation in substrates suitable for microscopic examination to analyse biofilm architecture (Ch.3), visualise the distribution of ligands for immune lectin receptors (Ch.4), and investigate Immune cells-biofilm interactions (Ch.5 and 6). Following several optimisation experiments as

summarised in the schematic diagram (Ch.3, Figure 3.12), we successfully generated biofilms under flow conditions in ibidi µ-Slide VI 0.4. From the confocal laser scanning microscopy data in (Ch.3) we determined that within our experimental settings, the most suitable biofilm generation conditions were when (1) PA cultures were inoculated on tissue culture slides and subjected to (2) continuous flow (1.6 ml/hr) of (3) pre-gassed X-Vivo-15 [48 hr prior usage as described in (Figure 3.7)].

Alongside optimising the biofilms formation, in another set of experiments in the same chapter (Ch.3), we confirmed and quantified the biofilm formation by PA Δ*wspF* strains and clinical isolates in two types of microtiter plates using a defined eukaryotic media (Figure 3.2 and Figure 3.3). The aim was to use these biofilms in testing the binding of C-type lectins and the analysis of biofilms-innate immune cells interaction (Chapters 4 and 5, respectively).

In all biofilm generation methods in this thesis, we utilised the defined eukaryotic media X-Vivo-15 which is generally used for the culture of eukaryotic cells but not for prokaryotic cells (Bethke et al., 2002, Dasgupta et al., 2007, Earle et al., 2005). The main aim was to utilise a media where we can co-culture both biofilms and innate immune cells. Since X-Vivo-15 was shown to support biofilm generation, it was considered appropriate for this study. The results obtained by exploiting these biofilm generation procedures are described in the following sections.

7.2. Recognition of *Pseudomonas aeruginosa* biofilms and purified biofilm-associated carbohydrate by Dectin-2 (Chapter 4).

The CLR Dectin-2 reportedly binds several pathogenic microorganisms, in all instances, the cell wall polysaccharides of these organisms contain high mannose structures (McGreal et al., 2006, Sato et al., 2006, Barrett et al., 2009, Brudner et al., 2013, Miyasaka et al., 2013, Ritter et al., 2010). Competition binding studies indicated that the Dectin-2 CRD binds to

monosaccharides with modest affinity and that affinity was significantly higher for mannose-linked (1–2) or (1– 4) to a second mannose residue (Feinberg et al., 2017). In Ch.4, we mainly investigated the possibility of Dectin-2 recognising PA biofilms and purified biofilm carbohydrates. A commercially available Dectin-2-Fc chimera protein comprising the mannose-binding region (CRD) of Dectin-2 fused to the Fc portion of human IgG1 was used to test the capability of Dectin-2 to bind PA biofilms and purified Psl in ELISA assays as described in (2.5). The functionality of the Dectin-2-Fc was confirmed in all assay conducted by testing the binding against the confirmed Dectin-2 ligand heat-killed *C.albicans* (HKCA) (Figure 4.7-Figure 4.11).

When Dectin-2-Fc was added to 96 well plates coated with PA LPS or fixed planktonic cells of PAO1 and *wspF* mutant lab strains, no binding was detected (Figure 4.14). The results were further confirmed by comparing Dectin-2-Fc and DC-SIGN-Fc binding to planktonic PAO1. DC-SIGN-Fc had been shown to bind planktonic cells using ELISA, and we confirmed these findings using confocal microscopy (Figure 4.15). This observation is in agreement with a previous study demonstrating no binding of Dectin-2 to PA LPS (Wittmann et al., 2016). On the other hand, when Dectin-2-Fc was incubated with biofilms formed by PAO1 or *wspF* mutant lab strains in 96 well plates, binding activity was detected in all tested strains except for the biofilm deficient strain Δ*wspF*Δ*pel*Δ*psl* (Figure 4.7). Dectin-2-Fc binding was not only observed with PAO1 and *wspF* lab strains but with biofilms formed by several wound isolates (Figure 4.8). Altogether these data suggested that PA display ligand(s) for Dectin-2 only as a biofilm. (Discussed in detail in 4.6.1)

The fact that Dectin-2-Fc binding was higher with strains that overexpress Psl compared to Pel only and PAO1 suggests that these strains might display more ligands for Dectin-2 (Figure 4.7). When Dectin-2-Fc was added to wells pre-coated with three different preparations of LMW-Psl and HMW-Psl, Dectin-2-Fc binding to all preparations was detected with stronger binding observed to HMW-Psl preparations (Figure 4.10). Initial NMR analysis indicated an

increased level of impurities in LMW-Psl compared to HMW-Psl (data not shown); hence all subsequent work apart from the assay in (Figure 4.10) utilised the HMW-Psl preparations.

Silver staining of two HMW-Psl preparations noted contamination with LPS (Figure 5.4 A). Thanks to substantial efforts of our lab colleagues (Sonali Singh and Darrel Jackson), the removal of LPS from HMW-Psl was successfully achieved using an endotoxin removal column and verified using SDS-PAGE (Figure 5.4 B) and TLR4-transduced cells (Data not shown). The ELISA binding assay showed that the ability to bind DC-SIGN and MR-CTLD4-7 and Dectin-2-Fc (Figure 5.4 C), respectively, was preserved in HMW-Psl$^{(LPS\text{-}free)}$. In agreement with the previous observations with biofilms, removal of calcium from the binding buffer diminished the binding of Dectin-2-Fc to HMW-Psl$^{(LPS\text{-}free)}$, suggesting contribution of the CRD domain to binding high mannose structures within HMW-Psl$^{(LPS\text{-}free)}$ (Figure 4.11). Pre-incubation of Dectin-2-Fc with Manα-1-2Man before performing the binding assay diminished Dectin-2-Fc binding to HMW-Psl$^{(LPS\text{-}free)}$ (Figure 4.12). This result correlates with Dectin-2 specificity for Manα-1-2Man mentioned in (Feinberg et al., 2017). Biolayer interferometry studies confirmed the binding of huDectin-2 to purified HMW-Psl (KD 20 nM) (Figure 4.13).

The Dectin-2-Fc binding to PA biofilms and purified Psl was in all cases lower compared to MR (CTLD-4-7-Fc) (Figure 4.7, Figure 4.10 and Figure 4.11), which correlate with the previous report showing lower affinity of Dectin-2 to mannose-rich structures compared to MR (CTLD-4-7-Fc) (McGreal et al., 2006). However, this was not the case when on PAO1 biofilms were developed on microscopic slides under continuous flow (Figure 4.9). In addition to the different binding profiles exhibited by each lectin, opposite of what was seen in the ELISA studies, Dectin-2 showed enhanced binding to biofilms generated under flow conditions compared to MR (Figure 4.9). It is possible to speculate that the different binding profiles are due to the two different biofilm generation methods which might alter biofilm structure (Azeredo et al., 2017). The enhanced DC-SIGN binding compared to both lectins might be attributed to the fact that DC-SIGN binds to planktonic cells, as observed previously in Alshahrani (2018) (discussed in detail in 5.6).

Overall, the most prominent finding to emerge from this chapter was that PA biofilms display ligands for Dectin-2 and that HMW-Psl behaves as Dectin-2 antagonist, which was unexpected. This would fit with a role for biofilm polysaccharides in dampening immune activation.

7.3. Interaction of human Dendritic cells with PA Biofilms (Chapter 5)

In Chapter 5, the initial aim was to find human myeloid cells that express DC-SIGN, MR and Dectin-2 to investigate their contributions to immune response after exposed to PA biofilms or purified Psl. Analysis of the expression of these receptors on human macrophages indicated that they would possibly be applicable to establish MR contribution to biofilm recognition, but not the contribution of DC-SIGN and Dectin-2 (Figure 5.2). On the other hand, analysis of expression of these lectins on moDCs indicated they are best suited to investigate the contribution of MR and DC-SIGN to biofilm recognition but not for investigating Dectin-2 contribution (Figure 5.3). Therefore chapter 5 focused mainly on DC-SIGN and MR. As shown in (5.4.2), a series of experiments were conducted to evaluate cytokine profiles produced by moDCs after interaction with biofilms. IL-1β, IL-23, IL-6, IL-10, MCP-1, Gro-α and TNF-α were quantified in supernatants collected after 4 hr of incubation. The time point was chosen based on the fact that LDH analysis showed no cytotoxicity at that time (Figure 5.10).

The most apparent results from this chapter were that HMW-Psl$^{(LPS\text{-}Free)}$ does not stimulate the production of cytokines by moDCs (Figure 5.5). Which is in agreement with the reports showing that both DC-SIGN and MR do not directly trigger an immune response, but rather modulate signalling by other PRRs, like TLRs (Gringhuis et al., 2007, Martinez-Pomares, 2012). However, HMW-Psl failed to influence moDCs cytokine responses to biofilms lacking Psl suggesting either that Psl does not play a role on the modulation of moDCs responses, or that the models implemented in this study were not suitable (Figure 5.5).

Although ManLam is a well-known DC-SIGN and MR ligand, Rivière et al. (2004) indicated that the modulatory effect resulted from the engagement of both MR or DC-SIGN is only obtained by ManLAM clusters and not by monomers ManLAM (Rivière et al., 2004). Therefore, to rule out the chance that the structure of our purified HMW-Psl$^{(LPS\text{-}free)}$ might not resemble that of Psl within PA biofilms, we co-cultured moDCs with PA biofilms formed by *wspF* mutant strains with distinct EPS components. However, data revealed no indication that the presence of Psl influenced moDCs cytokine responses to biofilms (Figure 5.6). We completed this investigation by assessing the effect of blocking DC-SIGN, MR and/or Dectin-2 on the cytokine response of moDCs to PA biofilms. No statistically significant changes could be detected (Figure 5.9). Together, these results suggest that there is either no role for Psl on the modulation of moDCs responses or the models implemented in this study are too limited. Recommendation of changes to existing models and suggestions on an alternative mouse model for the follow-up of this research can be found in (5.6.4).

Because both MR and DC-SIGN are considered important endocytic receptors expressed by antigen-presenting cells (Švajger et al., 2010). Dr. Sonali Singh conducted another set of experiments intended to determine whether two different HMW-Psl preparations HMW-Psl-1 and HMW-Psl-2 could interfere with moDCs endocytic activities. Data show distinct ability of HMW-Psl to modulate DC-SIGN-mediated endocytosis in moDCs independent of LPS (Figure 5.11 and Figure 5.12). These results prompted the launch of the microscopy-based investigation to study moDCs-HMW-Psl interaction.

It has been well established in the literature that DC-SIGN recognition of mannose-rich ligands such as HIV-1 envelope glycoprotein gp120 generates internalisation and cytoskeleton remodelling (Engering et al., 2002). Therefore, the aim was to assess if we could make similar observations when moDCs (DC-SIGN+, MR+, Dectin-1^{low}, Dectin-2$^{low/-}$, Figure 5.3) are incubated with biofilms formed by Psl-expressing strains or purified HMW-Psl$^{(LPS\text{-}Free)}$.

Curiously, results indicated that moDCs adopt rounded morphologies when incubated with biofilms (Figure 5.16). In agreement with this result, moDCs cultured with HMW-Psl$^{(LPS\text{-}free)}$ for 24 hr displayed a rounder morphology, characterised by higher circularity index and lowered perimeter (Figure 5.17). Together these results provide important insights into the Psl capability to interfere with moDCs activity and might indicate changes in the cytoskeleton.

In spite of limitations in this chapter with regards to moDCs cytokines analysis, the most obvious finding to emerge is that Psl have the capability to interfere with the activity of moDCs (DC-SIGN+, MR+, Dectin-1^{low} and Dectin-2$^{low/-}$) (Major finding.2).

7.4. Analysis of biofilm-human neutrophils interactions (Chapter 6)

About 50-70% percent of all circulating white blood cells in humans are neutrophils originated from myeloid precursor cells in the bone marrow (Doeing et al., 2003, Mestas and Hughes, 2004). These cells play an essential role in the complete resolution of lung infection as they function as effective phagocytic cells against extracellular bacteria and fungi (Segal, 2005). Neutrophils follow a variety of signals to reach sites of infection (de Oliveira et al., 2016). Although neutrophil infiltration is a hallmark of biofilm infection, the infection persists due to failure of neutrophils to eradicate the bacteria (Hänsch, 2012). Thanabalasuriar et al. (2019) reported that biofilm formation hindered neutrophils activity. Therefore, in Chapter 6 we mainly aimed to set up an *in vitro* microscopy-based model that enables us to examine neutrophils morphology and behaviour, as determined by live and confocal microscopy, following their interaction with PA, as planktonic or biofilms.

In this chapter, we utilised the biofilm formation method described in (Ch.3, Figure 3.9). Briefly, isolated human neutrophils were co-cultured with PA biofilm-forming strains (PAO1 and Δ*wspF*), or a biofilm-deficient strain (Δ*wspF*Δ*pel*Δ*psl*). To analyse the interaction, we acquired time-lapse images every 8 min using a DeltaVision microscope. Those images were then

uploaded to Fiji software with the aim to analyse neutrophils behaviour in each condition (Figure 6.4). Our data analysis mainly indicated that when neutrophils were exposed to fixed planktonic PA or biofilms, neutrophils motility was significantly lower when exposed to biofilms characterised as reduced velocity, net distance, MSD and speed. (Figures 6.7 and Figure 6.8). These results were in agreement with previous observations, indicating that biofilms restrict neutrophils activity (Thanabalasuriar et al., 2019).

While the added number of neutrophils and the location of image acquisition (Figure 6.5) were maintained constant. We found that the number of neutrophils cultured with biofilm-forming strains was lower than those cultured with biofilm-deficient cells, which may indicate that biofilm interferes with the adhesion of neutrophils (Figure 6.10). While there is no clear explanation of why this would occur, it possibly results from the presence of specific molecules that could kill the cells such as rhamnolipids. Alternatively, it may result from a reduction in the diffusion of certain molecules of chemoattractant that is necessary for the migration of neutrophils to the tested locations (please refer to 6.6.2).

Following live microscopy data acquisition, we stained the neutrophils biofilms co-cultures with HHA. The initial aim was to explore the possibility of neutrophils being attracted to high mannose structures. One unanticipated finding was the uptake of HHA staining by neutrophils (Figure 6.11), which was never reported before in the literature. This observation, (as discussed in 6.6.3) might result from form staining of paucimannosidic proteins within the neutrophils azurophilic granules. Based on this observation, we analysed the intensity of HHA labelling in each condition tested. Our data indicated that HHA staining intensity was higher for neutrophils incubated with biofilms-forming strains compared to biofilm-deficient strains (Figure 6.11). Overall, our findings indicated that HHA could possibly stain azurophilic granules within neutrophils, that HHA labelling was affected by the presence of biofilms and planktonic cells, and that biofilms could restrict the release of granules. (Please refer to 6.6.3 for further explanation).

Jesaitis et al. (2003) reported that neutrophils display rounded morphology when exposed to PA biofilms. Similarly, in Chapter 5, we observed that moDCs adopted a rounded morphology when exposed to PA biofilms or HMW-Psl (Figure 5.16Figure 5.17). Therefore, in this chapter, we examined whether neutrophils would also adopt a circular morphology when exposed to PA biofilms and whether the addition of the biofilm purified component, HMW-Psl to planktonic cells would influence neutrophils shape. Similar to moDCs, neutrophils retained circular shape after exposure to biofilms or HMW-Psl+ and showed higher phalloidin intensity, suggesting changes in the cytoskeleton (Figure 6.12). (discussed in detail in 6.6.4).

Discussion of limitations and future work can be found in (6.6.5). Overall, data in Chapter 6 identified possible factors that might affect neutrophils ability to eliminate biofilms.

7.5. Future prospects

7.5.1. Examination of the innate immune response to polymicrobial biofilms:

The current study data highlighted the engagement of CLRs in recognition of PA biofilms. However, data obtained *in vitro* with a single-species biofilm may not represent the whole scenario in clinical settings. Several reports have shown that many chronic biofilms-associated infections are polymicrobial composed of a collection of organisms (fungi and bacteria) (Peters et al., 2012, Mulcahy et al., 2014). Multi-species biofilms have been involved in cystic fibrosis pathogenesis and many hospital-acquired infections related to implanted medical devices, including urinary catheters (Coad et al., 2016, Sibley et al., 2008). Additionally, analysis of 30 human wounds showed the presence of diverse bacterial species (Dowd et al., 2008).

While It is evident that immune responses to bacteria or fungi alone are different, there is very little information about the host immune reactions to polymicrobial infections (Dhamgaye et al., 2016). Additionally, it was indicated that competition between organisms caused by close proximity and nutrient limitations could lead to changes in metabolism and virulence, which

might influence the host immunity (Tay et al., 2016, He et al., 2017). For example, PA is reported to secret the toxin pyocyanin to outcompete co-infecting microbes such as *Burkholderia cepacian* (Tomlin et al., 2001). However, the release of pyocyanin is reported to induce neutrophil apoptosis and the release of ROS (Manago et al., 2015).

It has been demonstrated that *C. albicans* colonisation of the respiratory tract may facilitate the establishment of PA-associated VAP (Azoulay et al., 2006). Additionally, the coexistence of *C. albicans* and PA has been linked to poor clinical outcomes in cystic fibrosis patients compared to mono-infection with PA alone (Navarro et al., 2001). This finding was validated by results by Roux et al. (2009) utilising a mouse model (Roux et al., 2009). Several studies have established the important role of CLRs in *C. albicans* infection. For example, mice lacking Dectin-2 were more susceptible to candida infection compared to WT mice (Ifrim et al., 2016). Early reports described the contribution of MR to cytokine release and killing of *C. albicans* by phagocytic cells (Szolnoky et al., 2001, Maródi et al., 1991, Yamamoto et al., 1997). Additionally, DC-SIGN was reported to bind the N-linked mannans in the cell wall of *C. albicans,* and mediate DC internalisation of this pathogen (Cambi et al., 2003).

In this study, we showed evidence that PA biofilms display ligand for DC-SIGN, MR and Dectin-2. Notably our data indicated, that Psl interferes with the biological function of these receptors, working as an antagonist for Dectin-2 and restricting MR and DC-SIGN ligands endocytosis (Ch.4 and Ch.5 respectively). Although this study focuses only on PA biofilms, these findings may well have a bearing on polymicrobial biofilm infections involving *C.albicans* and PA. In a mouse model, it was indicated that administration of fungal lysate from *C. albicans* caused the release of Th2 cytokines (IL-4, IL-5 and IL-13), eosinophilia and hypersecretion of mucus. On the other hand, administration of PA lysates only elicits the production of Th1 cytokines (IFN-γ) and associated with neutrophils dominated responses with no mucus secretion. Interestingly, co-stimulation with of both fungal and bacteria lysates shifted the fungal immune response (Th2) towards the bacterial (Th1) (Allard et al., 2009). Therefore,

further work needs to be done to establish whether CLRs response to *C.albicans* is altered in the presence of PA biofilms or purified Psl.

PA also often coexist with *S. aureus* within the context of biofilm-associated infection. Although the nature of this existence was reported to be competitional in some situations (Magalhães et al., 2019), some reports suggested that it might be advantageous. For example, it was indicated that antibiotic susceptible *S. aureus* might benefit from being surrounded by antibiotic resistance PA (Magalhães et al., 2019). (Dalton et al., 2011) studied the impact of co-infections of PA and S. aureus in a mouse model of polymicrobial wounds infection. In this study, an *in vitro* biofilms were transplanted into the wounds of mice. Data revealed that co-infection of both organisms caused delayed wound closure and hindered antibiotic treatments compared to infection with PA only (Dalton et al., 2011). The engagement of DC-SIGN, Dectin-2 and MR by *S. aureus* is not reported; preliminary observations in our lab indicated that DC-SIGN might recognise EPS purified form *S. aureus* (data not shown). Further research could also be conducted to determine how the coexistence of both organisms might influence the innate immune response.

7.5.2. Examination of the possibility of other lectins to also contribute to PA recognition:

In addition to MR, DC-SIGN and Dectin-2 other lectins among the CLRs family might potentially bind to PA biofilms and EPS components such as Dendritic cell immunoreceptor (DCIR) and Macrophage-inducible C-type lectin (Mincle).

7.5.2.1. Dendritic cell immunoreceptor (DCIR):

DCIR (CLECSF6, CLEC4A) belongs to the Dectin 2 family and is expressed on DC, monocytes, macrophages, B lymphocytes, and granulocytes (Bates et al., 1999). *In vitro*, DCIR expression was found to be high in moDCs, and was downregulated upon exposure to LPS (Bates et al., 1999). This CLR had a broad specificity for carbohydrates, mainly binding mannose and fucose (Nagae et al., 2016). In both pDCs and moDCs activation of DCIR with

a monoclonal antibody modulated TLR-9 and TLR-8 responses, respectively; reduced cytokines release (IFN-α and TNF-α for pDCs and IL-12 and TNF-α for moDCs) was detected when both (TLR-9 or TLR-8) and DCIR were co-stimulated (Tel et al., 2012, Meyer-Wentrup et al., 2009). Co-stimulation of DCIR and DC-SIGN was found to affect the internalisation of high mannose ligands. DC-SIGN internalisation and antigen presentation to T-Cells was reduced when DCIR was triggered simultaneously (García-Vallejo et al., 2015). In a mouse model of MTB infection Troegeler et al. (2017), found that DCIR deficiency inhibit type I IFN signalling in DCs, leading to enhanced production of IL-12 and increased T cell differentiation toward Th1. Although DCIR-deficient mice showed better ability to control MTB compared to WT mice, it developed higher inflammation characterised by increased release of TNF and inducible NOS (iNOS) in the lungs (Troegeler et al., 2017).

7.5.2.2. Macrophage-inducible C-type lectin (Mincle):

Mincle (CLECSF9, Clec4e) consists of a CTLD domain containing an EPN motif, thus able to recognise different carbohydrates, mainly α-mannose (Lee et al., 2011, Yamasaki et al., 2009). Similar to Dectin-2, Mincle is linked to the FcR-γ to transduce intracellular signalling (Yamasaki et al., 2008). Mincle is expressed by multiple innate immune cells including monocytes, macrophages and neutrophils (Flornes et al., 2004, Vijayan et al., 2012, Yamasaki et al., 2008, Lee et al., 2012, Kawata et al., 2012). Inflammatory stimuli, including LPS, TNF-α, IL-6 and IFN-γ, strongly induce Mincle expression in macrophages (Matsumoto et al., 1999). Human Mincle has shown a mutual expression pattern on neutrophils and monocytes from the same donor (Vijayan et al., 2012). Expression of Mincle in monocytes was shown to be essential for inflammatory cytokine responses; however, it is negatively correlated with fungal uptake and killing. On the other hand, the expression of Mincle in neutrophils aided fungal uptake and killing (Vijayan et al., 2012). Research have showed that TLRs can collaborate with Mincle synergistically to upregulate the production of inflammatory cytokines and expression of complement receptor 3 (CR3) (Yamasaki et al., 2008, da Glória Sousa et al., 2011). Mincle intracellular signalling through Syk, CARD9–Bcl10–Malt1 and mitogen-

activated protein kinase (MAPK) pathways will result in the induction of several cytokines and chemokines, including TNF-α, macrophage inflammatory protein 2 (MIP-2; CXCL2), keratinocyte-derived chemokine (KC; CXCL1) and IL-6 (Strasser et al., 2012, Yamasaki et al., 2008). Mincle binds ligands from several fungal and bacterial pathogens, implicating its role in anti-microbial immunity. Mincle binding to the cell wall of *C. albicans* triggers protective immune response including inflammatory cytokine production, fungal killing and phagocytosis (Vijayan et al., 2012, Wells et al., 2008).

7.5.3. Examination of the synergistic response of CLRs with other PPRs such as TLR-9:

In this study, we noted an extensive amount of eDNA within the biofilm matrix (Figure 3.10 and Figure 3.11), which is relevant to all biofilms (Montanaro et al., 2011). eDNA is a fundamental component of PA biofilms; treatment with DNase completely prevented biofilms formation by PAO1 (Swartjes et al., 2013). The source of eDNA in biofilms was initially reported to be autolysis of bacteria subpopulations within the biofilm community (Turnbull et al., 2016, Montanaro et al., 2011) which was supported by the detection of full bacterial genomic DNA in the EPS of PAO1 biofilms (Deng et al., 2020). However, a recent study found that PAO1 Δ*wspF* displayed a distinct mechanism of eDNA release independent of the suicidal path as previously reported in PAO1 (Deng et al., 2020).

The PPR, TLR-9, which resides in endosomes, is reported to bind microbial DNA in the endolysosomal compartments to prevent activation by self-DNA (Kawasaki and Kawai, 2019). Activation of TLR-9 with bacterial DNA triggers the release IL-8, which regulate neutrophils recruitment (Kawasaki and Kawai, 2019). Neutrophils also express TLR-9, and it was indicated that treatment of PA biofilms with DNase significantly reduced the release of IL-8, IL-1β, phagocytosis and NETs formation (Bass et al., 2010).

Two separate studies indicated that mice lacking TLR-9 exhibited better killing ability of PA (Benmohamed et al., 2014) and *S. aureus* (Parker and Prince, 2012). Additionally, it was

indicated that Syk activation is required for TLR-9 recruitment to β-1,3 glucan beads and fungal-containing phagosomes following ligation of Dectin-1 (Khan et al., 2016). Therefore, future investigation on TLR-9 contribution in the immune response against PA biofilms and the possible collaboration with other CLR such as DC-SIGN, MR and Dectin-2 is highly recommended. DC-SIGN transgenic mice with or without mutation in MR, Dectin-2 and TLR-9 would offer a possible tool for future investigation.

Summary

To conclude, we have shown that Dectin-2 binds to PA biofilms and different independent preparations of Psl. We also found that HMW-Psl$^{(LPS\text{-}Free)}$ works as Dectin-2 antagonist and interfere with moDCs morphology and endocytic activity of DC-SIGN and MR. Finally, we highlighted possible factors that might affect neutrophils capability in eliminating biofilms. Despite its limitations, this study certainly adds to our understanding of the interaction between innate immune cells and PA biofilms.

References

ABERDEIN, J., COLE, J., BEWLEY, M., MARRIOTT, H. & DOCKRELL, D. 2013. Alveolar macrophages in pulmonary host defence–the unrecognized role of apoptosis as a mechanism of intracellular bacterial killing. *Clinical & Experimental Immunology,* 174**,** 193-202.

ADAM, E. C., MITCHELL, B. S., SCHUMACHER, D. U., GRANT, G. & SCHUMACHER, U. 1997. Pseudomonas aeruginosa II lectin stops human ciliary beating: therapeutic implications of fucose. *American Journal of Respiratory and Critical Care Medicine,* 155**,** 2102-2104.

ADAMO, R., SOKOL, S., SOONG, G., GOMEZ, M. I. & PRINCE, A. 2004. Pseudomonas aeruginosa flagella activate airway epithelial cells through asialoGM1 and toll-like receptor 2 as well as toll-like receptor 5. *Am J Respir Cell Mol Biol,* 30**,** 627-34.

AGUINIGA, L. M., YAGGIE, R. E., SCHAEFFER, A. J. & KLUMPP, D. J. 2016. Lipopolysaccharide domains modulate urovirulence. *Infection and Immunity,* 84**,** 3131-3140.

AJUEBOR, M. N., DAS, A. M., VIRÁG, L., FLOWER, R. J., SZABÓ, C. & PERRETTI, M. 1999. Role of resident peritoneal macrophages and mast cells in chemokine production and neutrophil migration in acute inflammation: evidence for an inhibitory loop involving endogenous IL-10. *The Journal of Immunology,* 162**,** 1685-1691.

AKBARI, O., DEKRUYFF, R. H. & UMETSU, D. T. 2001. Pulmonary dendritic cells producing IL-10 mediate tolerance induced by respiratory exposure to antigen. *Nature Immunology,* 2**,** 725-731.

AKILOV, O. E., KASUBOSKI, R. E., CARTER, C. R. & MCDOWELL, M. A. 2007. The role of mannose receptor during experimental leishmaniasis. *Journal of Leukocyte Biology,* 81**,** 1188-1196.

ALARCON, I., EVANS, D. J. & FLEISZIG, S. M. 2009. The role of twitching motility in Pseudomonas aeruginosa exit from and translocation of corneal epithelial cells. *Investigative Ophthalmology & Visual Science,* 50**,** 2237-2244.

ALHEDE, M., BJARNSHOLT, T., GIVSKOV, M. & ALHEDE, M. 2014. Pseudomonas aeruginosa biofilms: mechanisms of immune evasion. *Advances in Applied Microbiology.* Elsevier.

ALI, J., SOHAIL, A., WANG, L., RIZWAN HAIDER, M., MULK, S. & PAN, G. 2018. Electro-microbiology as a promising approach towards renewable energy and environmental sustainability. *Energies,* 11**,** 1822.

ALKAWASH, M. A., SOOTHILL, J. S. & SCHILLER, N. L. 2006. Alginate lyase enhances antibiotic killing of mucoid Pseudomonas aeruginosa in biofilms. *Apmis,* 114**,** 131-138.

ALLARD, J. B., RINALDI, L., WARGO, M. J., ALLEN, G., AKIRA, S., UEMATSU, S., POYNTER, M. E., HOGAN, D. A., RINCON, M. & WHITTAKER, L. A. 2009. Th2 allergic immune response to inhaled fungal antigens is modulated by TLR‐4‐independent bacterial products. *European Journal of Immunology,* 39**,** 776-788.

ALLAVENA, P., CHIEPPA, M., MONTI, P. & PIEMONTI, L. 2004. From pattern recognition receptor to regulator of homeostasis: the double-faced macrophage mannose receptor. *Critical Reviews in Immunology,* 24.

ALLEN, L.-A. H. 2014. Immunofluorescence and confocal microscopy of neutrophils. *Neutrophil Methods and Protocols.* Springer.

ALLESEN-HOLM, M., BARKEN, K. B., YANG, L., KLAUSEN, M., WEBB, J. S., KJELLEBERG, S., MOLIN, S., GIVSKOV, M. & TOLKER‐NIELSEN, T. 2006. A characterization of DNA release in Pseudomonas aeruginosa cultures and biofilms. *Molecular Microbiology,* 59**,** 1114-1128.

ALSHAHRANI, M. 2018. *The role of C-type lectin receptors in the recognition of Pseudiminas aeruginosa.* University of Nottingham.

ALVAREZ, C. P., LASALA, F., CARRILLO, J., MUÑIZ, O., CORBÍ, A. L. & DELGADO, R. 2002. C-type lectins DC-SIGN and L-SIGN mediate cellular entry by Ebola virus in cis and in trans. *J Virol,* 76**,** 6841-4.

ARCIOLA, C. R., CAMPOCCIA, D., SPEZIALE, P., MONTANARO, L. & COSTERTON, J. W. 2012. Biofilm formation in Staphylococcus implant infections. A review of molecular mechanisms and implications for biofilm-resistant materials. *Biomaterials,* 33**,** 5967-5982.

ARDAVíN, C., MARTíNEZ DEL HOYO, G., MARTíN, P., ANJUÈRE, F., ARIAS, C. F., MARíN, A. R., RUIZ, S., PARRILLAS, V. & HERNÁNDEZ, H. 2001. Origin and differentiation of dendritic cells. *Trends in Immunology,* 22**,** 691-700.

ARIIZUMI, K., SHEN, G. L., SHIKANO, S., RITTER, R., 3RD, ZUKAS, P., EDELBAUM, D., MORITA, A. & TAKASHIMA, A. 2000. Cloning of a second dendritic cell-associated C-type lectin (dectin-2) and its alternatively spliced isoforms. *J Biol Chem,* 275**,** 11957-63.

ARLEHAMN, C. S. & EVANS, T. J. 2011. Pseudomonas aeruginosa pilin activates the inflammasome. *Cell Microbiol,* 13**,** 388-401.

ARMBRUSTER, C. R., LEE, C. K., PARKER-GILHAM, J., DE ANDA, J., XIA, A., ZHAO, K., MURAKAMI, K., TSENG, B. S., HOFFMAN, L. R. & JIN, F. 2019. Heterogeneity in surface sensing suggests a division of labor in Pseudomonas aeruginosa populations. *Elife,* 8**,** e45084.

ARORA, S. K., RITCHINGS, B. W., ALMIRA, E. C., LORY, S. & RAMPHAL, R. 1998. The Pseudomonas aeruginosa flagellar cap protein, FliD, is responsible for mucin adhesion. *Infection and Immunity,* 66**,** 1000-1007.

AURAY, G., KELLER, I., PYTHON, S., GERBER, M., BRUGGMANN, R., RUGGLI, N. & SUMMERFIELD, A. 2016. Characterization and transcriptomic analysis of porcine blood conventional and plasmacytoid dendritic cells reveals striking species-specific differences. *The Journal of Immunology,* 197**,** 4791-4806.

AZAD, A. K., TORRELLES, J. B. & SCHLESINGER, L. S. 2008. Mutation in the DC‐SIGN cytoplasmic triacidic cluster motif markedly attenuates receptor activity for phagocytosis and endocytosis of mannose‐containing ligands by human myeloid cells. *Journal of Leukocyte Biology,* 84**,** 1594-1603.

AZEREDO, J., AZEVEDO, N. F., BRIANDET, R., CERCA, N., COENYE, T., COSTA, A. R., DESVAUX, M., DI BONAVENTURA, G., HEBRAUD, M., JAGLIC, Z., KACANIOVA, M., KNOCHEL, S., LOURENCO, A., MERGULHAO, F., MEYER, R. L., NYCHAS, G., SIMOES, M., TRESSE, O. & STERNBERG, C. 2017. Critical review on biofilm methods. *Crit Rev Microbiol,* 43**,** 313-351.

AZOULAY, E., TIMSIT, J.-F., TAFFLET, M., DE LASSENCE, A., DARMON, M., ZAHAR, J.-R., ADRIE, C., GARROUSTE-ORGEAS, M., COHEN, Y. & MOURVILLIER, B. 2006. Candida colonization of the respiratory tract and subsequent pseudomonas ventilator-associated pneumonia. *Chest,* 129**,** 110-117.

BAILIN, A. 2017. *Regulation of the Pseudomonas aeruginosa type III secretion system by cyclic-di-GMP.* Master of Science, University of Iowa.

BAJOLET-LAUDINAT, O., GIROD-DE BENTZMANN, S., TOURNIER, J., MADOULET, C., PLOTKOWSKI, M., CHIPPAUX, C. & PUCHELLE, E. 1994. Cytotoxicity of Pseudomonas aeruginosa internal lectin PA-I to respiratory epithelial cells in primary culture. *Infection and Immunity,* 62**,** 4481-4487.

BALAMAYOORAN, G., BATRA, S., FESSLER, M. B., HAPPEL, K. I. & JEYASEELAN, S. 2010. Mechanisms of neutrophil accumulation in the lungs against bacteria. *American Journal of Respiratory Cell and Molecular Biology,* 43**,** 5-16.

BALCH, S. G., GREAVES, D. R., GORDON, S. & MCKNIGHT, A. J. 2002. Organization of the mouse macrophage C-type lectin (Mcl) gene and identification of a subgroup of related lectin molecules. *European Journal of Immunogenetics,* 29**,** 61-64.

BALES, P. M., RENKE, E. M., MAY, S. L., SHEN, Y. & NELSON, D. C. 2013. Purification and characterization of biofilm-associated EPS exopolysaccharides from ESKAPE organisms and other pathogens. *PloS One,* 8**,** e67950.

BALLOY, V., VERMA, A., KURAVI, S., SI-TAHAR, M., CHIGNARD, M. & RAMPHAL, R. 2007. The role of flagellin versus motility in acute lung disease caused by Pseudomonas aeruginosa. *The Journal of Infectious Diseases,* 196**,** 289-296.

BALZARINI, J., HATSE, S., VERMEIRE, K., PRINCEN, K., AQUARO, S., PERNO, C.-F., DE CLERCQ, E., EGBERINK, H., MOOTER, G. V. & PEUMANS, W. 2004. Mannose-specific plant lectins from the Amaryllidaceae family qualify as efficient microbicides for prevention of human immunodeficiency virus infection. *Antimicrobial Agents and Chemotherapy,* 48**,** 3858-3870.

BARANOV, M., TER BEEST, M., REINIEREN-BEEREN, I., CAMBI, A., FIGDOR, C. G. & VAN DEN BOGAART, G. 2014. Podosomes of dendritic cells facilitate antigen sampling. *Journal of Cell Science,* 127**,** 1052-1064.

BARAQUET, C. & HARWOOD, C. S. 2013. Cyclic diguanosine monophosphate represses bacterial flagella synthesis by interacting with the Walker A motif of the enhancer-binding protein FleQ. *Proceedings of the National Academy of Sciences,* 110**,** 18478-18483.

BARAQUET, C., MURAKAMI, K., PARSEK, M. R. & HARWOOD, C. S. 2012. The FleQ protein from Pseudomonas aeruginosa functions as both a repressor and an activator to control gene expression from the pel operon promoter in response to c-di-GMP. *Nucleic Acids Research,* 40**,** 7207-7218.

BARDOEL, B. W., VAN DER ENT, S., PEL, M. J., TOMMASSEN, J., PIETERSE, C. M., VAN KESSEL, K. P. & VAN STRIJP, J. A. 2011. Pseudomonas evades immune recognition of flagellin in both mammals and plants. *PLoS Pathog,* 7**,** e1002206.

BARRETT, N. A., MAEKAWA, A., RAHMAN, O. M., AUSTEN, K. F. & KANAOKA, Y. 2009. Dectin-2 recognition of house dust mite triggers cysteinyl leukotriene generation by dendritic cells. *Journal of Immunology* 182**,** 1119-1128.

BASHIROVA, A. A., GEIJTENBEEK, T. B., VAN DUIJNHOVEN, G. C., VAN VLIET, S. J., EILERING, J. B., MARTIN, M. P., WU, L., MARTIN, T. D., VIEBIG, N., KNOLLE, P. A., KEWALRAMANI, V. N., VAN KOOYK, Y. & CARRINGTON, M. 2001. A dendritic cell-specific intercellular adhesion molecule 3-grabbing nonintegrin (DC-SIGN)-related protein is highly expressed on human liver sinusoidal endothelial cells and promotes HIV-1 infection. *The Journal of Experimental Medicine,* 193**,** 671-678.

BASS, J. I. F., GABELLONI, M. L., ALVAREZ, M. E., VERMEULEN, M. E., RUSSO, D. M., ZORREGUIETA, A., GEFFNER, J. R. & TREVANI, A. S. 2008. Characterization of bacterial DNA binding to human neutrophil surface. *Laboratory Investigation,* 88**,** 926-937.

BASS, J. I. F., RUSSO, D. M., GABELLONI, M. L., GEFFNER, J. R., GIORDANO, M., CATALANO, M., ZORREGUIETA, Á. & TREVANI, A. S. 2010. Extracellular DNA: a major proinflammatory component of Pseudomonas aeruginosa biofilms. *The Journal of Immunology,* 184**,** 6386-6395.

BATES, E. E., FOURNIER, N., GARCIA, E., VALLADEAU, J., DURAND, I., PIN, J.-J., ZURAWSKI, S. M., PATEL, S., ABRAMS, J. S. & LEBECQUE, S. 1999. APCs express DCIR, a novel C-type lectin surface receptor containing an immunoreceptor tyrosine-based inhibitory motif. *The Journal of Immunology,* 163**,** 1973-1983.

BENDER, A., SAPP, M., SCHULER, G., STEINMAN, R. M. & BHARDWAJ, N. 1996. Improved methods for the generation of dendritic cells from nonproliferating progenitors in human blood. *J Immunol Methods,* 196**,** 121-35.

BENKO, S., PHILPOTT, D. J. & GIRARDIN, S. E. 2008. The microbial and danger signals that activate Nod-like receptors. *Cytokine,* 43**,** 368-373.

BENMOHAMED, F., MEDINA, M., WU, Y.-Z., MASCHALIDI, S., JOUVION, G., GUILLEMOT, L., CHIGNARD, M., MANOURY, B. & TOUQUI, L. 2014. Toll-like receptor 9 deficiency protects mice against Pseudomonas aeruginosa lung infection. *PloS One,* 9**,** e90466-e90466.

BERK, V., FONG, J. C., DEMPSEY, G. T., DEVELIOGLU, O. N., ZHUANG, X., LIPHARDT, J., YILDIZ, F. H. & CHU, S. 2012. Molecular architecture and assembly principles of Vibrio cholerae biofilms. *Science,* 337**,** 236-239.

BERNARDO, J., BILLINGSLEA, A. M., BLUMENTHAL, R. L., SEETOO, K. F., SIMONS, E. R. & FENTON, M. J. 1998. Differential responses of human mononuclear phagocytes to mycobacterial lipoarabinomannans: role of CD14 and the mannose receptor. *Infection and Immunity,* 66**,** 28-35.

BERSHADSKY, A. D., BALABAN, N. Q. & GEIGER, B. 2003. Adhesion-dependent cell mechanosensitivity. *Annual Review of Cell and Developmental Biology,* 19**,** 677-695.

BERUBE, B. J., RANGEL, S. M. & HAUSER, A. R. 2016. Pseudomonas aeruginosa: breaking down barriers. *Current Genetics,* 62**,** 109-113.

BETHKE, K., STAIB, F., DISTLER, M., SCHMITT, U., JONULEIT, H., ENK, A. H., GALLE, P. R. & HEIKE, M. 2002. Different efficiency of heat shock proteins (HSP) to activate human monocytes and dendritic cells: superiority of HSP60. *The Journal of Immunology,* 169**,** 6141-6148.

BEVERIDGE, T. J., MAKIN, S. A., KADURUGAMUWA, J. L. & LI, Z. 1997. Interactions between biofilms and the environment. *FEMS Microbiol Rev,* 20**,** 291-303.

BILLINGS, N., MILLAN, M. R., CALDARA, M., RUSCONI, R., TARASOVA, Y., STOCKER, R. & RIBBECK, K. 2013. The extracellular matrix component Psl provides fast-acting antibiotic defense in Pseudomonas aeruginosa biofilms. *PLoS Pathog,* 9**,** e1003526.

BJARNSHOLT, T., ALHEDE, M., ALHEDE, M., EICKHARDT-SØRENSEN, S. R., MOSER, C., KÜHL, M., JENSEN, P. Ø. & HØIBY, N. 2013. The in vivo biofilm. *Trends in Microbiology,* 21**,** 466-474.

BLEVES, S., SANA, T. G. & VOULHOUX, R. 2014. The target cell genus does not matter. *Trends in Microbiology,* 22**,** 304-306.

BÖL, M., EHRET, A. E., BOLEA ALBERO, A., HELLRIEGEL, J. & KRULL, R. 2013. Recent advances in mechanical characterisation of biofilm and their significance for material modelling. *Critical Reviews in Biotechnology,* 33**,** 145-171.

BORLEE, B. R., GOLDMAN, A. D., MURAKAMI, K., SAMUDRALA, R., WOZNIAK, D. J. & PARSEK, M. R. 2010. Pseudomonas aeruginosa uses a cyclic‐di‐GMP‐regulated adhesin to reinforce the biofilm extracellular matrix. *Molecular Microbiology,* 75**,** 827-842.

BORREGAARD, N. 2010. Neutrophils, from marrow to microbes. *Immunity,* 33**,** 657-670.

BOUGLÉ, A., FOUCRIER, A., DUPONT, H., MONTRAVERS, P., OUATTARA, A., KALFON, P., SQUARA, P., SIMON, T., AMOUR, J. & FOR THE I, D. S. G. 2017. Impact of the duration of antibiotics on clinical events in patients with Pseudomonas aeruginosa ventilator-associated pneumonia: study protocol for a randomized controlled study. *Trials,* 18**,** 37.

BOYD, A. & CHAKRABARTY, A. Á. 1994. Role of alginate lyase in cell detachment of Pseudomonas aeruginosa. *Applied and Environmental Microbiology,* 60**,** 2355-2359.

BRAGONZI, A., PARONI, M., NONIS, A., CRAMER, N., MONTANARI, S., REJMAN, J., DI SERIO, C., DÖRING, G. & TÜMMLER, B. 2009. Pseudomonas aeruginosa microevolution during cystic fibrosis lung infection establishes clones with adapted virulence. *American Journal of Respiratory and Critical Care Medicine,* 180**,** 138-145.

BRANDENBURG, K. S., CALDERON, D. F., KIERSKI, P. R., BROWN, A. L., SHAH, N. M., ABBOTT, N. L., SCHURR, M. J., MURPHY, C. J., MCANULTY, J. F. & CZUPRYNSKI, C. J. 2015. Inhibition of Pseudomonas aeruginosa biofilm formation on wound dressings. *Wound Repair Regen,* 23**,** 842-54.

BRIKEN, V., PORCELLI, S. A., BESRA, G. S. & KREMER, L. 2004. Mycobacterial lipoarabinomannan and related lipoglycans: from biogenesis to modulation of the immune response. *Mol Microbiol,* 53**,** 391-403.

BRILL-KARNIELY, Y., JIN, F., WONG, G. C. L., FRENKEL, D. & DOBNIKAR, J. 2017. Emergence of complex behavior in pili-based motility in early stages of P. aeruginosa surface adaptation. *Scientific Reports,* 7**,** 45467.

BRINKMANN, V., REICHARD, U., GOOSMANN, C., FAULER, B., UHLEMANN, Y., WEISS, D. S., WEINRAUCH, Y. & ZYCHLINSKY, A. 2004. Neutrophil extracellular traps kill bacteria. *Science,* 303**,** 1532-1535.

BROS, M., HAAS, K., MOLL, L. & GRABBE, S. 2019. RhoA as a key regulator of innate and adaptive immunity. *Cells,* 8**,** 733.

BROWN, G. D. 2006. Dectin-1: a signalling non-TLR pattern-recognition receptor. *Nature Reviews Immunology,* 6**,** 33-43.

BROWN, G. D. & GORDON, S. 2001. A new receptor for β-glucans. *Nature,* 413**,** 36-37.

BRUDNER, M., KARPEL, M., LEAR, C., CHEN, L., YANTOSCA, L. M., SCULLY, C., SARRAJU, A., SOKOLOVSKA, A., ZARIFFARD, M. R., EISEN, D. P., MUNGALL, B. A., KOTTON, D. N., OMARI, A., HUANG, I. C., FARZAN, M., TAKAHASHI, K., STUART, L., STAHL, G. L., EZEKOWITZ, A. B., SPEAR, G. T., OLINGER, G. G., SCHMIDT, E. V. & MICHELOW, I. C. 2013. Lectin-dependent enhancement of Ebola virus infection via soluble and transmembrane C-type lectin receptors. *PloS One,* 8**,** e60838-e60838.

BRUSCIA, E. M., ZHANG, P.-X., SATOH, A., CAPUTO, C., MEDZHITOV, R., SHENOY, A., EGAN, M. E. & KRAUSE, D. S. 2011. Abnormal trafficking and degradation of TLR4 underlie the elevated inflammatory response in cystic fibrosis. *The Journal of Immunology,* 186**,** 6990-6998.

BUCCIONE, R., ORTH, J. D. & MCNIVEN, M. A. 2004. Foot and mouth: podosomes, invadopodia and circular dorsal ruffles. *Nat Rev Mol Cell Biol,* 5**,** 647-57.

BUCIOR, I., PIELAGE, J. F. & ENGEL, J. N. 2012. Pseudomonas aeruginosa pili and flagella mediate distinct binding and signaling events at the apical and basolateral surface of airway epithelium. *PLoS Pathog,* 8**,** e1002616.

BURD, J. F. & USATEGUI-GOMEZ, M. 1973. A colorimetric assay for serum lactate dehydrogenase. *Clin Chim Acta,* 46**,** 223-7.

BURNS, J. L., GIBSON, R. L., MCNAMARA, S., YIM, D., EMERSON, J., ROSENFELD, M., HIATT, P., MCCOY, K., CASTILE, R., SMITH, A. L. & RAMSEY, B. W. 2001. Longitudinal Assessment of Pseudomonas aeruginosa in Young Children with Cystic Fibrosis. *The Journal of Infectious Diseases,* 183**,** 444-452.

BURROWS, L. L. 2012. Pseudomonas aeruginosa twitching motility: type IV pili in action. *Annual Review of Microbiology,* 66**,** 493-520.

BYRD, M. S., SADOVSKAYA, I., VINOGRADOV, E., LU, H., SPRINKLE, A. B., RICHARDSON, S. H., MA, L., RALSTON, B., PARSEK, M. R., ANDERSON, E. M., LAM, J. S. & WOZNIAK, D. J. 2009. Genetic and biochemical analyses of the Pseudomonas aeruginosa Psl exopolysaccharide reveal overlapping roles for polysaccharide synthesis enzymes in Psl and LPS production. *Molecular microbiology,* 73**,** 622-638.

BYSTROVA, O. V., KNIREL, Y. A., LINDNER, B., KOCHAROVA, N. A., KONDAKOVA, A. N., ZÄHRINGER, U. & PIER, G. B. 2006. Structures of the core oligosaccharide and O-units in the R-and SR-type lipopolysaccharides of reference strains of Pseudomonas aeruginosa O-serogroups. *FEMS Immunology & Medical Microbiology,* 46**,** 85-99.

CALDERONE, R. A. & CLANCY, C. J. 2011. *Candida and candidiasis*, American Society for Microbiology Press.

CALIZ, R., CANET, L. M., LUPIANEZ, C. B., CANHAO, H., ESCUDERO, A., FILIPESCU, I., SEGURA-CATENA, J., SOTO-PINO, M. J., EXPOSITO-RUIZ, M., FERRER, M. A., GARCIA, A., ROMANI, L., GONZALEZ-UTRILLA, A., VALLEJO, T., PEREZ-PAMPIN, E., HEMMINKI, K., FORSTI, A., COLLANTES, E., FONSECA, J. E. & SAINZ, J. 2013. Gender-specific effects of genetic variants within Th1 and Th17 cell-mediated immune response genes on the risk of developing rheumatoid arthritis. *PLoS One,* 8**,** e72732.

CAMBI, A., DE LANGE, F., VAN MAARSEVEEN, N. M., NIJHUIS, M., JOOSTEN, B., VAN DIJK, E. M. H. P., DE BAKKER, B. I., FRANSEN, J. A. M., BOVEE-GEURTS, P. H. M., VAN LEEUWEN, F. N., VAN HULST, N. F. & FIGDOR, C. G. 2004. Microdomains of the C-type lectin DC-SIGN are portals for virus entry into dendritic cells. *The Journal of Cell Biology,* 164**,** 145-155.

CAMBI, A., GIJZEN, K., DE VRIES, I. J. M., TORENSMA, R., JOOSTEN, B., ADEMA, G. J., NETEA, M. G., KULLBERG, B. J., ROMANI, L. & FIGDOR, C. G. 2003. The C‐type lectin DC‐SIGN (CD209) is an antigen‐uptake receptor for Candida albicans on dendritic cells. *European Journal of Immunology,* 33**,** 532-538.

CAROFF, M. & NOVIKOV, A. 2019. LPS Structure, Function, and Heterogeneity. *Endotoxin Detection and Control in Pharma, Limulus, and Mammalian Systems.* Springer.

CARTER, R. W., THOMPSON, C., REID, D. M., WONG, S. Y. C. & TOUGH, D. F. 2006. Induction of CD8+ T cell responses through targeting of antigen to Dectin-2. *Cellular Immunology,* 239**,** 87-91.

CARVALHO, A., GIOVANNINI, G., DE LUCA, A., D'ANGELO, C., CASAGRANDE, A., IANNITTI, R. G., RICCI, G., CUNHA, C. & ROMANI, L. 2012. Dectin-1 isoforms contribute to distinct Th1/Th17 cell activation in mucosal candidiasis. *Cellular & Molecular Immunology,* 9**,** 276-286.

CASTANHEIRA, F. V. S. & KUBES, P. 2019. Neutrophils and NETs in modulating acute and chronic inflammation. *Blood,* 133**,** 2178-2185.

CASTILLO‐ACOSTA, V. M., VIDAL, A. E., RUIZ‐PÉREZ, L. M., VAN DAMME, E. J., IGARASHI, Y., BALZARINI, J. & GONZÁLEZ‐PACANOWSKA, D. 2013. Carbohydrate‐binding agents act as potent trypanocidals that elicit modifications in VSG glycosylation and reduced virulence in T rypanosoma brucei. *Molecular Microbiology,* 90**,** 665-679.

CERI, H., OLSON, M. E., STREMICK, C., READ, R. R., MORCK, D. & BURET, A. 1999. The Calgary Biofilm Device: new technology for rapid determination of antibiotic susceptibilities of bacterial biofilms. *J Clin Microbiol,* 37**,** 1771-6.

CHAO, Y. & ZHANG, T. 2011. Optimization of fixation methods for observation of bacterial cell morphology and surface ultrastructures by atomic force microscopy. *Applied Microbiology and Biotechnology,* 92**,** 381-392.

CHAPUIS, F., ROSENZWAJG, M., YAGELLO, M., EKMAN, M., BIBERFELD, P. & GLUCKMAN, J. C. 1997. Differentiation of human dendritic cells from monocytes in vitro. *European Journal of Immunology,* 27**,** 431-441.

CHAVANT, P., GAILLARD-MARTINIE, B., TALON, R., HÉBRAUD, M. & BERNARDI, T. 2007. A new device for rapid evaluation of biofilm formation potential by bacteria. *Journal of Microbiological Methods,* 68**,** 605-612.

CHEMANI, C., IMBERTY, A., DE BENTZMANN, S., PIERRE, M., WIMMEROVÁ, M., GUERY, B. P. & FAURE, K. 2009. Role of LecA and LecB lectins in Pseudomonas aeruginosa-induced lung injury and effect of carbohydrate ligands. *Infection and Immunity,* 77**,** 2065-2075.

CHEN, G., SHAW, M. H., KIM, Y.-G. & NUÑEZ, G. 2009. NOD-like receptors: role in innate immunity and inflammatory disease. *Annual Review of Pathological Mechanical Disease,* 4**,** 365-398.

CHEN, L., ZOU, Y., KRONFL, A. A. & WU, Y. 2020. Type VI secretion system of Pseudomonas aeruginosa is associated with biofilm formation but not environmental adaptation. *Microbiology Open,* 9**,** e991.

CHEUNG, D. O., HALSEY, K. & SPEERT, D. P. 2000. Role of pulmonary alveolar macrophages in defense of the lung against Pseudomonas aeruginosa. *Infect Immun,* 68**,** 4585-92.

CHEW, S. C., KUNDUKAD, B., SEVIOUR, T., VAN DER MAAREL, J. R., YANG, L., RICE, S. A., DOYLE, P. & KJELLEBERG, S. 2014. Dynamic remodeling of microbial biofilms by functionally distinct exopolysaccharides. *MBio,* 5.

CHOI, H. W., BROOKING-DIXON, R., NEUPANE, S., LEE, C.-J., MIAO, E. A., STAATS, H. F. & ABRAHAM, S. N. 2013. Salmonella typhimurium impedes innate immunity with a mast-cell-suppressing protein tyrosine phosphatase, SptP. *Immunity,* 39**,** 1108-1120.

CHRISTENSEN, G. D., SIMPSON, W. A., YOUNGER, J., BADDOUR, L., BARRETT, F., MELTON, D. & BEACHEY, E. 1985. Adherence of coagulase-negative staphylococci to plastic tissue culture plates: a quantitative model for the adherence of staphylococci to medical devices. *Journal of Clinical Microbiology,* 22**,** 996-1006.

CHUA, S. L., SIVAKUMAR, K., RYBTKE, M., YUAN, M., ANDERSEN, J. B., NIELSEN, T. E., GIVSKOV, M., TOLKER-NIELSEN, T., CAO, B., KJELLEBERG, S. & YANG, L. 2015. C-di-GMP regulates Pseudomonas aeruginosa stress response to tellurite during both planktonic and biofilm modes of growth. *Scientific Reports,* 5**,** 10052.

CIANFANELLI, F. R., MONLEZUN, L. & COULTHURST, S. J. 2016. Aim, load, fire: the type VI secretion system, a bacterial nanoweapon. *Trends in microbiology,* 24**,** 51-62.

CIGANA, C., CURCURÙ, L., LEONE, M. R., IERANÒ, T., LORÈ, N. I., BIANCONI, I., SILIPO, A., COZZOLINO, F., LANZETTA, R. & MOLINARO, A. 2009. Pseudomonas aeruginosa exploits lipid A and muropeptides modification as a strategy to lower innate immunity during cystic fibrosis lung infection. *PLoS One,* 4**,** e8439.

CIORNEI, C. D., NOVIKOV, A., BELOIN, C., FITTING, C., CAROFF, M., GHIGO, J.-M., CAVAILLON, J.-M. & ADIB-CONQUY, M. 2010. Biofilm-forming Pseudomonas aeruginosa bacteria undergo lipopolysaccharide structural modifications and induce enhanced inflammatory cytokine response in human monocytes. *Innate Immunity,* 16**,** 288-301.

CISNEROS, J. M., ROSSO-FERNÁNDEZ, C. M., ROCA-OPORTO, C., DE PASCALE, G., JIMÉNEZ-JORGE, S., FERNÁNDEZ-HINOJOSA, E., MATTHAIOU, D. K., RAMÍREZ, P., DÍAZ-MIGUEL, R. O., ESTELLA, A., ANTONELLI, M., DIMOPOULOS, G., GARNACHO-MONTERO, J. & MAGIC BULLET WORKING GROUP, W. 2019. Colistin versus meropenem in the empirical treatment of ventilator-associated pneumonia (Magic Bullet study): an investigator-driven, open-label, randomized, noninferiority controlled trial. *Critical Care,* 23**,** 383.

COAD, B. R., GRIESSER, H. J., PELEG, A. Y. & TRAVEN, A. 2016. Anti-infective surface coatings: design and therapeutic promise against device-associated infections. *PLoS Pathogens,* 12**,** e1005598.

COBURN, B., SEKIROV, I. & FINLAY, B. B. 2007. Type III secretion systems and disease. *Clinical Microbiology Reviews,* 20**,** 535-549.

COGEN, A., NIZET, V. & GALLO, R. 2008. Skin microbiota: a source of disease or defence? *British Journal of Dermatology,* 158**,** 442-455.

COHEN, T. S. & PRINCE, A. 2012. Cystic fibrosis: a mucosal immunodeficiency syndrome. *Nature Medicine,* 18**,** 509-519.

COLVIN, K. M., GORDON, V. D., MURAKAMI, K., BORLEE, B. R., WOZNIAK, D. J., WONG, G. C. & PARSEK, M. R. 2011. The pel polysaccharide can serve a structural and protective role in the biofilm matrix of Pseudomonas aeruginosa. *PLoS Pathog,* 7**,** e1001264.

COLVIN, K. M., IRIE, Y., TART, C. S., URBANO, R., WHITNEY, J. C., RYDER, C., HOWELL, P. L., WOZNIAK, D. J. & PARSEK, M. R. 2012. The Pel and Psl polysaccharides provide Pseudomonas aeruginosa structural redundancy within the biofilm matrix. *Environmental Microbiology,* 14**,** 1913-1928.

COSTERTON, J. W., CHENG, K., GEESEY, G. G., LADD, T. I., NICKEL, J. C., DASGUPTA, M. & MARRIE, T. J. 1987. Bacterial biofilms in nature and disease. *Annual Reviews in Microbiology,* 41**,** 435-464.

COSTERTON, J. W., STEWART, P. S. & GREENBERG, E. P. 1999. Bacterial biofilms: a common cause of persistent infections. *Science,* 284**,** 1318-1322.

COTT, C., THUENAUER, R., LANDI, A., KÜHN, K., JUILLOT, S., IMBERTY, A., MADL, J., EIERHOFF, T. & RÖMER, W. 2016. Pseudomonas aeruginosa lectin LecB inhibits tissue repair processes by triggering β-catenin degradation. *Biochimica et Biophysica Acta (BBA)-Molecular Cell Research,* 1863**,** 1106-1118.

COWELL, B. A., CHEN, D. Y., FRANK, D. W., VALLIS, A. J. & FLEISZIG, S. M. 2000. ExoT of Cytotoxic Pseudomonas aeruginosaPrevents Uptake by Corneal Epithelial Cells. *Infection and Immunity,* 68**,** 403-406.

COWLAND, J. B. & BORREGAARD, N. 2016. Granulopoiesis and granules of human neutrophils. *Immunological reviews,* 273**,** 11-28.

CRONE, S., VIVES‐FLÓREZ, M., KVICH, L., SAUNDERS, A. M., MALONE, M., NICOLAISEN, M. H., MARTÍNEZ‐GARCÍA, E., ROJAS‐ACOSTA, C., CATALINA GOMEZ‐PUERTO, M. & CALUM, H. 2020. The environmental occurrence of Pseudomonas aeruginosa. *Apmis,* 128**,** 220-231.

CRUSZ, S. A., POPAT, R., RYBTKE, M. T., CAMARA, M., GIVSKOV, M., TOLKER-NIELSEN, T., DIGGLE, S. P. & WILLIAMS, P. 2012. Bursting the bubble on bacterial biofilms: a flow cell methodology. *Biofouling,* 28**,** 835-42.

CULLEN, L. & MCCLEAN, S. 2015. Bacterial Adaptation during Chronic Respiratory Infections. *Pathogens,* 4**,** 66-89.

DA GLÓRIA SOUSA, M., REID, D. M., SCHWEIGHOFFER, E., TYBULEWICZ, V., RULAND, J., LANGHORNE, J., YAMASAKI, S., TAYLOR, P. R., ALMEIDA, S. R. & BROWN, G. D. 2011. Restoration of pattern recognition receptor costimulation to treat chromoblastomycosis, a chronic fungal infection of the skin. *Cell host & microbe,* 9**,** 436-443.

DA SILVA, D. P., MATWICHUK, M. L., TOWNSEND, D. O., REICHHARDT, C., LAMBA, D., WOZNIAK, D. J. & PARSEK, M. R. 2019. The Pseudomonas aeruginosa lectin LecB binds to the exopolysaccharide Psl and stabilizes the biofilm matrix. *Nature Communications,* 10**,** 1-11.

DALOD, M., CHELBI, R., MALISSEN, B. & LAWRENCE, T. 2014. Dendritic cell maturation: functional specialization through signaling specificity and transcriptional programming. *The EMBO journal,* 33**,** 1104-1116.

DALTON, T., DOWD, S. E., WOLCOTT, R. D., SUN, Y., WATTERS, C., GRISWOLD, J. A. & RUMBAUGH, K. P. 2011. An in vivo polymicrobial biofilm wound infection model to study interspecies interactions. *PloS One,* 6**,** e27317.

DAMLUND, D. S. M., CHRISTOPHERSEN, L., JENSEN, P. Ø., ALHEDE, M., HØIBY, N. & MOSER, C. 2016. Activation of pulmonary and lymph node dendritic cells during chronic Pseudomonas aeruginosa lung infection in mice. *Apmis,* 124**,** 500-507.

DAPSON, R. W. 2007. Macromolecular changes caused by formalin fixation and antigen retrieval. *Biotech Histochem,* 82**,** 133-40.

DASGUPTA, S., REPESSÉ, Y., BAYRY, J., NAVARRETE, A.-M., WOOTLA, B., DELIGNAT, S., IRINOPOULOU, T., KAMATÉ, C., SAINT-REMY, J.-M. & JACQUEMIN, M. 2007. VWF protects FVIII from endocytosis by dendritic cells and subsequent presentation to immune effectors. *Blood,* 109**,** 610-612.

DAUER, M., OBERMAIER, B., HERTEN, J., HAERLE, C., POHL, K., ROTHENFUSSER, S., SCHNURR, M., ENDRES, S. & EIGLER, A. 2003. Mature dendritic cells derived from human monocytes within 48 hours: a novel strategy for dendritic cell differentiation from blood precursors. *The Journal of Immunology,* 170**,** 4069-4076.

DAVIES, D. G., PARSEK, M. R., PEARSON, J. P., IGLEWSKI, B. H., COSTERTON, J. W. & GREENBERG, E. P. 1998. The involvement of cell-to-cell signals in the development of a bacterial biofilm. *Science,* 280**,** 295-298.

DE BUHR, N. & VON KÖCKRITZ-BLICKWEDE, M. 2016. How neutrophil extracellular traps become visible. *Journal of Immunology Research,* 2016.

DE OLIVEIRA, S., ROSOWSKI, E. E. & HUTTENLOCHER, A. 2016. Neutrophil migration in infection and wound repair: going forward in reverse. *Nature reviews. Immunology,* 16**,** 378-391.

DELEO, F. R., RENEE, J., MCCORMICK, S., NAKAMURA, M., APICELLA, M., WEISS, J. P. & NAUSEEF, W. M. 1998. Neutrophils exposed to bacterial lipopolysaccharide upregulate NADPH oxidase assembly. *The Journal of Clinical Investigation,* 101**,** 455-463.

DELIGIANNI, E., PATTISON, S., BERRAR, D., TERNAN, N. G., HAYLOCK, R. W., MOORE, J. E., ELBORN, S. J. & DOOLEY, J. S. 2010. Pseudomonas aeruginosa cystic fibrosis isolates of similar RAPD genotype exhibit diversity in biofilm forming ability in vitro. *BMC microbiology,* 10**,** 38.

DENG, B., GHATAK, S., SARKAR, S., SINGH, K., GHATAK, P. D., MATHEW-STEINER, S. S., ROY, S., KHANNA, S., WOZNIAK, D. J. & MCCOMB, D. W. 2020. Novel Bacterial Diversity and Fragmented eDNA Identified in Hyperbiofilm-Forming Pseudomonas aeruginosa Rugose Small Colony Variant. *Iscience,* 23**,** 100827.

DENG, Z., MA, S., ZHOU, H., ZANG, A., FANG, Y., LI, T., SHI, H., LIU, M., DU, M., TAYLOR, P. R., ZHU, H. H., CHEN, J., MENG, G., LI, F., CHEN, C., ZHANG, Y., JIA, X.-M., LIN, X., ZHANG, X., PEARLMAN, E., LI, X., FENG, G.-S. & XIAO, H. 2015. Tyrosine phosphatase SHP-2 mediates C-type lectin receptor-induced activation of the kinase Syk and anti-fungal TH17 responses. *Nature Immunology,* 16**,** 642-652.

DERIY, L. V., GOMEZ, E. A., ZHANG, G., BEACHAM, D. W., HOPSON, J. A., GALLAN, A. J., SHEVCHENKO, P. D., BINDOKAS, V. P. & NELSON, D. J. 2009. Disease-causing mutations in the cystic fibrosis transmembrane conductance regulator determine the functional responses of alveolar macrophages. *J Biol Chem,* 284**,** 35926-38.

DHAMGAYE, S., QU, Y. & PELEG, A. Y. 2016. Polymicrobial infections involving clinically relevant Gram‐negative bacteria and fungi. *Cellular Microbiology,* 18**,** 1716-1722.

DI, A., BROWN, M. E., DERIY, L. V., LI, C., SZETO, F. L., CHEN, Y., HUANG, P., TONG, J., NAREN, A. P., BINDOKAS, V., PALFREY, H. C. & NELSON, D. J. 2006. CFTR regulates phagosome acidification in macrophages and alters bactericidal activity. *Nat Cell Biol,* 8**,** 933-44.

DI MARTINO, J., HENRIET, E., EZZOUKHRY, Z., GOETZ, J. G., MOREAU, V. & SALTEL, F. 2016. The microenvironment controls invadosome plasticity. *J Cell Sci,* 129**,** 1759-68.

DIACONU, O., SIRIOPOL, I., POLOȘANU, L. I. & GRIGORAȘ, I. 2018. Endotracheal Tube Biofilm and its Impact on the Pathogenesis of Ventilator-Associated

Pneumonia. *Journal of critical care medicine (Universitatea de Medicina si Farmacie din Targu-Mures),* 4**,** 50-55.
DIGGLE, S. P., STACEY, R. E., DODD, C., CÁMARA, M., WILLIAMS, P. & WINZER, K. 2006. The galactophilic lectin, LecA, contributes to biofilm development in Pseudomonas aeruginosa. *Environmental Microbiology,* 8**,** 1095-1104.
DIGIANDOMENICO, A., KELLER, A. E., GAO, C., RAINEY, G. J., WARRENER, P., CAMARA, M. M., BONNELL, J., FLEMING, R., BEZABEH, B., DIMASI, N., SELLMAN, B. R., HILLIARD, J., GUENTHER, C. M., DATTA, V., ZHAO, W., GAO, C., YU, X.-Q., SUZICH, J. A. & STOVER, C. K. 2014. A multifunctional bispecific antibody protects against Pseudomonas aeruginosa. *Science Translational Medicine,* 6**,** 262ra155-262ra155.
DIGIANDOMENICO, A., WARRENER, P., HAMILTON, M., GUILLARD, S., RAVN, P., MINTER, R., CAMARA, M. M., VENKATRAMAN, V., MACGILL, R. S., LIN, J., WANG, Q., KELLER, A. E., BONNELL, J. C., TOMICH, M., JERMUTUS, L., MCCARTHY, M. P., MELNICK, D. A., SUZICH, J. A. & STOVER, C. K. 2012. Identification of broadly protective human antibodies to Pseudomonas aeruginosa exopolysaccharide Psl by phenotypic screening. *Journal of Experimental Medicine,* 209**,** 1273-1287.
DIMANGO, E., ZAR, H. J., BRYAN, R. & PRINCE, A. 1995. Diverse Pseudomonas aeruginosa gene products stimulate respiratory epithelial cells to produce interleukin-8. *The Journal of Clinical Investigation,* 96**,** 2204-2210.
DINGEMANS, J., MONSIEURS, P., YU, S.-H., CRABBÉ, A., FÖRSTNER, K. U., MALFROOT, A., CORNELIS, P. & VAN HOUDT, R. 2016. Effect of shear stress on Pseudomonas aeruginosa isolated from the cystic fibrosis lung. *MBio,* 7.
DODGE, I. L., CARR, M. W., CERNADAS, M. & BRENNER, M. B. 2003. IL-6 production by pulmonary dendritic cells impedes Th1 immune responses. *The Journal of Immunology,* 170**,** 4457-4464.
DOEING, D. C., BOROWICZ, J. L. & CROCKETT, E. T. 2003. Gender dimorphism in differential peripheral blood leukocyte counts in mice using cardiac, tail, foot, and saphenous vein puncture methods. *BMC Clin Pathol,* 3**,** 3.
DOIG, P., TODD, T., SASTRY, P. A., LEE, K., HODGES, R. S., PARANCHYCH, W. & IRVIN, R. 1988. Role of pili in adhesion of Pseudomonas aeruginosa to human respiratory epithelial cells. *Infection and Immunity,* 56**,** 1641-1646.
DOMÍNGUEZ-SOTO, A., SIERRA-FILARDI, E., PUIG-KRÖGER, A., PÉREZ-MACEDA, B., GÓMEZ-AGUADO, F., CORCUERA, M. T., SÁNCHEZ-MATEOS, P. & CORBÍ, A. L. 2011. Dendritic Cell-Specific ICAM-3–Grabbing Nonintegrin Expression on M2-Polarized and Tumor-Associated Macrophages Is Macrophage-CSF Dependent and Enhanced by Tumor-Derived IL-6 and IL-10. *The Journal of Immunology,* 186**,** 2192-2200.
DONLAN, R. M. 2002. Biofilms: microbial life on surfaces. *Emerg Infect Dis,* 8**,** 881-90.
DONLAN, R. M. & COSTERTON, J. W. 2002. Biofilms: survival mechanisms of clinically relevant microorganisms. *Clinical Microbiology Reviews,* 15**,** 167-193.
DORHOI, A., DESEL, C., YEREMEEV, V., PRADL, L., BRINKMANN, V., MOLLENKOPF, H.-J., HANKE, K., GROSS, O., RULAND, J. & KAUFMANN, S. H. E. 2010. The adaptor molecule CARD9 is essential for tuberculosis control. *Journal of Experimental Medicine,* 207**,** 777-792.
DOSTERT, C. & TSCHOPP, J. 2007. Detecting fungal pathogens. *Nature Immunology,* 8**,** 17-18.

DOWD, S. E., SUN, Y., SECOR, P. R., RHOADS, D. D., WOLCOTT, B. M., JAMES, G. A. & WOLCOTT, R. D. 2008. Survey of bacterial diversity in chronic wounds using pyrosequencing, DGGE, and full ribosome shotgun sequencing. *BMC Microbiology,* 8**,** 43.

DRISCOLL, J. A., BRODY, S. L. & KOLLEF, M. H. 2007. The epidemiology, pathogenesis and treatment of Pseudomonas aeruginosa infections. *Drugs,* 67**,** 351-68.

DUEHOLM, M. S., SØNDERGAARD, M. T., NILSSON, M., CHRISTIANSEN, G., STENSBALLE, A., OVERGAARD, M. T., GIVSKOV, M., TOLKER‐NIELSEN, T., OTZEN, D. E. & NIELSEN, P. H. 2013. Expression of Fap amyloids in P seudomonas aeruginosa, P. fluorescens, and P. putida results in aggregation and increased biofilm formation. *Microbiologyopen,* 2**,** 365-382.

DURAND, M. & SEGURA, E. 2015. The known unknowns of the human dendritic cell network. *Frontiers in Immunology,* 6**,** 129.

DWYER, M., SHAN, Q., D'ORTONA, S., MAURER, R., MITCHELL, R., OLESEN, H., THIEL, S., HUEBNER, J. & GADJEVA, M. 2014. Cystic fibrosis sputum DNA has NETosis characteristics and neutrophil extracellular trap release is regulated by macrophage migration-inhibitory factor. *Journal of Innate Immunity,* 6**,** 765-779.

EADES-PERNER, A.-M., THOMPSON, J., VAN DER PUTTEN, H. & ZIMMERMANN, W. 1998. Mice transgenic for the human CGM6 gene express its product, the granulocyte marker CD66b, exclusively in granulocytes. *Blood, The Journal of the American Society of Hematology,* 91**,** 663-672.

EARLE, K., TANG, Q., ZHOU, X., LIU, W., ZHU, S., BONYHADI, M. & BLUESTONE, J. 2005. In vitro expanded human CD4+ CD25+ regulatory T cells suppress effector T cell proliferation. *Clinical Immunology,* 115**,** 3-9.

EDMONDS, J. M., COLLETT, P. J., VALDES, E. R., SKOWRONSKI, E. W., PELLAR, G. J. & EMANUEL, P. A. 2009. Surface sampling of spores in dry-deposition aerosols. *Appl Environ Microbiol,* 75**,** 39-44.

EDWARDSON, S. & CAIRNS, C. 2019. Nosocomial infections in the ICU. *Anaesthesia & Intensive Care Medicine,* 20**,** 14-18.

EHLERS, S. 2010. DC-SIGN and mannosylated surface structures of Mycobacterium tuberculosis: a deceptive liaison. *European Journal of Cell Biology,* 89**,** 95-101.

ENDESFELDER, U. & HEILEMANN, M. 2014. Art and artifacts in single-molecule localization microscopy: beyond attractive images. *Nat Methods,* 11**,** 235-8.

ENGERING, A., GEIJTENBEEK, T. B., VAN VLIET, S. J., WIJERS, M., VAN LIEMPT, E., DEMAUREX, N., LANZAVECCHIA, A., FRANSEN, J., FIGDOR, C. G. & PIGUET, V. 2002. The dendritic cell-specific adhesion receptor DC-SIGN internalizes antigen for presentation to T cells. *The Journal of Immunology,* 168**,** 2118-2126.

EPELMAN, S., BRUNO, T. F., NEELY, G. G., WOODS, D. E. & MODY, C. H. 2000. Pseudomonas aeruginosa exoenzyme S induces transcriptional expression of proinflammatory cytokines and chemokines. *Infect Immun,* 68**,** 4811-4.

ERNST, R. K., ADAMS, K. N., MOSKOWITZ, S. M., KRAIG, G. M., KAWASAKI, K., STEAD, C. M., TRENT, M. S. & MILLER, S. I. 2006. The Pseudomonas aeruginosa lipid A deacylase: selection for expression and loss within the cystic fibrosis airway. *Journal of Bacteriology,* 188**,** 191-201.

ERNST, R. K., EUGENE, C. Y., GUO, L., LIM, K. B., BURNS, J. L., HACKETT, M. & MILLER, S. I. 1999. Specific lipopolysaccharide found in cystic fibrosis airway Pseudomonas aeruginosa. *Science,* 286**,** 1561-1565.

ERNST, R. K., HAJJAR, A. M., TSAI, J. H., MOSKOWITZ, S. M., WILSON, C. B. & MILLER, S. I. 2003. Pseudomonas aeruginosa lipid A diversity and its recognition by Toll-like receptor 4. *Journal of Endotoxin Research,* 9**,** 395-400.

ESTENSEN, R. D., REUSCH, M. E., EPSTEIN, M. L. & HILL, H. R. 1976. Role of Ca2+ and Mg2+ in some human neutrophil functions as indicated by ionophore A23187. *Infection and Immunity,* 13**,** 146-151.

FAURE, E., MEAR, J. B., FAURE, K., NORMAND, S., COUTURIER-MAILLARD, A., GRANDJEAN, T., BALLOY, V., RYFFEL, B., DESSEIN, R., CHIGNARD, M., UYTTENHOVE, C., GUERY, B., GOSSET, P., CHAMAILLARD, M. & KIPNIS, E. 2014. Pseudomonas aeruginosa type-3 secretion system dampens host defense by exploiting the NLRC4-coupled inflammasome. *Am J Respir Crit Care Med,* 189**,** 799-811.

FEINBERG, H., JEGOUZO, S. A. F., REX, M. J., DRICKAMER, K., WEIS, W. I. & TAYLOR, M. E. 2017. Mechanism of pathogen recognition by human dectin-2. *J Biol Chem,* 292**,** 13402-13414.

FELTMAN, H., SCHULERT, G., KHAN, S., JAIN, M., PETERSON, L. & HAUSER, A. R. 2001. Prevalence of type III secretion genes in clinical and environmental isolates of Pseudomonas aeruginosa. *Microbiology,* 147**,** 2659-2669.

FERNANDES, M. J., FINNEGAN, A. A., SIRACUSA, L. D., BRENNER, C., ISCOVE, N. N. & CALABRETTA, B. 1999. Characterization of a novel receptor that maps near the natural killer gene complex: demonstration of carbohydrate binding and expression in hematopoietic cells. *Cancer Res,* 59**,** 2709-17.

FERRETTI, S., BONNEAU, O., DUBOIS, G. R., JONES, C. E. & TRIFILIEFF, A. 2003. IL-17, produced by lymphocytes and neutrophils, is necessary for lipopolysaccharide-induced airway neutrophilia: IL-15 as a possible trigger. *The Journal of Immunology,* 170**,** 2106-2112.

FERWERDA, B., FERWERDA, G., PLANTINGA, T. S., WILLMENT, J. A., VAN SPRIEL, A. B., VENSELAAR, H., ELBERS, C. C., JOHNSON, M. D., CAMBI, A. & HUYSAMEN, C. 2009. Human dectin-1 deficiency and mucocutaneous fungal infections. *New England Journal of Medicine,* 361**,** 1760-1767.

FEUILLET, V., MEDJANE, S., MONDOR, I., DEMARIA, O., PAGNI, P. P., GALÁN, J. E., FLAVELL, R. A. & ALEXOPOULOU, L. 2006. Involvement of Toll-like receptor 5 in the recognition of flagellated bacteria. *Proceedings of the National Academy of Sciences,* 103**,** 12487-12492.

FILLOUX, A. 2011. Protein secretion systems in Pseudomonas aeruginosa: an essay on diversity, evolution, and function. *Frontiers in Microbiology,* 2**,** 155.

FINKEL, S. E. & KOLTER, R. 2001. DNA as a nutrient: novel role for bacterial competence gene homologs. *Journal of Bacteriology,* 183**,** 6288-6293.

FISCHER, M., MÜLLER, J. P., SPIES‐WEISSHART, B., GRÄFE, C., KURZAI, O., HÜNNIGER, K., HOCHHAUS, A., SCHOLL, S. & SCHNETZKE, U. 2017. Isoform localization of Dectin‐1 regulates the signaling quality of anti‐fungal immunity. *European Journal of Immunology,* 47**,** 848-859.

FITZGERALD, K. A. & KAGAN, J. C. 2020. Toll-like Receptors and the Control of Immunity. *Cell,* 180**,** 1044-1066.

FLEMMING, H.-C. & WINGENDER, J. 2010. The biofilm matrix. *Nature Reviews Microbiology,* 8**,** 623-633.

FLEMMING, H.-C., WINGENDER, J., SZEWZYK, U., STEINBERG, P., RICE, S. A. & KJELLEBERG, S. 2016. Biofilms: an emergent form of bacterial life. *Nat Rev Micro,* 14**,** 563-575.

FLEMMING, H. C. & WUERTZ, S. 2019. Bacteria and archaea on Earth and their abundance in biofilms. *Nat Rev Microbiol,* 17**,** 247-260.
FLO, T. H., RYAN, L., LATZ, E., TAKEUCHI, O., MONKS, B. G., LIEN, E., HALAAS, O., AKIRA, S., SKJAK-BRAEK, G., GOLENBOCK, D. T. & ESPEVIK, T. 2002. Involvement of toll-like receptor (TLR) 2 and TLR4 in cell activation by mannuronic acid polymers. *J Biol Chem,* 277**,** 35489-95.
FLORNES, L. M., BRYCESON, Y. T., SPURKLAND, A., LORENTZEN, J. C., DISSEN, E. & FOSSUM, S. 2004. Identification of lectin-like receptors expressed by antigen presenting cells and neutrophils and their mapping to a novel gene complex. *Immunogenetics,* 56**,** 506-517.
FONG, J. N. & YILDIZ, F. H. 2015. Biofilm matrix proteins. *Microbial Biofilms***,** 201-222.
FOULKES, D. M., MCLEAN, K., HANEEF, A. S., FERNIG, D. G., WINSTANLEY, C., BERRY, N. & KAYE, S. B. 2019. Pseudomonas aeruginosa Toxin ExoU as a Therapeutic Target in the Treatment of Bacterial Infections. *Microorganisms,* 7**,** 707.
FOXALL, E., PIPILI, A., JONES, G. E. & WELLS, C. M. 2016. Significance of kinase activity in the dynamic invadosome. *Eur J Cell Biol,* 95**,** 483-492.
FRANCIS, V. I., STEVENSON, E. C. & PORTER, S. L. 2017. Two-component systems required for virulence in Pseudomonas aeruginosa. *FEMS Microbiology Letters,* 364**,** fnx104.
FRANK, K. L., GUITON, P. S., BARNES, A. M., MANIAS, D. A., CHUANG-SMITH, O. N., KOHLER, P. L., SPAULDING, A. R., HULTGREN, S. J., SCHLIEVERT, P. M. & DUNNY, G. M. 2013. AhrC and Eep are biofilm infection-associated virulence factors in Enterococcus faecalis. *Infection and immunity,* 81**,** 1696-1708.
FRANKLIN, M. J., NIVENS, D. E., WEADGE, J. T. & HOWELL, P. L. 2011. Biosynthesis of the Pseudomonas aeruginosa Extracellular Polysaccharides, Alginate, Pel, and Psl. *Front Microbiol,* 2**,** 167.
FRASER-PITT, D. & O'NEIL, D. 2015. Cystic fibrosis–a multiorgan protein misfolding disease. *Future Science OA,* 1.
FRIEDMAN, L. & KOLTER, R. 2004a. Genes involved in matrix formation in Pseudomonas aeruginosa PA14 biofilms. *Molecular Microbiology,* 51**,** 675-690.
FRIEDMAN, L. & KOLTER, R. 2004b. Two genetic loci produce distinct carbohydrate-rich structural components of the Pseudomonas aeruginosa biofilm matrix. *Journal of Bacteriology,* 186**,** 4457-4465.
FRISON, N., TAYLOR, M. E., SOILLEUX, E., BOUSSER, M.-T., MAYER, R., MONSIGNY, M., DRICKAMER, K. & ROCHE, A.-C. 2003. Oligolysine-based Oligosaccharide Clusters SELECTIVE RECOGNITION AND ENDOCYTOSIS BY THE MANNOSE RECEPTOR AND DENDRITIC CELL-SPECIFIC INTERCELLULAR ADHESION MOLECULE 3 (ICAM-3)-GRABBING NONINTEGRIN. *Journal of Biological Chemistry,* 278**,** 23922-23929.
FRITHZ-LINDSTEN, E., DU, Y., FORSBERG, A. & ROSQUIST, R. 1998. Intracellular Targeting of Exoenzyme S by Pseudomonas aeruginosa. *Zentralblatt Fur Bakteriologie-Supplement***,** 128-129.
FRITZ, J. H., FERRERO, R. L., PHILPOTT, D. J. & GIRARDIN, S. E. 2006. Nod-like proteins in immunity, inflammation and disease. *Nature immunology,* 7**,** 1250-1257.

FUJIKADO, N., SAIJO, S. & IWAKURA, Y. 2006. Identification of arthritis-related gene clusters by microarray analysis of two independent mouse models for rheumatoid arthritis. *Arthritis Research & Therapy,* 8**,** R100-R100.

FUJIMOTO, J., WIENER-KRONISH, J. P., HASHIMOTO, S. & SAWA, T. 2002. Effects of Cl2MDP-encapsulating liposomes in a murine model of Pseudomonas aeruginosa-induced sepsis. *Journal of liposome research,* 12**,** 239-257.

FUJIWARA, K. 1980. Techniques for localizing contractile proteins with fluorescent antibodies. *Curr Top Dev Biol,* 14**,** 271-96.

FUNKEN, H., BARTELS, K.-M., WILHELM, S., BROCKER, M., BOTT, M., BAINS, M., HANCOCK, R. E., ROSENAU, F. & JAEGER, K.-E. 2012. Specific association of lectin LecB with the surface of Pseudomonas aeruginosa: role of outer membrane protein OprF. *PloS One,* 7**,** e46857.

FURUKAWA, S., KUCHMA, S. & O'TOOLE, G. 2006. Keeping their options open: acute versus persistent infections. *Journal of Bacteriology,* 188**,** 1211-1217.

GAL, N., LECHTMAN-GOLDSTEIN, D. & WEIHS, D. 2013. Particle tracking in living cells: a review of the mean square displacement method and beyond. *Rheologica Acta,* 52**,** 425-443.

GALÁN, J. E. & ZHOU, D. 2000. Striking a balance: modulation of the actin cytoskeleton by Salmonella. *Proceedings of the National Academy of Sciences,* 97**,** 8754-8761.

GALIE, S., GARCÍA-GUTIÉRREZ, C., MIGUÉLEZ, E. M., VILLAR, C. J. & LOMBÓ, F. 2018. Biofilms in the food industry: health aspects and control methods. *Frontiers in Microbiology,* 9**,** 898.

GANTER, M. T., ROUX, J., SU, G., LYNCH, S. V., DEUTSCHMAN, C. S., WEISS, Y. G., CHRISTIAANS, S. C., MYAZAWA, B., KIPNIS, E., WIENER-KRONISH, J. P., HOWARD, M. & PITTET, J.-F. 2009. Role of Small GTPases and αvβ5 Integrin in Pseudomonas aeruginosa–Induced Increase in Lung Endothelial Permeability. *American Journal of Respiratory Cell and Molecular Biology,* 40**,** 108-118.

GARAI, P., BERRY, L., MOUSSOUNI, M., BLEVES, S. & BLANC-POTARD, A.-B. 2019. Killing from the inside: Intracellular role of T3SS in the fate of Pseudomonas aeruginosa within macrophages revealed by mgtC and oprF mutants. *PLoS Pathogens,* 15**,** e1007812.

GARCÍA-VALLEJO, J. J., BLOEM, K., KNIPPELS, L. M. J., GARSSEN, J., VAN VLIET, S. J. & VAN KOOYK, Y. 2015. The Consequences of Multiple Simultaneous C-Type Lectin-Ligand Interactions: DCIR Alters the Endo-Lysosomal Routing of DC-SIGN. *Frontiers in Immunology,* 6**,** 87-87.

GARCIA-VALLEJO, J. J. & VAN KOOYK, Y. 2013. The physiological role of DC-SIGN: a tale of mice and men. *Trends Immunol,* 34**,** 482-6.

GARCIA, M., MORELLO, E., GARNIER, J., BARRAULT, C., GARNIER, M., BURUCOA, C., LECRON, J. C., SI-TAHAR, M., BERNARD, F. X. & BODET, C. 2018. Pseudomonas aeruginosa flagellum is critical for invasion, cutaneous persistence and induction of inflammatory response of skin epidermis. *Virulence,* 9**,** 1163-1175.

GARRITY-RYAN, L., KAZMIERCZAK, B., KOWAL, R., COMOLLI, J., HAUSER, A. & ENGEL, J. 2000. The arginine finger domain of ExoT contributes to actin cytoskeleton disruption and inhibition of internalization of Pseudomonas aeruginosa by epithelial cells and macrophages. *Infection and Immunity,* 68**,** 7100-7113.

GAVINO, A. C., CHUNG, J. S., SATO, K., ARIIZUMI, K. & CRUZ, P. D., JR. 2005. Identification and expression profiling of a human C-type lectin, structurally homologous to mouse dectin-2. *Exp Dermatol,* 14**,** 281-8.

GAWDEN-BONE, C., ZHOU, Z., KING, E., PRESCOTT, A., WATTS, C. & LUCOCQ, J. 2010. Dendritic cell podosomes are protrusive and invade the extracellular matrix using metalloproteinase MMP-14. *Journal of Cell Science,* 123**,** 1427-1437.

GAZI, U. & MARTINEZ-POMARES, L. 2009. Influence of the mannose receptor in host immune responses. *Immunobiology,* 214**,** 554-561.

GEDDES-MCALISTER, J., KUGADAS, A. & GADJEVA, M. 2019. Tasked with a challenging objective: why do neutrophils fail to battle pseudomonas aeruginosa biofilms. *Pathogens,* 8**,** 283.

GEGINAT, J., NIZZOLI, G., PARONI, M., MAGLIE, S., LARGHI, P., PASCOLO, S. & ABRIGNANI, S. 2015. Immunity to pathogens taught by specialized human dendritic cell subsets. *Frontiers in Immunology,* 6**,** 527.

GEIJTENBEEK, T. B., KWON, D. S., TORENSMA, R., VAN VLIET, S. J., VAN DUIJNHOVEN, G. C., MIDDEL, J., CORNELISSEN, I. L., NOTTET, H. S., KEWALRAMANI, V. N., LITTMAN, D. R., FIGDOR, C. G. & VAN KOOYK, Y. 2000a. DC-SIGN, a dendritic cell-specific HIV-1-binding protein that enhances trans-infection of T cells. *Cell,* 100**,** 587-97.

GEIJTENBEEK, T. B., TORENSMA, R., VAN VLIET, S. J., VAN DUIJNHOVEN, G. C., ADEMA, G. J., VAN KOOYK, Y. & FIGDOR, C. G. 2000b. Identification of DC-SIGN, a novel dendritic cell–specific ICAM-3 receptor that supports primary immune responses. *Cell,* 100**,** 575-585.

GEIJTENBEEK, T. B. H. & GRINGHUIS, S. I. 2009. Signalling through C-type lectin receptors: shaping immune responses. *Nature Reviews Immunology,* 9**,** 465-479.

GEIJTENBEEK , T. B. H., VAN VLIET , S. J., KOPPEL , E. A., SANCHEZ-HERNANDEZ , M., VANDENBROUCKE-GRAULS , C. M. J. E., APPELMELK , B. & VAN KOOYK , Y. 2002. Mycobacteria Target DC-SIGN to Suppress Dendritic Cell Function. *Journal of Experimental Medicine,* 197**,** 7-17.

GELLATLY, S. L. & HANCOCK, R. E. 2013. Pseudomonas aeruginosa: new insights into pathogenesis and host defenses. *Pathogens and disease,* 67**,** 159-173.

GENEVAUX, P., MULLER, S. & BAUDA, P. 1996. A rapid screening procedure to identify mini-Tn10 insertion mutants of Escherichia coli K-12 with altered adhesion properties. *FEMS Microbiology Letters,* 142**,** 27-30.

GILL, C. & TAN, K. 1979. Effect of carbon dioxide on growth of Pseudomonas fluorescens. *Applied and Environmental Microbiology,* 38**,** 237-240.

GLICK, J. & GARBER, N. 1983. The intracellular localization of Pseudomonas aeruginosa lectins. *Microbiology,* 129**,** 3085-3090.

GLOAG, E. S., GERMAN, G. K., STOODLEY, P. & WOZNIAK, D. J. 2018. Viscoelastic properties of Pseudomonas aeruginosa variant biofilms. *Scientific Reports,* 8**,** 1-11.

GLOAG, E. S., TURNBULL, L., HUANG, A., VALLOTTON, P., WANG, H., NOLAN, L. M., MILILLI, L., HUNT, C., LU, J. & OSVATH, S. R. 2013. Self-organization of bacterial biofilms is facilitated by extracellular DNA. *Proceedings of the National Academy of Sciences,* 110**,** 11541-11546.

GLUCKSAM-GALNOY, Y., SANANES, R., SILBERSTEIN, N., KRIEF, P., KRAVCHENKO, V. V., MEIJLER, M. M. & ZOR, T. 2013. The bacterial quorum-sensing signal molecule N-3-oxo-dodecanoyl-L-homoserine lactone

reciprocally modulates pro- and anti-inflammatory cytokines in activated macrophages. *Journal of immunology (Baltimore, Md. : 1950),* 191**,** 337-344.
GOLTERMANN, L. & TOLKER-NIELSEN, T. 2017. Importance of the exopolysaccharide matrix in antimicrobial tolerance of Pseudomonas aeruginosa aggregates. *Antimicrobial Agents and Chemotherapy,* 61.
GOMES, L. C., MOREIRA, J. M., SIMOES, M., MELO, L. F. & MERGULHAO, F. J. 2014. Biofilm localization in the vertical wall of shaking 96-well plates. *Scientifica (Cairo),* 2014**,** 231083.
GOMEZ-LOPEZ, N., ROMERO, R., XU, Y., MILLER, D., UNKEL, R., SHAMAN, M., JACQUES, S. M., PANAITESCU, B., GARCIA-FLORES, V. & HASSAN, S. S. 2017. Neutrophil extracellular traps in the amniotic cavity of women with intra-amniotic infection: a new mechanism of host defense. *Reproductive Sciences,* 24**,** 1139-1153.
GOODMAN, A. L., KULASEKARA, B., RIETSCH, A., BOYD, D., SMITH, R. S. & LORY, S. 2004. A signaling network reciprocally regulates genes associated with acute infection and chronic persistence in Pseudomonas aeruginosa. *Developmental Cell,* 7**,** 745-754.
GOODRIDGE, H. S., REYES, C. N., BECKER, C. A., KATSUMOTO, T. R., MA, J., WOLF, A. J., BOSE, N., CHAN, A. S., MAGEE, A. S. & DANIELSON, M. E. 2011. Activation of the innate immune receptor Dectin-1 upon formation of a 'phagocytic synapse'. *Nature,* 472**,** 471-475.
GOODRIDGE, H. S., SIMMONS, R. M. & UNDERHILL, D. M. 2007. Dectin-1 stimulation by Candida albicans yeast or zymosan triggers NFAT activation in macrophages and dendritic cells. *The Journal of Immunology,* 178**,** 3107-3115.
GORDON, S. & MARTINEZ-POMARES, L. 2017. Physiological roles of macrophages. *Pflügers Archiv-European Journal of Physiology,* 469**,** 365-374.
GORDON, S. & MARTINEZ, F. O. 2010. Alternative activation of macrophages: mechanism and functions. *Immunity,* 32**,** 593-604.
GORELIK, R. & GAUTREAU, A. 2014. Quantitative and unbiased analysis of directional persistence in cell migration. *Nature Protocols,* 9**,** 1931.
GORVEL, J.-P. 2004. *Intracellular Pathogens in Membrane Interactions and Vacuole Biogenesis*, Springer Science & Business Media.
GOVAN, J. R. & DERETIC, V. 1996. Microbial pathogenesis in cystic fibrosis: mucoid Pseudomonas aeruginosa and Burkholderia cepacia. *Microbiological Reviews,* 60**,** 539-574.
GRAINGER, J. R., WOHLFERT, E. A., FUSS, I. J., BOULADOUX, N., ASKENASE, M. H., LEGRAND, F., KOO, L. Y., BRENCHLEY, J. M., FRASER, I. D. & BELKAID, Y. 2013. Inflammatory monocytes regulate pathologic responses to commensals during acute gastrointestinal infection. *Nature Medicine,* 19**,** 713.
GRAND, I., BELLON-FONTAINE, M. N., HERRY, J. M., HILAIRE, D., MORICONI, F. X. & NAÏTALI, M. 2011. Possible overestimation of surface disinfection efficiency by assessment methods based on liquid sampling procedures as demonstrated by in situ quantification of spore viability. *Applied and Environmental Microbiology,* 77**,** 6208-6214.
GRAUS, M. S., WESTER, M. J., LOWMAN, D. W., WILLIAMS, D. L., KRUPPA, M. D., MARTINEZ, C. M., YOUNG, J. M., PAPPAS, H. C., LIDKE, K. A. & NEUMANN, A. K. 2018. Mannan Molecular Substructures Control Nanoscale Glucan Exposure in Candida. *Cell Rep,* 24**,** 2432-2442.e5.
GRINGHUIS, S. I., DEN DUNNEN, J., LITJENS, M., VAN DER VLIST, M. & GEIJTENBEEK, T. B. 2009. Carbohydrate-specific signaling through the DC-

SIGN signalosome tailors immunity to Mycobacterium tuberculosis, HIV-1 and Helicobacter pylori. *Nature Immunology,* 10**,** 1081-1088.
GRINGHUIS, S. I., DEN DUNNEN, J., LITJENS, M., VAN HET HOF, B., VAN KOOYK, Y. & GEIJTENBEEK, T. B. 2007. C-type lectin DC-SIGN modulates Toll-like receptor signaling via Raf-1 kinase-dependent acetylation of transcription factor NF-κB. *Immunity,* 26**,** 605-616.
GRINGHUIS, S. I., KAPTEIN, T. M., WEVERS, B. A., MESMAN, A. W. & GEIJTENBEEK, T. B. 2014. Fucose-specific DC-SIGN signalling directs T helper cell type-2 responses via IKKε-and CYLD-dependent Bcl3 activation. *Nature Communications,* 5**,** 1-13.
GUENTHER, F., STROH, P., WAGNER, C., OBST, U. & HÄNSCH, G. M. 2009. Phagocytosis of staphylococci biofilms by polymorphonuclear neutrophils: S. aureus and S. epidermidis differ with regard to their susceptibility towards the host defense. *The International Journal of Artificial Organs,* 32**,** 565-573.
GUILLIAMS, M., DUTERTRE, C.-A., SCOTT, C. L., MCGOVERN, N., SICHIEN, D., CHAKAROV, S., VAN GASSEN, S., CHEN, J., POIDINGER, M. & DE PRIJCK, S. 2016. Unsupervised high-dimensional analysis aligns dendritic cells across tissues and species. *Immunity,* 45**,** 669-684.
HA, D.-G. & O'TOOLE, G. A. 2015. c-di-GMP and its Effects on Biofilm Formation and Dispersion: a Pseudomonas Aeruginosa Review. *Microbiology Spectrum,* 3**,** 10.1128/microbiolspec.MB-0003-2014-2014.
HA, T. & TINNEFELD, P. 2012. Photophysics of fluorescent probes for single-molecule biophysics and super-resolution imaging. *Annu Rev Phys Chem,* 63**,** 595-617.
HÄGER, M., COWLAND, J. & BORREGAARD, N. 2010. Neutrophil granules in health and disease. *Journal of internal medicine,* 268**,** 25-34.
HAIKO, J. & WESTERLUND-WIKSTRÖM, B. 2013. The role of the bacterial flagellum in adhesion and virulence. *Biology* 2**,** 1242-67.
HAJJAR, A. M., ERNST, R. K., TSAI, J. H., WILSON, C. B. & MILLER, S. I. 2002. Human Toll-like receptor 4 recognizes host-specific LPS modifications. *Nature Immunology,* 3**,** 354-359.
HALARY, F., AMARA, A., LORTAT-JACOB, H., MESSERLE, M., DELAUNAY, T., HOULÈS, C., FIESCHI, F., ARENZANA-SEISDEDOS, F., MOREAU, J. F. & DÉCHANET-MERVILLE, J. 2002. Human cytomegalovirus binding to DC-SIGN is required for dendritic cell infection and target cell trans-infection. *Immunity,* 17**,** 653-64.
HALL-STOODLEY, L., COSTERTON, J. W. & STOODLEY, P. 2004. Bacterial biofilms: from the natural environment to infectious diseases. *Nature Reviews Microbiology,* 2**,** 95-108.
HALL, S., MCDERMOTT, C., ANOOPKUMAR-DUKIE, S., MCFARLAND, A. J., FORBES, A., PERKINS, A. V., DAVEY, A. K., CHESS-WILLIAMS, R., KIEFEL, M. J., ARORA, D. & GRANT, G. D. 2016. Cellular Effects of Pyocyanin, a Secreted Virulence Factor of Pseudomonas aeruginosa. *Toxins,* 8**,** 236.
HAMILTON, J. A. 2008. Colony-stimulating factors in inflammation and autoimmunity. *Nature Reviews Immunology,* 8**,** 533-544.
HANKE, M. L. & KIELIAN, T. 2012. Deciphering mechanisms of staphylococcal biofilm evasion of host immunity. *Frontiers in Cellular and Infection Microbiology,* 2**,** 62.
HÄNSCH, G., BRENNER-WEISS, G., PRIOR, B., WAGNER, C. & OBST, U. 2008. The extracellular polymer substance of Pseudomonas aeruginosa: too slippery

for neutrophils to migrate on? *The International Journal of Artificial Organs,* 31**,** 796-803.
HÄNSCH, G. M. 2012. Host Defence against Bacterial Biofilms: “Mission Impossible”? *ISRN Immunology,* 2012**,** 853123.
HARA, H., ISHIHARA, C., TAKEUCHI, A., IMANISHI, T., XUE, L., MORRIS, S. W., INUI, M., TAKAI, T., SHIBUYA, A., SAIJO, S., IWAKURA, Y., OHNO, N., KOSEKI, H., YOSHIDA, H., PENNINGER, J. M. & SAITO, T. 2007. The adaptor protein CARD9 is essential for the activation of myeloid cells through ITAM-associated and Toll-like receptors. *Nat Immunol,* 8**,** 619-29.
HARDING, C. V. & SONG, R. 1994. Phagocytic processing of exogenous particulate antigens by macrophages for presentation by class I MHC molecules. *The Journal of Immunology,* 153**,** 4925-4933.
HARTL, D., GAGGAR, A., BRUSCIA, E., HECTOR, A., MARCOS, V., JUNG, A., GREENE, C., MCELVANEY, G., MALL, M. & DÖRING, G. 2012. Innate immunity in cystic fibrosis lung disease. *Journal of Cystic Fibrosis,* 11**,** 363-382.
HASHIMOTO, S., PITTET, J. F., HONG, K., FOLKESSON, H., BAGBY, G., KOBZIK, L., FREVERT, C., WATANABE, K., TSURUFUJI, S. & WIENER-KRONISH, J. 1996. Depletion of alveolar macrophages decreases neutrophil chemotaxis to Pseudomonas airspace infections. *Am J Physiol,* 270**,** L819-28.
HASTIE, A. T., HINGLEY, S. T., HIGGINS, M. L., KUEPPERS, F. & SHRYOCK, T. 1986. Rhamnolipid from Pseudomonas aeruginosa inactivates mammalian tracheal ciliary axonemes. *Cell Motility,* 6**,** 502-509.
HAUBER, H.-P., SCHULZ, M., PFORTE, A., MACK, D., ZABEL, P. & SCHUMACHER, U. 2008. Inhalation with fucose and galactose for treatment of Pseudomonas aeruginosa in cystic fibrosis patients. *International Journal of Medical Sciences,* 5**,** 371.
HAUSER, A. R. 2009. The type III secretion system of Pseudomonas aeruginosa: infection by injection. *Nature Reviews. Microbiology,* 7**,** 654-665.
HAY, I. D., REMMINGHORST, U. & REHM, B. H. 2009. MucR, a novel membrane-associated regulator of alginate biosynthesis in Pseudomonas aeruginosa. *Applied and Environmental Microbiology,* 75**,** 1110-1120.
HAYASHI, F., SMITH, K. D., OZINSKY, A., HAWN, T. R., EUGENE, C. Y., GOODLETT, D. R., ENG, J. K., AKIRA, S., UNDERHILL, D. M. & ADEREM, A. 2001. The innate immune response to bacterial flagellin is mediated by Toll-like receptor 5. *Nature,* 410**,** 1099-1103.
HE, J., KIM, D., ZHOU, X., AHN, S.-J., BURNE, R. A., RICHARDS, V. P. & KOO, H. 2017. RNA-seq reveals enhanced sugar metabolism in Streptococcus mutans co-cultured with Candida albicans within mixed-species biofilms. *Frontiers in Microbiology,* 8**,** 1036.
HEALE, J. P., POLLARD, A. J., STOKES, R. W., SIMPSON, D., TSANG, A., MASSING, B. & SPEERT, D. P. 2001. Two distinct receptors mediate nonopsonic phagocytosis of different strains of Pseudomonas aeruginosa. *J Infect Dis,* 183**,** 1214-20.
HEEB, S., FLETCHER, M. P., CHHABRA, S. R., DIGGLE, S. P., WILLIAMS, P. & CÁMARA, M. 2011. Quinolones: from antibiotics to autoinducers. *FEMS Microbiol Rev,* 35**,** 247-74.
HEIDKAMP, G. F., SANDER, J., LEHMANN, C. H., HEGER, L., EISSING, N., BARANSKA, A., LÜHR, J. J., HOFFMANN, A., REIMER, K. C. & LUX, A. 2016. Human lymphoid organ dendritic cell identity is predominantly dictated by ontogeny, not tissue microenvironment. *Science Immunology,* 1.

HEINSBROEK, S. E., TAYLOR, P. R., ROSAS, M., WILLMENT, J. A., WILLIAMS, D. L., GORDON, S. & BROWN, G. D. 2006. Expression of functionally different dectin-1 isoforms by murine macrophages. *The Journal of Immunology,* 176**,** 5513-5518.

HENGGE, R. 2009. Principles of c-di-GMP signalling in bacteria. *Nature Reviews Microbiology,* 7**,** 263-273.

HEYDORN, A., ERSBØLL, B. K., HENTZER, M., PARSEK, M. R., GIVSKOV, M. & MOLIN, S. 2000a. Experimental reproducibility in flow-chamber biofilms. *Microbiology,* 146**,** 2409-2415.

HEYDORN, A., NIELSEN, A. T., HENTZER, M., STERNBERG, C., GIVSKOV, M., ERSBØLL, B. K. & MOLIN, S. 2000b. Quantification of biofilm structures by the novel computer program COMSTAT. *Microbiology,* 146**,** 2395-2407.

HICKMAN, J. W. & HARWOOD, C. S. 2008. Identification of FleQ from Pseudomonas aeruginosa as ac‐di‐GMP‐responsive transcription factor. *Molecular Microbiology,* 69**,** 376-389.

HICKMAN, J. W., TIFREA, D. F. & HARWOOD, C. S. 2005. A chemosensory system that regulates biofilm formation through modulation of cyclic diguanylate levels. *Proc Natl Acad Sci U S A,* 102**,** 14422-7.

HILL, D. B., LONG, R. F., KISSNER, W. J., ATIEH, E., GARBARINE, I. C., MARKOVETZ, M. R., FONTANA, N. C., CHRISTY, M., HABIBPOUR, M. & TARRAN, R. 2018. Pathological mucus and impaired mucus clearance in cystic fibrosis patients result from increased concentration, not altered pH. *European Respiratory Journal,* 52**,** 1801297.

HIRCHE, T. O., BENABID, R., DESLEE, G., GANGLOFF, S., ACHILEFU, S., GUENOUNOU, M., LEBARGY, F., HANCOCK, R. E. & BELAAOUAJ, A. 2008. Neutrophil elastase mediates innate host protection against Pseudomonas aeruginosa. *The Journal of Immunology,* 181**,** 4945-4954.

HODGES, A., SHARROCKS, K., EDELMANN, M., BABAN, D., MORIS, A., SCHWARTZ, O., DRAKESMITH, H., DAVIES, K., KESSLER, B. & MCMICHAEL, A. 2007. Activation of the lectin DC-SIGN induces an immature dendritic cell phenotype triggering Rho-GTPase activity required for HIV-1 replication. *Nature Immunology,* 8**,** 569-577.

HOGARDT, M. & HEESEMANN, J. 2010. Adaptation of Pseudomonas aeruginosa during persistence in the cystic fibrosis lung. *International Journal of Medical Microbiology,* 300**,** 557-562.

HØIBY, N. 2011. Recent advances in the treatment of Pseudomonas aeruginosainfections in cystic fibrosis. *BMC Medicine,* 9**,** 32.

HOLLOWAY, B. W., KRISHNAPILLAI, V. & MORGAN, A. F. 1979. Chromosomal Genetics of Pseudomonas. *Microbiological Reviews,* 43**,** 73-102.

HOLM, A. & VIKSTRÖM, E. 2014. Quorum sensing communication between bacteria and human cells: signals, targets, and functions. *Frontiers in Plant Science,* 5**,** 309.

HONG, W., JUNEAU, R. A., PANG, B. & SWORDS, W. E. 2009. Survival of bacterial biofilms within neutrophil extracellular traps promotes nontypeable Haemophilus influenzae persistence in the chinchilla model for otitis media. *Journal of Innate Immunity,* 1**,** 215-224.

HORREVORTS, S. K., DUINKERKEN, S., BLOEM, K., SECADES, P., KALAY, H., MUSTERS, R. J., VAN VLIET, S. J., GARCÍA-VALLEJO, J. J. & VAN KOOYK, Y. 2018. Toll-Like Receptor 4 Triggering Promotes Cytosolic Routing of DC-

SIGN-Targeted Antigens for Presentation on MHC Class I. *Frontiers in Immunology,* 9**,** 1231-1231.
HUQ, A., SACK, R. B., NIZAM, A., LONGINI, I. M., NAIR, G. B., ALI, A., MORRIS, J. G., KHAN, M. H., SIDDIQUE, A. K. & YUNUS, M. 2005. Critical factors influencing the occurrence of Vibrio cholerae in the environment of Bangladesh. *Applied and Environmental Microbiology,* 71**,** 4645-4654.
HUSZCZYNSKI, S. M., LAM, J. S. & KHURSIGARA, C. M. 2020. The role of Pseudomonas aeruginosa lipopolysaccharide in bacterial pathogenesis and physiology. *Pathogens,* 9**,** 6.
IFRIM, D. C., QUINTIN, J., COURJOL, F., VERSCHUEREN, I., VAN KRIEKEN, J. H., KOENTGEN, F., FRADIN, C., GOW, N. A., JOOSTEN, L. A. & VAN DER MEER, J. W. 2016. The role of dectin-2 for host defense against disseminated candidiasis. *Journal of Interferon & Cytokine Research,* 36**,** 267-276.
INABA, K., INABA, M., ROMANI, N., AYA, H., DEGUCHI, M., IKEHARA, S., MURAMATSU, S. & STEINMAN, R. M. 1992. Generation of large numbers of dendritic cells from mouse bone marrow cultures supplemented with granulocyte/macrophage colony-stimulating factor. *J Exp Med,* 176**,** 1693-702.
IRANKHAH, S., ABDI ALI, A., MALLAVARAPU, M., SOUDI, M. R., SUBASHCHANDRABOSE, S., GHARAVI, S. & AYATI, B. 2019. Ecological role of Acinetobacter calcoaceticus GSN3 in natural biofilm formation and its advantages in bioremediation. *Biofouling,* 35**,** 377-391.
IRIE, Y., BORLEE, B. R., O'CONNOR, J. R., HILL, P. J., HARWOOD, C. S., WOZNIAK, D. J. & PARSEK, M. R. 2012. Self-produced exopolysaccharide is a signal that stimulates biofilm formation in Pseudomonas aeruginosa. *Proc Natl Acad Sci U S A,* 109**,** 20632-6.
IRIE, Y., ROBERTS, A. E. L., KRAGH, K. N., GORDON, V. D., HUTCHISON, J., ALLEN, R. J., MELAUGH, G., BJARNSHOLT, T., WEST, S. A. & DIGGLE, S. P. 2017. The Pseudomonas aeruginosa PSL Polysaccharide Is a Social but Noncheatable Trait in Biofilms. *Mbio,* 8**,** e00374-17.
IRIE, Y., STARKEY, M., EDWARDS, A. N., WOZNIAK, D. J., ROMEO, T. & PARSEK, M. R. 2010. Pseudomonas aeruginosa biofilm matrix polysaccharide Psl is regulated transcriptionally by RpoS and post-transcriptionally by RsmA. *Molecular microbiology,* 78**,** 158-172.
ISHIKAWA, E., ISHIKAWA, T., MORITA, Y. S., TOYONAGA, K., YAMADA, H., TAKEUCHI, O., KINOSHITA, T., AKIRA, S., YOSHIKAI, Y. & YAMASAKI, S. 2009. Direct recognition of the mycobacterial glycolipid, trehalose dimycolate, by C-type lectin Mincle. *J Exp Med,* 206**,** 2879-88.
ISHIKAWA, T., ITOH, F., YOSHIDA, S., SAIJO, S., MATSUZAWA, T., GONOI, T., SAITO, T., OKAWA, Y., SHIBATA, N., MIYAMOTO, T. & YAMASAKI, S. 2013. Identification of distinct ligands for the C-type lectin receptors Mincle and Dectin-2 in the pathogenic fungus Malassezia. *Cell Host Microbe,* 13**,** 477-88.
IWAKURA, Y., ISHIGAME, H., SAIJO, S. & NAKAE, S. 2011. Functional specialization of interleukin-17 family members. *Immunity,* 34**,** 149-162.
JACKSON, K. D., STARKEY, M., KREMER, S., PARSEK, M. R. & WOZNIAK, D. J. 2004. Identification of psl, a locus encoding a potential exopolysaccharide that is essential for Pseudomonas aeruginosa PAO1 biofilm formation. *Journal of Bacteriology,* 186**,** 4466-4475.
JAHAGIRDAR, P., LOKHANDE, A. S., DANDEKAR, P. & DEVARAJAN, P. V. 2019. Mannose Receptor and Targeting Strategies. *Targeted intracellular drug delivery by receptor mediated endocytosis.* Springer.

JANEWAY, C. A., JR. & MEDZHITOV, R. 2002. Innate immune recognition. *Annu Rev Immunol,* 20**,** 197-216.

JANSSENS, S. & BEYAERT, R. 2003. Role of Toll-like receptors in pathogen recognition. *Clinical microbiology reviews,* 16**,** 637-646.

JEFFERSON, K. K. 2004. What drives bacteria to produce a biofilm? *FEMS Microbiology Letters,* 236**,** 163-173.

JENNINGS, L. K., STOREK, K. M., LEDVINA, H. E., COULON, C., MARMONT, L. S., SADOVSKAYA, I., SECOR, P. R., TSENG, B. S., SCIAN, M. & FILLOUX, A. 2015. Pel is a cationic exopolysaccharide that cross-links extracellular DNA in the Pseudomonas aeruginosa biofilm matrix. *Proceedings of the National Academy of Sciences,* 112**,** 11353-11358.

JENSEN, P. Ø., BJARNSHOLT, T., PHIPPS, R., RASMUSSEN, T. B., CALUM, H., CHRISTOFFERSEN, L., MOSER, C., WILLIAMS, P., PRESSLER, T., GIVSKOV, M. & HØIBY, N. 2007. Rapid necrotic killing of polymorphonuclear leukocytes is caused by quorum-sensing-controlled production of rhamnolipid by Pseudomonas aeruginosa. *Microbiology,* 153**,** 1329-1338.

JESAITIS, A. J., FRANKLIN, M. J., BERGLUND, D., SASAKI, M., LORD, C. I., BLEAZARD, J. B., DUFFY, J. E., BEYENAL, H. & LEWANDOWSKI, Z. 2003. Compromised host defense on Pseudomonas aeruginosa biofilms: characterization of neutrophil and biofilm interactions. *J Immunol,* 171**,** 4329-39.

JIANG, F., WATERFIELD, N. R., YANG, J., YANG, G. & JIN, Q. 2014. A Pseudomonas aeruginosa type VI secretion phospholipase D effector targets both prokaryotic and eukaryotic cells. *Cell host & microbe,* 15**,** 600-610.

JONES, C. J. & WOZNIAK, D. J. 2017. Psl Produced by Mucoid *Pseudomonas aeruginosa* Contributes to the Establishment of Biofilms and Immune Evasion. *Mbio,* 8**,** e00864-17.

JONES, D., TOBLER, D., SCHAPERDOTH, I., MAINIERO, M. & MACALADY, J. 2010. Community structure of subsurface biofilms in the thermal sulfidic caves of Acquasanta Terme, Italy. *Applied and environmental microbiology,* 76**,** 5902-5910.

JYOT, J., SONAWANE, A., WU, W. & RAMPHAL, R. 2007. Genetic mechanisms involved in the repression of flagellar assembly by Pseudomonas aeruginosa in human mucus. *Molecular Microbiology,* 63**,** 1026-1038.

KAGAMI, S., RIZZO, H. L., KURTZ, S. E., MILLER, L. S. & BLAUVELT, A. 2010. IL-23 and IL-17A, but not IL-12 and IL-22, are required for optimal skin host defense against Candida albicans. *The Journal of Immunology,* 185**,** 5453-5462.

KANG, P. B., AZAD, A. K., TORRELLES, J. B., KAUFMAN, T. M., BEHARKA, A., TIBESAR, E., DESJARDIN, L. E. & SCHLESINGER, L. S. 2005. The human macrophage mannose receptor directs Mycobacterium tuberculosis lipoarabinomannan-mediated phagosome biogenesis. *The Journal of Experimental Medicine,* 202**,** 987-999.

KANNAN, S., AUDET, A., HUANG, H., CHEN, L. J. & WU, M. 2008. Cholesterol-rich membrane rafts and Lyn are involved in phagocytosis during Pseudomonas aeruginosa infection. *J Immunol,* 180**,** 2396-408.

KARLSSON, T., MUSSE, F., MAGNUSSON, K. E. & VIKSTRÖM, E. 2012. N‐Acylhomoserine lactones are potent neutrophil chemoattractants that act via calcium mobilization and actin remodeling. *Journal of Leukocyte Biology,* 91**,** 15-26.

KAROSI, T., CSOMOR, P., HEGYI, Z. & SZIKLAI, I. 2013. The presence of CD209 expressing dendritic cells correlates with biofilm positivity in chronic rhinosinusitis with nasal polyposis. *European Archives of Oto-Rhino-Laryngology,* 270**,** 2455-2463.
KAWASAKI, T. & KAWAI, T. 2014. Toll-like receptor signaling pathways. *Frontiers in Immunology,* 5**,** 461-461.
KAWASAKI, T. & KAWAI, T. 2019. Discrimination Between Self and Non-Self-Nucleic Acids by the Innate Immune System. *International Review of Cell and Molecular Biology,* 344**,** 1-30.
KAWATA, K., ILLARIONOV, P., YANG, G.-X., KENNY, T. P., ZHANG, W., TSUDA, M., ANDO, Y., LEUNG, P. S., ANSARI, A. A. & GERSHWIN, M. E. 2012. Mincle and human B cell function. *Journal of autoimmunity,* 39**,** 315-322.
KAZMIERCZAK, B. & ENGEL, J. 2002. Pseudomonas aeruginosa ExoT acts in vivo as a GTPase-activating protein for RhoA, Rac1, and Cdc42. *Infection and Immunity,* 70**,** 2198-2205.
KERRIGAN, A. M. & BROWN, G. D. 2009. C-type lectins and phagocytosis. *Immunobiology,* 214**,** 562-575.
KERSCHER, B., WILLMENT, J. A. & BROWN, G. D. 2013. The Dectin-2 family of C-type lectin-like receptors: an update. *Int Immunol,* 25**,** 271-7.
KHAN, N. S., KASPERKOVITZ, P. V., TIMMONS, A. K., MANSOUR, M. K., TAM, J. M., SEWARD, M. W., REEDY, J. L., PURANAM, S., FELIU, M. & VYAS, J. M. 2016. Dectin-1 Controls TLR9 Trafficking to Phagosomes Containing β-1,3 Glucan. *Journal of Immunology* 196**,** 2249-2261.
KHAN, W., BERNIER, S. P., KUCHMA, S. L., HAMMOND, J. H., HASAN, F. & O'TOOLE, G. A. 2010. Aminoglycoside resistance of Pseudomonas aeruginosa biofilms modulated by extracellular polysaccharide. *International Microbiology: the Official Journal of the Spanish Society for Microbiology,* 13**,** 207.
KING, J. D., KOCÍNCOVÁ, D., WESTMAN, E. L. & LAM, J. S. 2009. Lipopolysaccharide biosynthesis in Pseudomonas aeruginosa. *Innate Immunity,* 15**,** 261-312.
KING JR, A. D. & NAGEL, C. W. 1975. Influence of carbon dioxide upon the metabolism of Pseudomonas aeruginosa. *Journal of Food Science,* 40**,** 362-366.
KIRISITS, M. J., PROST, L., STARKEY, M. & PARSEK, M. R. 2005. Characterization of colony morphology variants isolated from Pseudomonas aeruginosa biofilms. *Applied and Environmental Microbiology,* 71**,** 4809-4821.
KLAPPER, I., RUPP, C. J., CARGO, R., PURVEDORJ, B. & STOODLEY, P. 2002. Viscoelastic fluid description of bacterial biofilm material properties. *Biotechnology and Bioengineering,* 80**,** 289-296.
KLOCKGETHER, J. & TÜMMLER, B. 2017. Recent advances in understanding Pseudomonas aeruginosa as a pathogen. *F1000Research,* 6.
KLOTH, C., SCHIRMER, B., MUNDER, A., STELZER, T., ROTHSCHUH, J. & SEIFERT, R. 2018. The role of Pseudomonas aeruginosa ExoY in an acute mouse lung infection model. *Toxins,* 10**,** 185.
KOCH, C. & HOIBY, N. 1993. Pathogenesis of cystic fibrosis. *The Lancet,* 341**,** 1065-1069.
KOCINCOVA, D. & LAM, J. 2011. Structural diversity of the core oligosaccharide domain of Pseudomonas aeruginosa lipopolysaccharide. *Biochemistry (Moscow),* 76**,** 755-760.

KOFOED, E. M. & VANCE, R. E. 2011. Innate immune recognition of bacterial ligands by NAIPs determines inflammasome specificity. *Nature,* 477**,** 592-595.

KOH, A. Y., PRIEBE, G. P., RAY, C., VAN ROOIJEN, N. & PIER, G. B. 2009. Inescapable need for neutrophils as mediators of cellular innate immunity to acute Pseudomonas aeruginosa pneumonia. *Infection and Immunity,* 77**,** 5300-5310.

KÖHLER, T., CURTY, L. K., BARJA, F., VAN DELDEN, C. & PECHÈRE, J.-C. 2000. Swarming of Pseudomonas aeruginosa is dependent on cell-to-cell signaling and requires flagella and pili. *Journal of bacteriology,* 182**,** 5990-5996.

KOLACZKOWSKA, E. & KUBES, P. 2013. Neutrophil recruitment and function in health and inflammation. *Nature Reviews Immunology,* 13**,** 159-175.

KOOGUCHI, K., HASHIMOTO, S., KOBAYASHI, A., KITAMURA, Y., KUDOH, I., WIENER-KRONISH, J. & SAWA, T. 1998. Role of alveolar macrophages in initiation and regulation of inflammation in Pseudomonas aeruginosa pneumonia. *Infect Immun,* 66**,** 3164-9.

KORN, T., OUKKA, M., KUCHROO, V. & BETTELLI, E. Th17 cells: effector T cells with inflammatory properties. Seminars in immunology, 2007. Elsevier, 362-371.

KORNEEV, K. V., ARBATSKY, N. P., MOLINARO, A., PALMIGIANO, A., SHAIKHUTDINOVA, R. Z., SHNEIDER, M. M., PIER, G. B., KONDAKOVA, A. N., SVIRIAEVA, E. N. & STURIALE, L. 2015. Structural relationship of the lipid A acyl groups to activation of murine toll-like receptor 4 by lipopolysaccharides from pathogenic strains of Burkholderia mallei, Acinetobacter baumannii, and Pseudomonas aeruginosa. *Frontiers in Immunology,* 6**,** 595.

KOUNNAS, M. Z., MORRIS, R. E., THOMPSON, M. R., FITZGERALD, D. J., STRICKLAND, D. K. & SAELINGER, C. B. 1992. The alpha 2-macroglobulin receptor/low density lipoprotein receptor-related protein binds and internalizes Pseudomonas exotoxin A. *J Biol Chem,* 267**,** 12420-3.

KOVACH, K., DAVIS-FIELDS, M., IRIE, Y., JAIN, K., DOORWAR, S., VUONG, K., DHAMANI, N., MOHANTY, K., TOUHAMI, A. & GORDON, V. D. 2017. Evolutionary adaptations of biofilms infecting cystic fibrosis lungs promote mechanical toughness by adjusting polysaccharide production. *Npj Biofilms and Microbiomes,* 3**,** 1-9.

KRAGH, K. N., ALHEDE, M., JENSEN, P. Ø., MOSER, C., SCHEIKE, T., JACOBSEN, C. S., POULSEN, S. S., EICKHARDT-SØRENSEN, S. R., TRØSTRUP, H. & CHRISTOFFERSEN, L. 2014. Polymorphonuclear leukocytes restrict growth of Pseudomonas aeruginosa in the lungs of cystic fibrosis patients. *Infection and Immunity,* 82**,** 4477-4486.

KRAGH, K. N., ALHEDE, M., KVICH, L. & BJARNSHOLT, T. 2019. Into the well—A close look at the complex structures of a microtiter biofilm and the crystal violet assay. *Biofilm,* 1**,** 100006.

KROKEN, A. R., CHEN, C. K., EVANS, D. J., YAHR, T. L. & FLEISZIG, S. M. 2018. The impact of ExoS on Pseudomonas aeruginosa internalization by epithelial cells is independent of fleQ and correlates with bistability of type three secretion system gene expression. *Mbio,* 9.

KUGADAS, A., GEDDES‐MCALISTER, J., GUY, E., DIGIANDOMENICO, A., SYKES, D. B., MANSOUR, M. K., MIRCHEV, R. & GADJEVA, M. 2019. Frontline Science: Employing enzymatic treatment options for management of ocular biofilm‐based infections. *Journal of Leukocyte Biology,* 105**,** 1099-1110.

KULASEKARA, H. D., VENTRE, I., KULASEKARA, B. R., LAZDUNSKI, A., FILLOUX, A. & LORY, S. 2005. A novel two‐component system controls the expression of Pseudomonas aeruginosa fimbrial cup genes. *Molecular Microbiology,* 55**,** 368-380.

KUZMICH, N. N., SIVAK, K. V., CHUBAREV, V. N., POROZOV, Y. B., SAVATEEVA-LYUBIMOVA, T. N. & PERI, F. 2017. TLR4 signaling pathway modulators as potential therapeutics in inflammation and sepsis. *Vaccines,* 5**,** 34.

LAGOUMINTZIS, G., XAPLANTERI, P., DIMITRACOPOULOS, G. & PALIOGIANNI, F. 2008. TNF-alpha induction by Pseudomonas aeruginosa lipopolysaccharide or slime-glycolipoprotein in human monocytes is regulated at the level of Mitogen-activated Protein Kinase activity: a distinct role of Toll-like receptor 2 and 4. *Scand J Immunol,* 67**,** 193-203.

LAHARRAGUE, P., CORBERAND, J., FILLOLA, G., GLEIZES, B., FONTANILLES, A. & GYRARD, E. 1984. In vitro effect of the slime of Pseudomonas aeruginosa on the function of human polymorphonuclear neutrophils. *Infection and Immunity,* 44**,** 760-762.

LAM, J. S., TAYLOR, V. L., ISLAM, S. T., HAO, Y. & KOCÍNCOVÁ, D. 2011. Genetic and functional diversity of Pseudomonas aeruginosa lipopolysaccharide. *Frontiers in Microbiology,* 2**,** 118.

LAM, M. Y., MCGROARTY, E. J., KROPINSKI, A. M., MACDONALD, L. A., PEDERSEN, S. S., HØIBY, N. & LAM, J. S. 1989. Occurrence of a common lipopolysaccharide antigen in standard and clinical strains of Pseudomonas aeruginosa. *Journal of Clinical Microbiology,* 27**,** 962-967.

LAMBERT, A. A., GILBERT, C., RICHARD, M., BEAULIEU, A. D. & TREMBLAY, M. J. 2008. The C-type lectin surface receptor DCIR acts as a new attachment factor for HIV-1 in dendritic cells and contributes to trans- and cis-infection pathways. *Blood,* 112**,** 1299-307.

LAUGHLIN, R. S., MUSCH, M. W., HOLLBROOK, C. J., ROCHA, F. M., CHANG, E. B. & ALVERDY, J. C. 2000. The key role of Pseudomonas aeruginosa PA-I lectin on experimental gut-derived sepsis. *Annals of Surgery,* 232**,** 133.

LAVOIE, E. G., WANGDI, T. & KAZMIERCZAK, B. I. 2011. Innate immune responses to Pseudomonas aeruginosa infection. *Microbes and Infection,* 13**,** 1133-1145.

LE CABEC, V., EMORINE, L. J., TOESCA, I., COUGOULE, C. & MARIDONNEAU‐PARINI, I. 2005. The human macrophage mannose receptor is not a professional phagocytic receptor. *Journal of Leukocyte Biology,* 77**,** 934-943.

LEE, B., HAAGENSEN, J. A. J., CIOFU, O., ANDERSEN, J. B., HØIBY, N. & MOLIN, S. 2005. Heterogeneity of biofilms formed by nonmucoid Pseudomonas aeruginosa isolates from patients with cystic fibrosis. *Journal of Clinical Microbiology,* 43**,** 5247-5255.

LEE, J., WU, J., DENG, Y., WANG, J., WANG, C., WANG, J., CHANG, C., DONG, Y., WILLIAMS, P. & ZHANG, L. H. 2013a. A cell-cell communication signal integrates quorum sensing and stress response. *Nat Chem Biol,* 9**,** 339-43.

LEE, J. & ZHANG, L. 2015. The hierarchy quorum sensing network in Pseudomonas aeruginosa. *Protein Cell,* 6**,** 26-41.

LEE, P. Y., WANG, J. X., PARISINI, E., DASCHER, C. C. & NIGROVIC, P. A. 2013b. Ly6 family proteins in neutrophil biology. *Journal of Leukocyte Biology,* 94**,** 585-594.

LEE, R. T., HSU, T.-L., HUANG, S. K., HSIEH, S.-L., WONG, C.-H. & LEE, Y. C. 2011. Survey of immune-related, mannose/fucose-binding C-type lectin receptors reveals widely divergent sugar-binding specificities. *Glycobiology,* 21**,** 512-520.

LEE, S. J., ZHENG, N.-Y., CLAVIJO, M. & NUSSENZWEIG, M. C. 2003. Normal host defense during systemic candidiasis in mannose receptor-deficient mice. *Infection and Immunity,* 71**,** 437-445.
LEE, W.-B., KANG, J.-S., YAN, J.-J., LEE, M. S., JEON, B.-Y., CHO, S.-N. & KIM, Y.-J. 2012. Neutrophils promote mycobacterial trehalose dimycolate-induced lung inflammation via the Mincle pathway. *PLoS Pathog,* 8**,** e1002614.
LEID, J. G., WILLSON, C. J., SHIRTLIFF, M. E., HASSETT, D. J., PARSEK, M. R. & JEFFERS, A. K. 2005. The exopolysaccharide alginate protects Pseudomonas aeruginosa biofilm bacteria from IFN-γ-mediated macrophage killing. *The Journal of Immunology,* 175**,** 7512-7518.
LEIGHTON, T. L., BUENSUCESO, R. N., HOWELL, P. L. & BURROWS, L. L. 2015. Biogenesis of P seudomonas aeruginosa type IV pili and regulation of their function. *Environmental Microbiology,* 17**,** 4148-4163.
LEQUETTE, Y., ROLLET, E., DELANGLE, A., GREENBERG, E. P. & BOHIN, J.-P. 2007. Linear osmoregulated periplasmic glucans are encoded by the opgGH locus of Pseudomonas aeruginosa. *Microbiology,* 153**,** 3255-3263.
LEVENTAL, I., GEORGES, P. C. & JANMEY, P. A. 2007. Soft biological materials and their impact on cell function. *Soft Matter,* 3**,** 299-306.
LEY, K., SMITH, E. & STARK, M. A. 2006. IL-17A-producing neutrophil-regulatory Tn lymphocytes. *Immunologic research,* 34**,** 229-242.
LEYTON-PUIG, D., KEDZIORA, K. M., ISOGAI, T., VAN DEN BROEK, B., JALINK, K. & INNOCENTI, M. 2016. PFA fixation enables artifact-free super-resolution imaging of the actin cytoskeleton and associated proteins. *Biology Open,* 5**,** 1001-1009.
LI, H., MO, K.-F., WANG, Q., STOVER, C. K., DIGIANDOMENICO, A. & BOONS, G.-J. 2013. Epitope Mapping of Monoclonal Antibodies using Synthetic Oligosaccharides Uncovers Novel Aspects of Immune Recognition of the Psl Exopolysaccharide of Pseudomonas aeruginosa. *Chemistry* 19**,** 17425-17431.
LI, J., JOHNSON, X. D., IAZVOVSKAIA, S., TAN, A., LIN, A. & HERSHENSON, M. B. 2003. Signaling intermediates required for NF-κB activation and IL-8 expression in CF bronchial epithelial cells. *American Journal of Physiology-Lung Cellular and Molecular Physiology,* 284**,** L307-L315.
LI, X.-H. & LEE, J.-H. 2019. Quorum sensing-dependent post-secretional activation of extracellular proteases in Pseudomonas aeruginosa. *The Journal of Biological Chemistry,* 294**,** 19635-19644.
LI, Y., OOSTING, M., DEELEN, P., RICAÑO-PONCE, I., SMEEKENS, S., JAEGER, M., MATZARAKI, V., SWERTZ, M. A., XAVIER, R. J., FRANKE, L., WIJMENGA, C., JOOSTEN, L. A. B., KUMAR, V. & NETEA, M. G. 2016. Inter-individual variability and genetic influences on cytokine responses to bacteria and fungi. *Nature Medicine,* 22**,** 952-960.
LI, Z., KOSOROK, M. R., FARRELL, P. M., LAXOVA, A., WEST, S. E., GREEN, C. G., COLLINS, J., ROCK, M. J. & SPLAINGARD, M. L. 2005. Longitudinal development of mucoid Pseudomonas aeruginosa infection and lung disease progression in children with cystic fibrosis. *Jama,* 293**,** 581-588.
LIESSE IYAMBA, J.-M., SEIL, M., DEVLEESCHOUWER, M., TAKAISI KIKUNI, N. & DEHAYE, J.-P. 2011. Study of the formation of a biofilm by clinical strains of Staphylococcus aureus. *Biofouling,* 27**,** 811-821.
LIMOLI, D. H., JONES, C. J. & WOZNIAK, D. J. 2015. Bacterial Extracellular Polysaccharides in Biofilm Formation and Function. *Microbiology Spectrum,* 3**,** 10.1128/microbiolspec.MB-0011-2014.

LIMOLI, D. H., WHITFIELD, G. B., KITAO, T., IVEY, M. L., DAVIS, M. R., GRAHL, N., HOGAN, D. A., RAHME, L. G., HOWELL, P. L. & O'TOOLE, G. A. 2017. Pseudomonas aeruginosa alginate overproduction promotes coexistence with Staphylococcus aureus in a model of cystic fibrosis respiratory infection. *Mbio,* 8.

LIN, A. M., RUBIN, C. J., KHANDPUR, R., WANG, J. Y., RIBLETT, M., YALAVARTHI, S., VILLANUEVA, E. C., SHAH, P., KAPLAN, M. J. & BRUCE, A. T. 2011. Mast cells and neutrophils release IL-17 through extracellular trap formation in psoriasis. *The Journal of Immunology,* 187**,** 490-500.

LIN CHUA, S., LIU, Y., LI, Y., JUN TING, H., KOHLI, G. S., CAI, Z., SUWANCHAIKASEM, P., KAU KIT GOH, K., PIN NG, S., TOLKER-NIELSEN, T., YANG, L. & GIVSKOV, M. 2017. Reduced Intracellular c-di-GMP Content Increases Expression of Quorum Sensing-Regulated Genes in Pseudomonas aeruginosa. *Frontiers in Cellular and Infection Microbiology,* 7.

LIN, G., SIMMONS, G., PÖHLMANN, S., BARIBAUD, F., NI, H., LESLIE, G. J., HAGGARTY, B. S., BATES, P., WEISSMAN, D. & HOXIE, J. A. 2003. Differential N-linked glycosylation of human immunodeficiency virus and Ebola virus envelope glycoproteins modulates interactions with DC-SIGN and DC-SIGNR. *Journal of Virology,* 77**,** 1337-1346.

LINDEN, A., LAAN, M. & ANDERSON, G. 2005. Neutrophils, interleukin-17A and lung disease. *European Respiratory Journal,* 25**,** 159-172.

LINDER, S. & AEPFELBACHER, M. 2003. Podosomes: adhesion hot-spots of invasive cells. *Trends Cell Biol,* 13**,** 376-85.

LINEHAN, S. A., MARTÍNEZ‐POMARES, L., SILVA, R. P. D. & GORDON, S. 2001. Endogenous ligands of carbohydrate recognition domains of the mannose receptor in murine macrophages, endothelial cells and secretory cells; potential relevance to inflammation and immunity. *European Journal of Immunology,* 31**,** 1857-1866.

LIPINSKI, S., TILL, A., SINA, C., ARLT, A., GRASBERGER, H., SCHREIBER, S. & ROSENSTIEL, P. 2009. DUOX2-derived reactive oxygen species are effectors of NOD2-mediated antibacterial responses. *Journal of cell science,* 122**,** 3522-3530.

LISTER, P. D., WOLTER, D. J. & HANSON, N. D. 2009. Antibacterial-resistant Pseudomonas aeruginosa: clinical impact and complex regulation of chromosomally encoded resistance mechanisms. *Clin Microbiol Rev,* 22**,** 582-610.

LIU, Y.-C., HUSSAIN, F., NEGM, O., PAIVA, A. C., HALLIDAY, N., DUBERN, J.-F., SINGH, S., MUNTAKA, S., WHELDON, L. & LUCKETT, J. 2018. Contribution of the alkylquinolone quorum-sensing system to the interaction of Pseudomonas aeruginosa with bronchial epithelial cells. *Frontiers in Microbiology,* 9**,** 3018.

LOOD, C., BLANCO, L. P., PURMALEK, M. M., CARMONA-RIVERA, C., DE RAVIN, S. S., SMITH, C. K., MALECH, H. L., LEDBETTER, J. A., ELKON, K. B. & KAPLAN, M. J. 2016. Neutrophil extracellular traps enriched in oxidized mitochondrial DNA are interferogenic and contribute to lupus-like disease. *Nature Medicine,* 22**,** 146.

LOONEY, M. R., THORNTON, E. E., SEN, D., LAMM, W. J., GLENNY, R. W. & KRUMMEL, M. F. 2011. Stabilized imaging of immune surveillance in the mouse lung. *Nature Methods,* 8**,** 91-96.

LORÈ, N. I., CIGANA, C., DE FINO, I., RIVA, C., JUHAS, M., SCHWAGER, S., EBERL, L. & BRAGONZI, A. 2012. Cystic Fibrosis-Niche Adaptation of Pseudomonas aeruginosa Reduces Virulence in Multiple Infection Hosts. *PLoS One,* 7**,** e35648.

LOURES, F. V., ARAÚJO, E. F., FERIOTTI, C., BAZAN, S. B. & CALICH, V. L. 2015. TLR-4 cooperates with Dectin-1 and mannose receptor to expand Th17 and Tc17 cells induced by Paracoccidioides brasiliensis stimulated dendritic cells. *Frontiers in Microbiology,* 6**,** 261.

LOWMAN, D. W., ENSLEY, H. E., GREENE, R. R., KNAGGE, K. J., WILLIAMS, D. L. & KRUPPA, M. D. 2011. Mannan structural complexity is decreased when Candida albicans is cultivated in blood or serum at physiological temperature. *Carbohydrate Research,* 346**,** 2752-2759.

LUDWIG, I. S., LEKKERKERKER, A. N., DEPLA, E., BOSMAN, F., MUSTERS, R. J. P., DEPRAETERE, S., VAN KOOYK, Y. & GEIJTENBEEK, T. B. H. 2004. Hepatitis C Virus Targets DC-SIGN and L-SIGN To Escape Lysosomal Degradation. *Journal of Virology,* 78**,** 8322.

LUND-PALAU, H., TURNBULL, A. R., BUSH, A., BARDIN, E., CAMERON, L., SOREN, O., WIERRE-GORE, N., ALTON, E. W., BUNDY, J. G. & CONNETT, G. 2016. Pseudomonas aeruginosa infection in cystic fibrosis: pathophysiological mechanisms and therapeutic approaches. *Expert Review of Respiratory Medicine,* 10**,** 685-697.

LUTZ, M. B., STROBL, H., SCHULER, G. & ROMANI, N. 2017. GM-CSF monocyte-derived cells and Langerhans cells as part of the dendritic cell family. *Frontiers in Immunology,* 8**,** 1388.

LYCZAK, J. B., CANNON, C. L. & PIER, G. B. 2000. Establishment of Pseudomonas aeruginosa infection: lessons from a versatile opportunist. *Microbes Infect,* 2**,** 1051-60.

LYNCH, A. S. & ROBERTSON, G. T. 2008. Bacterial and fungal biofilm infections. *Annu Rev Med,* 59**,** 415-28.

MA, F., YI, L., YU, N., WANG, G., MA, Z., LIN, H. & FAN, H. 2017. Streptococcus suis serotype 2 biofilms inhibit the formation of neutrophil extracellular traps. *Frontiers in Cellular and Infection Microbiology,* 7**,** 86.

MA, J., BECKER, C., LOWELL, C. A. & UNDERHILL, D. M. 2012. Dectin-1-triggered recruitment of light chain 3 protein to phagosomes facilitates major histocompatibility complex class II presentation of fungal-derived antigens. *Journal of Biological Chemistry,* 287**,** 34149-34156.

MA, L., CONOVER, M., LU, H., PARSEK, M. R., BAYLES, K. & WOZNIAK, D. J. 2009. Assembly and development of the Pseudomonas aeruginosa biofilm matrix. *PLoS Pathog,* 5**,** e1000354.

MA, L., JACKSON, K. D., LANDRY, R. M., PARSEK, M. R. & WOZNIAK, D. J. 2006. Analysis of Pseudomonas aeruginosa conditional psl variants reveals roles for the psl polysaccharide in adhesion and maintaining biofilm structure postattachment. *Journal of Bacteriology,* 188**,** 8213-8221.

MA, L., LU, H., SPRINKLE, A., PARSEK, M. R. & WOZNIAK, D. J. 2007. Pseudomonas aeruginosa Psl is a galactose-and mannose-rich exopolysaccharide. *Journal of bacteriology,* 189**,** 8353-8356.

MADIANOS, P., BOBETSIS, Y. & KINANE, D. 2005. Generation of inflammatory stimuli: how bacteria set up inflammatory responses in the gingiva. *Journal of Clinical Periodontology,* 32**,** 57-71.

MAGALHÃES, A. P., JORGE, P. & PEREIRA, M. O. 2019. Pseudomonas aeruginosa and Staphylococcus aureus communication in biofilm infections: insights through network and database construction. *Critical Reviews in Microbiology,* 45**,** 712-728.

MAGANA, M., SERETI, C., IOANNIDIS, A., MITCHELL, C. A., BALL, A. R., MAGIORKINIS, E., CHATZIPANAGIOTOU, S., HAMBLIN, M. R., HADJIFRANGISKOU, M. & TEGOS, G. P. 2018. Options and Limitations in Clinical Investigation of Bacterial Biofilms. *Clin Microbiol Rev,* 31.

MAHENTHIRALINGAM, E., CAMPBELL, M. E., FOSTER, J., LAM, J. S. & SPEERT, D. P. 1996. Random amplified polymorphic DNA typing of Pseudomonas aeruginosa isolates recovered from patients with cystic fibrosis. *Journal of clinical microbiology,* 34**,** 1129-1135.

MALHOTRA, S., LIMOLI, D. H., ENGLISH, A. E., PARSEK, M. R. & WOZNIAK, D. J. 2018. Mixed communities of mucoid and nonmucoid Pseudomonas aeruginosa exhibit enhanced resistance to host antimicrobials. *Mbio,* 9.

MANAGO, A., BECKER, K. A., CARPINTEIRO, A., WILKER, B., SODDEMANN, M., SEITZ, A. P., EDWARDS, M. J., GRASSMÉ, H., SZABO, I. & GULBINS, E. 2015. Pseudomonas aeruginosa pyocyanin induces neutrophil death via mitochondrial reactive oxygen species and mitochondrial acid sphingomyelinase. *Antioxidants & redox signaling,* 22**,** 1097-1110.

MANLEY, H. R., KEIGHTLEY, M. C. & LIESCHKE, G. J. 2018. The Neutrophil Nucleus: An Important Influence on Neutrophil Migration and Function. *Frontiers in immunology,* 9**,** 2867-2867.

MANN, E. E. & WOZNIAK, D. J. 2012. Pseudomonas biofilm matrix composition and niche biology. *FEMS microbiology reviews,* 36**,** 893-916.

MANTOPOULOS, D., CRUZAT, A. & HAMRAH, P. In vivo imaging of corneal inflammation: new tools for clinical practice and research. Seminars in ophthalmology, 2010. Taylor & Francis, 178-185.

MANTOVANI, A., CASSATELLA, M. A., COSTANTINI, C. & JAILLON, S. 2011. Neutrophils in the activation and regulation of innate and adaptive immunity. *Nature reviews immunology,* 11**,** 519-531.

MAO, Y. 2016. Nearest neighbor distances calculation with ImageJ.

MARÓDI, L., KORCHAK, H. M. & JOHNSTON, R. B. 1991. Mechanisms of host defense against Candida species. I. Phagocytosis by monocytes and monocyte-derived macrophages. *The Journal of Immunology,* 146**,** 2783-2789.

MARTIN, D., SCHURR, M., MUDD, M., GOVAN, J., HOLLOWAY, B. & DERETIC, V. 1993. Mechanism of conversion to mucoidy in Pseudomonas aeruginosa infecting cystic fibrosis patients. *Proceedings of the National Academy of Sciences,* 90**,** 8377-8381.

MARTINEZ-POMARES, L. 2012. The mannose receptor. *Journal of Leukocyte Biology,* 92**,** 1177-1186.

MARTINEZ-POMARES, L., WIENKE, D., STILLION, R., MCKENZIE, E. J., ARNOLD, J. N., HARRIS, J., MCGREAL, E., SIM, R. B., ISACKE, C. M. & GORDON, S. 2006. Carbohydrate-independent recognition of collagens by the macrophage mannose receptor. *European Journal of Immunology,* 36**,** 1074-1082.

MARTINEZ, F. O. & GORDON, S. 2014. The M1 and M2 paradigm of macrophage activation: time for reassessment. *F1000prime reports,* 6**,** 13-13.

MATHY-HARTERT, M., DEBY-DUPONT, G., MELIN, P., LAMY, M. & DEBY, C. 1996. Bactericidal activity againstPseudomonas aeruginosa is acquired by cultured

human monocyte-derived macrophages after uptake of myeloperoxidase. *Experientia,* 52**,** 167-174.
MATSUI, H., VERGHESE, M. W., KESIMER, M., SCHWAB, U. E., RANDELL, S. H., SHEEHAN, J. K., GRUBB, B. R. & BOUCHER, R. C. 2005. Reduced three-dimensional motility in dehydrated airway mucus prevents neutrophil capture and killing bacteria on airway epithelial surfaces. *The journal of immunology,* 175**,** 1090-1099.
MATSUMOTO, M., TANAKA, T., KAISHO, T., SANJO, H., COPELAND, N. G., GILBERT, D. J., JENKINS, N. A. & AKIRA, S. 1999. A novel LPS-inducible C-type lectin is a transcriptional target of NF-IL6 in macrophages. *The Journal of Immunology,* 163**,** 5039-5048.
MATTICK, J. S. 2002. Type IV pili and twitching motility. *Annual Reviews in Microbiology,* 56**,** 289-314.
MAUNDERS, E. & WELCH, M. 2017. Matrix exopolysaccharides; the sticky side of biofilm formation. *FEMS Microbiology Letters,* 364.
MAZUREK, J., IGNATOWICZ, L., KALLENIUS, G., SVENSON, S. B., PAWLOWSKI, A. & HAMASUR, B. 2012. Divergent effects of mycobacterial cell wall glycolipids on maturation and function of human monocyte-derived dendritic cells. *PLoS One,* 7**,** e42515.
MCCARTHY, R. R., MAZON-MOYA, M. J., MOSCOSO, J. A., HAO, Y., LAM, J. S., BORDI, C., MOSTOWY, S. & FILLOUX, A. 2017. Cyclic-di-GMP regulates lipopolysaccharide modification and contributes to Pseudomonas aeruginosa immune evasion. *Nature Microbiology,* 2**,** 17027.
MCCORMICK, B., CHU, J. Y. & VERMEREN, S. 2019. Cross-talk between Rho GTPases and PI3K in the neutrophil. *Small GTPases,* 10**,** 187-195.
MCDONALD, J. U., ROSAS, M., BROWN, G. D., JONES, S. A. & TAYLOR, P. R. 2012. Differential dependencies of monocytes and neutrophils on dectin-1, dectin-2 and complement for the recognition of fungal particles in inflammation. *PLoS One,* 7**,** e45781.
MCGOVERN, N., SCHLITZER, A., GUNAWAN, M., JARDINE, L., SHIN, A., POYNER, E., GREEN, K., DICKINSON, R., WANG, X.-N. & LOW, D. 2014. Human dermal CD14+ cells are a transient population of monocyte-derived macrophages. *Immunity,* 41**,** 465-477.
MCGOVERN, N., SCHLITZER, A., GUNAWAN, M., JARDINE, L., SHIN, A., POYNER, E., GREEN, K., DICKINSON, R., WANG, X.-N. & LOW, D. 2015. Population of Monocyte-Derived Macrophages. *Immunity,* 42**,** 391.
MCGREAL, E. P., ROSAS, M., BROWN, G. D., ZAMZE, S., WONG, S. Y., GORDON, S., MARTINEZ-POMARES, L. & TAYLOR, P. R. 2006. The carbohydrate-recognition domain of Dectin-2 is a C-type lectin with specificity for high mannose. *Glycobiology,* 16**,** 422-30.
MCKNIGHT, S. L., IGLEWSKI, B. H. & PESCI, E. C. 2000. The Pseudomonas quinolone signal regulates rhl quorum sensing in Pseudomonas aeruginosa. *J Bacteriol,* 182**,** 2702-8.
MCMACKIN, E. A. W., DJAPGNE, L., CORLEY, J. M. & YAHR, T. L. 2019. Fitting pieces into the puzzle of Pseudomonas aeruginosa type III secretion system gene expression. *Journal of bacteriology,* 201.
MCRAE, B. L., NAGAI, T., SEMNANI, R. T., VAN SEVENTER, J. M. & VAN SEVENTER, G. A. 2000. Interferon-α and -β inhibit the in vitro differentiation of immunocompetent human dendritic cells from CD14+ precursors. *Blood,* 96**,** 210-217.

MEADE, A. D., CLARKE, C., DRAUX, F., SOCKALINGUM, G. D., MANFAIT, M., LYNG, F. M. & BYRNE, H. J. 2010. Studies of chemical fixation effects in human cell lines using Raman microspectroscopy. *Anal Bioanal Chem,* 396**,** 1781-91.

MEDZHITOV, R. 2007. Recognition of microorganisms and activation of the immune response. *Nature,* 449**,** 819-826.

MENNINK-KERSTEN, M. A., RUEGEBRINK, D. & VERWEIJ, P. E. 2008. Pseudomonas aeruginosa as a cause of 1, 3-β-d-glucan assay reactivity. *Clinical Infectious Diseases,* 46**,** 1930-1931.

MERAD, M., SATHE, P., HELFT, J., MILLER, J. & MORTHA, A. 2013. The dendritic cell lineage: ontogeny and function of dendritic cells and their subsets in the steady state and the inflamed setting. *Annual Review of Immunology,* 31**,** 563-604.

MERIGHI, M., LEE, V. T., HYODO, M., HAYAKAWA, Y. & LORY, S. 2007. The second messenger bis‐(3′‐5′)‐cyclic‐GMP and its PilZ domain‐containing receptor Alg44 are required for alginate biosynthesis in Pseudomonas aeruginosa. *Molecular Microbiology,* 65**,** 876-895.

MESTAS, J. & HUGHES, C. C. 2004. Of mice and not men: differences between mouse and human immunology. *J Immunol,* 172**,** 2731-8.

MEYER-WENTRUP, F., CAMBI, A., JOOSTEN, B., LOOMAN, M. W., DE VRIES, I. J., FIGDOR, C. G. & ADEMA, G. J. 2009. DCIR is endocytosed into human dendritic cells and inhibits TLR8-mediated cytokine production. *J Leukoc Biol,* 85**,** 518-25.

MIAO, E. A., ERNST, R. K., DORS, M., MAO, D. P. & ADEREM, A. 2008. Pseudomonas aeruginosa activates caspase 1 through Ipaf. *Proc Natl Acad Sci U S A,* 105**,** 2562-7.

MIAO, E. A., MAO, D. P., YUDKOVSKY, N., BONNEAU, R., LORANG, C. G., WARREN, S. E., LEAF, I. A. & ADEREM, A. 2010. Innate immune detection of the type III secretion apparatus through the NLRC4 inflammasome. *Proc Natl Acad Sci U S A,* 107**,** 3076-80.

MICHALSKA, M. & WOLF, P. 2015. Pseudomonas Exotoxin A: optimized by evolution for effective killing. *Frontiers in Microbiology,* 6**,** 963-963.

MISHRA, A. K., DRIESSEN, N. N., APPELMELK, B. J. & BESRA, G. S. 2011. Lipoarabinomannan and related glycoconjugates: structure, biogenesis and role in Mycobacterium tuberculosis physiology and host-pathogen interaction. *FEMS Microbiology Reviews,* 35**,** 1126-1157.

MISHRA, M., BYRD, M. S., SERGEANT, S., AZAD, A. K., PARSEK, M. R., MCPHAIL, L., SCHLESINGER, L. S. & WOZNIAK, D. J. 2012. Pseudomonas aeruginosa Psl polysaccharide reduces neutrophil phagocytosis and the oxidative response by limiting complement-mediated opsonization. *Cell Microbiol,* 14**,** 95-106.

MITCHELL, E. P., SABIN, C., ŠNAJDROVÁ, L., POKORNÁ, M., PERRET, S., GAUTIER, C., HOFR, C., GILBOA‐GARBER, N., KOČA, J. & WIMMEROVÁ, M. 2005. High affinity fucose binding of Pseudomonas aeruginosa lectin PA‐IIL: 1.0 Å resolution crystal structure of the complex combined with thermodynamics and computational chemistry approaches. *Proteins: Structure, Function, and Bioinformatics,* 58**,** 735-746.

MIURA, T., KAWAKAMI, K., KANNO, E., TANNO, H., TADA, H., SATO, N., MASAKI, A., YOKOYAMA, R., KAWAMURA, K., KITAI, Y., TAKAGI, N., YAMAGUCHI, K., YAMAGUCHI, N., KYO, Y., ISHII, K., IMAI, Y., SAIJO, S., IWAKURA, Y. &

TACHI, M. 2019. Dectin-2-Mediated Signaling Leads to Delayed Skin Wound Healing through Enhanced Neutrophilic Inflammatory Response and Neutrophil Extracellular Trap Formation. *J Invest Dermatol,* 139**,** 702-711.
MIYAKE, Y., TOYONAGA, K., MORI, D., KAKUTA, S., HOSHINO, Y., OYAMADA, A., YAMADA, H., ONO, K.-I., SUYAMA, M. & IWAKURA, Y. 2013. C-type lectin MCL is an FcRγ-coupled receptor that mediates the adjuvanticity of mycobacterial cord factor. *Immunity,* 38**,** 1050-1062.
MIYASAKA, T., AKAHORI, Y., TOYAMA, M., MIYAMURA, N., ISHII, K., SAIJO, S., IWAKURA, Y., KINJO, Y., MIYAZAKI, Y., OISHI, K. & KAWAKAMI, K. 2013. Dectin-2-dependent NKT cell activation and serotype-specific antibody production in mice immunized with pneumococcal polysaccharide vaccine. *PLoS One,* 8**,** e78611.
MOGENSEN, T. H. 2009. Pathogen Recognition and Inflammatory Signaling in Innate Immune Defenses. *Clinical Microbiology Reviews,* 22**,** 240-273.
MONTANARO, L., POGGI, A., VISAI, L., RAVAIOLI, S., CAMPOCCIA, D., SPEZIALE, P. & ARCIOLA, C. R. 2011. Extracellular DNA in biofilms. *The International Journal of Artificial Organs,* 34**,** 824-831.
MORADALI, M. F., GHODS, S. & REHM, B. H. 2017. Pseudomonas aeruginosa lifestyle: a paradigm for adaptation, survival, and persistence. *Frontiers in Cellular and Infection Microbiology,* 7**,** 39.
MORIS, A., PAJOT, A., BLANCHET, F., GUIVEL-BENHASSINE, F., SALCEDO, M. & SCHWARTZ, O. 2006. Dendritic cells and HIV-specific CD4+ T cells: HIV antigen presentation, T-cell activation, and viral transfer. *Blood,* 108**,** 1643-1651.
MORRIS, J. D., HEWITT, J. L., WOLFE, L. G., KAMATKAR, N. G., CHAPMAN, S. M., DIENER, J. M., COURTNEY, A. J., LEEVY, W. M. & SHROUT, J. D. 2011. Imaging and analysis of Pseudomonas aeruginosa swarming and rhamnolipid production. *Applied and Environmental Microbiology,* 77**,** 8310-8317.
MOSCOSO, J. A., MIKKELSEN, H., HEEB, S., WILLIAMS, P. & FILLOUX, A. 2011. The Pseudomonas aeruginosa sensor RetS switches type III and type VI secretion via c‐di‐GMP signalling. *Environmental Microbiology,* 13**,** 3128-3138.
MOSER, C., KJAERGAARD, S., PRESSLER, T., KHARAZMI, A., KOCH, C. & HØIBY, N. 2000. The immune response to chronic Pseudomonas aeruginosa lung infection in cystic fibrosis patients is predominantly of the Th2 type. *Apmis,* 108**,** 329-335.
MOSS, R., HSU, Y. P. & OLDS, L. 2000. Cytokine dysregulation in activated cystic fibrosis (CF) peripheral lymphocytes. *Clinical & Experimental Immunology,* 120**,** 518-525.
MOUTSOPOULOS, N. M., KONKEL, J., SARMADI, M., ESKAN, M. A., WILD, T., DUTZAN, N., ABUSLEME, L., ZENOBIA, C., HOSUR, K. B. & ABE, T. 2014. Defective neutrophil recruitment in leukocyte adhesion deficiency type I disease causes local IL-17–driven inflammatory bone loss. *Science Translational Medicine,* 6**,** 229ra40-229ra40.
MUHAMMAD, M. H., IDRIS, A. L., FAN, X., GUO, Y., YU, Y., JIN, X., QIU, J., GUAN, X. & HUANG, T. 2020. Beyond Risk: Bacterial Biofilms and Their Regulating Approaches. *Frontiers in Microbiology,* 11.
MULCAHY, H., CHARRON-MAZENOD, L. & LEWENZA, S. 2008. Extracellular DNA chelates cations and induces antibiotic resistance in Pseudomonas aeruginosa biofilms. *PLoS Pathog,* 4**,** e1000213.

MULCAHY, H., CHARRON‐MAZENOD, L. & LEWENZA, S. 2010. Pseudomonas aeruginosa produces an extracellular deoxyribonuclease that is required for utilization of DNA as a nutrient source. *Environmental Microbiology,* 12**,** 1621-1629.

MULCAHY, L. R., ISABELLA, V. M. & LEWIS, K. 2014. Pseudomonas aeruginosa biofilms in disease. *Microb Ecol,* 68**,** 1-12.

MULLER, P., GUGGENHEIM, B., ATTIN, T., MARLINGHAUS, E. & SCHMIDLIN, P. R. 2011. Potential of shock waves to remove calculus and biofilm. *Clin Oral Investig,* 15**,** 959-65.

MUMMIDI, S., CATANO, G., LAM, L., HOEFLE, A., TELLES, V., BEGUM, K., JIMENEZ, F., AHUJA, S. S. & AHUJA, S. K. 2001. Extensive repertoire of membrane-bound and soluble dendritic cell-specific ICAM-3-grabbing nonintegrin 1 (DC-SIGN1) and DC-SIGN2 isoforms. Inter-individual variation in expression of DC-SIGN transcripts. *J Biol Chem,* 276**,** 33196-212.

MUNDER, A., ROTHSCHUH, J., SCHIRMER, B., KLOCKGETHER, J., KAEVER, V., TÜMMLER, B., SEIFERT, R. & KLOTH, C. 2018. The Pseudomonas aeruginosa ExoY phenotype of high-copy-number recombinants is not detectable in natural isolates. *Open Biology,* 8**,** 170250.

MUNTAKA, S., ALMUHANNA, Y., JACKSON, D., SINGH, S., AFRYIE-ASANTE, A., CÁMARA, M. & MARTÍNEZ-POMARES, L. 2019. Gamma interferon and interleukin-17A differentially influence the response of human macrophages and neutrophils to Pseudomonas aeruginosa infection. *Infection and Immunity,* 87**,** e00814-18.

MURPHY, D. A. & COURTNEIDGE, S. A. 2011. The 'ins' and 'outs' of podosomes and invadopodia: characteristics, formation and function. *Nat Rev Mol Cell Biol,* 12**,** 413-26.

NAGAE, M., IKEDA, A., HANASHIMA, S., KOJIMA, T., MATSUMOTO, N., YAMAMOTO, K. & YAMAGUCHI, Y. 2016. Crystal structure of human dendritic cell inhibitory receptor C-type lectin domain reveals the binding mode with N-glycan. *FEBS letters,* 590**,** 1280-1288.

NAKAMURA, S., HIGASHIYAMA, Y., IZUMIKAWA, K., SEKI, M., KAKEYA, H., YAMAMOTO, Y., YANAGIHARA, K., MIYAZAKI, Y., MIZUTA, Y. & KOHNO, S. 2008. The roles of the quorum-sensing system in the release of extracellular DNA, lipopolysaccharide, and membrane vesicles from Pseudomonas aeruginosa. *Jpn J Infect Dis,* 61**,** 375-8.

NAVARRO, J., RAINISIO, M., HARMS, H., HODSON, M., KOCH, C., MASTELLA, G., STRANDVIK, B. & MCKENZIE, S. 2001. Factors associated with poor pulmonary function: cross-sectional analysis of data from the ERCF. *European Respiratory Journal,* 18**,** 298-305.

NEU, T. R., SWERHONE, G. D. & LAWRENCE, J. R. 2001. Assessment of lectin-binding analysis for in situ detection of glycoconjugates in biofilm systems. *Microbiology,* 147**,** 299-313.

NEWTON, K. & DIXIT, V. M. 2012. Signaling in innate immunity and inflammation. *Cold Spring Harbor Perspectives in Biology,* 4**,** a006049.

NG, L. G., QIN, J. S., ROEDIGER, B., WANG, Y., JAIN, R., CAVANAGH, L. L., SMITH, A. L., JONES, C. A., DE VEER, M. & GRIMBALDESTON, M. A. 2011. Visualizing the neutrophil response to sterile tissue injury in mouse dermis reveals a three-phase cascade of events. *Journal of Investigative Dermatology,* 131**,** 2058-2068.

NGUYEN, D. G. & HILDRETH, J. E. 2003. Involvement of macrophage mannose receptor in the binding and transmission of HIV by macrophages. *Eur J Immunol,* 33**,** 483-93.
NGUYEN, S. T., NGUYEN, H. L., PHAM, V. Q., NGUYEN, G. T., TRAN, C. D.-T., PHAN, N. K. & PHAM, P. V. 2015. Targeting specificity of dendritic cells on breast cancer stem cells: in vitro and in vivo evaluations. *OncoTargets and therapy,* 8**,** 323-334.
NIVENS, D. E., OHMAN, D. E., WILLIAMS, J. & FRANKLIN, M. J. 2001. Role of alginate and its O acetylation in formation of Pseudomonas aeruginosa microcolonies and biofilms. *J Bacteriol,* 183**,** 1047-57.
O'CONNOR, J. R., KUWADA, N. J., HUANGYUTITHAM, V., WIGGINS, P. A. & HARWOOD, C. S. 2012. Surface sensing and lateral subcellular localization of WspA, the receptor in a chemosensory-like system leading to c-di-GMP production. *Molecular Microbiology,* 86**,** 720-729.
O'SULLIVAN, B. P. & FREEDMAN, S. D. 2009. Cystic fibrosis. *The Lancet,* 373**,** 1891-1904.
O'TOOLE, G. 2011. Microtiter dish biofilm formation assay. JoVE. 47.
O'TOOLE, G. A. & KOLTER, R. 1998a. Flagellar and twitching motility are necessary for Pseudomonas aeruginosa biofilm development. *Molecular Microbiology,* 30**,** 295-304.
O'TOOLE, G. A. & KOLTER, R. 1998b. Initiation of biofilm formation in Pseudomonas fluorescens WCS365 proceeds via multiple, convergent signalling pathways: a genetic analysis. *Molecular Microbiology,* 28**,** 449-461.
OH, H., SIANO, B. & DIAMOND, S. 2008. Neutrophil isolation protocol. *Journal of Visualized Experiments***,** e745.
OJIELO, C. I., COOKE, K., MANCUSO, P., STANDIFORD, T. J., OLKIEWICZ, K. M., CLOUTHIER, S., CORRION, L., BALLINGER, M. N., TOEWS, G. B. & PAINE, R. 2003. Defective phagocytosis and clearance of Pseudomonas aeruginosa in the lung following bone marrow transplantation. *The Journal of Immunology,* 171**,** 4416-4424.
OPITZ, B., VAN LAAK, V., EITEL, J. & SUTTORP, N. 2010. Innate immune recognition in infectious and noninfectious diseases of the lung. *American journal of respiratory and critical care medicine,* 181**,** 1294-1309.
OVCHINNIKOV, D. A. 2008. Macrophages in the embryo and beyond: much more than just giant phagocytes. *Genesis,* 46**,** 447-462.
OVERHAGE, J., BAINS, M., BRAZAS, M. D. & HANCOCK, R. E. 2008. Swarming of Pseudomonas aeruginosa is a complex adaptation leading to increased production of virulence factors and antibiotic resistance. *Journal of Bacteriology,* 190**,** 2671-2679.
PAINTER, R. G., BONVILLAIN, R. W., VALENTINE, V. G., LOMBARD, G. A., LAPLACE, S. G., NAUSEEF, W. M. & WANG, G. 2008. The role of chloride anion and CFTR in killing of Pseudomonas aeruginosa by normal and CF neutrophils. *J Leukoc Biol,* 83**,** 1345-53.
PAINTER, R. G., MARRERO, L., LOMBARD, G. A., VALENTINE, V. G., NAUSEEF, W. M. & WANG, G. 2010. CFTR-mediated halide transport in phagosomes of human neutrophils. *J Leukoc Biol,* 87**,** 933-42.
PALOMO, J., MARCHIOL, T., PIOTET, J., FAUCONNIER, L., ROBINET, M., REVERCHON, F., LE BERT, M., TOGBE, D., BUIJS-OFFERMAN, R., STOLARCZYK, M., QUESNIAUX, V. F. J., SCHOLTE, B. J. & RYFFEL, B.

2014. Role of IL-1β in Experimental Cystic Fibrosis upon P. aeruginosa Infection. *PLoS One,* 9**,** e114884.
PAPAYANNOPOULOS, V. 2018. Neutrophil extracellular traps in immunity and disease. *Nature Reviews Immunology,* 18**,** 134.
PAPENFORT, K. & BASSLER, B. L. 2016. Quorum sensing signal-response systems in Gram-negative bacteria. *Nature reviews. Microbiology,* 14**,** 576-588.
PARK, B. S. & LEE, J.-O. 2013. Recognition of lipopolysaccharide pattern by TLR4 complexes. *Experimental & Molecular Medicine,* 45**,** e66-e66.
PARK, B. S., SONG, D. H., KIM, H. M., CHOI, B.-S., LEE, H. & LEE, J.-O. 2009. The structural basis of lipopolysaccharide recognition by the TLR4–MD-2 complex. *Nature,* 458**,** 1191-1195.
PARKER, D., COHEN, T. S., ALHEDE, M., HARFENIST, B. S., MARTIN, F. J. & PRINCE, A. 2012a. Induction of type I interferon signaling by Pseudomonas aeruginosa is diminished in cystic fibrosis epithelial cells. *American Journal of Respiratory Cell and Molecular Biology,* 46**,** 6-13.
PARKER, D. & PRINCE, A. 2011. Innate Immunity in the Respiratory Epithelium. *American Journal of Respiratory Cell and Molecular Biology,* 45**,** 189-201.
PARKER, D. & PRINCE, A. 2012. Staphylococcus aureus Induces Type I IFN Signaling in Dendritic Cells Via TLR9. *The Journal of Immunology,* 189**,** 4040.
PARKER, H., ALBRETT, A. M., KETTLE, A. J. & WINTERBOURN, C. C. 2012b. Myeloperoxidase associated with neutrophil extracellular traps is active and mediates bacterial killing in the presence of hydrogen peroxide. *Journal of Leukocyte Biology,* 91**,** 369-376.
PARKHURST, M. R. & SALTZMAN, W. M. 1992. Quantification of human neutrophil motility in three-dimensional collagen gels. Effect of collagen concentration. *Biophysical Journal,* 61**,** 306-315.
PARKHURST, M. R. & SALTZMAN, W. M. 1994. Leukocytes migrate through three-dimensional gels of midcycle cervical mucus. *Cellular Immunology,* 156**,** 77-94.
PARKS, Q. M., YOUNG, R. L., POCH, K. R., MALCOLM, K. C., VASIL, M. L. & NICK, J. A. 2009. Neutrophil enhancement of Pseudomonas aeruginosa biofilm development: human F-actin and DNA as targets for therapy. *Journal of Medical Microbiology,* 58**,** 492.
PASSADOR, L., COOK, J. M., GAMBELLO, M. J., RUST, L. & IGLEWSKI, B. H. 1993. Expression of Pseudomonas aeruginosa virulence genes requires cell-to-cell communication. *Science,* 260**,** 1127-1130.
PAZOS, M. A., LANTER, B. B., YONKER, L. M., EATON, A. D., PIRZAI, W., GRONERT, K., BONVENTRE, J. V. & HURLEY, B. P. 2017. Pseudomonas aeruginosa ExoU augments neutrophil transepithelial migration. *PLoS Pathogens,* 13**,** e1006548.
PEETERS, E., NELIS, H. J. & COENYE, T. 2008. Comparison of multiple methods for quantification of microbial biofilms grown in microtiter plates. *Journal of Microbiological Methods,* 72**,** 157-165.
PEREIRA, P. M., ALBRECHT, D., CULLEY, S., JACOBS, C., MARSH, M., MERCER, J. & HENRIQUES, R. 2019. Fix Your Membrane Receptor Imaging: Actin Cytoskeleton and CD4 Membrane Organization Disruption by Chemical Fixation. *Frontiers in Immunology,* 10**,** 675-675.
PESTRAK, M. J., CHANEY, S. B., EGGLESTON, H. C., DELLOS-NOLAN, S., DIXIT, S., MATHEW-STEINER, S. S., ROY, S., PARSEK, M. R., SEN, C. K. & WOZNIAK, D. J. 2018. Pseudomonas aeruginosa rugose small-colony variants

evade host clearance, are hyper-inflammatory, and persist in multiple host environments. *PLoS Pathogens,* 14**,** e1006842.
PETERS, B. M., JABRA-RIZK, M. A., GRAEME, A., COSTERTON, J. W. & SHIRTLIFF, M. E. 2012. Polymicrobial interactions: impact on pathogenesis and human disease. *Clinical Microbiology Reviews,* 25**,** 193-213.
PHAM, C. T. 2006. Neutrophil serine proteases: specific regulators of inflammation. *Nature Reviews Immunology,* 6**,** 541-550.
PIER, G. B. 1998. Pseudomonas aeruginosa: a key problem in cystic fibrosis. *Asm News,* 64**,** 339-347.
PIER, G. B., BOYER, D., PRESTON, M., COLEMAN, F. T., LLOSA, N., MUESCHENBORN-KOGLIN, S., THEILACKER, C., GOLDENBERG, H., UCHIN, J. & PRIEBE, G. P. 2004. Human monoclonal antibodies to Pseudomonas aeruginosa alginate that protect against infection by both mucoid and nonmucoid strains. *The Journal of Immunology,* 173**,** 5671-5678.
PIER, G. B., SAUNDERS, J. M., AMES, P., EDWARDS, M. S., AUERBACH, H., GOLDFARB, J., SPEERT, D. P. & HURWITCH, S. 1987. Opsonophagocytic killing antibody to Pseudomonas aeruginosa mucoid exopolysaccharide in older noncolonized patients with cystic fibrosis. *New England Journal of Medicine,* 317**,** 793-798.
PIETERSE, E., ROTHER, N., YANGINLAR, C., HILBRANDS, L. B. & VAN DER VLAG, J. 2016. Neutrophils discriminate between lipopolysaccharides of different bacterial sources and selectively release neutrophil extracellular traps. *Frontiers in Immunology,* 7**,** 484.
PLANQUETTE, B., TIMSIT, J. F., MISSET, B. Y., SCHWEBEL, C., AZOULAY, E., ADRIE, C., VESIN, A., JAMALI, S., ZAHAR, J. R., ALLAOUCHICHE, B., SOUWEINE, B., DARMON, M., DUMENIL, A. S., GOLDGRAN-TOLEDANO, D., MOURVILLIER, B. H. & BÉDOS, J. P. 2013. Pseudomonas aeruginosa ventilator-associated pneumonia. predictive factors of treatment failure. *Am J Respir Crit Care Med,* 188**,** 69-76.
PLANTINGA, M., DE HAAR, C. & NIERKENS, S. 2015. Dendritic Cells. *The Impact of Food Bioactives on Health.* Springer, Cham.
PNEUMATIKOS, I. A., DRAGOUMANIS, C. K. & BOUROS, D. E. 2009. Ventilator-associated pneumonia or endotracheal tube-associated pneumonia? An approach to the pathogenesis and preventive strategies emphasizing the importance of endotracheal tube. *Anesthesiology,* 110**,** 673-80.
PÖHLMANN, S., ZHANG, J., BARIBAUD, F., CHEN, Z., LESLIE, G. J., LIN, G., GRANELLI-PIPERNO, A., DOMS, R. W., RICE, C. M. & MCKEATING, J. A. 2003. Hepatitis C virus glycoproteins interact with DC-SIGN and DC-SIGNR. *Journal of Virology,* 77**,** 4070-4080.
POWELL, L. C., PRITCHARD, M. F., FERGUSON, E. L., POWELL, K. A., PATEL, S. U., RYE, P. D., SAKELLAKOU, S.-M., BUURMA, N. J., BRILLIANT, C. D. & COPPING, J. M. 2018. Targeted disruption of the extracellular polymeric network of Pseudomonas aeruginosa biofilms by alginate oligosaccharides. *Npj Biofilms and Microbiomes,* 4**,** 1-10.
PUEL, A., CYPOWYJ, S., BUSTAMANTE, J., WRIGHT, J. F., LIU, L., LIM, H. K., MIGAUD, M., ISRAEL, L., CHRABIEH, M. & AUDRY, M. 2011. Chronic mucocutaneous candidiasis in humans with inborn errors of interleukin-17 immunity. *Science,* 332**,** 65-68.
RAHMAN, T. 2016. *Interaction of Pseudomonas aeruginosa biofilm with inflammatory cytokines and immune cells.* University of Nottingham.

RAJARAM, M. V., ARNETT, E., AZAD, A. K., GUIRADO, E., NI, B., GERBERICK, A. D., HE, L.-Z., KELER, T., THOMAS, L. J. & LAFUSE, W. P. 2017. M. tuberculosis-initiated human mannose receptor signaling regulates macrophage recognition and vesicle trafficking by FcRγ-Chain, Grb2, and SHP-1. *Cell Reports,* 21**,** 126-140.

RAMPHAL, R., BALLOY, V., HUERRE, M., SI-TAHAR, M. & CHIGNARD, M. 2005. TLRs 2 and 4 are not involved in hypersusceptibility to acute Pseudomonas aeruginosa lung infections. *The Journal of Immunology,* 175**,** 3927-3934.

RANGEL, S. M., DIAZ, M. H., KNOTEN, C. A., ZHANG, A. & HAUSER, A. R. 2015. The role of ExoS in dissemination of Pseudomonas aeruginosa during pneumonia. *PLoS Pathogens,* 11**,** e1004945.

RAO, J., DAMRON, F. H., BASLER, M., DIGIANDOMENICO, A., SHERMAN, N. E., FOX, J. W., MEKALANOS, J. J. & GOLDBERG, J. B. 2011. Comparisons of two proteomic analyses of non-mucoid and mucoid Pseudomonas aeruginosa clinical isolates from a cystic fibrosis patient. *Frontiers in Microbiology,* 2**,** 162.

RAOUST, E., BALLOY, V., GARCIA-VERDUGO, I., TOUQUI, L., RAMPHAL, R. & CHIGNARD, M. 2009. Pseudomonas aeruginosa LPS or flagellin are sufficient to activate TLR-dependent signaling in murine alveolar macrophages and airway epithelial cells. *PloS One,* 4**,** e7259.

RASAMIRAVAKA, T., LABTANI, Q., DUEZ, P. & EL JAZIRI, M. 2015. The formation of biofilms by Pseudomonas aeruginosa: a review of the natural and synthetic compounds interfering with control mechanisms. *BioMed Research International,* 2015.

RASHID, M. H. & KORNBERG, A. 2000. Inorganic polyphosphate is needed for swimming, swarming, and twitching motilities of Pseudomonas aeruginosa. *Proceedings of the National Academy of Sciences,* 97**,** 4885-4890.

RATNER, D. & MUELLER, C. 2012. Immune responses in cystic fibrosis: are they intrinsically defective? *Am J Respir Cell Mol Biol,* 46**,** 715-22.

RAY, V. A., HILL, P. J., STOVER, C. K., ROY, S., SEN, C. K., YU, L., WOZNIAK, D. J. & DIGIANDOMENICO, A. 2017. Anti-Psl Targeting of Pseudomonas aeruginosa Biofilms for Neutrophil-Mediated Disruption. *Scientific Reports,* 7**,** 16065.

REBERNICK, R., FAHMY, L., GLOVER, C., BAWADEKAR, M., SHIM, D., HOLMES, C. L., RADEMACHER, N., POTLURI, H., BARTELS, C. M. & SHELEF, M. A. 2018. DNA Area and NETosis Analysis (DANA): a high-throughput method to quantify neutrophil extracellular traps in fluorescent microscope images. *Biological Procedures Online,* 20**,** 7.

REICHHARDT, C., JACOBS, H. M., MATWICHUK, M., WONG, C., WOZNIAK, D. J. & PARSEK, M. R. 2020. The versatile Pseudomonas aeruginosa biofilm matrix protein CdrA promotes aggregation through different extracellular EPS interactions. *Journal of Bacteriology*.

REICHHARDT, C. & PARSEK, M. R. 2019. Confocal Laser Scanning Microscopy for Analysis of Pseudomonas aeruginosa Biofilm Architecture and Matrix Localization. *Frontiers in Microbiology,* 10**,** 677-677.

REICHHARDT, C., WONG, C., DA SILVA, D. P., WOZNIAK, D. J. & PARSEK, M. R. 2018. CdrA interactions within the Pseudomonas aeruginosa biofilm matrix safeguard it from proteolysis and promote cellular packing. *MBio,* 9.

REIDING, K. R., FRANC, V., HUITEMA, M. G., BROUWER, E., HEERINGA, P. & HECK, A. J. 2019. Neutrophil myeloperoxidase harbors distinct site-specific

peculiarities in its glycosylation. *Journal of Biological Chemistry,* 294**,** 20233-20245.
RELLOSO, M., PUIG-KRÖGER, A., PELLO, O. M., RODRÍGUEZ-FERNÁNDEZ, J. L., DE LA ROSA, G., LONGO, N., NAVARRO, J., MUÑOZ-FERNÁNDEZ, M. A., SÁNCHEZ-MATEOS, P. & CORBÍ, A. L. 2002. DC-SIGN (CD209) expression is IL-4 dependent and is negatively regulated by IFN, TGF-beta, and anti-inflammatory agents. *J Immunol,* 168**,** 2634-43.
REYNOLDS, G. & HANIFFA, M. Human and Mouse Mononuclear Phagocyte Networks: A Tale of Two Species? Front Immunol. 2015; 6: 330. Epub 2015/07/01. doi: 10.3389/fimmu. 2015.00330 PMID: 26124761.
RICH, J. 2016. *Pseudomonas aeruginosa Exopolysaccharide Biosynthesis and Immunosuppressive Role in Vivo.* Graduate Studies.
RITTER, M., GROSS, O., KAYS, S., RULAND, J., NIMMERJAHN, F., SAIJO, S., TSCHOPP, J., LAYLAND, L. E. & PRAZERES DA COSTA, C. 2010. Schistosoma mansoni triggers Dectin-2, which activates the Nlrp3 inflammasome and alters adaptive immune responses. *Proc Natl Acad Sci U S A,* 107**,** 20459-64.
RIVIÈRE, M., MOISAND, A., LOPEZ, A. & PUZO, G. 2004. Highly ordered supra-molecular organization of the mycobacterial lipoarabinomannans in solution. Evidence of a relationship between supra-molecular organization and biological activity. *J Mol Biol,* 344**,** 907-18.
ROBINSON, M. J., OSORIO, F., ROSAS, M., FREITAS, R. P., SCHWEIGHOFFER, E., GROSS, O., VERBEEK, J. S., RULAND, J., TYBULEWICZ, V., BROWN, G. D., MOITA, L. F., TAYLOR, P. R. & REIS E SOUSA, C. 2009. Dectin-2 is a Syk-coupled pattern recognition receptor crucial for Th17 responses to fungal infection. *J Exp Med,* 206**,** 2037-51.
ROBINSON, R. W. & SNYDER, J. A. 2004. An innovative fixative for cytoskeletal components allows high resolution in colocalization studies using immunofluorescence techniques. *Histochem Cell Biol,* 122**,** 1-5.
ROHWEDDER, I., KURZ, A. R., PRUENSTER, M., IMMLER, R., PICK, R., EGGERSMANN, T., KLAPPROTH, S., JOHNSON, J. L., ALSINA, S. M. & LOWELL, C. A. 2019. Src family kinase-mediated vesicle trafficking is critical for neutrophil basement membrane penetration. *Haematologica*.
ROLÁN, H. G., DURAND, E. A. & MECSAS, J. 2013. Identifying Yersinia YopH-targeted signal transduction pathways that impair neutrophil responses during in vivo murine infection. *Cell host & microbe,* 14**,** 306-317.
ROMANI, N., REIDER, D., HEUER, M., EBNER, S., KÄMPGEN, E., EIBL, B., NIEDERWIESER, D. & SCHULER, G. 1996. Generation of mature dendritic cells from human blood. An improved method with special regard to clinical applicability. *J Immunol Methods,* 196**,** 137-51.
ROMERO, P. A., LUSSIER, M., VERONNEAU, S., SDICU, A.-M., HERSCOVICS, A. & BUSSEY, H. 1999. Mnt2p and Mnt3p of Saccharomyces cerevisiae are members of the Mnn1p family of α-1, 3-mannosyltransferases responsible for adding the terminal mannose residues of O-linked oligosaccharides. *Glycobiology,* 9**,** 1045-1051.
RÖMLING, U. & BALSALOBRE, C. 2012. Biofilm infections, their resilience to therapy and innovative treatment strategies. *Journal of Internal Medicine,* 272**,** 541-561.
ROSCHE, B., LI, X. Z., HAUER, B., SCHMID, A. & BUEHLER, K. 2009. Microbial biofilms: a concept for industrial catalysis? *Trends Biotechnol,* 27**,** 636-43.

ROSENTHAL, V. D., AL-ABDELY, H. M., EL-KHOLY, A. A., ALKHAWAJA, S. A. A., LEBLEBICIOGLU, H., MEHTA, Y., RAI, V., HUNG, N. V., KANJ, S. S. & SALAMA, M. F. 2016. International Nosocomial Infection Control Consortium report, data summary of 50 countries for 2010-2015: Device-associated module. *American Journal of Infection Control,* 44**,** 1495-1504.

ROSSI, M. & YOUNG, J. W. 2005. Human Dendritic Cells: Potent Antigen-Presenting Cells at the Crossroads of Innate and Adaptive Immunity. *The Journal of Immunology,* 175**,** 1373-1381.

ROUX, D., GAUDRY, S., DREYFUSS, D., EL-BENNA, J., DE PROST, N., DENAMUR, E., SAUMON, G. & RICARD, J.-D. 2009. Candida albicans impairs macrophage function and facilitates Pseudomonas aeruginosa pneumonia in rat. *Critical Care Medicine,* 37**,** 1062-1067.

ROWE, S. M., MILLER, S. & SORSCHER, E. J. 2005. Cystic Fibrosis. *New England Journal of Medicine,* 352**,** 1992-2001.

RUCHAUD‐SPARAGANO, M. H., MILLS, R., SCOTT, J. & SIMPSON, A. J. 2014. MPLA inhibits release of cytotoxic mediators from human neutrophils while preserving efficient bacterial killing. *Immunology and Cell Biology,* 92**,** 799-809.

RUFFIN, M. & BROCHIERO, E. 2019. Repair Process Impairment by Pseudomonas aeruginosa in Epithelial Tissues: Major Features and Potential Therapeutic Avenues. *Frontiers in Cellular and Infection Microbiology,* 9.

RUSSELL, A. B., HOOD, R. D., BUI, N. K., LEROUX, M., VOLLMER, W. & MOUGOUS, J. D. 2011. Type VI secretion delivers bacteriolytic effectors to target cells. *Nature,* 475**,** 343-347.

RYBTKE, M., BERTHELSEN, J., YANG, L., HØIBY, N., GIVSKOV, M. & TOLKER‐NIELSEN, T. 2015a. The LapG protein plays a role in Pseudomonas aeruginosa biofilm formation by controlling the presence of the CdrA adhesin on the cell surface. *Microbiologyopen,* 4**,** 917-930.

RYBTKE, M., HULTQVIST, L. D., GIVSKOV, M. & TOLKER-NIELSEN, T. 2015b. Pseudomonas aeruginosa biofilm infections: community structure, antimicrobial tolerance and immune response. *Journal of Molecular Biology,* 427**,** 3628-3645.

RYDER, C., BYRD, M. & WOZNIAK, D. J. 2007. Role of polysaccharides in Pseudomonas aeruginosa biofilm development. *Current Opinion in Microbiology,* 10**,** 644-648.

SABIN, C., MITCHELL, E. P., POKORNÁ, M., GAUTIER, C., UTILLE, J.-P., WIMMEROVÁ, M. & IMBERTY, A. 2006. Binding of different monosaccharides by lectin PA-IIL from Pseudomonas aeruginosa: thermodynamics data correlated with X-ray structures. *FEBS letters,* 580**,** 982-987.

SAFDAR, N., CRNICH, C. J. & MAKI, D. G. 2005. The pathogenesis of ventilator-associated pneumonia: its relevance to developing effective strategies for prevention. *Respir Care,* 50**,** 725-39; discussion 739-41.

SAIJO, S., IKEDA, S., YAMABE, K., KAKUTA, S., ISHIGAME, H., AKITSU, A., FUJIKADO, N., KUSAKA, T., KUBO, S., CHUNG, S. H., KOMATSU, R., MIURA, N., ADACHI, Y., OHNO, N., SHIBUYA, K., YAMAMOTO, N., KAWAKAMI, K., YAMASAKI, S., SAITO, T., AKIRA, S. & IWAKURA, Y. 2010. Dectin-2 recognition of alpha-mannans and induction of Th17 cell differentiation is essential for host defense against Candida albicans. *Immunity,* 32**,** 681-91.

SAIJO, S. & IWAKURA, Y. 2011. Dectin-1 and Dectin-2 in innate immunity against fungi. *Int Immunol,* 23**,** 467-72.

SAINT-CRIQ, V. & GRAY, M. A. 2017. Role of CFTR in epithelial physiology. *Cellular and Molecular Life Sciences,* 74**,** 93-115.

SAITOH, T., KOMANO, J., SAITOH, Y., MISAWA, T., TAKAHAMA, M., KOZAKI, T., UEHATA, T., IWASAKI, H., OMORI, H. & YAMAOKA, S. 2012. Neutrophil extracellular traps mediate a host defense response to human immunodeficiency virus-1. *Cell Host & Microbe,* 12**,** 109-116.

SAKURAGI, Y. & KOLTER, R. 2007. Quorum-sensing regulation of the biofilm matrix genes (pel) of Pseudomonas aeruginosa. *J Bacteriol,* 189**,** 5383-6.

SALLUSTO, F., CELLA, M., DANIELI, C. & LANZAVECCHIA, A. 1995. Dendritic cells use macropinocytosis and the mannose receptor to concentrate macromolecules in the major histocompatibility complex class II compartment: downregulation by cytokines and bacterial products. *The Journal of Experimental Medicine,* 182**,** 389-400.

SALLUSTO, F. & LANZAVECCHIA, A. 1994. Efficient presentation of soluble antigen by cultured human dendritic cells is maintained by granulocyte/macrophage colony-stimulating factor plus interleukin 4 and downregulated by tumor necrosis factor alpha. *J Exp Med,* 179**,** 1109-18.

SANA, T. G., BERNI, B. & BLEVES, S. 2016. The T6SSs of Pseudomonas aeruginosa strain PAO1 and their effectors: beyond bacterial-cell targeting. *Frontiers in cellular and infection microbiology,* 6**,** 61.

SANA, T. G., HACHANI, A., BUCIOR, I., SOSCIA, C., GARVIS, S., TERMINE, E., ENGEL, J., FILLOUX, A. & BLEVES, S. 2012. The second type VI secretion system of Pseudomonas aeruginosa strain PAO1 is regulated by quorum sensing and Fur and modulates internalization in epithelial cells. *Journal of Biological Chemistry,* 287**,** 27095-27105.

SATO, K., YANG, X. L., YUDATE, T., CHUNG, J. S., WU, J., LUBY-PHELPS, K., KIMBERLY, R. P., UNDERHILL, D., CRUZ, P. D., JR. & ARIIZUMI, K. 2006. Dectin-2 is a pattern recognition receptor for fungi that couples with the Fc receptor gamma chain to induce innate immune responses. *J Biol Chem,* 281**,** 38854-66.

SCHELSTRAETE, P., HAERYNCK, F., DESEYNE, S. & DE BAETS, F. 2013. Eradication therapy for Pseudomonas aeruginosa colonization episodes in cystic fibrosis patients not chronically colonized by P. aeruginosa. *Journal of Cystic Fibrosis,* 12**,** 1-8.

SCHINDELIN, J., ARGANDA-CARRERAS, I., FRISE, E., KAYNIG, V., LONGAIR, M., PIETZSCH, T., PREIBISCH, S., RUEDEN, C., SAALFELD, S. & SCHMID, B. 2012. Fiji: an open-source platform for biological-image analysis. *Nature methods,* 9**,** 676-682.

SCHLESINGER, L. S., HULL, S. R. & KAUFMAN, T. M. 1994. Binding of the terminal mannosyl units of lipoarabinomannan from a virulent strain of Mycobacterium tuberculosis to human macrophages. *The Journal of Immunology,* 152**,** 4070-4079.

SCHROEDER, T. H., LEE, M. M., YACONO, P. W., CANNON, C. L., GERÇEKER, A. A., GOLAN, D. E. & PIER, G. B. 2002. CFTR is a pattern recognition molecule that extracts Pseudomonas aeruginosa LPS from the outer membrane into epithelial cells and activates NF-κB translocation. *Proceedings of the National Academy of Sciences,* 99**,** 6907-6912.

SCHUREK, K. N., BREIDENSTEIN, E. B. & HANCOCK, R. E. 2012. Pseudomonas aeruginosa: a persistent pathogen in cystic fibrosis and hospital-associated infections. *Antibiotic Discovery and Development.* Springer.

SCHUSTER, M. & GREENBERG, E. P. 2006. A network of networks: quorum-sensing gene regulation in Pseudomonas aeruginosa. *Int J Med Microbiol,* 296**,** 73-81.
SCHUSTER, M., LOSTROH, C. P., OGI, T. & GREENBERG, E. P. 2003. Identification, timing, and signal specificity of Pseudomonas aeruginosa quorum-controlled genes: a transcriptome analysis. *J Bacteriol,* 185**,** 2066-79.
SCHWEIZER, A., STAHL, P. D. & ROHRER, J. 2000. A di-aromatic motif in the cytosolic tail of the mannose receptor mediates endosomal sorting. *Journal of Biological Chemistry,* 275**,** 29694-29700.
SCHWIEBERT, E. M., BENOS, D. J., EGAN, M. E., STUTTS, M. J. & GUGGINO, W. B. 1999. CFTR is a conductance regulator as well as a chloride channel. *Physiological reviews,* 79**,** S145-S166.
SEEDS, R. E., GORDON, S. & MILLER, J. L. 2009. Characterisation of myeloid receptor expression and interferon alpha/beta production in murine plasmacytoid dendritic cells by flow cytomtery. *J Immunol Methods,* 350**,** 106-17.
SEGAL, A. W. 2005. How neutrophils kill microbes. *Annu Rev Immunol,* 23**,** 197-223.
SEGURA, E., TOUZOT, M., BOHINEUST, A., CAPPUCCIO, A., CHIOCCHIA, G., HOSMALIN, A., DALOD, M., SOUMELIS, V. & AMIGORENA, S. 2013. Human inflammatory dendritic cells induce Th17 cell differentiation. *Immunity,* 38**,** 336-348.
SENGUPTA, S., HITTLE, L. E., ERNST, R. K., URIARTE, S. M. & MITCHELL, T. C. 2016. A Pseudomonas aeruginosa hepta‐acylated lipid A variant associated with cystic fibrosis selectively activates human neutrophils. *Journal of Leukocyte Biology,* 100**,** 1047-1059.
SERRA, R., GRANDE, R., BUTRICO, L., ROSSI, A., SETTIMIO, U. F., CAROLEO, B., AMATO, B., GALLELLI, L. & DE FRANCISCIS, S. 2015. Chronic wound infections: the role of Pseudomonas aeruginosa and Staphylococcus aureus. *Expert Review of Anti-infective Therapy,* 13**,** 605-613.
SHEETZ, M. P., FELSENFELD, D. P. & GALBRAITH, C. G. 1998. Cell migration: regulation of force on extracellular-matrix-integrin complexes. *Trends in Cell Biology,* 8**,** 51-54.
SHENOY, A., KOPIC, S., MUREK, M., CAPUTO, C., GEIBEL, J. P. & EGAN, M. E. 2011. Calcium-modulated chloride pathways contribute to chloride flux in murine cystic fibrosis-affected macrophages. *Pediatr Res,* 70**,** 447-52.
SHEPHERD, V. L. & HOIDAL, J. R. 1990. Clearance of neutrophil-derived myeloperoxidase by the macrophage mannose receptor. *Am J Respir Cell Mol Biol,* 2**,** 335-340.
SHEPPARD, D. N. & WELSH, M. J. 1999. Structure and function of the CFTR chloride channel. *Physiological reviews,* 79**,** S23-S45.
SHIBATA, N., AKAGI, R., HOSOYA, T., KAWAHARA, K., SUZUKI, A., IKUTA, K., KOBAYASHI, H., HISAMICHI, K., OKAWA, Y. & SUZUKI, S. 1996. Existence of novel branched side chains containing-1, 2 and-1, 6 linkages corresponding to antigenic factor 9 in the mannan of Candida guilliermondii. *Journal of Biological Chemistry,* 271**,** 9259-9266.
SHIBATA, N., KOBAYASHI, H. & SUZUKI, S. 2012. Immunochemistry of pathogenic yeast, Candida species, focusing on mannan. *Proc Jpn Acad Ser B Phys Biol Sci,* 88**,** 250-65.
SHINOHARA, H., NAGI-MIURA, N., ISHIBASHI, K., ADACHI, Y., ISHIDA-OKAWARA, A., OHARASEKI, T., TAKAHASHI, K., NAOE, S., SUZUKI, K. & OHNO, N. 2006. Beta-mannosyl linkages negatively regulate anaphylaxis and vasculitis in

mice, induced by CAWS, fungal PAMPS composed of mannoprotein-beta-glucan complex secreted by Candida albicans. *Biol Pharm Bull,* 29**,** 1854-61.
SHIRTLIFF, M., LEID, J. G. & SHIRTLIFF, M. 2009. *The Role of Biofilms in Device-Related Infections*, Springer.
SHOCHAT, E., ROM-KEDAR, V. & SEGEL, L. 2007. G-CSF control of neutrophils dynamics in the blood. *Bulletin of Mathematical Biology,* 69**,** 2299-2338.
SHROUT, J. D., CHOPP, D. L., JUST, C. L., HENTZER, M., GIVSKOV, M. & PARSEK, M. R. 2006. The impact of quorum sensing and swarming motility on Pseudomonas aeruginosa biofilm formation is nutritionally conditional. *Mol Microbiol,* 62**,** 1264-77.
SIBLEY, C. D., PARKINS, M. D., RABIN, H. R., DUAN, K., NORGAARD, J. C. & SURETTE, M. G. 2008. A polymicrobial perspective of pulmonary infections exposes an enigmatic pathogen in cystic fibrosis patients. *Proceedings of the National Academy of Sciences,* 105**,** 15070-15075.
SICHIEN, D., LAMBRECHT, B., GUILLIAMS, M. & SCOTT, C. 2017. Development of conventional dendritic cells: from common bone marrow progenitors to multiple subsets in peripheral tissues. *Mucosal immunology,* 10**,** 831-844.
SIDDIQUI, A. R. & BERNSTEIN, J. M. 2010. Chronic wound infection: facts and controversies. *Clinics in Dermatology,* 28**,** 519-526.
SILHAVY, T. J., KAHNE, D. & WALKER, S. 2010. The bacterial cell envelope. *Cold Spring Harbor perspectives in biology,* 2**,** a000414.
SILVA, M. T. 2011. Macrophage phagocytosis of neutrophils at inflammatory/infectious foci: a cooperative mechanism in the control of infection and infectious inflammation. *Journal of Leukocyte Biology,* 89**,** 675-683.
SIMMONS, G., REEVES, J. D., GROGAN, C. C., VANDENBERGHE, L. H., BARIBAUD, F., WHITBECK, J. C., BURKE, E., BUCHMEIER, M. J., SOILLEUX, E. J., RILEY, J. L., DOMS, R. W., BATES, P. & PÖHLMANN, S. 2003. DC-SIGN and DC-SIGNR bind ebola glycoproteins and enhance infection of macrophages and endothelial cells. *Virology,* 305**,** 115-23.
SINGH, P. K., YADAV, V. K., KALIA, M., SHARMA, D., PANDEY, D. & AGARWAL, V. 2019. Pseudomonas aeruginosa quorum-sensing molecule N-(3-oxo-dodecanoyl)-l-homoserine lactone triggers mitochondrial dysfunction and apoptosis in neutrophils through calcium signaling. *Medical Microbiology and Immunology,* 208**,** 855-868.
SINGH, S., ALMUHANNA, Y., ALSHAHRANI, M. Y., LOWMAN, D., RICE, P. J., GELL, C., MA, Z., GRAVES, B., JACKSON, D., LEE, K., KELKAR, R., KORANTENG, J., MITCHELL, D., SILVA, A. D., HUSSAIN, F., YILMAZ, G., MASTROTTO, F., IRIE, Y., WILLIAMS, P., WILLIAMS, D., CAMARA, M. & MARTINEZ-POMARES, L. 2020. Pseudomonas aeruginosa biofilms display carbohydrate ligands for CD206 and CD209 that interfere with their receptor function. *bioRxiv***,** 2020.04.20.051292.
SINGH, S., BARR, H., LIU, Y.-C., ROBINS, A., HEEB, S., WILLIAMS, P., FOGARTY, A., CÁMARA, M. & MARTINEZ-POMARES, L. 2015. Granulocyte-macrophage colony stimulatory factor enhances the pro-inflammatory response of interferon-γ-treated macrophages to Pseudomonas aeruginosa infection. *PLoS One,* 10**,** e0117447.
SIT, S. T. & MANSER, E. 2011. Rho GTPases and their role in organizing the actin cytoskeleton. *J Cell Sci,* 124**,** 679-83.
SKINDERSOE, M. E., ZEUTHEN, L. H., BRIX, S., FINK, L. N., LAZENBY, J., WHITTALL, C., WILLIAMS, P., DIGGLE, S. P., FROEKIAER, H., COOLEY, M.

& GIVSKOV, M. 2009. Pseudomonas aeruginosa quorum-sensing signal molecules interfere with dendritic cell-induced T-cell proliferation. *FEMS Immunology & Medical Microbiology,* 55**,** 335-345.

SMITH, A. J., GRAVES, B., CHILD, R., RICE, P. J., MA, Z., LOWMAN, D. W., ENSLEY, H. E., RYTER, K. T., EVANS, J. T. & WILLIAMS, D. L. 2018a. Immunoregulatory activity of the natural product laminarin varies widely as a result of its physical properties. *The Journal of Immunology,* 200**,** 788-799.

SMITH, A. L., GANESH, L., LEUNG, K., JONGSTRA-BILEN, J., JONGSTRA, J. & NABEL, G. J. 2007. Leukocyte-specific protein 1 interacts with DC-SIGN and mediates transport of HIV to the proteasome in dendritic cells. *The Journal of Experimental Medicine,* 204**,** 421-430.

SMITH, E. E., BUCKLEY, D. G., WU, Z., SAENPHIMMACHAK, C., HOFFMAN, L. R., D'ARGENIO, D. A., MILLER, S. I., RAMSEY, B. W., SPEERT, D. P., MOSKOWITZ, S. M., BURNS, J. L., KAUL, R. & OLSON, M. V. 2006. Genetic adaptation by Pseudomonas aeruginosa to the airways of cystic fibrosis patients. *Proc Natl Acad Sci U S A,* 103**,** 8487-92.

SMITH, S. R., SCHAAF, K., RAJABALEE, N., WAGNER, F., DUVERGER, A., KUTSCH, O. & SUN, J. 2018b. The phosphatase PPM1A controls monocyte-to-macrophage differentiation. *Scientific Reports,* 8**,** 1-14.

SOEHNLEIN, O. & LINDBOM, L. 2010. Phagocyte partnership during the onset and resolution of inflammation. *Nature Reviews Immunology,* 10**,** 427-439.

SOILLEUX, E. J., MORRIS, L. S., LESLIE, G., CHEHIMI, J., LUO, Q., LEVRONEY, E., TROWSDALE, J., MONTANER, L. J., DOMS, R. W., WEISSMAN, D., COLEMAN, N. & LEE, B. 2002. Constitutive and induced expression of DC-SIGN on dendritic cell and macrophage subpopulations in situ and in vitro. *Journal of Leukocyte Biology,* 71**,** 445-457.

SØNDERHOLM, M., KRAGH, K. N., KOREN, K., JAKOBSEN, T. H., DARCH, S. E., ALHEDE, M., JENSEN, P. Ø., WHITELEY, M., KÜHL, M. & BJARNSHOLT, T. 2017. Pseudomonas aeruginosa aggregate formation in an alginate bead model system exhibits in vivo-like characteristics. *Appl. Environ. Microbiol.,* 83**,** e00113-17.

SOONG, G., REDDY, B., SOKOL, S., ADAMO, R. & PRINCE, A. 2004. TLR2 is mobilized into an apical lipid raft receptor complex to signal infection in airway epithelial cells. *The Journal of Clinical Investigation,* 113**,** 1482-1489.

SOUSA, A. M. & PEREIRA, M. O. 2014. Pseudomonas aeruginosa Diversification during Infection Development in Cystic Fibrosis Lungs-A Review. *Pathogens,* 3**,** 680-703.

SPEERT, D. P. & GORDON, S. 1992. Phagocytosis of unopsonized Pseudomonas aeruginosa by murine macrophages is a two-step process requiring glucose. *J Clin Invest,* 90**,** 1085-92.

SPEERT, D. P., WRIGHT, S. D., SILVERSTEIN, S. C. & MAH, B. 1988. Functional characterization of macrophage receptors for in vitro phagocytosis of unopsonized Pseudomonas aeruginosa. *J Clin Invest,* 82**,** 872-9.

SRIVASTAVA, D. & WATERS, C. M. 2012. A Tangled Web: Regulatory Connections between Quorum Sensing and Cyclic Di-GMP. *Journal of Bacteriology,* 194**,** 4485.

ST-LAURENT, J., BOULAY, M. E., PRINCE, P., BISSONNETTE, E. & BOULET, L. P. 2006. Comparison of cell fixation methods of induced sputum specimens: an immunocytochemical analysis. *J Immunol Methods,* 308**,** 36-42.

STAREK, M., KOLEV, K. I., BERTHIAUME, L., YEUNG, C. W., SLEEP, B. E., WOLFAARDT, G. M. & HAUSNER, M. 2011. A flow cell simulating a subsurface rock fracture for investigations of groundwater-derived biofilms. *Int Microbiol,* 14**,** 163-71.

STARKEY, M., HICKMAN, J. H., MA, L., ZHANG, N., DE LONG, S., HINZ, A., PALACIOS, S., MANOIL, C., KIRISITS, M. J. & STARNER, T. D. 2009. Pseudomonas aeruginosa rugose small-colony variants have adaptations that likely promote persistence in the cystic fibrosis lung. *Journal of Bacteriology,* 191**,** 3492-3503.

STEICHEN, A. L., BINSTOCK, B. J., MISHRA, B. B. & SHARMA, J. 2013. C-type lectin receptor Clec4d plays a protective role in resolution of Gram-negative pneumonia. *Journal of Leukocyte Biology,* 94**,** 393-398.

STEIN, M., KESHAV, S., HARRIS, N. & GORDON, S. 1992. Interleukin 4 potently enhances murine macrophage mannose receptor activity: a marker of alternative immunologic macrophage activation. *J Exp Med,* 176**,** 287-92.

STEINMAN, R. M. & INABA, K. 1999. Myeloid dendritic cells. *J Leukoc Biol,* 66**,** 205-8.

STEPANOVIĆ, S., VUKOVIĆ, D., DAKIĆ, I., SAVIĆ, B. & ŠVABIĆ-VLAHOVIĆ, M. 2000. A modified microtiter-plate test for quantification of staphylococcal biofilm formation. *Journal of Microbiological Methods,* 40**,** 175-179.

STEWART, P. S. 2014. Biophysics of biofilm infection. *Pathogens and Disease,* 70**,** 212-218.

STOODLEY, P., SAUER, K., DAVIES, D. G. & COSTERTON, J. W. 2002. Biofilms as complex differentiated communities. *Annu Rev Microbiol,* 56**,** 187-209.

STOVER, C. K., PHAM, X. Q., ERWIN, A., MIZOGUCHI, S., WARRENER, P., HICKEY, M., BRINKMAN, F., HUFNAGLE, W., KOWALIK, D. & LAGROU, M. 2000. Complete genome sequence of Pseudomonas aeruginosa PAO1, an opportunistic pathogen. *Nature,* 406**,** 959-964.

STRASSER, D., NEUMANN, K., BERGMANN, H., MARAKALALA, M. J., GULER, R., ROJOWSKA, A., HOPFNER, K.-P., BROMBACHER, F., URLAUB, H. & BAIER, G. 2012. Syk kinase-coupled C-type lectin receptors engage protein kinase C-δ to elicit Card9 adaptor-mediated innate immunity. *Immunity,* 36**,** 32-42.

STRATHMANN, M., WINGENDER, J. & FLEMMING, H.-C. 2002. Application of fluorescently labelled lectins for the visualization and biochemical characterization of polysaccharides in biofilms of Pseudomonas aeruginosa. *Journal of Microbiological Methods,* 50**,** 237-248.

SUAREZ-CUARTIN, G., SMITH, A., ABO-LEYAH, H., RODRIGO-TROYANO, A., PEREA, L., VIDAL, S., PLAZA, V., FARDON, T. C., SIBILA, O. & CHALMERS, J. D. 2017. Anti-Pseudomonas aeruginosa IgG antibodies and chronic airway infection in bronchiectasis. *Respiratory Medicine,* 128**,** 1-6.

SUMMERS, C., RANKIN, S. M., CONDLIFFE, A. M., SINGH, N., PETERS, A. M. & CHILVERS, E. R. 2010. Neutrophil kinetics in health and disease. *Trends in Immunology,* 31**,** 318-324.

SUTTERWALA, F. S., MIJARES, L. A., LI, L., OGURA, Y., KAZMIERCZAK, B. I. & FLAVELL, R. A. 2007. Immune recognition of Pseudomonas aeruginosa mediated by the IPAF/NLRC4 inflammasome. *J Exp Med,* 204**,** 3235-45.

ŠVAJGER, U., ANDERLUH, M., JERAS, M. & OBERMAJER, N. 2010. C-type lectin DC-SIGN: an adhesion, signalling and antigen-uptake molecule that guides dendritic cells in immunity. *Cellular signalling,* 22**,** 1397-1405.

SWARTJES, J. J., DAS, T., SHARIFI, S., SUBBIAHDOSS, G., SHARMA, P. K., KROM, B. P., BUSSCHER, H. J. & VAN DER MEI, H. C. 2013. A functional DNase I coating to prevent adhesion of bacteria and the formation of biofilm. *Advanced Functional Materials,* 23**,** 2843-2849.

SWETMAN ANDERSEN, C. A., HANDLEY, M., POLLARA, G., RIDLEY, A. J., KATZ, D. R. & CHAIN, B. M. 2006. β1-Integrins determine the dendritic morphology which enhances DC-SIGN-mediated particle capture by dendritic cells. *International Immunology,* 18**,** 1295-1303.

SWIECKI, M. & COLONNA, M. 2015. The multifaceted biology of plasmacytoid dendritic cells. *Nature Reviews Immunology,* 15**,** 471-485.

SZOLNOKY, G., BATA-CSÖRGÖ, Z., KENDERESSY, A. S., KISS, M., PIVARCSI, A., NOVÁK, Z., NEWMAN, K. N., MICHEL, G., RUZICKA, T. & MARÓDI, L. 2001. A mannose-binding receptor is expressed on human keratinocytes and mediates killing of Candida albicans. *Journal of Investigative Dermatology,* 117**,** 205-213.

TABOR, D., OGANESYAN, V., KELLER, A., YU, L., MCLAUGHLIN, R., SONG, E., WARRENER, P., ROSENTHAL, K., ESSER, M. & QI, Y. 2018. Pseudomonas aeruginosa PcrV and Psl, the molecular targets of bispecific antibody MEDI3902, are conserved among diverse global clinical isolates. *The Journal of Infectious Diseases,* 218**,** 1983-1994.

TACCONELLI, E., MAGRINI, N., KAHLMETER, G. & SINGH, N. 2017. Global priority list of antibiotic-resistant bacteria to guide research, discovery, and development of new antibiotics. *World Health Organization,* 27**,** 318-327.

TACKEN, P. J., GINTER, W., BEROD, L., CRUZ, L. J., JOOSTEN, B., SPARWASSER, T., FIGDOR, C. G. & CAMBI, A. 2011. Targeting DC-SIGN via its neck region leads to prolonged antigen residence in early endosomes, delayed lysosomal degradation, and cross-presentation. *Blood,* 118**,** 4111-4119.

TAHERI, N., FAHLGREN, A. & FÄLLMAN, M. 2016. Yersinia pseudotuberculosis blocks neutrophil degranulation. *Infection and immunity,* 84**,** 3369-3378.

TAKEUCHI, O. & AKIRA, S. 2010. Pattern recognition receptors and inflammation. *Cell,* 140**,** 805-20.

TALLANT, T., DEB, A., KAR, N., LUPICA, J., DE VEER, M. J. & DIDONATO, J. A. 2004. Flagellin acting via TLR5 is the major activator of key signaling pathways leading to NF-κB and proinflammatory gene program activation in intestinal epithelial cells. *BMC Microbiology,* 4**,** 1-24.

TANG, H., KAYS, M. & PRINCE, A. 1995. Role of Pseudomonas aeruginosa pili in acute pulmonary infection. *Infection and Immunity,* 63**,** 1278-1285.

TANG, L.-L., ZHANG, Z., ZHENG, J.-S., SHENG, J.-F. & LIU, K.-Z. 2005. Phenotypic and functional characteristics of dendritic cells derived from human peripheral blood monocytes. *Journal of Zhejiang University. Science. B,* 6**,** 1176-1181.

TAY, W. H., CHONG, K. K. L. & KLINE, K. A. 2016. Polymicrobial–host interactions during infection. *Journal of molecular biology,* 428**,** 3355-3371.

TAYLOR, P. R., BROWN, G. D., REID, D. M., WILLMENT, J. A., MARTINEZ-POMARES, L., GORDON, S. & WONG, S. Y. 2002. The β-glucan receptor, dectin-1, is predominantly expressed on the surface of cells of the monocyte/macrophage and neutrophil lineages. *The Journal of Immunology,* 169**,** 3876-3882.

TAYLOR, P. R., GORDON, S. & MARTINEZ-POMARES, L. 2005a. The mannose receptor: linking homeostasis and immunity through sugar recognition. *Trends in Immunology,* 26**,** 104-110.

TAYLOR, P. R., REID, D. M., HEINSBROEK, S. E., BROWN, G. D., GORDON, S. & WONG, S. Y. 2005b. Dectin-2 is predominantly myeloid restricted and exhibits unique activation-dependent expression on maturing inflammatory monocytes elicited in vivo. *Eur J Immunol,* 35**,** 2163-74.

TAYLOR, P. R., ROY, S., LEAL JR, S. M., SUN, Y., HOWELL, S. J., COBB, B. A., LI, X. & PEARLMAN, E. 2014. Activation of neutrophils by autocrine IL-17A-IL-17RC interactions during fungal infection is regulated by IL-6, IL-23, ROR [gamma] t and dectin-2. *Nature immunology,* 15**,** 143-151.

TAYLOR, P. R., TSONI, S. V., WILLMENT, J. A., DENNEHY, K. M., ROSAS, M., FINDON, H., HAYNES, K., STEELE, C., BOTTO, M. & GORDON, S. 2007. Dectin-1 is required for β-glucan recognition and control of fungal infection. *Nature Immunology,* 8**,** 31-38.

TEL, J., VAN DER LEUN, A. M., FIGDOR, C. G., TORENSMA, R. & DE VRIES, I. J. M. 2012. Harnessing human plasmacytoid dendritic cells as professional APCs. *Cancer Immunology, Immunotherapy,* 61**,** 1279-1288.

THADEN, J. T., KELLER, A. E., SHIRE, N. J., CAMARA, M. M., OTTERSON, L., HUBAND, M., GUENTHER, C. M., ZHAO, W., WARRENER, P., STOVER, C. K., FOWLER, V. G., JR & DIGIANDOMENICO, A. 2015. Pseudomonas aeruginosa Bacteremic Patients Exhibit Nonprotective Antibody Titers Against Therapeutic Antibody Targets PcrV and Psl Exopolysaccharide. *The Journal of Infectious Diseases,* 213**,** 640-648.

THANABALASURIAR, A., SCOTT, B. N. V., PEISELER, M., WILLSON, M. E., ZENG, Z., WARRENER, P., KELLER, A. E., SUREWAARD, B. G. J., DOZIER, E. A., KORHONEN, J. T., CHENG, L. I., GADJEVA, M., STOVER, C. K., DIGIANDOMENICO, A. & KUBES, P. 2019. Neutrophil Extracellular Traps Confine Pseudomonas aeruginosa Ocular Biofilms and Restrict Brain Invasion. *Cell Host Microbe,* 25**,** 526-536.e4.

THAYSEN-ANDERSEN, M., VENKATAKRISHNAN, V., LOKE, I., LAURINI, C., DIESTEL, S., PARKER, B. L. & PACKER, N. H. 2015. Human neutrophils secrete bioactive paucimannosidic proteins from azurophilic granules into pathogen-infected sputum. *J Biol Chem,* 290**,** 8789-802.

THOMEN, P., ROBERT, J., MONMEYRAN, A., BITBOL, A.-F., DOUARCHE, C. & HENRY, N. 2017. Bacterial biofilm under flow: first a physical struggle to stay, then a matter of breathing. *PloS one,* 12**,** e0175197.

TIELKER, D., HACKER, S., LORIS, R., STRATHMANN, M., WINGENDER, J., WILHELM, S., ROSENAU, F. & JAEGER, K.-E. 2005. Pseudomonas aeruginosa lectin LecB is located in the outer membrane and is involved in biofilm formation. *Microbiology,* 151**,** 1313-1323.

TILLEY, A. E., WALTERS, M. S., SHAYKHIEV, R. & CRYSTAL, R. G. 2015. Cilia dysfunction in lung disease. *Annual Review of Physiology,* 77**,** 379-406.

TIMMUSK, S., BEHERS, L., MUTHONI, J., MURAYA, A. & ARONSSON, A.-C. 2017. Perspectives and Challenges of Microbial Application for Crop Improvement. *Frontiers in Plant Science,* 8.

TINEVEZ, J.-Y., PERRY, N., SCHINDELIN, J., HOOPES, G. M., REYNOLDS, G. D., LAPLANTINE, E., BEDNAREK, S. Y., SHORTE, S. L. & ELICEIRI, K. W. 2017. TrackMate: An open and extensible platform for single-particle tracking. *Methods,* 115**,** 80-90.

TOMLIN, K. L., COLL, O. P. & CERI, H. 2001. Interspecies biofilms of Pseudomonas aeruginosa and Burkholderia cepacia. *Canadian Journal of Microbiology,* 47**,** 949-954.

TONE, K., STAPPERS, M. H., WILLMENT, J. A. & BROWN, G. D. 2019. C‐type lectin receptors of the Dectin‐1 cluster: Physiological roles and involvement in disease. *European Journal of Immunology,* 49**,** 2127-2133.

TOYJANOVA, J., FLORES-CORTEZ, E., REICHNER, J. S. & FRANCK, C. 2015. Matrix confinement plays a pivotal role in regulating neutrophil-generated tractions, speed, and integrin utilization. *Journal of Biological Chemistry,* 290**,** 3752-3763.

TOYOFUKU, M., ROSCHITZKI, B., RIEDEL, K. & EBERL, L. 2012. Identification of proteins associated with the Pseudomonas aeruginosa biofilm extracellular matrix. *Journal of Proteome Research,* 11**,** 4906-4915.

TRAVASSOS, L. H., CARNEIRO, L. A., GIRARDIN, S. E., BONECA, I. G., LEMOS, R., BOZZA, M. T., DOMINGUES, R. C., COYLE, A. J., BERTIN, J. & PHILPOTT, D. J. 2005. Nod1 participates in the innate immune response to Pseudomonas aeruginosa. *Journal of Biological Chemistry,* 280**,** 36714-36718.

TROEGELER, A., MERCIER, I., COUGOULE, C., PIETRETTI, D., COLOM, A., DUVAL, C., VU MANH, T.-P., CAPILLA, F., POINCLOUX, R., PINGRIS, K., NIGOU, J., RADEMANN, J., DALOD, M., VERRECK, F. A. W., AL SAATI, T., LUGO-VILLARINO, G., LEPENIES, B., HUDRISIER, D. & NEYROLLES, O. 2017. C-type lectin receptor DCIR modulates immunity to tuberculosis by sustaining type I interferon signaling in dendritic cells. *Proceedings of the National Academy of Sciences of the United States of America,* 114**,** E540-E549.

TSAI, W. C., STRIETER, R. M., MEHRAD, B., NEWSTEAD, M. W., ZENG, X. & STANDIFORD, T. J. 2000. CXC Chemokine Receptor CXCR2 Is Essential for Protective Innate Host Response in Murine Pseudomonas aeruginosaPneumonia. *Infection and Immunity,* 68**,** 4289-4296.

TSENG, B. S., REICHHARDT, C., MERRIHEW, G. E., ARAUJO-HERNANDEZ, S. A., HARRISON, J. J., MACCOSS, M. J. & PARSEK, M. R. 2018. A biofilm matrix-associated protease inhibitor protects Pseudomonas aeruginosa from proteolytic attack. *Mbio,* 9.

TSENG, B. S., ZHANG, W., HARRISON, J. J., QUACH, T. P., SONG, J. L., PENTERMAN, J., SINGH, P. K., CHOPP, D. L., PACKMAN, A. I. & PARSEK, M. R. 2013. The extracellular matrix protects P seudomonas aeruginosa biofilms by limiting the penetration of tobramycin. *Environmental Microbiology,* 15**,** 2865-2878.

TURKINA, M. V. & VIKSTRÖM, E. 2019. Bacteria-Host Crosstalk: Sensing of the Quorum in the Context of Pseudomonas aeruginosa Infections. *J Innate Immun,* 11**,** 263-279.

TURNBULL, L., TOYOFUKU, M., HYNEN, A. L., KUROSAWA, M., PESSI, G., PETTY, N. K., OSVATH, S. R., CÁRCAMO-OYARCE, G., GLOAG, E. S. & SHIMONI, R. 2016. Explosive cell lysis as a mechanism for the biogenesis of bacterial membrane vesicles and biofilms. *Nature Communications,* 7**,** 1-13.

TURNER, J. & TORRELLES, J. B. 2018. Mannose-capped lipoarabinomannan in Mycobacterium tuberculosis pathogenesis. *Pathogens and Disease,* 76**,** fty026.

TURNER, K. H., EVERETT, J., TRIVEDI, U., RUMBAUGH, K. P. & WHITELEY, M. 2014. Requirements for Pseudomonas aeruginosa acute burn and chronic surgical wound infection. *PLoS Genetics,* 10.

UEDA, A. & WOOD, T. K. 2009. Connecting quorum sensing, c-di-GMP, pel polysaccharide, and biofilm formation in Pseudomonas aeruginosa through tyrosine phosphatase TpbA (PA3885). *PLoS Pathog,* 5**,** e1000483.

UEDA, A. & WOOD, T. K. 2010. Tyrosine phosphatase TpbA of Pseudomonas aeruginosa controls extracellular DNA via cyclic diguanylic acid concentrations. *Environmental Microbiology Reports,* 2**,** 449-455.

URBAN, C. F., REICHARD, U., BRINKMANN, V. & ZYCHLINSKY, A. 2006. Neutrophil extracellular traps capture and kill Candida albicans yeast and hyphal forms. *Cellular Microbiology,* 8**,** 668-676.

VALENTINI, M., GONZALEZ, D., MAVRIDOU, D. A. & FILLOUX, A. 2018. Lifestyle transitions and adaptive pathogenesis of Pseudomonas aeruginosa. *Current Opinion in Microbiology,* 41**,** 15-20.

VALLET, I., DIGGLE, S. P., STACEY, R. E., CÁMARA, M., VENTRE, I., LORY, S., LAZDUNSKI, A., WILLIAMS, P. & FILLOUX, A. 2004. Biofilm formation in Pseudomonas aeruginosa: fimbrial cup gene clusters are controlled by the transcriptional regulator MvaT. *Journal of Bacteriology,* 186**,** 2880-2890.

VALLET, I., OLSON, J. W., LORY, S., LAZDUNSKI, A. & FILLOUX, A. 2001. The chaperone/usher pathways of Pseudomonas aeruginosa: identification of fimbrial gene clusters (cup) and their involvement in biofilm formation. *Proceedings of the National Academy of Sciences,* 98**,** 6911-6916.

VAN DE LAAR, L., COFFER, P. J. & WOLTMAN, A. M. 2012. Regulation of dendritic cell development by GM-CSF: molecular control and implications for immune homeostasis and therapy. *Blood,* 119**,** 3383-93.

VAN DE LINDE, S., WOLTER, S., HEILEMANN, M. & SAUER, M. 2010. The effect of photoswitching kinetics and labeling densities on super-resolution fluorescence imaging. *J Biotechnol,* 149**,** 260-6.

VAN DER VEEN, B. S., DE WINTHER, M. P. & HEERINGA, P. 2009. Myeloperoxidase: molecular mechanisms of action and their relevance to human health and disease. *Antioxidants & redox signaling,* 11**,** 2899-2937.

VAN HAASTERT, P. J. & DEVREOTES, P. N. 2004. Chemotaxis: signalling the way forward. *Nature reviews Molecular cell biology,* 5**,** 626-634.

VAN KOOYK, Y. & GEIJTENBEEK, T. B. 2003. DC-SIGN: escape mechanism for pathogens. *Nature Reviews Immunology,* 3**,** 697-709.

VAN SCHAIK, E. J., GILTNER, C. L., AUDETTE, G. F., KEIZER, D. W., BAUTISTA, D. L., SLUPSKY, C. M., SYKES, B. D. & IRVIN, R. T. 2005. DNA binding: a novel function of Pseudomonas aeruginosa type IV pili. *Journal of Bacteriology,* 187**,** 1455-1464.

VASSEUR, P., VALLET-GELY, I., SOSCIA, C., GENIN, S. & FILLOUX, A. 2005. The pel genes of the Pseudomonas aeruginosa PAK strain are involved at early and late stages of biofilm formation. *Microbiology,* 151**,** 985-997.

VEESENMEYER, J. L., HAUSER, A. R., LISBOA, T. & RELLO, J. 2009. Pseudomonas aeruginosa virulence and therapy: evolving translational strategies. *Critical Care Medicine,* 37**,** 1777.

VESTWEBER, D. 2015. How leukocytes cross the vascular endothelium. *Nature Reviews Immunology,* 15**,** 692-704.

VIEIRA, S., LEMOS, H., GRESPAN, R., NAPIMOGA, M., DAL‐SECCO, D., FREITAS, A., CUNHA, T., VERRI JR, W., SOUZA‐JUNIOR, D. & JAMUR, M. 2009. A crucial role for TNF‐α in mediating neutrophil influx induced by endogenously generated or exogenous chemokines, KC/CXCL1 and LIX/CXCL5. *British journal of pharmacology,* 158**,** 779-789.

VIJAYAN, D., RADFORD, K. J., BECKHOUSE, A. G., ASHMAN, R. B. & WELLS, C. A. 2012. Mincle polarizes human monocyte and neutrophil responses to Candida albicans. *Immunology and cell biology,* 90**,** 889-895.
VILAPLANA, L. & MARCO, M. P. 2020. Phenazines as potential biomarkers of Pseudomonas aeruginosa infections: synthesis regulation, pathogenesis and analytical methods for their detection. *Analytical and Bioanalytical Chemistry*.
VISWESHWARAN, S. P. & MARITZEN, T. 2019. A simple 3D cellular chemotaxis assay and analysis workflow suitable for a wide range of migrating cells. *MethodsX,* 6**,** 2807-2821.
VOLLMER, J. 2006. TLR9 in health and disease. *Int Rev Immunol,* 25**,** 155-81.
VON BISMARCK, P., SCHNEPPENHEIM, R. & SCHUMACHER, U. 2001. Successful treatment of Pseudomonas aeruginosa respiratory tract infection with a sugar solution-a case report on a lectin based therapeutic principle. *Klinische Pädiatrie,* 213**,** 285-287.
VON CHAMIER, L., LAINE, R. F. & HENRIQUES, R. 2019. Artificial intelligence for microscopy: what you should know. *Biochemical Society Transactions,* 47**,** 1029-1040.
VU, B., CHEN, M., CRAWFORD, R. J. & IVANOVA, E. P. 2009. Bacterial extracellular polysaccharides involved in biofilm formation. *Molecules,* 14**,** 2535-2554.
WAGENER, M., HOVING, J. C., NDLOVU, H. & MARAKALALA, M. J. 2018. Dectin-1-Syk-CARD9 signaling pathway in TB immunity. *Frontiers in Immunology,* 9**,** 225.
WAGNER, J. G. & ROTH, R. A. 2000. Neutrophil migration mechanisms, with an emphasis on the pulmonary vasculature. *Pharmacological Reviews,* 52**,** 349-374.
WAGNER, V. E., BUSHNELL, D., PASSADOR, L., BROOKS, A. I. & IGLEWSKI, B. H. 2003. Microarray analysis of Pseudomonas aeruginosa quorum-sensing regulons: effects of growth phase and environment. *J Bacteriol,* 185**,** 2080-95.
WALKER, T. S., TOMLIN, K. L., WORTHEN, G. S., POCH, K. R., LIEBER, J. G., SAAVEDRA, M. T., FESSLER, M. B., MALCOLM, K. C., VASIL, M. L. & NICK, J. A. 2005. Enhanced Pseudomonas aeruginosa biofilm development mediated by human neutrophils. *Infection and Immunity,* 73**,** 3693-3701.
WANDSTRAT, A. & WAKELAND, E. 2001. The genetics of complex autoimmune diseases: non-MHC susceptibility genes. *Nat Immunol,* 2**,** 802-9.
WANG, J.-X., BAIR, A. M., KING, S. L., SHNAYDER, R., HUANG, Y.-F., SHIEH, C.-C., SOBERMAN, R. J., FUHLBRIGGE, R. C. & NIGROVIC, P. A. 2012. Ly6G ligation blocks recruitment of neutrophils via a β2-integrin–dependent mechanism. *Blood, The Journal of the American Society of Hematology,* 120**,** 1489-1498.
WANG, J., HOSSAIN, M., THANABALASURIAR, A., GUNZER, M., MEININGER, C. & KUBES, P. 2017. Visualizing the function and fate of neutrophils in sterile injury and repair. *Science,* 358**,** 111-116.
WARD, R. A., NAKAMURA, M. & MCLEISH, K. R. 2000. Priming of the neutrophil respiratory burst involves p38 mitogen-activated protein kinase-dependent exocytosis of flavocytochrome b 558-containing granules. *Journal of Biological Chemistry,* 275**,** 36713-36719.
WARGO, M. J., GROSS, M. J., RAJAMANI, S., ALLARD, J. L., LUNDBLAD, L. K. A., ALLEN, G. B., VASIL, M. L., LECLAIR, L. W. & HOGAN, D. A. 2011. Hemolytic phospholipase C inhibition protects lung function during Pseudomonas

aeruginosa infection. *American Journal of Respiratory and Critical Care Medicine,* 184**,** 345-354.
WARTHA, F., BEITER, K., ALBIGER, B., FERNEBRO, J., ZYCHLINSKY, A., NORMARK, S. & HENRIQUES‐NORMARK, B. 2007. Capsule and D‐alanylated lipoteichoic acids protect Streptococcus pneumoniae against neutrophil extracellular traps. *Cellular Microbiology,* 9**,** 1162-1171.
WEI, Q. & MA, L. Z. 2013. Biofilm matrix and its regulation in Pseudomonas aeruginosa. *International Journal of Molecular Sciences,* 14**,** 20983-21005.
WEIS, W. I., TAYLOR, M. E. & DRICKAMER, K. 1998. The C-type lectin superfamily in the immune system. *Immunol Rev,* 163**,** 19-34.
WEISS, J. & BARKER, J. 2018. Diverse pro-inflammatory endotoxin recognition systems of mammalian innate immunity. *F1000Research,* 7.
WELLS, C. A., SALVAGE-JONES, J. A., LI, X., HITCHENS, K., BUTCHER, S., MURRAY, R. Z., BECKHOUSE, A. G., MANZANERO, S., COBBOLD, C. & SCHRODER, K. 2008. The macrophage-inducible C-type lectin, mincle, is an essential component of the innate immune response to Candida albicans. *The Journal of Immunology,* 180**,** 7404-7413.
WELSH, M., TSUI, L. & BOAT, T. 1995. In Scriver, CR, Beaudet, AL, Sly, WS and Valle, D. *The Metabolic and Molecular Bases of Inherited Disease***,** 3799-3876.
WHITCHURCH, C. B., TOLKER-NIELSEN, T., RAGAS, P. C. & MATTICK, J. S. 2002. Extracellular DNA Required for Bacterial Biofilm Formation. *Science,* 295**,** 1487.
WHITESON, K., AGRAWAL, S. & AGRAWAL, A. 2017. Differential responses of human dendritic cells to metabolites from the oral/airway microbiome. *Clinical & Experimental Immunology,* 188**,** 371-379.
WIJESINGHE, G., DILHARI, A., GAYANI, B., KOTTEGODA, N., SAMARANAYAKE, L. & WEERASEKERA, M. 2019. Influence of laboratory culture media on in vitro growth, adhesion, and biofilm formation of Pseudomonas aeruginosa and Staphylococcus aureus. *Medical Principles and Practice,* 28**,** 28-35.
WILKING, J. N., ANGELINI, T. E., SEMINARA, A., BRENNER, M. P. & WEITZ, D. A. 2011. Biofilms as complex fluids. *MRS bulletin,* 36**,** 385-391.
WILLIAMS, B. J., DEHNBOSTEL, J. & BLACKWELL, T. S. 2010. Pseudomonas aeruginosa: host defence in lung diseases. *Respirology,* 15**,** 1037-1056.
WILLIAMS, P. & CÁMARA, M. 2009. Quorum sensing and environmental adaptation in Pseudomonas aeruginosa: a tale of regulatory networks and multifunctional signal molecules. *Current Opinion in Microbiology,* 12**,** 182-191.
WILLMENT, J. A., LIN, H.-H., REID, D. M., TAYLOR, P. R., WILLIAMS, D. L., WONG, S. Y. C., GORDON, S. & BROWN, G. D. 2003. Dectin-1 Expression and Function Are Enhanced on Alternatively Activated and GM-CSF-Treated Macrophages and Are Negatively Regulated by IL-10, Dexamethasone, and Lipopolysaccharide. *The Journal of Immunology,* 171**,** 4569.
WINZER, K., FALCONER, C., GARBER, N. C., DIGGLE, S. P., CAMARA, M. & WILLIAMS, P. 2000. The Pseudomonas aeruginosa lectins PA-IL and PA-IIL are controlled by quorum sensing and by RpoS. *J Bacteriol,* 182**,** 6401-11.
WITTMANN, A., LAMPRINAKI, D., BOWLES, K. M., KATZENELLENBOGEN, E., KNIREL, Y. A., WHITFIELD, C., NISHIMURA, T., MATSUMOTO, N., YAMAMOTO, K. & IWAKURA, Y. 2016. Dectin-2 recognizes mannosylated O-antigens of human opportunistic pathogens and augments lipopolysaccharide activation of myeloid cells. *Journal of Biological Chemistry,* 291**,** 17629-17638.

WOLCOTT, R. D., RHOADS, D. D., BENNETT, M. E., WOLCOTT, B. M., GOGOKHIA, L., COSTERTON, J. W. & DOWD, S. E. 2010. Chronic wounds and the medical biofilm paradigm. *J Wound Care,* 19**,** 45-6, 48-50, 52-3.

WOLCOTT, R. D., RHOADS, D. D. & DOWD, S. E. 2008. Biofilms and chronic wound inflammation. *Journal of Wound Care,* 17**,** 333-341.

WOLFAARDT, G. M., LAWRENCE, J. R., ROBARTS, R. D., CALDWELL, S. J. & CALDWELL, D. E. 1994. Multicellular organization in a degradative biofilm community. *Appl Environ Microbiol,* 60**,** 434-46.

WOLFGANG, M. C., JYOT, J., GOODMAN, A. L., RAMPHAL, R. & LORY, S. 2004. Pseudomonas aeruginosa regulates flagellin expression as part of a global response to airway fluid from cystic fibrosis patients. *Proceedings of the National Academy of Sciences,* 101**,** 6664-6668.

WOOD, S. J., GOLDUFSKY, J. W., BELLO, D., MASOOD, S. & SHAFIKHANI, S. H. 2015. Pseudomonas aeruginosa ExoT induces mitochondrial apoptosis in target host cells in a manner that depends on its GTPase-activating protein (GAP) domain activity. *Journal of Biological Chemistry,* 290**,** 29063-29073.

WOZNIAK, D. J., WYCKOFF, T. J., STARKEY, M., KEYSER, R., AZADI, P., O'TOOLE, G. A. & PARSEK, M. R. 2003. Alginate is not a significant component of the extracellular polysaccharide matrix of PA14 and PAO1 Pseudomonas aeruginosa biofilms. *Proc Natl Acad Sci U S A,* 100**,** 7907-12.

WU, H., MOSER, C., WANG, H.-Z., HØIBY, N. & SONG, Z.-J. 2015. Strategies for combating bacterial biofilm infections. *International journal of oral science,* 7**,** 1.

WU, H., WANG, D., TANG, M. & MA, L. Z. 2019. The advance of assembly of exopolysaccharide Psl biosynthesis machinery in Pseudomonas aeruginosa. *Microbiology Open,* 8**,** e857.

XU, S. & SHINOHARA, M. L. 2017. Tissue-resident macrophages in fungal infections. *Frontiers in Immunology,* 8**,** 1798.

YAMAMOTO, Y., KLEIN, T. W. & FRIEDMAN, H. 1997. Involvement of mannose receptor in cytokine interleukin-1beta (IL-1beta), IL-6, and granulocyte-macrophage colony-stimulating factor responses, but not in chemokine macrophage inflammatory protein 1beta (MIP-1beta), MIP-2, and KC responses, caused by attachment of Candida albicans to macrophages. *Infection and Immunity,* 65**,** 1077-1082.

YAMASAKI, S. 2016. *C-type Lectin Receptors in Immunity*, Springer.

YAMASAKI, S., ISHIKAWA, E., SAKUMA, M., HARA, H., OGATA, K. & SAITO, T. 2008. Mincle is an ITAM-coupled activating receptor that senses damaged cells. *Nature Immunology,* 9**,** 1179-1188.

YAMASAKI, S., MATSUMOTO, M., TAKEUCHI, O., MATSUZAWA, T., ISHIKAWA, E., SAKUMA, M., TATENO, H., UNO, J., HIRABAYASHI, J. & MIKAMI, Y. 2009. C-type lectin Mincle is an activating receptor for pathogenic fungus, Malassezia. *Proceedings of the National Academy of Sciences,* 106**,** 1897-1902.

YANG, J., ZHAO, H.-L., RAN, L.-Y., LI, C.-Y., ZHANG, X.-Y., SU, H.-N., SHI, M., ZHOU, B.-C., CHEN, X.-L. & ZHANG, Y.-Z. 2015. Mechanistic insights into elastin degradation by pseudolysin, the major virulence factor of the opportunistic pathogen Pseudomonas aeruginosa. *Scientific reports,* 5**,** 9936.

YANG, S.-J., OH, H.-M., CHUNG, S. & CHO, J.-C. 2009. Antarcticimonas flava gen. nov., sp. nov., isolated from Antarctic coastal seawater. *The Journal of Microbiology,* 47**,** 517-523.

YOKOTA, S. I., KAYA, S., SAWADA, S., KAWAMURA, T., ARAKI, Y. & ITO, E. 1987. Characterization of a polysaccharide component of lipopolysaccharide from

Pseudomonas aeruginosa IID 1008 (ATCC 27584) as D‐rhamnan. *European Journal of Biochemistry,* 167**,** 203-209.
YONEKAWA, A., SAIJO, S., HOSHINO, Y., MIYAKE, Y., ISHIKAWA, E., SUZUKAWA, M., INOUE, H., TANAKA, M., YONEYAMA, M., OH-HORA, M., AKASHI, K. & YAMASAKI, S. 2014. Dectin-2 is a direct receptor for mannose-capped lipoarabinomannan of mycobacteria. *Immunity,* 41**,** 402-413.
YOUNG, R. L., MALCOLM, K. C., KRET, J. E., CACERES, S. M., POCH, K. R., NICHOLS, D. P., TAYLOR-COUSAR, J. L., SAAVEDRA, M. T., RANDELL, S. H. & VASIL, M. L. 2011. Neutrophil extracellular trap (NET)-mediated killing of Pseudomonas aeruginosa: evidence of acquired resistance within the CF airway, independent of CFTR. *PloS One,* 6.
YOUSEFI, S. & SIMON, H.-U. 2016. NETosis–does it really represent nature's "suicide bomber"? *Frontiers in Immunology,* 7**,** 328.
ZEGANS, M. E., DIGIANDOMENICO, A., RAY, K., NAIMIE, A., KELLER, A. E., STOVER, C. K., LALITHA, P., SRINIVASAN, M., ACHARYA, N. R. & LIETMAN, T. M. 2016. Association of Biofilm Formation, Psl Exopolysaccharide Expression, and Clinical Outcomes in Pseudomonas aeruginosa Keratitis: Analysis of Isolates in the Steroids for Corneal Ulcers Trial. *JAMA Ophthalmology,* 134**,** 383-389.
ZEGANS, M. E., WOZNIAK, D., GRIFFIN, E., TOUTAIN-KIDD, C. M., HAMMOND, J. H., GARFOOT, A. & LAM, J. S. 2012. Pseudomonas aeruginosa exopolysaccharide Psl promotes resistance to the biofilm inhibitor polysorbate 80. *Antimicrobial Agents and Chemotherapy,* 56**,** 4112-4122.
ZELENSKY, A. N. & GREADY, J. E. 2005. The C-type lectin-like domain superfamily. *FEBS J,* 272**,** 6179-217.
ZHAN, Y., VEGA-RAMOS, J., CARRINGTON, E. M., VILLADANGOS, J. A., LEW, A. M. & XU, Y. 2012a. The inflammatory cytokine, GM-CSF, alters the developmental outcome of murine dendritic cells. *Eur J Immunol,* 42**,** 2889-900.
ZHAN, Y., XU, Y. & LEW, A. M. 2012b. The regulation of the development and function of dendritic cell subsets by GM-CSF: more than a hematopoietic growth factor. *Mol Immunol,* 52**,** 30-7.
ZHANG, R., NEU, T. R., BELLENBERG, S., KUHLICKE, U., SAND, W. & VERA, M. 2015. Use of lectins to in situ visualize glycoconjugates of extracellular polymeric substances in acidophilic archaeal biofilms. *Microbial Biotechnology,* 8**,** 448-461.
ZHANG, X., BISHOP, P. L. & KUPFERLE, M. J. 1998. Measurement of polysaccharides and proteins in biofilm extracellular polymers. *Water Science and Technology,* 37**,** 345-348.
ZHANG, Z., LOUBOUTIN, J.-P., WEINER, D. J., GOLDBERG, J. B. & WILSON, J. M. 2005. Human airway epithelial cells sense Pseudomonas aeruginosa infection via recognition of flagellin by Toll-like receptor 5. *Infection and Immunity,* 73**,** 7151-7160.
ZHANG, Z., REENSTRA, W., WEINER, D. J., LOUBOUTIN, J.-P. & WILSON, J. M. 2007. The p38 mitogen-activated protein kinase signaling pathway is coupled to Toll-like receptor 5 to mediate gene regulation in response to Pseudomonas aeruginosa infection in human airway epithelial cells. *Infection and Immunity,* 75**,** 5985-5992.
ZHAO, K., TSENG, B. S., BECKERMAN, B., JIN, F., GIBIANSKY, M. L., HARRISON, J. J., LUIJTEN, E., PARSEK, M. R. & WONG, G. C. L. 2013. Psl trails guide

exploration and microcolony formation in Pseudomonas aeruginosa biofilms. *Nature,* 497**,** 388-391.
ZHAO, Y., CHEN, H., WANG, Y. & LI, Q. 2016. Effect of sodium alginate and its guluronic acid/mannuronic acid ratio on the physicochemical properties of high‐amylose cornstarch. *Starch‐Stärke,* 68**,** 1215-1223.
ZHOU, K. L., LI, X., ZHANG, X. L. & PAN, Q. 2019. Mycobacterial mannose-capped lipoarabinomannan: a modulator bridging innate and adaptive immunity. *Emerg Microbes Infect,* 8**,** 1168-1177.
ZHU, L.-L., ZHAO, X.-Q., JIANG, C., YOU, Y., CHEN, X.-P., JIANG, Y.-Y., JIA, X.-M. & LIN, X. 2013. C-type lectin receptors Dectin-3 and Dectin-2 form a heterodimeric pattern-recognition receptor for host defense against fungal infection. *Immunity,* 39**,** 324-334.